UNIVERSITY OF SOUTHAMPTON

A COMPUTATIONAL FLUID DYNAMICS INVESTIGATION INTO THE PARTICULATE EROSION OF OILFIELD CONTROL VALVES

VOLUME 2

BY

ALISTER FRANK FORDER

A dissertation submitted in the partial fulfillment of the requirements for the degree of Doctor of Philosophy at the University of Southampton

Faculty of Engineering and Applied Science January 2001

UNIVERSITY OF SOUTHAMPTON

SUMMARY OF APPENDICES

FACULTY OF ENGINEERING AND APPLIED SCIENCE
DEPARTMENT OF MECHANICAL ENGINEERING

Doctor of Philosophy

A COMPUTATIONAL FLUID DYNAMICS INVESTIGATION INTO THE PARTICULATE EROSION OF OILFIELD CONTROL VALVES

by Alister Frank Forder

Due to size constraints upon the binding of the thesis, the necessity for extensive appendices has arisen. This approach has been beneficial in that a broad array of supporting material has been included and that the numerous graphical representations have been stored in a separate binder, facilitating ease of reference with the main text.

The Appendices table of contents included herewith, details the topic range deemed to hold value to this study.

Appendices Table of Contents

List of Appendices Figures and Pictures

Appendix A Summary of the Effects of Erodent Velocity on Erosion

ERODENT	TARGET MATERIAL	IMPINGEMENT ANGLE	ERODENT VELOCITY	VELOCITY EXPONENT 'N'	REFERENCE
Steel Shot	Annealed glass, Glass, Porcelain	90°	100-300 ft/s	6.5, 5.5, 3.3	Finnie
Steel Shot No.70 No.110	Glass, MgO, Graphite	90°	100-1000 ft/s	4.37, 2.73, 2.67	Sheldon
Carbon tetrachloride	Nickel	Variable	100-210 m/s	4.8	Rochester & Brunton
Ash	Mild Steel	45°	30-40 m/s	3.5	Raask
Arizona road dust	410 SS, 17-7 PH	37.5, 60°	650-1100 ft/s	0.3 - 1.64	Smeltzer
Silica slurry	Chromel	Variable	1-9 ft/s	2.6	Jackson
Silica flour	Tempered C-1050 Steel	40°	100-1000 ft/s	2	Miller & Coyle
Diamond	11% Cr. Steel, Al-Alloy	90°	100-1000 ft/s	2.3	Tilly & Sage
SiC, Glass shot, Quartz	Al, Cu, Steel	20, 30, 90°	1000 ft/s	2.05 - 2.9	Sheldon & Kanhere
Quartz	Mild steel	30-45°	30-40 m/s	2.5	Raask
Quartz	11% Cr.-Steel	20, 90°	200-1800 ft/s	2.0 - 2.3	Tilly
Quartz	Many materials	90°	200-1800 ft/s	2.3	Tilly
Quartz	Many materials	90°	800 ft/s	0.2 - 10	Tilly & Sage
Quartz	11% Cr.-Steel, Al-Alloy	90°	100-1000 ft/s	2.3, 2.3	Tilly & Sage
Glass	11% Cr.-Steel, Al-Alloy	90°	100-1000 ft/s	3.4, 2.4	Tilly & Sage
SiC (220 mesh)	Aluminium	Variable	97-164 ft/s	2	Bridwell
SiC (46 mesh)	1020 Steel	20°	100-300 ft/s	2	Finnie
SiC (60 mesh)	Tool/Mild Steel	20°	450-2500 ft/s	2.05 - 2.44	Finnie
SiC (60, 120 mesh)	Plate Glass	90°	100-1000 ft/s	3.0	Sheldon
SiC (60, 120 mesh)	Glass, MgO, Steel, Al_2O_3	90°	100-1000 ft/s	3.0, 2.74, 2.69, 2.53, 2.62	Sheldon
SiC (60, 180 mesh)	6061-0 Al	20°	< 500 ft/s	2.36	Sheldon
SiC (60, 180 mesh)	1215 Steel	20°	< 500 ft/s	2.48, 2.69	Sheldon
SiC (60, 180 mesh)	Copper	20°	< 500 ft/s	2.36	Sheldon
Sand (200-250μm)	28 materials	7.5, 22.5, 90°	22, 55, 320 m/s	0.9 - 3.4	Haugen
Sand (200-250μm)	1020 steel	30, 45 ,60, 75, 90°	~ 8 m/s	2.54	Forder [Chp. 9]
Sand (200-250μm)	Various WC	30, 45 ,60, 75, 90°	~ 8 m/s	3.8 - 3.9	Forder [Chp. 9]

Appendix B Summary of the Dependency of Erosion upon the Impingement Angle

ERODENT	TARGET MATERIAL	ERODENT VELOCITY	CRITICAL ANGLE	OTHER RELATIONS	REFERENCE
Cast Iron Pellets	Annealed Glass	990.6 cm/s	$\alpha_c = 90°$	$\varepsilon \sim 0$ for $\alpha < 20°$ ε inc. with α 20-90°	Bitter
Cast Iron Pellets	Annealed Glass	3048 cm/s	$\alpha_c = 90°$	$\varepsilon \sim 0$ for $\alpha < 10°$ ε inc. with α 10-90°	Bitter
Cast Iron Pellets	Glass	3048 cm/s	$\alpha_c = 90°$	$\varepsilon \sim 0$ for $\alpha < 10°$ ε inc. with α 10-90°	Bitter
Cast Iron Pellets	Aluminium	10 m/s	$\alpha_c = 15°$	-	Bitter
SiC	Aluminium, Copper, 1055 Steel	107 m/s	$\alpha_c = 12, 13, 25°$	-	Bitter
SiC, Al_2O_3	Aluminium, Copper, 1055 Steel	250 ft/s	$\alpha_c = 20°$	-	Finnie
SiC	Many Metals	250 ft/s	$\alpha_c = 20°$	-	Finnie
Al_2O_3	Glass	260, 316, 354 ft/s	$\alpha_c = 90°$	ε inc. with α 0-90°	Neilson & Gilchrist
Glass	Glass	260 ft/s	-	$\varepsilon \sim 0$ for $\alpha < 35°$ ε inc. with α 35-90°	Neilson & Gilchrist
Al_2O_3	Graphite, Perspex	363, 420 ft/s	$\alpha_c = 50°$	ε inc. with α 0-90°	Neilson & Gilchrist
Quartz	Mild Steel	20 m/s	$30° < \alpha_c < 45°$	-	Raask
SiC	Some brittle materials	500 ft/s	$\alpha_c = 60°$	-	Sheldon
SiC	Some ductile materials	500 ft/s	$\alpha_c = 50°$	-	Sheldon
Al_2O_3, Arizona road dust	Number of alloys	500, 600 ft/s	$\alpha_c = 45°$	-	Smeltzer
Arizona road dust	2024 Al	1100, 650 ft/s	-	ε inc. with α 0-90°	Smeltzer
Quartz	Aluminium, 11% Cr.-Steel, Glass	340 ft/s	$\alpha_c = 45°$	ε inc. with α 0-90°	Tilly
Al_2O_3 flourite	302 SS	300 m/s	$\alpha_c = 30°$	-	Head
Al_2O_3 flourite	6061-T6 Al	300 m/s	$\alpha_c = 30°$	-	Head
Alundum, Crystolon, Glass beads, Silica	Many Materials	200-700 ft/s	variable	-	Head & Harr
Glass, Quartz, Corundum	Steel	120 m/s	$\alpha_c = 30°$	-	Kleis
Variable	Aluminium, Mild steel	100-400 ft/s	$\alpha_c = 20°$	$\varepsilon \sim 0$ for $\alpha < 5°$ ε inc. with α 5-90°	Neilson & Gilchrist

ERODENT	TARGET MATERIAL	ERODENT VELOCITY	CRITICAL ANGLE	OTHER RELATIONS	REFERENCE
Variable	Various materials	100-400 ft/s	$\alpha_c = 20°$	$\varepsilon \sim 0$ for $\alpha < 5°$ ε inc. with α 5-90°	Neilson & Gilchrist
Al_2O_3	Ceramics	100-400 ft/s	$\alpha_c = 90°$	ε inc. with α 0-90°	Neilson & Gilchrist
Al_2O_3	Aluminium	424, 494, 354 ft/s	$\alpha_c = 20°$	-	Neilson & Gilchrist
Glass	Aluminium	354 ft/s	$\alpha_c = 20°$	-	Neilson & Gilchrist
Quartz	H46 Steel	1200 ft/s	$\alpha_c = 30°$	-	Tilly
Glass, Quartz	Al-Alloy	800 ft/s	$\alpha_c = 30°$	-	Tilly & Sage
Sand	Steel	30, 80 m/s	$\alpha_c = 30°$	ε inc. with α 0-90°	Uuemois
Sand	Various metals	5 m/s	-	ε inc. with α 0-90°	Wellinger & Uetz
Sand	Steel	-	$\alpha_c = 60°$	ε inc. with α 0-60°	Wellinger & Brockstedt
SiC (120, 1000 mesh)	1100-OAI	500 ft/s	$\alpha_c = 20°$	-	Sheldon
SiC (120, 500, 1000 mesh)	Plate glass	500 ft/s	$\alpha_c = 80, 85, 25°$	-	Sheldon
SiC (120, 1000 mesh)	Tool steel	500 ft/s	$\alpha_c = 20, 50°$	-	Sheldon
SiC (120, 1000 mesh)	Magnesia	500 ft/s	$\alpha_c = 80, 50°$	-	Sheldon
SiC (120, 1000 mesh)	Graphite	500 ft/s	$\alpha_c = 75, 40°$	-	Sheldon
SiC (120, 1000 mesh)	Aluminium	500 ft/s	$\alpha_c = 70°$	ε inc. with α 0-70°	Sheldon
Silica flour	C-1050 Steel	835 ft/s	$\alpha_c = 20°$	-	Miller & Coyle
Sand (200-250μm)	1020 Steel, 316-Steel, Duplex	22, 55, 320 m/s	$\alpha_c = 30°$	ε inc. for α 0-30° ε dec. for α 30-90°	Haugen
Sand (200-250μm)	Various ceramics	22, 55, 320 m/s	$\alpha_c = 90°$	ε inc. with α 0-90°	Haugen
Sand (200-250μm)	Stellite	22, 55, 320 m/s	$\alpha_c = 90°$	ε inc. with α 0-90°	Haugen
Sand (200-250μm)	Hot sprayed WC (60, 40% Ni)	22, 55, 320 m/s	$\alpha_c = 90°$	ε inc. with α 0-90°	Haugen
Sand (200-250μm)	WC (6, 11% Ni)	22, 55, 320 m/s	$\alpha_c = 90°$	ε inc. with α 0-90°	Haugen
Sand (200-250μm)	1020 Steel	~ 8 m/s	$\alpha_c = 35°$	ε inc. for α 0-35° ε dec. for α 35-90°	Forder [Chp. 9]
Sand (200-250μm)	WC (6, 11% Ni)	~ 8 m/s	$\alpha_c = 90°$	ε inc. with α 0-90°	Forder [Chp. 9]

Appendix C Summary of Predictive Erosion Models

EQ.NO	BASIS	EQUATION DEVELOPED	REFERENCE
C.0	Cutting	$\varepsilon = \frac{MpU^2}{\sigma\psi K}(\sin 2\alpha - \frac{6}{K}\sin^2\alpha)$	Finnie
C.1	Cutting	$\varepsilon = \frac{fpU^2}{4P\left(1+\frac{MpRf^2}{Ip}\right)}\cos^2\alpha$	Finnie
C.2	Cutting	$\varepsilon = \frac{7}{\pi}\left(\frac{U}{Ck}\right)^n \sin 2\alpha\sqrt{\sin\alpha}$	Hashish
C.3	Cutting	$\varepsilon = \frac{M(U\sin\alpha - Ck)^2}{\sqrt{U\sin\alpha}}\left[U\cos\alpha - \frac{C_1(U\sin\alpha - Ck)^2}{\sqrt{U\sin\alpha}}Ec\right]$	Bitter
C.4	Deformation	$\varepsilon = \frac{(U\sin\alpha - Dk)^2}{2Ef}$	Bitter
C.5	Cutting and deformation	$\varepsilon = \frac{(U^2\cos^2\alpha - Uh^2)}{2Ec} + \frac{(U\sin\alpha - K')^2}{2Ef}$	Neilson
C.6	Cutting and particle fragmentation	$\varepsilon = \varepsilon_1\left(\frac{U}{Ur}\right)^2\left[1-\left(\frac{do}{d}\right)^{3/2}\left(\frac{Uo}{U}\right)\right]^2 + \varepsilon_2\left(\frac{U}{Ur}\right)^2 F_{du}$	Tilly
C.7	Dimensional analysis with regression	$\varepsilon = 0.00023 - 0.00016Rf - 0.00024\ln(Hp/E) - 0.00021\ln(Ht/E)$ $+0.0016(U^2/E)^2 + 0.0083\sin\alpha + 0.00003[\ln(Hp/E)]^2$ $-0.001(U^2/E)Rf + 0.0001Rf\ln(Ht/E) - 0.0014\ln(Ht/E)\cos\alpha$	Head & Harr
C.8	Empirical Particle Dynamics	$\varepsilon = k_1 f(\alpha)U^2\cos^2\alpha(1-R_t^2) + k_2(U\sin\alpha)^4$	Grant
C.9	Dimensional analysis	$\varepsilon = \left(\frac{K_t^{5/2}}{Rf}\frac{m^{1/3}}{\rho t^{1/3}kTm\Delta Hm}\right)S$	Jennings
C.10	Indentation hardness	$\varepsilon = C_1\left(\frac{dp^3U^3\rho p^{3/2}}{Ht^{3/2}}\right)$	Sheldon
C.11	Low cycle fatigue	$\varepsilon = 0.033\left(\frac{Fv\rho t\rho p^{1/2}U^3}{Ec^2Ht^{3/2}}\right)$	Hutchings
C.12	Work of shear force	$\varepsilon = \left[\tau + \left(\frac{\phi}{2}\right)^{1/2}Ht\right]\phi^{5/2}\cos^2\alpha\sin^{1/2}\alpha + \left[\tau + \frac{(2\phi)^{1/2}}{1-\phi}Ht\right]\phi^2\sin^2\alpha$	Beckmann
C.13	Shear localisation	$\varepsilon = \frac{(6.5e-3)U^{5/2}\rho p^{1/4}}{CpTm^{3/4}Ht^{1/4}}$	Shewmon

SOUTHAMPTON UNIVERSITY OF LIBRARY

Appendix D Generic Designs of Control Chokes

The Needle and Seat Choke

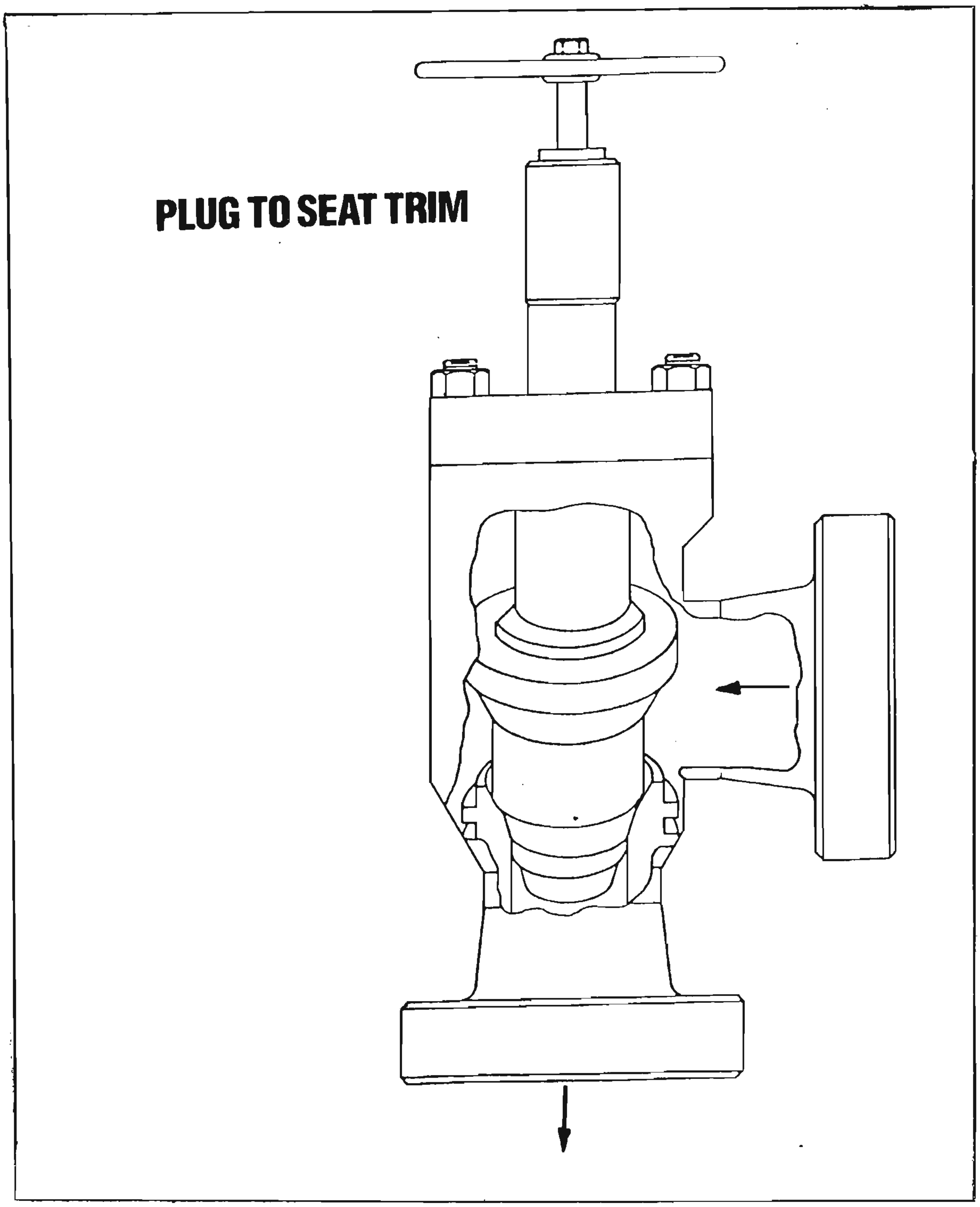

The Internal Plug and Cage Choke

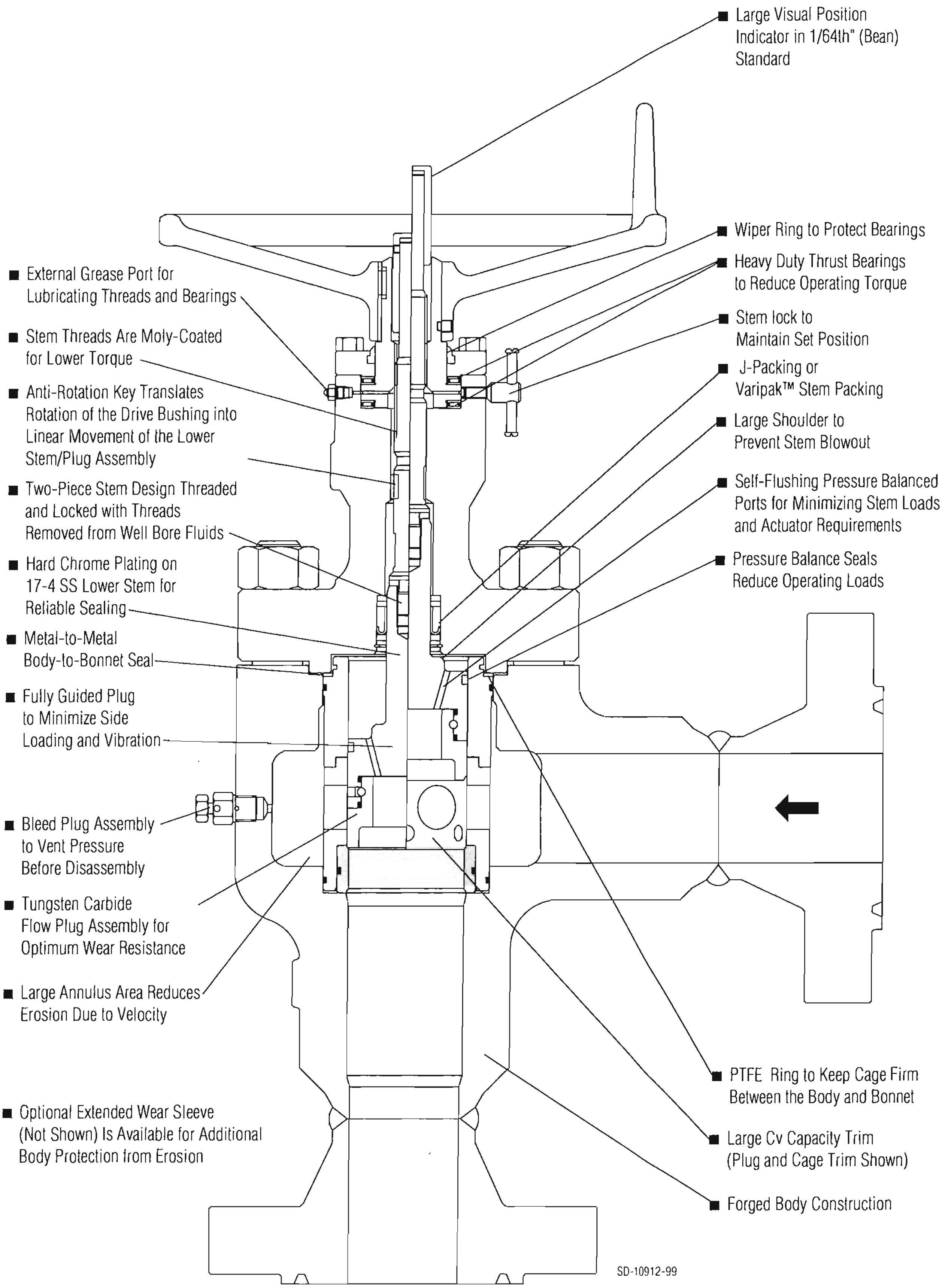

The External Sleeve and Cage Choke

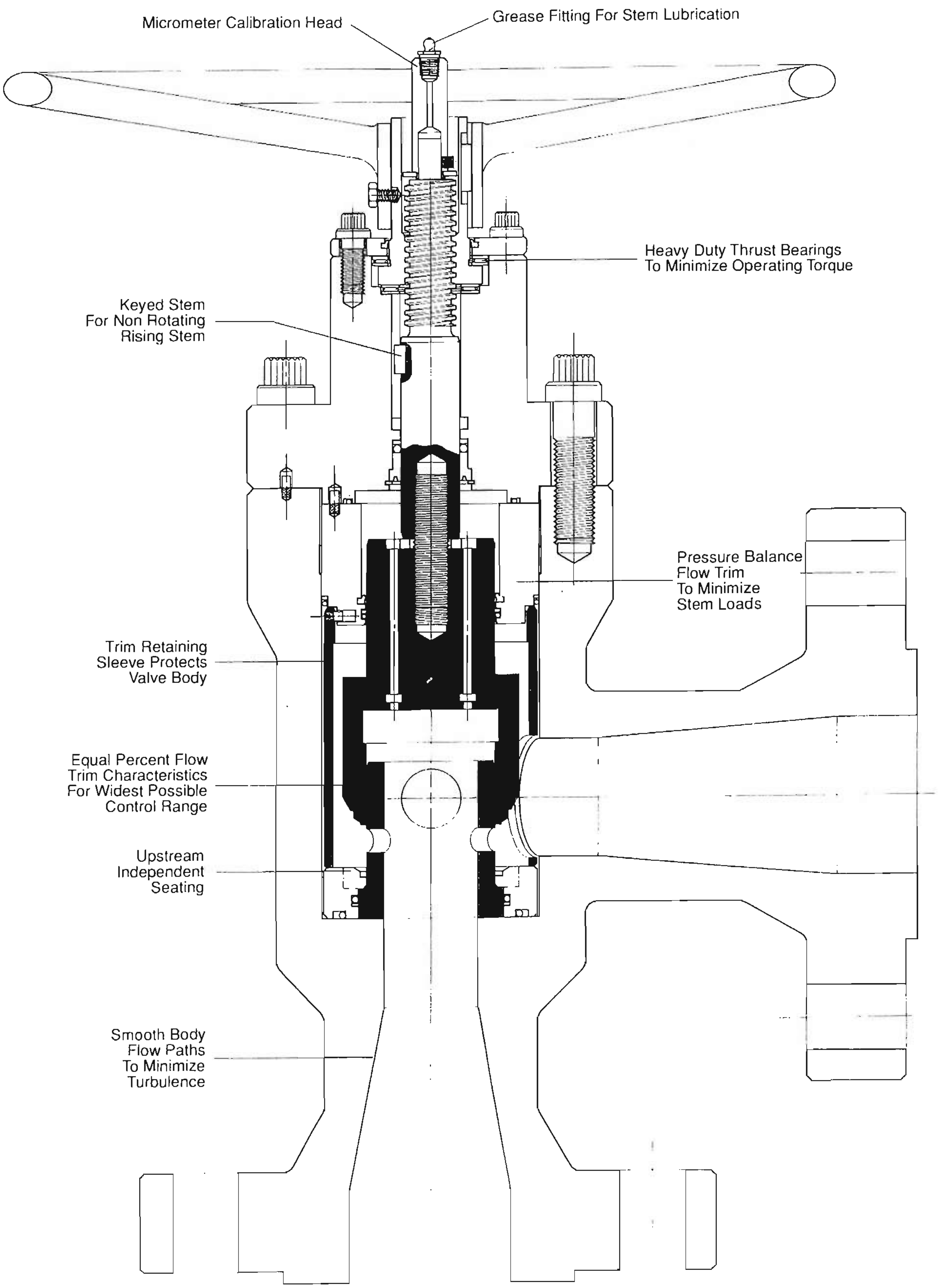

The Multiple Orifice Valve (MOV)

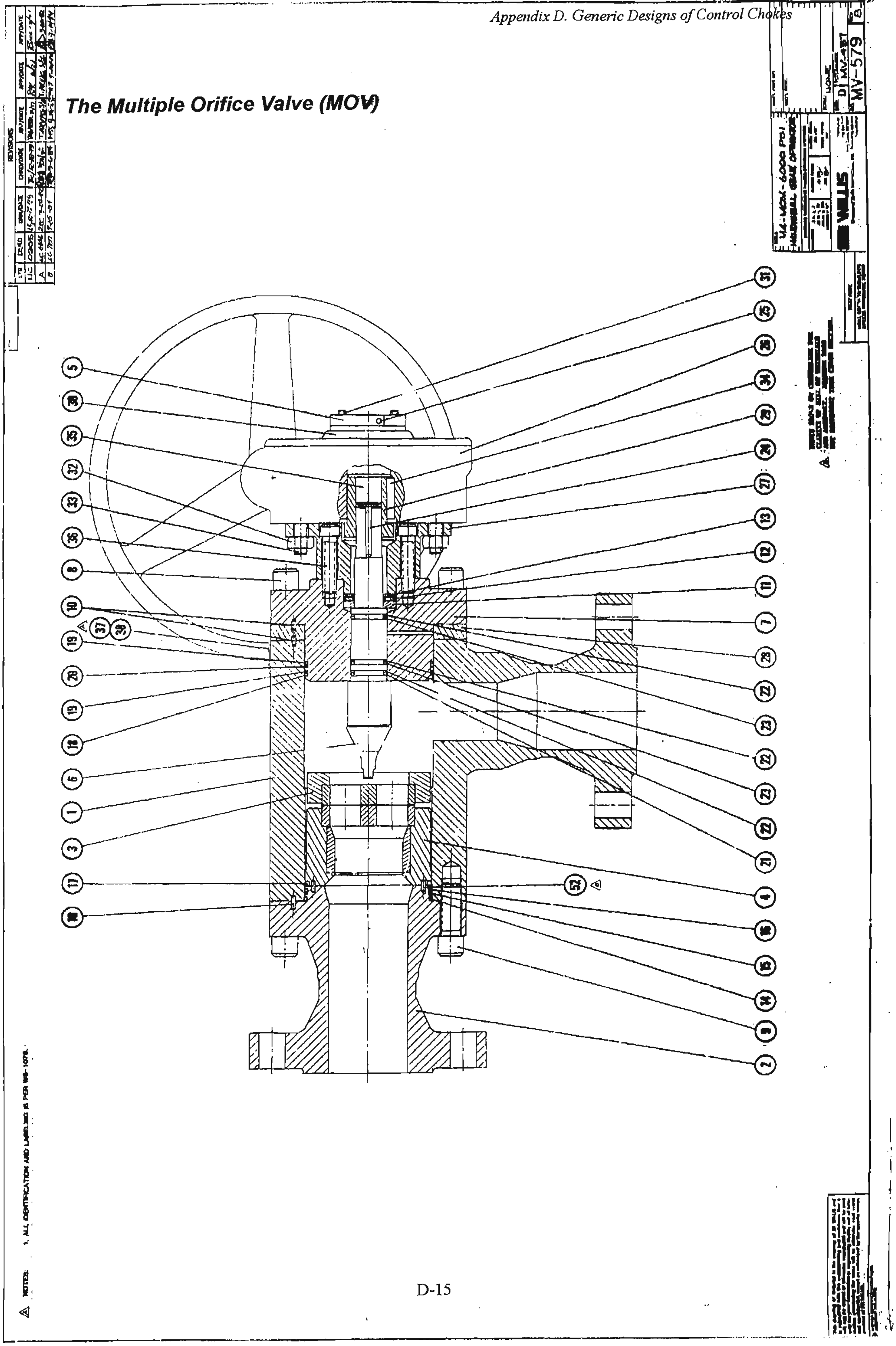

Appendix E Definition of Cv

Cv denotes the number of US gallons per minute of water that will flow through the choke with a pressure drop of 1 psi. The valve flow coefficient is used to determine the size of valve and the trim style required, providing the capacity and control for a particular flow configuration and pressure drop. A *Cv* calculation should be performed at maximum, normal and minimum operating conditions of the field to ensure both rangeability and maximum capacity can be achieved. The design *Cv* should be selected to give suitable valve openings at normal operating conditions.

The selection of a valve with too large a *Cv* will result in the valve being operated near the choked condition; see section 3.5.1. Such a situation induces the highest flow velocities at the vena contracta, hence the greatest erosive potential. Further, from an erosive viewpoint, if small *CVs* are to be expected it is advisable that an equal percentage trim be used. Such trims provide finer control at small *Cv*, thus avoiding the need to choke the flow hard to obtain the desired pressure drop; promoting a uniform flow field and a reduced erosive potential. *Cv* can be defined by the following equation, which allows valve sizing to be achieved. By volume for incompressible flows;

Equation E-1

$$Cv = 1.16Q\sqrt{\frac{Sg}{\Delta p}}$$

By volume for compressible flows following the ideal gas law;

Equation E-2

$$Cv = 0.0366\frac{K_E Q}{V_H}\sqrt{\frac{1}{v_1 \Delta p}}$$

where the expansion correction factor K_E

Equation E-3

$$K_E = S_1\left(1 - \frac{\Delta p}{C_f^2 P_1}\right)^y$$

the multi-stage correction factor V_H

single stage $V_H = 1$

two stages $V_H = 1 + 0.33\frac{\Delta p}{P_1}$

Equation E-4 three stages $V_H = 1 + 0.48\frac{\Delta p}{P_1}$

the inlet specific volume v_1

Equation E-5

$$v_1 = \frac{Z.8314(273 + T_1)}{M_W . P_1 x 10^5}$$

Appendix F An Example of the CFX-F3D Command File

```
>>FLOW3D
  >>SET LIMITS
      TOTAL INTEGER WORK SPACE 50000000
      TOTAL CHARACTER WORK SPACE 10000000
      TOTAL REAL WORK SPACE 80000000
      MAXIMUM NUMBER OF BLOCKS 600
      MAXIMUM NUMBER OF PATCHES 4000
      MAXIMUM NUMBER OF INTER BLOCK BOUNDARIES 1500
 >>OPTIONS
    THREE DIMENSIONS
    BODY FITTED GRID
    CARTESIAN COORDINATES
    TURBULENT FLOW
    ISOTHERMAL FLOW
    INCOMPRESSIBLE FLOW
    STEADY STATE
    /* NO COMBUSTION */
    /* NO COAL COMBUSTION */
    /* NO DELTA FUNCTION */
    USER SCALAR EQUATIONS 3
    MAXIMUM NUMBER OF MATERIAL TYPES 10
    NUMBER OF PHASES 1
    PARTICLE TRANSPORT
    PARTICLE BUOYANCY
 >>VARIABLE NAMES
    USER SCALAR1 'USRDCC ERODED'
    USER SCALAR2 'USRDCC VEL'
    USER SCALAR3 'USRDCC ANG'
>>MODEL TOPOLOGY
  >>INPUT TOPOLOGY
     READ GEOMETRY FILE
>>MODEL DATA
  >>SET INITIAL GUESS
    >>INPUT FROM FILE
       READ DUMP FILE
 >>PARTICLE TRANSPORT MODEL
   >>MODEL CHARACTERISTICS
      MAXIMUM NUMBER OF PARTICLES 1000
      NUMBER OF ITERATIONS 1
      TURBULENT PARTICLE DISPERSION
      PRESSURE GRADIENT FORCE
      CROSS SECTION FACTOR 1.4000E+00
      SURFACE AREA FACTOR 1.2000E+00
  >>INTEGRATION PARAMETERS
     TIME LIMIT 4.0000E+00
     COEFFICIENT OF RESTITUTION 7.5000E-01
     SIMPLE INTERPOLATION AT BLOCK BOUNDARIES
     MINIMUM FRACTION OF CELL CROSSED BETWEEN BOUNDARIES 3.0E-04
     NO PRINTING OF TRACKS
  >>PARTICLE PROPERTIES
     BASE PARTICLE DENSITY 2.650E+03
     PARTICLE TEMPERATURE 3.4000E+02
>>PHYSICAL PROPERTIES
  >>BUOYANCY PARAMETERS
      GRAVITY VECTOR 0.0 8.0 0.0
  >>STANDARD FLUID
      FLUID 'WATER'
      STANDARD FLUID REFERENCE TEMPERATURE 3.3000E+02
  >>TURBULENCE PARAMETERS
    >>TURBULENCE MODEL
        TURBULENCE MODEL 'ALGEBRAIC STRESS'
```

```
>>SOLVER DATA
  >>PROGRAM CONTROL
     MAXIMUM NUMBER OF ITERATIONS 1
     PRESSURE REFERENCE POINT BLOCK 'BLOCK-NUMBER-2'
     PRESSURE REFERENCE POINT 1 1 1
     OUTPUT MONITOR BLOCK 'BLOCK-NUMBER-8'
     OUTPUT MONITOR POINT 1 1 1
     MASS SOURCE TOLERANCE 1.0000E-04
     ITERATIONS OF TURBULENCE EQUATIONS 1
     ITERATIONS OF VELOCITY AND PRESSURE EQUATIONS 1
     ITERATIONS OF TEMPERATURE AND SCALAR EQUATIONS 1
     ITERATIONS OF HYDRODYNAMIC EQUATIONS 1
     SOLVER DEBUG PRINT STREAM 20
  >>EQUATION SOLVERS
     PRESSURE 'AMG'
  >>DEFERRED CORRECTION
     K START 70
     K END 1000
     EPSILON START 70
     EPSILON END 1000
  >>FALSE TIMESTEPS
     K 1.0000E-01
     EPSILON 1.0000E-02
  >>UNDER RELAXATION FACTORS
     U VELOCITY 3.5000E-01
     V VELOCITY 3.5000E-01
     W VELOCITY 3.5000E-01
     PRESSURE 6.5000E-01
     DENSITY 2.0000E-01
     VISCOSITY 1.0000E+00
     K 2.0000E-01
     EPSILON 1.0000E-01
>>CREATE GRID
  >>INPUT GRID
     READ GRID FILE
>>MODEL BOUNDARY CONDITIONS
  >>PARTICLE TRANSPORT BOUNDARY CONDITIONS
    >>PARTICLES ON PATCH
       PATCH NAME 'INLET1'
       EACH CELL CENTRE
       NUMBER OF SIZES 3
       DIAMETER DISTRIBUTION TYPE 'UNIFORM IN DIAMETER'
       DIAMETER DISTRIBUTION PARAMETERS 63E-06 20E-6
       TOTAL MASS FLOW RATE ON PATCH 1.7E-03
       VELOCITY ON PATCH 1.6 0.0 0.0
  >>SET VARIABLES
     PATCH NAME 'INLET'
     U VELOCITY 1.6700E+00
     V VELOCITY 0.0000E+00
     W VELOCITY 0.0000E+00
     PRESSURE 1.0000E+07
     K 8.0000E-03
     EPSILON 3.13E-02
  >>SET VARIABLES
     PATCH NAME 'INLET1'
     U VELOCITY 1.6700E+00
     V VELOCITY 0.0000E+00
     W VELOCITY 0.0000E+00
     PRESSURE 1.00E+07
     K 8.00E-03
     EPSILON 3.13E-02
  >>MASS FLOW BOUNDARY CONDITIONS
     FRACTIONAL MASS FLOW SPECIFIED
     FLUXES 1.0
```

Appendix G The *k*-Epsilon Closure Model of Turbulence

The *k*-Epsilon model solves for the mechanisms which influence the turbulence, convection and diffusion. Estimates are made for the levels of turbulent kinetic energy per unit mass. Initially a number of definitions are required to facilitate the subsequent derivation of the *k* and Epsilon equations and the terms involved within them. These definitions include matrix algebra for the mean rate of deformation of a fluid element and the stresses acting. The reader is referred to Appendix J and K for these details.

The Governing Equation for the Mean Flow Kinetic Energy K

Tennekes and Lumley [**Ref. 86**] devised a time-averaged equation that governs the mean kinetic energy of the flow. In words the structure of the equation is;

Rate of change of K	+	Transport of K by convection	=	Transport of K by pressure gradient	+	Transport of K by viscous flow	+	Transport of K by Reynolds stresses	-	Rate of dissipation of K stresses	+	Turbulence production

Numerically, the governing equation can be obtained by multiplying the Reynolds equations (Equation G-14 to Equation G-16) with their respective mean velocity components, i.e. multiply the x-component of the momentum equation by U. The results of these multiplication's are summed and simplified using some extensive algebra, thus resulting in the time-averaged mean flow kinetic energy equation. Refer to Tennekes and Lumley [**Ref. 86**] for a description of the algebra utilised.

Equation G-6 $$\frac{\partial(\rho K)}{\partial t} + div(\rho K\mathrm{U}) = div\left(-P\mathrm{U} + 2\mu \mathrm{U} E_{ij} - \rho \mathrm{U}\,\overline{u_i' u_j'}\right) - 2\mu E_{ij}.E_{ij} + \rho\overline{u_i' u_j'}.E_{ij}$$

(1) (2) (3) (4) (5) (6) (7)

Here the transport terms 2, 3, 4 and 5, all have *div* in common, so to simplify the equation we place these terms together. The viscous stresses are incorporated within *K*, through terms 4 and 6. Term 4 provides transport of *K* through the action of the viscous stresses, with term 6 providing destruction of *K* by viscous dissipation. The action of the Reynolds stresses are incorporated through terms 5 and 7. Term 5 represents the transport of *K* by the Reynolds stresses, whilst term 7 represents the net decrease of *K* due to the deformation work generated by the production of the Reynolds stresses. In highly turbulent flows the Reynolds stresses, terms 5 and 7, are always far in excess of the viscous stresses, terms 4 and 6.

The Governing Equation for the Turbulent Kinetic Energy k

As an aid to an understanding of the implications of solving the mean as opposed to the instantaneous transport equation for the kinetic energy of the flow, we derive the instantaneous turbulent kinetic energy equation. This equation cannot be solved directly due to the presence of the fluctuating components, however, it displays that the structure of the two equations are similar.

The derivation involved in determining the instantaneous turbulent kinetic energy of the flow is very in-depth, as such only a summary of the procedure will be given here. The interested reader is once again referred to Tennekes and Lumley.

First we must multiply the instantaneous Navier-Stokes equations by the respective fluctuating velocity component. The resulting equations are then summed. As with the mean flow kinetic energy equation, each of the Reynolds equations are multiplied by the appropriate fluctuating velocity component. These multiplied Reynolds equations are then summed. The two summed equation are then subtracted from one another and the use of some very substantial re-arrangement generates the equation for the turbulent kinetic energy k.

In words the turbulent kinetic energy is given by;

Rate of change of k	+	Transport of k by convection	=	Transport of k by pressure	+	Transport of k by viscous	+	Transport of k by Reynolds stresses	-	Rate of dissipation of k stresses	+	Turbulence production

or

Equation G-7

$$\frac{\partial(\rho k)}{\partial t} + div(\rho k \mathrm{U}) = div\left(-\overline{p'\mathrm{u}'} + 2\mu\overline{\mathrm{u}'e_{ij}'} - \rho\tfrac{1}{2}\overline{u_i'.u_i'u_j'}\right) - 2\mu\overline{e_{ij}'.e_{ij}'} - \rho\overline{u_i'u_j'}.E_{ij}$$

(1) (2) (3) (4) (5) (6) (7)

The equations for mean, K, and instantaneous, k, kinetic energy are similar apart from the appearance of the fluctuating components in k and the change of sign of term 7. As such in the turbulent kinetic energy equation, Equation G-7, term 7 represents the production of turbulent kinetic energy as it is positive. Inversely, in the mean flow kinetic energy equation, Equation G-6, term 7 represents the destruction of mean flow kinetic energy as it is negative. This sign change between K and k mathematically expresses the process of turbulence kinetic energy generation by the extraction of kinetic energy from the mean flow.

Of great importance to the study of turbulence and its modelling is the rate of dissipation of turbulent kinetic energy, as given by term 5 of Equation G-7. The viscous dissipation term gives a negative contribution to Equation G-7 due to the appearance of the sum squared fluctuating deformation rates e_{ij}'.

Equation G-8 $$-2\mu\overline{e_{ij}'.e_{ij}'} = -2\mu\left(\overline{e_{11}'^2} + \overline{e_{22}'^2} + \overline{e_{33}'^2} + \overline{e_{12}'^2} + \overline{e_{13}'^2} + \overline{e_{23}'^2}\right)$$

This term represents the dissipation work done by the smallest eddies against the viscous stresses. The rate of dissipation per unit mass is denoted by ε, having the units m^2/s^2.

Equation G-9 $$\varepsilon = 2\nu\overline{e_{ij}'.e_{ij}'}$$

This term is always the main dissipation term in the turbulent kinetic energy equation, never being negligible, having a order of magnitude assumed to be similar to the production term.

The k - Epsilon Model Equations

As with the transport equations developed for k and K, it is possible to produce such transport equations for other turbulent flow properties, including the rate of viscous dissipation, ε. The derivation of this transport equation is extremely complex, with the equation containing many assumptions regarding unknown and non-measurable terms. Readers interested in the development of the ε equation are referred to Bradshaw *et al* **[Ref. 15]**. Based upon our best knowledge of the processes causing changes to the flow variables we can generate transport equations for k and Epsilon. Thus, we can develop a set of transport equations that describe turbulent flow, providing closure by time-averaging.

These transport equations can be used to define large scale turbulence by using scales to describe velocity and length, using ϑ and l respectfully.

Equation G-10 $$\vartheta = k^{1/2} \qquad l = \frac{k^{3/2}}{\varepsilon}$$

One may note that ε denotes dissipation of turbulent energy by the work or retardation of the smallest eddies against the viscous stresses. Hence, we are using a term directly related to the smallest eddies to describe the action of the largest eddies. We can make this assumption due to the presence of the energy cascade of turbulence. Here at high Reynolds numbers the rate at which the largest eddies extract energy from the mean flow equals the rate of energy transfer across the entire spectrum, i.e. the rate at which energy is passed from the largest to the smallest eddies of turbulence. Thus the rate at which turbulence is produced from the mean flow in the form of the largest eddies, exactly equals the rate at which turbulence is destroyed by the action of viscous stresses on the smallest eddies. If this were not the case, then some scales of turbulence could grow or diminish without limit, thus we can justify the use of ε in the definition of l.

Furthermore, through the use of ε and l once more we can obtain a definition for the eddy viscosity of turbulence.

Equation G-11 $$\mu_t = C_\mu \rho \vartheta l = \rho C_\mu \frac{k^2}{\varepsilon}$$

Here C_μ is a dimensionless constant.

Now that we have developed the relevant transport equations and the terms required to solve them, we can write the transport equations used for k and Epsilon used in the standard k-Epsilon turbulence closure model.

Equation G-12 $$\frac{\partial(\rho k)}{\partial t} + div(\rho k\mathrm{U}) = div\left(\frac{\mu_t}{\sigma_k} grad.k\right) + 2\mu_t E_{ij}.E_{ij} - \rho\varepsilon$$

Equation G-13

$$\frac{\partial(\rho\varepsilon)}{\partial t} + div(\rho\varepsilon\mathrm{U}) = div\left(\frac{\mu_t}{\sigma_\varepsilon} grad.\varepsilon\right) + C_{1\varepsilon}\frac{\varepsilon}{k}2\mu_t E_{ij}.E_{ij} - C_{2\varepsilon}\rho\frac{\varepsilon^2}{k}$$

We can express this in writing as;

Rate of change of k or ε	+	Transport of of k or ε by convection	=	Transport of of k or ε by diffusion	+	Rate of production of k or	-	Rate of destruction of k or ε

One may note that there are five empirical constants which have been arrived at by data fitting for a large number of turbulent flows. The values assigned to each constant can be adjusted, however, the following values are strongly recommended for solutions of general engineering problems [**Ref. 18**].

$C_\mu = 0.09$; $\sigma_k = 1.00$; $\sigma_\varepsilon = 1.30$; $C_{1\varepsilon} = 1.44$; $C_{2\varepsilon} = 1.92$

Here, σ_k and σ_ε, represent the Prandtl numbers which connect the diffusivities of k and ε to the eddy viscosity given by Equation G-11. The production and destruction of turbulent kinetic energy must be closely linked, or else non-physical results will be obtained. Simply, when ε is large, k must also be large. As stated previously, the ε equation is largely generated through assumption. One of the main assumptions is that the production and destruction terms of ε, which cannot be measured, are proportional to those experienced in the k equation.

By using k and the Kronecker delta, [**Ref. 76**] we can compute the isotropic Reynolds stress, Equation G-15. The Kronecker delta, Equation G-14, has the value of either 1 or 0. $\delta_{ij} = 1$ if $i = j$ or $\delta_{ij} = 0$ if $i \neq j$. This term forces Equation G-15 to be applicable to the normal Reynolds stresses when $i = j$, i.e. $\tau_{xx} = -\rho\overline{u'^2}$ $\tau_{yy} = -\rho\overline{v'^2}$ $\tau_{zz} = -\rho\overline{w'^2}$.

Equation G-14
$$\delta_{ij} = \begin{bmatrix} 1 & 0 & 0 \\ 0 & 1 & 0 \\ 0 & 0 & 1 \end{bmatrix}$$

Equation G-15
$$-\rho \overline{u_i' u_j'} = \mu_t \left(\frac{\partial U_i}{\partial x_j} + \frac{\partial U_j}{\partial x_i} \right) - \frac{2}{3} \rho k \delta_{ij} = 2 \mu_t E_{ij} - \frac{2}{3} \rho k \delta_{ij}$$

Boundary Conditions The* k *- Epsilon Model Equations

Due to the gradient diffusion term of equations k and ε the equations are elliptic, and hence require boundary conditions for their solution. There are four sets of boundary conditions that are required, including;

1. walls - wall functions or low Reynolds number k-ε model.
2. free stream - k and ε both equal zero.
3. inlet - distribution of k and ε across the inlet required.
4. outlet/symmetry plane - dk/dn and $d\varepsilon/dn$ equal zero.

The most important of the boundary conditions is the distribution of k and ε at the inlet. Here values for k and ε must be set, however it is normally not practical to measure them experimentally. Thus crude approximations have been developed which allow these distributions to be set. Those included in CFX-F3D **[Ref. 18]** are as follows;

Equation G-16
$$k = 0.002 U^2 \qquad \varepsilon = \frac{k^{1.5}}{0.3 d}$$

,where d is the diameter of the inlet pipe. These distributions are assumed uniform, as with the velocity distribution at inlet. Common *CFD* practice is that at least 6 pipe diameters upstream of the flow feature of interest be included to ensure the flow has sufficient time to develop.

Many variables vary rapidly in the near wall regions of the flow. To avoid the need for very fine grids in these regions, wall functions can be used. Thus, at high Reynolds numbers the k-Epsilon model avoids the need to integrate right up to the wall through the application of these wall functions which describe the viscous sub-layer. If we define y to be that co-ordinate normal to the wall, the mean velocity at any near wall point is satisfied by the log-law for Reynolds numbers between $30<y_p^+<500$. Further, near wall measurements of the turbulent kinetic energy show that its rate of production equals the rate of turbulent dissipation **[Ref. 15]**. Thus, through the application of these assumption and the eddy viscosity equation, Equation G-11, the following wall functions can be developed as used within CFX-F3D.

Equation G-17
$$u^+ = \frac{U}{u_\tau} = \frac{1}{\kappa} \ln\left(E y_p^+\right) \qquad k = \frac{u_\tau^2}{\sqrt{C_\mu}} \qquad \varepsilon = \frac{u_\tau^3}{\kappa y}$$

The transition between the viscous sub-layer and the integration region of the flow problem is given by the upper root of the normal co-ordinate.

Equation G-18

$$y_p^+ = \frac{1}{\kappa}\log\left(Ey_p^+\right)$$

For Equation G-17 and Equation G-18, the Von Karman constant $\kappa = 0.41$ and the wall roughness parameter $E = 9.8$ for smooth walls. This wall roughness parameter can be varied to simulate rough walls.

Appendix H The Reynolds Stress Closure Model of Turbulence

The major limitation of the *k*-Epsilon model is its inability to predict flows with high shear rates, such as those experienced in the throttling regions within control chokes. Here the individual Reynolds stresses are poorly represented by the isotropic Reynolds equation of the *k*-Epsilon model, Equation G-15, even when the turbulent kinetic energy, k, is well resolved. However, by the inclusion of the exact Reynolds stresses transport equations, the directional effects of such a high shear rate can be resolved.

Such an approach has given rise to the most complex of the classic closure models of turbulence, known as the Reynolds stress model or the second order closure model due to the inclusion of the Reynolds stress.

Following the convention of the literature, the Reynolds stresses are denoted by $R_{ij} = \overline{u_i' u_j'}$, with the exact equation for R_{ij} having the form;

Equation H-19
$$\frac{DR_{ij}}{Dt} = P_{ij} + D_{ij} - \varepsilon_{ij} + \Pi_{ij} + \Omega_{ij}$$

(1) (2) (3) (4) (5) (6)

or in its full written form;

Rate of change of R_{ij}	+	Transport of R_{ij} by convection	=	Rate of production of R_{ij}	+	Transport of R_{ij} by diffusion of R_{ij}	-	Rate of dissipation	+	Transport of R_{ij} due to turbulent pressure-strain interactions
	+	Transport of R_{ij} due to rotation								

If we compare Equation H-19 with the exact transport equation for the turbulent kinetic energy, Equation G-6, we observe that two further physical terms have been included within the Reynolds stress equation, i.e. term 5 and 6. These terms represent pressure strain correlation and rotation transport. Thus to obtain a solution to Reynolds equation we need to derive terms for each of the above.

The production term, P_{ij}, retains its exact solution.

Equation H-20
$$P_{ij} = -\left(R_{im} \frac{\partial U_j}{\partial x_m} + R_{jm} \frac{\partial U_i}{\partial x_m} \right)$$

The diffusion term, D_{ij}, uses the concept of gradient diffusion which is common in turbulence modelling. Here we assume that the transport rate of the Reynolds stresses is proportional to the gradient of the Reynolds stresses.

Equation H-21 $$D_{ij} = \frac{\partial}{\partial x_m}\left(\frac{\nu_t}{\sigma_k}.\frac{\partial R_{ij}}{\partial x_m}\right) = div\left(\frac{\nu_t}{\sigma_k} grad\left(R_{ij}\right)\right)$$

where: $\nu_t = C_\mu \frac{k^2}{\varepsilon}$; $C_\mu = 0.09$; $\sigma_k = 1.0$

The rate of turbulent dissipation, ε_{ij}, is modelled by assuming the that small dissipative eddies, that operate against the viscous stress of the fluid, behave in a isotropic fashion. Only affecting the normal Reynolds stresses, this is achieved using the Kronecker delta, δ_{ij}, as with the *k*-Epsilon model.

Equation H-22 $$\varepsilon_{ij} = \frac{2}{3}\varepsilon\delta_{ij}$$

The pressure-strain correlation is that term most important to capture accurately, whilst at the same time it is the term most difficult to model. The term models pressure fluctuations as generated by the action of the Reynolds stresses. This process occurs through two distinct paths. Firstly, those pressure fluctuations as generated by the interaction of the largest eddies with the mean flow properties of the fluid. Secondly, the interaction of the eddies against one another. The overall action of the pressure-strain term is the distribution of turbulent kinetic energy. Here the term tends to promote the distribution of energy amongst the normal Reynolds stresses ($i = j$), making them more isotropic, whilst reducing the Reynolds shear stresses.

Whilst one is considering the Reynolds stresses, thought must be given to the influence of the wall proximity on the pressure-strain relationship. This correlation of the pressure-strain term is different in nature from the wall-functions described for the *k*-Epsilon model. This difference lies in the fact that the wall proximity term of the pressure-strain correlation must be applied irrespective of the Reynolds number of the mean flow.

Measurements of near wall turbulence have indicated that wall effects tend to increase the anisotropy of the normal Reynolds stresses, whilst decreasing the magnitude of the Reynolds shear stresses. This arises through the suppression of eddy fluctuations in the direction normal to the wall.

Thus, the pressure-strain correlation term commonly used within commercial *CFD* packages has the following form **[Ref. 18]**;

Equation H-23 $$\Pi_{ij} = -C_1\frac{\varepsilon}{k}\left(R_{ij} - \frac{2}{3}k\delta_{ij}\right) - C_2\left(P_{ij} - \frac{2}{3}k\delta_{ij}\right)$$

where $C_1 = 1.8$; $C_2 = 0.6$

Finally the rotational term, Ω_{ij}, is given by **[Ref. 18]**;

Equation H-24 $$\Omega_{ij} = -2\omega_k\left(R_{jm}e_{ikm} + R_{im}e_{jkm}\right)$$

Here, ω_k, is the rotation vector and e_{ijk} is a rotation dependent constant. $e_{ijk} = 1$ if I, j and k are all different and in cyclic order. $e_{ijk} = -1$ if I, j and k are all different and in anti-cyclic order. Finally $e_{ijk} = 0$ if any two of the indices are equal, irrespective of rotation.

The transport of turbulent kinetic energy, k, can be computed directly from the normal Reynolds stresses, as these terms are known.

Equation H-25
$$k = \frac{1}{2}\left(\overline{u_1'^2} + \overline{u_2'^2} + \overline{u_3'^2}\right) = \frac{1}{2}\left(R_{11} + R_{22} + R_{33}\right)$$

Thus we can now propose the transport equation of Epsilon, or turbulent dissipation due to the action of the smallest eddies against the viscous stresses of the fluid **[Ref. 18]**.

Equation H-26
$$\frac{D\varepsilon}{Dt} = div\left(\frac{\nu_t}{\sigma_\varepsilon} grad\varepsilon\right) + C_{1\varepsilon}\frac{\varepsilon}{k}2\nu_t E_{ij}.E_{ij} - C_{2\varepsilon}\frac{\varepsilon^2}{k}$$

where $C_{1\varepsilon} = 1.44$; $C_{2\varepsilon} = 1.92$

Or in written form;

Rate of		Transport of		Transport of		Rate of		Rate of
change	+	ε by convection	=	ε by diffusion	+	production	-	destruction
of ε						of ε		of ε

As with the k-Epsilon model, the transport equations are elliptic, so they require the usual boundary conditions;

1. walls - wall functions or low Reynolds number k-ε model.
2. free stream - k and ε both equal zero.
3. inlet - distribution of k and ε across the inlet required.
4. outlet/symmetry plane - dk/dn and $d\varepsilon/dn$ equal zero.

For computations at high Reynolds numbers wall-functions are used which are very similar to those of the k-Epsilon model, see equation 5.40. Low Reynolds number modifications to the model can be incorporated to include the effects of molecular viscosity to the diffusion terms, accounting for an anisotropic dissipation rate in the Reynolds stress equations, i.e. R_{ij}.

Finally the inlet distribution of k and ε must be set using inlet approximations **[Ref. 18]**, see Equation G-16.

Appendix I The Algebraic Stress Closure Model of Turbulence

The k-Epsilon model has the failing that it assumes that the turbulent flow field is isotropic. This allows solutions to be reached efficiently, however, the assumption produces poor results in general. The Reynolds stress model allows the anisotropy of the turbulent flow field to be considered. However, it has a very large computational cost associated with the inclusion of the gradients of the Reynolds stresses in the convective and diffusive transport terms. Bradshaw proposed that if the convective and diffusive transport terms are removed or simplified, then the Reynolds stress equations can be reduced to a set of algebraic equations.

Thus, the algebraic stress model was developed, providing an economical method for the inclusion of anisotropic turbulence effects without the need to solve in full the Reynolds stress transport equations.

The simplest method of generating the algebraic equations is to ignore the convective and diffusive transport terms completely. However, the results produced in this fashion are poor. The common approach, which produces a model of wide applicability, is to assume that the sum of the convective and diffusive terms of the Reynolds stress equations equals the sum of the convective and diffusive terms of the turbulent kinetic energy equation. This assumption can be made as the Reynolds stresses and the turbulent kinetic energy are closely related turbulence properties. The accuracy of the approximation can be assessed using $\overline{u_i'u_j'}/k$. Provided this ratio does not vary rapidly across the flow, then the assumption is valid.

We can then propose, using the exact solution for k;

Equation I-27

$$\frac{D\overline{u_i'u_j'}}{Dt} - D_{ij} \approx \frac{\overline{u_i'u_j'}}{k}.\begin{pmatrix} \frac{Dk}{Dt} - div\left(-\overline{p'\mathrm{u}'} + 2\mu\overline{\mathrm{u}'e_{ij}'} - \rho\tfrac{1}{2}\overline{u_i'.u_i'u_j'}\right) \\ -2\mu\overline{e_{ij}'.e_{ij}'} - \rho\overline{u_i'u_j'}.E_{ij} - div(\rho k\mathrm{U}) \end{pmatrix}$$

Equation I-28

$$\frac{D\overline{u_i'u_j'}}{Dt} - D_{ij} = \frac{\overline{u_i'u_j'}}{k}.\left(-\overline{u_i'u_j'}.E_{ij} - \varepsilon\right)$$

Here the large term on the right hand side represents the production and dissipation rate for the turbulent kinetic energy as obtained from Equation G-7. Further improvements to the accuracy of the modelling process may be obtained by independently relating the convective transport term and the diffusion transport term to the transport of turbulent kinetic energy, as opposed to the summation assumption.

Thus, we can utilise the assumptions made above, that introduced the approximation equation, Equation I-27, within the Reynolds stress transport equation, Equation H-19. Here we incorporate into the equation, the production term, Equation H-20, the dissipation rate due to rotation, Equation H-24 and the pressure-strain correlation term, Equation H-23. Through extensive re-arrangement we produce an equation which describes the Reynolds stresses in algebraic form.

Equation I-29

$$R_{ij} = \overline{u_i' u_j'} = \frac{2}{3}k\delta_{ij} + \left(\frac{C_D}{C_1 - 1 + \dfrac{P}{\varepsilon}}\right)\left(P_{ij} - \frac{2}{3}P\delta_{ij}\right)\frac{k}{\varepsilon}$$

The Reynolds stresses appear on either side of the above, hence producing a set of six simultaneous algebraic equations for each of the unknown Reynolds stresses. On the right, the stresses are contained within the P_{ij} term. These algebraic equations can then be solved by an iterative method if k and ε are known. Thus we solve these formulae in conjunction with the standard k and ε transport equations, i.e. Equation G-12 and Equation G-13, respectively.

The constants in Equation I-29 are present to accommodate physical losses in the assumption that the convective and diffusion terms of the Reynolds stresses are proportional to those within the turbulent kinetic energy equation, i.e. the basis of the algebraic stress turbulence model. The values assigned to these constants are recommended to be [**Ref. 18**];

$C_D = 0.55$; and $C_1 = 2.2$

Appendix J Navier-Stokes and Continuity Equations

Here the Navier-Stokes and Continuity equations are present for incompressible flow with constant viscosity to simplify the case. The equations are presented in vector notation for compactness.

Equation J-1 $$div\,\mathbf{u} = \frac{\partial u}{\partial x} + \frac{\partial v}{\partial y} + \frac{\partial w}{\partial z} = 0$$

Equation J-2 $$\frac{\partial u}{\partial t} + div(u\mathbf{u}) = -\frac{1}{\rho}\frac{\partial p}{\partial x} + v.div.grad.u$$

Equation J-3 $$\frac{\partial v}{\partial t} + div(v\mathbf{u}) = -\frac{1}{\rho}\frac{\partial p}{\partial y} + v.div.grad.v$$

Equation J-4 $$\frac{\partial w}{\partial t} + div(w\mathbf{u}) = -\frac{1}{\rho}\frac{\partial p}{\partial z} + v.div.grad.w$$

Here the velocity vector $\boldsymbol{u}$ represents the instantaneous features of the flow, Cartesian co-ordinates are taken so that $\boldsymbol{u}$ has x-component u, y-component v and z-component w. To include the effects of turbulence we utilise Reynolds decomposition, such that the variables now become;

Equation J-5
$$u = U + u'$$
$$u = U + u'$$
$$v = V + v'$$
$$w = W + w'$$
$$p = P + p'$$

Now we consider the implications of the time-averaging process on the Navier-Stokes and continuity equations. First we consider the continuity equation. We note that $div\boldsymbol{u} = divU$, thus through time-averaging to obtain the mean flow properties yields;

Equation J-6 $$divU = 0$$

Now we can undertake a similar process for the x, y and z-momentum equations. If we consider the x-momentum equation as the example, the time-averaging process yields the following terms;

Equation J-7 $$\overline{\frac{\partial u}{\partial t}} = \frac{\partial U}{\partial t}$$

Equation J-8 $$\overline{div(uu)} = div(UU) + div(\overline{u'u'})$$

Equation J-9 $$-\frac{\bar{1}}{\rho}\frac{\overline{\partial p}}{\partial x} = -\frac{1}{\rho}\frac{\partial P}{\partial x}$$

Equation J-10 $$\overline{v.div.grad.u} = v.div.grad.U$$

Thus the time-averaged x-momentum equation becomes;

Equation J-11 $$\frac{\partial U}{\partial t} + div(UU) + div(\overline{u'u'}) = -\frac{1}{\rho}\frac{\partial P}{\partial x} + v.div.grad.U$$

Repeating the process for the y and z-momentum equations yields;

Equation J-12 $$\frac{\partial V}{\partial t} + div(VU) + div(\overline{v'u'}) = -\frac{1}{\rho}\frac{\partial P}{\partial y} + v.div.grad.V$$

Equation J-13 $$\frac{\partial W}{\partial t} + div(WU) + div(\overline{w'u'}) = -\frac{1}{\rho}\frac{\partial P}{\partial z} + v.div.grad.W$$

The significant thing to note regarding the time-averaging process is the introduction of new terms in the resulting momentum equations. It can be seen that the new terms involve products of the fluctuating velocities, as such these new terms constitute convective momentum generating additional turbulent stresses on each of the mean velocity components u, v and w.

As these new terms are turbulent stress generators, it is customary to place the new terms on the right of the equations. Thus the time-averaged momentum equations can be rewritten to display this. Below, only the new terms have been written out in full, the remainder has been shown in the compact vector notation.

Equation J-14
$$\frac{\partial U}{\partial t} + div(UU) = -\frac{1}{\rho}\frac{\partial P}{\partial x} + v.div.grad.U + \left[-\frac{\partial \overline{u'^2}}{\partial x} - \frac{\partial \overline{u'v'}}{\partial y} - \frac{\partial \overline{u'w'}}{\partial z}\right]$$

Equation J-15
$$\frac{\partial V}{\partial t} + div(VU) = -\frac{1}{\rho}\frac{\partial P}{\partial y} + v.div.grad.V + \left[-\frac{\partial \overline{u'v'}}{\partial x} - \frac{\partial \overline{v'^2}}{\partial y} - \frac{\partial \overline{v'w'}}{\partial z}\right]$$

Equation J-16

$$\frac{\partial W}{\partial t} + div(W\mathrm{U}) = -\frac{1}{\rho}\frac{\partial P}{\partial z} + v.div.grad.W + \left[-\frac{\partial \overline{u'w'}}{\partial x} - \frac{\partial \overline{v'w'}}{\partial y} - \frac{\partial \overline{w'^2}}{\partial z} \right]$$

Thus the addition of the new terms has given rise to the Reynolds stress tensors, being three normal stresses and three shear stresses. If we include the effects of compressible flow through the addition of density terms, we can write the normal and shear stresses as;

Normal stresses: $\tau_{xx} = -\rho\overline{u'^2}$ $\tau_{yy} = -\rho\overline{v'^2}$ $\tau_{zz} = -\rho\overline{w'^2}$

Shear stresses: $\tau_{xy} = \tau_{yx} - \rho\overline{u'v'}$ $\tau_{xz} = \tau_{zx} - \rho\overline{u'w'}$ $\tau_{yz} = \tau_{zy} - \rho\overline{v'w'}$

The Reynolds stress tensor, under the influence of turbulent fluctuations, are always non-zero. The normal stresses are always non-zero due to the inclusion of the squared velocity fluctuations. The shear stresses provide correlation between different velocity components, once again they are always non-zero and large compared to the viscous stresses within the flow.

Extending this theory to include arbitrary scalar quantities, we obtain the time-averaged transport equation for a scalar;

Equation J-17

$$\frac{\partial \Phi}{\partial t} + div(\Phi\mathrm{U}) = div\left(\Gamma_{\Phi} grad.\Phi\right) + \left[-\frac{\partial \overline{u'\varphi'}}{\partial x} - \frac{\partial \overline{v'\varphi'}}{\partial y} - \frac{\partial \overline{w'\varphi}}{\partial z} \right] + S_{\Phi}$$

Thus far, the momentum equations have been considered to be incompressible with constant density. However, in flows of practical interest the mean density is likely to vary from point to point if the flow is gaseous, with the instantaneous density always varying due to localised turbulent fluctuations. Bradshaw *et al*[15] noted that small density fluctuations did not appear to significantly affect the mean flow characteristics. In free turbulent flows the rms. velocity fluctuations can be in the order of 20% of the mean velocity for density fluctuation to be assumed negligible. However, in the confined turbulent flows of the choke valve, that is of interest, given an rms. velocity fluctuation value of 5% of the mean flow, Bradshaw also showed that density fluctuations are unimportant.

We may utilise the density weighted averaged form of the mean flow equations for compressible flow. Here the instantaneous density fluctuations due to velocity fluctuations are assumed negligible, whilst we give consideration to mean density variations from point to point. Such a situation is acceptable as the computational requirements to directly simulate all density fluctuations would be extremely large. Such a form for the continuity and momentum equations is that commonly used in commercial *CFD* codes.

Continuity

Equation J-18
$$\frac{\partial p}{\partial t} + div(\rho U) = 0$$

Reynolds Equation

Equation J-19
$$\frac{\partial(\rho U)}{\partial t} + div(\rho U\mathrm{U}) = -\frac{\partial P}{\partial x} + div(\mu.grad.U) + \left[-\frac{\partial\left(\overline{\rho u'^2}\right)}{\partial x} - \frac{\partial\left(\overline{\rho u'v'}\right)}{\partial y} - \frac{\partial\left(\overline{\rho u'w'}\right)}{\partial z} \right] + S_{Mx}$$

Equation J-20
$$\frac{\partial(\rho V)}{\partial t} + div(\rho V\mathrm{U}) = -\frac{\partial P}{\partial y} + div(\mu.grad.V) + \left[-\frac{\partial\left(\overline{\rho u'v'}\right)}{\partial x} - \frac{\partial\left(\overline{\rho v'^2}\right)}{\partial y} - \frac{\partial\left(\overline{\rho v'w'}\right)}{\partial z} \right] + S_{My}$$

Equation J-21
$$\frac{\partial(\rho W)}{\partial t} + div(\rho W\mathrm{U}) = -\frac{\partial P}{\partial z} + div(\mu.grad.W) + \left[-\frac{\partial\left(\overline{\rho u'w'}\right)}{\partial x} - \frac{\partial\left(\overline{\rho v'w'}\right)}{\partial y} - \frac{\partial\left(\overline{\rho w'^2}\right)}{\partial z} \right] + S_{Mz}$$

Scalar Transport Equation

Equation J-22
$$\frac{\partial(\rho\Phi)}{\partial t} + div(\rho\Phi\mathrm{U}) = div(\Gamma_{\Phi} grad.\Phi) + \left[-\frac{\partial\left(\overline{\rho u'\varphi'}\right)}{\partial x} - \frac{\partial\left(\overline{\rho v'\varphi'}\right)}{\partial y} - \frac{\partial\left(\overline{\rho w'\varphi'}\right)}{\partial z} \right] + S_{\Phi}$$

Appendix K Matrix Algebra k/ε

The mean rate of deformation of a fluid element and the stresses acting on that element is given by;

$$e_{ij} = \begin{pmatrix} e_{xx} & e_{xy} & e_{xz} \\ e_{yx} & e_{yy} & e_{yz} \\ e_{zx} & e_{zy} & e_{zz} \end{pmatrix} \qquad \text{and} \qquad \tau_{ij} = \begin{pmatrix} \tau_{xx} & \tau_{xy} & \tau_{xz} \\ \tau_{yx} & \tau_{yy} & \tau_{yz} \\ \tau_{zx} & \tau_{zy} & \tau_{zz} \end{pmatrix}$$

The same approach is taken to determine the product of each matrix, thus consideration will only be given to the rate of deformation of a fluid element. We decompose the instantaneous rate of deformation into the mean and fluctuating components, i.e.

$$e_{ij}(t) = E_{ij} + e'_{ij}$$

Substituting this back into the matrix provides the following element;

$$e_{xx}(t) = E_{xx} + e'_{xx} = \frac{\partial U}{\partial x} + \frac{\partial u'}{\partial x}$$

$$e_{yy}(t) = E_{yy} + e'_{yy} = \frac{\partial V}{\partial y} + \frac{\partial v'}{\partial y}$$

$$e_{zz}(t) = E_{zz} + e'_{zz} = \frac{\partial W}{\partial z} + \frac{\partial w'}{\partial z}$$

$$e_{xy}(t) = e_{yx}(t) = E_{xy} + e'_{xy} = \frac{1}{2}\left[\frac{\partial U}{\partial y} + \frac{\partial V}{\partial x}\right] + \frac{1}{2}\left[\frac{\partial u'}{\partial y} + \frac{\partial v'}{\partial x}\right]$$

$$e_{xz}(t) = e_{zx}(t) = E_{xz} + e'_{xz} = \frac{1}{2}\left[\frac{\partial U}{\partial z} + \frac{\partial W}{\partial x}\right] + \frac{1}{2}\left[\frac{\partial u'}{\partial z} + \frac{\partial w'}{\partial x}\right]$$

$$e_{yz}(t) = e_{zy}(t) = E_{yz} + e'_{yz} = \frac{1}{2}\left[\frac{\partial V}{\partial z} + \frac{\partial W}{\partial y}\right] + \frac{1}{2}\left[\frac{\partial v'}{\partial z} + \frac{\partial w'}{\partial y}\right]$$

These elements can be written into the matrix, then the rules of matrix algebra applied to find the product of a vector a and a tensor b_{ij} is given by vector c_j, i.e.

$$\mathbf{a}b_{ij} \equiv a_i b_{ij} = \begin{pmatrix} a_1 & a_2 & a_3 \end{pmatrix} \begin{pmatrix} b_{11} & b_{12} & b_{13} \\ b_{21} & b_{22} & b_{23} \\ b_{31} & b_{32} & b_{33} \end{pmatrix} = \begin{pmatrix} a_1 b_{11} & a_2 b_{21} & a_3 b_{31} \\ a_1 b_{12} & a_2 b_{22} & a_3 b_{32} \\ a_1 b_{13} & a_2 b_{23} & a_3 b_{33} \end{pmatrix}^T = \begin{pmatrix} c_1 \\ c_2 \\ c_3 \end{pmatrix}^T = c_j = \mathbf{c}$$

Furthermore, the scalar product of the two tensors a_{ij} and b_{ij} is given by;

$$a_{ij}.b_{ij} = a_{11}.b_{11} + a_{12}.b_{11} + a_{13}.b_{13} + a_{21}.b_{21} + a_{22}.b_{22} + a_{23}.b_{23}$$
$$+ a_{31}.b_{31} + a_{32}.b_{32} + a_{33}.b_{33}$$

Appendix L Modified CFX Particle Tracking FORTRAN Routines - PARCAL, TRACK & BCSPAR

```
      SUBROUTINE PARCAL(IPART,RPART,PNUM,YPART,YPDER,VARV,VINTG,AMFG
     +           ,VDIFF,RHOPAR,CPPAR,CPVAP,VAP0
     +           ,COV,NCVD,SUP,SPS,PURF
     +           ,CFACE,CFACEP,CBLK,IBLKF,IBLK,INDBLK,NCVBLK
     +           ,AREA,VOL,VPOR,PVFRAC
     +           ,WORK,IWORK,CWORK)
C
C***********************************************************************
C
C  THIS SUBROUTINE IS THE MAIN ROUTINE FOR THE PARTICLE TRANSPORT
C  MODEL
C
C***********************************************************************
C
C  THIS SUBROUTINE IS CALLED BY THE FOLLOWING SUBROUTINES
C      PARCL1
C
C***********************************************************************
C  CREATED
C    03/01/92  NSW  COPIED FROM SPRAY IN RELEASE 2.4
C  MODIFIED
C    14/07/92  NSW  DEFAULT AMDC IN COAL MODEL
C    29/01/93  NSW  PRINT PARTICLE TRANSPORT ITERATION NUMBER
C    29/06/93  DSC  INCLUDE COMMON BLOCK /FUELM/ FOR NOX MODEL
C    15/10/93  NSW  INCLUDE OIL COMBUSTION
C    23/11/93  CSH  REPLACE 1H0,1H1 WITH / FORMAT
C    11/01/94  NSW  INCLUDE CFACEP, CBLK, VOL AND PVFRAC PASSING
C                   CFACEP, CBLK AND PVFRAC TO TRACK.
C                   CALCULATE VOLUME FRACTION OF PARTICLES.
C                   INCLUDE STOP FLOW3D FACILITY.
C                   REMOVE COMMON /NCVPR/.
C    07/02/94  FHW  CHANGES INVOLVING NPARTM FOR NEW PARTICLE
C                   TRANSPORT COMMAND LANGUAGE
C    11/03/94  IRH  MAKE DIVISION BY VOLUME SAFE
C    26/01/95  NSW  INCREASE NUMBER OF PARAMETERS FOR COLOURING
C    21/02/95  NSW  PASS VOLUME AND POROUS VOLUME TO TRACK
C    15/03/95  NSW  CHANGE WIDTH OF COLOURING PARAMETERS TO 20
C    20/12/95  NSW  INCLUDE SGI COMPILER DIRECTIVES
C
C***********************************************************************
C
      CHARACTER*(*) CWORK,CBLK
      CHARACTER*8  CFACE
      CHARACTER*20  CTRK(10)
      CHARACTER*32  CFACEP
C
      LOGICAL LMASS,LHEAT,LCOAL,LSPRAY,LPBUOY,LPTURB,LPGRAD,LTWSTP
      LOGICAL LSTOP
C
      DOUBLE PRECISION DB1,DB2
C
      COMMON
     + /ALL/   NBLOCK,NCELL,NBDRY,NNODE,NFACE,NVERT,NDIM
     + /COAL/   AV,EV,AFC,EFC,ASTAR,TSTAR,AMC,AMO2,SWELL,VOIDS,HOLES
     +        ,DCOEFF,DIP,DENV,DENA,C,AMV,AMA,AMFC,FO2,RDROP0
     +        ,FHCHAR,FV,FA,Y1,AV1,EV1,Y2,AV2,EV2,LTWSTP
     + /CPART/  FAT,FVT,FFCT
     + /DEVICE/ NREAD,NWRITE,NRDISK,NWDISK
     + /FUELM/  SUMMS1,SUMMS2
     + /IGRAF/  IWRT,NWTRKS
     + /IMOIST/ SMOIST,SMASS
     + /INTEGR/ NEQ,NTER,IPTT,IPTS,NSUP,NMASS,NVARV
     + /IPART/  NPART,NPARTM,NRP
     + /LOGPAR/ LMASS,LHEAT,LCOAL,LSPRAY,LPBUOY,LPTURB,LPGRAD
     + /OILCMB/ IOILC
     + /RPART/  DIAM,AMDC,RHO,CPBPAR,TVAP
     + /SPRIT/  ITER
     + /TOTMAS/ SUMMS
C
      DIMENSION IPART(NPARTM,4),RPART(NPARTM,NRP),PNUM(NPARTM)
```

```
     +,YPART(NEQ),YPDER(NEQ),VARV(NVERT,NVARV),VINTG(NVARV),AMFG(*)
     +,VDIFF(*),RHOPAR(*),CPPAR(*),CPVAP(*),VAP0(*)
     +,COV(NVERT,2,2,2,3),NCVD(NCELL)
     +,SUP(NCELL,NSUP),SPS(NCELL,NSUP),PURF(NSUP)
     +,CFACE(NFACE),CFACEP(NFACE),CBLK(*)
     +,IBLKF(NFACE),IBLK(5,NBLOCK),INDBLK(*)
     +,AREA(NFACE,3),VOL(NCELL),VPOR(NCELL),PVFRAC(NCELL)
     +,WORK(*),IWORK(*),CWORK(*)
      DIMENSION IPOS(4)
C
      DATA PI / 3.1415926 /
C
C----HEADING
C
      WRITE(NWRITE,600) ITER
      IF (IWRT.EQ.1) THEN
        IF (LCOAL) THEN
          NCOL = 3
          CTRK(1) = 'TEMPERATURE       '
          CTRK(2) = 'TOTAL MASS        '
          CTRK(3) = 'DIAMETER          '
        ELSE IF (LSPRAY) THEN
          NCOL = 3
          CTRK(1) = 'DIAMETER          '
          CTRK(2) = 'TEMPERATURE       '
          CTRK(3) = 'TOTAL MASS        '
        ELSE IF (LMASS.AND.LHEAT) THEN
          NCOL = 3
          CTRK(1) = 'TOTAL MASS        '
          CTRK(2) = 'TEMPERATURE       '
          CTRK(3) = 'DIAMETER          '
        ELSE IF (LMASS) THEN
          NCOL = 2
          CTRK(1) = 'TOTAL MASS        '
          CTRK(2) = 'DIAMETER          '
        ELSE IF (LHEAT) THEN
          NCOL = 2
          CTRK(1) = 'DIAMETER          '
          CTRK(2) = 'TEMPERATURE       '
        ELSE
          NCOL = 1
          CTRK(1) = 'DIAMETER          '
        END IF
        CTRK(NCOL+1) = 'U VELOCITY        '
        CTRK(NCOL+2) = 'V VELOCITY        '
        CTRK(NCOL+3) = 'W VELOCITY        '
        CTRK(NCOL+4) = 'SPEED             '
        NCOL = NCOL + 4
        WRITE(NWTRKS,605) NCOL
      END IF
C
      LSTOP = .FALSE.
C
C----INITIALISE
C
      DO 110 ISUP=1,NSUP
C$DOACROSS LOCAL(ICELL)
      DO 100 ICELL=1,NCELL
      SUP(ICELL,ISUP) = 0.0
  100 CONTINUE
  110 CONTINUE
C
C$DOACROSS LOCAL(ICELL)
      DO 115 ICELL=1,NCELL
      PVFRAC(ICELL) = 0.0
  115 CONTINUE
C
C----INTERPOLATE CONTINUUM PHASE VARIABLES TO VERTICES
C
      CALL VARVRT(VARV,WORK,IWORK,CWORK)
C
C----CARRY OUT CALCULATION FOR DROP NN
C
      DO 140 NN=1,NPART
C
C----REAL INITIAL CONDITIONS FOR DROP NN
```

```
C
      DO 120 II=1,NEQ-3
      YPART(II) = RPART(NN,II)
 120  CONTINUE
C
      IF (LCOAL) THEN
C
        AMV  = RPART(NN,9)
        AMFC = RPART(NN,10)
        AMA  = RPART(NN,11)
        IF (LTWSTP) YPART(11) = 0.0
        RDROP0 = YPART(8)/2.0
C
        AMPART = AMV+AMA+AMFC
        FVT = AMV/AMPART
        FAT = AMA/AMPART
        FFCT = AMFC/AMPART
C
        DB1 = YPART(7)
        DB2 = YPART(8)
        CALL DPROPC(DB1,DB2)
C
        DIAM = YPART(8)
C
        AMDC = 0.0
C
      ELSE IF (LSPRAY) THEN
C
        SMASS = RPART(NN,7)
        SMOIST = RPART(NN,9)
        FMOIST = SMOIST/100.0
        VOLP = SMASS*(FMOIST/RHOPAR(1) + (1.0-FMOIST)/RHO)
        DIAM = (6.0*VOLP/PI)**(1.0/3.0)
C
        AMDC = SMASS*(1.0-FMOIST)
        AMPART = SMASS
C
      ELSE
C
        AMMF = 0.0
        DO 125 IMASS=1,NMASS
C
          AMMF = AMMF+RPART(NN,6+IMASS)
C
 125    CONTINUE
C
        AMPART = RPART(NN,IPTT+1)
        AMDC = AMPART-AMMF
        DIAM = RPART(NN,IPTT+2)
C
      END IF
C
C----NUMBER OF PARTICLES/SECOND
C
      PNUMS = PNUM(NN)
C
C----INTEGER INFORMATION FOR DROP NN
C
      DO 130 II=1,4
      IPOS(II) = IPART(NN,II)
 130  CONTINUE
C
C----PRINT HEADING
C
      PMASS = PNUMS*AMPART
      WRITE(NWRITE,610) NN,DIAM,AMPART,PMASS
C
C----CALL PARTICLE TRACKING ROUTINE
C
      CALL TRACK(NN,IPOS,YPART,YPDER,PNUMS,PMASS,VARV,VINTG,AMFG
     +          ,VDIFF,RHOPAR,CPPAR,CPVAP,VAP0,COV,NCVD,SUP
     +          ,CFACE,CFACEP,CBLK,IBLKF,IBLK,INDBLK,NCVBLK
     +          ,AREA,VOL,VPOR,PVFRAC,LSTOP,WORK,IWORK,CWORK)
C
      IF (LSTOP) THEN
        CALL TERMIN('DUMP-SOLUTION-STOP',' ','NOW'
```

```
     +              ,'STOPPED BY USERS REQUEST.'
     +              ,' ',1,WORK,IWORK,CWORK)
       END IF
C
       IF (IWRT.EQ.1) WRITE(NWTRKS,615) (CTRK(ICOL),ICOL=1,NCOL)
C
 140 CONTINUE
C
C----PARTICLE SOURCE TERMS ARE STORED IN SPS
C
      DO 170 ISUP=1,NSUP
C$DOACROSS LOCAL(ICELL)
      DO 160 ICELL=1,NCELL
C
C----UNDER-RELAXATION OF SOURCE TERMS
C
      SPS(ICELL,ISUP) = SPS(ICELL,ISUP)
     +               +PURF(ISUP)*(SUP(ICELL,ISUP)-SPS(ICELL,ISUP))
C
 160 CONTINUE
 170 CONTINUE
C
C----CALCULATE TOTAL MASS SOURCE
C
      SUMMS = 0.0
      IF (LCOAL) THEN
C
        SUMMS1 = 0.0
        SUMMS2 = 0.0
C
        DO 180 ICELL=1,NCELL
C
        SUMMS1 = SUMMS1+SPS(ICELL,4)
        IF(IOILC.NE.1) SUMMS2 = SUMMS2+SPS(ICELL,6)
C
 180   CONTINUE
C
        SUMMS = SUMMS1+SUMMS2
C
        WRITE(NWRITE,620) SUMMS1
        IF(IOILC.NE.1) WRITE(NWRITE,630) SUMMS2
C
      ELSE IF (LSPRAY.OR.LMASS) THEN
C
        DO 200 IMASS=1,NMASS
          DO 190 ICELL=1,NCELL
C
          SUMMS = SUMMS+SPS(ICELL,3+IMASS)
C
 190     CONTINUE
 200   CONTINUE
C
        WRITE(NWRITE,640) SUMMS
C
      END IF
C
C----CALCULATE PARTICLE VOLUME FRACTION
C
C$DOACROSS LOCAL(ICELL)
      DO 210 ICELL=1,NCELL
C
        PVFRAC(ICELL) = PVFRAC(ICELL)/MAX(VOL(ICELL),1.0E-20)
C
 210 CONTINUE
C
      RETURN
C
 600 FORMAT(//,' PARTICLE TRANSPORT CALCULATION - ITERATION NO. ',I3)
 605 FORMAT(1X,I3)
 610 FORMAT(/,' PARTICLE NO.',1X,I5,' DIAMETER =',1PE11.3,
     +       ' MASS =',1PE11.3,' MASS FLOW RATE =',1PE11.3)
 615 FORMAT('/*',10A20)
 620 FORMAT(/,' TOTAL MASS OF VOLATILE GASES =',1PE11.3)
 630 FORMAT(1H ,' TOTAL MASS OF CHAR REACTED =',1PE11.3)
 640 FORMAT(/,' TOTAL MASS FROM PARTICLES =',1PE11.3)
C
```

```
      END
      SUBROUTINE TRACK(NN,IPOS,YPART,YPDER,PNUM,PMASS,VARV,VINTG,AMFG
     +            ,VDIFF,RHOPAR,CPPAR,CPVAP,VAP0,COV,NCVD,SUP
     +            ,CFACE,CFACEP,CBLK,IBLKF,IBLK,INDBLK,NCVBLK
     +            ,AREA,VOL,VPOR,PVFRAC,LSTOP,WORK,IWORK,CWORK)
C
C***********************************************************************
C
C  THIS SUBROUTINE, THE DROPLET TRACKING ROUTINE,
C     TRACKS EACH DROPLET THROUGH THE FLOW DOMAIN AND SETS UP
C     THE PROBLEM FOR THE INTEGRATING ROUTINE WORKING IN
C     COMPUTATIONAL SPACE.
C     IT CHECKS THAT A DROP HAS NEITHER STRUCK A SURFACE NOR IS
C     WITHIN A SOLID CONTROL VOLUME.
C
C***********************************************************************
C
C  THIS SUBROUTINE IS CALLED BY THE FOLLOWING SUBROUTINES
C     PARCAL
C
C***********************************************************************
C  CREATED
C    28/02/92  NSW  COPIED FROM CSSRMY VERSION OF RELEASE 2.4
C  MODIFIED
C    09/06/92  NSW  ENSURE PARTICLES START REMOTE FROM CELL EDGES
C                   SET NEDDY AND PASS TO INTEG
C    16/06/92  NSW  REFLECT TURBULENT EDDY AT SYMMETRY PLANES
C    14/07/92  NSW  MAKE IBPATH CONSTANT WITH SUBPATH
C    01/09/92  PHA  REPLACE COMMON BOUNCE BY BOUNCI AND BOUNCR
C    01/12/92  NSW  CORRECT BLOCK BOUNDARY TREATMENT AND TIME LIMIT
C                   CORRECT TREATMENT OF COAL PARTICLES AT WALLS
C                   CHANGE ARGUMENT LIST OF BCSPAR
C                   INCLUDE TRAP ON SLOW INCREASE OF TIME AND SPACE
C                   INCLUDE MESSAGE FOR STATIONARY PARTICLE
C                   CHECK ON JUMPING OUT OF INTEG INTERPOLATION LOOP
C    14/09/93  NSW  START NEW EDDY WHEN PARTICLE HITS WALL
C                   BUT NOT AT SYMMETRY PLANES AND BLOCK BOUNDARIES
C    23/11/93  CSH  REPLACE 1H0,1H1 WITH / FORMAT
C    11/01/94  NSW  INCLUDE CBLK AND CFACEP FOR INCLUSION IN CALL
C                   TO NEW USER ROUTINE USRPBM FOR MONITORING
C                   PARTICLES AT BOUNDARIES.
C                   INCLUDE PVFRAC AND PASS WITH OTHER ARGUMENTS
C                   TO PARSRC.
C                   CORRECT TREATMENT OF NEAR STATIONARY PARTICLES
C                   AND PARTICLES WITH INTERPOLATION ERROR.
C                   MODIFY METHOD OF CALCULATING PREVIOUS CONTROL
C                   VOLUME WHEN BOUNCING OFF WALLS TO ENSURE IT
C                   IS INSIDE THE FLOW.
C                   MOVE PARTICLES SLIGHTLY AWAY FROM WALL WHEN
C                   BOUNCING TO AVOID ROUNDING ERROR PROBLEMS.
C                   INCLUDE STOP FLOW3D FACILITY.
C                   INCLUDE USER CONTROL OF NEAR STATIONARY PARTICLES.
C                   INCLUDE USER CONTROL OF TRACK PRINTING.
C    26/02/94  NSW  CHANGE MAXPTH TO 30
C    24/10/94  NSW  MODIFY CALL TO USRPBM TO ALLOW INITIALISATION
C                   AND FINAL OUTPUT
C    16/11/94  NSW  ALLOW NO PRINTING OF TRACKS
C    02/12/94  NSW  INCLUDE COMMON /IPART/
C    21/02/95  NSW  INCLUDE TEST ON POROUS REGIONS. VOLUME AND POROUS
C                   VOLUME INCLUDED IN ARGUMENT LIST.
C    16/03/95  NSW  PASS CONTROL OF OUTPUT FILE PRINTING TO PRINTD
C    25/03/96  NSW  CORRECT MESSAGE FOR OIL DROPS
C
C***********************************************************************
C
      PARAMETER (MAXNEQ=30,MAXPTH=30)
C
      CHARACTER*(*) CBLK
      CHARACTER*6 CCALL
      CHARACTER*8 CFACE,CFAC
      CHARACTER*32 CFACEP,CFACP,CBLOCK
C
      LOGICAL LDEN,LVIS,LTURB,LTEMP,LBUOY,LSCAL,LCOMP
     +     ,LRECT,LCYN,LAXIS,LPOROS,LTRANS
      LOGICAL LMASS,LHEAT,LCOAL,LSPRAY,LPBUOY,LPTURB,LPGRAD
      LOGICAL LSTOP
```

```
C
      COMMON
     + /ALL/   NBLOCK,NCELL,NBDRY,NNODE,NFACE,NVERT,NDIM
     + /BOUNCI/ IBOUNC
     + /BOUNCR/ RESTCF
     + /DEVICE/ NREAD,NWRITE,NRDISK,NWDISK
     + /DTURB/  TLE,UGF,VGF,WGF
     + /INTEGR/ NEQ,NTER,IPTT,IPTS,NSUP,NMASS,NVARV
     + /INTPAR/ TLIM,ER1,DMIN,TOL
     + /IPART/  NPART,NPARTM,NRP
     + /IPORPA/ IPORPA
     + /LOGIC/  LDEN,LVIS,LTURB,LTEMP,LBUOY,LSCAL,LCOMP
     +          ,LRECT,LCYN,LAXIS,LPOROS,LTRANS
     + /LOGPAR/ LMASS,LHEAT,LCOAL,LSPRAY,LPBUOY,LPTURB,LPGRAD
     + /NIJKB/  NIB,NJB,NKB,IPCB,IPVB
     + /OILCMB/ IOILC
     + /PARFRC/ TFRAC,CVFRAC
     + /SPARM/  SMALL,SORMAX,NITER,INDPRI,MAXIT,NODREF,NODMON
     + /SPRIT/  ITER
     + /USRNNN/ NN1,PDAT,CFAC,CFACP,I,J,K
     + /MLTGRD/ MLEVEL,NLEVEL,ILEVEL
C
      DIMENSION IPOS(4),YPART(NEQ),YPDER(NEQ)
     +,VARV(NVERT,NVARV),VINTG(NVARV),AMFG(*)
     +,VDIFF(*),RHOPAR(*),CPPAR(*),CPVAP(*),VAP0(*)
     +,COV(NVERT,2,2,2,3),NCVD(NCELL),SUP(NCELL,NSUP)
     +,CFACE(NFACE),CFACEP(NFACE),CBLK(*)
     +,IBLKF(NFACE),IBLK(5,NBLOCK),INDBLK(*)
     +,AREA(NFACE,3),VOL(NCELL),VPOR(NCELL),PVFRAC(NCELL)
     +,WORK(*),IWORK(*),CWORK(*)
C
      DIMENSION RPAR(1),IPAR(1),IFLAG(2)
      DIMENSION YFACE(MAXNEQ,MAXPTH),TFACE(MAXPTH),JFACE(MAXPTH)
      DIMENSION IPATH(3,MAXPTH)
      DIMENSION NWLMIN(6),SGNWL(6),COLD(3),FRAC(3)
C
      DATA NWLMIN / 1, 2, 3, 1, 2, 3 /
      DATA SGNWL / 1.0, 1.0, 1.0, -1.0, -1.0, -1.0 /
      SAVE LFIRST
      DATA LFIRST/.TRUE./
C
C INITIALISE THE PATH
C
      NN1 = NN
      ISLOW  = 0
      ICOUNT = 1
      LNEW   = 2
      NEDDY  = 1
      T      = 0.0
      IPAR(1) = 0
      RPAR(1) = 1.0
C
      TLE = -1.0
      UGF =  0.0
      VGF =  0.0
      WGF =  0.0
C
      IBPATH = IPOS(1)
      CBLOCK = CBLK(IBPATH)
      DO 10 II=1,3
       IPATH(II,1) = IPOS(II+1)+1
       YPART(II+3) = MAX(MIN(YPART(II+3),0.9999),0.0001)+IPOS(II+1)+1
   10 CONTINUE
C
      NIB = IBLK(1,IBPATH)
      NJB = IBLK(2,IBPATH)
      NKB = IBLK(3,IBPATH)
      IPCB = IBLK(4,IBPATH)
      IPVB = IBLK(5,IBPATH)
C
      NPATH1 = 1
C
C INITIALISE MOMENTUM SOURCES
C
      DO 122 II=IPTS,NEQ
       YPART(II) = 0.0
```

```
 122 CONTINUE
C
C  INITIALISE SOURCE TERMS
C
      IFLAG(1) =  0
      IFLAG(2) = -1
      CALL PARSRC(IFLAG,IPATH,NPATH1,YPART,SUP,PNUM,RHOPAR,CPPAR,CPVAP
     +        ,VAP0,PVFRAC,T,TFOLD,VOLOLD)
      TFOLD = T
C
C  PRINT HEADING
C
      CALL PRINTD(0,T,YPART,COV,NCVD)
C
C  INITIAL CALL TO USRPBM
C
      IF (NN.EQ.1 .AND. ITER.EQ.1) THEN
       CCALL = 'FIRST '
       E = 1.0
       CFAC = ''
       CFACP = ''
       CBLOCK = ''
       I1 = 1
       J1 = 1
       K1 = 1
       CALL USRPBM(CCALL,E,CFAC,CFACP,CBLOCK,I1,J1,K1
     +         ,T,YPART,YPDER,AMFG)
      END IF
C
C  GET A NEW SUB-PATH
C
  40 IPATH(1,1) = IPATH(1,NPATH1)
      IPATH(2,1) = IPATH(2,NPATH1)
      IPATH(3,1) = IPATH(3,NPATH1)
C
      TOLD = T
      YPIOLD = YPART(4)
      YPJOLD = YPART(5)
      YPKOLD = YPART(6)
C
      CALL INTEG(LNEW,NEDDY,RPAR,VARV,VINTG,AMFG,VDIFF
     +       ,RHOPAR,CPPAR,CPVAP,VAP0
     +       ,COV,NCVD,IPAR,T,YPART,YPDER
     +       ,ICOUNT,IPATH,YFACE,TFACE,JFACE,IFT)
C
C  OPENING A USER FILE FOR RESIDENCE TIME
C
      IF (LFIRST) THEN
      ISEQF = 0
      CALL FILCON('TRACK','impact3','OPEN','FORMATTED','NEW',
     +         IOCAT,ISEQF,IOST,IERR1)
      LFIRST = .FALSE.
      ENDIF
C
C  GETTING SCALAR ARRAY
C
      CALL GETADD('TRACK ','ITOPOL','IPNODB',ILEVEL,JPNODB)
      CALL GETADD('TRACK ','VAR   ','SCAL  ',ILEVEL,JSCAL)
C
C  CHECK IF FLOW3D IS BEING STOPPED
C
      IF(IFT.EQ.-12) LSTOP = .TRUE.
C
C  CHECK IF PARTICLE IS NOT ADVANCING FAR IN TIME AND SPACE
C
      ARCL = (YPART(4)-YPIOLD)**2 + (YPART(5)-YPJOLD)**2
     +             + (YPART(6)-YPKOLD)**2
      IF((T-TOLD).LE.TFRAC*TLIM .AND. ARCL.LE.CVFRAC**2
     +             .AND. IFT.NE.-1) THEN
C
       ISLOW = ISLOW + 1
       IF (ISLOW.EQ.2) THEN
         IFLAG(1) = 1
         IFLAG(2) = 0
         ILAST   = 2
         IFT     = -10
```

```
        GO TO 800
       END IF
C
      ELSE
C
       ISLOW = 0
C
      END IF
C
C  CHECK FOR JUMP OUT OF INTEG INTERPOLATION LOOP
C
      IF(IFT.EQ.-8 .OR. IFT.EQ.-9 .OR. IFT.EQ.-11) THEN
C
       IFLAG(1) = 1
       IFLAG(2) = 0
       ILAST    = 2
       GO TO 800
C
      END IF
C
C  ITERATE OVER CURRENT SUB-PATH
C
      DO 50 NPATH=1,ICOUNT
C
       NPATH1 = NPATH+1
C
       I = IPATH(1,NPATH1)
       J = IPATH(2,NPATH1)
       K = IPATH(3,NPATH1)
C
       CFAC = CFACE(JFACE(NPATH))
       CFACP = CFACEP(JFACE(NPATH))
C
C  CHECK WHETHER PARTICLE HAS CROSSED A BOUNDARY FACE
C
       IF(CFAC.EQ.'INTERIOR') THEN
C
C  PARTICLE IS IN INTERIOR OF PRESENT BLOCK
C
C  CHECK IF TIME LIMIT EXCEEDED
C
        IF(T.GE.TLIM) THEN
C
         IFLAG(1) = 1
         IFLAG(2) = 0
         ILAST    = NPATH1
         IFT      = -2
         GO TO 800
C
        END IF
C
        IFLAG(1) =  1
        IFLAG(2) = -1
C
       ELSE
C
C  RESET VARIABLES AND TIME TO VALUES ON FACE CROSSED
C
        T = TFACE(NPATH)
        DO 200 II=1,NEQ
         YPART(II) = YFACE(II,NPATH)
 200    CONTINUE
C
C  CHECK IF TIME LIMIT EXCEEDED
C
        IF(T.GE.TLIM) THEN
C
         IFLAG(1) = 1
         IFLAG(2) = 0
         ILAST    = NPATH1
         IFT      = -2
         GO TO 800
C
        END IF
C
        IF((CFAC.EQ.'INLET   ').OR.(CFAC.EQ.'OUTLET  ')
```

```
     +            .OR.(CFAC.EQ.'PRESSURE')) THEN
C
C CALL USER ROUTINE FOR PARTICLE MONITORING AT BOUNDARIES
C
        CCALL = 'NORMAL'
        E = 1.0
        I1 = IPATH(1,NPATH)-1
        J1 = IPATH(2,NPATH)-1
        K1 = IPATH(3,NPATH)-1
        CALL USRPBM(CCALL,E,CFAC,CFACP,CBLOCK,I1,J1,K1
     +            ,T,YPART,YPDER,AMFG)
C
C PARTICLE EXITS THROUGH INLET/OUTLET/PRESSURE BOUNDARY
C
        IFLAG(1) = 1
        IFLAG(2) = 0
        ILAST   = NPATH1
        IFT     = 2
        GO TO 800
C
      ELSE IF(CFAC.EQ.'WALL    ') THEN
C
C PARTICLE HITS WALL
C
C CALL USER ROUTINE FOR PARTICLE MONITORING AT BOUNDARIES AND
C SPECIFICATION OF COEFFICIENT OF RESTITUTION
C
        CCALL = 'NORMAL'
        E = RESTCF
        I1 = IPATH(1,NPATH)-1
        J1 = IPATH(2,NPATH)-1
        K1 = IPATH(3,NPATH)-1
        CALL USRPBM(CCALL,E,CFAC,CFACP,CBLOCK,I1,J1,K1
     +            ,T,YPART,YPDER,AMFG)
C
        IF(IBOUNC.GT.0) THEN
C
C RETURN TO PREVIOUS CONTROL VOLUME
C
         IPTH = (JFACE(NPATH)-1)/NCELL+1
         CSTEP = YPART(3+IPTH)-IPATH(IPTH,NPATH1)
         CSTEP = 2.0*(CSTEP-0.5)
         IPATH(IPTH,NPATH1) = IPATH(IPTH,NPATH1)+NINT(CSTEP)
C
C REFLECT VELOCITY GET COEFFICIENT OF RESTITUTION
C
         I2 = IPATH(1,NPATH)
         J2 = IPATH(2,NPATH)
         K2 = IPATH(3,NPATH)
         CALL BCSPAR(E,I2,J2,K2,YPART(1),YPART(2),YPART(3)
     +             ,YPART,COV,NCVD,JFACE(NPATH)
     +             ,IWORK(JPNODB),WORK(JSCAL),PMASS)
C
C MOVE PARTICLE AWAY FROM WALL
C
         DIST = YPART(3+IPTH)-IPATH(IPTH,NPATH1)
         YPART(3+IPTH) = IPATH(IPTH,NPATH1)
     +             + MIN(MAX(DIST,0.00005),0.99995)
C
C FORCE A RESTART
C
         LNEW = 1
         NEDDY = 1
C
         IFLAG(1) = 1
         IFLAG(2) = -1
C
        ELSE
C
         IF(.NOT.LCOAL) THEN
          IFLAG(1) = 1
          IFLAG(2) = 0
          ILAST   = NPATH1
          IFT     = 3
          GO TO 800
         ENDIF
```

```
C
        IF(RPAR(1).GT.0.0) THEN
         IF(IOILC.NE.1) WRITE(NWRITE,605)
         IF(IOILC.EQ.1) WRITE(NWRITE,606)
        ENDIF
C
C  RETURN TO PREVIOUS CONTROL VOLUME
C
        IPATH(1,NPATH1) = IPATH(1,NPATH)
        IPATH(2,NPATH1) = IPATH(2,NPATH)
        IPATH(3,NPATH1) = IPATH(3,NPATH)
C
C  MOVE PARTICLE AWAY FROM WALL
C
        DO 300 ID=1,3
        DIST = YPART(ID+3)-IPATH(ID,NPATH)
        YPART(ID+3) = IPATH(ID,NPATH)+MIN(MAX(DIST,0.0001),0.9999)
 300      CONTINUE
C
C  TURN ADVECTION EQUATIONS OFF
C
        RPAR(1) = 0.0
C
C  SET VELOCITY TO ZERO
C
        YPART(1) = 0.0
        YPART(2) = 0.0
        YPART(3) = 0.0
C
C  FORCE A RESTART
C
        LNEW = 1
        NEDDY = 0
C
        IFLAG(1) = 1
        IFLAG(2) = -1
C
       END IF
C
     ELSE IF(CFAC.EQ.'SYMMETRY') THEN
C
C  PARTICLE CROSSES SYMMETRY PLANE
C
C  RETURN TO PREVIOUS CONTROL VOLUME
C
       IPATH(1,NPATH1) = IPATH(1,NPATH)
       IPATH(2,NPATH1) = IPATH(2,NPATH)
       IPATH(3,NPATH1) = IPATH(3,NPATH)
C
C  REFLECT VELOCITY - COEFFICIENT OF RESTITUTION = 1
C  IF TURBULENT DISPERSION INCLUDED - REFLECT EDDY
C
       E = 1.0
       CALL BCSPAR(E,I2,J2,K2,YPART(1),YPART(2),YPART(3)
   +            ,YPART,COV,NCVD,JFACE(NPATH)
   +            ,IWORK(JPNODB),WORK(JSCAL),PMASS)
       IF (LPTURB) CALL BCSPAR(E,I2,J2,K2,UGF,VGF,WGF
   +                    ,YPART,COV,NCVD,JFACE(NPATH)
   +                    ,IWORK(JPNODB),WORK(JSCAL)
   +                    ,PMASS)
C
C  FORCE A RESTART
C
       LNEW = 1
       NEDDY = 0
C
       IFLAG(1) = 1
       IFLAG(2) = -1
C
     ELSE IF(CFAC.EQ.'BLKBDY  ') THEN
C
C  CALCULATE SOURCE ON LEAVING BLOCK
C
       IFLAG(1) = 1
       IFLAG(2) = 0
C
```

```
        CALL PARSRC(IFLAG,IPATH,NPATH1,YFACE(1,NPATH),SUP,PNUM
     +         ,RHOPAR,CPPAR,CPVAP,VAP0
     +         ,PVFRAC,TFACE(NPATH),TFOLD,VOLOLD)
        TFOLD = TFACE(NPATH)
C
C PARTICLE CROSSES BLOCK BOUNDARY
C
        COLD(1) = YPART(4)-I
        COLD(2) = YPART(5)-J
        COLD(3) = YPART(6)-K
C
C RESET PARTICLE IN COMPUTATIONAL SPACE
C
        LCV = IBLKF(JFACE(NPATH))
C
        CALL BLKPAR(INDBLK,NCVBLK,LCV,NWL1,NWL2,NWL3
     +         ,IBLK,IBPATH,I,J,K)
C
        CBLOCK = CBLK(IBPATH)
        IPATH(1,NPATH1) = I
        IPATH(2,NPATH1) = J
        IPATH(3,NPATH1) = K
        FRAC(NWLMIN(NWL1)) = 0.5+SGNWL(NWL1)*(COLD(1)-0.5)
        FRAC(NWLMIN(NWL2)) = 0.5+SGNWL(NWL2)*(COLD(2)-0.5)
        FRAC(NWLMIN(NWL3)) = 0.5+SGNWL(NWL3)*(COLD(3)-0.5)
        YPART(4) = FRAC(1)+I
        YPART(5) = FRAC(2)+J
        YPART(6) = FRAC(3)+K
        YFACE(4,NPATH) = YPART(4)
        YFACE(5,NPATH) = YPART(5)
        YFACE(6,NPATH) = YPART(6)
C
C FORCE A RESTART
C
        LNEW = 1
        NEDDY = 0
C
        IFLAG(1) = 0
        IFLAG(2) = -1
C
       ENDIF
C
      ENDIF
C
      IF (LPOROS .AND. IPORPA.EQ.0) THEN
C
       NC = IPCB + (I-1) + (J-1)*NIB + (K-1)*NIB*NJB
       IF (VPOR(NC)/MAX(VOL(NC),SMALL).LT.0.9999) THEN
        IFLAG(1) = 1
        IFLAG(2) = 0
        ILAST   = NPATH1
        IFT     = 4
        GO TO 800
       END IF
C
      END IF
C
C UPDATE SOURCE TERMS AND CONTINUE ALONG SUB-PATH
C
      CALL PARSRC(IFLAG,IPATH,NPATH1,YFACE(1,NPATH),SUP,PNUM
     +        ,RHOPAR,CPPAR,CPVAP,VAP0
     +        ,PVFRAC,TFACE(NPATH),TFOLD,VOLOLD)
      TFOLD = TFACE(NPATH)
C
      CALL PRINTD(1,TFACE(NPATH),YFACE(1,NPATH),COV,NCVD)
C
C CHECK WHETHER STARTING NEW SUB-PATH
C
      IF(LNEW.GT.0) GO TO 40
C
 50 CONTINUE
C
C CHECK WHETHER CURRENT PATH COMPLETED
C
    IF(IFT.EQ.0) GO TO 40
C
```

```
C  FINISH OFF THE CURRENT PATH
C
C  FINALISE SOURCE TERMS
C
      ILAST = ICOUNT+2
      IFLAG(1) = 1
      IFLAG(2) = 0
C
 800 CALL PARSRC(IFLAG,IPATH,ILAST,YPART,SUP,PNUM,RHOPAR,CPPAR,CPVAP
     +        ,VAP0,PVFRAC,T,TFOLD,VOLOLD)
C
      CALL PRINTD(1,T,YPART,COV,NCVD)
C
C  FINAL CALL TO USRPBM
C
      IF (NN.EQ.NPART .AND. ITER.EQ.NTER) THEN
        CCALL = 'LAST  '
        E = 1.0
        CFAC = ' '
        CFACP = ' '
        CBLOCK = ' '
        I1 = 1
        J1 = 1
        K1 = 1
        CALL USRPBM(CCALL,E,CFAC,CFACP,CBLOCK,I1,J1,K1
     +          ,T,YPART,YPDER,AMFG)
      END IF
C
      IF(IFT.EQ.3) THEN
        WRITE(NWRITE,610)
        WRITE(IOCAT,610)
      ELSE IF(IFT.EQ.2) THEN
        WRITE(NWRITE,600)
        WRITE(IOCAT,600)
      ELSE IF(IFT.EQ.1) THEN
        WRITE(NWRITE,620)
        WRITE(IOCAT,620)
      ELSE IF(IFT.EQ.4) THEN
        WRITE(NWRITE,622)
        WRITE(IOCAT,622)
      ELSE IF(IFT.EQ.-1) THEN
        WRITE(NWRITE,625)
        WRITE(IOCAT,625)
      ELSE IF(IFT.EQ.-2) THEN
        WRITE(NWRITE,630)
        WRITE(IOCAT,630)
      ELSE IF(IFT.EQ.-10) THEN
        WRITE(NWRITE,640)
        WRITE(IOCAT,640)
      ENDIF
C
C  WRITNG DATA TO THE USER FILE
C
      WRITE(IOCAT,670)NN
      WRITE(IOCAT,650)
      WRITE(IOCAT,660)T
      WRITE(IOCAT,680)
C
      RETURN
C
C  FORMAT STATEMENTS
C
 600 FORMAT(/,' PARTICLE LEAVES FLOW DOMAIN')
 605 FORMAT(/,' COAL PARTICLE IS ON WALL')
 606 FORMAT(/,' OIL DROPLET IS ON WALL')
 610 FORMAT(/,' PARTICLE IS ON WALL')
 620 FORMAT(/,' PARTICLE HAS EVAPORATED')
 622 FORMAT(/,' PARTICLE HAS ENTERED POROUS REGION')
 625 FORMAT(/,' PARTICLE IS ALMOST STATIONARY')
 630 FORMAT(/,' T HAS EXCEEDED TIME-LIMIT')
 640 FORMAT(/,' TIME/SPACE ADVANCING SLOWLY '
     +          ,'- PARTICLE ALMOST STATIONARY')
 650 FORMAT('    Residence Time of Particle')
 660 FORMAT(E18.4)
 670 FORMAT(I9)
 680 FORMAT('  ')
```

```
C
      END
      SUBROUTINE BCSPAR(E,I2,J2,K2,U,V,W,YPART,COV
     +          ,NCVD,IFACE,IPNODB,SCAL,PMASS)
C
C***********************************************************************
C
C  SUBROUTINE TO REFLECT VELOCITY OF PARTICLES AT A SYMMETRY PLANE
C  OR A WALL WITH A COEFFICIENT OF RESTITUTION
C
C***********************************************************************
C
C  THIS SUBROUTINE IS CALLED BY THE FOLLOWING SUBROUTINES
C    TRACK
C
C***********************************************************************
C
      DOUBLE PRECISION UPART
C
      CHARACTER*8 CFAC
      CHARACTER*32 CFACP
C
      LOGICAL LDEN,LVIS,LTURB,LTEMP,LBUOY,LSCAL,LCOMP
     +     ,LRECT,LCYN,LAXIS,LPOROS,LTRANS
C
      COMMON
     + /ALL/   NBLOCK,NCELL,NBDRY,NNODE,NFACE,NVERT,NDIM
     + /LOGIC/  LDEN,LVIS,LTURB,LTEMP,LBUOY,LSCAL,LCOMP
     +       ,LRECT,LCYN,LAXIS,LPOROS,LTRANS
     + /ADDIMS/ NPHASE,NSCAL
     + /RPART/  DIAM,AMDC,RHO,CPBPAR,TVAP
     + /NIJKB/  NIB,NJB,NKB,IPCB
     + /USRNNN/ NN,PDAT,CFAC,CFACP,I,J,K
C
      REAL VOL,VER,SPD
C
      SAVE LFIRST
      DATA LFIRST/.TRUE./
      SAVE ICOUNT
      DATA ICOUNT/1/
      SAVE ICOUNT1
      DATA ICOUNT1/0/
      SAVE ICOUNT2
      DATA ICOUNT2/0/
      SAVE ICOUNT3
      DATA ICOUNT3/0/
C
      DIMENSION NCVD(NCELL),COV(NVERT,2,2,2,3),YPART(6)
      DIMENSION XP(3),RJAC(3,3),UPART(6)
      DIMENSION VOL(12000,3),VER(12000,3),SPD(12000,3)
      DIMENSION SCAL(NNODE,NPHASE,NSCAL)
      DIMENSION IPNODB(NBDRY,4)
C
      SAVE VOL,VER,SPD
C
C DETERMINING NODE NUMBER
C
      INODE = IPCB+(K2-1)*NIB*NJB+(J2-1)*NIB+(I2-1)
C
C FLUID AND PARTICLE PARAMETERS (WATER SETUP)
C
      DENP = AMDC/(4.18879*((DIAM/2)**3))
      PRF = 0.5
      QP = 0.227
      EP = 59.2E+09
      DENF = 984.6
      VISC = 4.807E-03
      D = 10
C
C MATERIAL CONSTANTS FOR CAGE (6%)
C
      IF(CFACP.EQ.'TUNG') THEN
      TRS = 3.0E+09
      ET = 624.0E+09
      QT = 0.21
      EF = 1.38E+11
```

```
      S = 3.0
      POW = ((1/EP*(1-QP**2))+(1/ET*(1-QT**2)))**2
      C = 2.5066*(TRS**2.4)*SQRT(PRF/DENP)*(POW)
      CK = SQRT((10*TRS*(PRF**0.6))/DENP)
      ENDIF
C
C MATERIAL CONSTANTS FOR PLUG (6%)
C
      IF(CFACP.EQ.'PLUG') THEN
      TRS = 3.0E+09
      ET = 624.0E+09
      QT = 0.21
      EF = 1.38E+11
      S = 3.0
      POW = ((1/EP*(1-QP**2))+(1/ET*(1-QT**2)))**2
      C = 2.5066*(TRS**2.4)*SQRT(PRF/DENP)*(POW)
      CK = SQRT((10*TRS*(PRF**0.6))/DENP)
      ENDIF
C
C MATERIAL CONSTANTS FOR BODY
C
      IF(CFACP.NE.'TUNG') THEN
      IF(CFACP.NE.'PLUG') THEN
      YS = 320.0E+06
      ET = 207.0E+09
      QT = 0.293
      EF = 1.9E+10
      S = 2.8
      POW = ((1/EP*(1-QP**2))+(1/ET*(1-QT**2)))**2
      C = 2.0466*(YS**2.6)*SQRT(PRF/DENP)*(POW)
      CK = SQRT((21*YS*(PRF**0.6))/DENP)
      ENDIF
      ENDIF
C
C-- OPENING A FILE TO WHICH DATA CAN BE WRITEN ABOUT PARTICLE IMPACTS
C
      IF (LFIRST) THEN
      ISEQF=0
      CALL FILCON('BCSPAR','impact1','OPEN','FORMATTED','NEW',
     +        IODAT,ISEQF,IOST,IERR1)
      CALL FILCON('BCSPAR','impact2','OPEN','FORMATTED','NEW',
     +        IOBAT,ISEQF,IOST,IERR1)
      LFIRST=.FALSE.
      WRITE(IODAT,230)
      ENDIF
C
C-- USE TRI-CUBIC INTERPOLATION TO FIND POSITION AND JACOBIAN
C
      DO 110 I=1,3
      DO 100 J=1,3
      RJAC(I,J) = 0.0
  100 CONTINUE
  110 CONTINUE
C
      UPART(4) = YPART(4)
      UPART(5) = YPART(5)
      UPART(6) = YPART(6)
C
      CALL LOCATE(UPART,NU,NV,NW,DU,DV,DW)
C
      CALL TCUINT(COV,NCVD,NU,NV,NW,DU,DV,DW,XP,RJAC)
C
C CALCULATE THE RADIAL POSITION (PERP. DISTANCE FROM CYLINDER AXIS)
C
      IF (LCYN) THEN
       RAD = XP(2)
      ELSE
       RAD = 1.0
      ENDIF
C
C FIND AREA OF BOUNDARY FACE IN PHYSICAL SPACE
C
C GET FACE DIRECTIONS
C
      NWL = (IFACE-1)/NCELL + 1
      NW2 = MOD(NWL,3)+1
```

```
      NW3 = MOD(NWL+1,3)+1
C
      AREAX = RAD*(RJAC(2,NW2)*RJAC(3,NW3)-RJAC(2,NW3)*RJAC(3,NW2))
      AREAY = RAD*(RJAC(3,NW2)*RJAC(1,NW3)-RJAC(3,NW3)*RJAC(1,NW2))
      AREAZ = RJAC(1,NW2)*RJAC(2,NW3)-RJAC(1,NW3)*RJAC(2,NW2)
C
C REFLECT VELOCITY
C
      AREASQ = AREAX**2 + AREAY**2 + AREAZ**2
C
C COMPUTE COMPONENTS OF VELOCITY PERPENDICULAR TO THE SYMMETRY PLANE
C
      FLUX  = U*AREAX + V*AREAY + W*AREAZ
      UPERP = FLUX * AREAX / AREASQ
      VPERP = FLUX * AREAY / AREASQ
      WPERP = FLUX * AREAZ / AREASQ
C
C COMPUTE COMPONENTS OF VELOCITY PARALLEL TO THE SYMMETRY PLANE
C
      UPAR  = U - UPERP
      VPAR  = V - VPERP
      WPAR  = W - WPERP
C
C CHECK FOR SYMMETRY PLANES
C
      IF(CFACP.NE.'NO') THEN
C
      IF(CFAC.NE.'SYMMETRY') THEN
C
C COMPUTE THE SPEED OF THE PARTICLE AT IMPACT GIVEN CONSIDERATION TO SQUEEZE FILM EFFECTS
C
      SPEED = SQRT(U**2 + V**2 + W**2)
      SPEPP = SQRT(UPERP**2+VPERP**2+WPERP**2)
      CON = 8*((2*DENP/DENF)+1)
      REP = (DENF*SPEPP*DIAM)/VISC
      REPC = 12*(D**2)/CON
      RF1 = 12*(D**2/(CON+D))*(1/REP)
      RF = SQRT((RF1-(CON/(CON+D)))**2)
      SPEED1 = RF*SPEED
C
C FILTER LOOP FOR LOW ANGLES OF IMPACT
C
      IF(REP.GT.REPC) THEN
C
C COMPUTE THE ANGLE OF THE PARTICLE IMPACT FROM THE SURFACE
C
      ANGLE = ASIN(ABS(FLUX/(SQRT(AREASQ)*SPEED)))
      ANGLE2 = ANGLE*57.29578
C
C COMPUTE PARTICLE MOMENTUM AND KINETIC ENERGY
C
      PMOME = AMDC*SPEED1
      PKE = 0.5*AMDC*SPEED1**2
C
C COMPUTE EROSION VOLUME PER IMPACT FOR DEFORMATION AND CUTTING WEAR
C
      WD = (AMDC*((SPEED1*SIN(ANGLE))-C)**2)/(2*EF)
C
      WC = 9.333*((DIAM/2)**3)*((SPEED1/CK)**S)*SIN(2*ANGLE)
     +     *(SQRT(SIN(ANGLE)))
C
      WT = (WD + WC)*1E+09
C
C NUMBER OF PARTICLES EACH TRAJECTORY CALCULATION REPRESENTS
C
      NPART = PMASS/AMDC
C
C PROJECTED EROSION PER TRAJECTORY PER hour
C
      PROJ = WT*NPART*3600
C
C CALCULATING THE COEFFICIENT OF RESTITUTIONS
C
      IF(CFACP.EQ.'TUNG') THEN
      EPAR = 1-0.49*ANGLE+0.62*ANGLE**2-0.2*ANGLE**3
      EPP = 0.998-0.59*ANGLE+0.16*ANGLE**2-0.026*ANGLE**3
```

```
     +    +0.024*ANGLE**4
      ENDIF
C
      IF(CFACP.EQ.'PLUG') THEN
      EPAR = 1-0.49*ANGLE+0.62*ANGLE**2-0.2*ANGLE**3
      EPP = 0.998-0.59*ANGLE+0.16*ANGLE**2-0.026*ANGLE**3
     +    +0.024*ANGLE**4
      ENDIF
C
      IF(CFACP.NE.'TUNG') THEN
      IF(CFACP.NE.'PLUG') THEN
      EPAR = 1-0.78*ANGLE+0.84*ANGLE**2-0.21*ANGLE**3
     +    +0.028*ANGLE**4-0.022*ANGLE**5
      EPP = 0.988-0.78*ANGLE+0.19*ANGLE**2-0.024*ANGLE**3
     +    +0.027*ANGLE**4
      ENDIF
      ENDIF
C
C DATA MANIPULATION FOR BODY
C
      IF(CFACP.NE.'TUNG') THEN
      IF(CFACP.NE.'PLUG') THEN
      ICOUNT1 = ICOUNT1+1
      VOL(ICOUNT1,1) = PROJ
      VER(ICOUNT1,1) = ANGLE2
      SPD(ICOUNT1,1) = SPEED
C
      SUM1 = 0.0
      DO 120 I = 1,ICOUNT1
       SUM1 = (SUM1 + VOL(I,1))
  120 CONTINUE
      SUM2 = 0.0
      DO 130 I = 1,ICOUNT1
       SUM2 = (SUM2 + VER(I,1))
  130 CONTINUE
      SUM3 = 0.0
      DO 140 I = 1,ICOUNT1
       SUM3 = (SUM3 + SPD(I,1))
  140 CONTINUE
C
      AVEA1 = SUM2/FLOAT(ICOUNT1)
      AVES1 = SUM3/FLOAT(ICOUNT1)
      ENDIF
      ENDIF
C
C DATA MANIPULATION FOR CAGE
C
      IF(CFACP.EQ.'TUNG') THEN
      ICOUNT2 = ICOUNT2+1
      VOL(ICOUNT2,2) = PROJ
      VER(ICOUNT2,2) = ANGLE2
      SPD(ICOUNT2,2) = SPEED
C
      SUM4 = 0.0
      DO 150 I = 1,ICOUNT2
       SUM4 = (SUM4 + VOL(I,2))
  150 CONTINUE
      SUM5 = 0.0
      DO 160 I = 1,ICOUNT2
       SUM5 = (SUM5 + VER(I,2))
  160 CONTINUE
      SUM6 = 0.0
      DO 170 I = 1,ICOUNT2
       SUM6 = (SUM6 + SPD(I,2))
  170 CONTINUE
C
      AVEA2 = SUM5/FLOAT(ICOUNT2)
      AVES2 = SUM6/FLOAT(ICOUNT2)
      ENDIF
C
C DATA MANIPULATION FOR PLUG
C
      IF(CFACP.EQ.'PLUG') THEN
      ICOUNT3 = ICOUNT3+1
      VOL(ICOUNT3,3) = PROJ
      VER(ICOUNT3,3) = ANGLE2
```

```
      SPD(ICOUNT3,3) = SPEED
C
      SUM7 = 0.0
      DO 600 I = 1,ICOUNT3
       SUM7 = (SUM7 + VOL(I,3))
  600 CONTINUE
      SUM8 = 0.0
      DO 610 I = 1,ICOUNT3
       SUM8 = (SUM8 + VER(I,3))
  610 CONTINUE
      SUM9 = 0.0
      DO 620 I = 1,ICOUNT3
       SUM9 = (SUM9 + SPD(I,3))
  620 CONTINUE
C
      AVEA3 = SUM8/FLOAT(ICOUNT3)
      AVES3 = SUM9/FLOAT(ICOUNT3)
      ENDIF
C
C WRITING DATA TO THE SCALAR ARRAY
C
      SCAL(INODE,NPHASE,1) = SCAL(INODE,NPHASE,1)+PROJ
      SCAL(INODE,NPHASE,2) = SCAL(INODE,NPHASE,2)+PKE
      SCAL(INODE,NPHASE,2) = SPEED
      SCAL(INODE,NPHASE,3) = ANGLE2
C
C WRITING PARTICLE NUMBER, MASS, DIAMETER AND IMPACT NUMBER
C
      WRITE(IODAT,190)
      WRITE(IODAT,260)ICOUNT
      WRITE(IODAT,350)
      WRITE(IODAT,360)NN
      WRITE(IODAT,270)
      WRITE(IODAT,200)DIAM,AMDC
      WRITE(IOBAT,190)
      WRITE(IOBAT,260)ICOUNT,ICOUNT1,ICOUNT2,ICOUNT3
      WRITE(IOBAT,350)
      WRITE(IOBAT,360)NN
C
C WRITING X,Y,Y POSITIONS OF THE PARTICLE IMPACT
C
      WRITE(IODAT,240)
      WRITE(IODAT,200)XP(1),XP(2),XP(3)
C
C WRITING PARTICLE IMPACT VELOCITIES U,V,W AND SPEED
C
      WRITE(IODAT,250)
      WRITE(IODAT,200)U,V,W
      WRITE(IODAT,320)
      WRITE(IODAT,340)SPEED
C
C WRITING THE ANGLE OF IMPACT
C
      WRITE(IODAT,300)
      WRITE(IODAT,310)ANGLE2
C
C WRITING MOMENTUM AND KINETIC ENERGY OF THE PARTICLE
C
      WRITE(IODAT,280)
      WRITE(IODAT,290)PMOME,PKE
C
C WRITING ERODED VOLUME PER IMPACT
C
      WRITE(IODAT,390)
      WRITE(IODAT,330)WT
C       WRITE(6,500)
C
C WRITING CUMULATIVE ERODED VOLUME, AVERAGE ANGLE OF IMPACT, SPEED AND EROSION
C
      WRITE(IOBAT,520)
      WRITE(IOBAT,310)SUM1,SUM4,SUM7
      WRITE(IOBAT,540)
      WRITE(IOBAT,310)AVEA1,AVEA2,AVEA3
      WRITE(IOBAT,560)
      WRITE(IOBAT,340)AVES1,AVES2,AVES3
C
```

```
      ICOUNT = ICOUNT+1
C
      ENDIF
C
C COMPUTE REFLECTED VELOCITY COMPONENTS
C
      IF(REPC.GE.REP)THEN
      U = UPAR - E*UPERP
      V = VPAR - E*VPERP
      W = WPAR - E*WPERP
      ENDIF
C
      IF(REP.GT.REPC)THEN
      U = EPAR*UPAR - EPP*UPERP
      V = EPAR*VPAR - EPP*VPERP
      W = EPAR*WPAR - EPP*WPERP
      ENDIF
      ENDIF
      ENDIF
C
      IF(CFACP.EQ.'NO') THEN
      U = UPAR - E*UPERP
      V = VPAR - E*VPERP
      W = WPAR - E*WPERP
      ENDIF
C
      IF(CFAC.EQ.'SYMMETRY') THEN
      U = UPAR - E*UPERP
      V = VPAR - E*VPERP
      W = WPAR - E*WPERP
      ENDIF
C
C  FORMAT LIMITS
C
 190 FORMAT("----------------------------------------------------")
 200 FORMAT(3E17.4)
 230 FORMAT("Particle Impact Data")
 240 FORMAT("     X(m)          Y(m)          Z(m)")
 250 FORMAT("     U(m/s)        V(m/s)        W(m/s)")
 260 FORMAT(I4)
 270 FORMAT("     Diameter(m)     Mass(kg)")
 280 FORMAT("     Momentum(kgm/s)  Kinetic Energy(j)")
 290 FORMAT(2E17.4)
 300 FORMAT("     Angle of Impact(deg)")
 310 FORMAT(F18.3)
 320 FORMAT("     Speed(m/s)")
 330 FORMAT(E18.4)
 340 FORMAT(F18.3)
 350 FORMAT("     Particle Number")
 360 FORMAT(I11)
 390 FORMAT("     Eroded Volume at Impact (mm**3)")
 500 FORMAT("A particle impact has occured")
 520 FORMAT("     Projected Erosion m**3/hour (Body/Cage/Plug)")
 540 FORMAT("     Average Angle of Impact (Body/Cage/Plug)")
 560 FORMAT("     Average Speed at Impact (Body/Cage/Plug)")
      RETURN
      END
```

Appendix M Numerical Investigation of Erosion and Control Choke Erosion

Incorporated within this Appendix are the graphical outputs generated by the findings of Chapter 8. The topics covered by Chapter 8 include;

1. Code Modifications to Facilitate Liquid Droplet Erosion.
2. A detailed Investigation of Erosion with a 90° Bend.
3. Investigation of Erosion within a Needle and Seat Choke.
4. A Design Evolution of a Needle and Seat Choke.
5. A Comparative Study of Cage Type Control Chokes.

Code Modifications to Facilitate Liquid Droplet Erosion

REVERSE FLOW CONDITIONS THROUGH THE CAMERON CC40

Fluid - **Wet Gas** (Fully Compressible)
Choke Opening ~ **28/64**th
Inlet Pressure - **480** Barg
Pressure Drop - **192** Barg
Droplet Size Range - **0.6-1.0** mm
Droplet Type - **Water** (Incompressible)
Droplet Flux Rate - **1%** by wt.

Figure 1 - Surface Contour Plot of Droplet Impact Velocities (m/s)

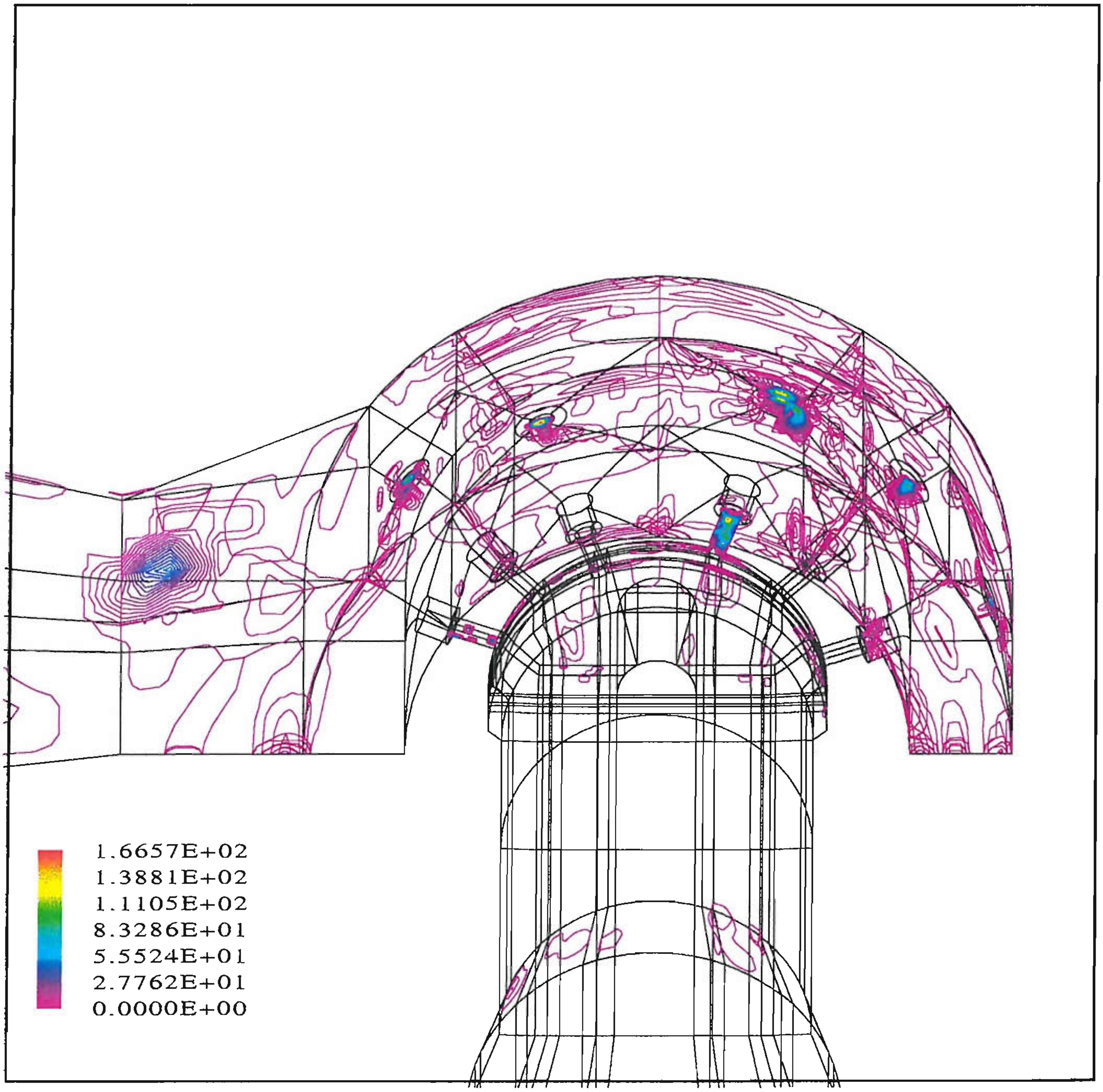

REVERSE FLOW CONDITIONS THROUGH THE CAMERON CC40

Fluid - **Wet Gas** (Fully Compressible)
Choke Opening ~ **28/64th**
Inlet Pressure - **480** Barg
Pressure Drop - **192** Barg
Droplet Size Range - **0.6-1.0** mm
Droplet Type - **Water** (Incompressible)
Droplet Flux Rate - **1%** by wt.

Figure 2 - Surface Contour Plot of Droplet Impact Angles (deg)

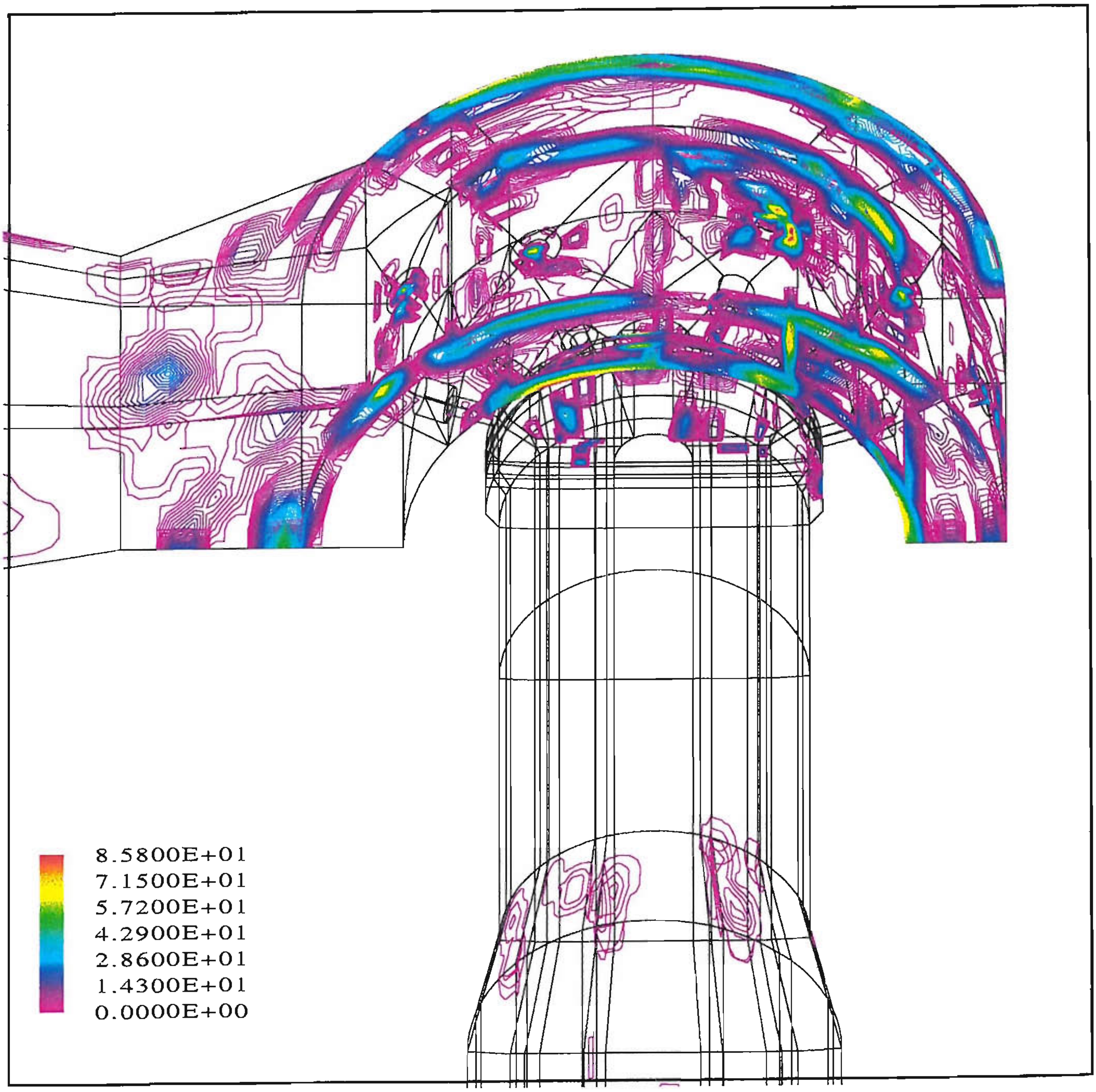

REVERSE FLOW CONDITIONS THROUGH THE CAMERON CC40

Fluid - **Wet Gas** (Fully Compressible)
Choke Opening ~ **28/64**th
Inlet Pressure - **480** Barg
Pressure Drop - **192** Barg
Droplet Size Range - **0.6-1.0** mm
Droplet Type - **Water** (Incompressible)
Droplet Flux Rate - **1%** by wt.

Figure 3 - Surface Contour Plot of Normalised Droplet Erosion Ratio

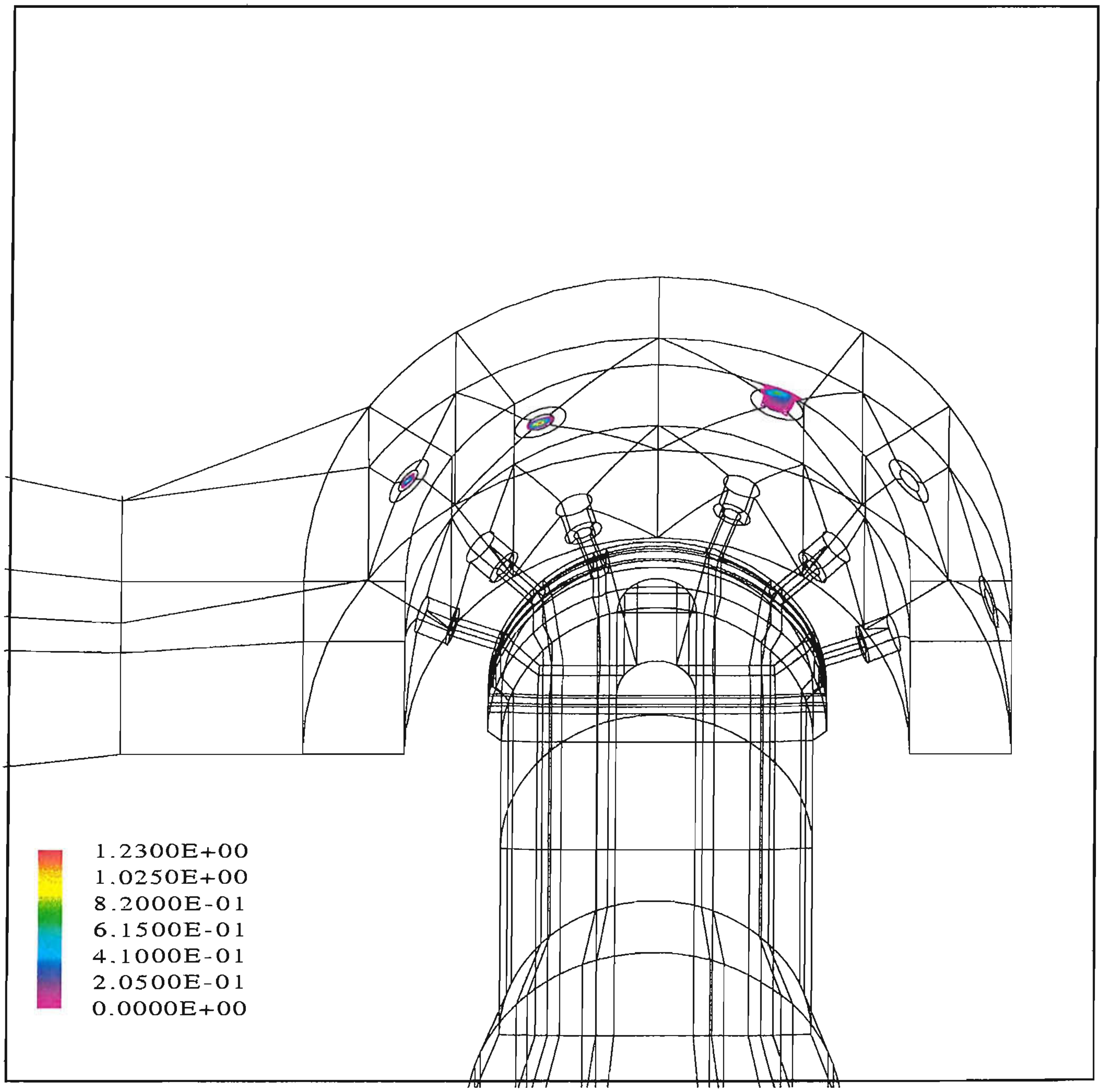

REVERSE FLOW CONDITIONS THROUGH THE CAMERON CC40

Fluid - **Wet Gas** (Fully Compressible)
Choke Opening ~ **28/64th**
Inlet Pressure - **480** Barg
Pressure Drop - **192** Barg
Droplet Size Range - **0.6-1.0** mm
Droplet Type - **Water** (Incompressible)
Droplet Flux Rate - **1%** by wt.

Figure 4 - Surface Contour Plot of Droplet Erosion Rates (mm^3/hr)

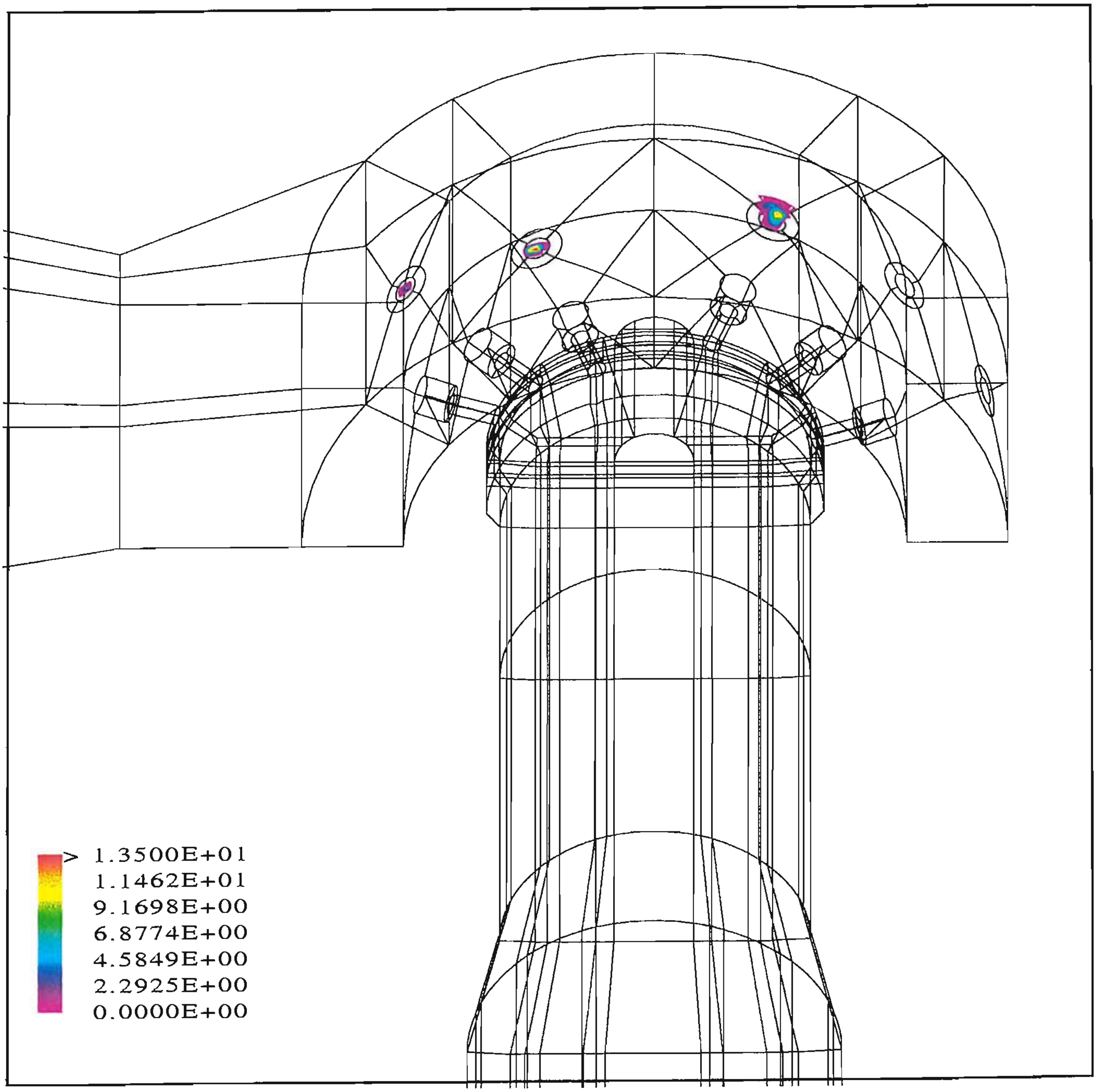

REVERSE FLOW CONDITIONS THROUGH THE CAMERON CC40

Fluid - **Wet Gas** (Fully Compressible)
Initial Density - **332.6** kg/m3
Viscosity - **0.047** cP
Choke Opening ~ **28/64th**
Inlet Pressure - **480** Barg
Pressure Drop - **192** Barg

Figure 5 - Pressure Contours on Surfaces (N/m^3)

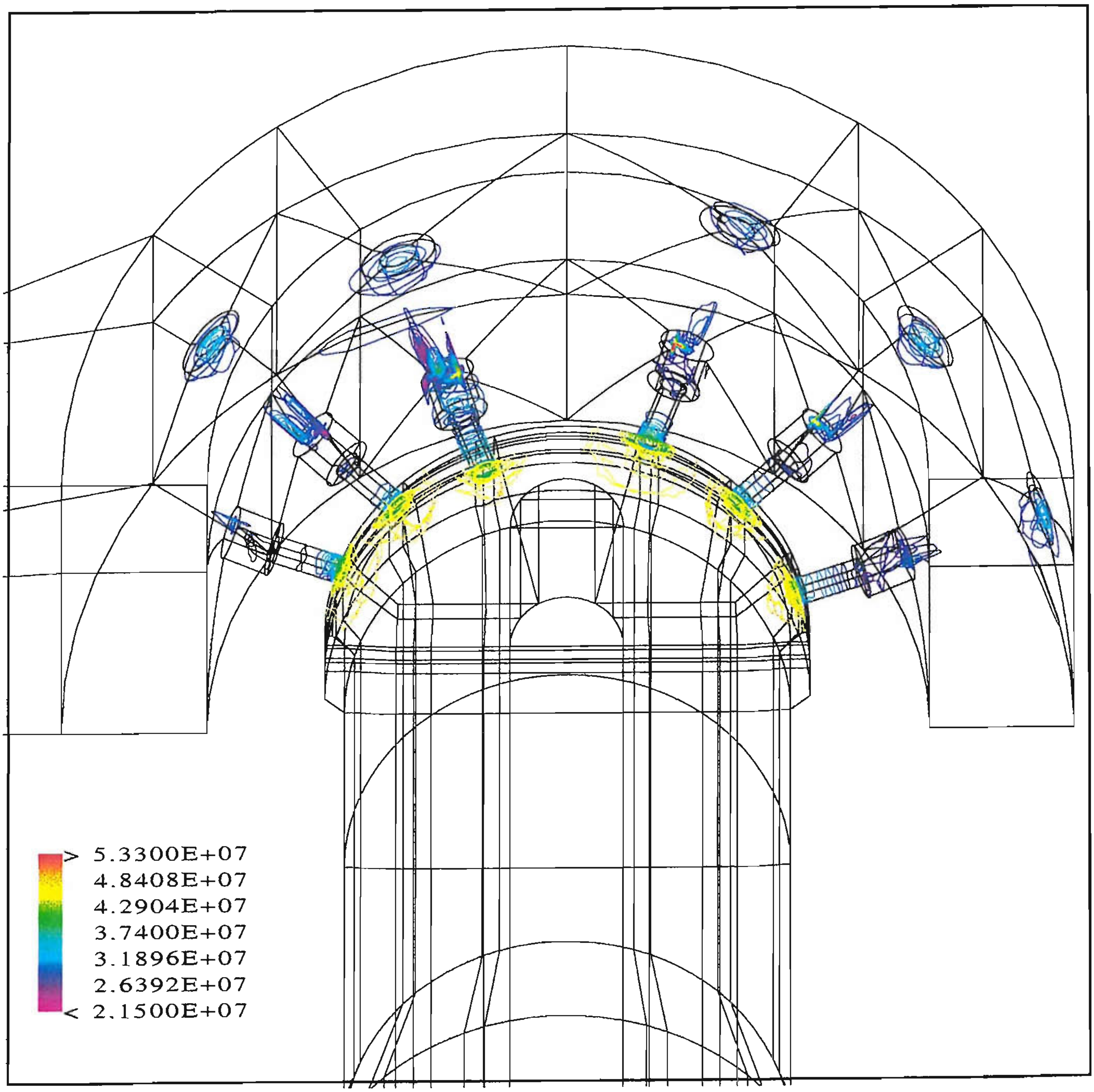

REVERSE FLOW CONDITIONS THROUGH THE CAMERON CC40

Fluid - **Wet Gas** (Fully Compressible)
Initial Density - **332.6** kg/m3
Viscosity - **0.047** cP
Choke Opening ~ **28/64th**
Inlet Pressure - **480** Barg
Pressure Drop - **192** Barg

Figure 6 - Speed Contours on Surfaces (m/s)

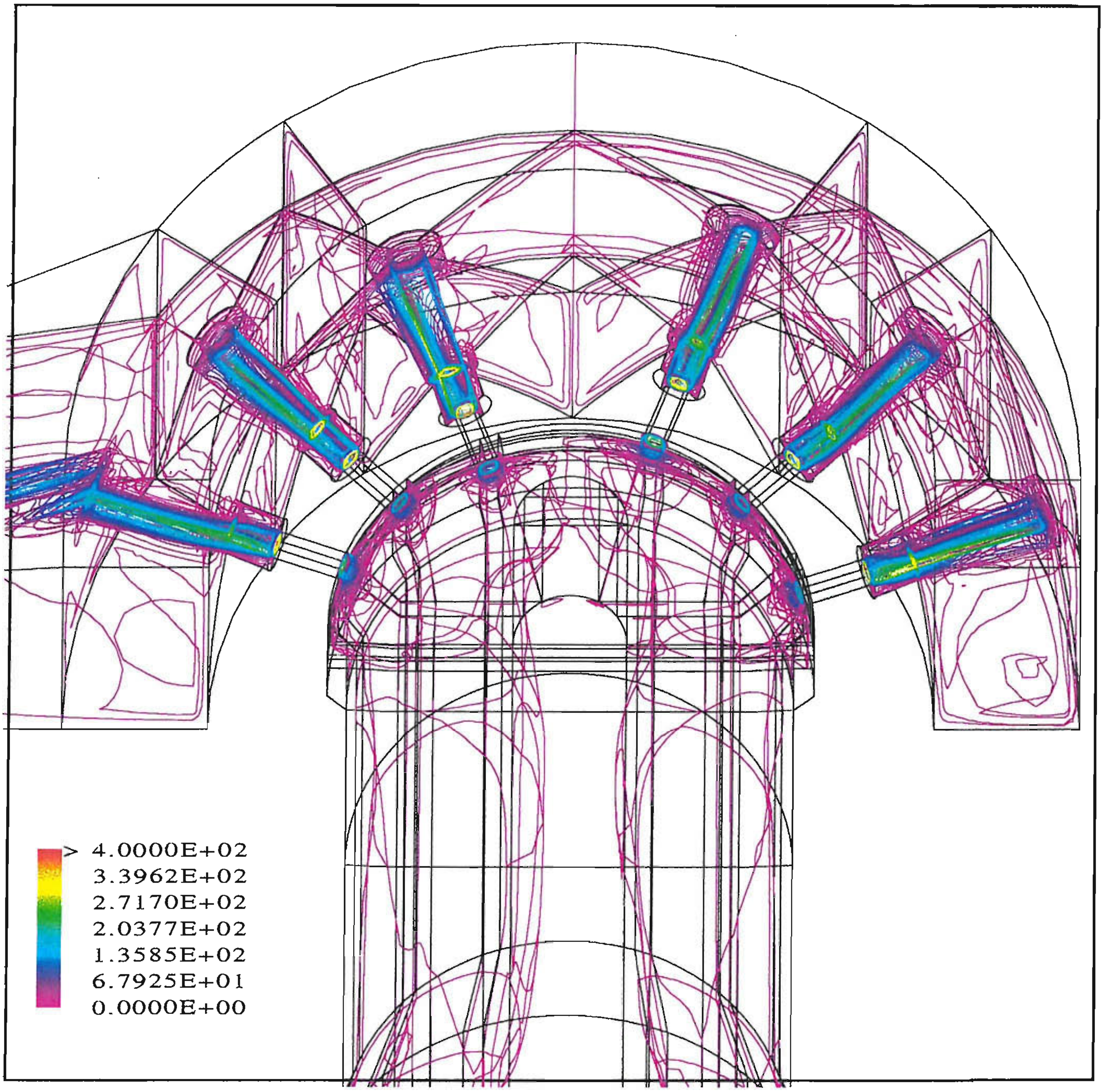

Reverse Flow Conditions Through the Cameron CC40

Fluid - **Wet Gas** (Fully Compressible)
Initial Density - **332.6** kg/m3
Viscosity - **0.047** cP
Choke Opening ~ **28/64th**
Inlet Pressure - **480** Barg
Pressure Drop - **192** Barg

Figure 7 - Mach Number Contours on Surfaces

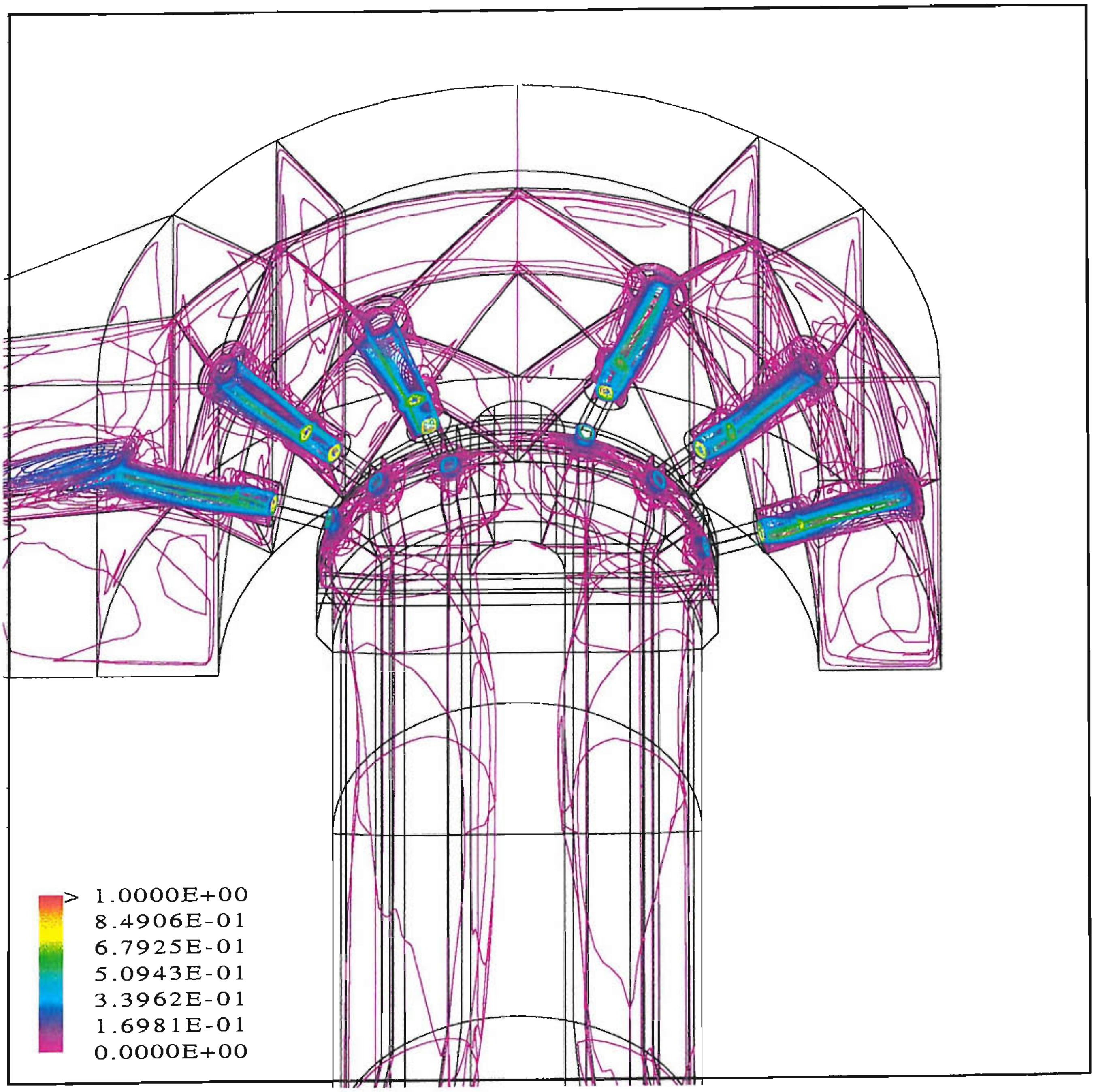

REVERSE FLOW CONDITIONS THROUGH THE CAMERON CC40

Fluid - **Wet Gas** (Fully Compressible)
Choke Opening ~ **28/64**th
Inlet Pressure - **480** Barg
Pressure Drop - **192** Barg
Droplet Size Range - **0.6-1.0** mm
Droplet Type - **Water** (Incompressible)
Droplet Flux Rate - **1%** by wt.

Figure 8 - Fluid Velocity Vector Slice and Droplet Trajectory & Velocity History (m/s)

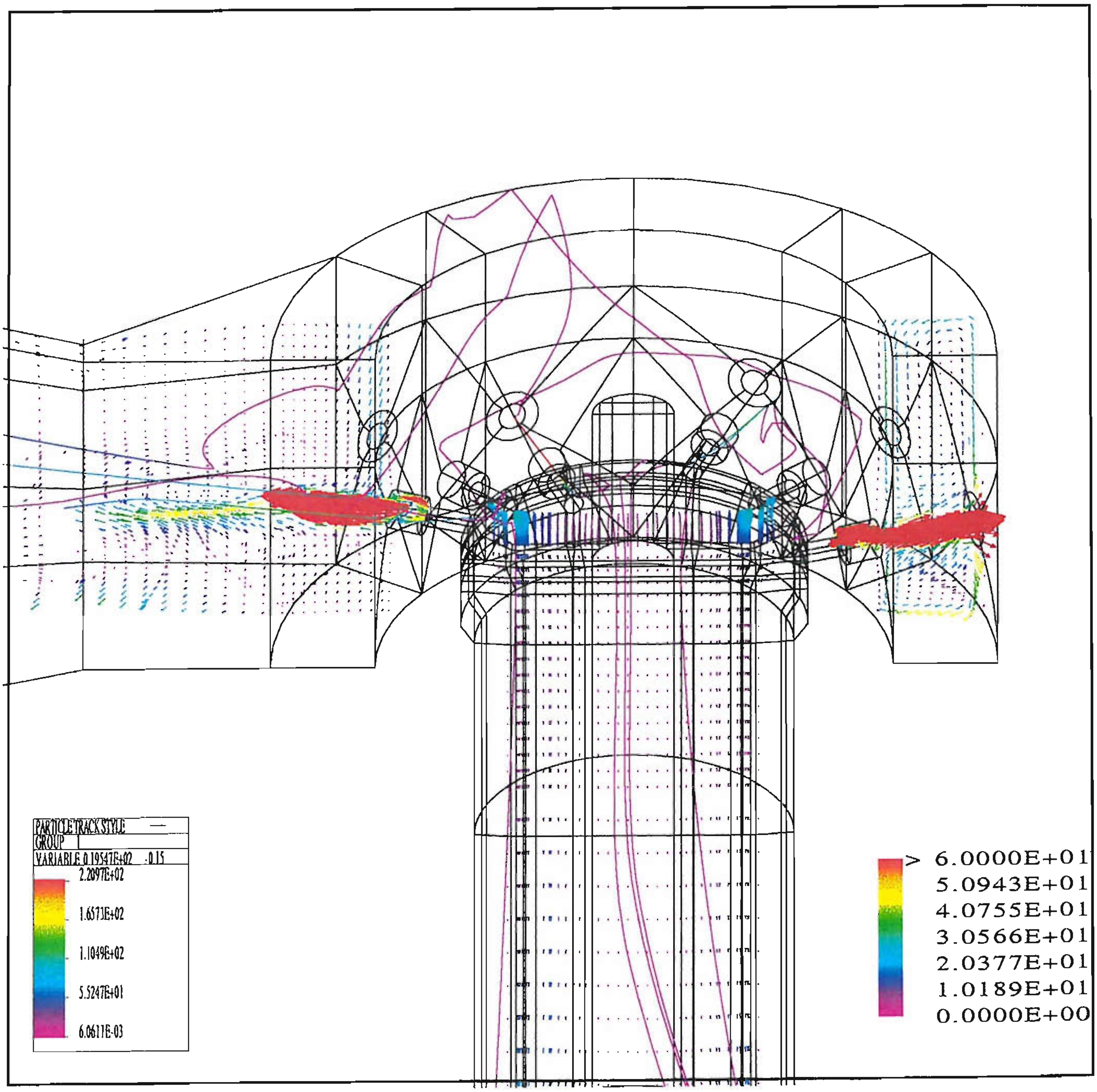

Reverse Flow Conditions Through the Cameron CC40

Fluid - **Wet Gas** (Fully Compressible)
Choke Opening ~ **28/64th**
Inlet Pressure - **480** Barg
Pressure Drop - **192** Barg
Droplet Size Range - **0.6-1.0** mm
Droplet Type - **Water** (Incompressible)
Droplet Flux Rate - **1%** by wt.

Figure 9 - Fluid Velocity Vector Slice and Droplet Trajectory & Velocity History (m/s)

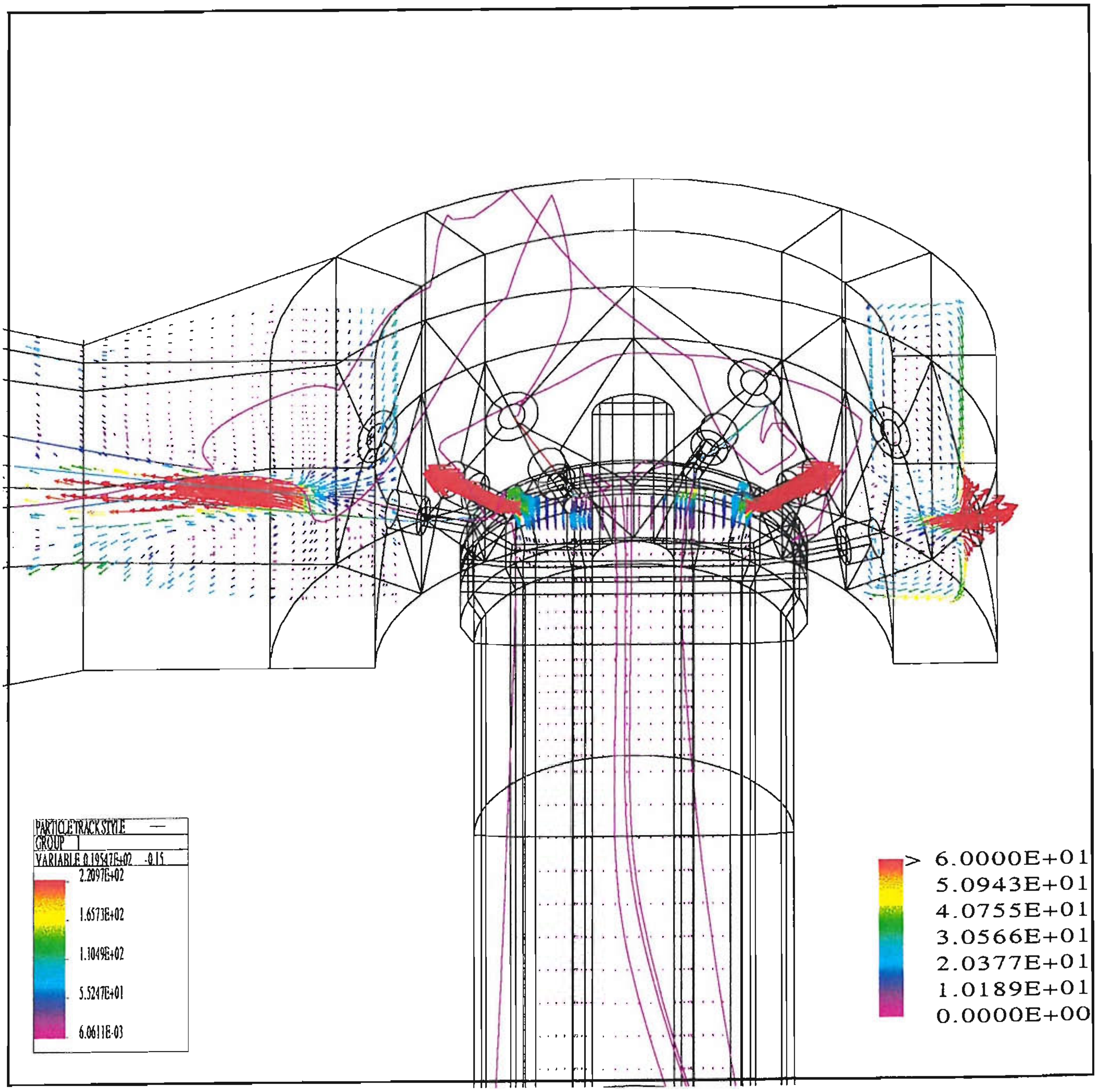

REVERSE FLOW CONDITIONS THROUGH THE CAMERON CC40

Fluid - **Wet Gas** (Fully Compressible)
Choke Opening ~ **28/64th**
Inlet Pressure - **480** Barg
Pressure Drop - **192** Barg
Droplet Size Range - **0.6-1.0** mm
Droplet Type - **Water** (Incompressible)
Droplet Flux Rate - **1%** by wt.

Figure 10 - Fluid Velocity Vector Slice and Droplet Trajectory & Velocity History (m/s)

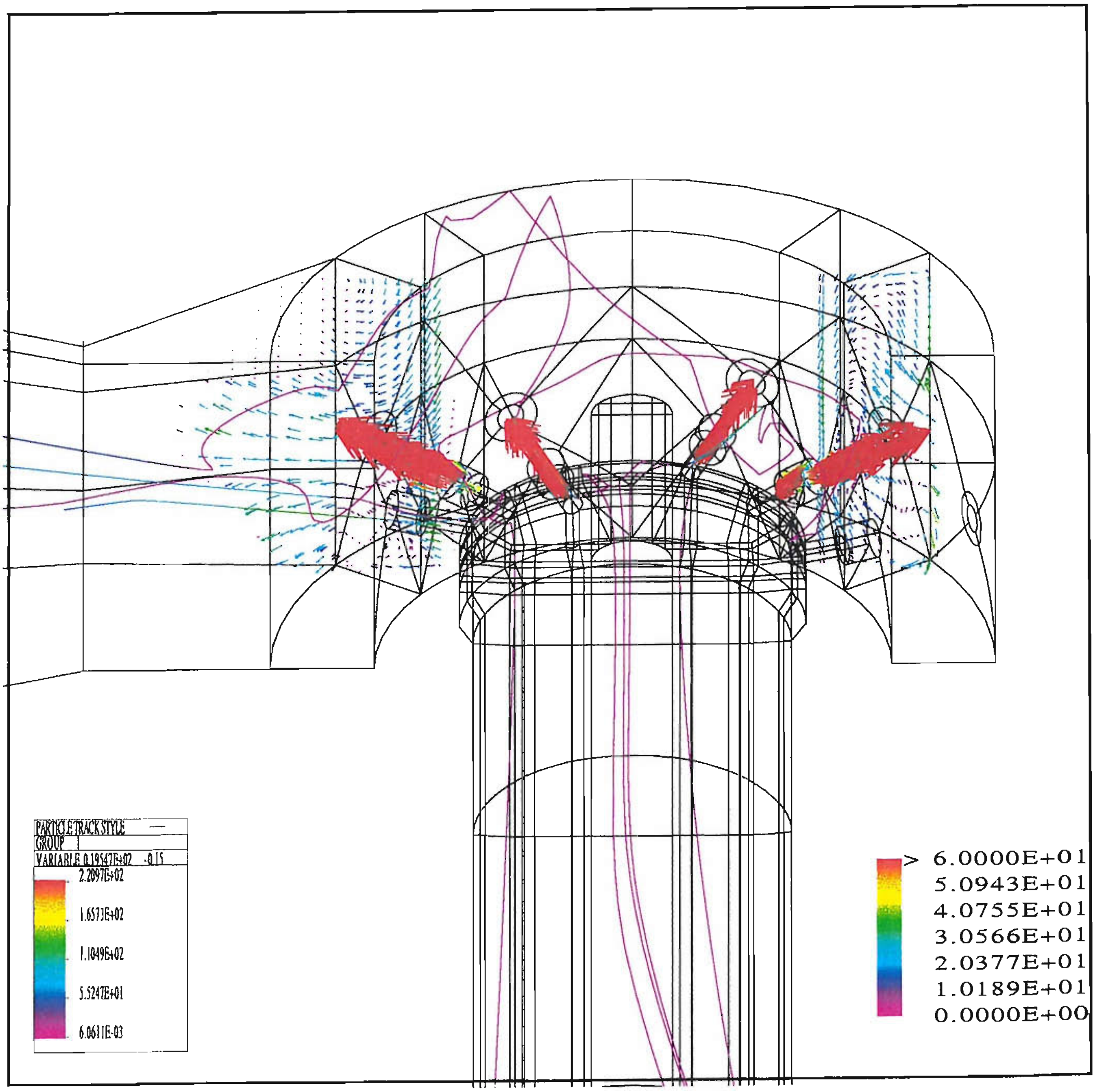

REVERSE FLOW CONDITIONS THROUGH THE CAMERON CC40

Fluid - **Wet Gas** (Fully Compressible)
Choke Opening ~ **28/64th**
Inlet Pressure - **480** Barg
Pressure Drop - **192** Barg
Droplet Size Range - **0.6-1.0** mm
Droplet Type - **Water** (Incompressible)
Droplet Flux Rate - **1%** by wt.

Figure 11 - Fluid Velocity Vector Slice and Droplet Trajectory & Velocity History (m/s)

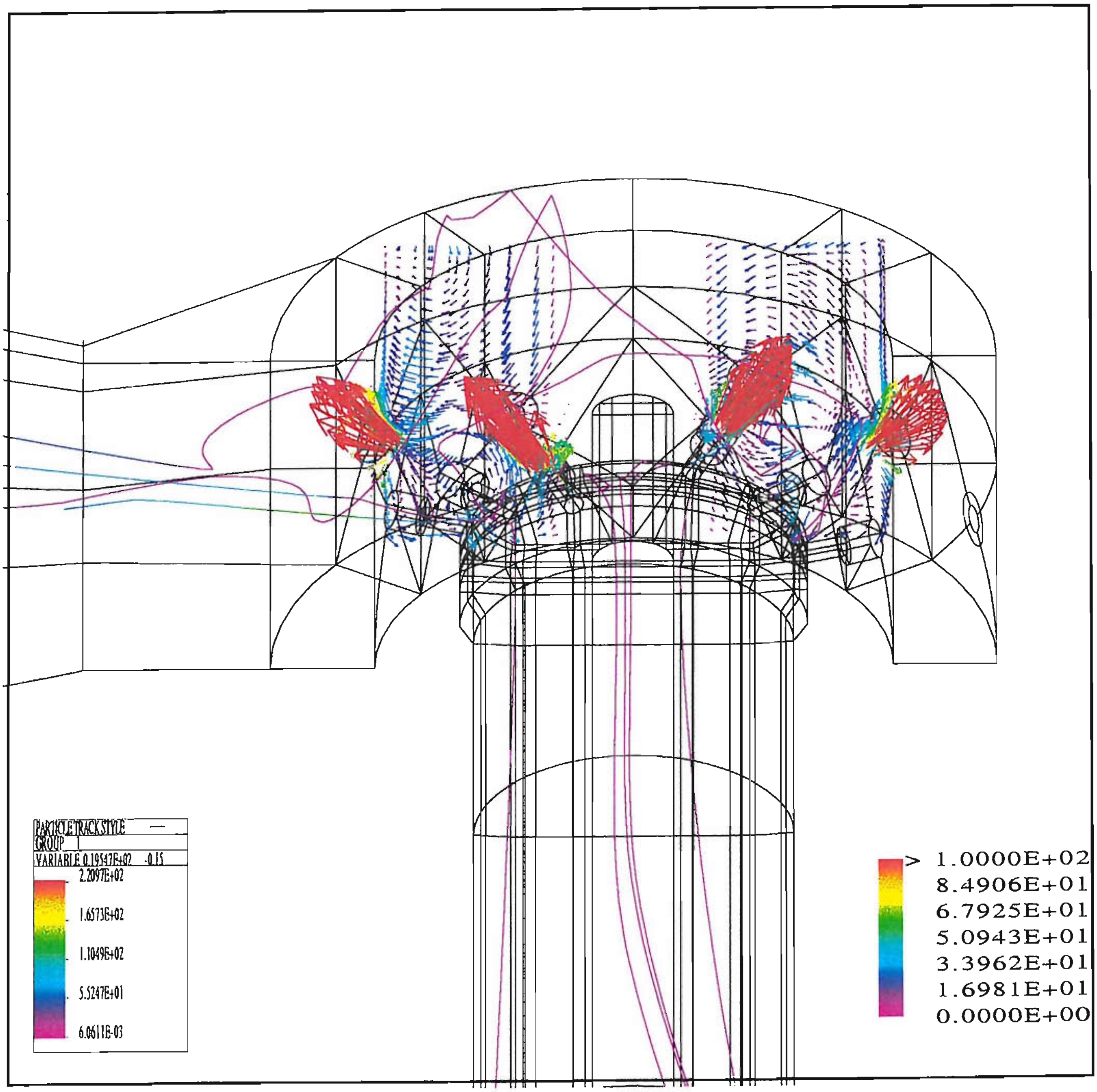

Reverse Flow Conditions Through the Cameron CC40

Fluid - **Wet Gas** (Fully Compressible)
Choke Opening ~ **28/64th**
Inlet Pressure - **480** Barg
Pressure Drop - **192** Barg
Droplet Size Range - **0.6-1.0** mm
Droplet Type - **Water** (Incompressible)
Droplet Flux Rate - **1%** by wt.

Figure 12 - Fluid Velocity Vector Slice and Droplet Trajectory & Velocity History (m/s)

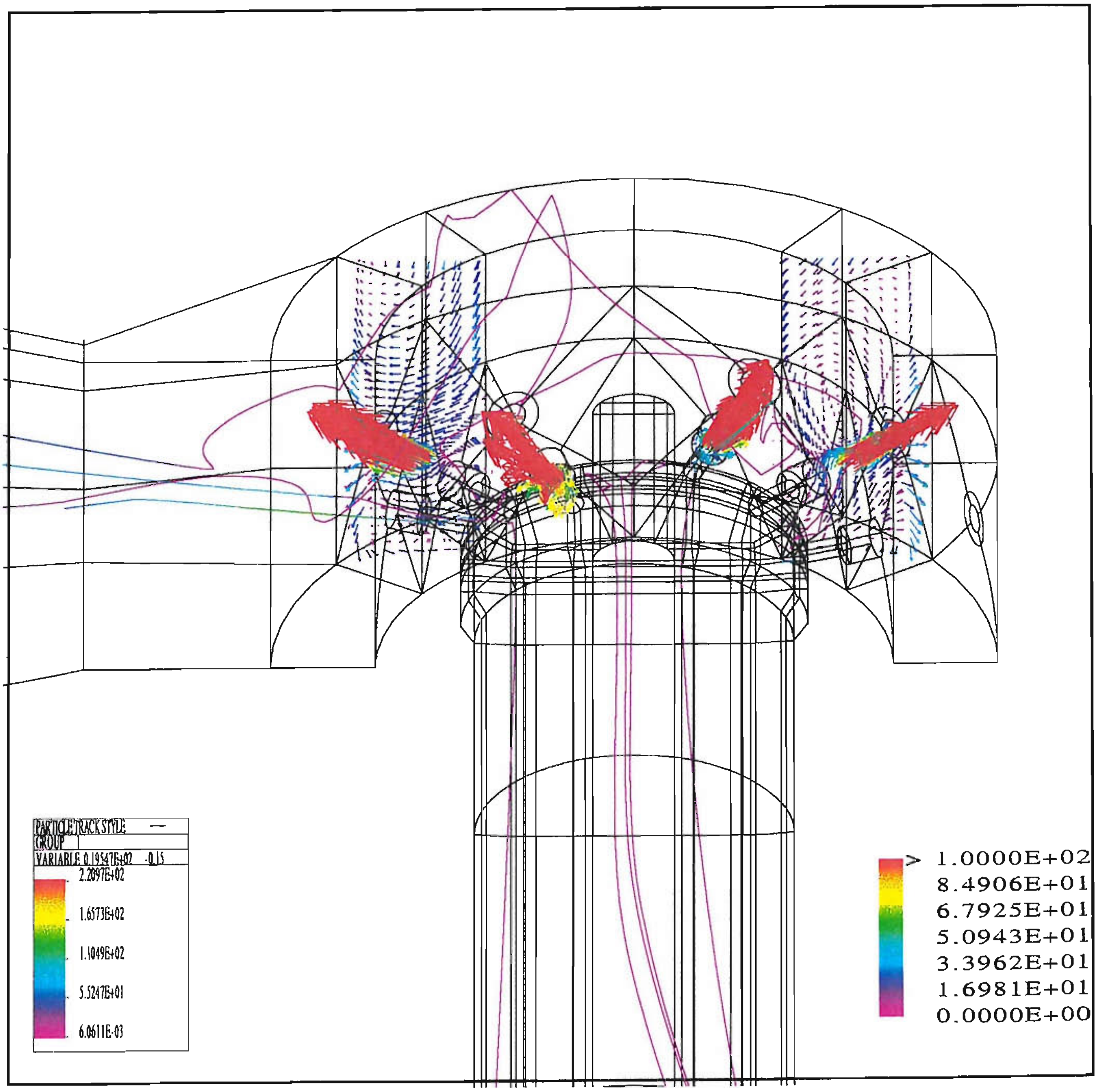

REVERSE FLOW CONDITIONS THROUGH THE CAMERON CC40

Fluid - **Wet Gas** (Fully Compressible)
Choke Opening ~ **28/64th**
Inlet Pressure - **480** Barg
Pressure Drop - **192** Barg
Droplet Size Range - **0.6-1.0** mm
Droplet Type - **Water** (Incompressible)
Droplet Flux Rate - **1%** by wt.

Figure 13 - Fluid Velocity Vector Slice and Droplet Trajectory & Velocity History (m/s)

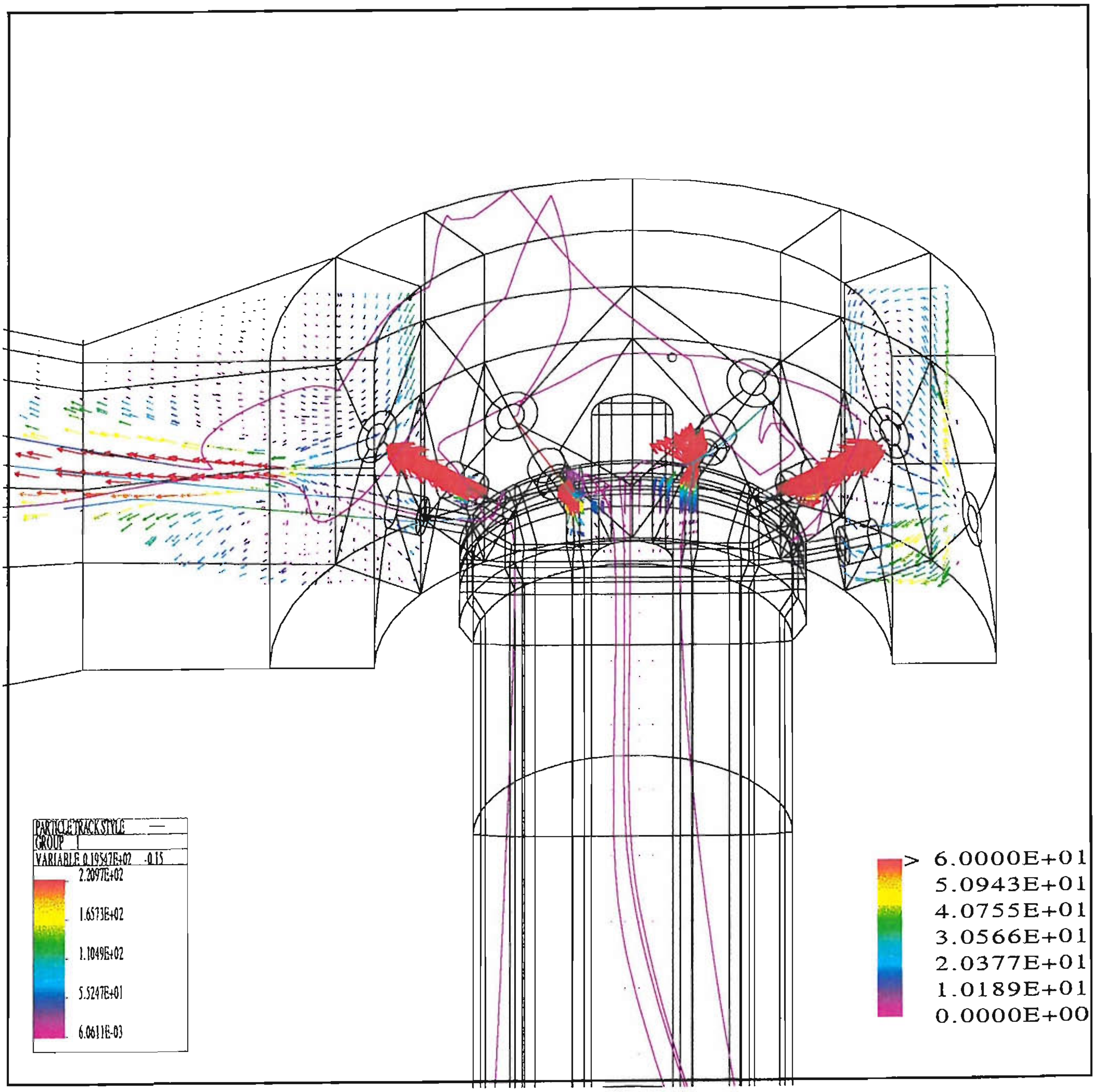

A detailed Investigation of Erosion with a 90° Bend

EROSION WITHIN A 50 MM, 1.5D RADIUS 90° BEND

Fluid - **Dry Air**
Average Gas Velocity - **32** m/s
Particle Size Range - **100-500** μm
No. of Particle Sizes - **4**
Particle Type - **Sand**
Particle Flux Rate - **112.7** kg/hr
Particle Roundness Factor - **0.5**

Figure 14 - Surface Contour Plot of 90° Bend Particle Impact Velocities (m/s)

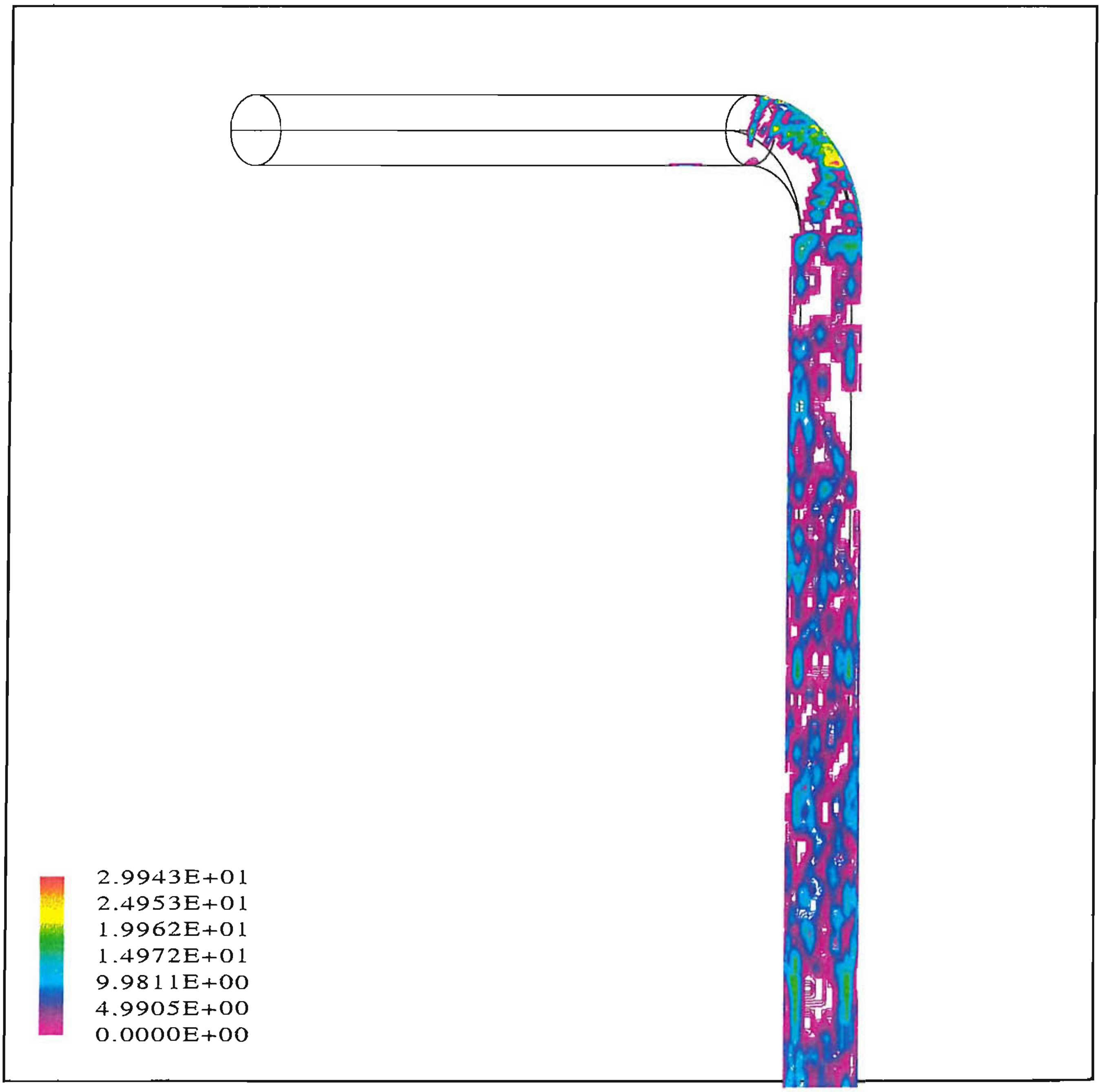

EROSION WITHIN A 50 MM, 1.5D RADIUS 90° BEND

Fluid - **Dry Air**
Average Gas Velocity - **32** m/s
Particle Size Range - **100-500** μm
No. of Particle Sizes - **4**
Particle Type - **Sand**
Particle Flux Rate - **112.7** kg/hr
Particle Roundness Factor - **0.5**

Figure 15 - Surface Contour Plot of 90° Bend Particle Impact Velocities (m/s)

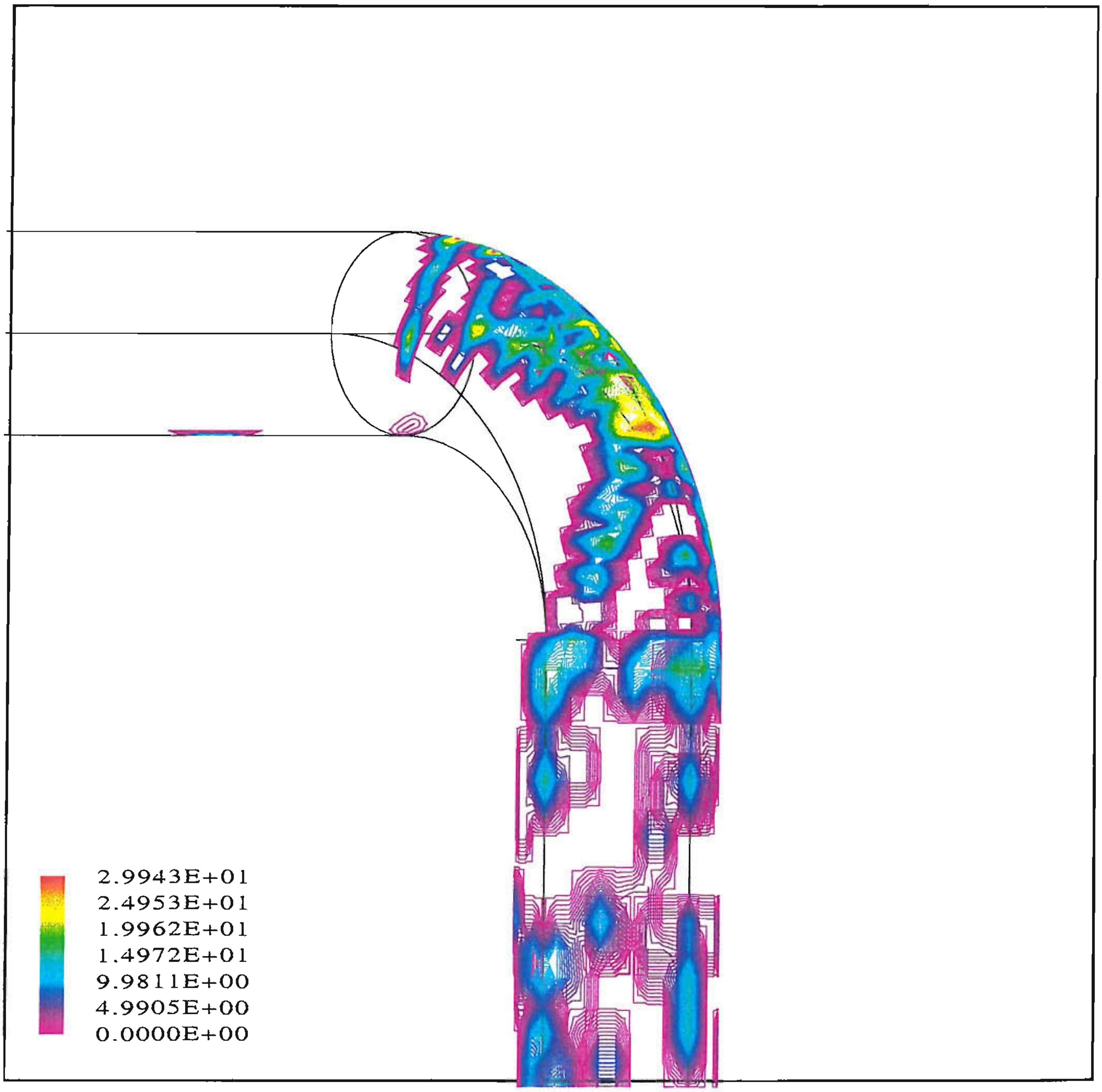

EROSION WITHIN A 50 MM, 1.5D RADIUS 90° BEND

Fluid - **Dry Air**
Average Gas Velocity - **32** m/s
Particle Size Range - **100-500** μm
No. of Particle Sizes - **4**
Particle Type - **Sand**
Particle Flux Rate - **112.7** kg/hr
Particle Roundness Factor - **0.5**

Figure 16 - Surface Contour Plot of 90° Bend Particle Impact Angle (Deg)

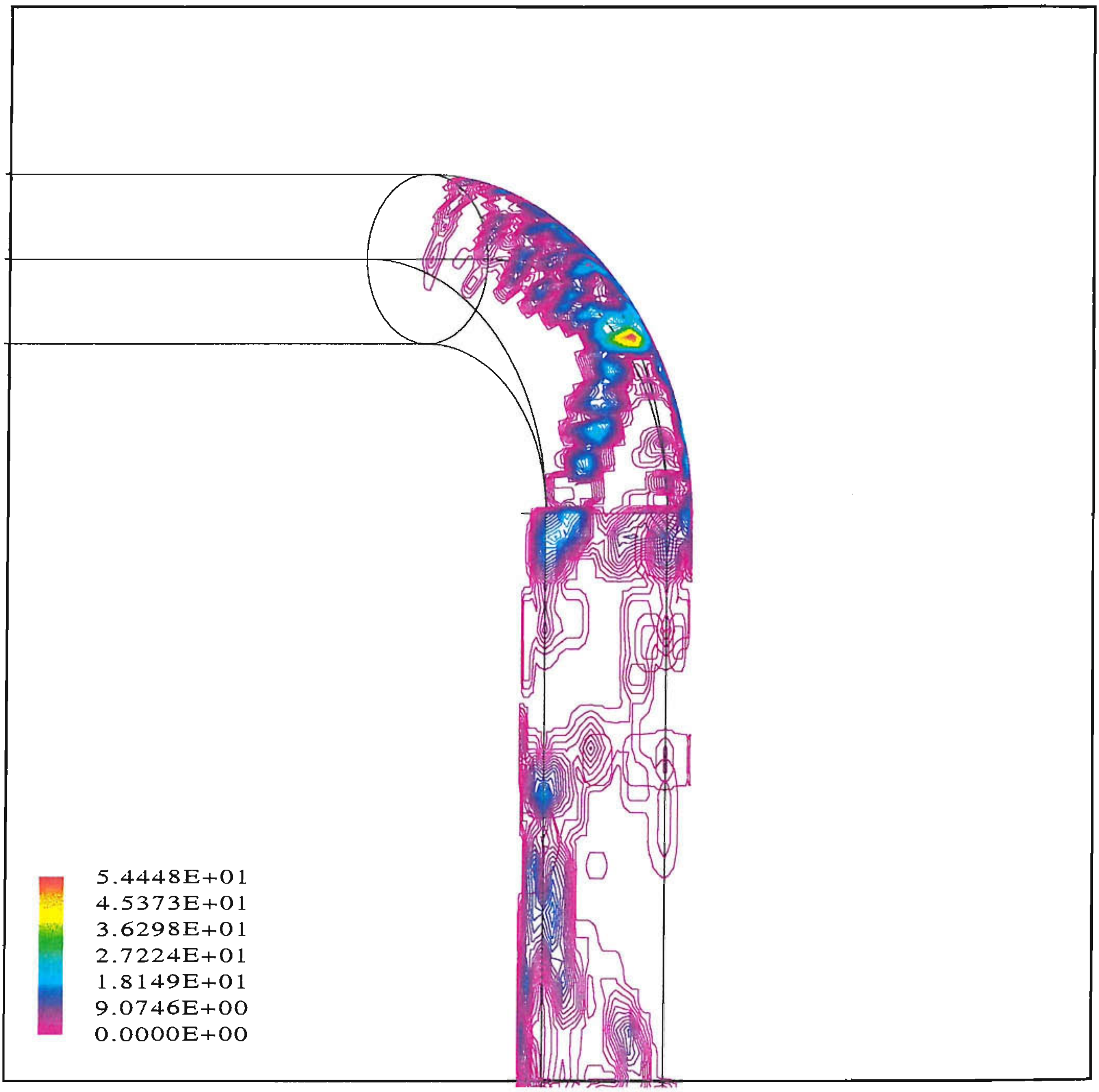

EROSION WITHIN A 50 MM, 1.5D RADIUS 90° BEND

Fluid - **Dry Air**
Average Gas Velocity - **32** m/s
Particle Size Range - **100-500** μm
No. of Particle Sizes - **4**
Particle Type - **Sand**
Particle Flux Rate - **112.7** kg/hr
Particle Roundness Factor - **0.5**

Figure 17 - Surface Contour Plot of 90° Bend Particle Erosion Rate (mm/hr)

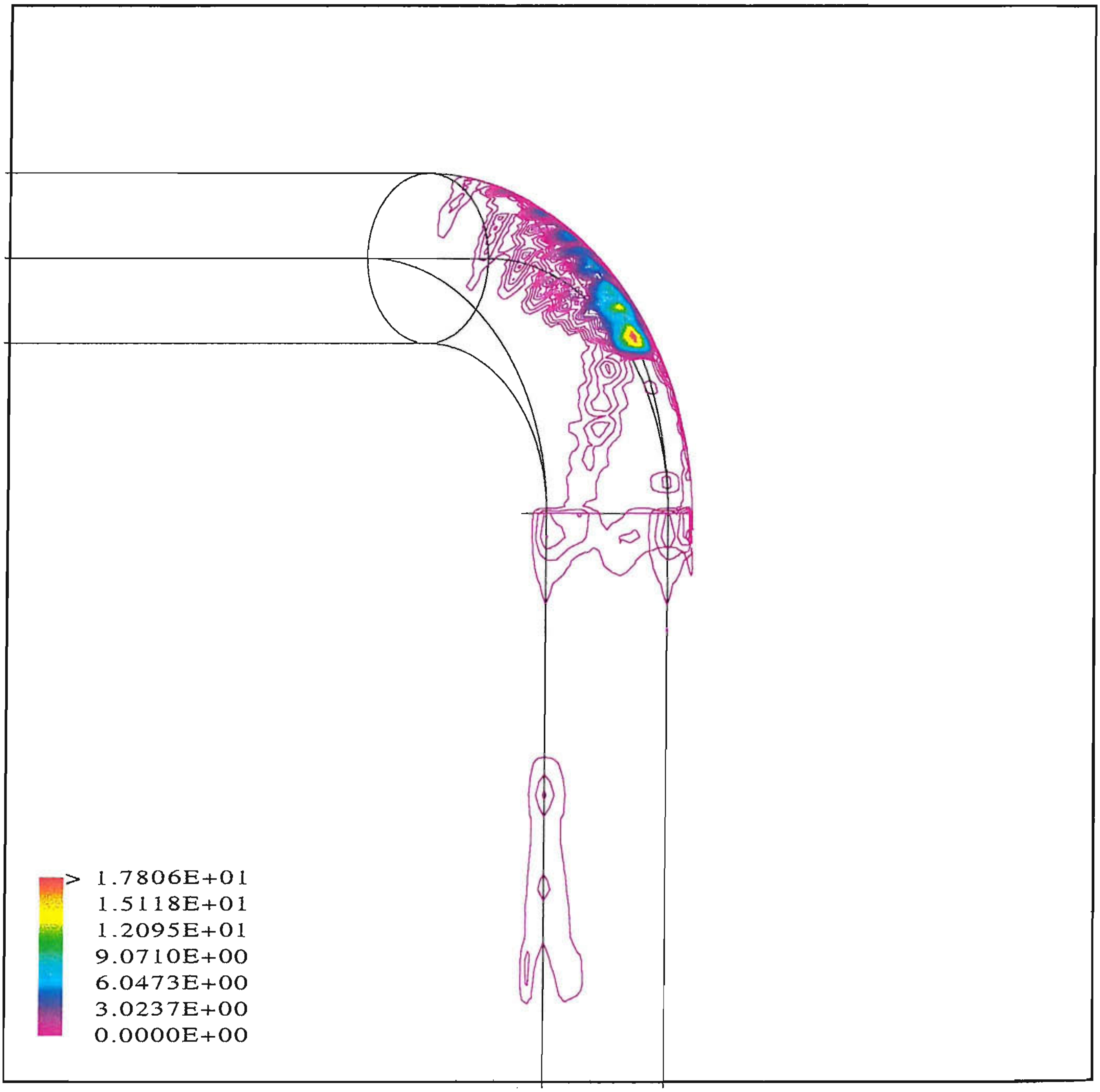

EROSION WITHIN A 50 MM, 1.5D RADIUS 90° BEND

Fluid - **Dry Air**
Average Gas Velocity - **32** m/s
Particle Size Range - **100-500** μm
No. of Particle Sizes - **4**
Particle Type - **Sand**
Particle Flux Rate - **112.7** kg/hr
Particle Roundness Factor - **0.5**

Figure 18 - Surface Contour Plot of 90° Bend Particle Erosion Rate (mm/hr)

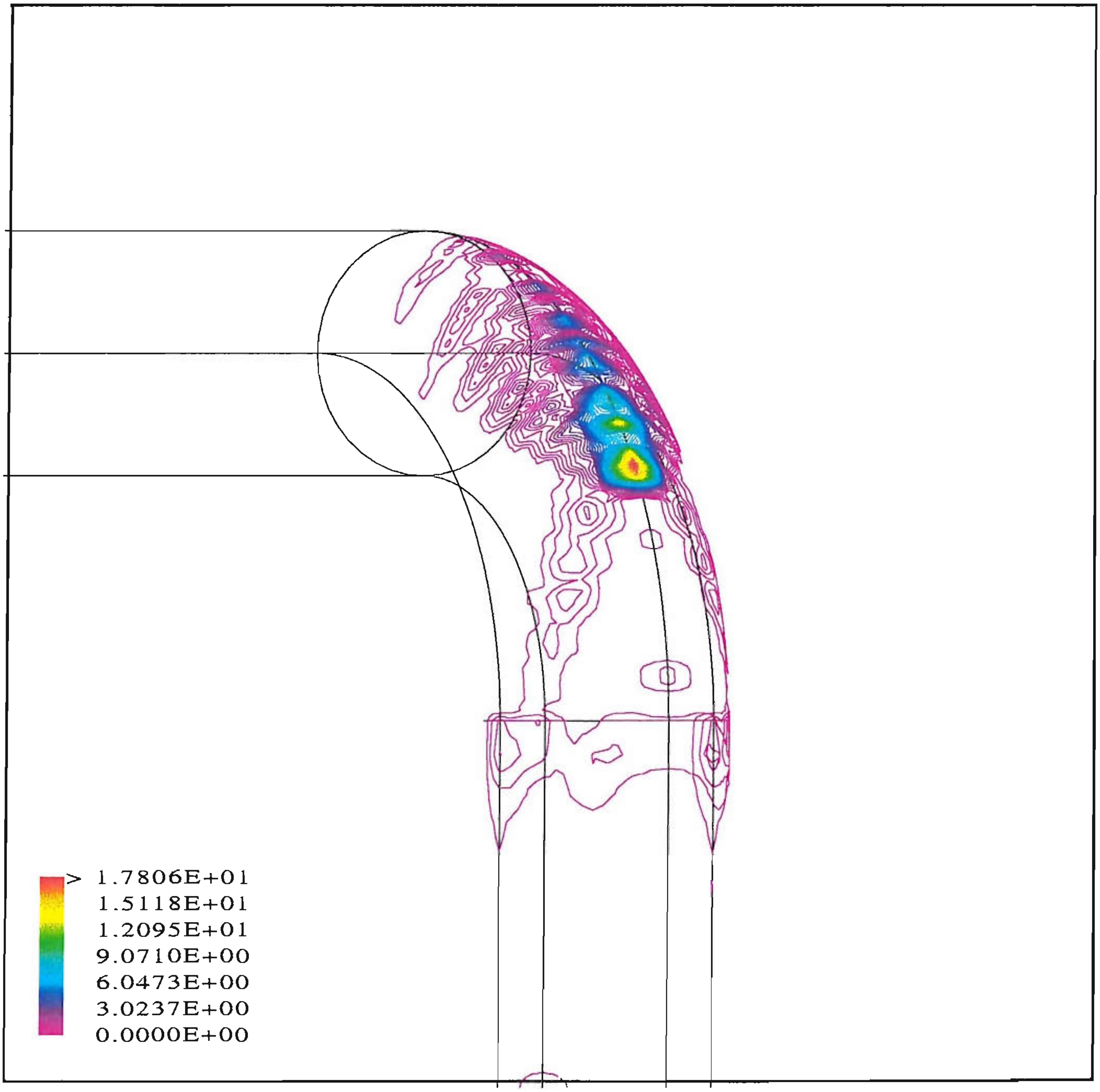

Investigation of Erosion within a Needle and Seat Choke

FLOW FIELD OF A CONVENTIONAL NEEDLE AND SEAT CHOKE (K-EPSILON MODEL)

Fluid - **Dry Air**
Inlet Diameter - **75** mm
Throat Diameter - **25** mm
Taper Angle of Needle - **45°**
Choke Opening - **25** % (Linear)
Pressure Drop - **68** Bar
Mass Flow Rate (air) - **178** kg/hr

Appendix Figure 19 - *k*-Epsilon Model Velocity Contour Plot of Needle & Seat Choke (m/s)

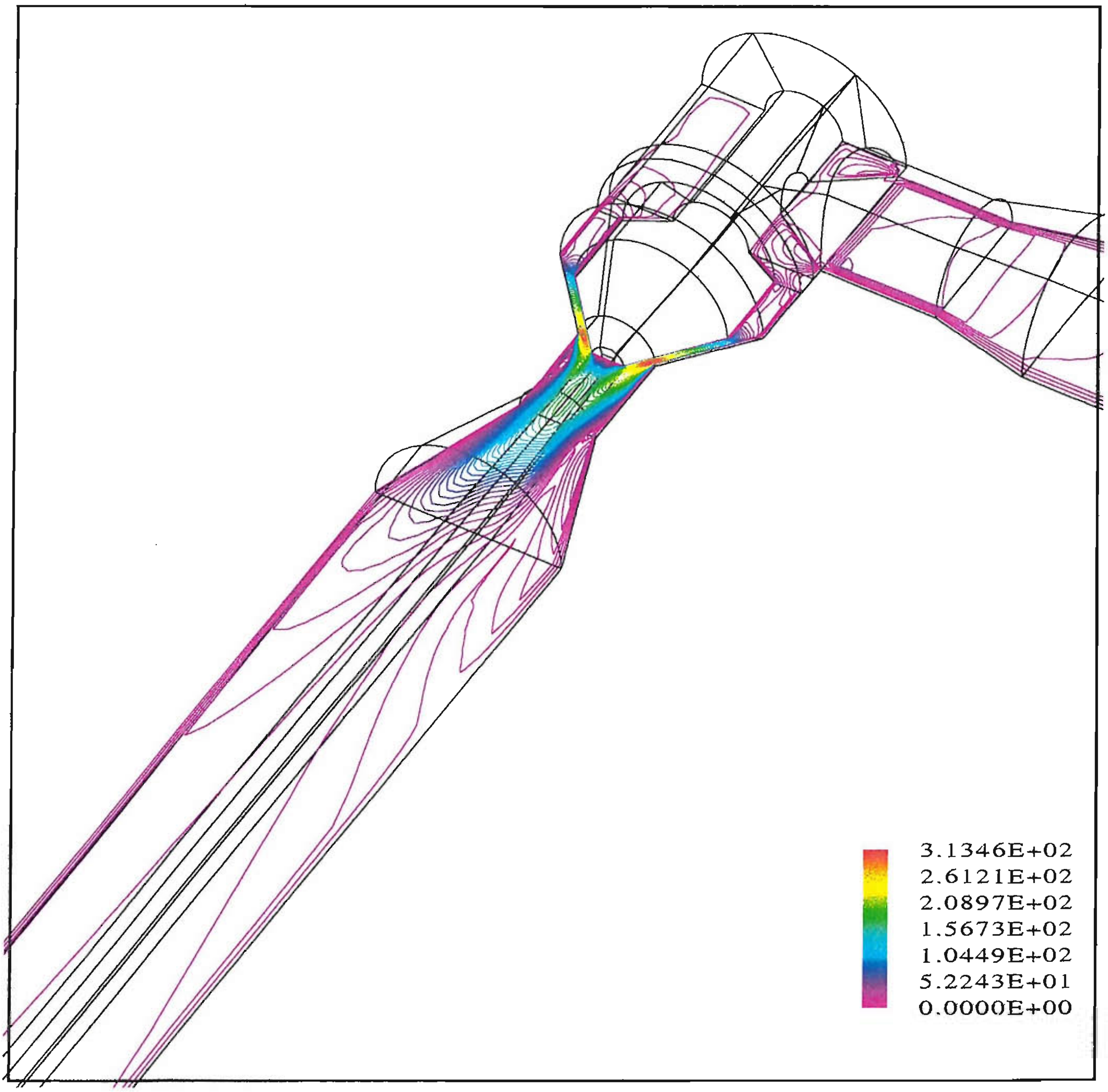

Flow Field of a Conventional Needle and Seat Choke (K-Epsilon Model)

Fluid - **Dry Air**
Inlet Diameter - **75** mm
Throat Diameter - **25** mm
Taper Angle of Needle - **45°**
Choke Opening - **25** % (Linear)
Pressure Drop - **68** Bar
Mass Flow Rate (air) - **178** kg/hr

Appendix Figure 20 - *k*-Epsilon Model Velocity Contour Plot of Needle & Seat Choke (m/s)

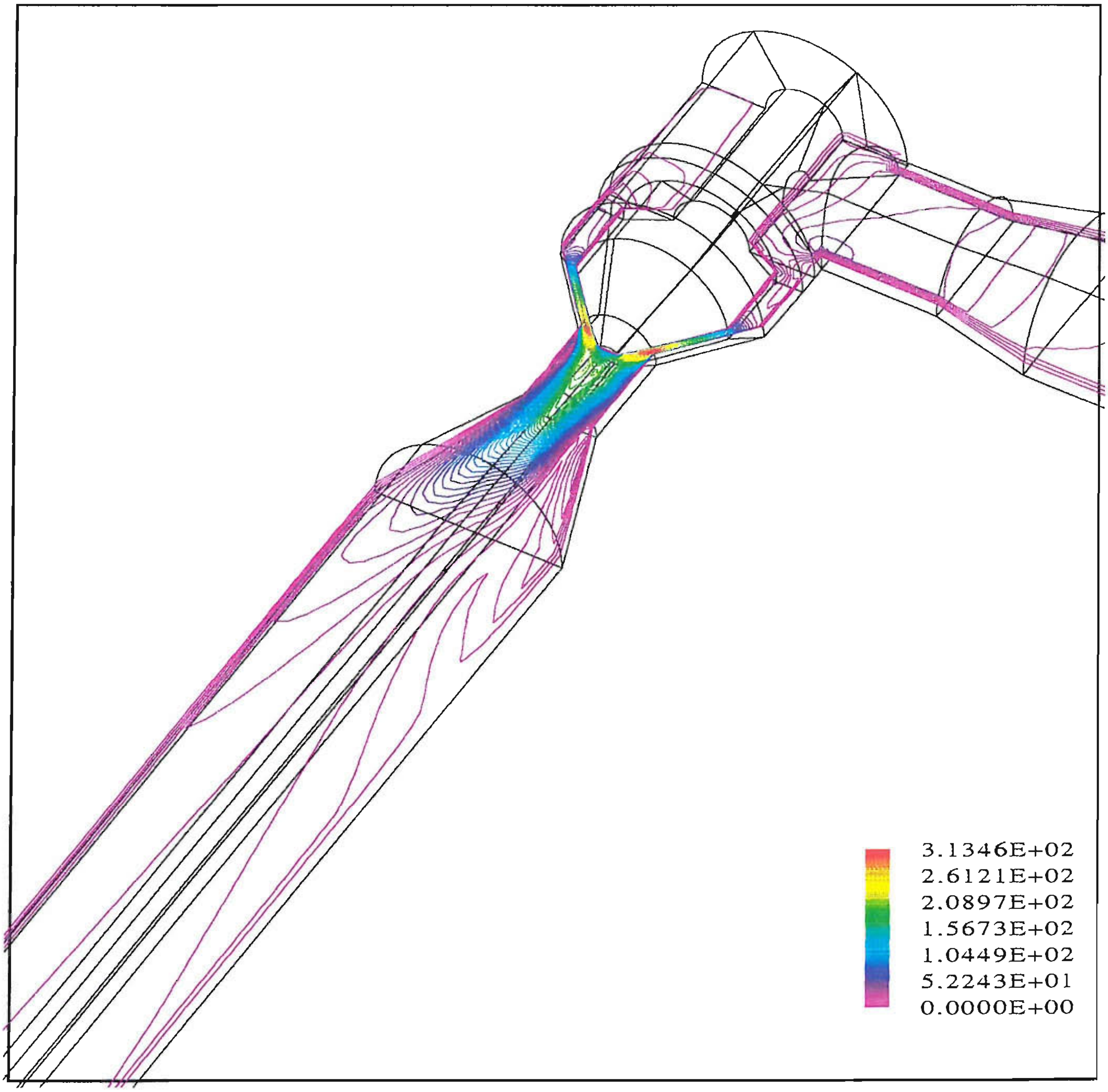

FLOW FIELD OF A CONVENTIONAL NEEDLE AND SEAT CHOKE (K-EPSILON MODEL)

Fluid - **Dry Air**
Inlet Diameter - **75** mm
Throat Diameter - **25** mm
Taper Angle of Needle - **45°**
Choke Opening - **25** % (Linear)
Pressure Drop - **68** Bar
Mass Flow Rate (air) - **178** kg/hr

Appendix Figure 21 - *k*-Epsilon Model Velocity Contour Plot of Needle & Seat Choke (m/s)

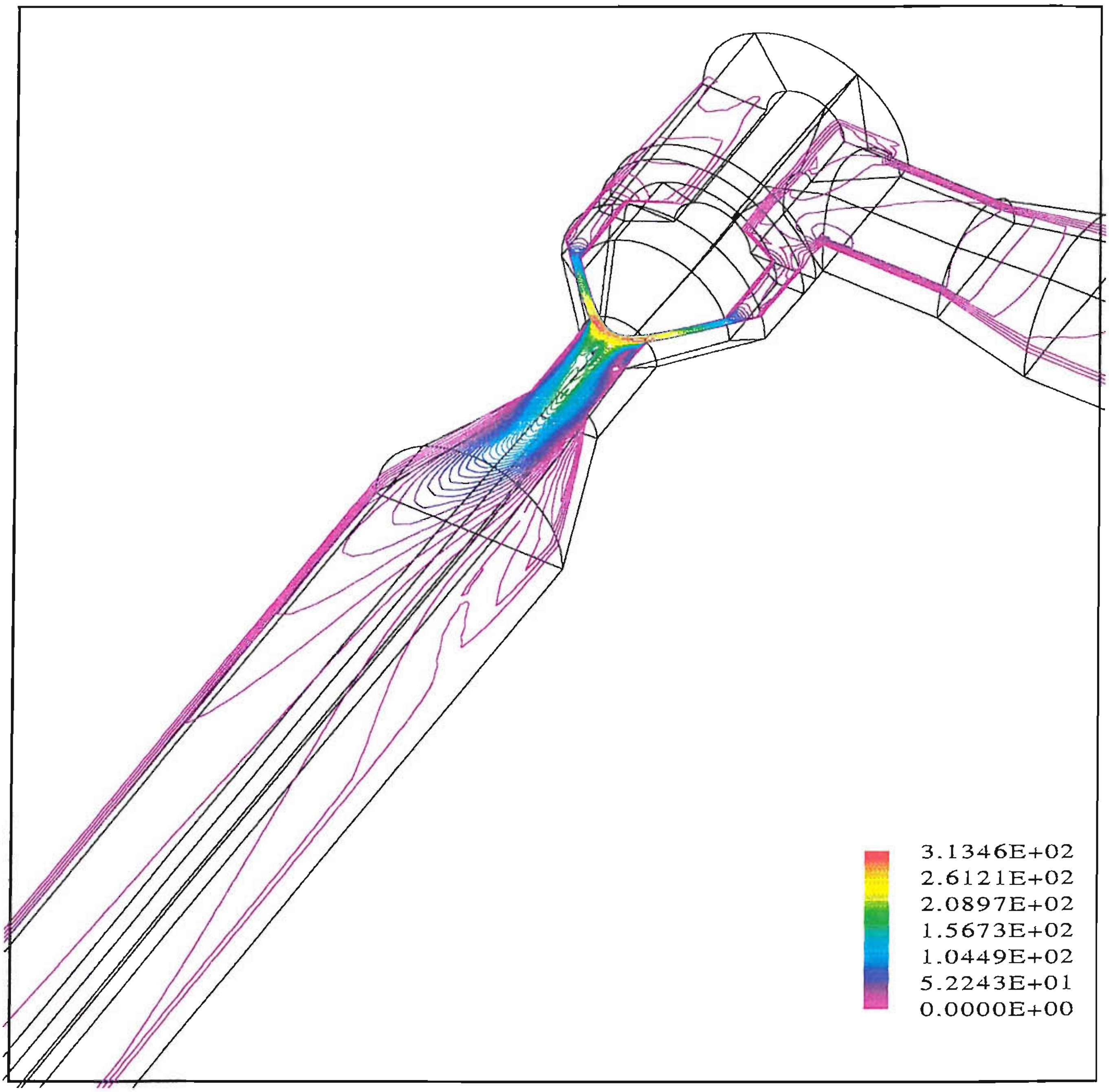

FLOW FIELD OF A CONVENTIONAL NEEDLE AND SEAT CHOKE (K-EPSILON MODEL)

Fluid - **Dry Air**
Inlet Diameter - **75** mm
Throat Diameter - **25** mm
Taper Angle of Needle - **45°**
Choke Opening - **25** % (Linear)
Pressure Drop - **68** Bar
Mass Flow Rate (air) - **178** kg/hr

Appendix Figure 22 - *k*-Epsilon Model Velocity Contour Plot of Needle & Seat Choke (m/s)

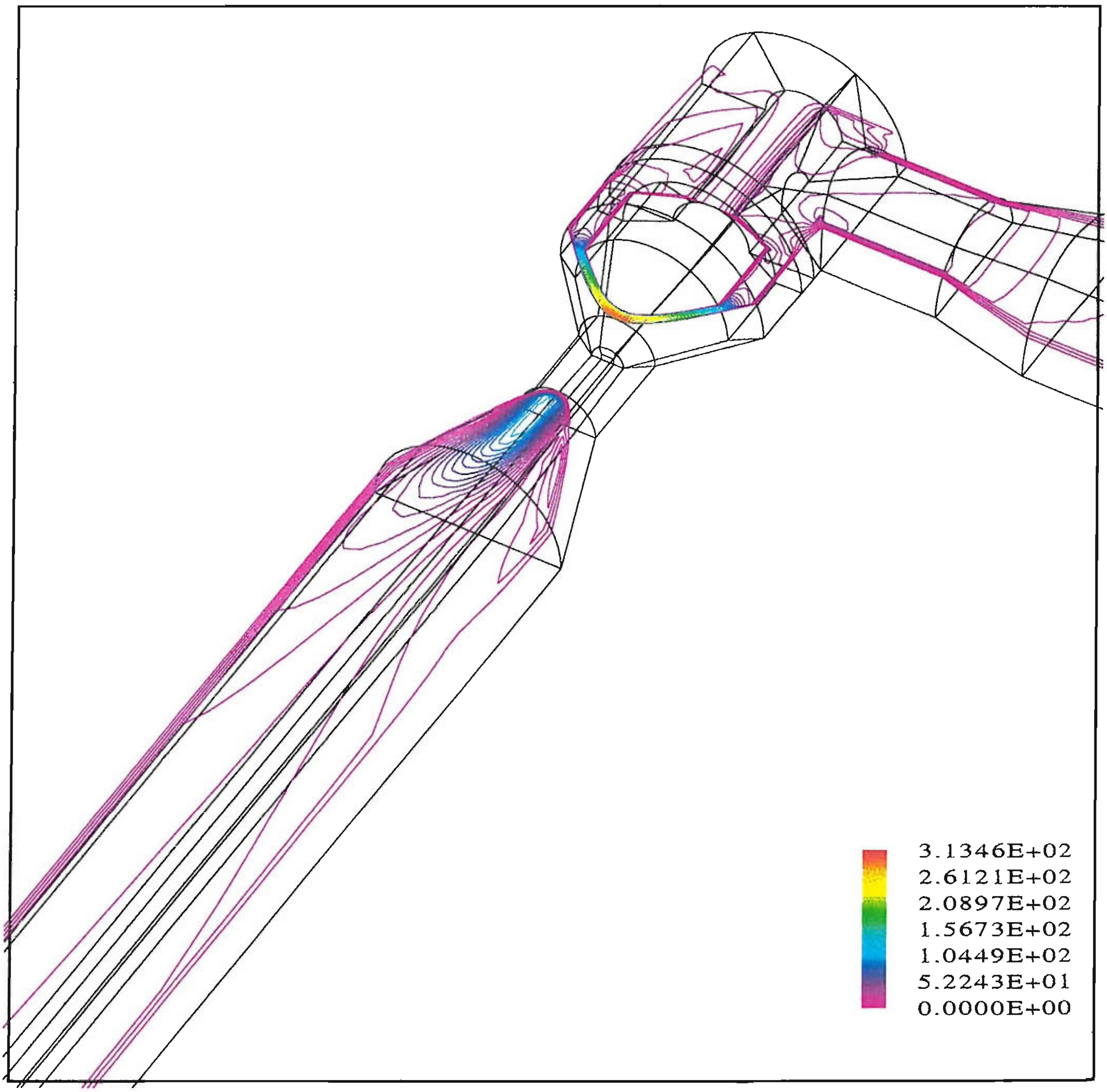

FLOW FIELD OF A CONVENTIONAL NEEDLE AND SEAT CHOKE (K-EPSILON MODEL)

Fluid - **Dry Air**
Inlet Diameter - **75** mm
Throat Diameter - **25** mm
Taper Angle of Needle - **45°**
Choke Opening - **25** % (Linear)
Pressure Drop - **68** Bar
Mass Flow Rate (air) - **178** kg/hr

Appendix Figure 23 - *k*-Epsilon Model Turbulent Kinetic Energy Contour Plot of Needle & Seat Choke

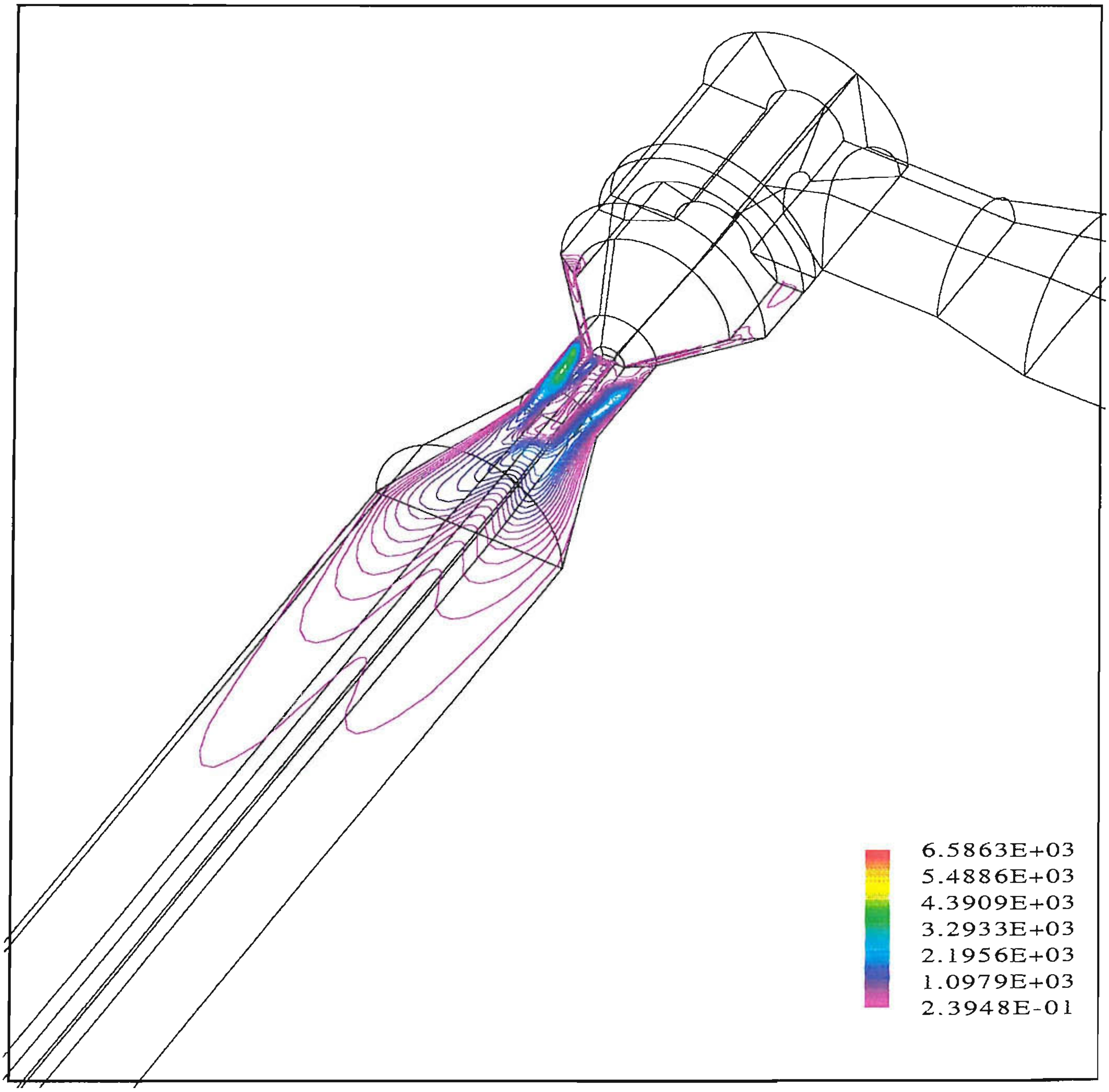

EROSIONAL TRENDS OF A CONVENTIONAL NEEDLE AND SEAT CHOKE (K-EPSILON MODEL)

Test Number - **1**
Particle Type - **Sand**
Particle Roundness Factor - **0.5**
Particle Flux Rate - **1** % by wt.
Number of Particle Sizes - **6**
Particle Size Range - **50-100** μm
Turbulent Dispersion - **Yes**

Appendix Figure 24 - *k*-Epsilon Model Surface Contour Plot of Needle & Seat Choke Particle Impact Velocities (m/s)

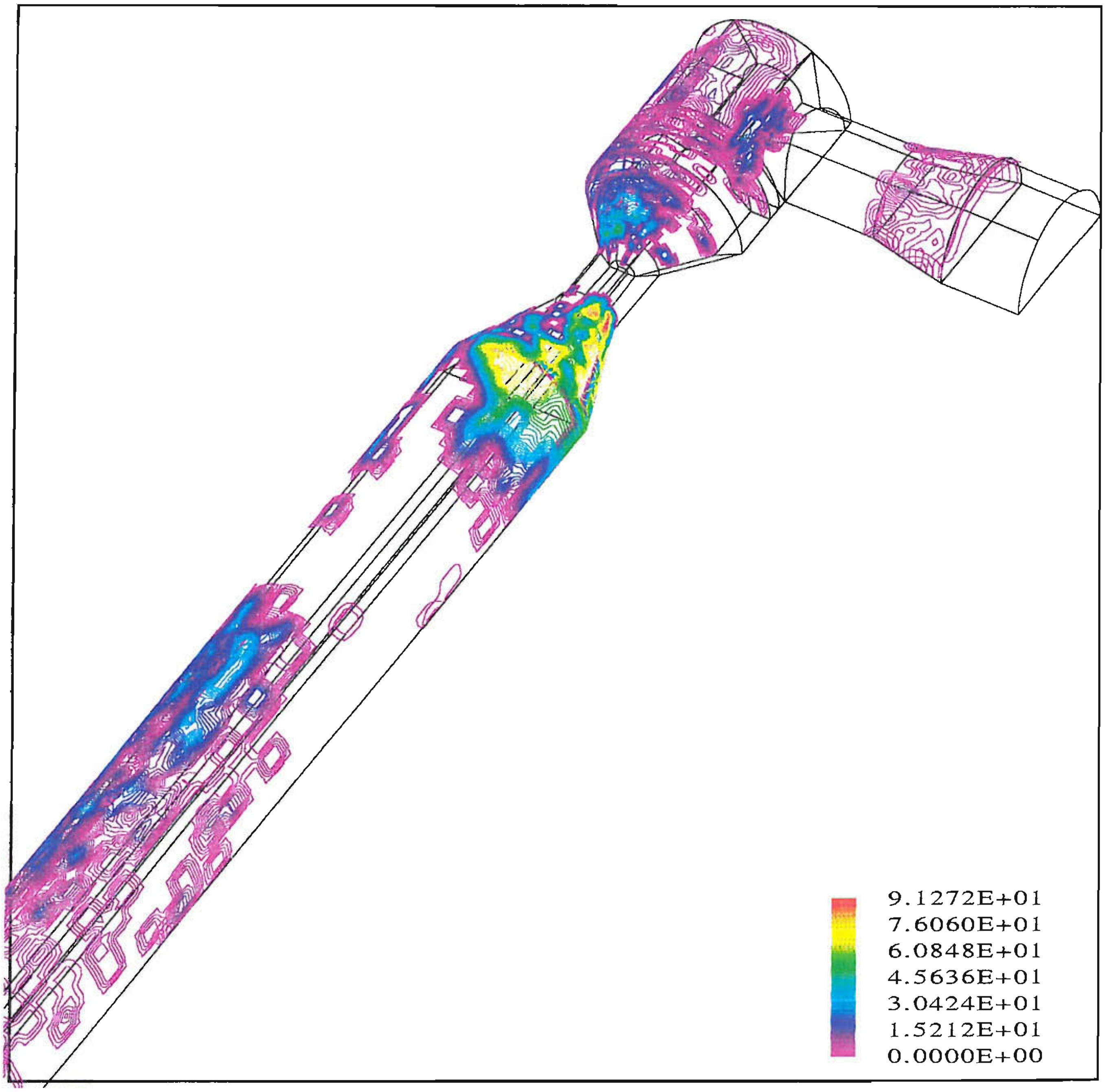

EROSIONAL TRENDS OF A CONVENTIONAL NEEDLE AND SEAT CHOKE (K-EPSILON MODEL)

Test Number - **1**
Particle Type - **Sand**
Particle Roundness Factor - **0.5**
Particle Flux Rate - **1** % by wt.
Number of Particle Sizes - **6**
Particle Size Range - **50-100** μm
Turbulent Dispersion - **Yes**

Appendix Figure 25 - *k*-Epsilon Model Surface Contour Plot of Needle & Seat Choke Particle Impact Angles (Deg)

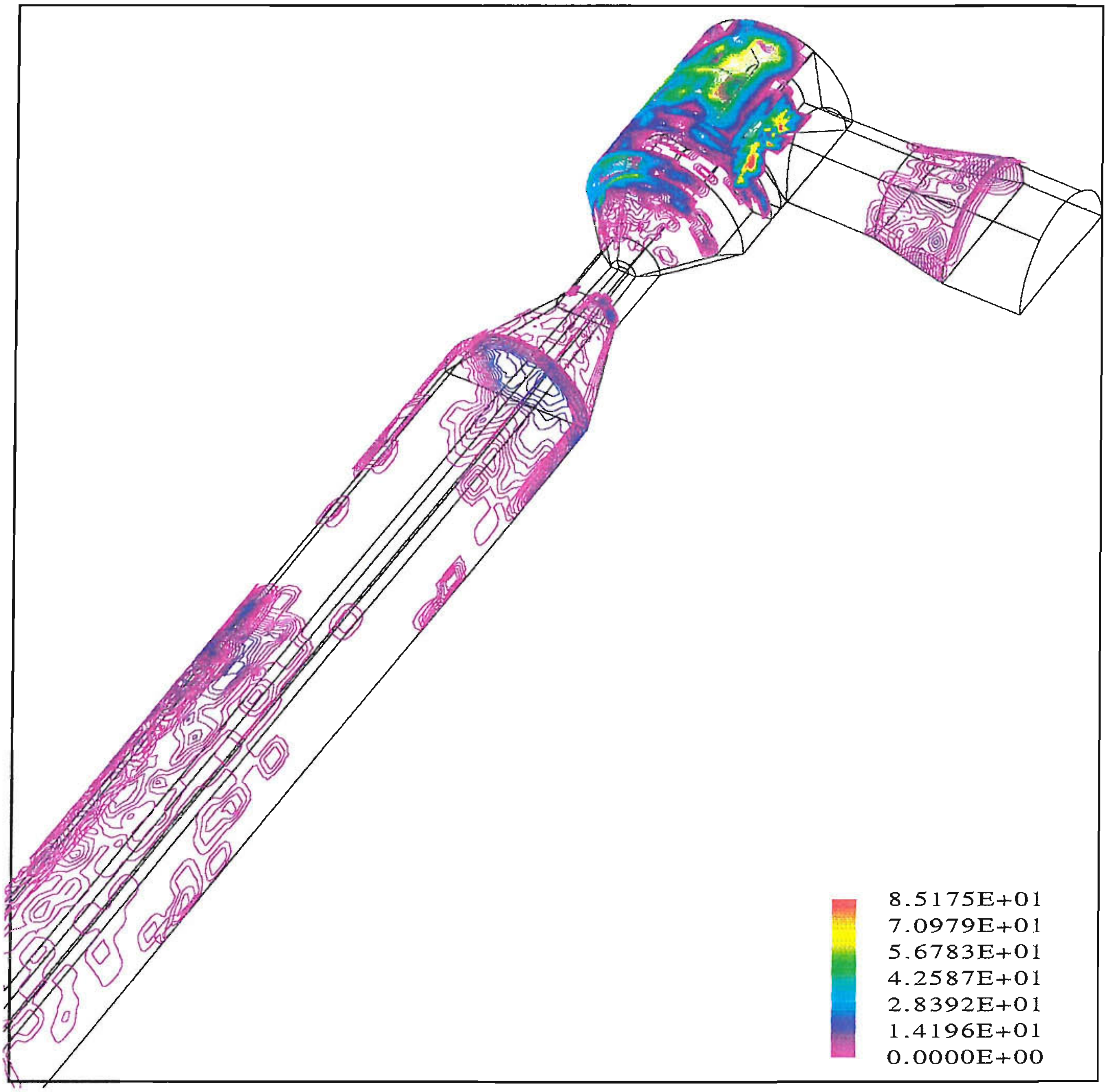

EROSIONAL TRENDS OF A CONVENTIONAL NEEDLE AND SEAT CHOKE (K-EPSILON MODEL)

Test Number - **1**
Particle Type - **Sand**
Particle Roundness Factor - **0.5**
Particle Flux Rate - **1** % by wt.
Number of Particle Sizes - **6**
Particle Size Range - **50-100** μm
Turbulent Dispersion - **Yes**

Appendix Figure 26 - *k*-Epsilon Model Surface Contour Plot of Needle & Seat Choke Particle Impact Kinetic Energy (J)

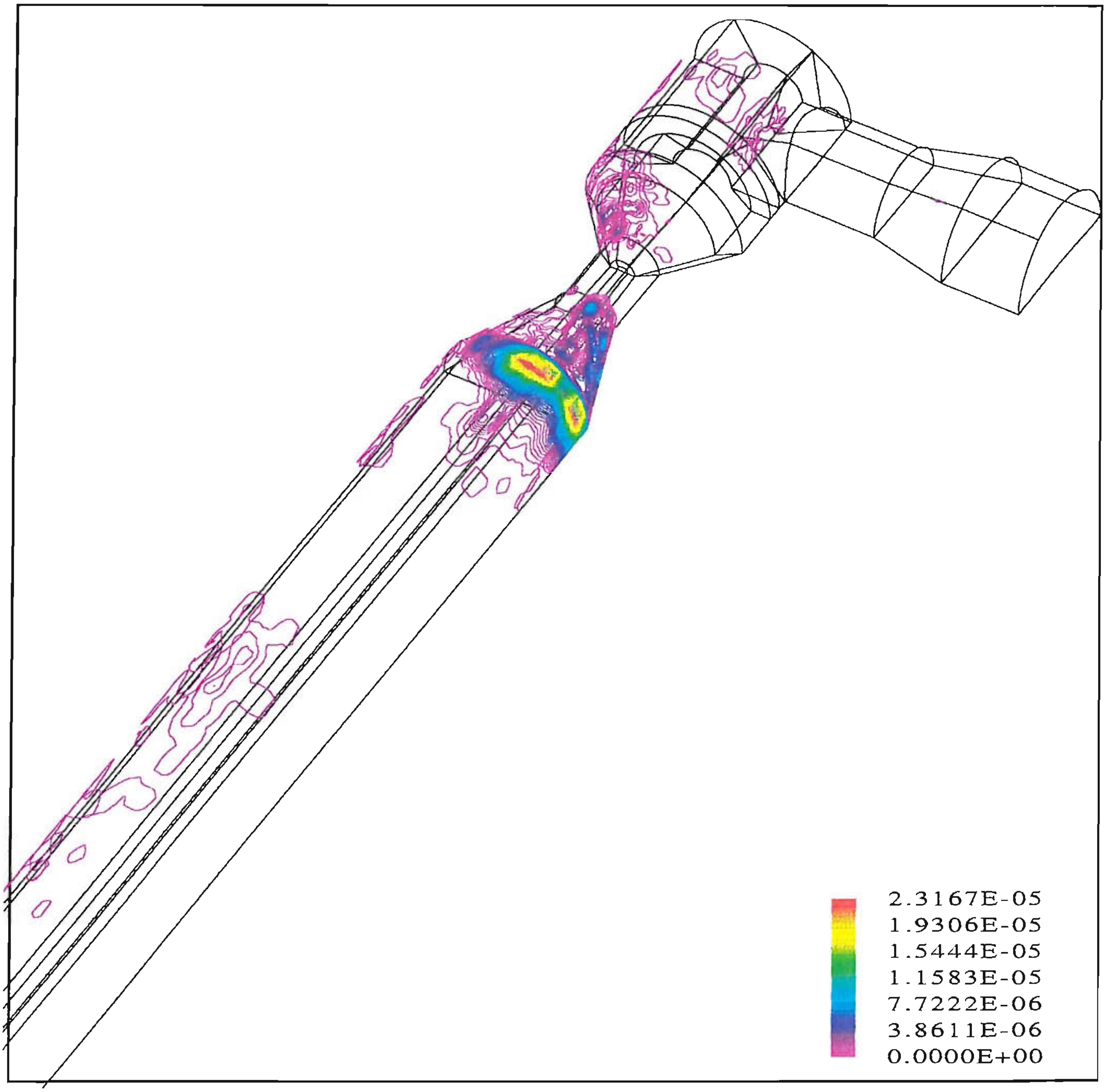

EROSIONAL TRENDS OF A CONVENTIONAL NEEDLE AND SEAT CHOKE (K-EPSILON MODEL)

Test Number - **1**
Particle Type - **Sand**
Particle Roundness Factor - **0.5**
Particle Flux Rate - **1** % by wt.
Number of Particle Sizes - **6**
Particle Size Range - **50-100** μm
Turbulent Dispersion - **Yes**

Appendix Figure 27 - *k*-Epsilon Model Surface Contour Plot of Needle & Seat Choke Particle Erosion Rates (mm^3/hr)

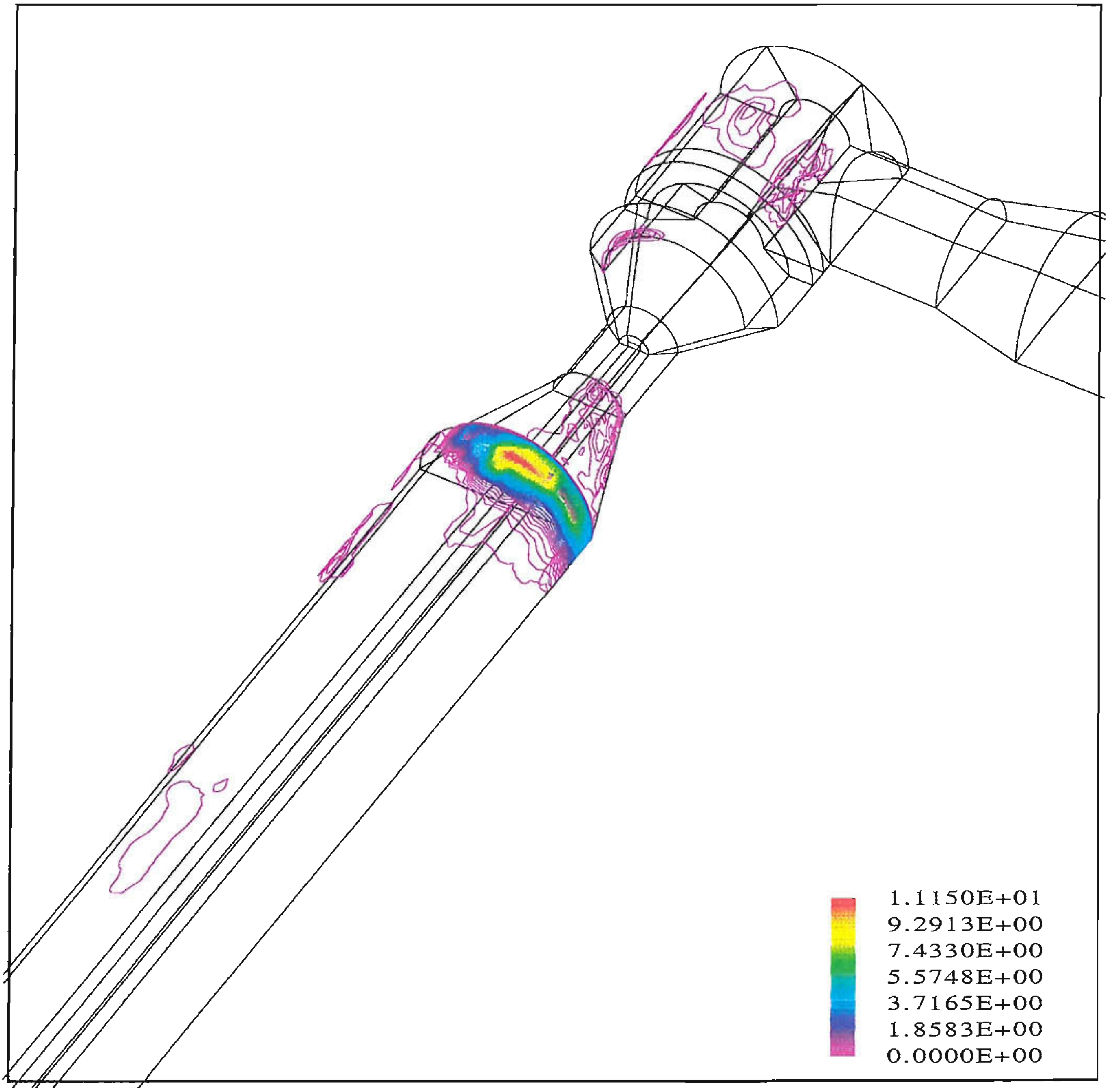

EROSIONAL TRENDS OF A CONVENTIONAL NEEDLE AND SEAT CHOKE (K-EPSILON MODEL)

Test Number - **1**
Particle Type - **Sand**
Particle Roundness Factor - **0.5**
Particle Flux Rate - **1** % by wt.
Number of Particle Sizes - **6**
Particle Size Range - **50-100** μm
Turbulent Dispersion - **Yes**

Appendix Figure 28 - ***k*-Epsilon Model Surface Contour Plot of Needle & Seat Choke Particle Erosion Rates (mm³/hr)**

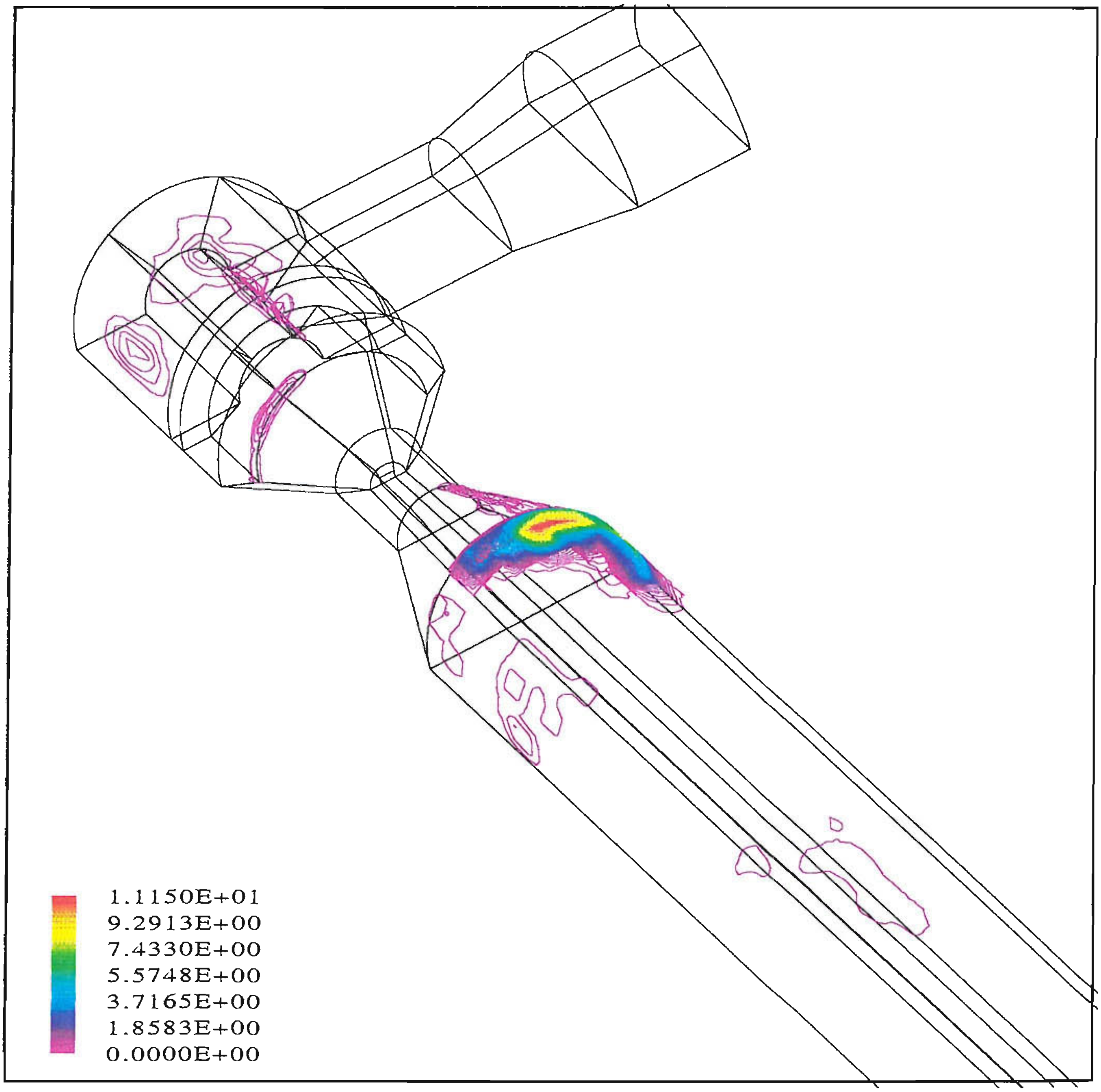

EROSIONAL TRENDS OF A CONVENTIONAL NEEDLE AND SEAT CHOKE (K-EPSILON MODEL)

Test Number - **2**
Particle Type - **Sand**
Particle Roundness Factor - **0.5**
Particle Flux Rate - **1** % by wt.
Number of Particle Sizes - **6**
Particle Size Range - **50-100** μm
Turbulent Dispersion - **No**

Appendix Figure 29 - *k*-Epsilon Model Surface Contour Plot of Needle & Seat Choke Particle Impact Velocities (m/s)

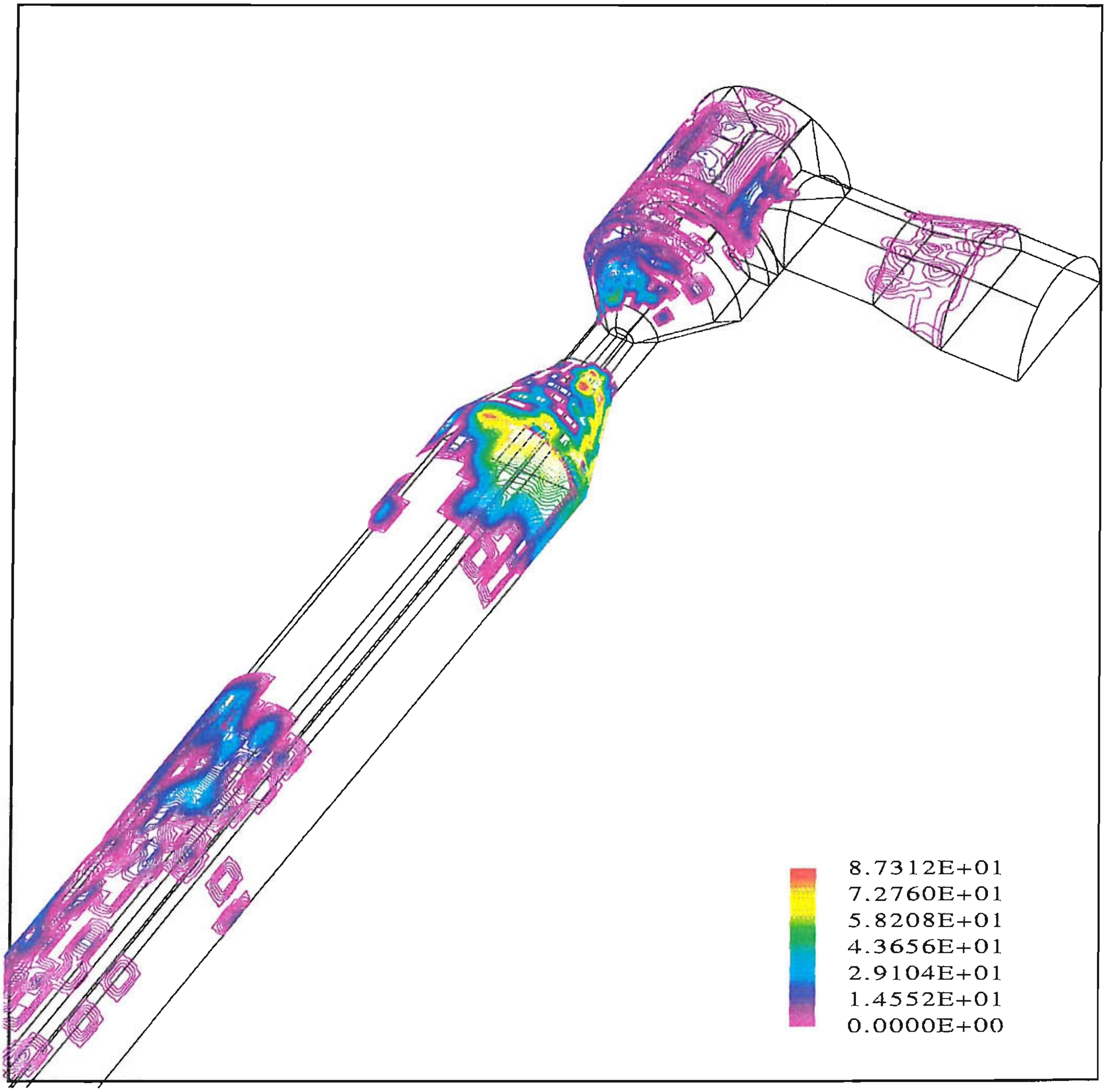

EROSIONAL TRENDS OF A CONVENTIONAL NEEDLE AND SEAT CHOKE (K-EPSILON MODEL)

Test Number - **2**
Particle Type - **Sand**
Particle Roundness Factor - **0.5**
Particle Flux Rate - **1** % by wt.
Number of Particle Sizes - **6**
Particle Size Range - **50-100** μm
Turbulent Dispersion - **No**

Appendix Figure 30 - *k*-Epsilon Model Surface Contour Plot of Needle & Seat Choke Particle Impact Angles (Deg)

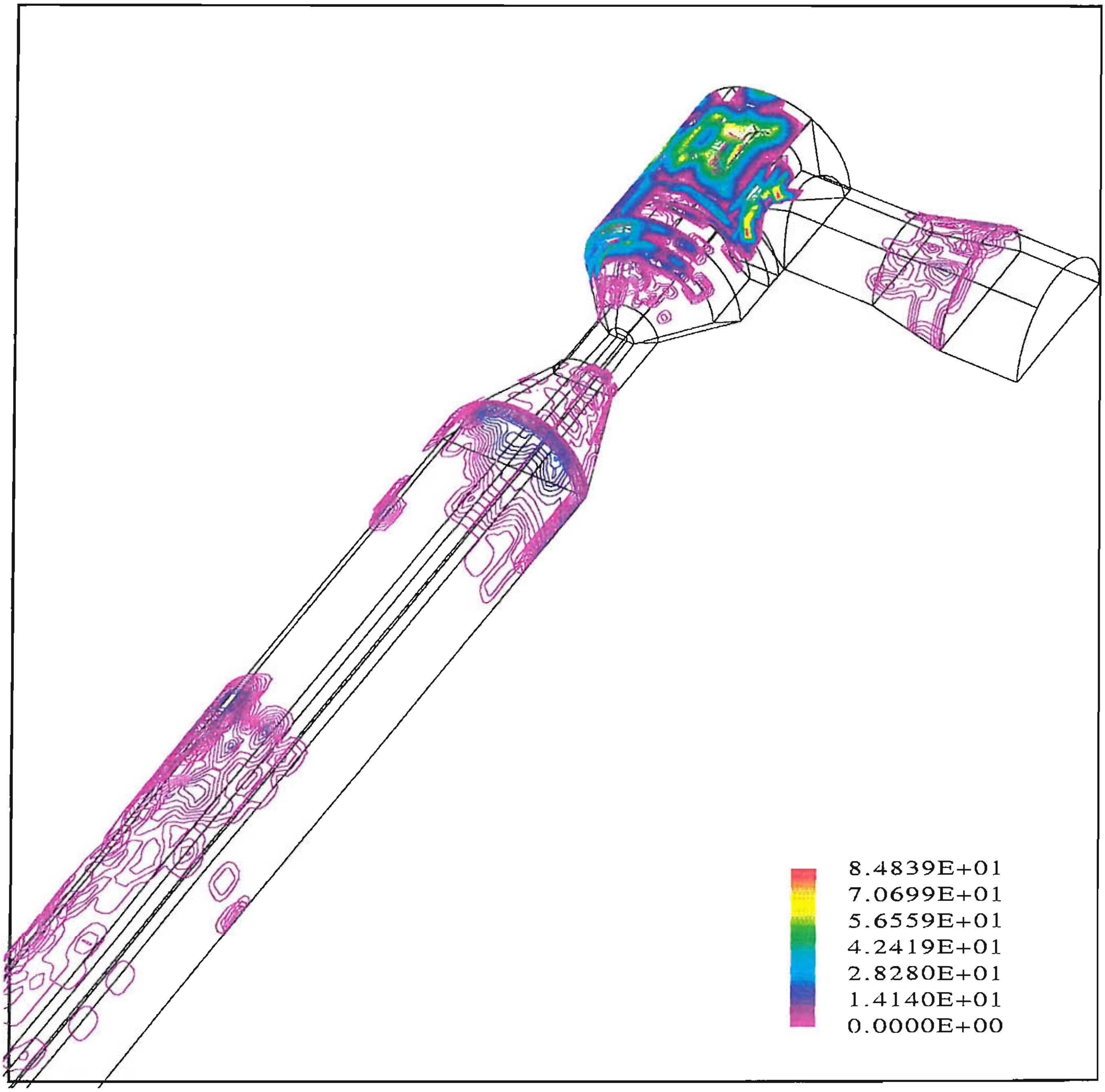

EROSIONAL TRENDS OF A CONVENTIONAL NEEDLE AND SEAT CHOKE (K-EPSILON MODEL)

Test Number - **2**
Particle Type - **Sand**
Particle Roundness Factor - **0.5**
Particle Flux Rate - **1** % by wt.
Number of Particle Sizes - **6**
Particle Size Range - **50-100** µm
Turbulent Dispersion - **No**

Appendix Figure 31 - *k*-Epsilon Model Surface Contour Plot of Needle & Seat Choke Particle Impact Kinetic Energy (J)

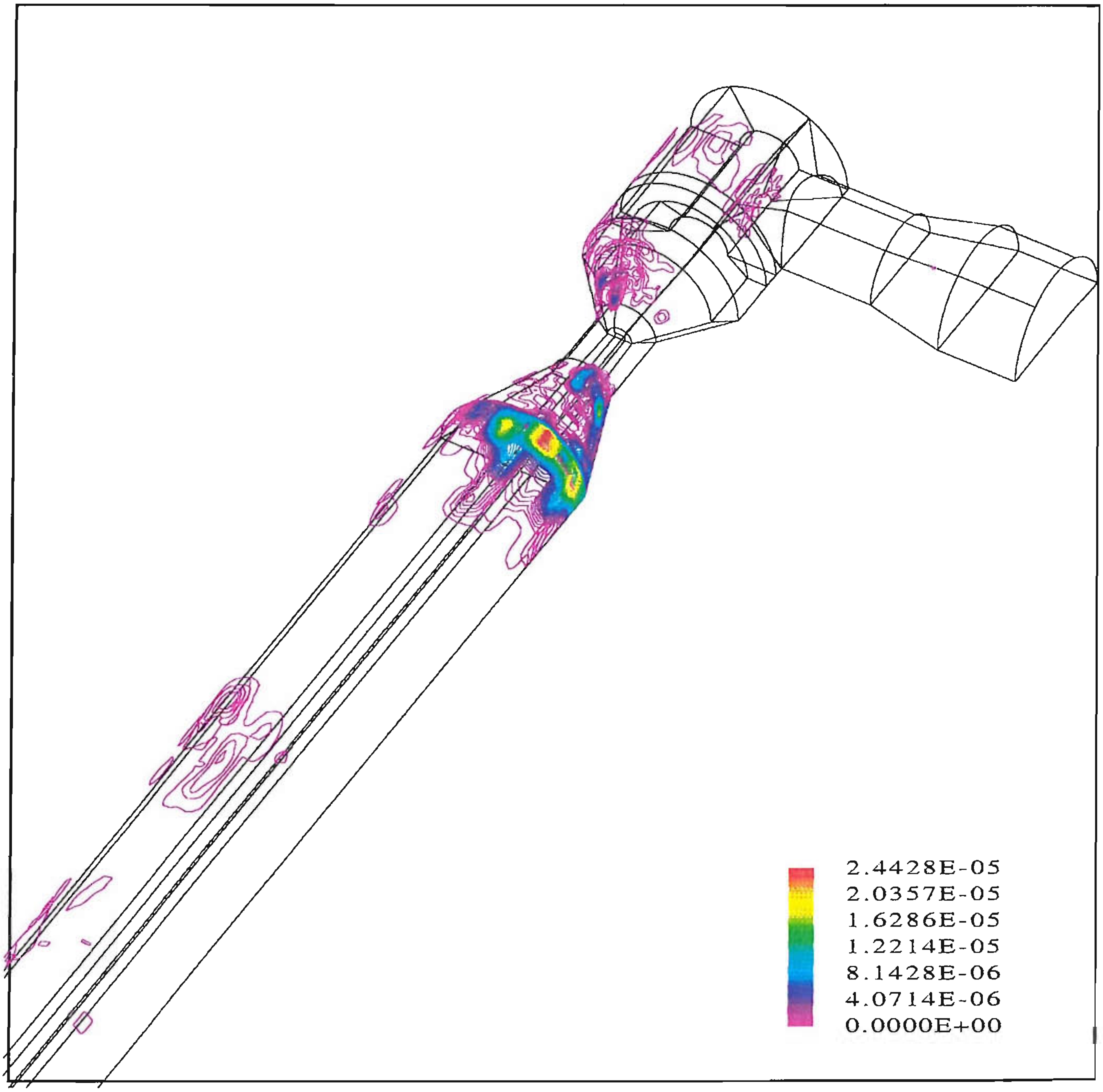

EROSIONAL TRENDS OF A CONVENTIONAL NEEDLE AND SEAT CHOKE (K-EPSILON MODEL)

Test Number - **2**
Particle Type - **Sand**
Particle Roundness Factor - **0.5**
Particle Flux Rate - **1** % by wt.
Number of Particle Sizes - **6**
Particle Size Range - **50-100** μm
Turbulent Dispersion - **No**

Appendix Figure 32 - *k*-Epsilon Model Surface Contour Plot of Needle & Seat Choke Particle Erosion Rates (mm^3/hr)

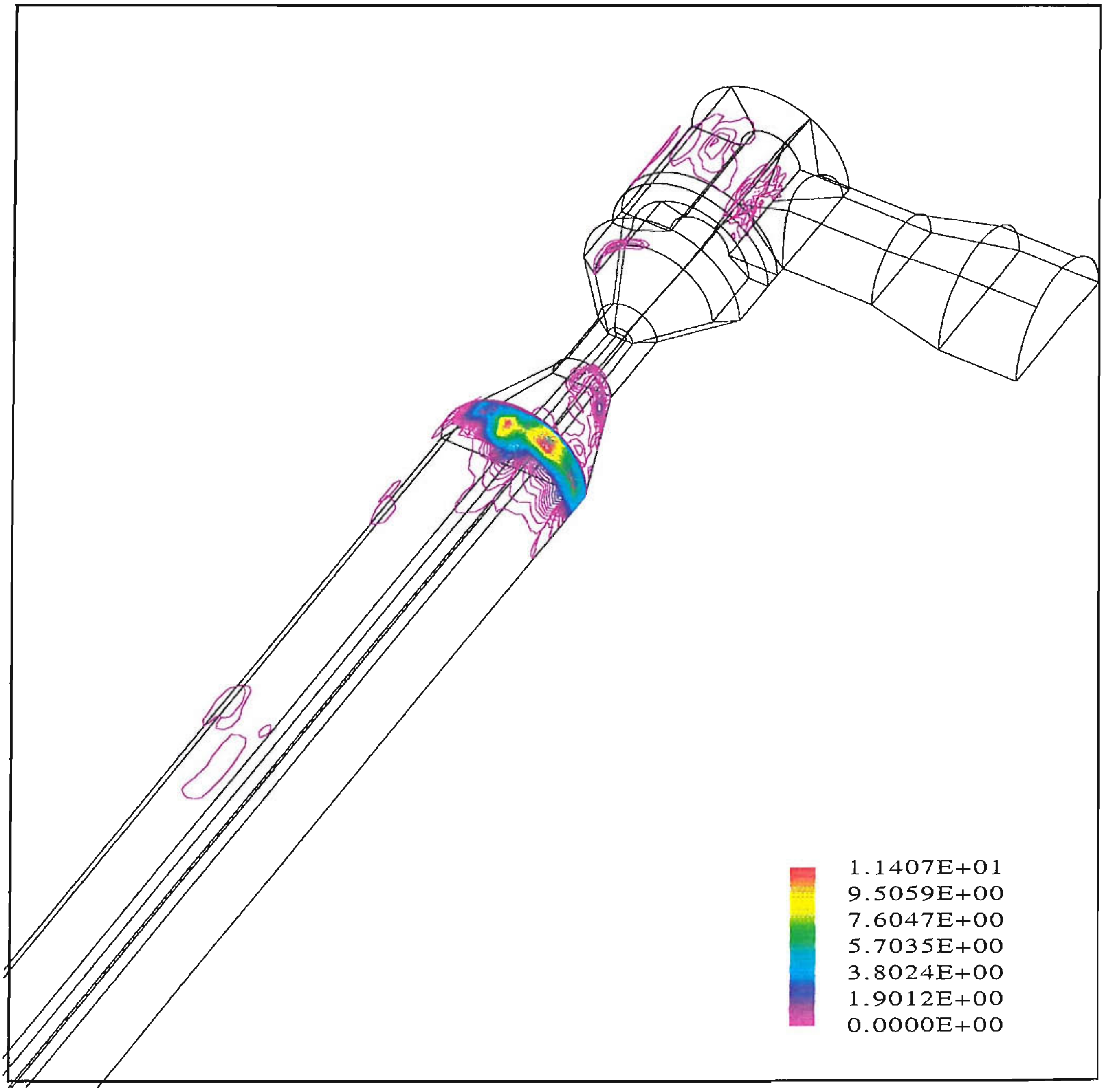

EROSIONAL TRENDS OF A CONVENTIONAL NEEDLE AND SEAT CHOKE (K-EPSILON MODEL)

Test Number - **2**
Particle Type - **Sand**
Particle Roundness Factor - **0.5**
Particle Flux Rate - **1** % by wt.
Number of Particle Sizes - **6**
Particle Size Range - **50-100** μm
Turbulent Dispersion - **No**

Appendix Figure 33 - *k*-Epsilon Model Surface Contour Plot of Needle & Seat Choke Particle Erosion Rates (mm^3/hr)

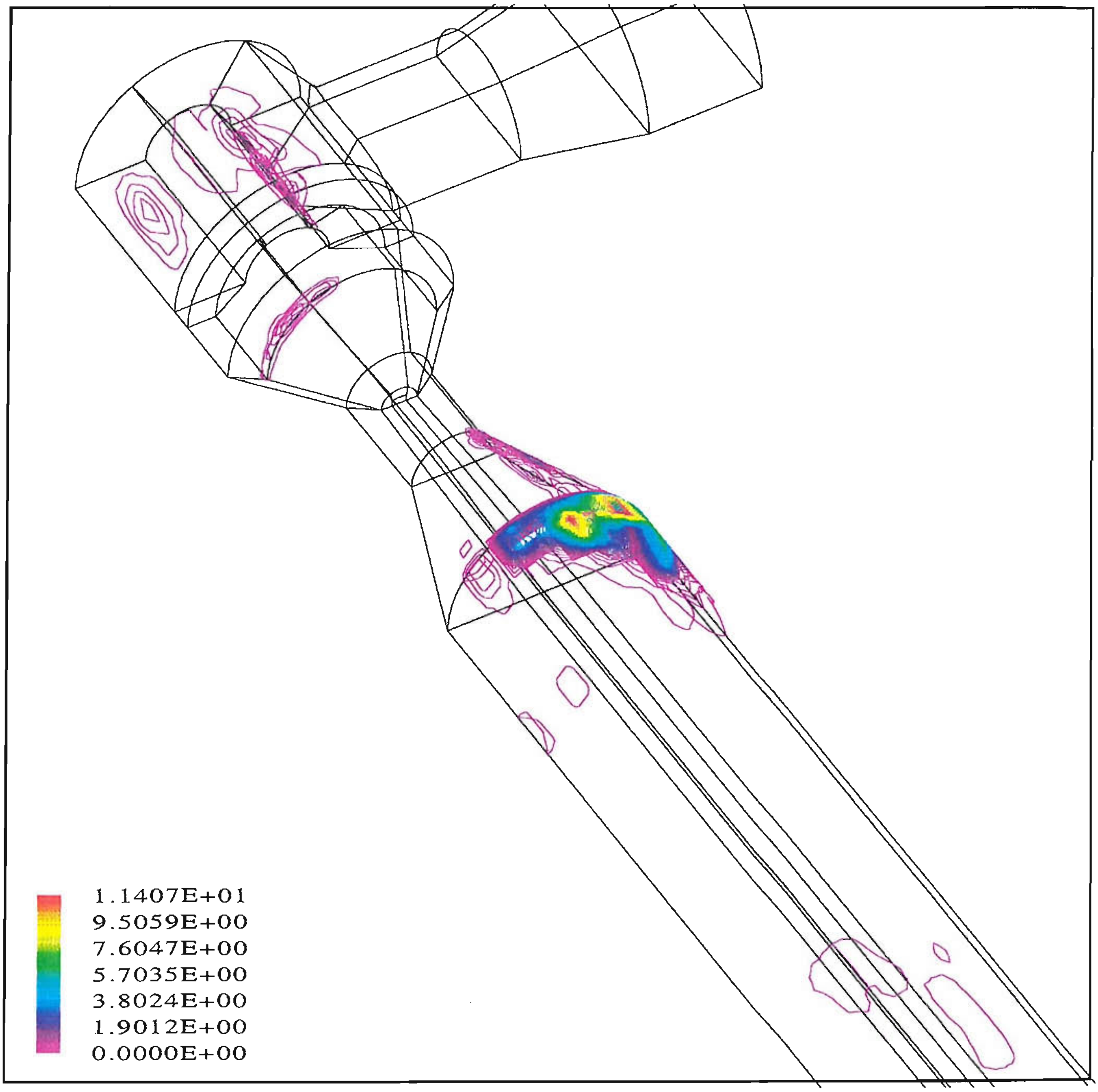

EROSIONAL TRENDS OF A CONVENTIONAL NEEDLE AND SEAT CHOKE (K-EPSILON MODEL)

Test Number - **3**
Particle Type - **Sand**
Particle Roundness Factor - **0.5**
Particle Flux Rate - **1** % by wt.
Number of Particle Sizes - **6**
Particle Size Range - **150-200** μm
Turbulent Dispersion - **Yes**

Appendix Figure 34 - *k*-Epsilon Model Surface Contour Plot of Needle & Seat Choke Particle Impact Velocities (m/s)

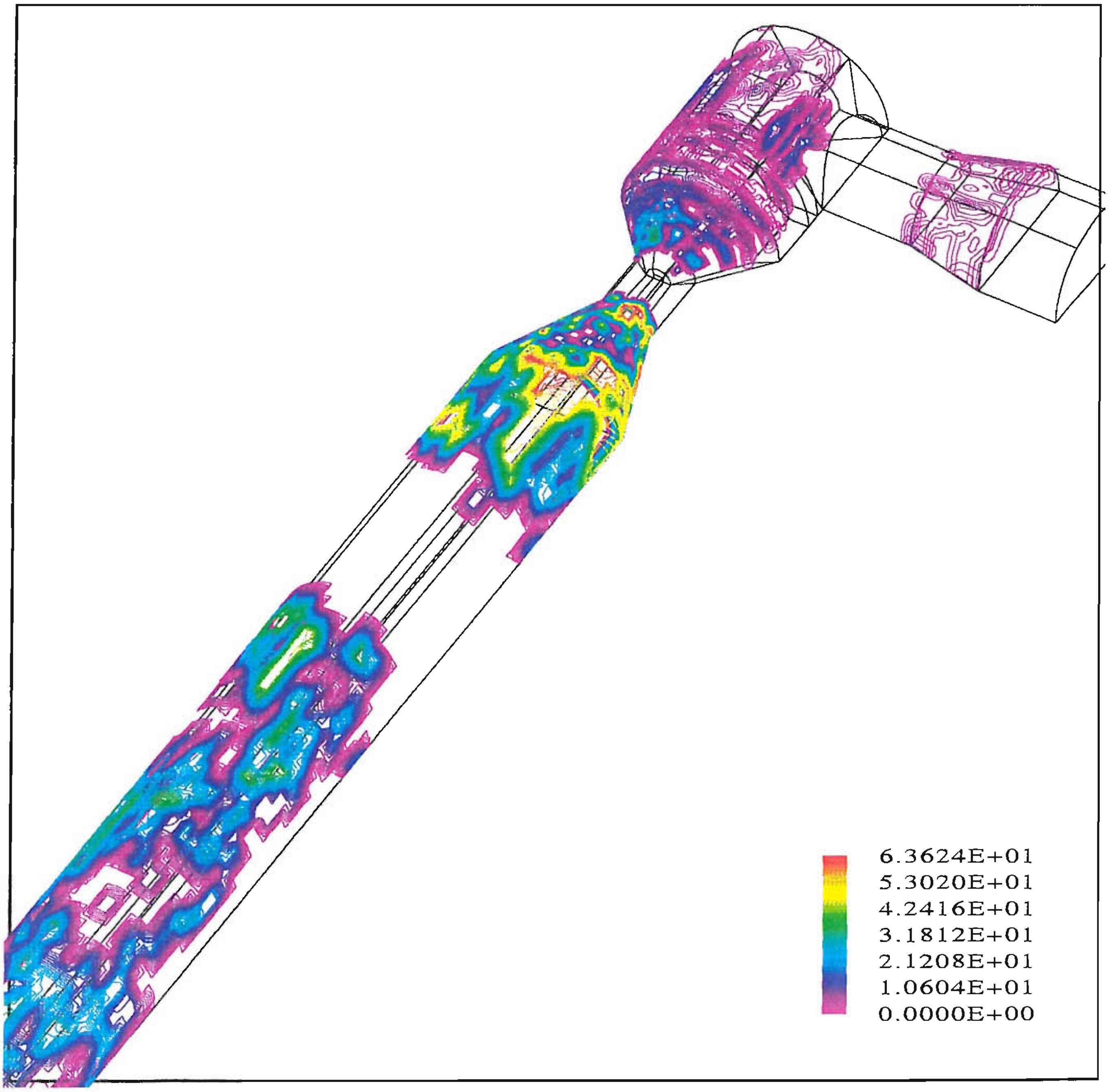

EROSIONAL TRENDS OF A CONVENTIONAL NEEDLE AND SEAT CHOKE (K-EPSILON MODEL)

Test Number - **3**
Particle Type - **Sand**
Particle Roundness Factor - **0.5**
Particle Flux Rate - **1** % by wt.
Number of Particle Sizes - **6**
Particle Size Range - **150-200** μm
Turbulent Dispersion - **Yes**

Appendix Figure 35 - *k*-Epsilon Model Surface Contour Plot of Needle & Seat Choke Particle Impact Angles (Deg)

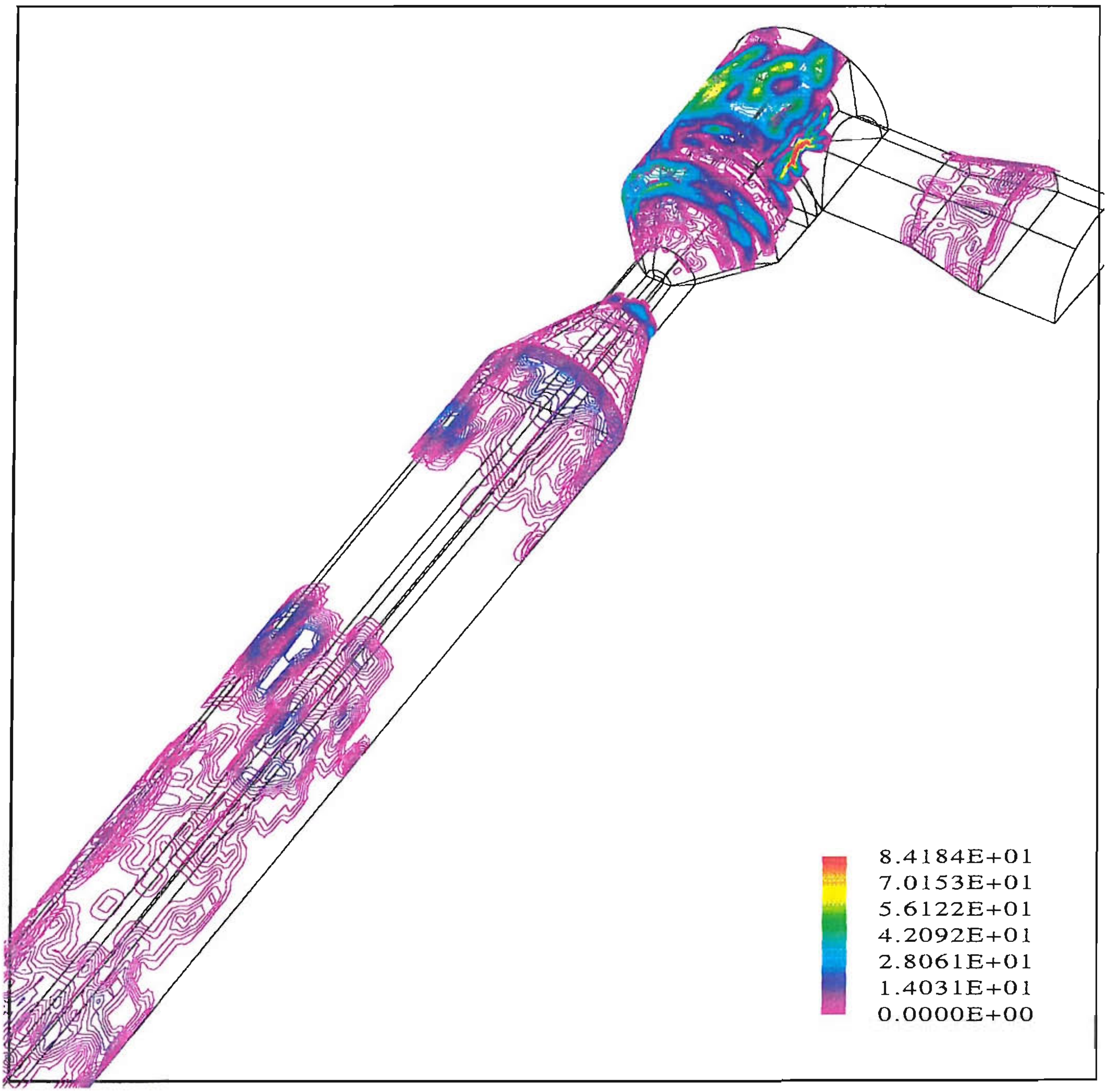

Erosional Trends of a Conventional Needle and Seat Choke (k-Epsilon Model)

Test Number - **3**
Particle Type - **Sand**
Particle Roundness Factor - **0.5**
Particle Flux Rate - **1** % by wt.
Number of Particle Sizes - **6**
Particle Size Range - **150-200** μm
Turbulent Dispersion - **Yes**

Appendix Figure 36 - *k*-Epsilon Model Surface Contour Plot of Needle & Seat Choke Particle Impact Kinetic Energy (J)

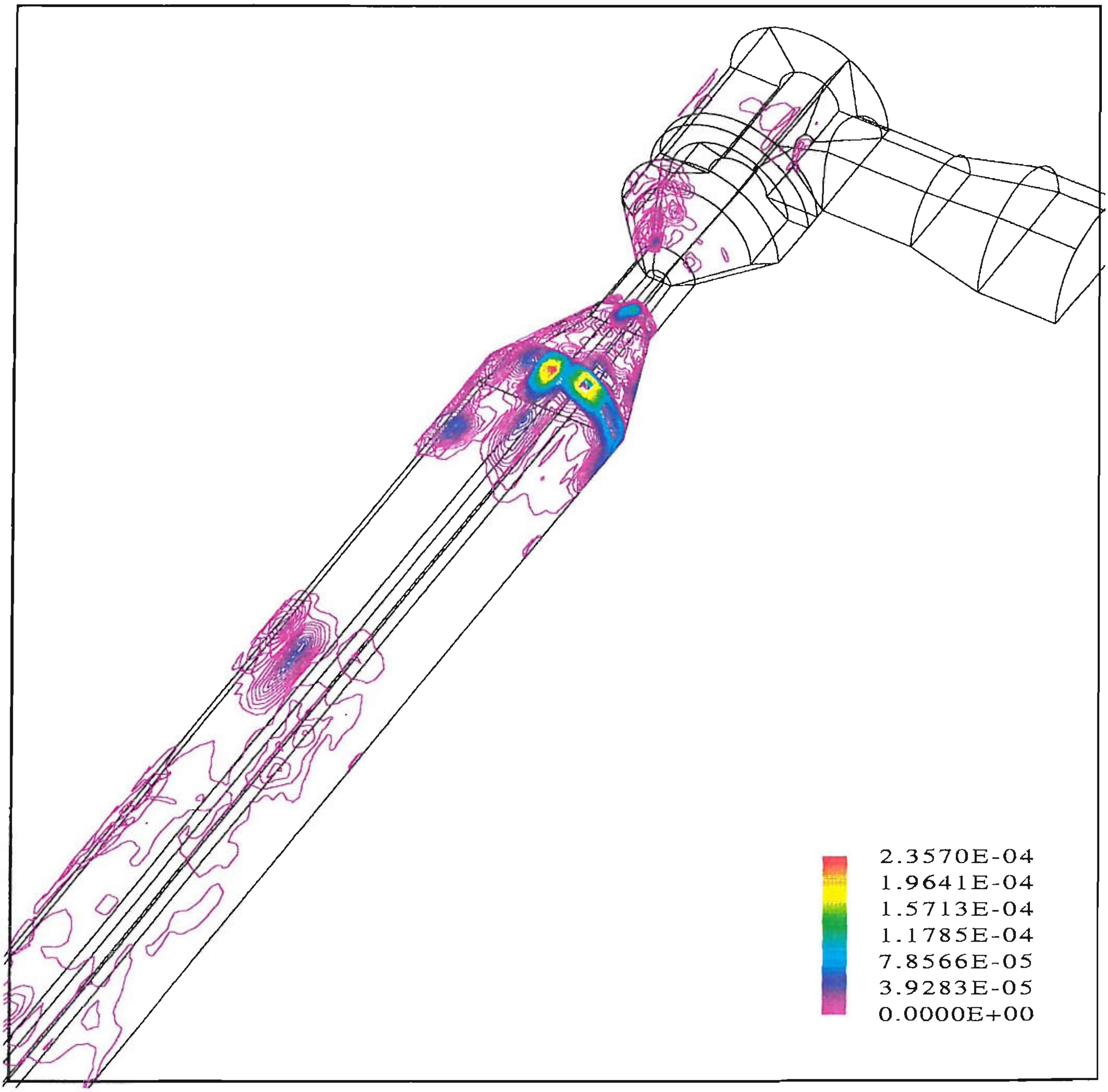

Erosional Trends of a Conventional Needle and Seat Choke (k-Epsilon Model)

Test Number - **3**
Particle Type - **Sand**
Particle Roundness Factor - **0.5**
Particle Flux Rate - **1** % by wt.
Number of Particle Sizes - **6**
Particle Size Range - **150-200** µm
Turbulent Dispersion - **Yes**

Appendix Figure 37 - *k*-Epsilon Model Surface Contour Plot of Needle & Seat Choke Particle Erosion Rates (mm³/hr)

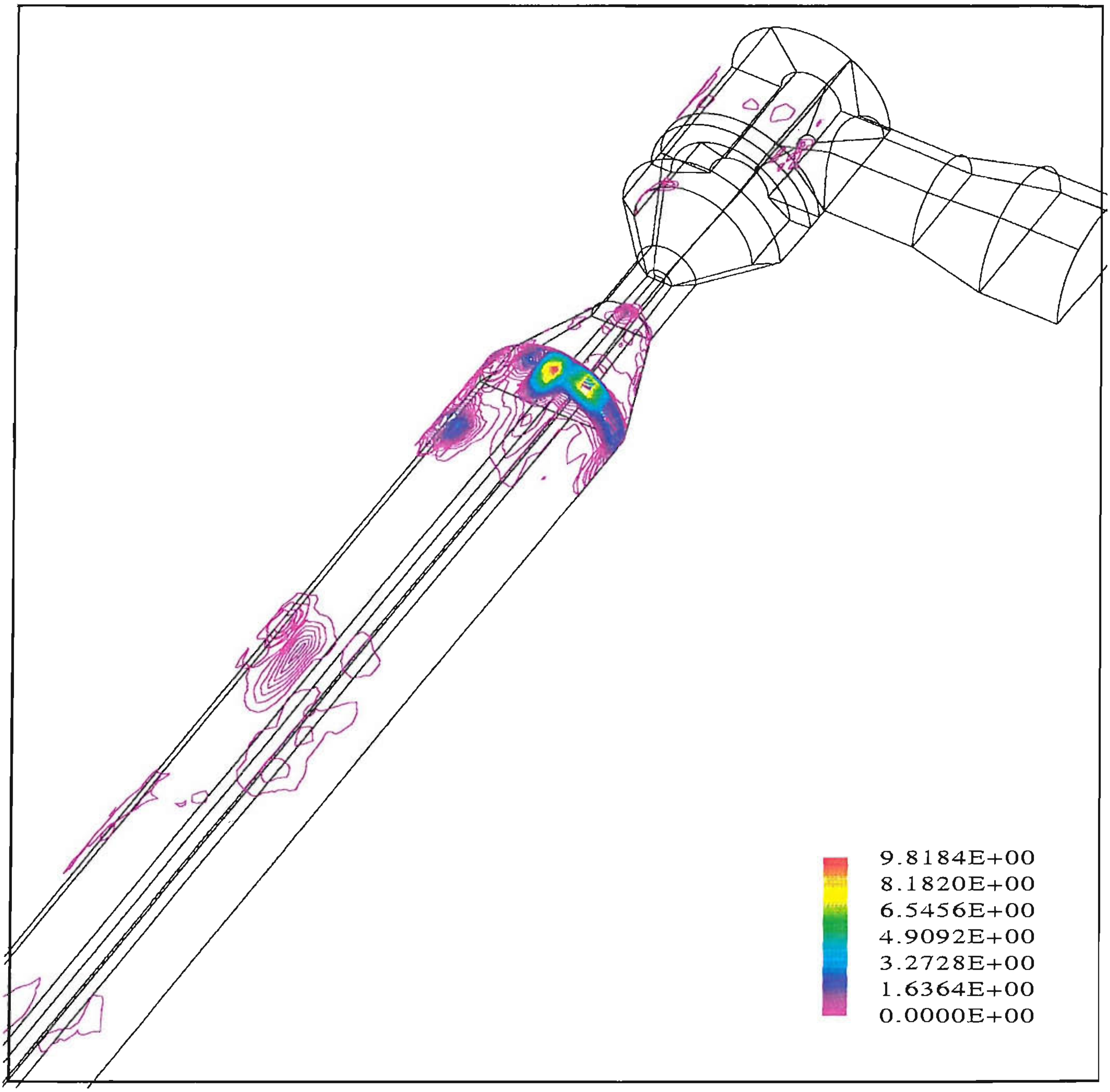

EROSIONAL TRENDS OF A CONVENTIONAL NEEDLE AND SEAT CHOKE (K-EPSILON MODEL)

Test Number - **3**
Particle Type - **Sand**
Particle Roundness Factor - **0.5**
Particle Flux Rate - **1** % by wt.
Number of Particle Sizes - **6**
Particle Size Range - **150-200** μm
Turbulent Dispersion - **Yes**

Appendix Figure 38 - *k*-Epsilon Model Surface Contour Plot of Needle & Seat Choke Particle Erosion Rates (mm³/hr)

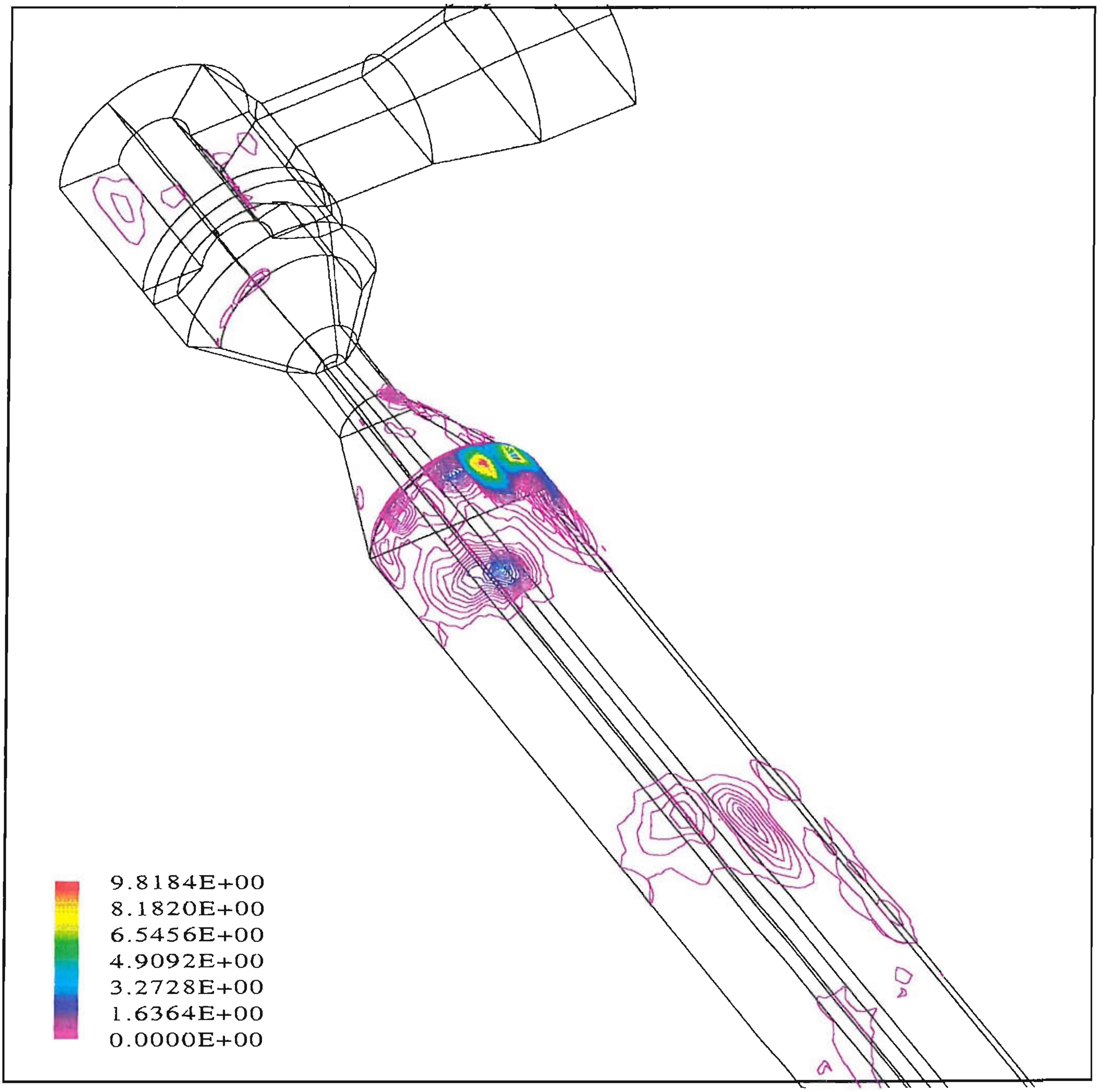

EROSIONAL TRENDS OF A CONVENTIONAL NEEDLE AND SEAT CHOKE (K-EPSILON MODEL)

Test Number - **4**
Particle Type - **Sand**
Particle Roundness Factor - **0.5**
Particle Flux Rate - **1** % by wt.
Number of Particle Sizes - **6**
Particle Size Range - **150-200** μm
Turbulent Dispersion - **No**

Appendix Figure 39 - *k*-Epsilon Model Surface Contour Plot of Needle & Seat Choke Particle Impact Velocities (m/s)

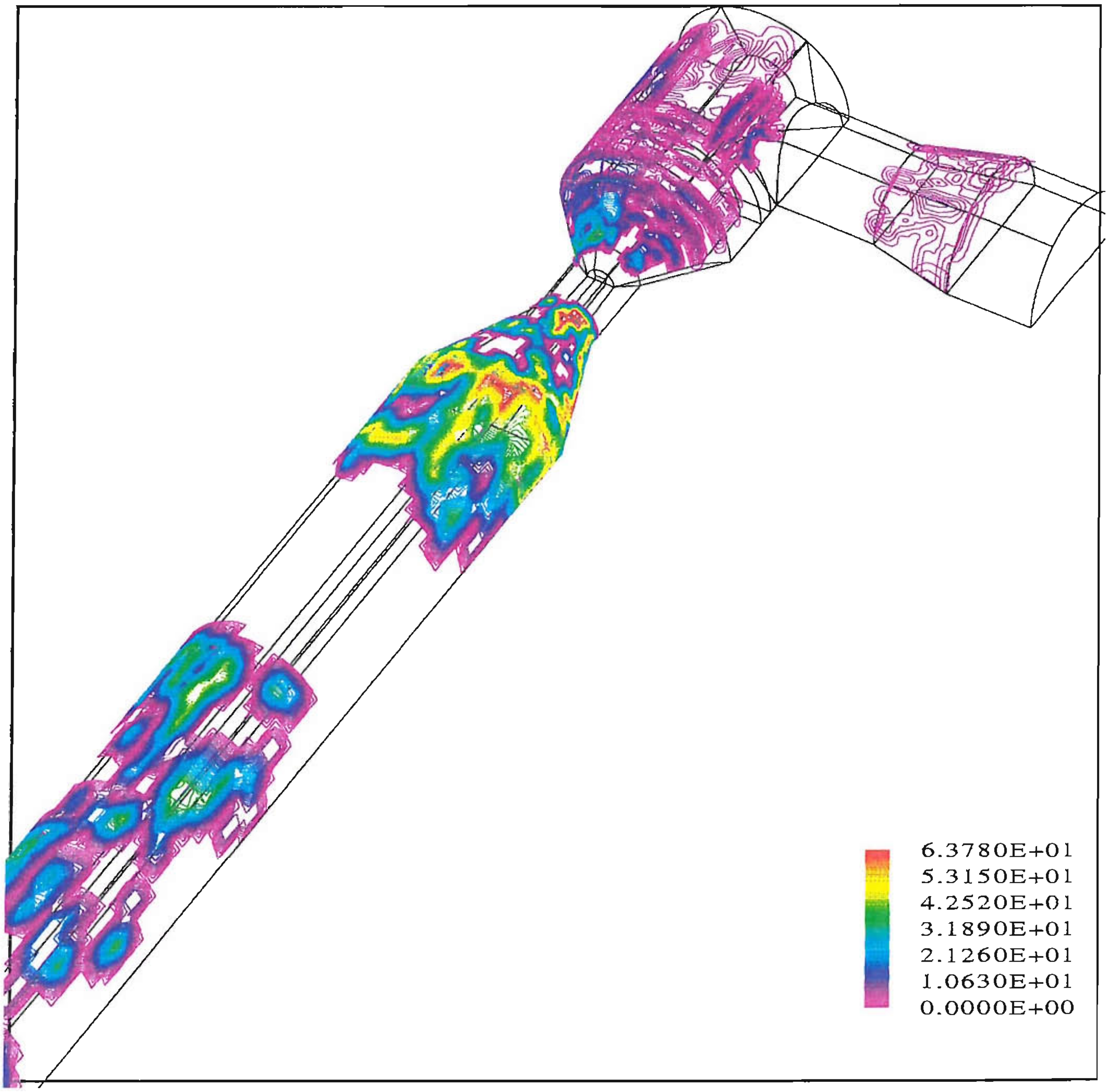

EROSIONAL TRENDS OF A CONVENTIONAL NEEDLE AND SEAT CHOKE (K-EPSILON MODEL)

Test Number - **4**
Particle Type - **Sand**
Particle Roundness Factor - **0.5**
Particle Flux Rate - **1** % by wt.
Number of Particle Sizes - **6**
Particle Size Range - **150-200** μm
Turbulent Dispersion - **No**

Appendix Figure 40 - *k*-Epsilon Model Surface Contour Plot of Needle & Seat Choke Particle Impact Angles (Deg)

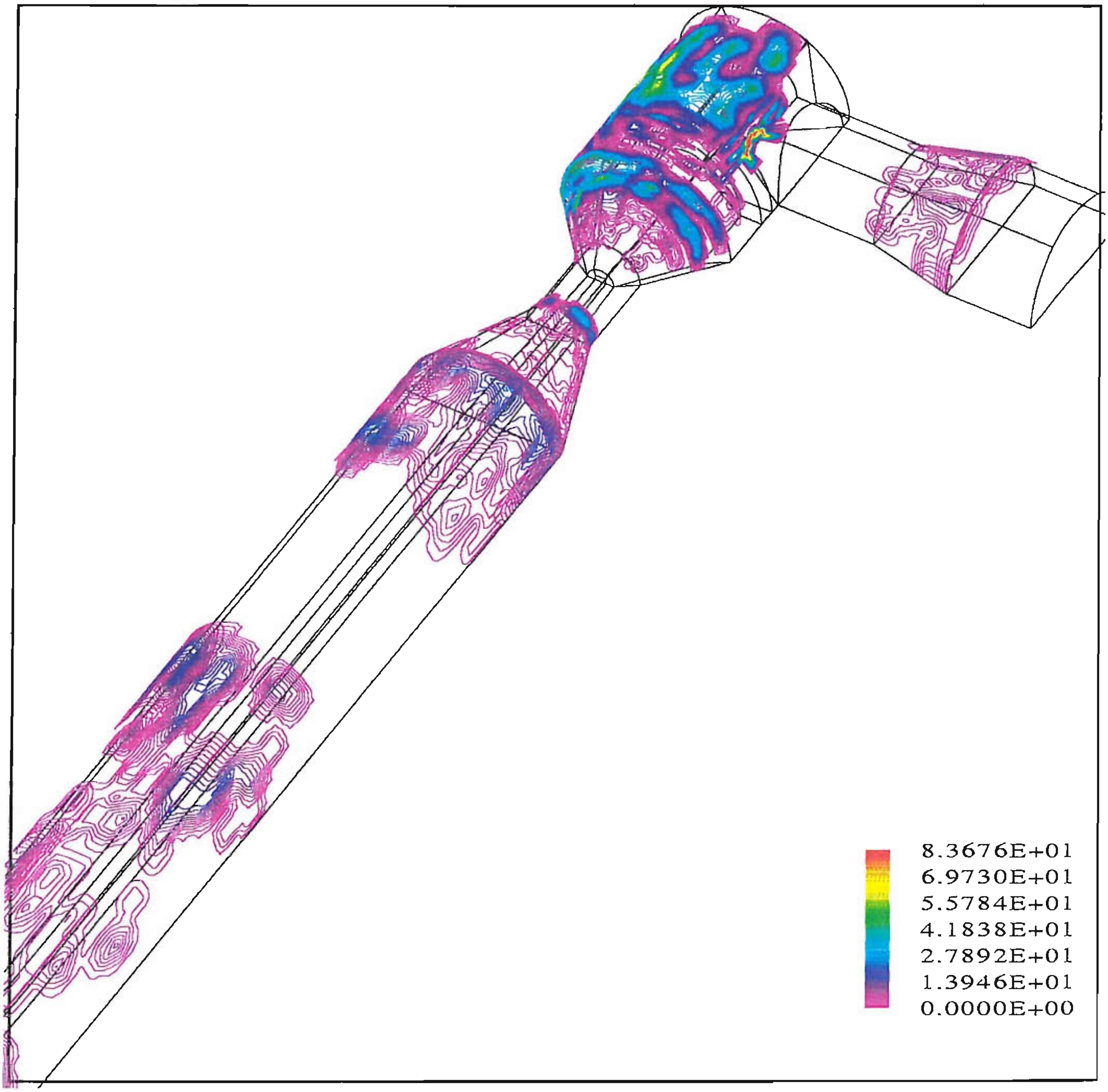

EROSIONAL TRENDS OF A CONVENTIONAL NEEDLE AND SEAT CHOKE (K-EPSILON MODEL)

Test Number - **4**
Particle Type - **Sand**
Particle Roundness Factor - **0.5**
Particle Flux Rate - **1** % by wt.
Number of Particle Sizes - **6**
Particle Size Range - **150-200** µm
Turbulent Dispersion - **No**

Appendix Figure 41 - *k*-Epsilon Model Surface Contour Plot of Needle & Seat Choke Particle Impact Kinetic Energy (J)

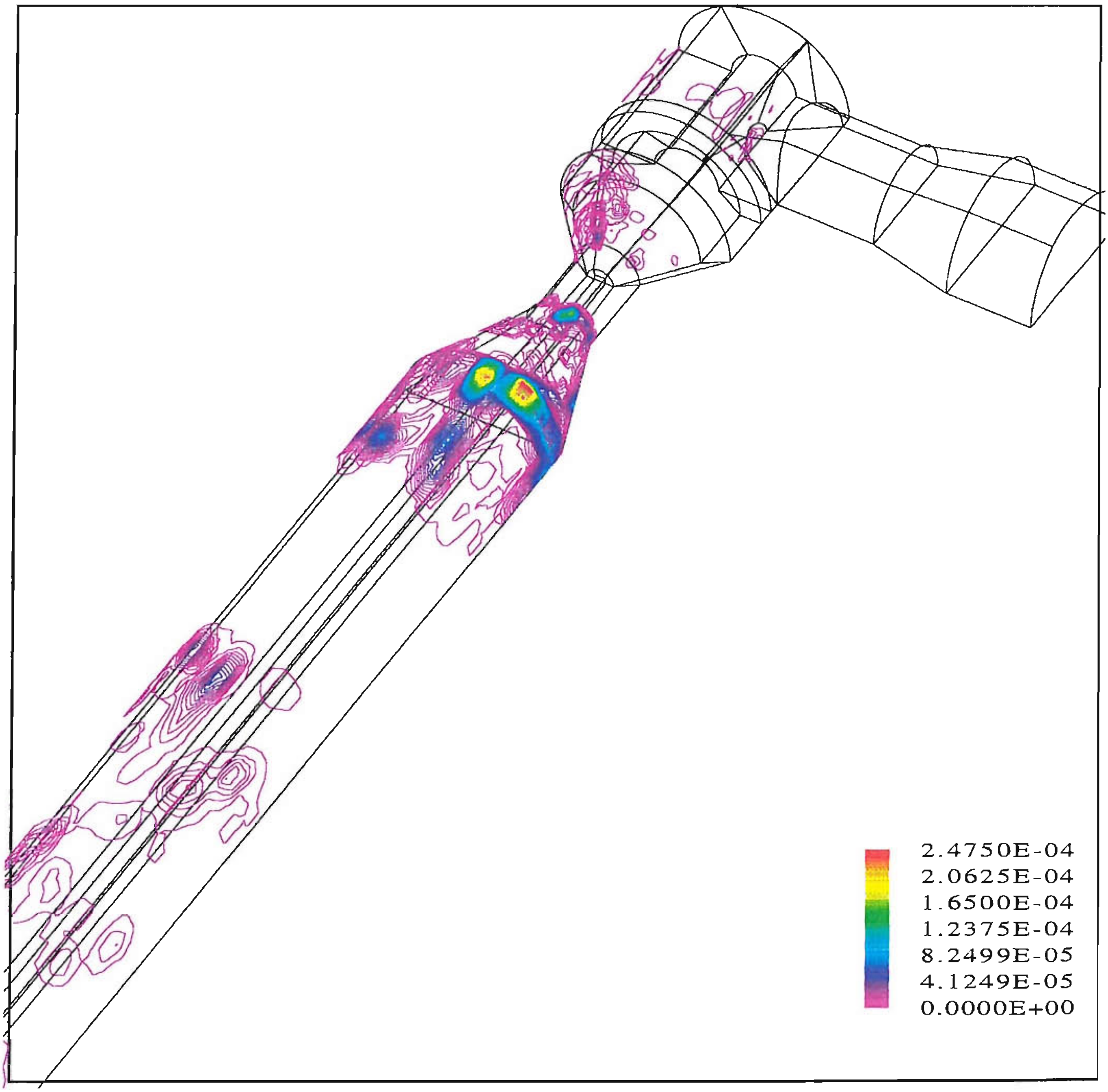

EROSIONAL TRENDS OF A CONVENTIONAL NEEDLE AND SEAT CHOKE (K-EPSILON MODEL)

Test Number - **4**
Particle Type - **Sand**
Particle Roundness Factor - **0.5**
Particle Flux Rate - **1** % by wt.
Number of Particle Sizes - **6**
Particle Size Range - **150-200** μm
Turbulent Dispersion - **No**

Appendix Figure 42 - *k*-Epsilon Model Surface Contour Plot of Needle & Seat Choke Particle Erosion Rates (mm^3/hr)

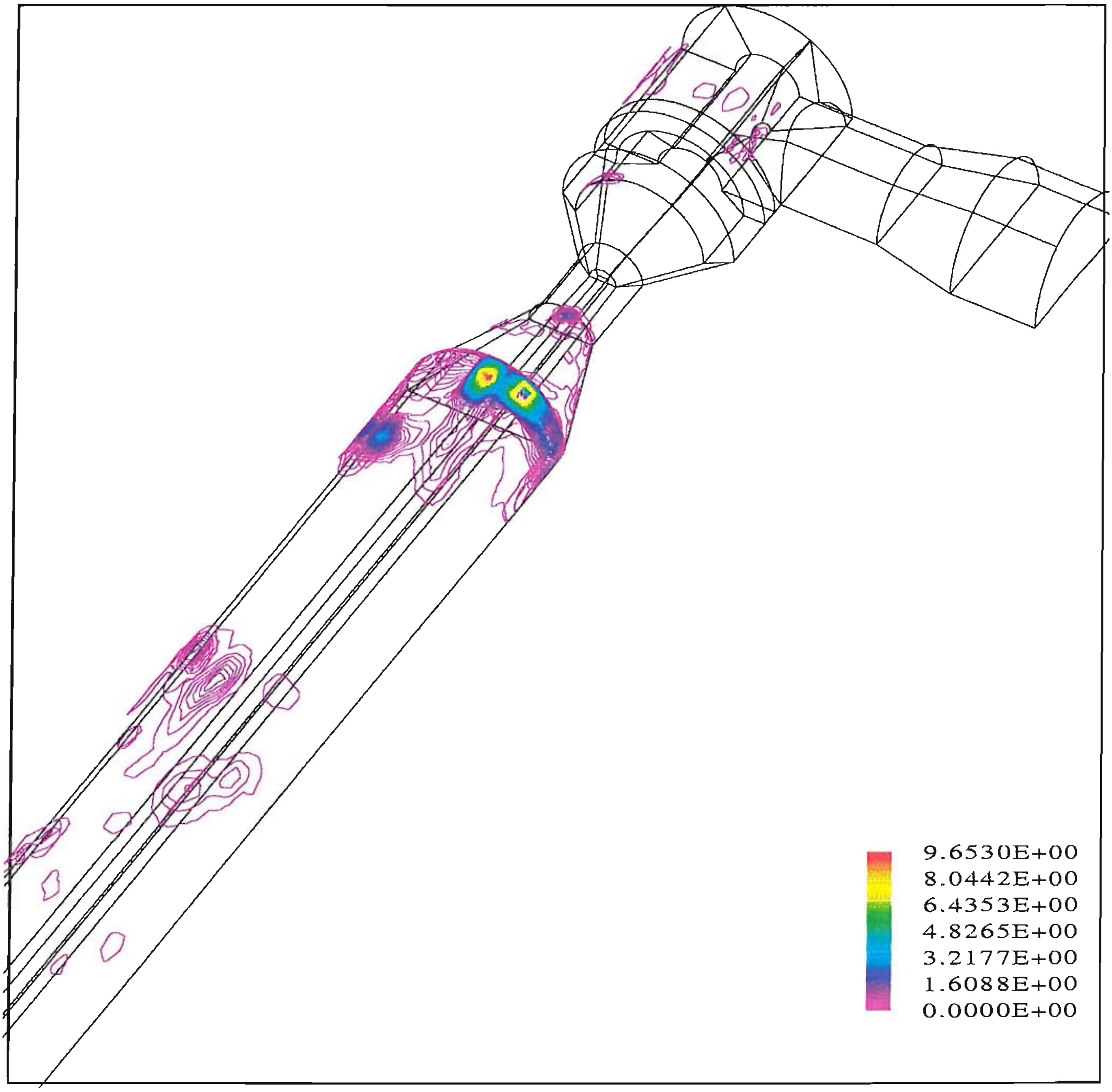

EROSIONAL TRENDS OF A CONVENTIONAL NEEDLE AND SEAT CHOKE (K-EPSILON MODEL)

Test Number - **4**
Particle Type - **Sand**
Particle Roundness Factor - **0.5**
Particle Flux Rate - **1** % by wt.
Number of Particle Sizes - **6**
Particle Size Range - **150-200** μm
Turbulent Dispersion - **No**

Appendix Figure 43 - *k*-Epsilon Model Surface Contour Plot of Needle & Seat Choke Particle Erosion Rates (mm^3/hr)

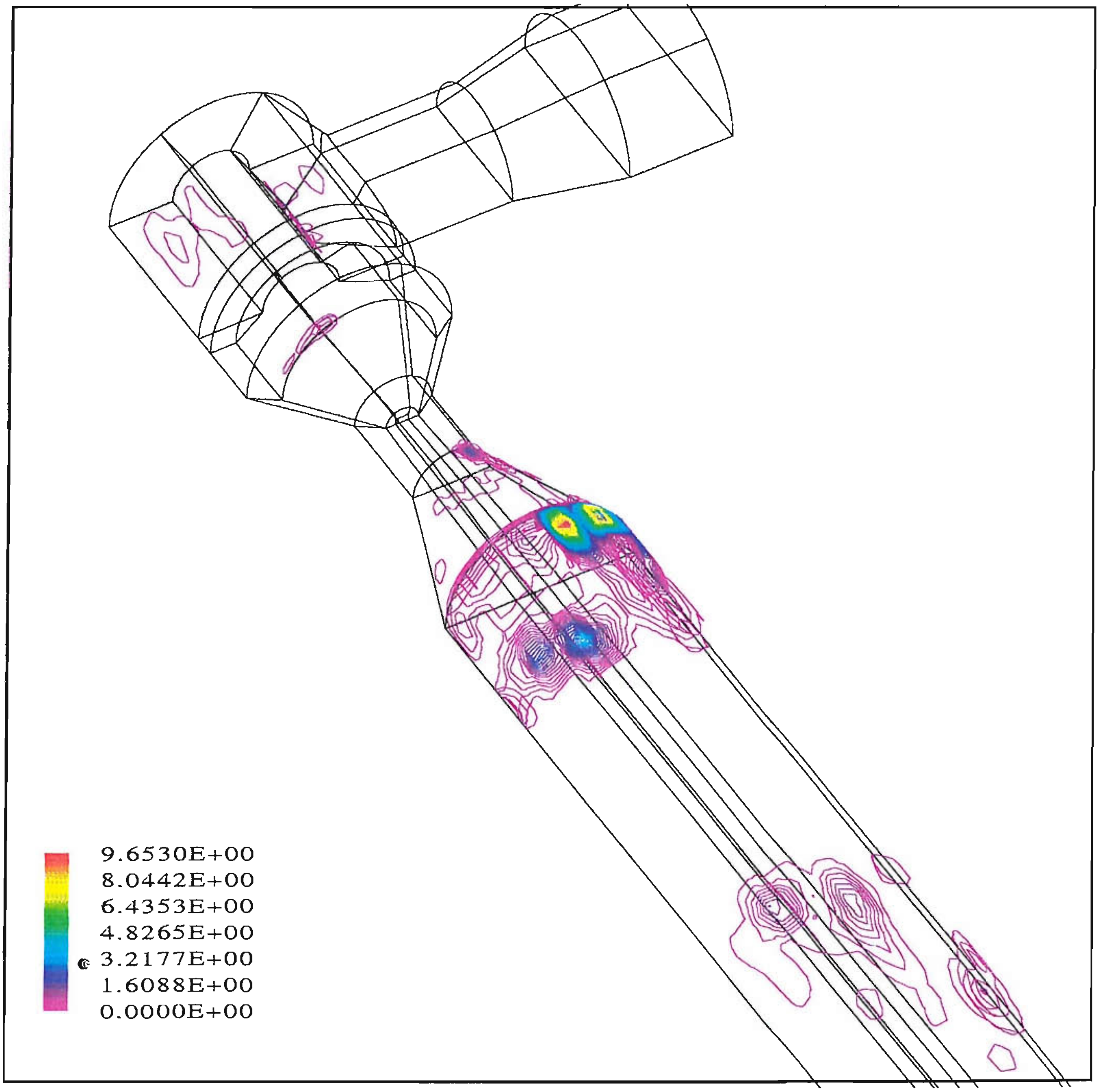

FLOW FIELD OF A CONVENTIONAL NEEDLE AND SEAT CHOKE (DIFFERENTIAL STRESS MODEL)

Fluid - **Dry Air**
Inlet Diameter - **75** mm
Throat Diameter - **25** mm
Taper Angle of Needle - **45°**
Choke Opening - **25** % (Linear)
Pressure Drop - **68** Bar
Mass Flow Rate (air) - **178** kg/hr

Appendix Figure 44 - Differential Stress Model Velocity Contour Plot of Needle & Seat Choke (m/s)

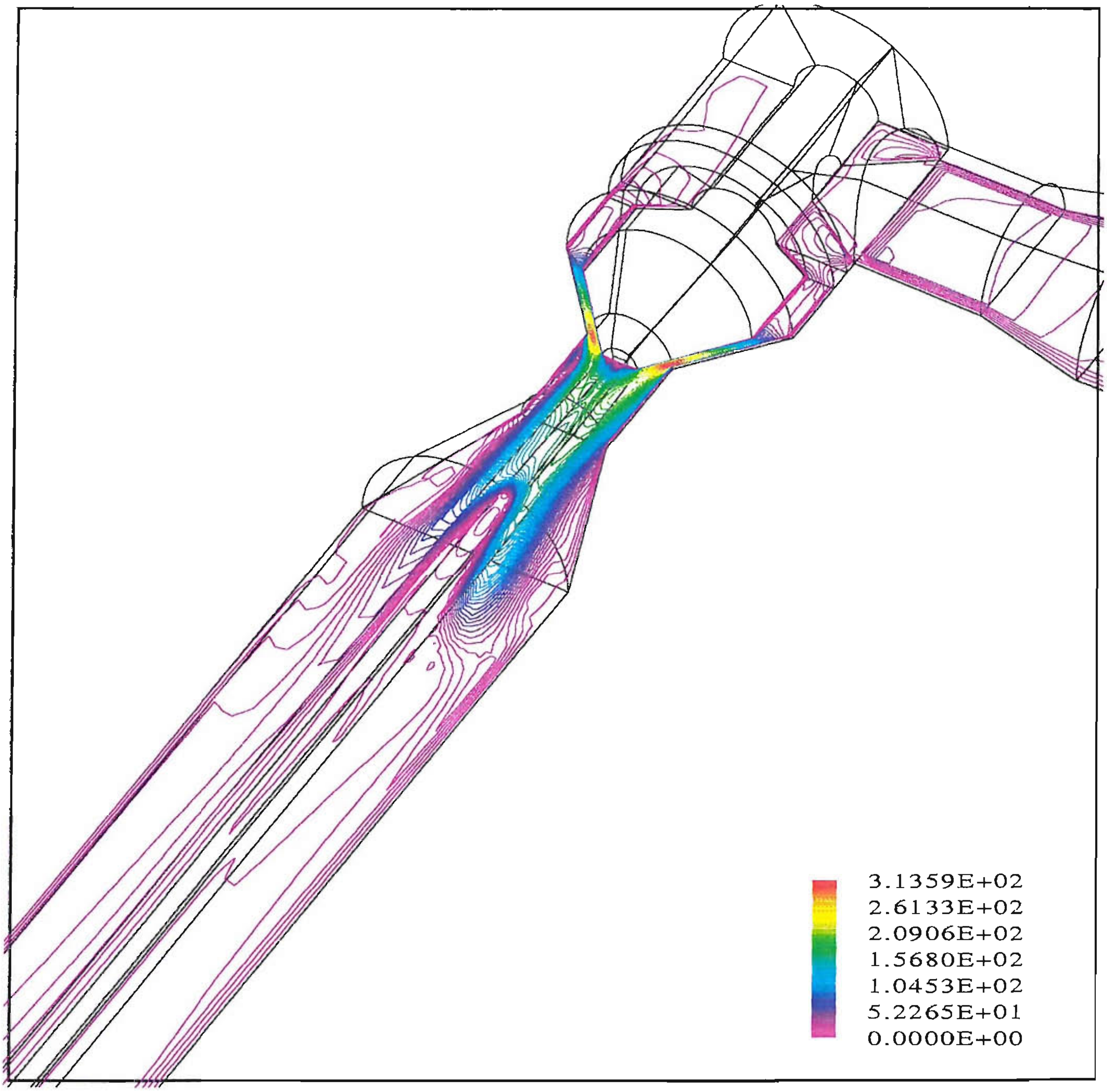

FLOW FIELD OF A CONVENTIONAL NEEDLE AND SEAT CHOKE (DIFFERENTIAL STRESS MODEL)

Fluid - **Dry Air**
Inlet Diameter - **75** mm
Throat Diameter - **25** mm
Taper Angle of Needle - **45°**
Choke Opening - **25** % (Linear)
Pressure Drop - **68** Bar
Mass Flow Rate (air) - **178** kg/hr

Appendix Figure 45 - Differential Stress Model Velocity Contour Plot of Needle & Seat Choke (m/s)

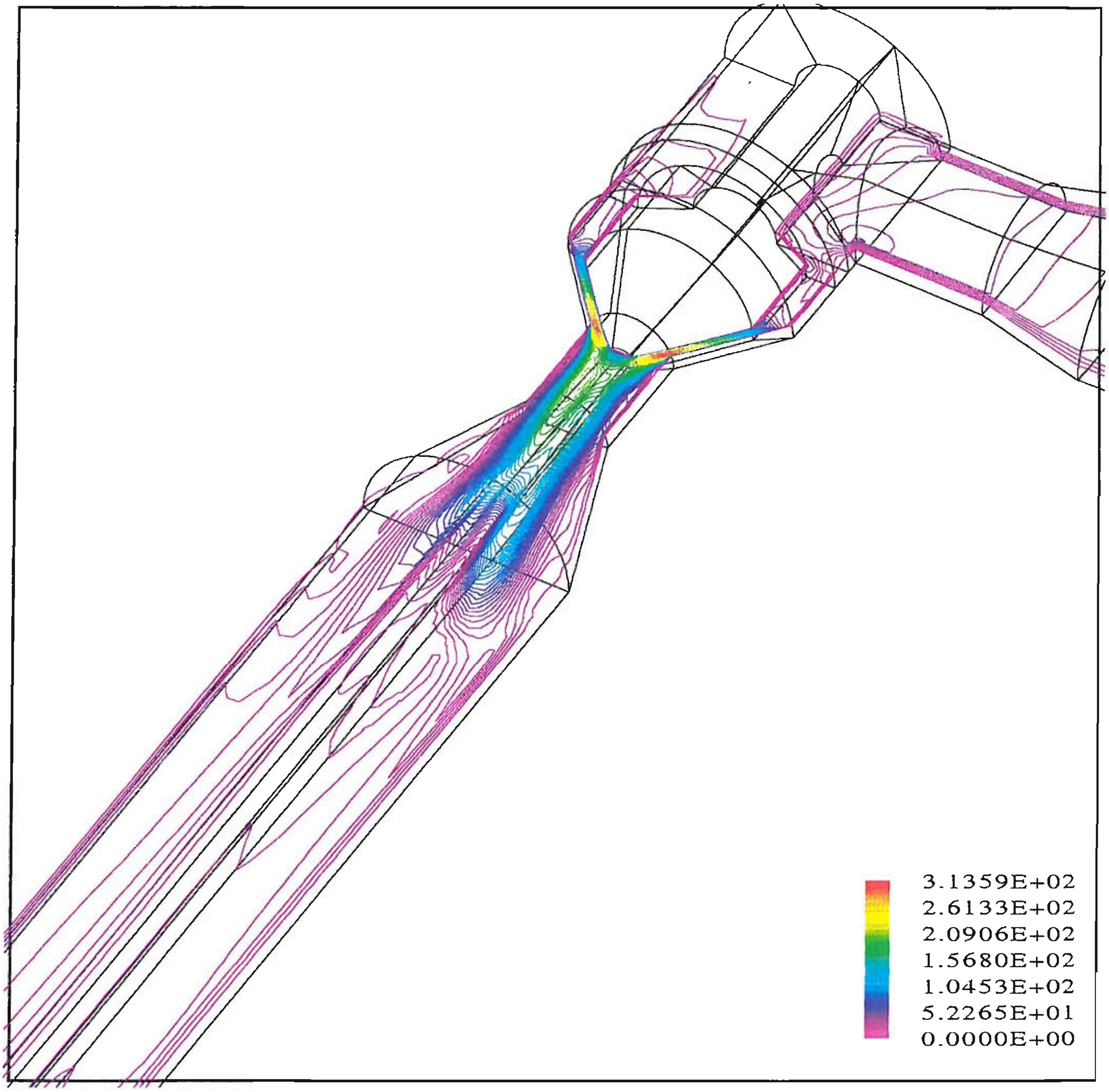

Flow Field of a Conventional Needle and Seat Choke (Differential Stress Model)

Fluid - **Dry Air**
Inlet Diameter - **75** mm
Throat Diameter - **25** mm
Taper Angle of Needle - **45°**
Choke Opening - **25** % (Linear)
Pressure Drop - **68** Bar
Mass Flow Rate (air) - **178** kg/hr

Appendix Figure 46 - Differential Stress Model Velocity Contour Plot of Needle & Seat Choke (m/s)

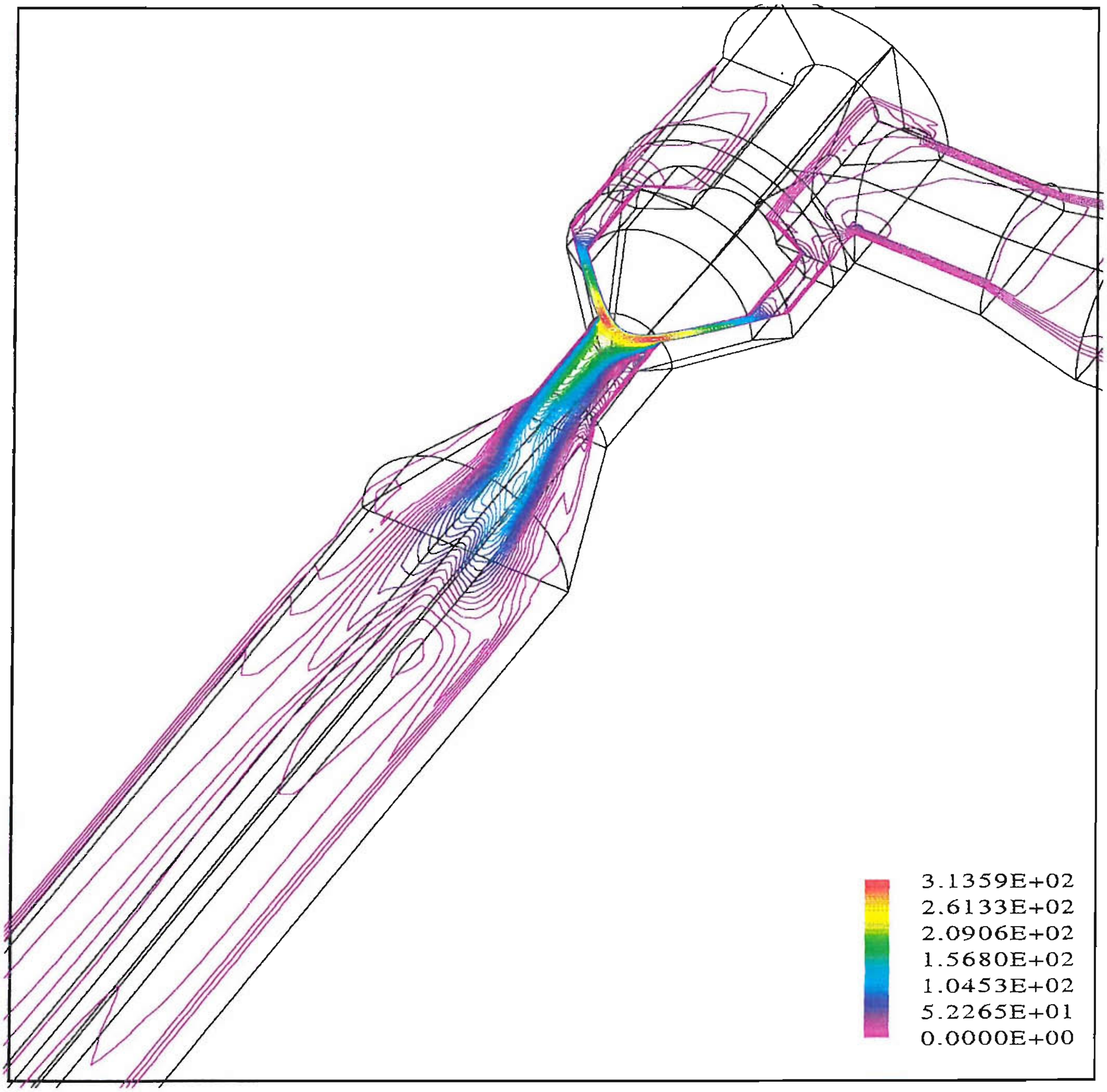

FLOW FIELD OF A CONVENTIONAL NEEDLE AND SEAT CHOKE (DIFFERENTIAL STRESS MODEL)

Fluid - **Dry Air**
Inlet Diameter - **75** mm
Throat Diameter - **25** mm
Taper Angle of Needle - **45°**
Choke Opening - **25** % (Linear)
Pressure Drop - **68** Bar
Mass Flow Rate (air) - **178** kg/hr

Appendix Figure 47 - Differential Stress Model Turbulent Kinetic Energy Contour Plot of Needle & Seat Choke

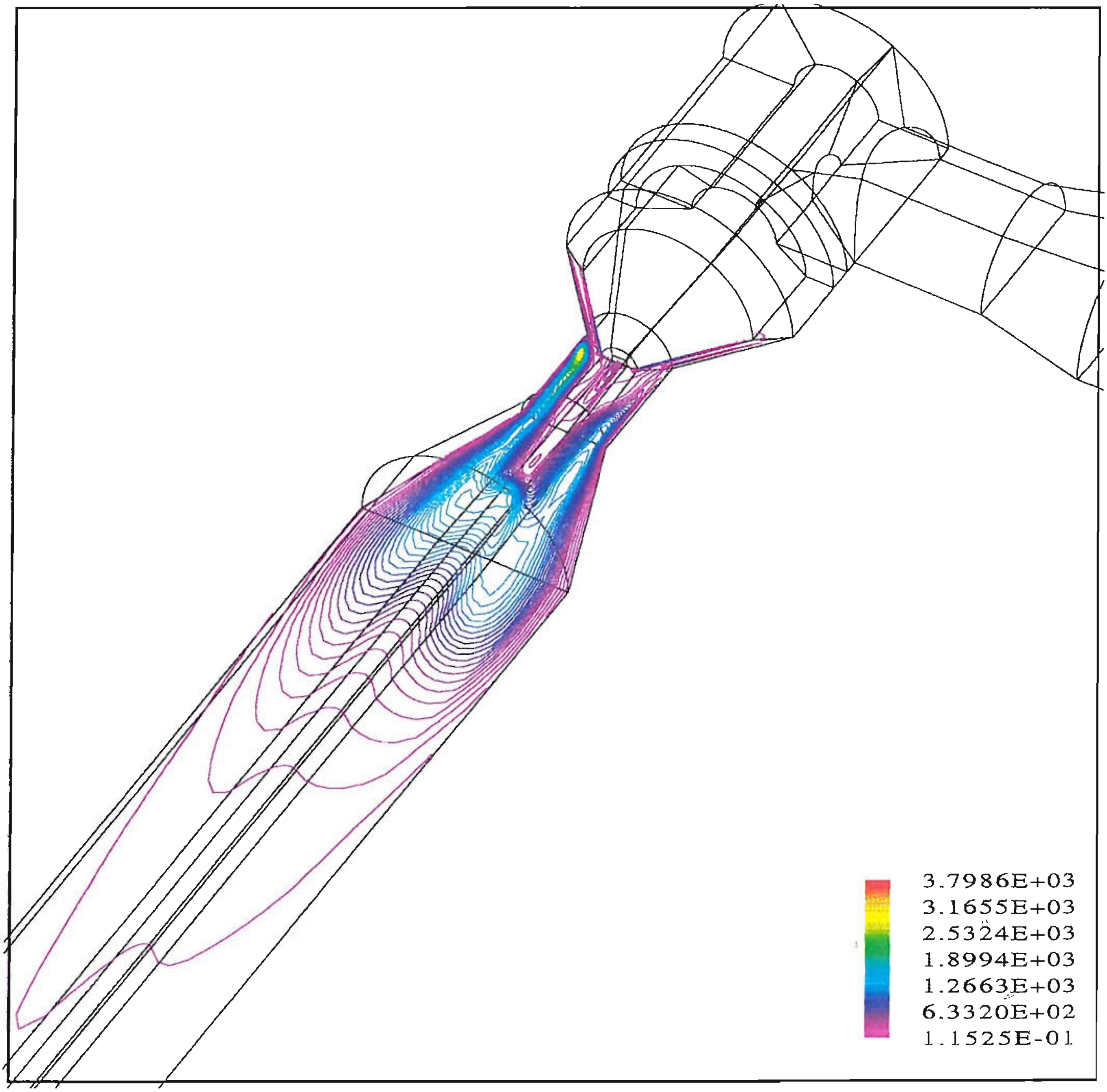

EROSIONAL TRENDS OF A CONVENTIONAL NEEDLE AND SEAT CHOKE (DIFFERENTIAL STRESS MODEL)

Test Number - **5**
Particle Type - **Sand**
Particle Roundness Factor - **0.5**
Particle Flux Rate - **1** % by wt.
Number of Particle Sizes - **6**
Particle Size Range - **50-100** μm
Turbulent Dispersion - **Yes**

Appendix Figure 48 - Differential Stress Model Surface Contour Plot of Needle & Seat Choke Particle Impact Velocities (m/s)

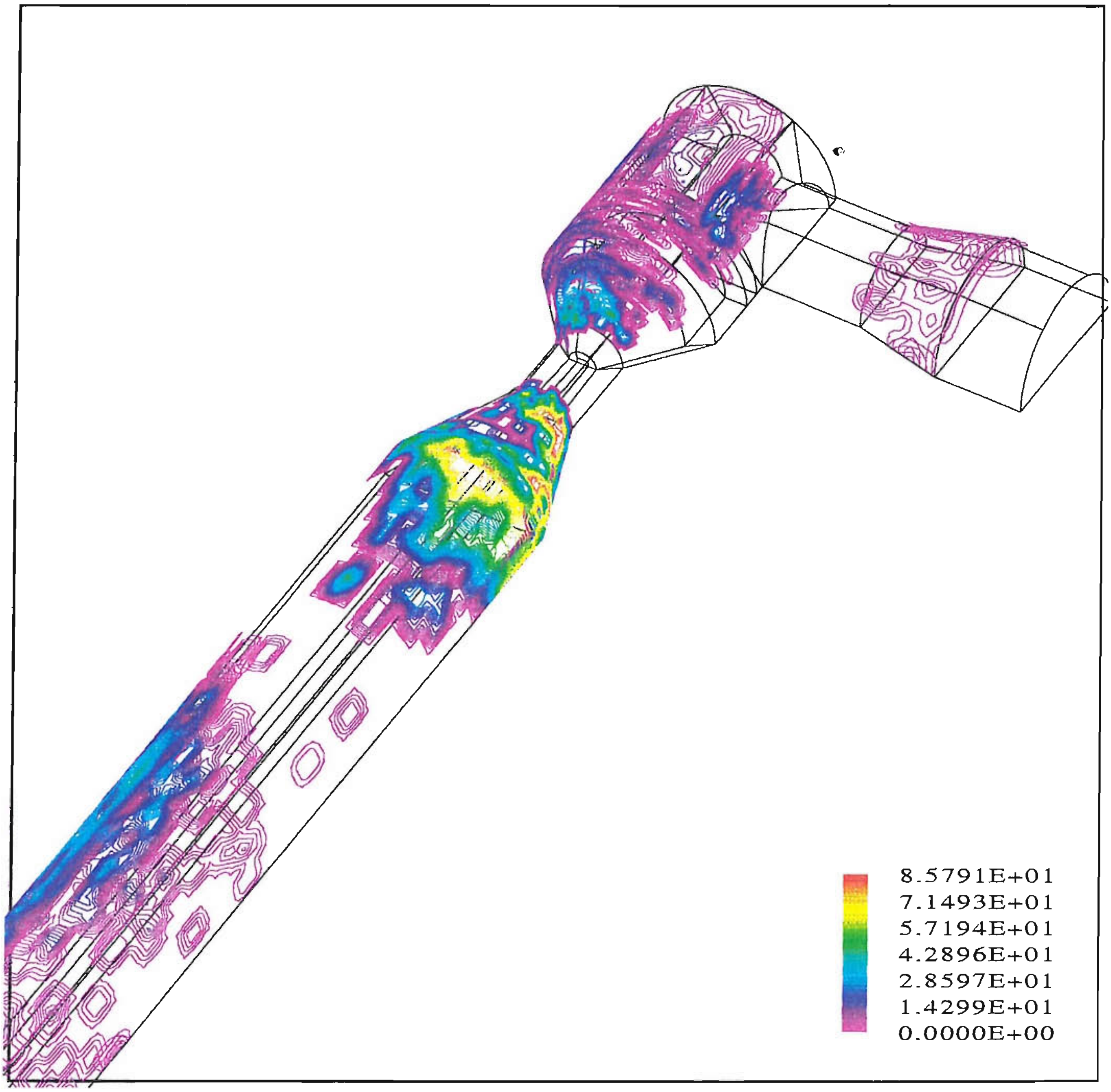

EROSIONAL TRENDS OF A CONVENTIONAL NEEDLE AND SEAT CHOKE (DIFFERENTIAL STRESS MODEL)

Test Number - **5**
Particle Type - **Sand**
Particle Roundness Factor - **0.5**
Particle Flux Rate - **1** % by wt.
Number of Particle Sizes - **6**
Particle Size Range - **50-100** μm
Turbulent Dispersion - **Yes**

Appendix Figure 49 - Differential Stress Model Surface Contour Plot of Needle & Seat Choke Particle Impact Angles (Deg)

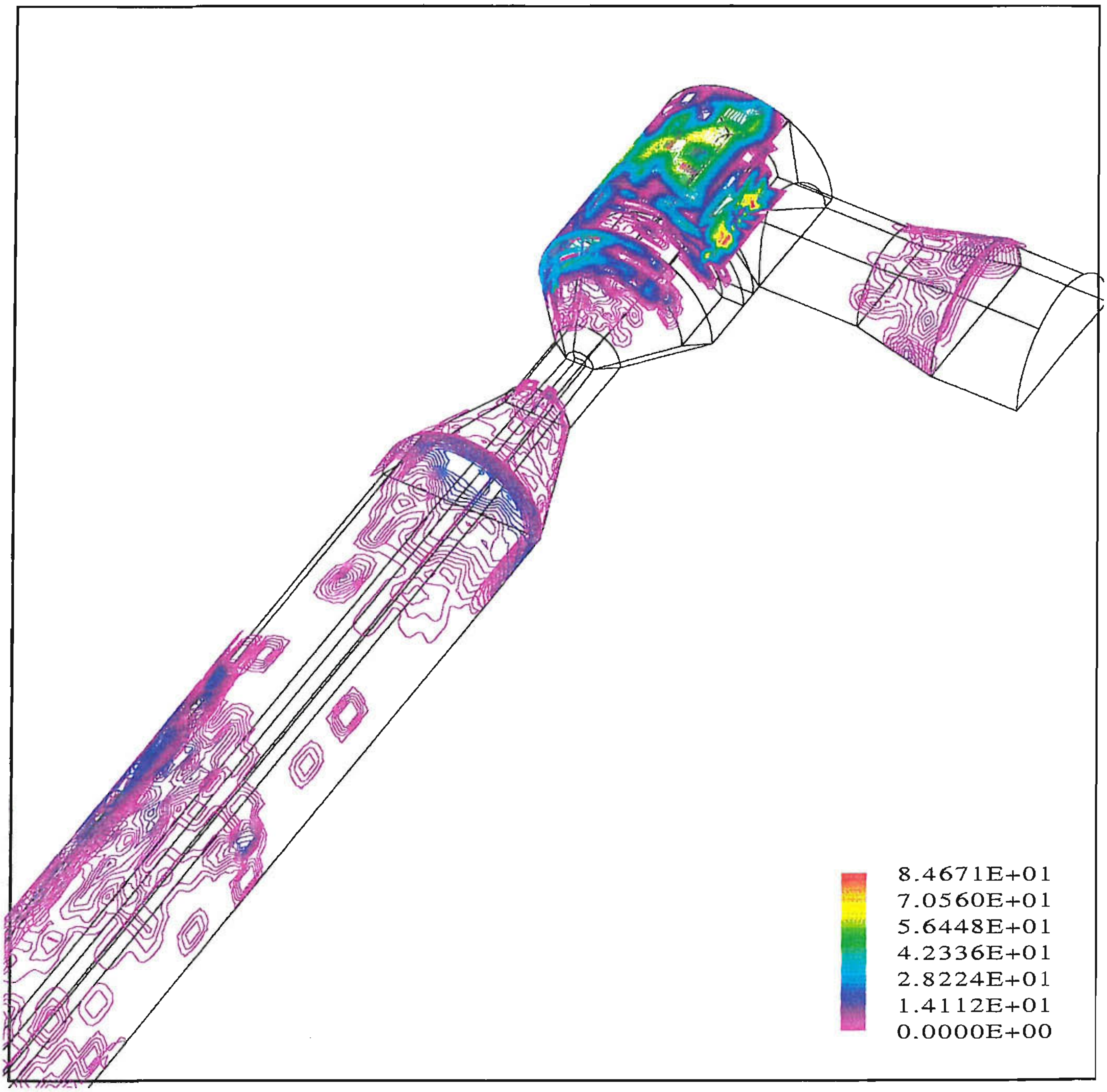

EROSIONAL TRENDS OF A CONVENTIONAL NEEDLE AND SEAT CHOKE (DIFFERENTIAL STRESS MODEL)

Test Number - **5**
Particle Type - **Sand**
Particle Roundness Factor - **0.5**
Particle Flux Rate - **1** % by wt.
Number of Particle Sizes - **6**
Particle Size Range - **50-100** μm
Turbulent Dispersion - **Yes**

Appendix Figure 50 - Differential Stress Model Surface Contour Plot of Needle & Seat Choke Particle Impact Kinetic Energy (J)

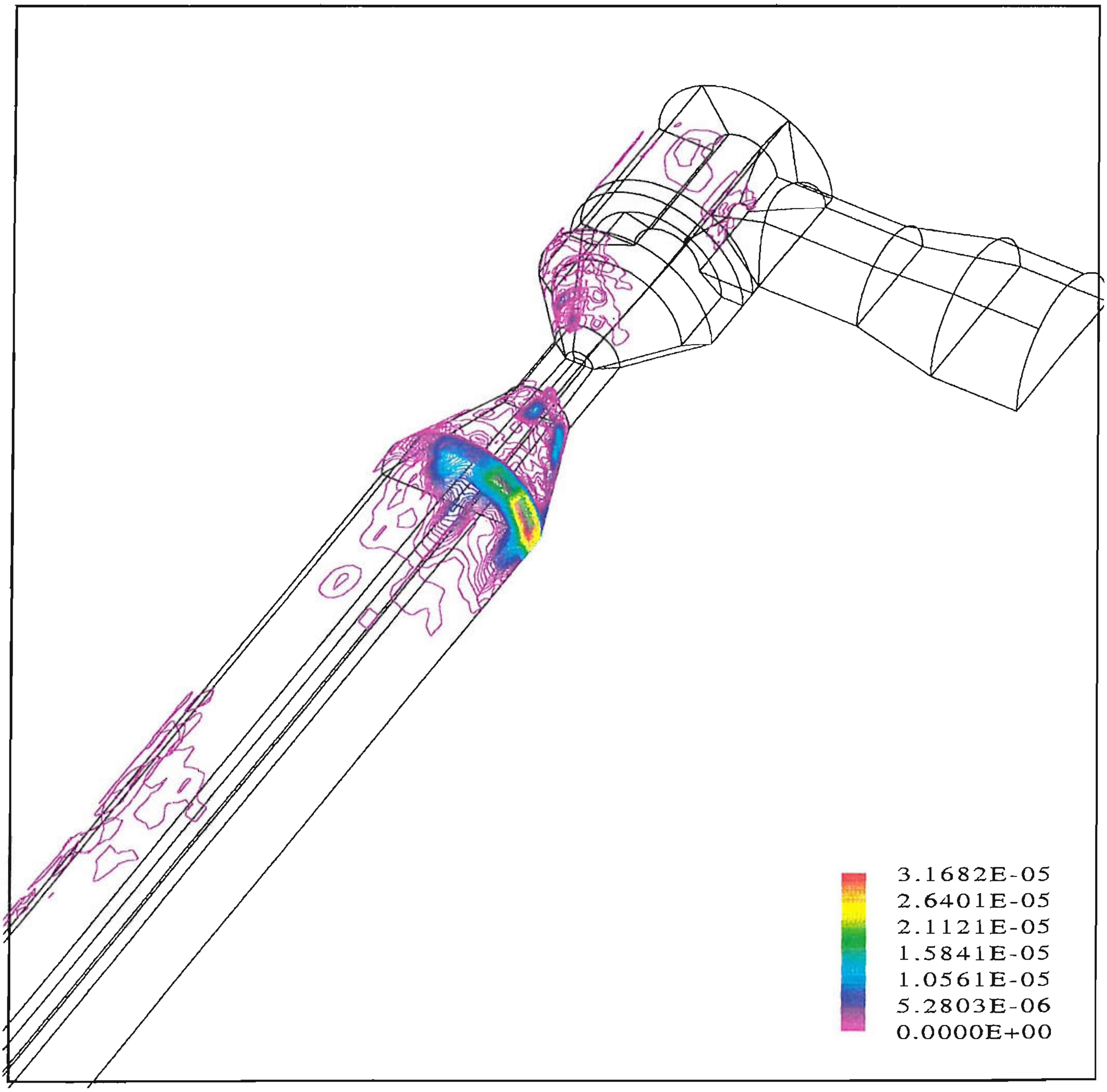

EROSIONAL TRENDS OF A CONVENTIONAL NEEDLE AND SEAT CHOKE (DIFFERENTIAL STRESS MODEL)

Test Number - **5**
Particle Type - **Sand**
Particle Roundness Factor - **0.5**
Particle Flux Rate - **1** % by wt.
Number of Particle Sizes - **6**
Particle Size Range - **50-100** μm
Turbulent Dispersion - **Yes**

Appendix Figure 51 - Differential Stress Model Surface Contour Plot of Needle & Seat Choke Particle Erosion Rates (mm^3/hr)

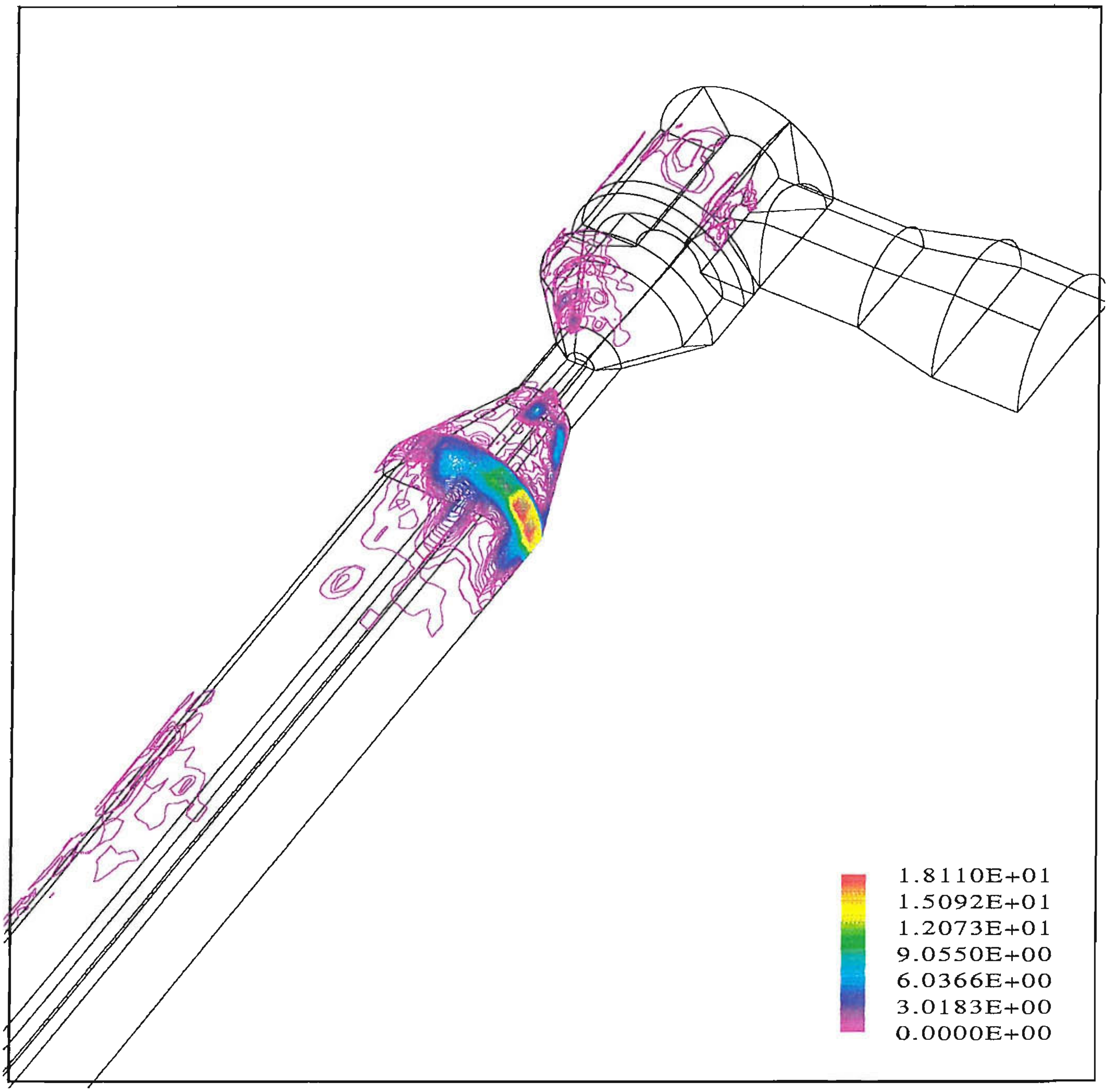

EROSIONAL TRENDS OF A CONVENTIONAL NEEDLE AND SEAT CHOKE (DIFFERENTIAL STRESS MODEL)

Test Number - **5**
Particle Type - **Sand**
Particle Roundness Factor - **0.5**
Particle Flux Rate - **1** % by wt.
Number of Particle Sizes - **6**
Particle Size Range - **50-100** μm
Turbulent Dispersion - **Yes**

Appendix Figure 52 - Differential Stress Model Surface Contour Plot of Needle & Seat Choke Particle Erosion Rates (mm³/hr)

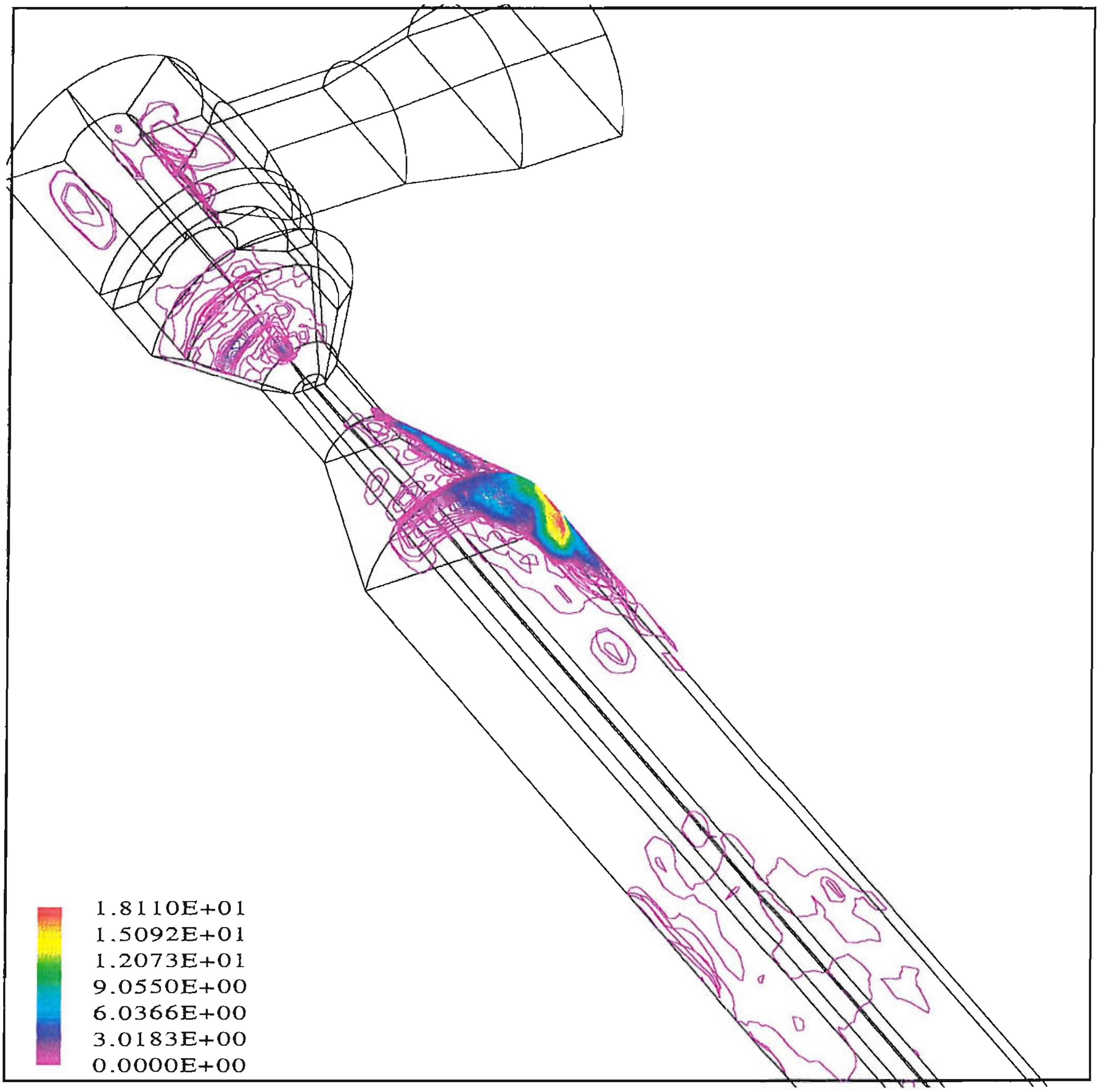

EROSIONAL TRENDS OF A CONVENTIONAL NEEDLE AND SEAT CHOKE (DIFFERENTIAL STRESS MODEL)

Test Number - **6**
Particle Type - **Sand**
Particle Roundness Factor - **0.5**
Particle Flux Rate - **1** % by wt.
Number of Particle Sizes - **6**
Particle Size Range - **50-100** μm
Turbulent Dispersion - **No**

Appendix Figure 53 - Differential Stress Model Surface Contour Plot of Needle & Seat Choke Particle Impact Velocities (m/s)

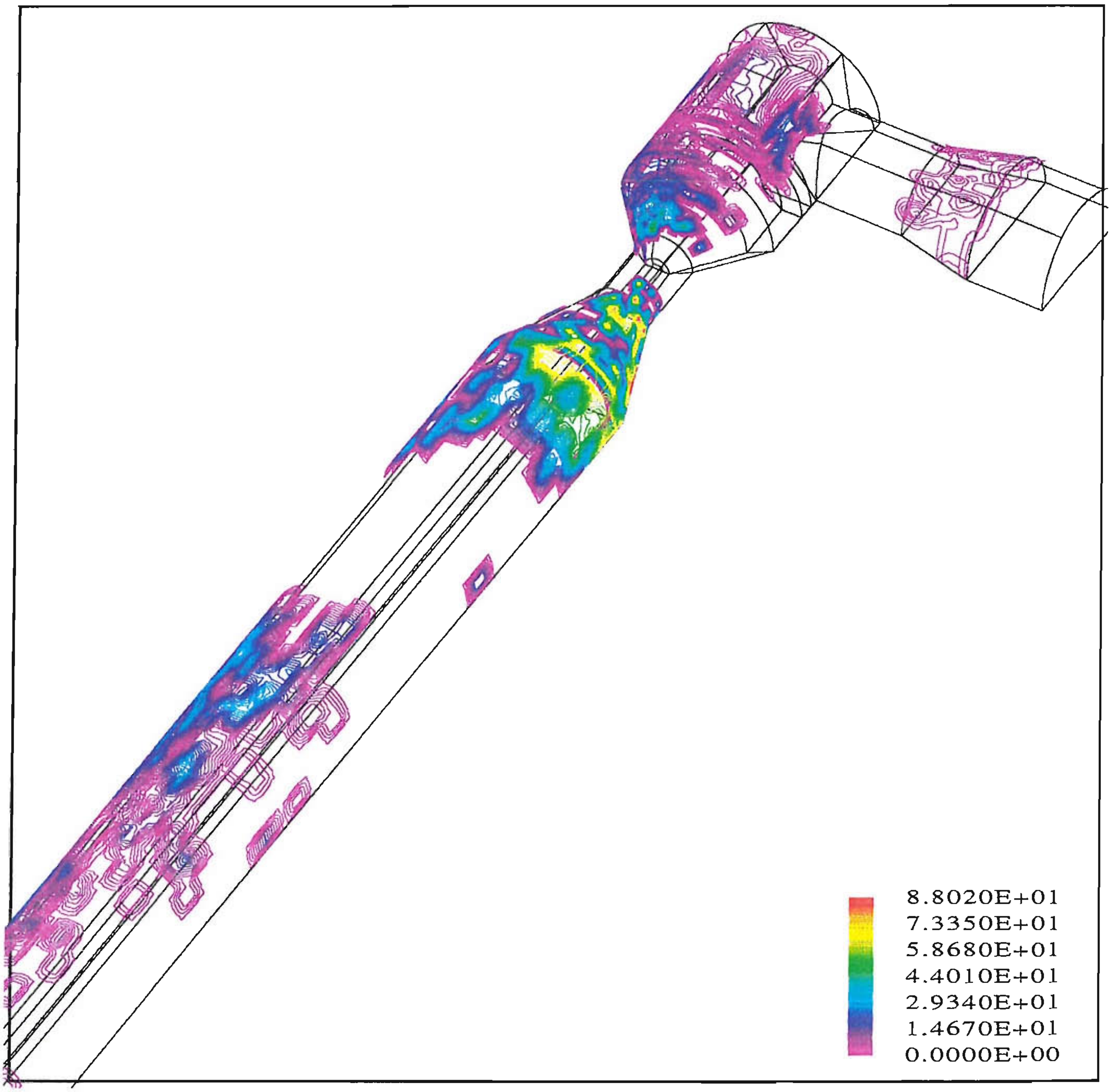

EROSIONAL TRENDS OF A CONVENTIONAL NEEDLE AND SEAT CHOKE (DIFFERENTIAL STRESS MODEL)

Test Number - **6**
Particle Type - **Sand**
Particle Roundness Factor - **0.5**
Particle Flux Rate - **1** % by wt.
Number of Particle Sizes - **6**
Particle Size Range - **50-100** µm
Turbulent Dispersion - **No**

Appendix Figure 54 - Differential Stress Model Surface Contour Plot of Needle & Seat Choke Particle Impact Angles (Deg)

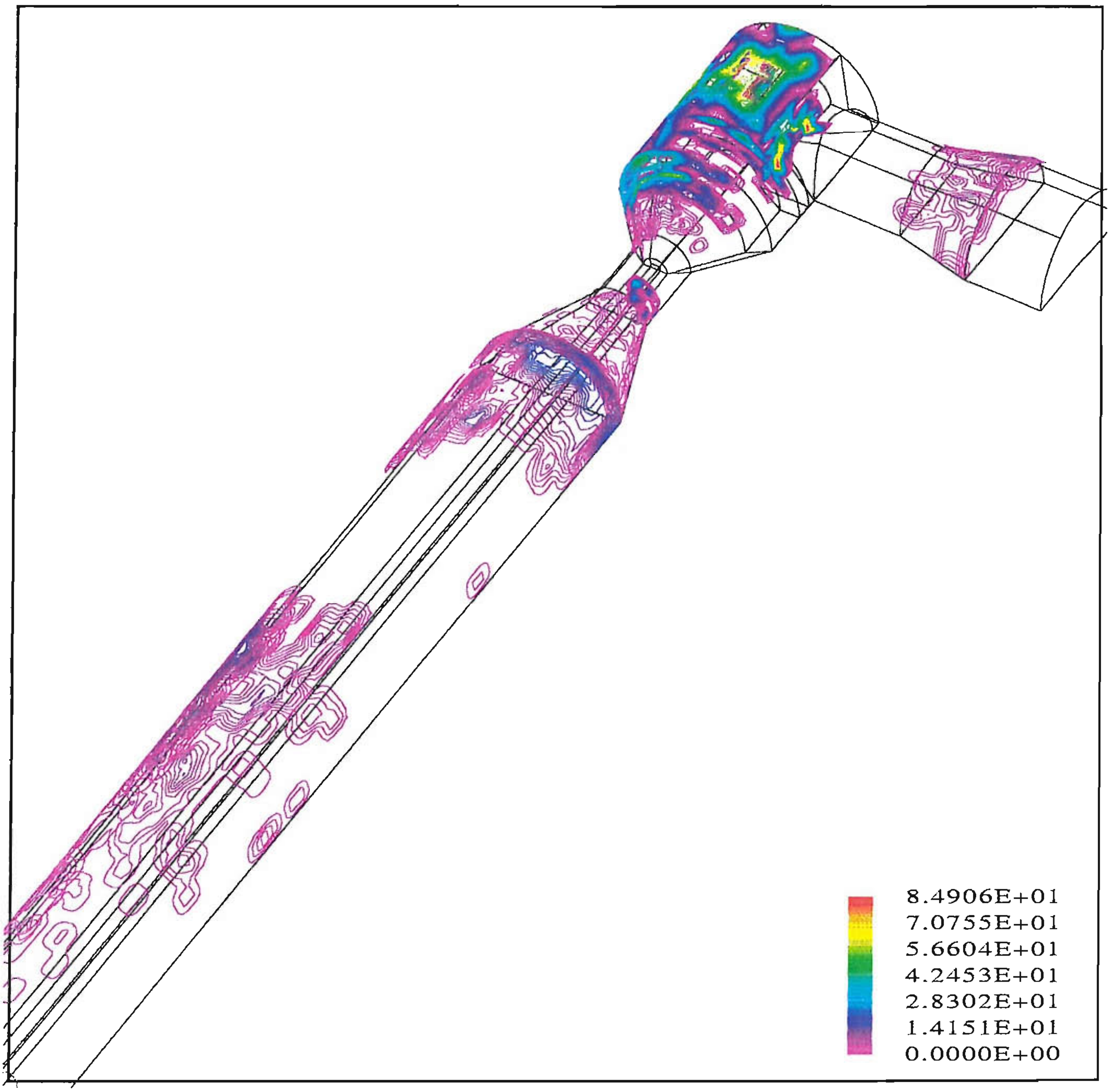

EROSIONAL TRENDS OF A CONVENTIONAL NEEDLE AND SEAT CHOKE (DIFFERENTIAL STRESS MODEL)

Test Number - **6**
Particle Type - **Sand**
Particle Roundness Factor - **0.5**
Particle Flux Rate - **1** % by wt.
Number of Particle Sizes - **6**
Particle Size Range - **50-100** μm
Turbulent Dispersion - **No**

Appendix Figure 55 - Differential Stress Model Surface Contour Plot of Needle & Seat Choke Particle Impact Kinetic Energy (J)

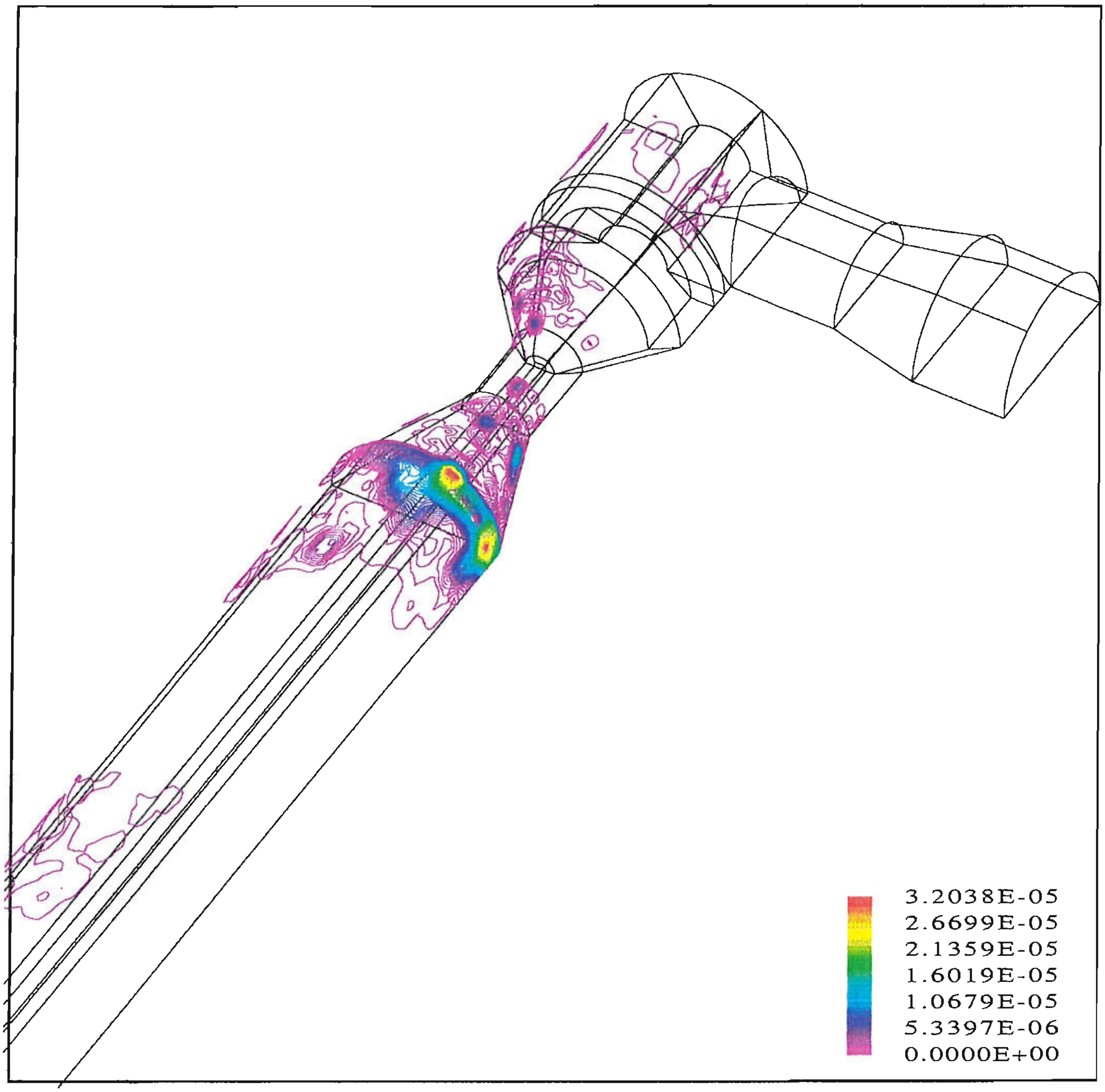

EROSIONAL TRENDS OF A CONVENTIONAL NEEDLE AND SEAT CHOKE (DIFFERENTIAL STRESS MODEL)

Test Number - **6**
Particle Type - **Sand**
Particle Roundness Factor - **0.5**
Particle Flux Rate - **1** % by wt.
Number of Particle Sizes - **6**
Particle Size Range - **50-100** μm
Turbulent Dispersion - **No**

Appendix Figure 56 - Differential Stress Model Surface Contour Plot of Needle & Seat Choke Particle Erosion Rates (mm^3/hr)

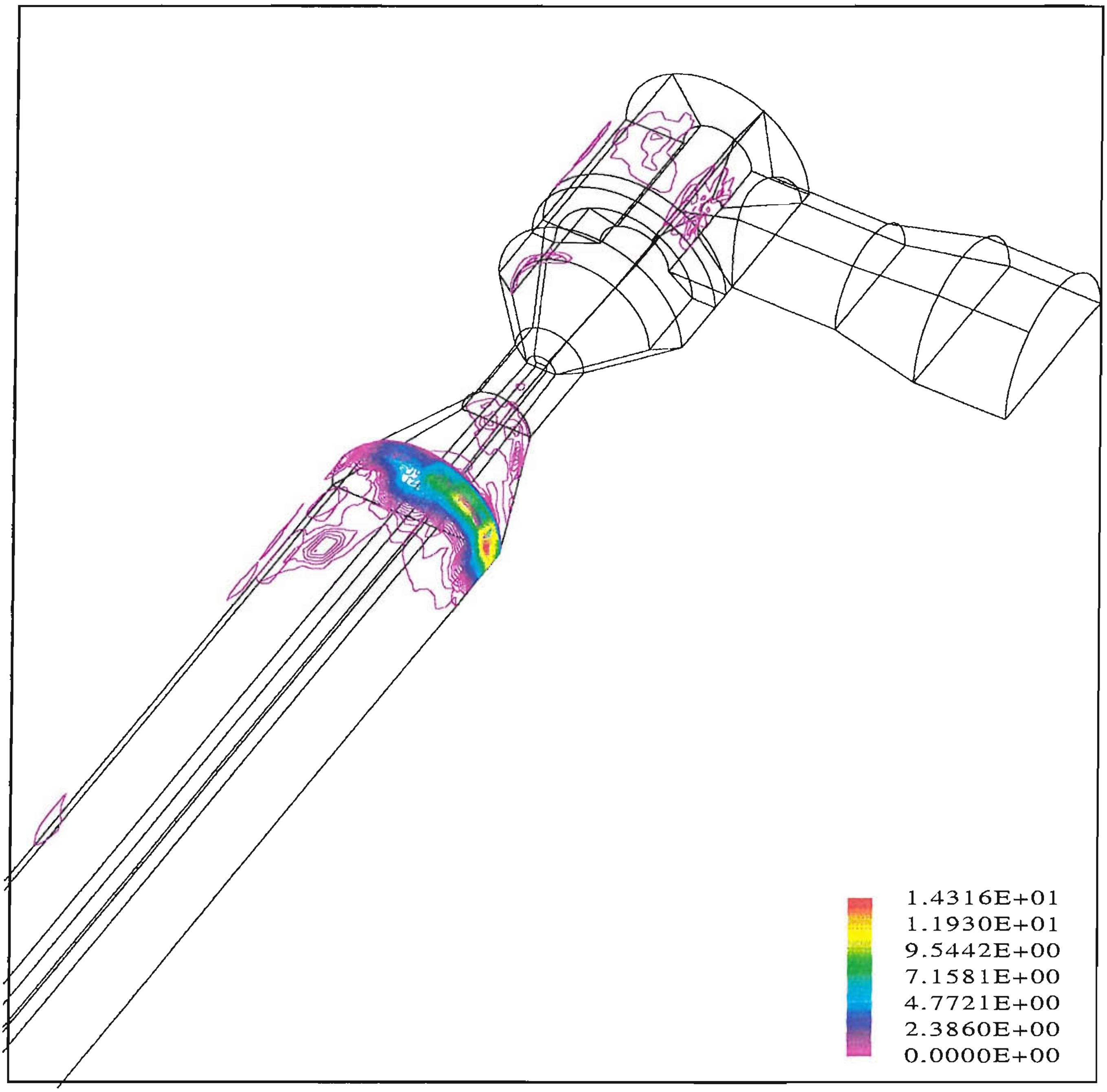

EROSIONAL TRENDS OF A CONVENTIONAL NEEDLE AND SEAT CHOKE (DIFFERENTIAL STRESS MODEL)

Test Number - **6**
Particle Type - **Sand**
Particle Roundness Factor - **0.5**
Particle Flux Rate - **1** % by wt.
Number of Particle Sizes - **6**
Particle Size Range - **50-100** μm
Turbulent Dispersion - **No**

Appendix Figure 57 - Differential Stress Model Surface Contour Plot of Needle & Seat Choke Particle Erosion Rates (mm^3/hr)

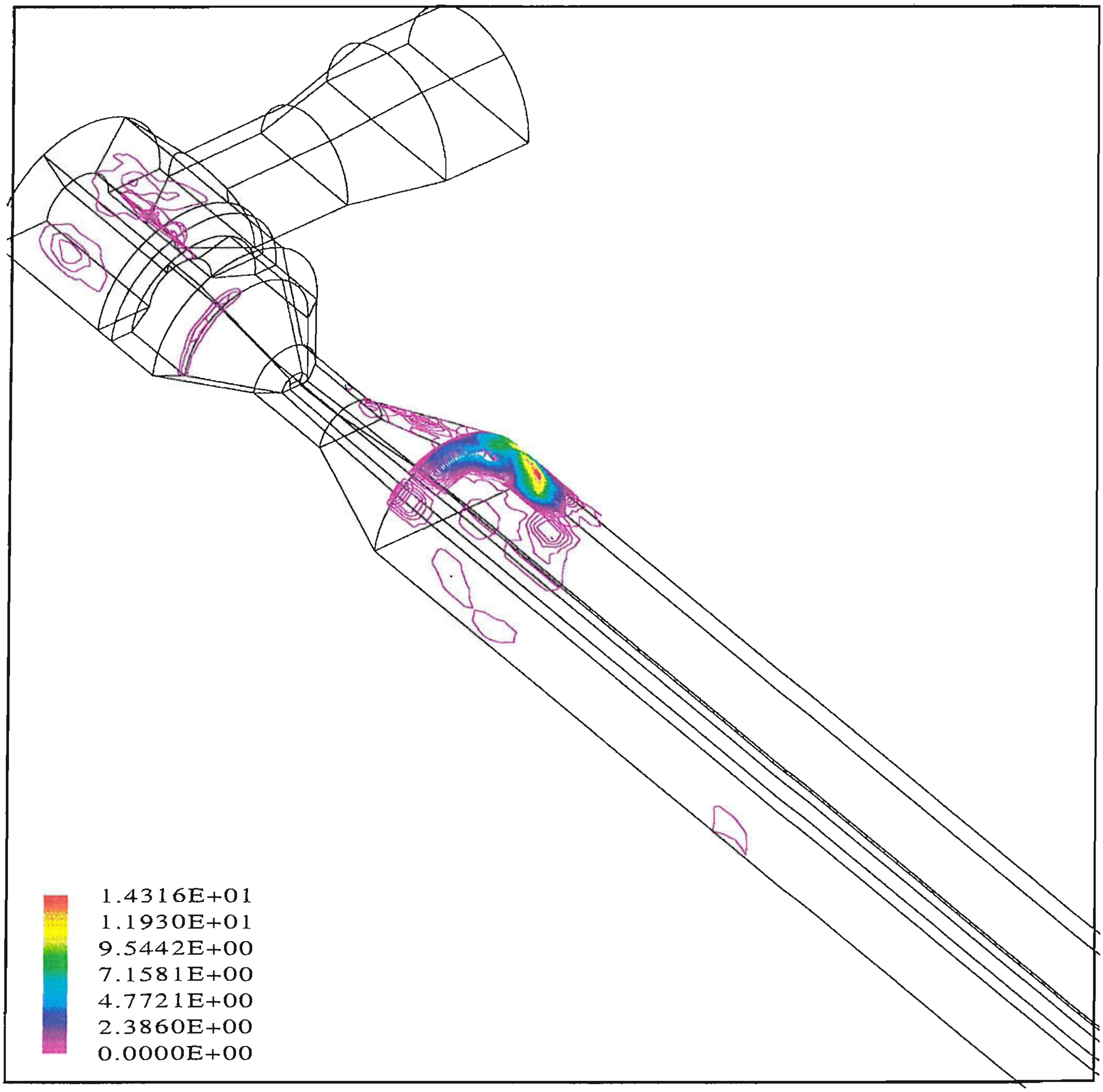

EROSIONAL TRENDS OF A CONVENTIONAL NEEDLE AND SEAT CHOKE (DIFFERENTIAL STRESS MODEL)

Test Number - **7**
Particle Type - **Sand**
Particle Roundness Factor - **0.5**
Particle Flux Rate - **1** % by wt.
Number of Particle Sizes - **6**
Particle Size Range - **150-200** μm
Turbulent Dispersion - **Yes**

Appendix Figure 58 - Differential Stress Model Surface Contour Plot of Needle & Seat Choke Particle Impact Velocities (m/s)

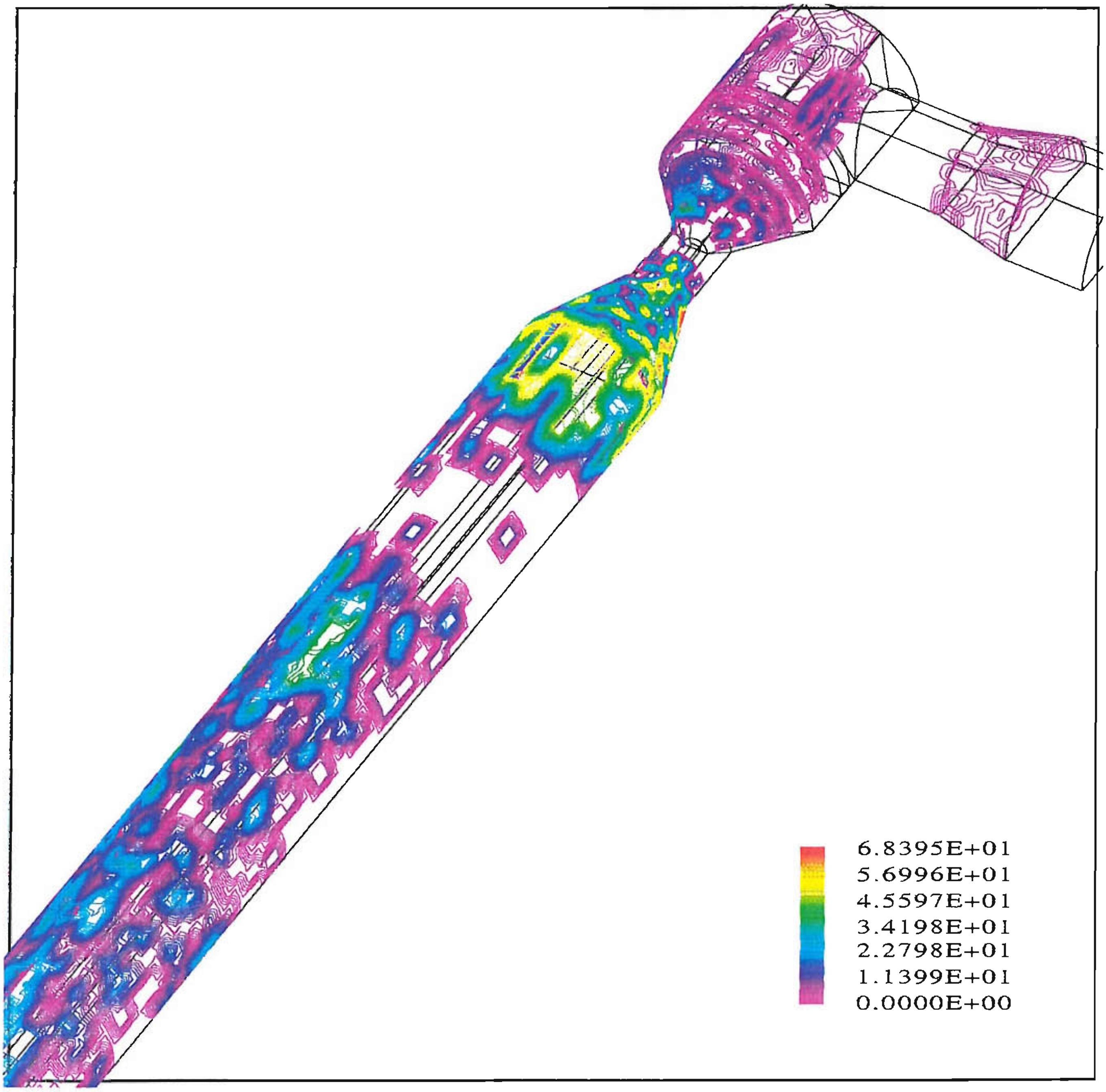

EROSIONAL TRENDS OF A CONVENTIONAL NEEDLE AND SEAT CHOKE (DIFFERENTIAL STRESS MODEL)

Test Number - **7**
Particle Type - **Sand**
Particle Roundness Factor - **0.5**
Particle Flux Rate - **1** % by wt.
Number of Particle Sizes - **6**
Particle Size Range - **150-200** μm
Turbulent Dispersion - **Yes**

Appendix Figure 59 - Differential Stress Model Surface Contour Plot of Needle & Seat Choke Particle Impact Angles (Deg)

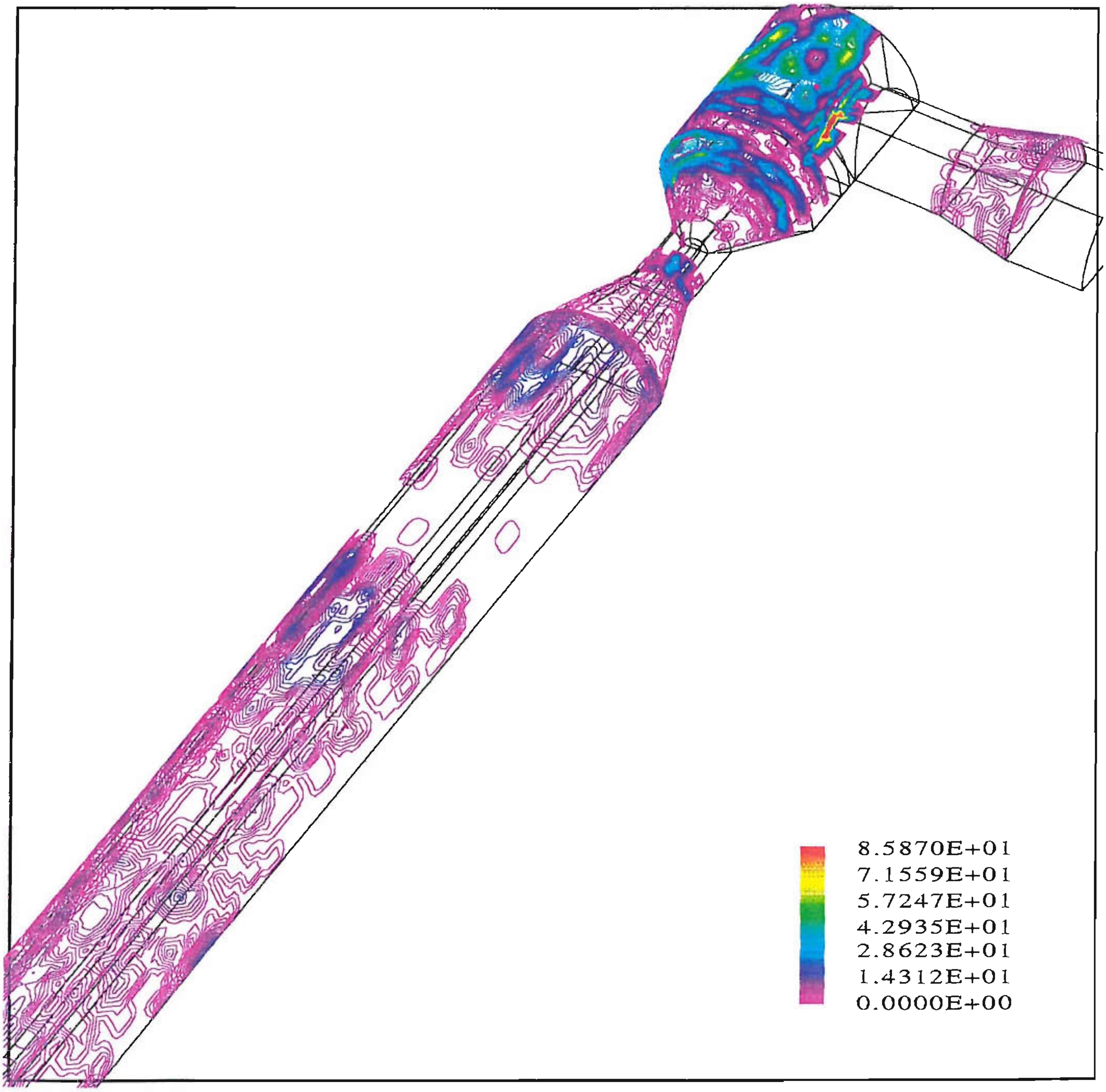

EROSIONAL TRENDS OF A CONVENTIONAL NEEDLE AND SEAT CHOKE (DIFFERENTIAL STRESS MODEL)

Test Number - **7**
Particle Type - **Sand**
Particle Roundness Factor - **0.5**
Particle Flux Rate - **1** % by wt.
Number of Particle Sizes - **6**
Particle Size Range - **150-200** μm
Turbulent Dispersion - **Yes**

Appendix Figure 60 - Differential Stress Model Surface Contour Plot of Needle & Seat Choke Particle Impact Kinetic Energy (J)

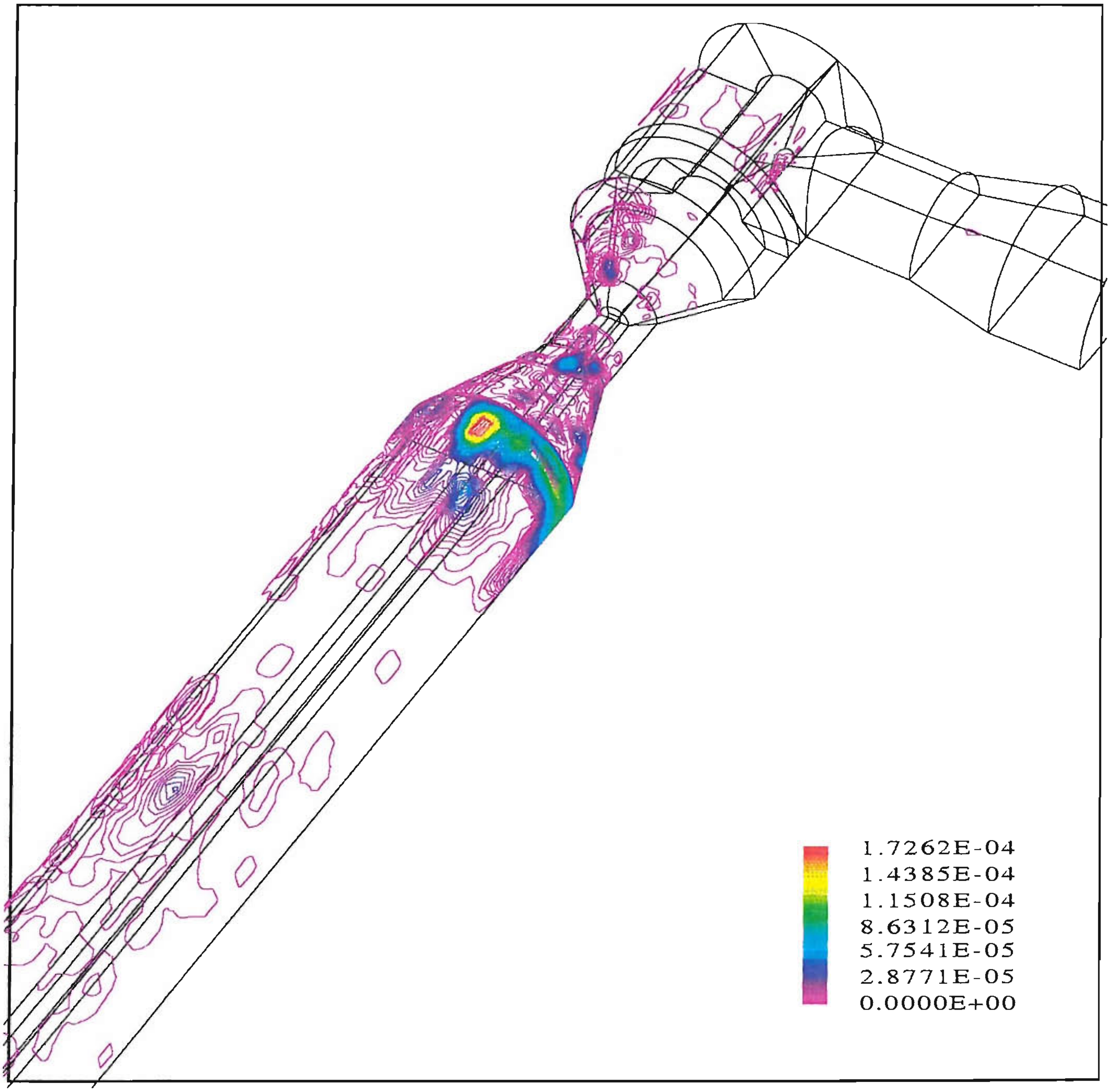

EROSIONAL TRENDS OF A CONVENTIONAL NEEDLE AND SEAT CHOKE (DIFFERENTIAL STRESS MODEL)

Test Number - **7**
Particle Type - **Sand**
Particle Roundness Factor - **0.5**
Particle Flux Rate - **1** % by wt.
Number of Particle Sizes - **6**
Particle Size Range - **150-200** μm
Turbulent Dispersion - **Yes**

Appendix Figure 61 - Differential Stress Model Surface Contour Plot of Needle & Seat Choke Particle Erosion Rates (mm^3/hr)

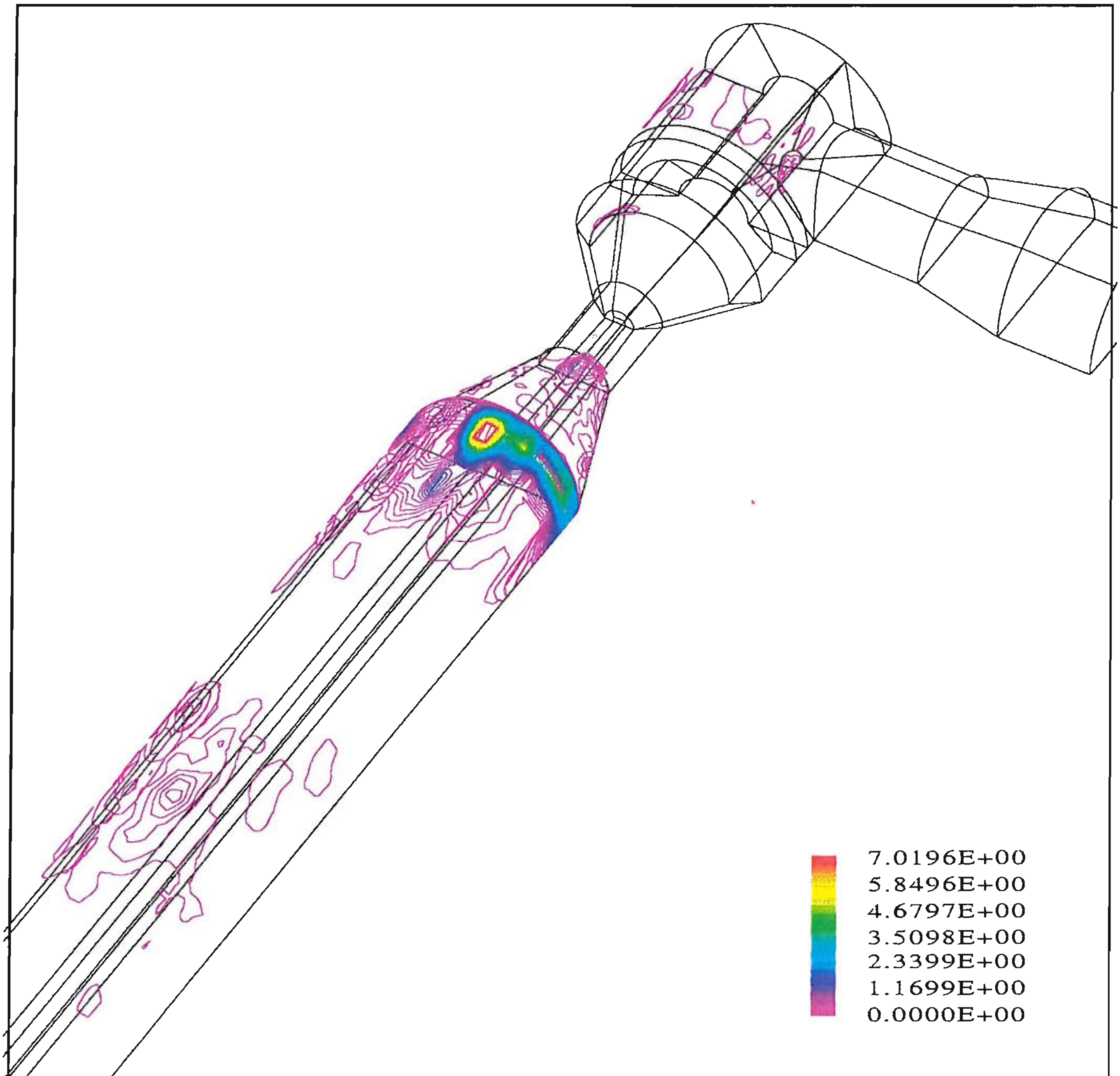

EROSIONAL TRENDS OF A CONVENTIONAL NEEDLE AND SEAT CHOKE (DIFFERENTIAL STRESS MODEL)

Test Number - **7**
Particle Type - **Sand**
Particle Roundness Factor - **0.5**
Particle Flux Rate - **1** % by wt.
Number of Particle Sizes - **6**
Particle Size Range - **150-200** μm
Turbulent Dispersion - **Yes**

Appendix Figure 62 - Differential Stress Model Surface Contour Plot of Needle & Seat Choke Particle Erosion Rates (mm^3/hr)

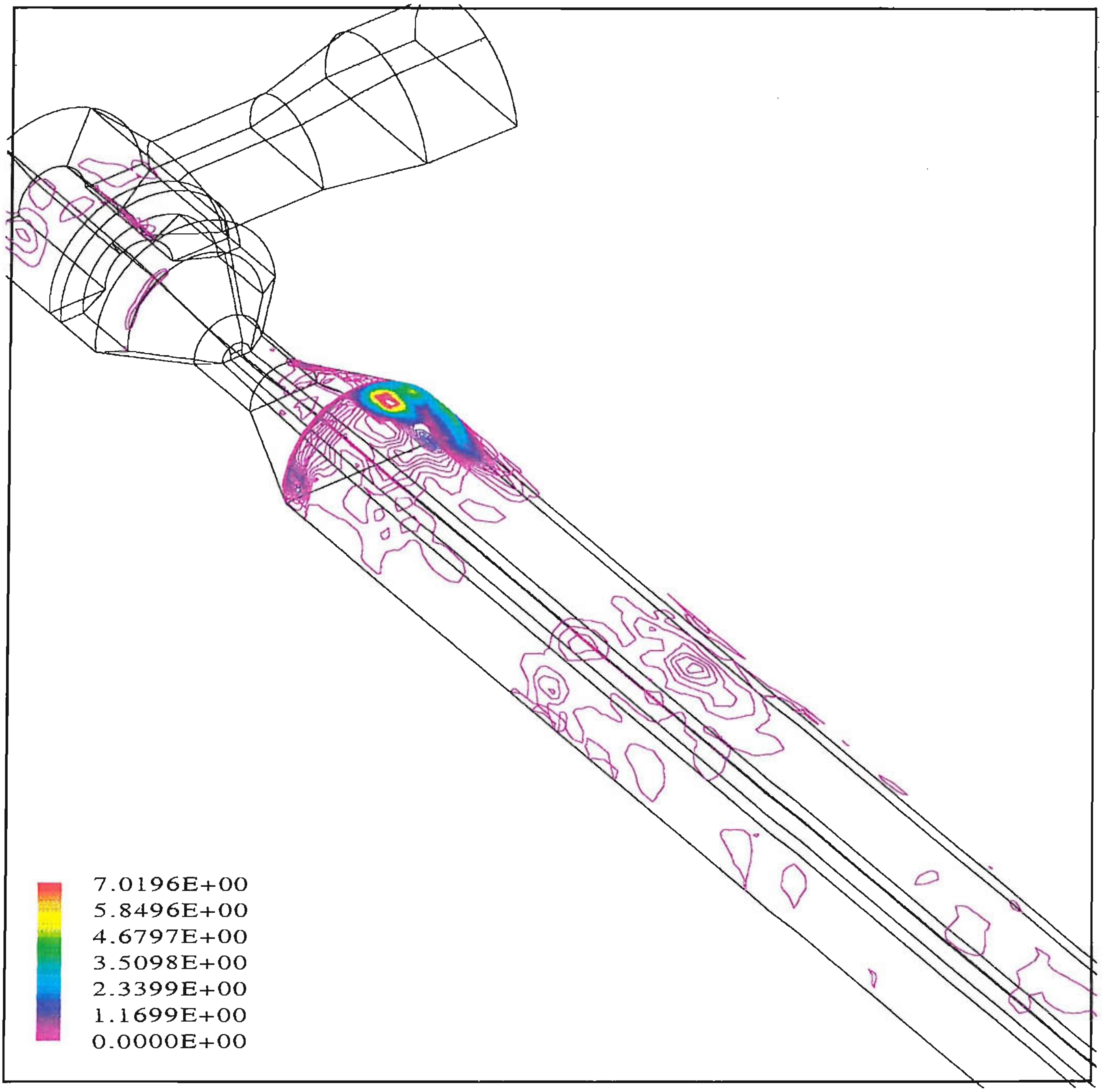

EROSIONAL TRENDS OF A CONVENTIONAL NEEDLE AND SEAT CHOKE (DIFFERENTIAL STRESS MODEL)

Test Number - **8**
Particle Type - **Sand**
Particle Roundness Factor - **0.5**
Particle Flux Rate - **1** % by wt.
Number of Particle Sizes - **6**
Particle Size Range - **150-200** μm
Turbulent Dispersion - **No**

Appendix Figure 63 - Differential Stress Model Surface Contour Plot of Needle & Seat Choke Particle Impact Velocities (m/s)

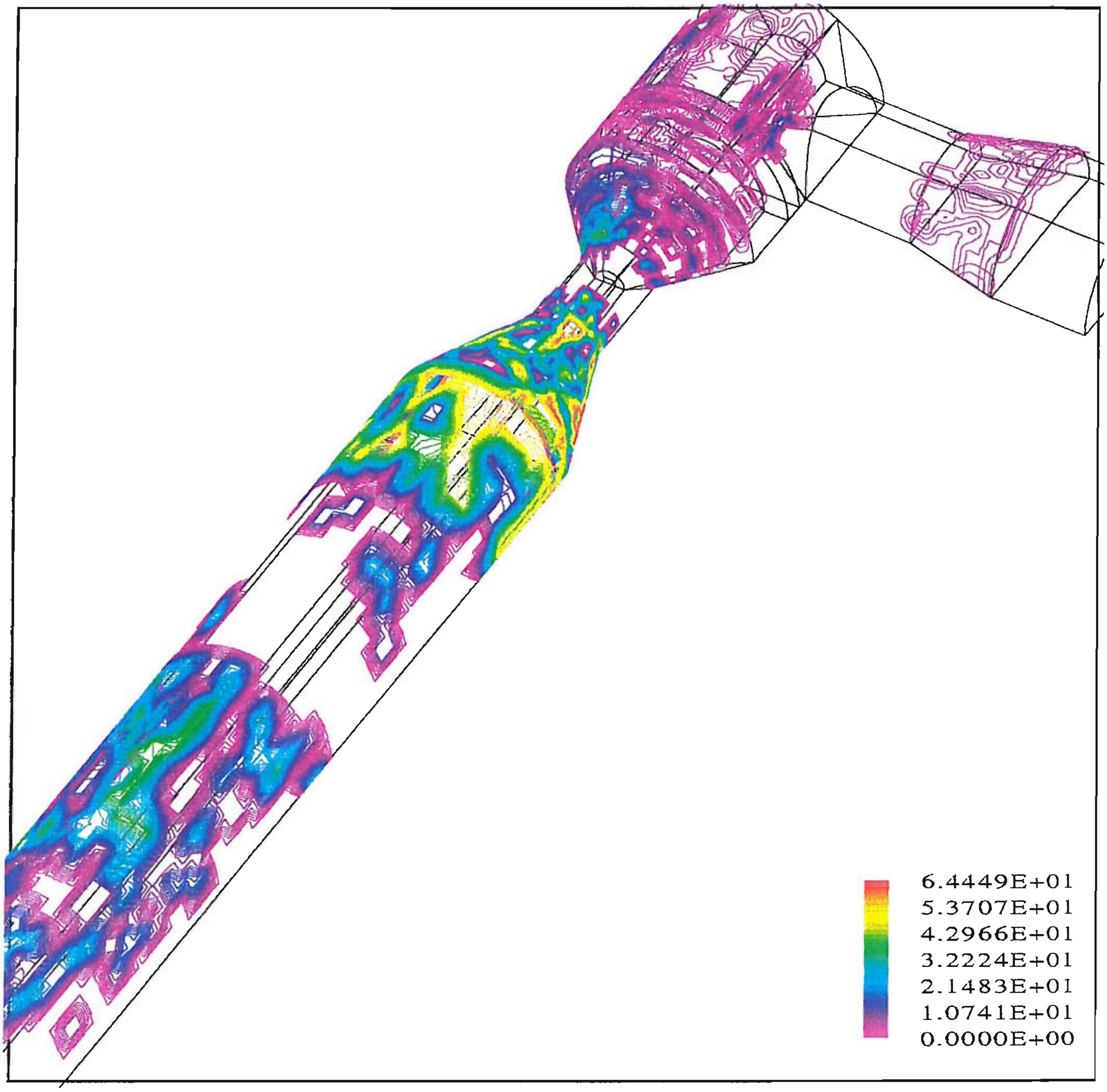

EROSIONAL TRENDS OF A CONVENTIONAL NEEDLE AND SEAT CHOKE (DIFFERENTIAL STRESS MODEL)

Test Number - **8**
Particle Type - **Sand**
Particle Roundness Factor - **0.5**
Particle Flux Rate - **1** % by wt.
Number of Particle Sizes - **6**
Particle Size Range - **150-200** µm
Turbulent Dispersion - **No**

Appendix Figure 64 - Differential Stress Model Surface Contour Plot of Needle & Seat Choke Particle Impact Angles (Deg)

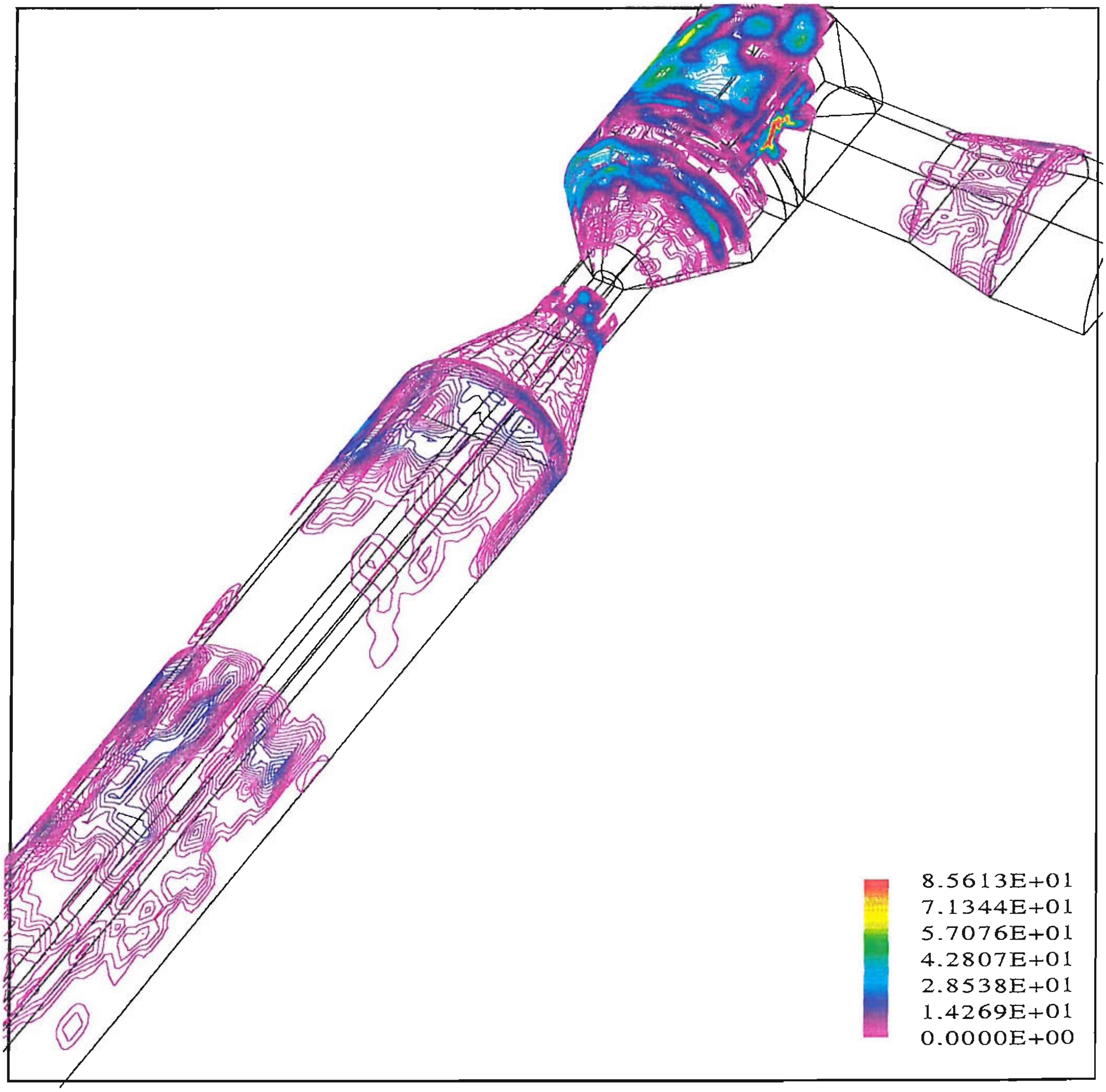

Erosional Trends of a Conventional Needle and Seat Choke (Differential Stress Model)

Test Number - **8**

Particle Type - **Sand**

Particle Roundness Factor - **0.5**

Particle Flux Rate - **1 % by wt.**

Number of Particle Sizes - **6**

Particle Size Range - **150-200** μm

Turbulent Dispersion - **No**

Appendix Figure 65 - Differential Stress Model Surface Contour Plot of Needle & Seat Choke Particle Impact Kinetic Energy (J)

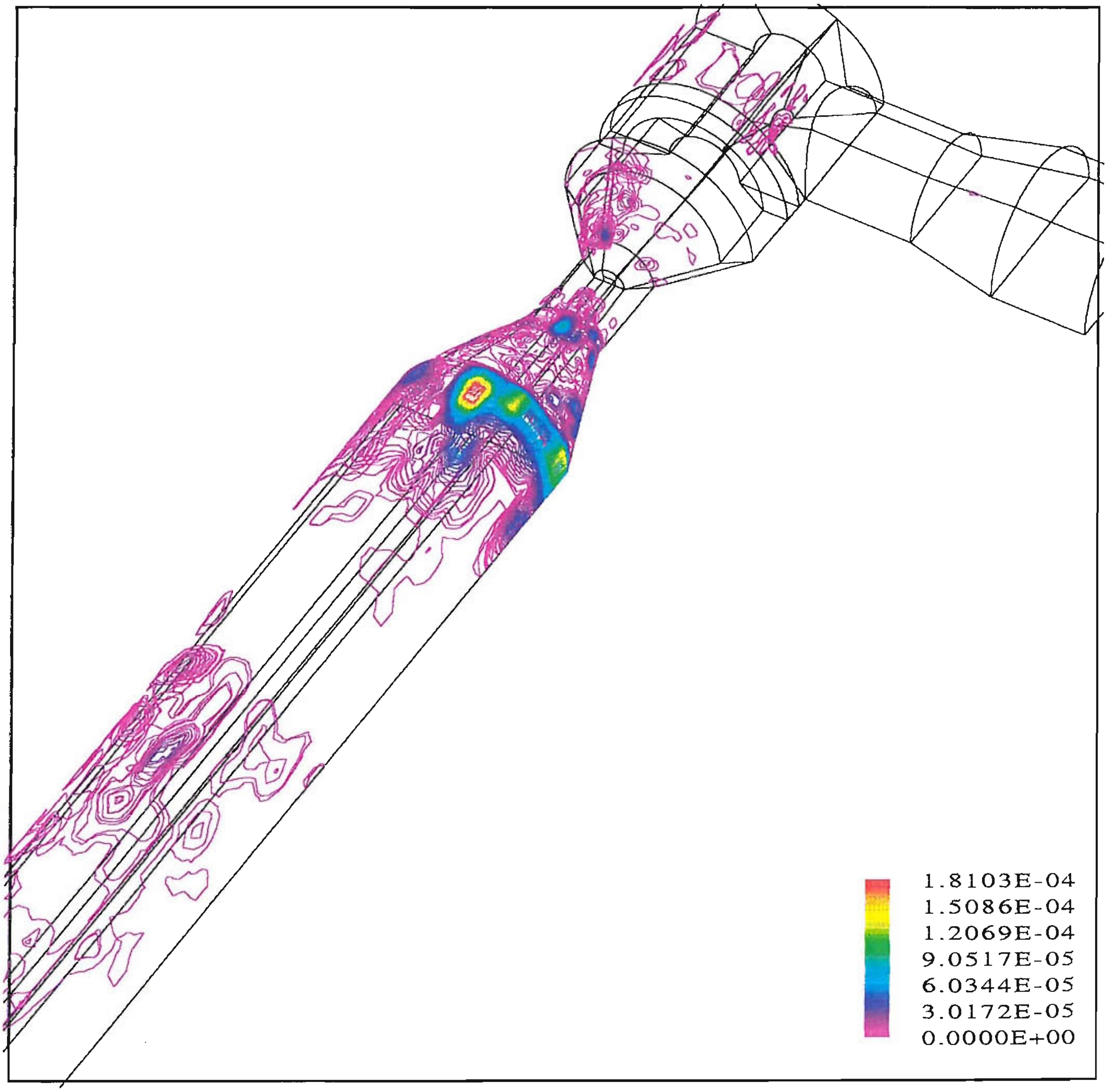

EROSIONAL TRENDS OF A CONVENTIONAL NEEDLE AND SEAT CHOKE (DIFFERENTIAL STRESS MODEL)

Test Number - **8**
Particle Type - **Sand**
Particle Roundness Factor - **0.5**
Particle Flux Rate - **1** % by wt.
Number of Particle Sizes - **6**
Particle Size Range - **150-200** μm
Turbulent Dispersion - **No**

Appendix Figure 66 - Differential Stress Model Surface Contour Plot of Needle & Seat Choke Particle Erosion Rates (mm³/hr)

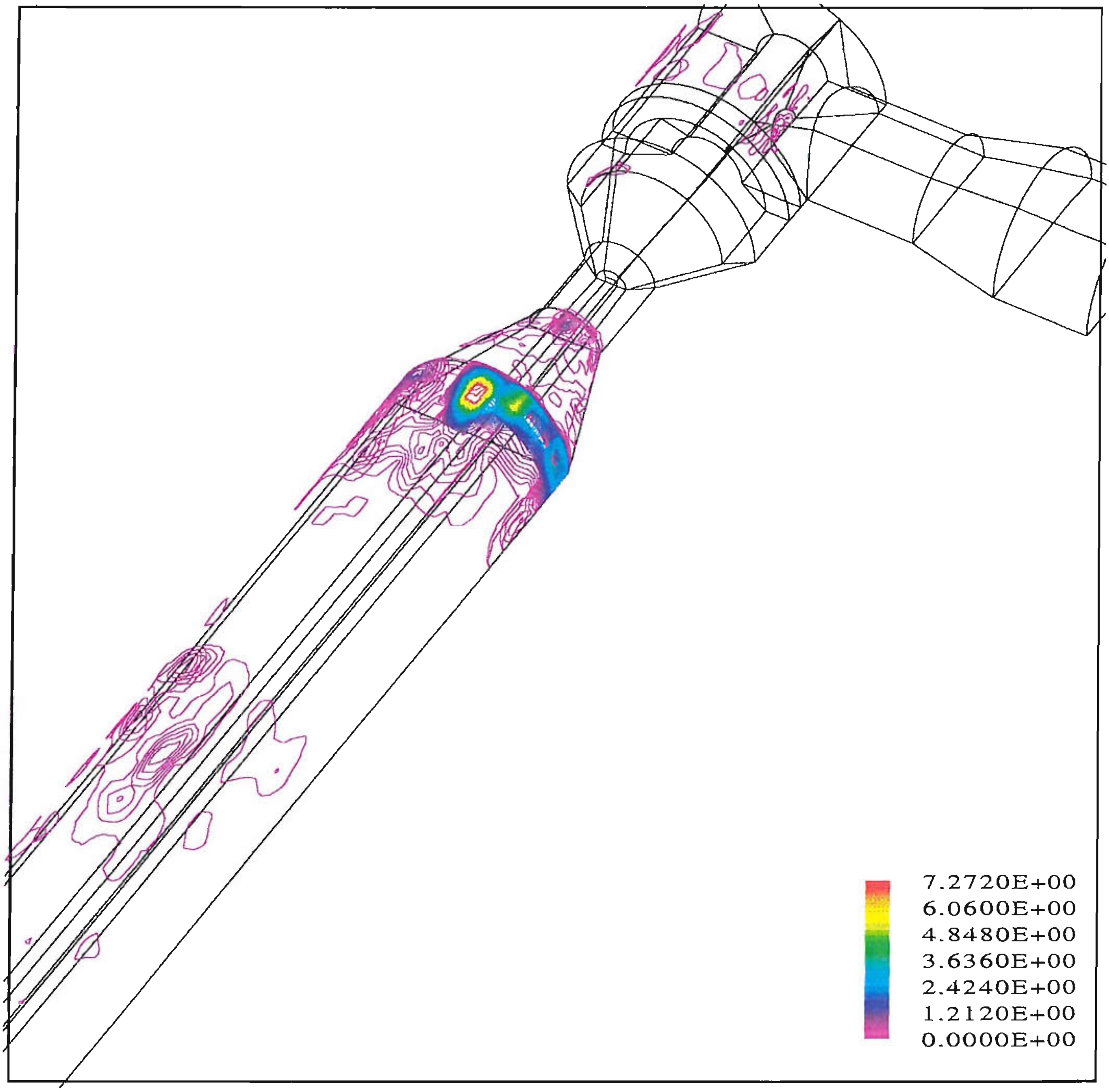

EROSIONAL TRENDS OF A CONVENTIONAL NEEDLE AND SEAT CHOKE (DIFFERENTIAL STRESS MODEL)

Test Number - **8**
Particle Type - **Sand**
Particle Roundness Factor - **0.5**
Particle Flux Rate - **1** % by wt.
Number of Particle Sizes - **6**
Particle Size Range - **150-200** μm
Turbulent Dispersion - **No**

Appendix Figure 67 - Differential Stress Model Surface Contour Plot of Needle & Seat Choke Particle Erosion Rates (mm^3/hr)

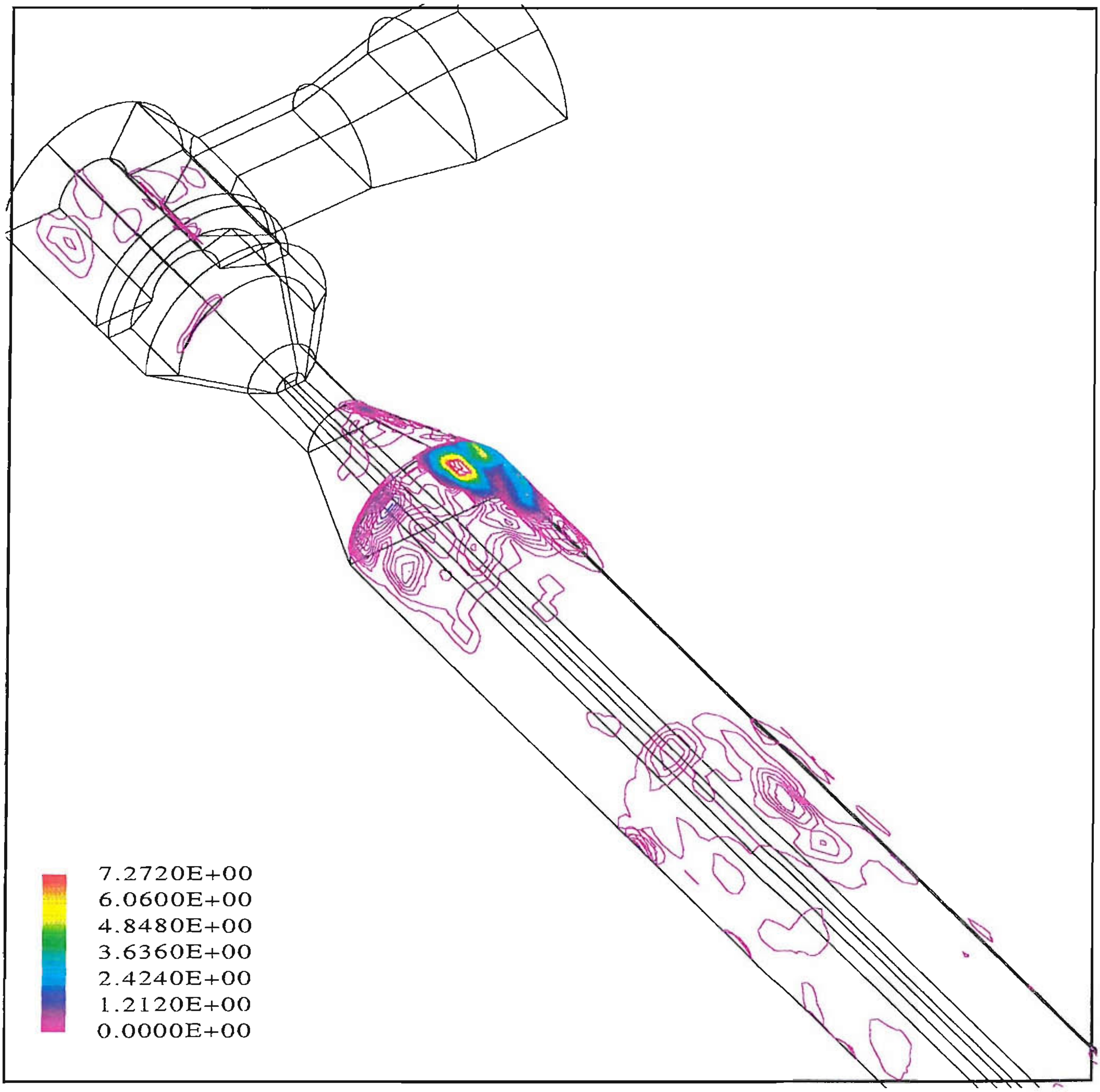

FLOW FIELD OF A EVOLUTION NEEDLE AND SEAT CHOKE (K-EPSILON MODEL)

Fluid - **Dry Air**
Inlet Diameter - **75** mm
Throat Diameter - **25** mm
Taper Angle of Needle - **15°**
Choke Opening - **25** % (Linear)
Pressure Drop - **68** Bar
Mass Flow Rate (air) - **178** kg/hr

Appendix Figure 68 - *k*-Epsilon Model Velocity Contour Plot of Needle & Seat Choke (m/s)

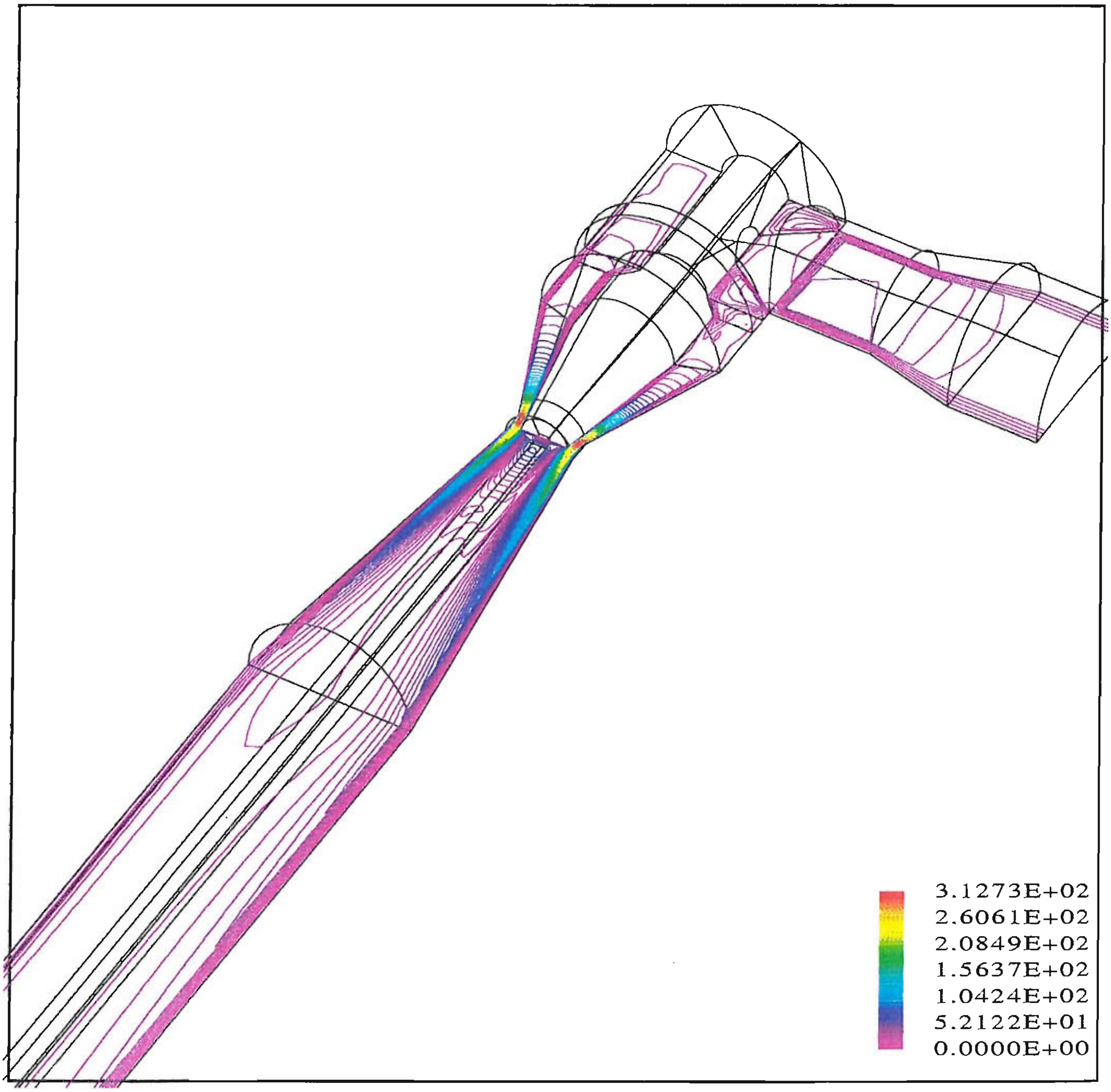

FLOW FIELD OF A EVOLUTION NEEDLE AND SEAT CHOKE (K-EPSILON MODEL)

Fluid - **Dry Air**
Inlet Diameter - **75** mm
Throat Diameter - **25** mm
Taper Angle of Needle - **15°**
Choke Opening - **25** % (Linear)
Pressure Drop - **68** Bar
Mass Flow Rate (air) - **178** kg/hr

Appendix Figure 69 - *k*-Epsilon Model Velocity Contour Plot of Needle & Seat Choke (m/s)

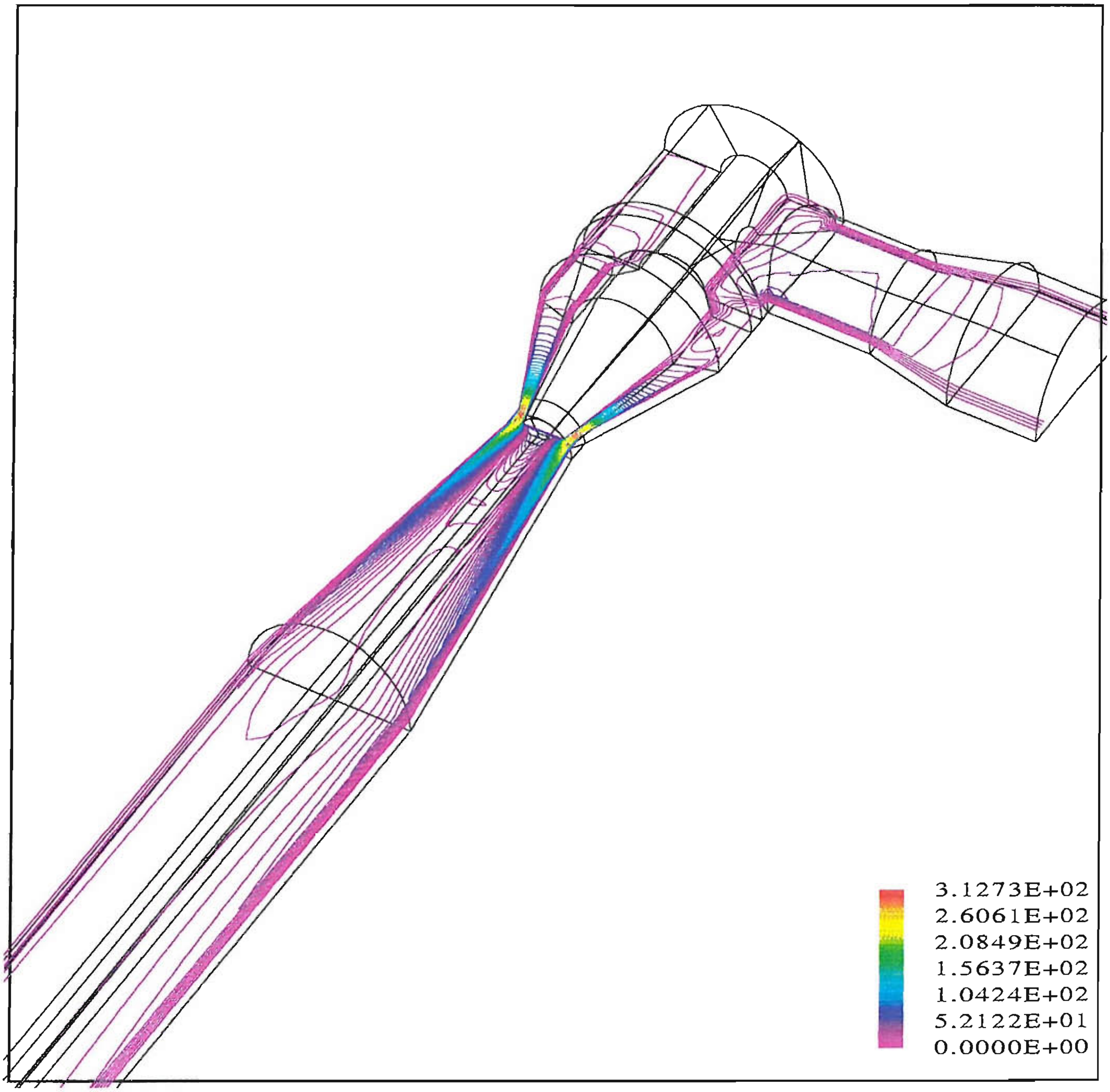

FLOW FIELD OF A EVOLUTION NEEDLE AND SEAT CHOKE (K-EPSILON MODEL)

Fluid - **Dry Air**
Inlet Diameter - **75** mm
Throat Diameter - **25** mm
Taper Angle of Needle - **15°**
Choke Opening - **25** % (Linear)
Pressure Drop - **68** Bar
Mass Flow Rate (air) - **178** kg/hr

Appendix Figure 70 - *k*-Epsilon Model Velocity Contour Plot of Needle & Seat Choke (m/s)

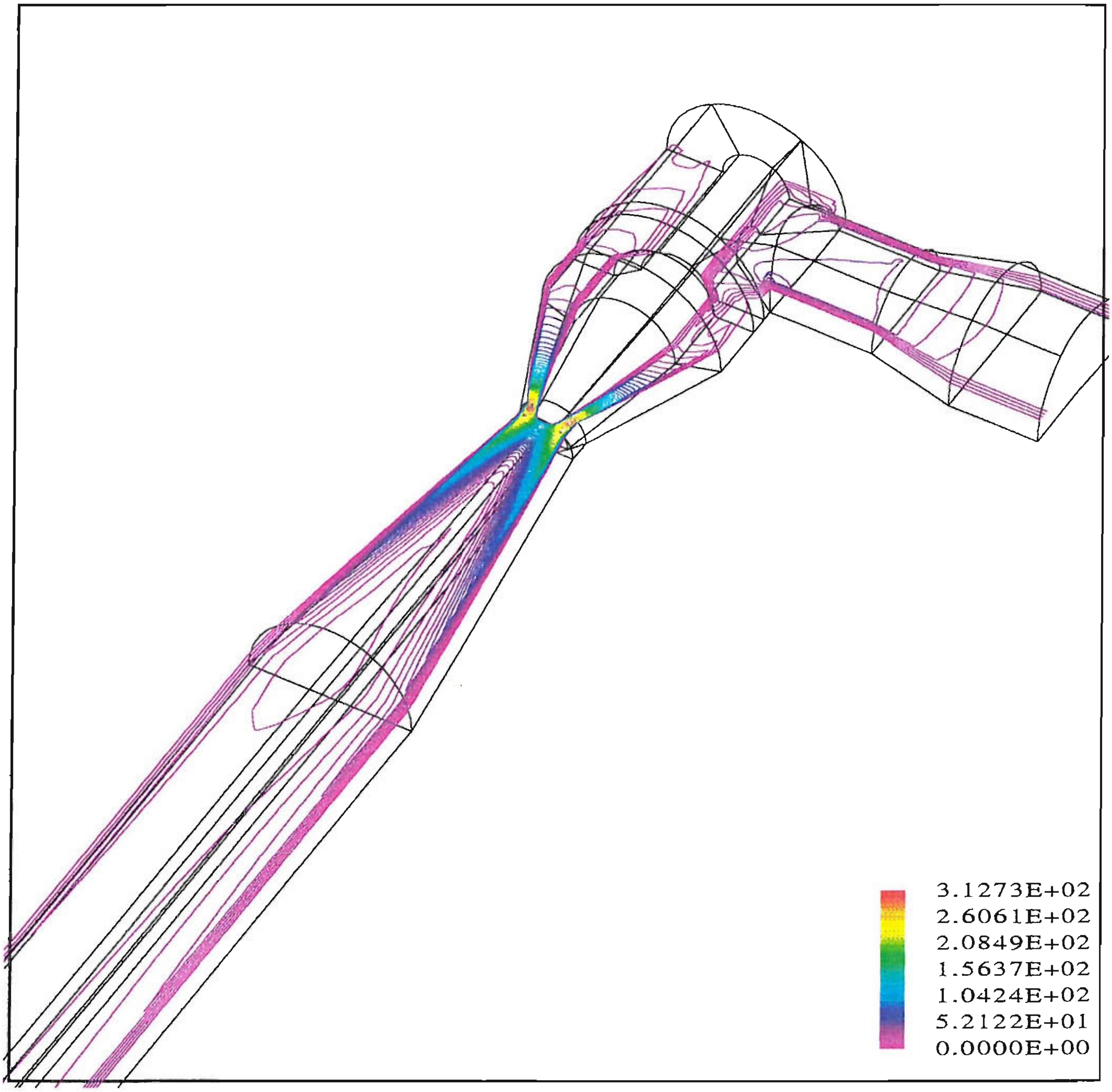

FLOW FIELD OF A EVOLUTION NEEDLE AND SEAT CHOKE (K-EPSILON MODEL)

Fluid - **Dry Air**
Inlet Diameter - **75** mm
Throat Diameter - **25** mm
Taper Angle of Needle - **15°**
Choke Opening - **25** % (Linear)
Pressure Drop - **68** Bar
Mass Flow Rate (air) - **178** kg/hr

Appendix Figure 71 - *k*-Epsilon Model Velocity Contour Plot of Needle & Seat Choke (m/s)

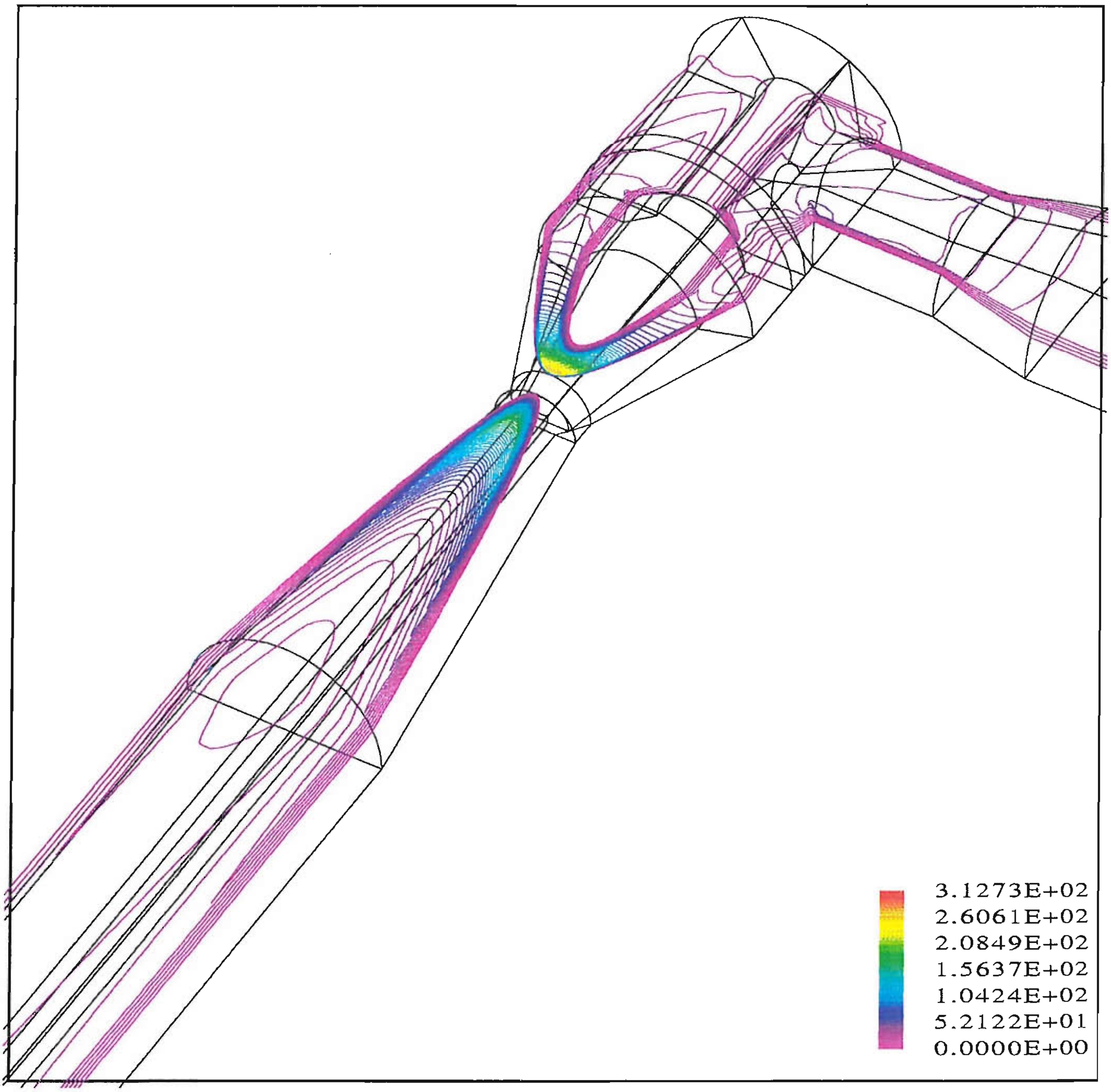

Flow Field of a Evolution Needle and Seat Choke (k-Epsilon Model)

Fluid - **Dry Air**
Inlet Diameter - **75** mm
Throat Diameter - **25** mm
Taper Angle of Needle - **15°**
Choke Opening - **25** % (Linear)
Pressure Drop - **68** Bar
Mass Flow Rate (air) - **178** kg/hr

Appendix Figure 72 - *k*-Epsilon Model Turbulent Kinetic Energy Contour Plot of Needle & Seat Choke

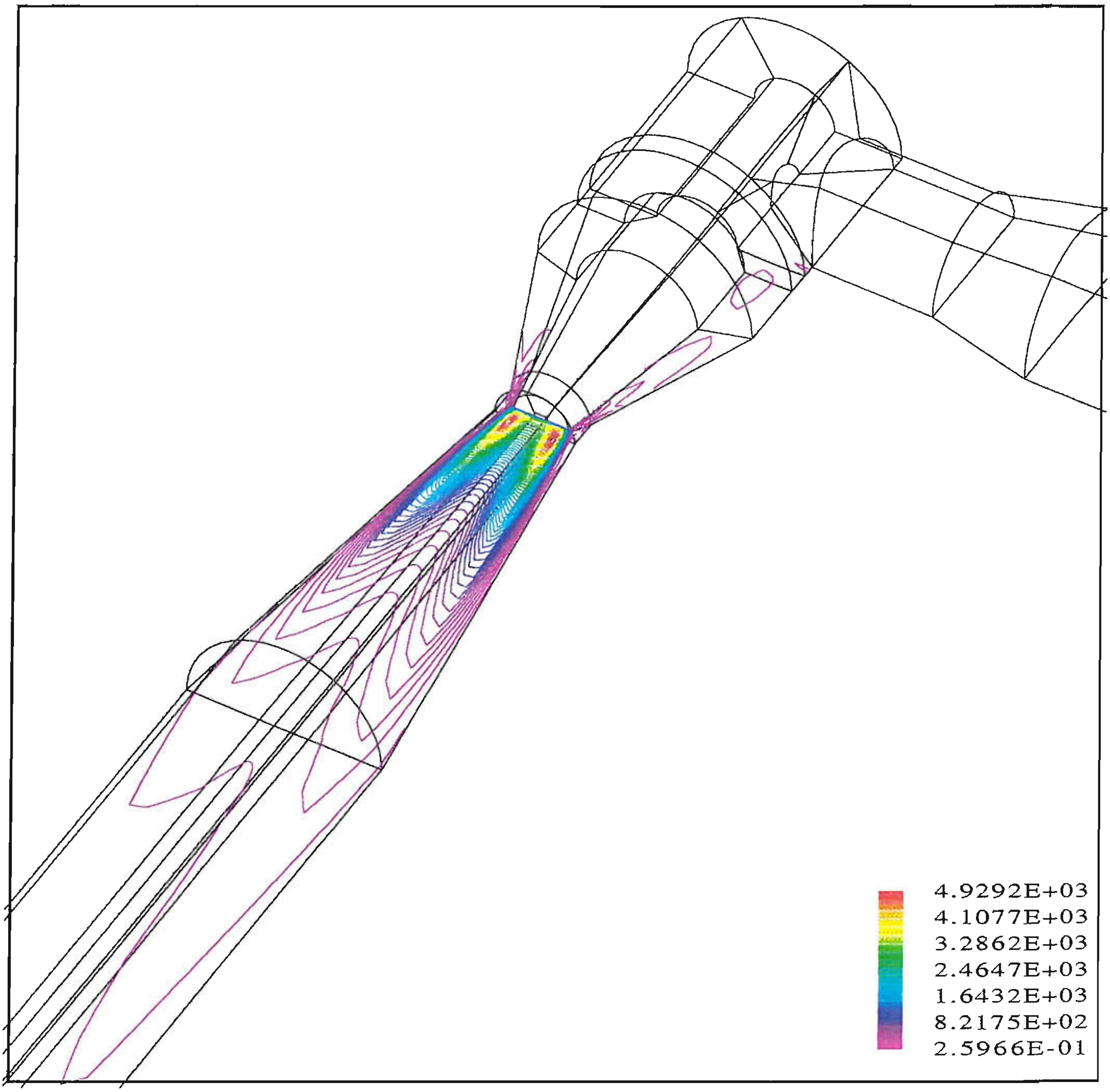

EROSIONAL TRENDS OF A EVOLUTION NEEDLE AND SEAT CHOKE (K-EPSILON MODEL)

Particle Type - **Sand**
Particle Roundness Factor - **0.5**
Particle Flux Rate - **1** % by wt.
Number of Particle Sizes - **6**
Particle Size Range - **150-200** μm
Turbulent Dispersion - **Yes**

Appendix Figure 73 - *k*-Epsilon Model Surface Contour Plot of Needle & Seat Choke Particle Impact Velocities (m/s)

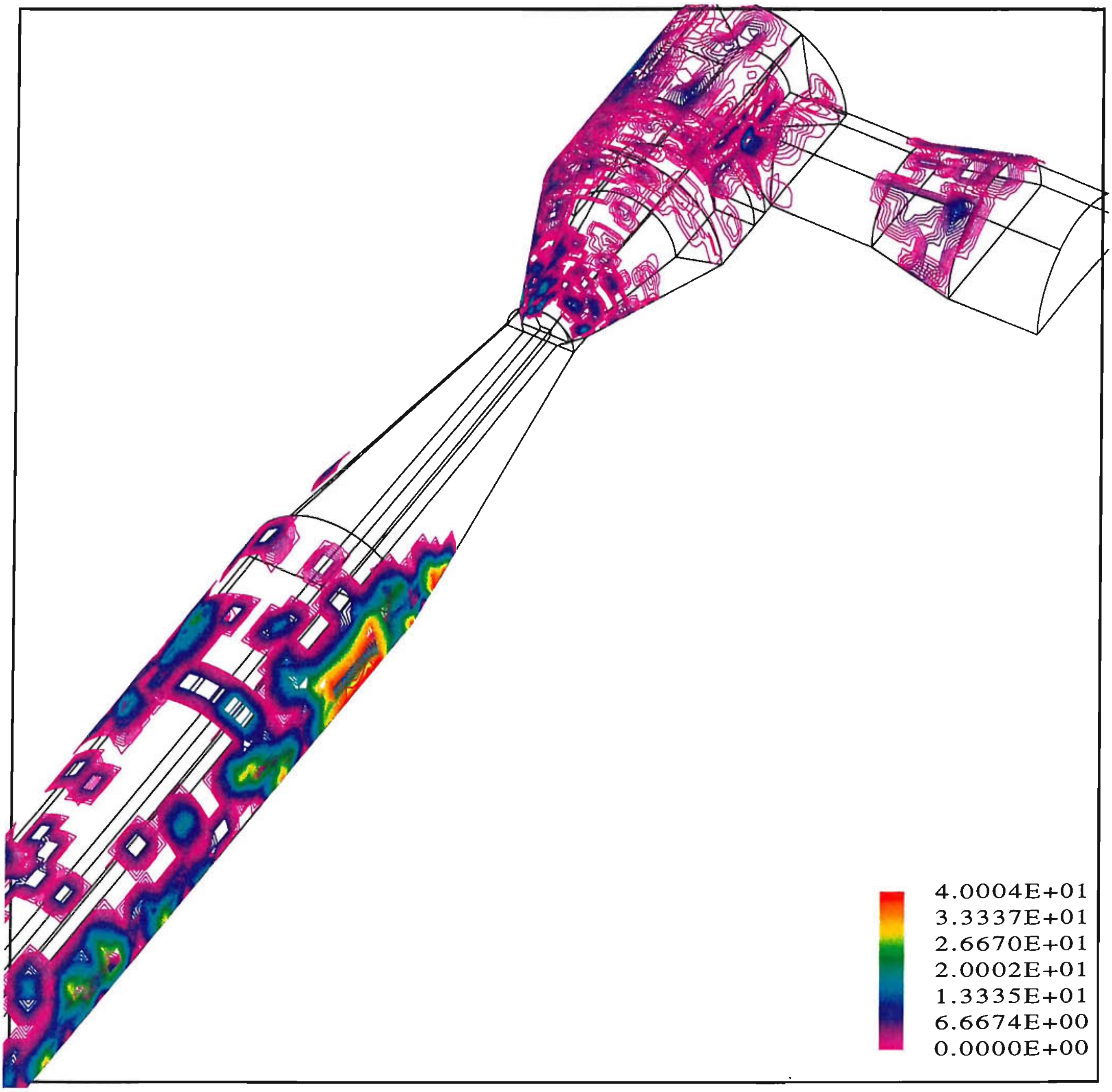

EROSIONAL TRENDS OF A EVOLUTION NEEDLE AND SEAT CHOKE (K-EPSILON MODEL)

Particle Type - **Sand**
Particle Roundness Factor - **0.5**
Particle Flux Rate - **1 %** by wt.
Number of Particle Sizes - **6**
Particle Size Range - **150-200** μm
Turbulent Dispersion - **Yes**

Appendix Figure 74 - *k*-Epsilon Model Surface Contour Plot of Needle & Seat Choke Particle Impact Angles (Deg)

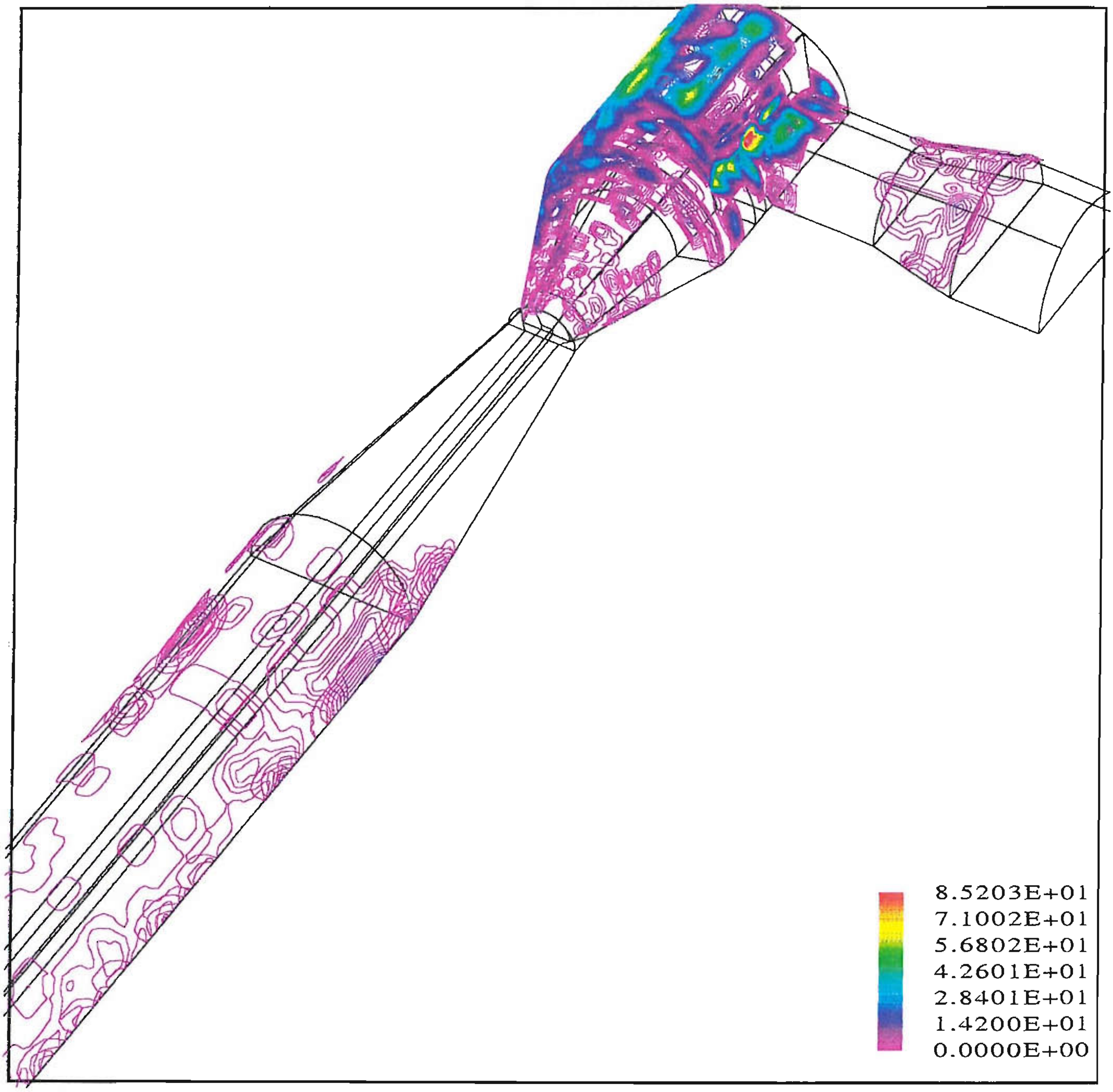

EROSIONAL TRENDS OF A EVOLUTION NEEDLE AND SEAT CHOKE (K-EPSILON MODEL)

Particle Type - **Sand**
Particle Roundness Factor - **0.5**
Particle Flux Rate - **1** % by wt.
Number of Particle Sizes - **6**
Particle Size Range - **150-200** μm
Turbulent Dispersion - **Yes**

Appendix Figure 75 - *k*-Epsilon Model Surface Contour Plot of Needle & Seat Choke Particle Impact Kinetic Energy (J)

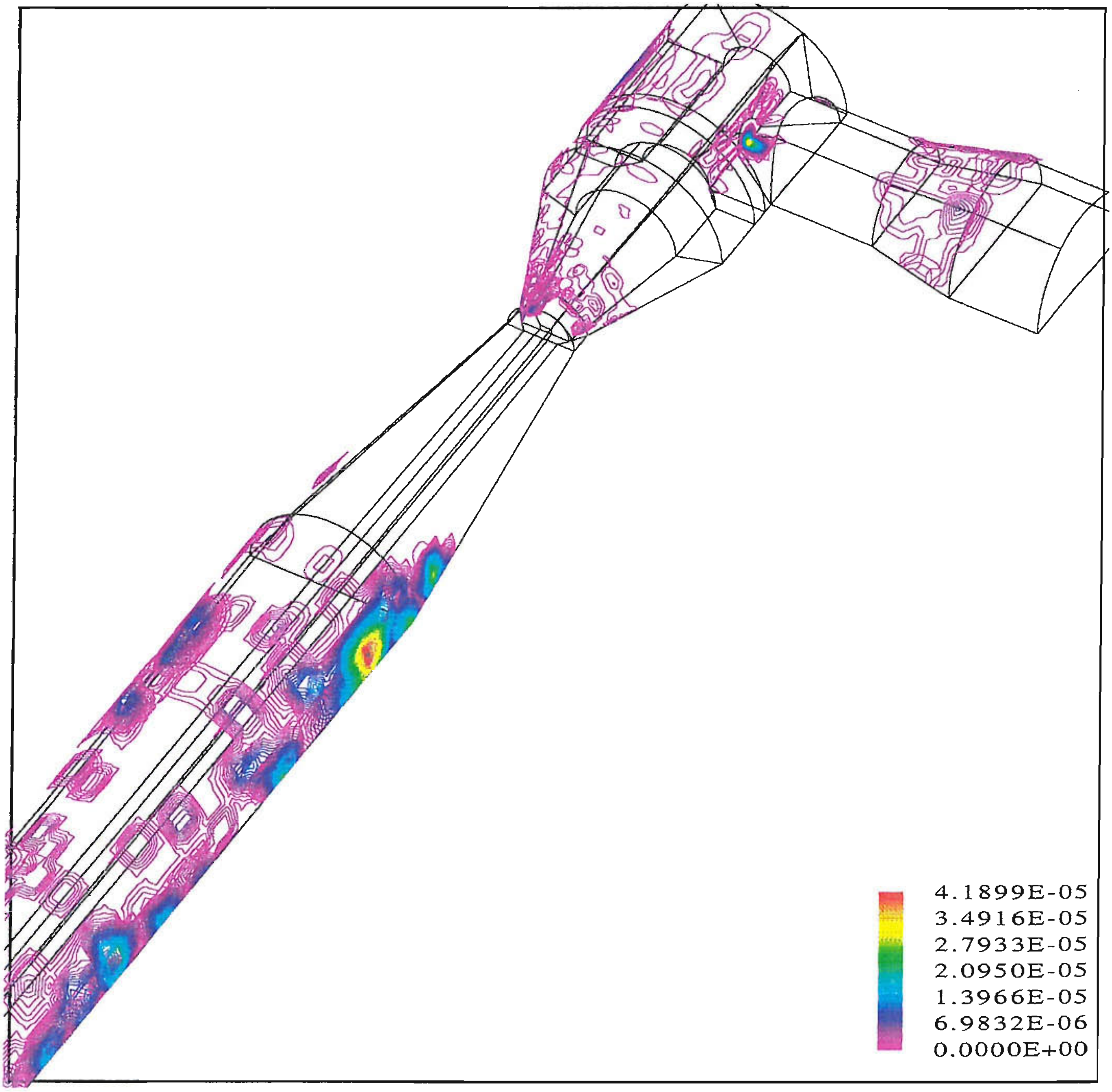

EROSIONAL TRENDS OF A EVOLUTION NEEDLE AND SEAT CHOKE (K-EPSILON MODEL)

Particle Type - **Sand**
Particle Roundness Factor - **0.5**
Particle Flux Rate - **1** % by wt.
Number of Particle Sizes - **6**
Particle Size Range - **150-200** μm
Turbulent Dispersion - **Yes**

Appendix Figure 76 - *k*-Epsilon Model Surface Contour Plot of Needle & Seat Choke Particle Erosion Rates (mm³/hr)

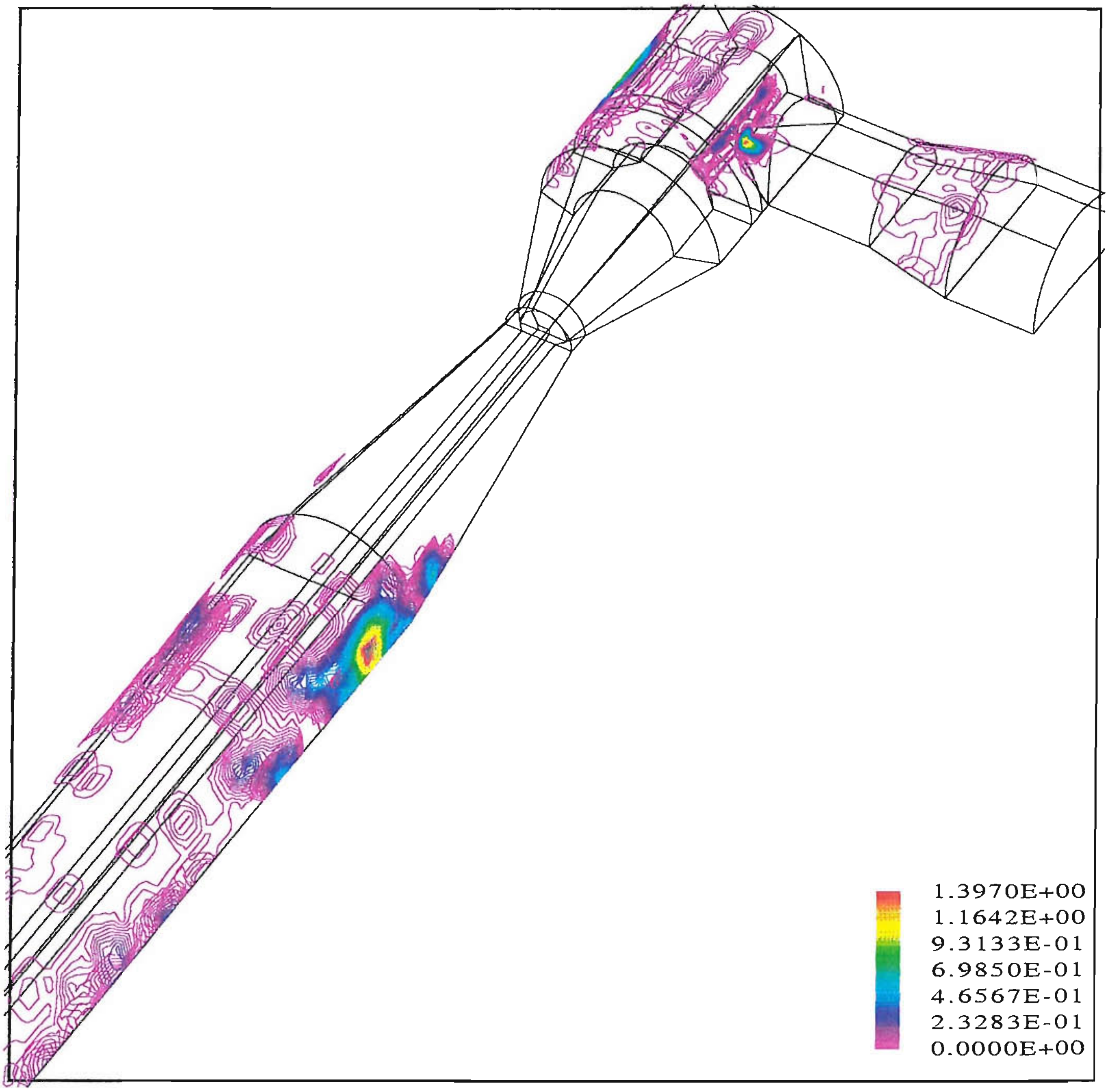

EROSIONAL TRENDS OF A EVOLUTION NEEDLE AND SEAT CHOKE (K-EPSILON MODEL)

Particle Type - **Sand**
Particle Roundness Factor - **0.5**
Particle Flux Rate - **1** % by wt.
Number of Particle Sizes - **6**
Particle Size Range - **150-200** μm
Turbulent Dispersion - **Yes**

Appendix Figure 77 - *k*-Epsilon Model Surface Contour Plot of Needle & Seat Choke Particle Erosion Rates (mm^3/hr)

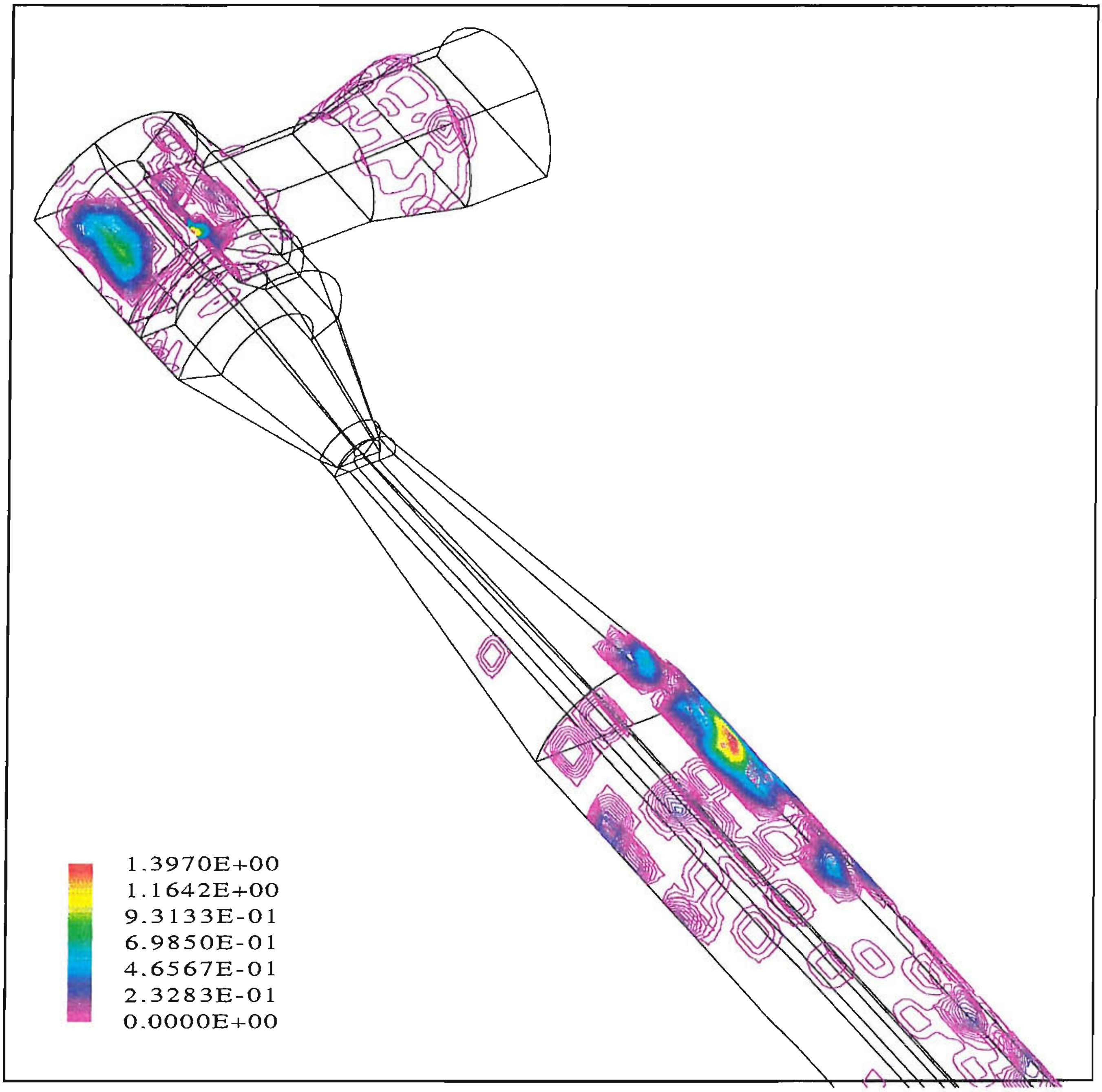

INVESTIGATION OF EROSION WITHIN CAGE TYPE CONTROL CHOKES

Fluid - **Crude Oil**
Inlet Diameter - **75** mm
Port Diameters - **12.5** & **25** mm
Taper Angle on Sleeve - **15°**
Choke Opening - **75** %
Pressure Drop - **50** Bar
Volumetric Flow Rate (Oil) - **240** m^3/hr

Appendix Figure 78 - Velocity Contour Plot of External Sleeve Control Choke (m/s)

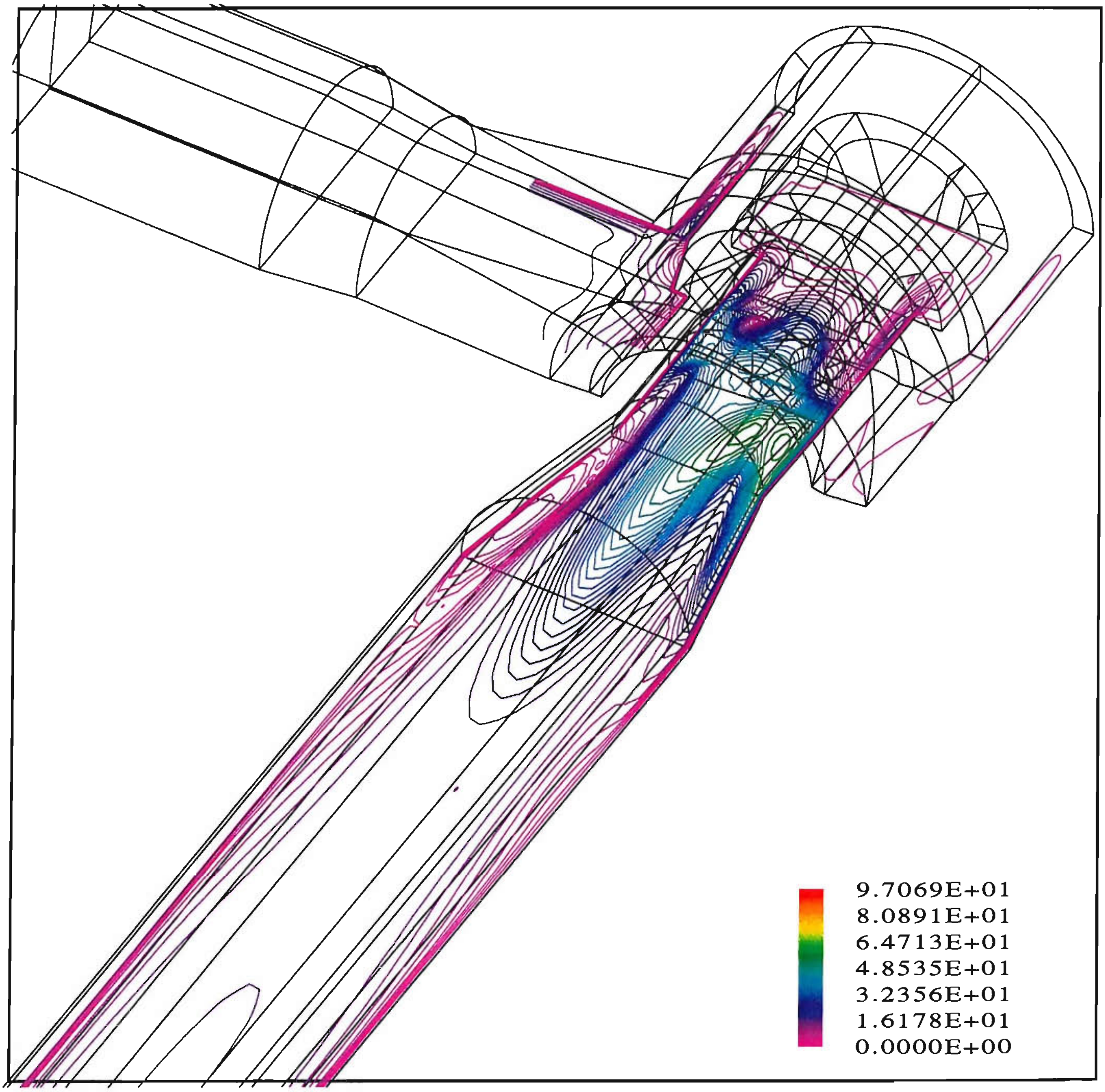

INVESTIGATION OF EROSION WITHIN CAGE TYPE CONTROL CHOKES - LIQUIDS

Particle Type - **Sand**　　Test No - **1**
Particle Flux Rate - **54** Wppm.
Particle Roundness Factor - **0.5**
Number of Particle Sizes - **8**
Particle Size Range - **75-165** μm
Turbulent Dispersion - **Yes**
Modified Coefficient of Restitution - **Yes**
Squeeze Film Retardation - **Yes**

Appendix Figure 79 - Surface Contour Plot of External Sleeve Particle Impact Velocities (m/s)

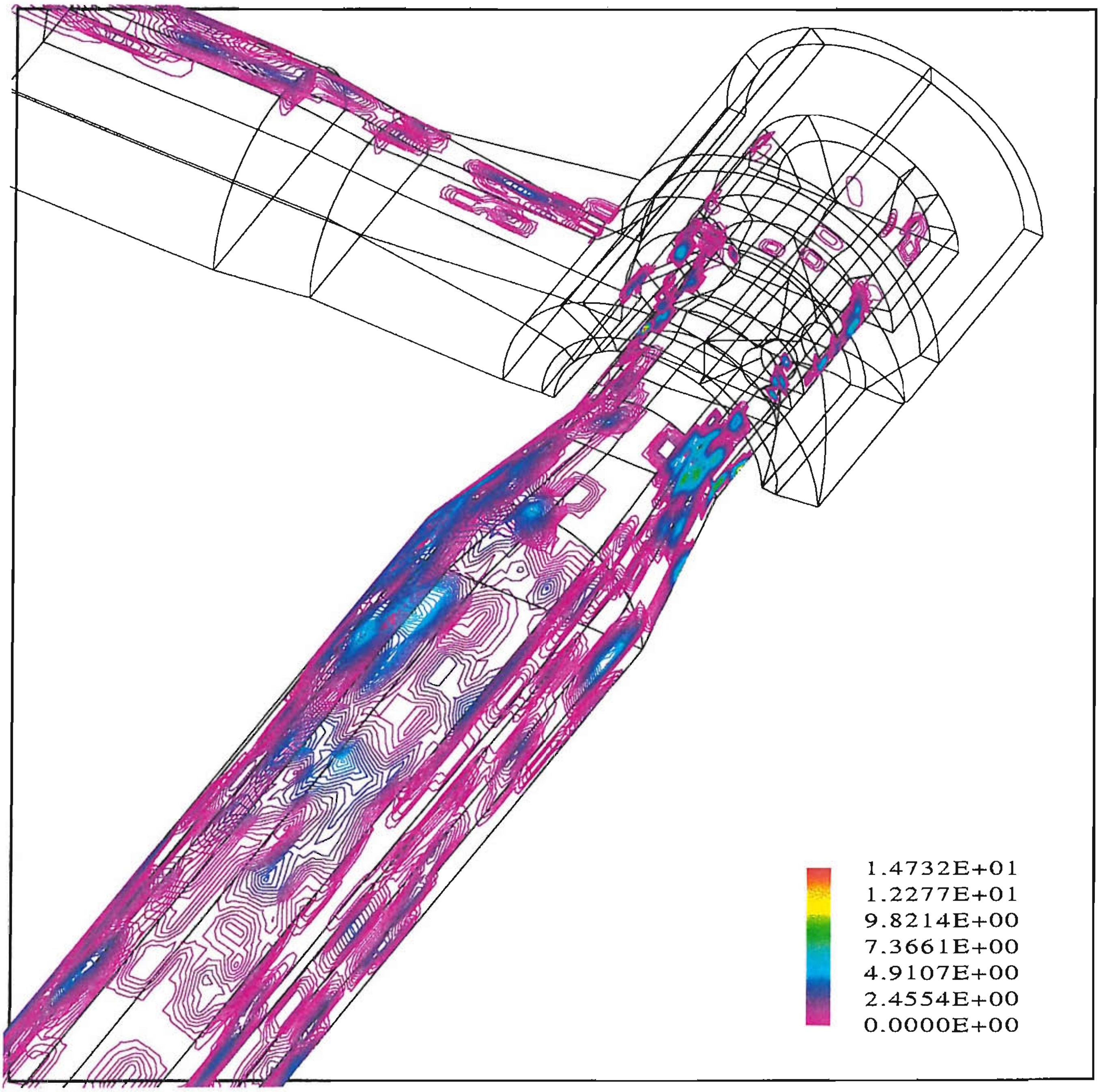

INVESTIGATION OF EROSION WITHIN CAGE TYPE CONTROL CHOKES - LIQUIDS

Particle Type - **Sand**
Test No - **1**
Particle Flux Rate - **54** Wppm.
Particle Roundness Factor - **0.5**
Number of Particle Sizes - **8**
Particle Size Range - **75-165** μm
Turbulent Dispersion - **Yes**
Modified Coefficient of Restitution - **Yes**
Squeeze Film Retardation - **Yes**

Appendix Figure 80 - Surface Contour Plot of External Sleeve Particle Impact Angle (deg)

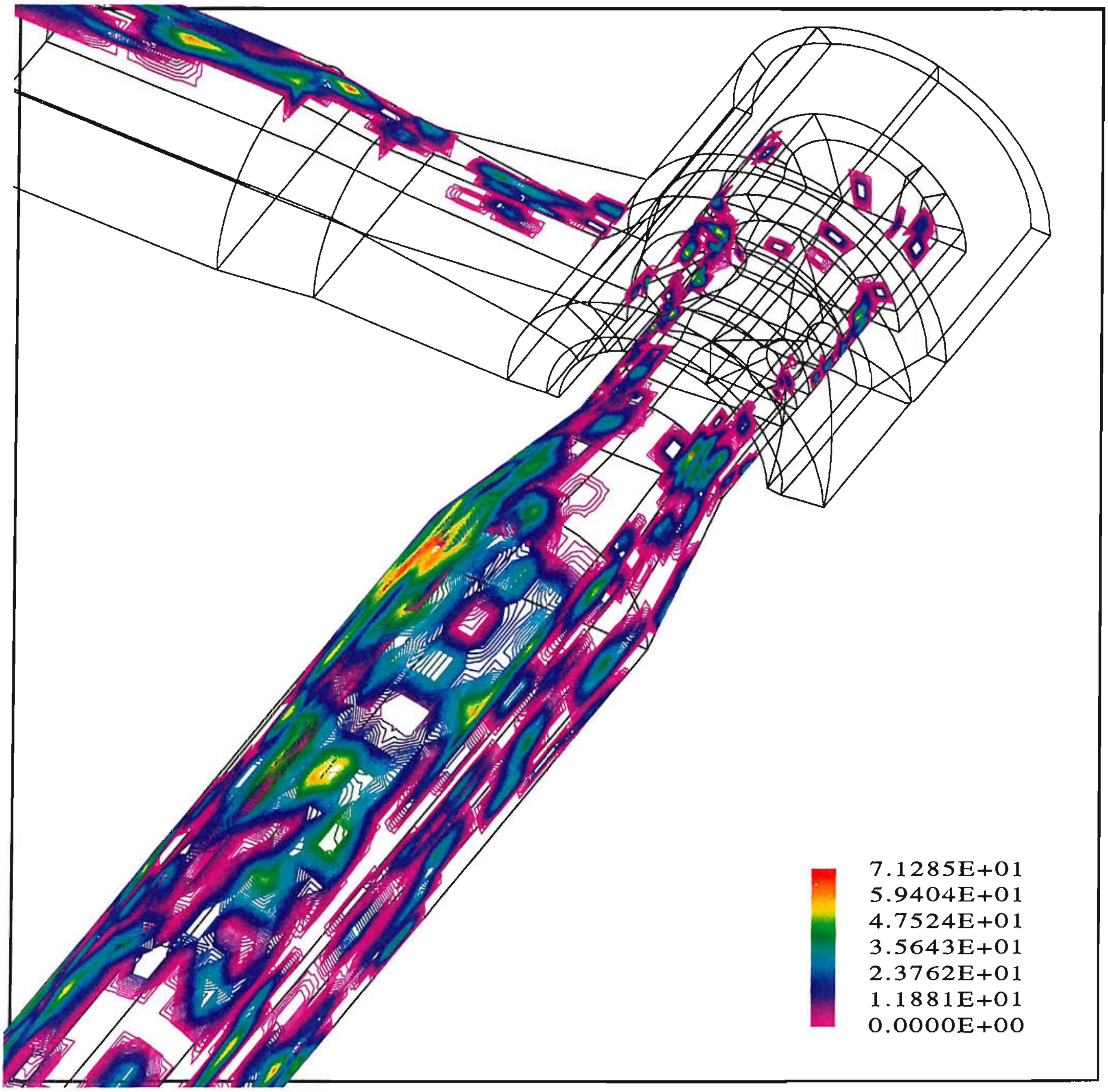

INVESTIGATION OF EROSION WITHIN CAGE TYPE CONTROL CHOKES - LIQUIDS

Particle Type - **Sand** Test No - **1**
Particle Flux Rate - **54** Wppm.
Particle Roundness Factor - **0.5**
Number of Particle Sizes - **8**
Particle Size Range - **75-165** μm
Turbulent Dispersion - **Yes**
Modified Coefficient of Restitution - **Yes**
Squeeze Film Retardation - **Yes**

Appendix Figure 81 - Surface Contour Plot of External Sleeve Particle Erosion Rates (mm^3/hr)

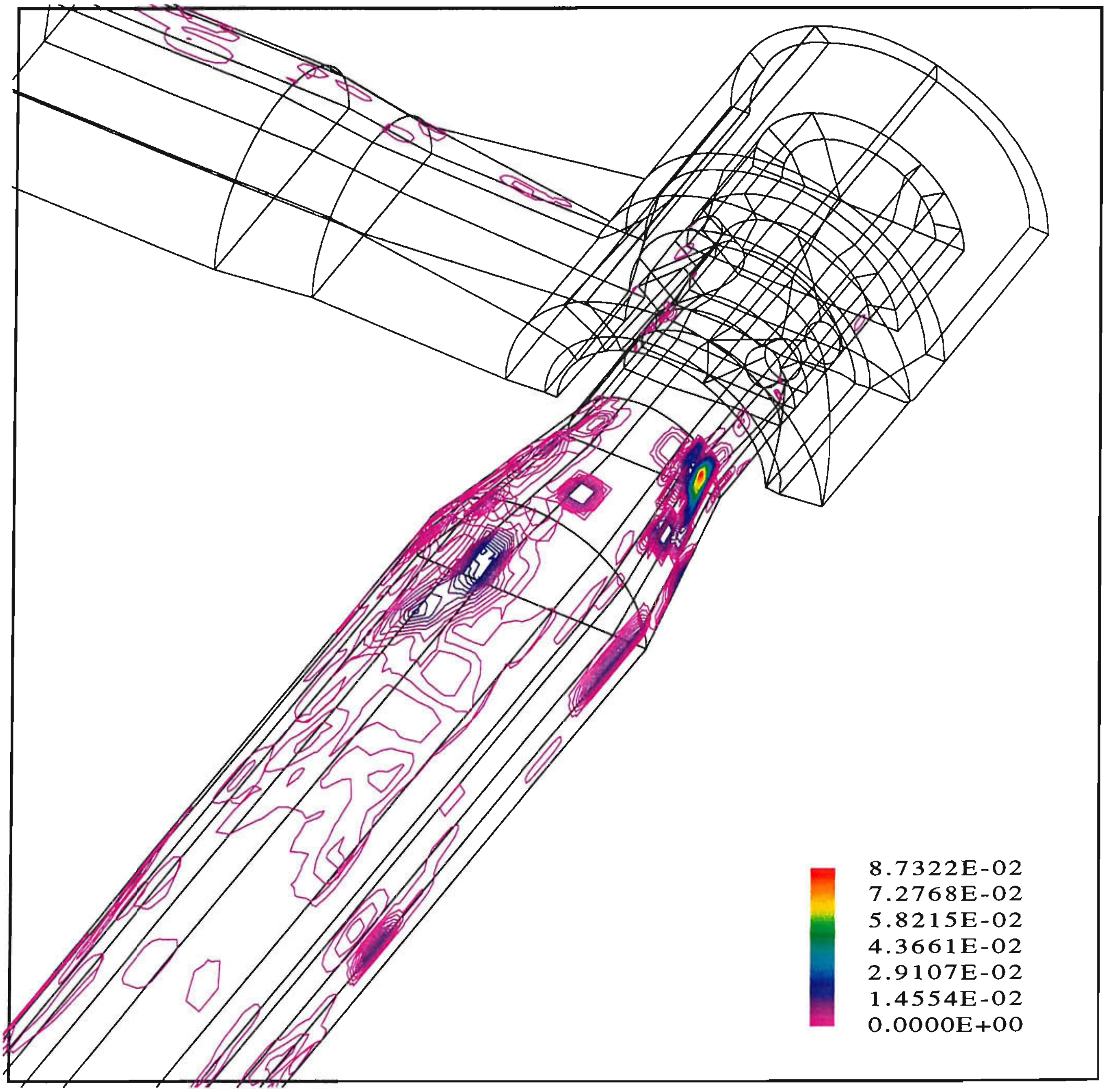

INVESTIGATION OF EROSION WITHIN CAGE TYPE CONTROL CHOKES - LIQUIDS

Particle Type - **Sand** Test No - **1**
Particle Flux Rate - **54** Wppm.
Particle Roundness Factor - **0.5**
Number of Particle Sizes - **8**
Particle Size Range - **75-165** μm
Turbulent Dispersion - **Yes**
Modified Coefficient of Restitution - **Yes**
Squeeze Film Retardation - **Yes**

Appendix Figure 82 - Surface Contour Plot of External Sleeve Particle Erosion Rates (mm^3/hr)

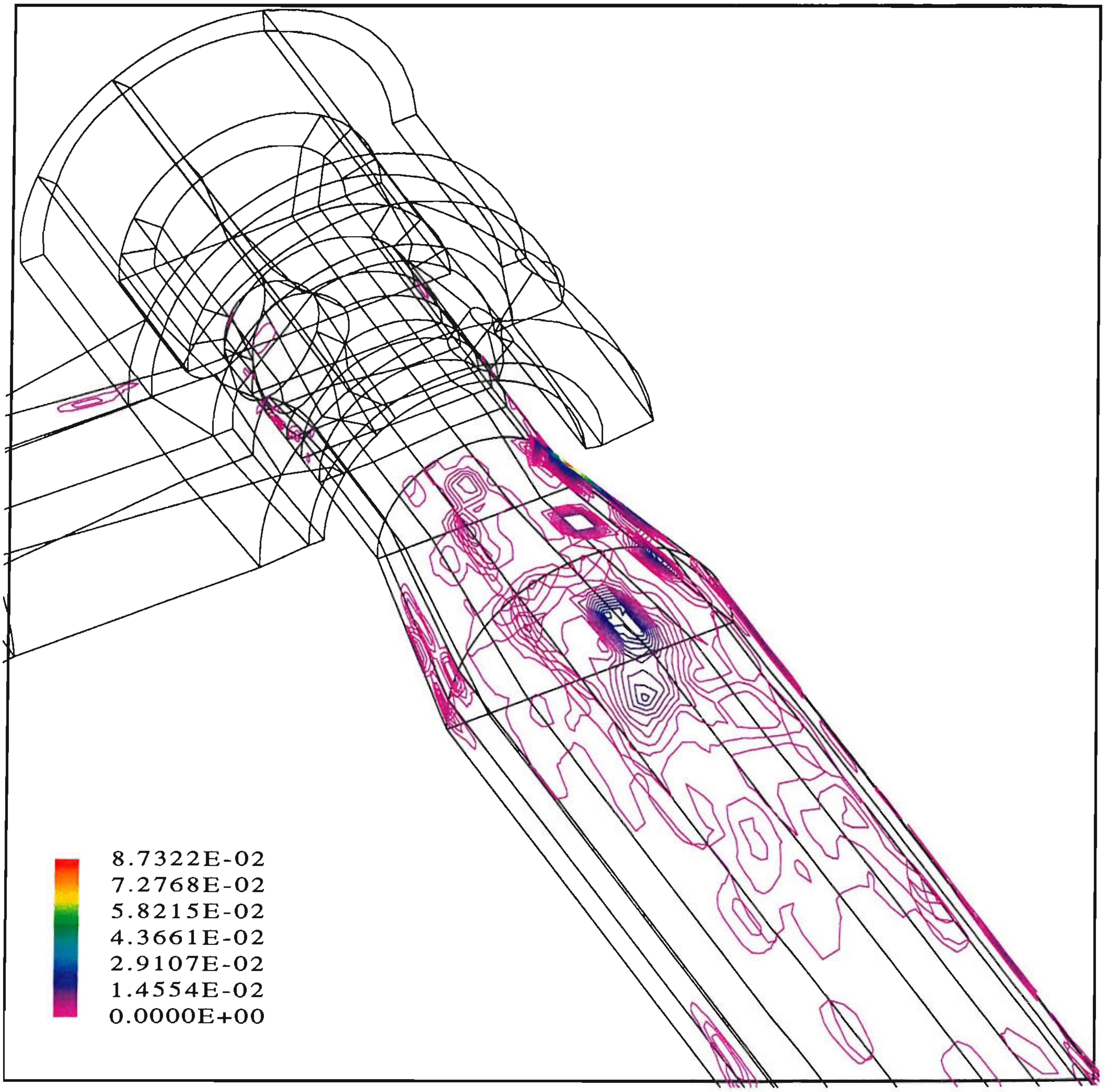

INVESTIGATION OF EROSION WITHIN CAGE TYPE CONTROL CHOKES - LIQUIDS

Particle Type - **Sand**
Test No - **3**
Particle Flux Rate - **54** Wppm.
Particle Roundness Factor - **0.5**
Number of Particle Sizes - **8**
Particle Size Range - **170-260** μm
Turbulent Dispersion - **Yes**
Modified Coefficient of Restitution - **Yes**
Squeeze Film Retardation - **Yes**

Appendix Figure 83 - Surface Contour Plot of External Sleeve Particle Impact Velocities (m/s)

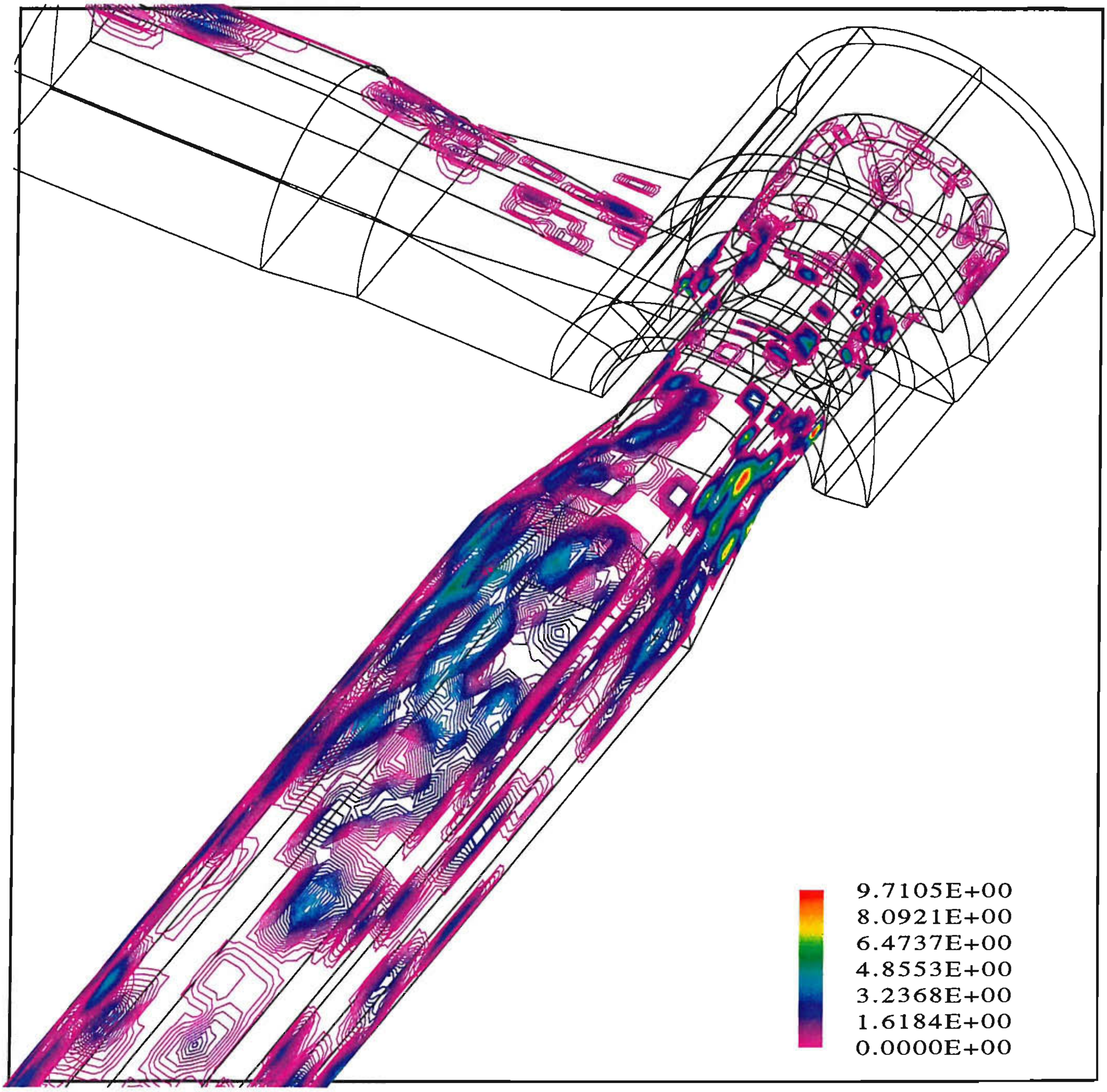

INVESTIGATION OF EROSION WITHIN CAGE TYPE CONTROL CHOKES - LIQUIDS

Particle Type - **Sand**

Test No - **3**

Particle Flux Rate - **54** Wppm.
Particle Roundness Factor - **0.5**
Number of Particle Sizes - **8**
Particle Size Range - **170-260** μm
Turbulent Dispersion - **Yes**
Modified Coefficient of Restitution - **Yes**
Squeeze Film Retardation - **Yes**

Appendix Figure 84 - Surface Contour Plot of External Sleeve Particle Impact Angle (deg)

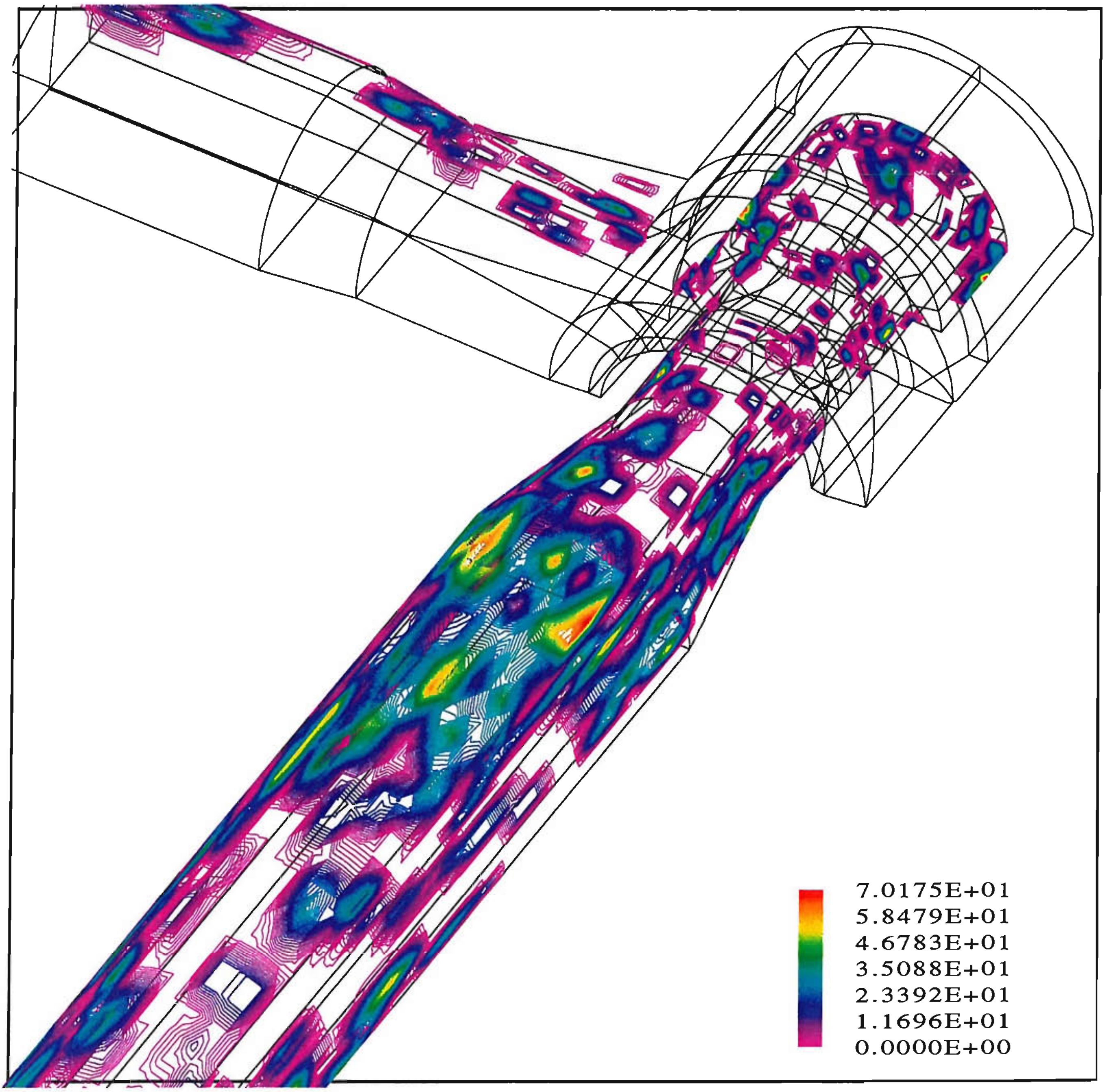

INVESTIGATION OF EROSION WITHIN CAGE TYPE CONTROL CHOKES - LIQUIDS

Particle Type - **Sand**

Test No - **3**

Particle Flux Rate - **54** Wppm.
Particle Roundness Factor - **0.5**
Number of Particle Sizes - **8**
Particle Size Range - **170-260** μm
Turbulent Dispersion - **Yes**
Modified Coefficient of Restitution - **Yes**
Squeeze Film Retardation - **Yes**

Appendix Figure 85 - Surface Contour Plot of External Sleeve Particle Erosion Rates (mm^3/hr)

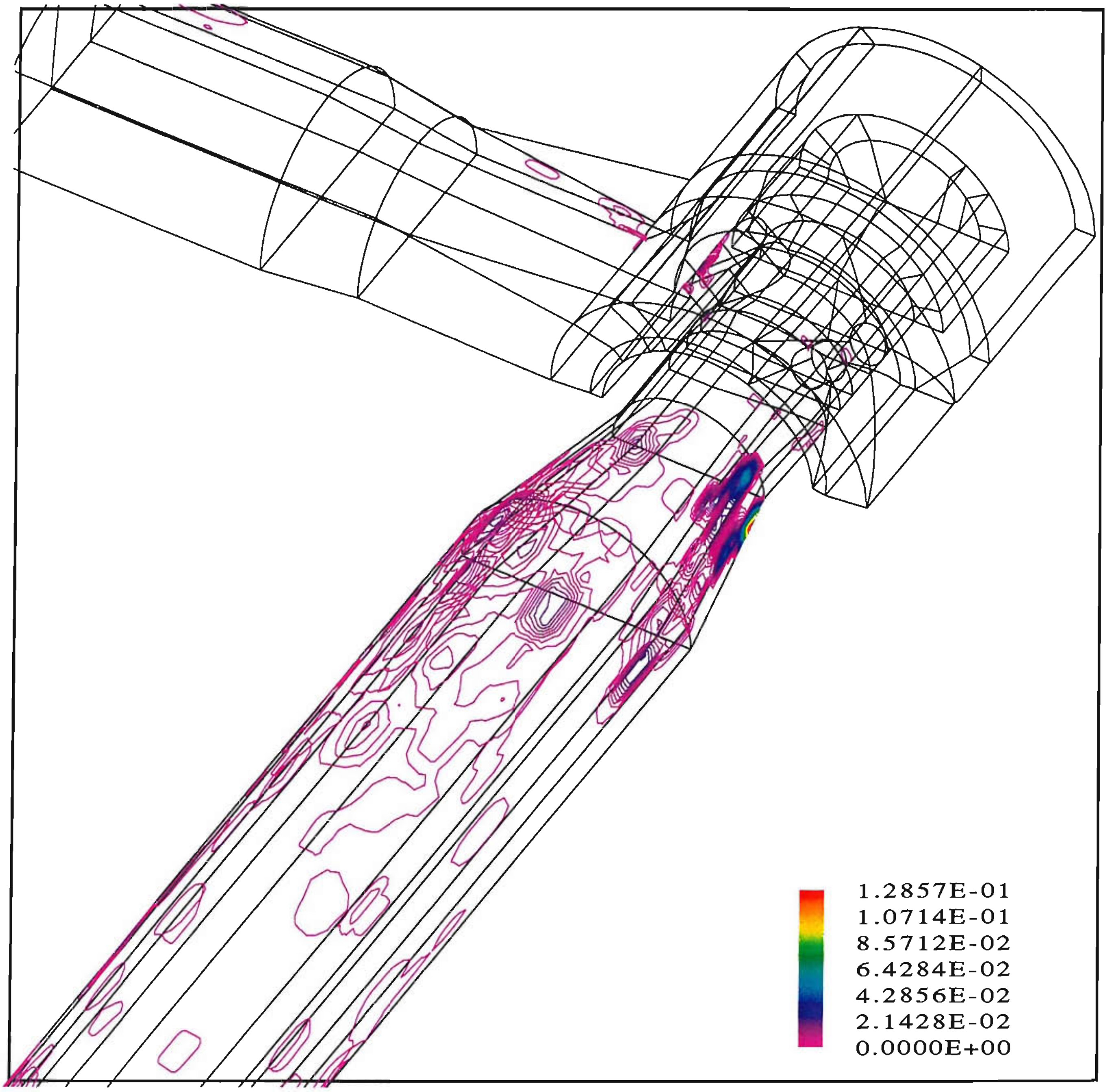

INVESTIGATION OF EROSION WITHIN CAGE TYPE CONTROL CHOKES - LIQUIDS

Particle Type - **Sand** Test No - **3**
Particle Flux Rate - **54** Wppm.
Particle Roundness Factor - **0.5**
Number of Particle Sizes - **8**
Particle Size Range - **170-260** μm
Turbulent Dispersion - **Yes**
Modified Coefficient of Restitution - **Yes**
Squeeze Film Retardation - **Yes**

Appendix Figure 86 - Surface Contour Plot of External Sleeve Particle Erosion Rates (mm^3/hr)

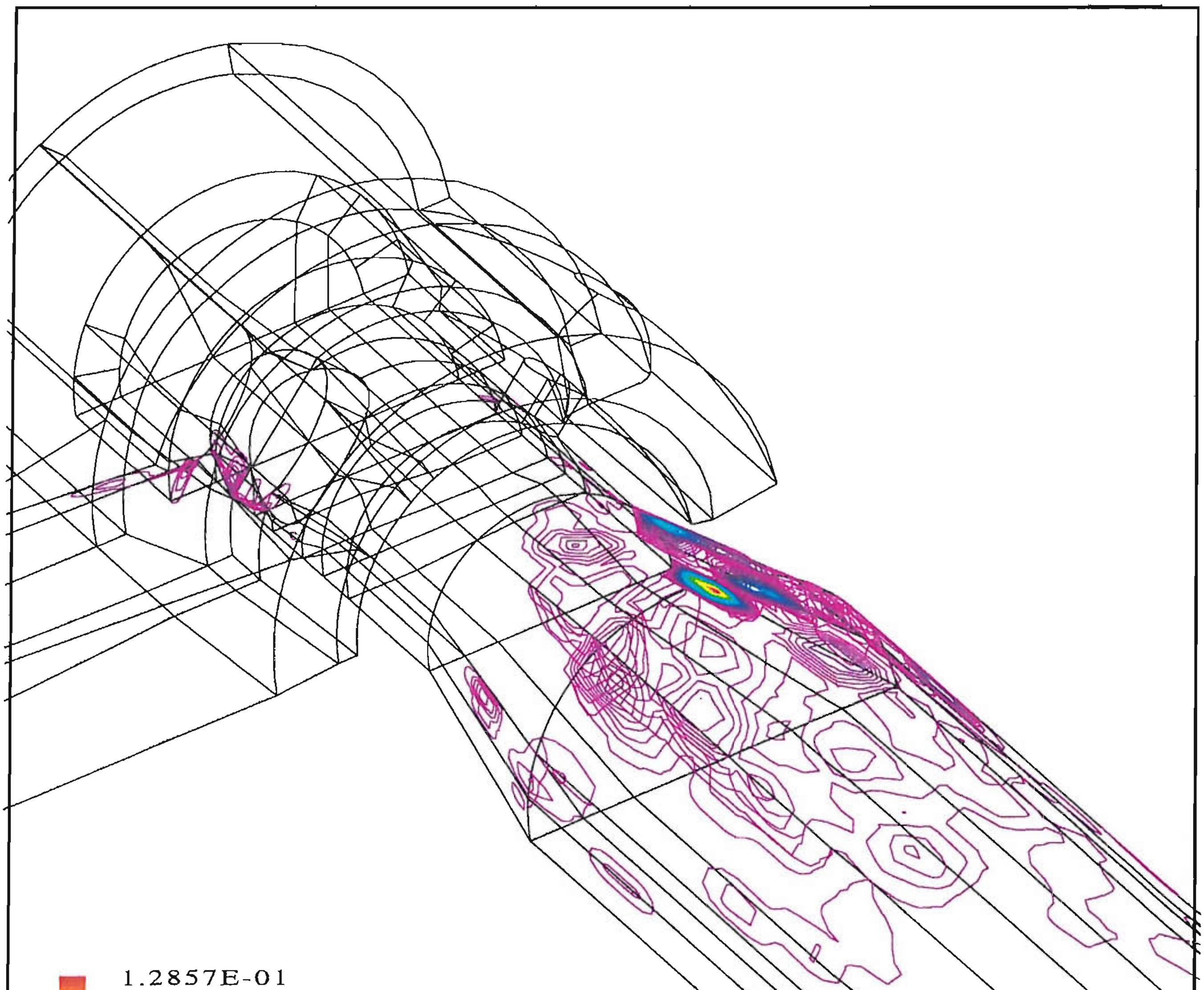

INVESTIGATION OF EROSION WITHIN CAGE TYPE CONTROL CHOKES

Fluid - **Crude Oil**
Inlet Diameter - **75** mm
Port Diameters - **12.5** & **25** mm
Plug Edge - **Sharp**
Choke Opening - **75** %
Pressure Drop - **50** Bar
Volumetric Flow Rate (Oil) - **240** m^3/hr

Appendix Figure 87 - Velocity Contour Plot of Internal Plug Control Choke (m/s)

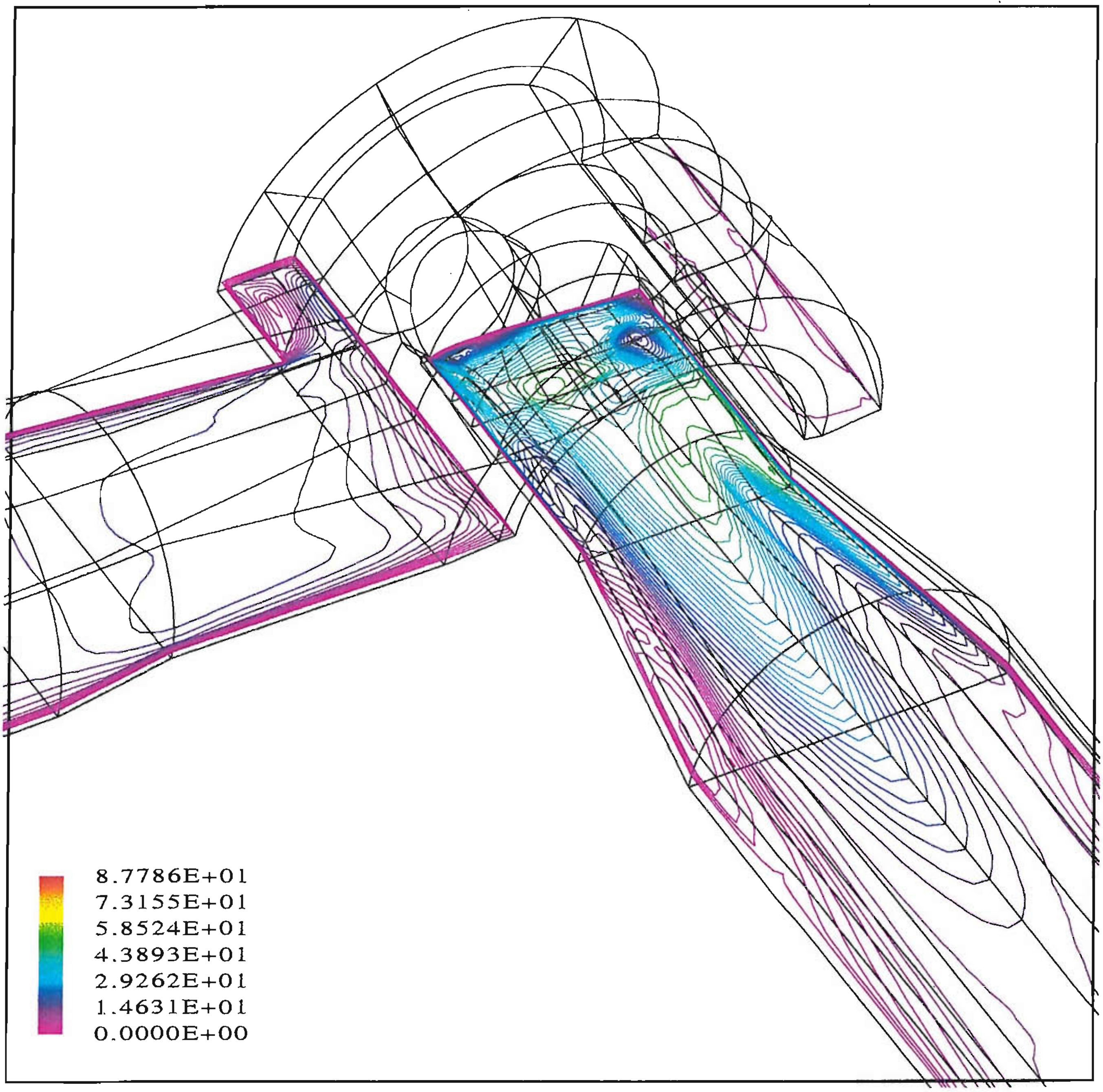

INVESTIGATION OF EROSION WITHIN CAGE TYPE CONTROL CHOKES

Fluid - **Crude Oil**
Inlet Diameter - **75** mm
Port Diameters - **12.5** & **25** mm
Plug Edge - **Sharp**
Choke Opening - **75** %
Pressure Drop - **50** Bar
Volumetric Flow Rate (Oil) - **240** m^3/hr

Appendix Figure 88 - Velocity Contour Plot of Internal Plug Control Choke (m/s)

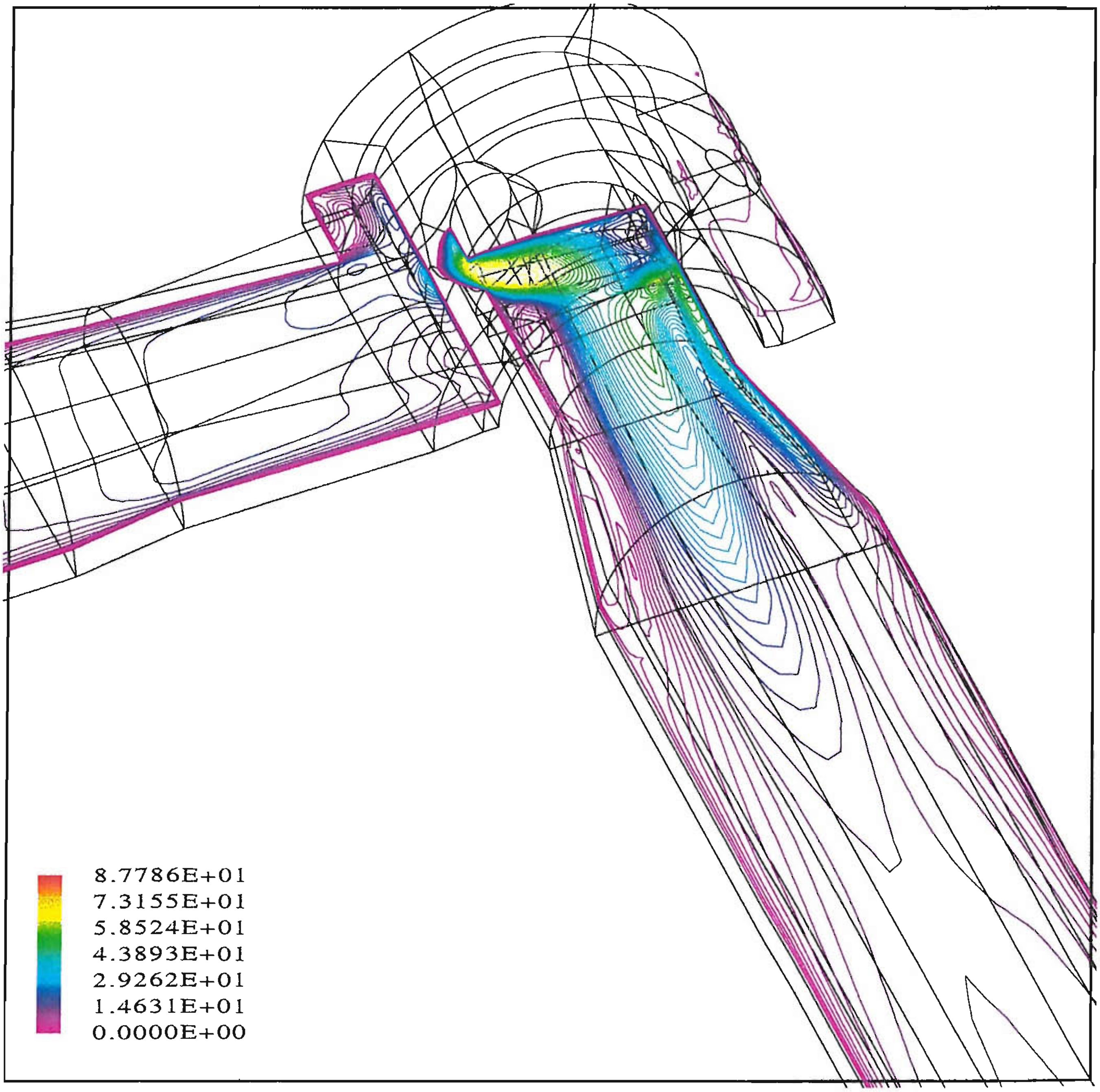

INVESTIGATION OF EROSION WITHIN CAGE TYPE CONTROL CHOKES

Fluid - **Crude Oil**
Inlet Diameter - **75** mm
Port Diameters - **12.5** & **25** mm
Plug Edge - **Sharp**
Choke Opening - **75** %
Pressure Drop - **50** Bar
Volumetric Flow Rate (Oil) - **240** m^3/hr

Appendix Figure 89 - Velocity Contour Plot of Internal Plug Control Choke (m/s)

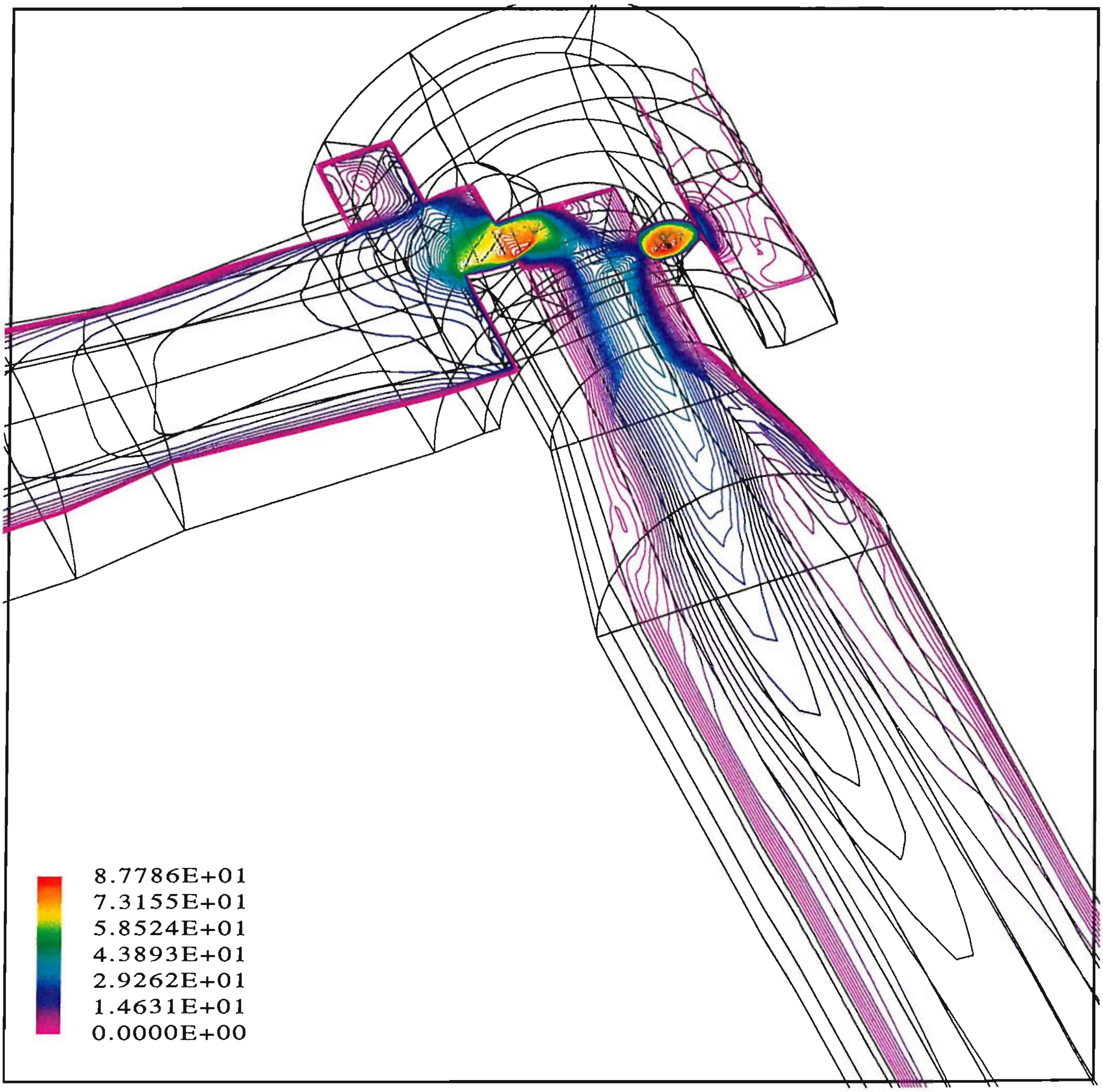

INVESTIGATION OF EROSION WITHIN CAGE TYPE CONTROL CHOKES

Fluid - **Crude Oil**
Inlet Diameter - **75** mm
Port Diameters - **12.5 & 25** mm
Plug Edge - **Sharp**
Choke Opening - **75** %
Pressure Drop - **50** Bar
Volumetric Flow Rate (Oil) - **240** m^3/hr

Appendix Figure 90 - Turbulent Kinetic Energy Contour Plot of Internal Plug Control Choke

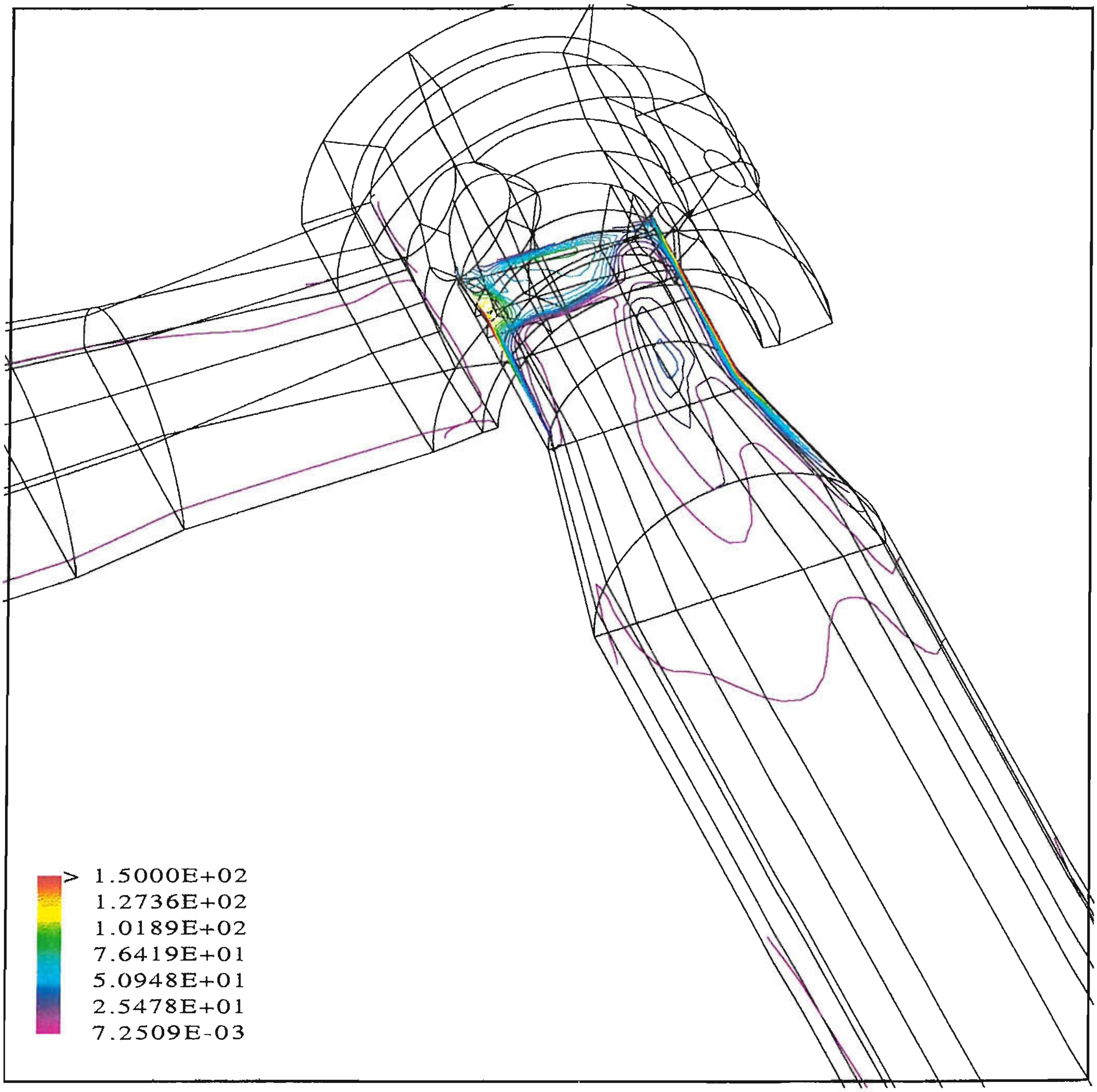

INVESTIGATION OF EROSION WITHIN CAGE TYPE CONTROL CHOKES - LIQUIDS

Particle Type - **Sand**
Test No - **2**
Particle Flux Rate - **54** Wppm.
Particle Roundness Factor - **0.5**
Number of Particle Sizes - **8**
Particle Size Range - **75-165** μm
Turbulent Dispersion - **Yes**
Modified Coefficient of Restitution - **Yes**
Squeeze Film Retardation - **Yes**

Appendix Figure 91 - Surface Contour Plot of Internal Plug Particle Impact Velocities (m/s)

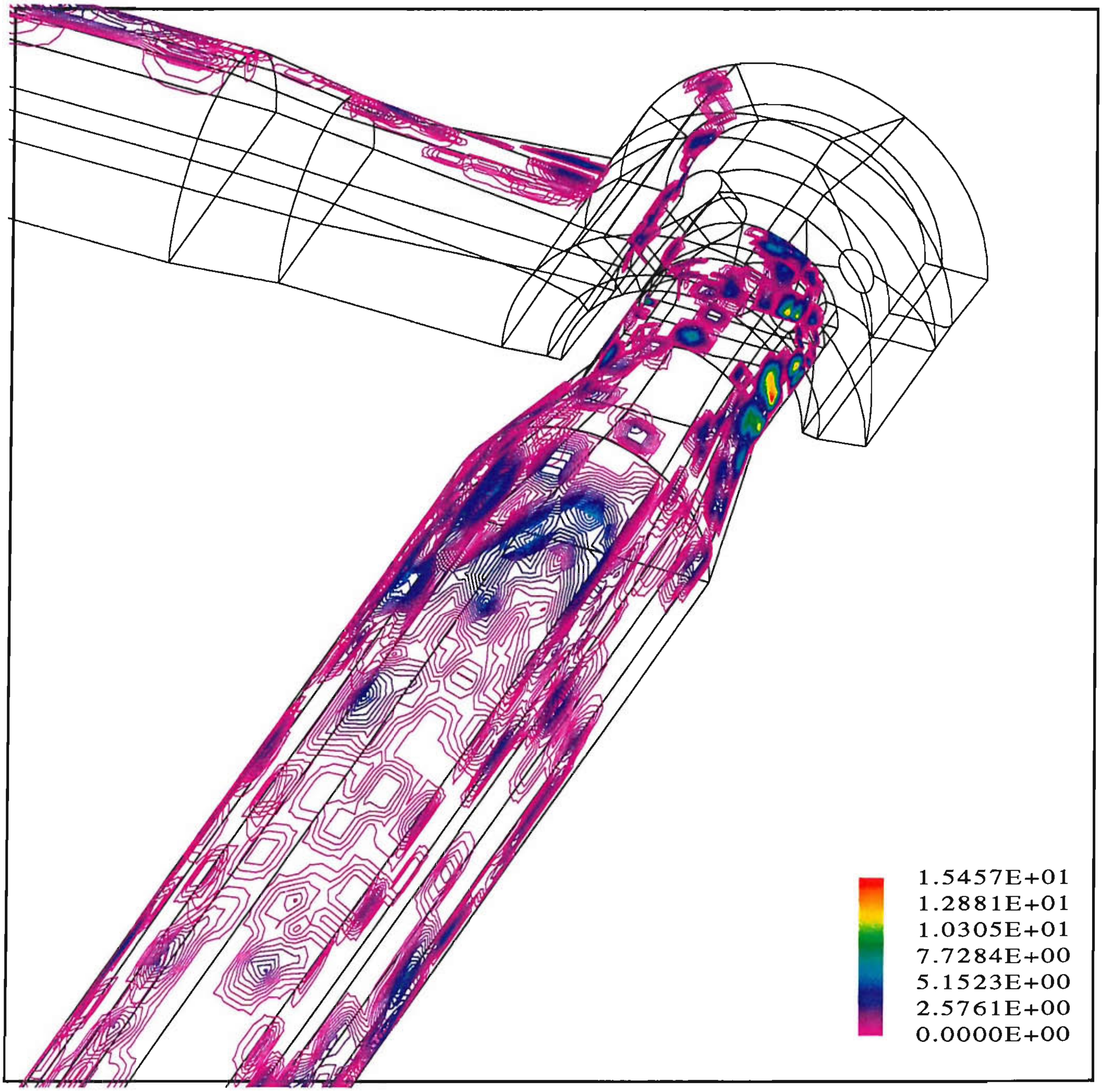

INVESTIGATION OF EROSION WITHIN CAGE TYPE CONTROL CHOKES - LIQUIDS

Particle Type - **Sand** Test No - **2**
Particle Flux Rate - **54** Wppm.
Particle Roundness Factor - **0.5**
Number of Particle Sizes - **8**
Particle Size Range - **75-165** μm
Turbulent Dispersion - **Yes**
Modified Coefficient of Restitution - **Yes**
Squeeze Film Retardation - **Yes**

Appendix Figure 92 - Surface Contour Plot of Internal Plug Particle Impact Angle (deg)

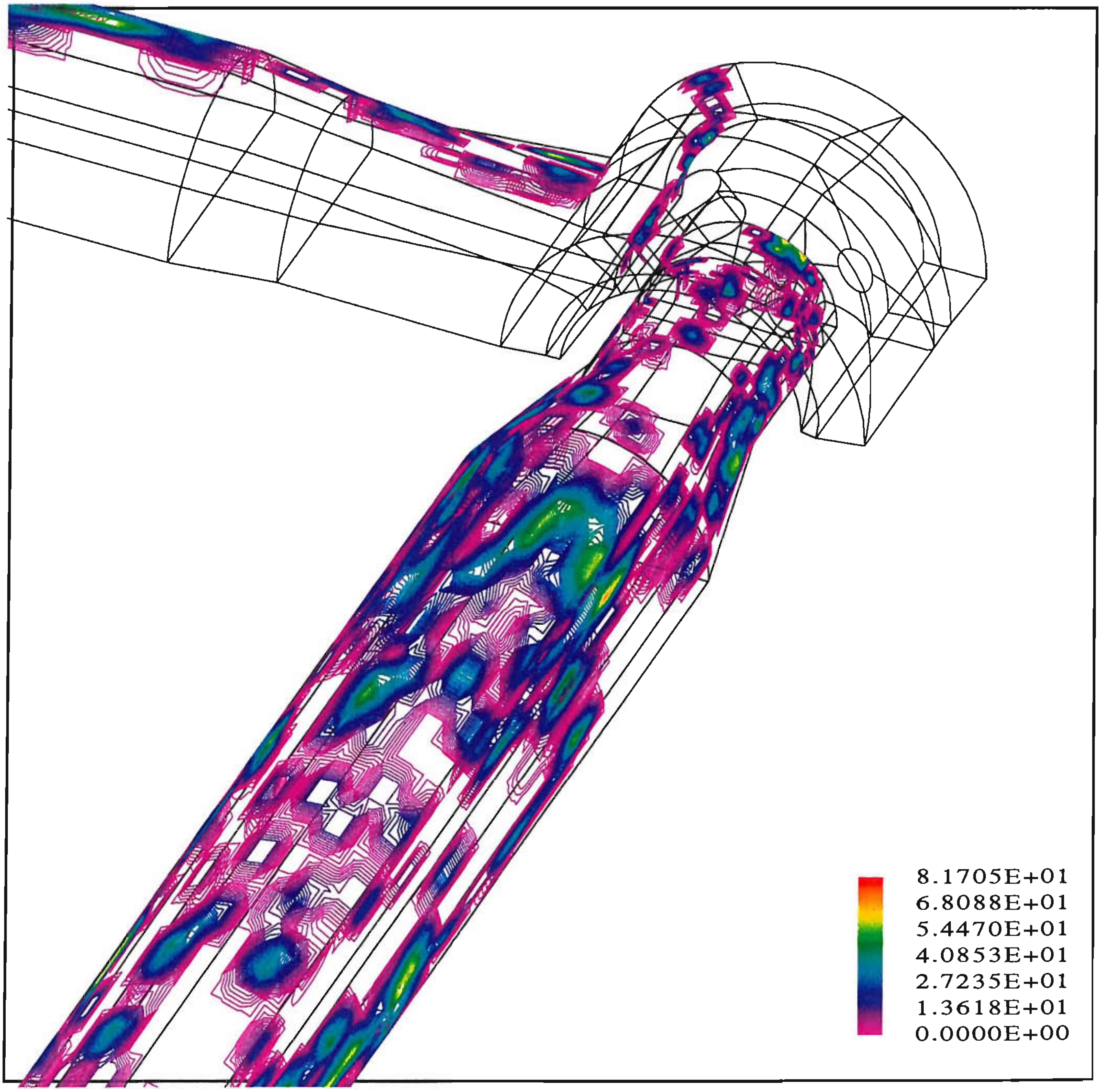

INVESTIGATION OF EROSION WITHIN CAGE TYPE CONTROL CHOKES - LIQUIDS

Particle Type - **Sand** Test No - **2**
Particle Flux Rate - **54** Wppm.
Particle Roundness Factor - **0.5**
Number of Particle Sizes - **8**
Particle Size Range - **75-165** μm
Turbulent Dispersion - **Yes**
Modified Coefficient of Restitution - **Yes**
Squeeze Film Retardation - **Yes**

Appendix Figure 93 - Surface Contour Plot of Internal Plug Particle Erosion Rates (mm³/hr)

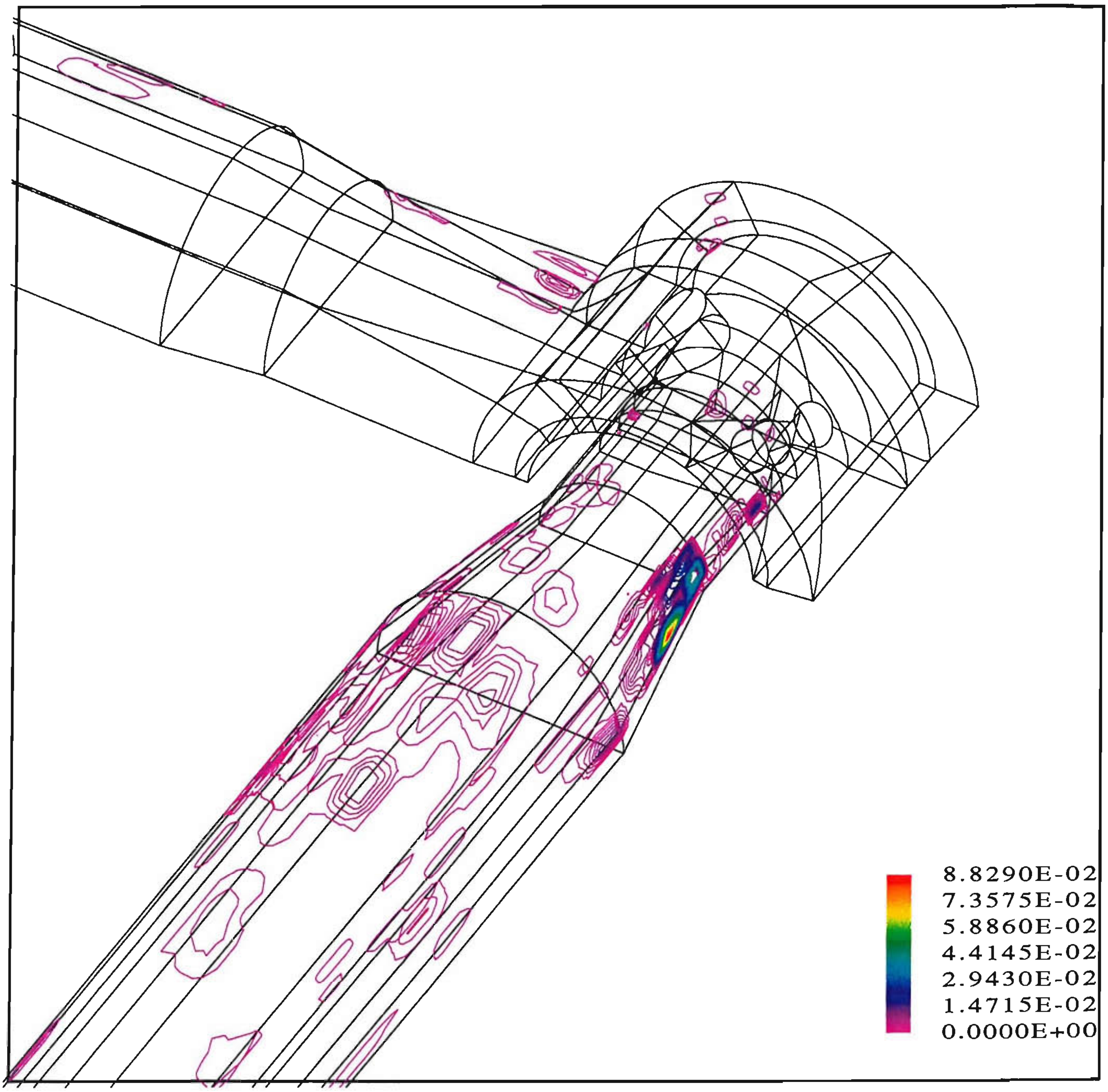

INVESTIGATION OF EROSION WITHIN CAGE TYPE CONTROL CHOKES - LIQUIDS

Particle Type - **Sand**
Test No - **2**
Particle Flux Rate - **54** Wppm.
Particle Roundness Factor - **0.5**
Number of Particle Sizes - **8**
Particle Size Range - **75-165** µm
Turbulent Dispersion - **Yes**
Modified Coefficient of Restitution - **Yes**
Squeeze Film Retardation - **Yes**

Appendix Figure 94 - Surface Contour Plot of Internal Plug Particle Erosion Rates (mm^3/hr)

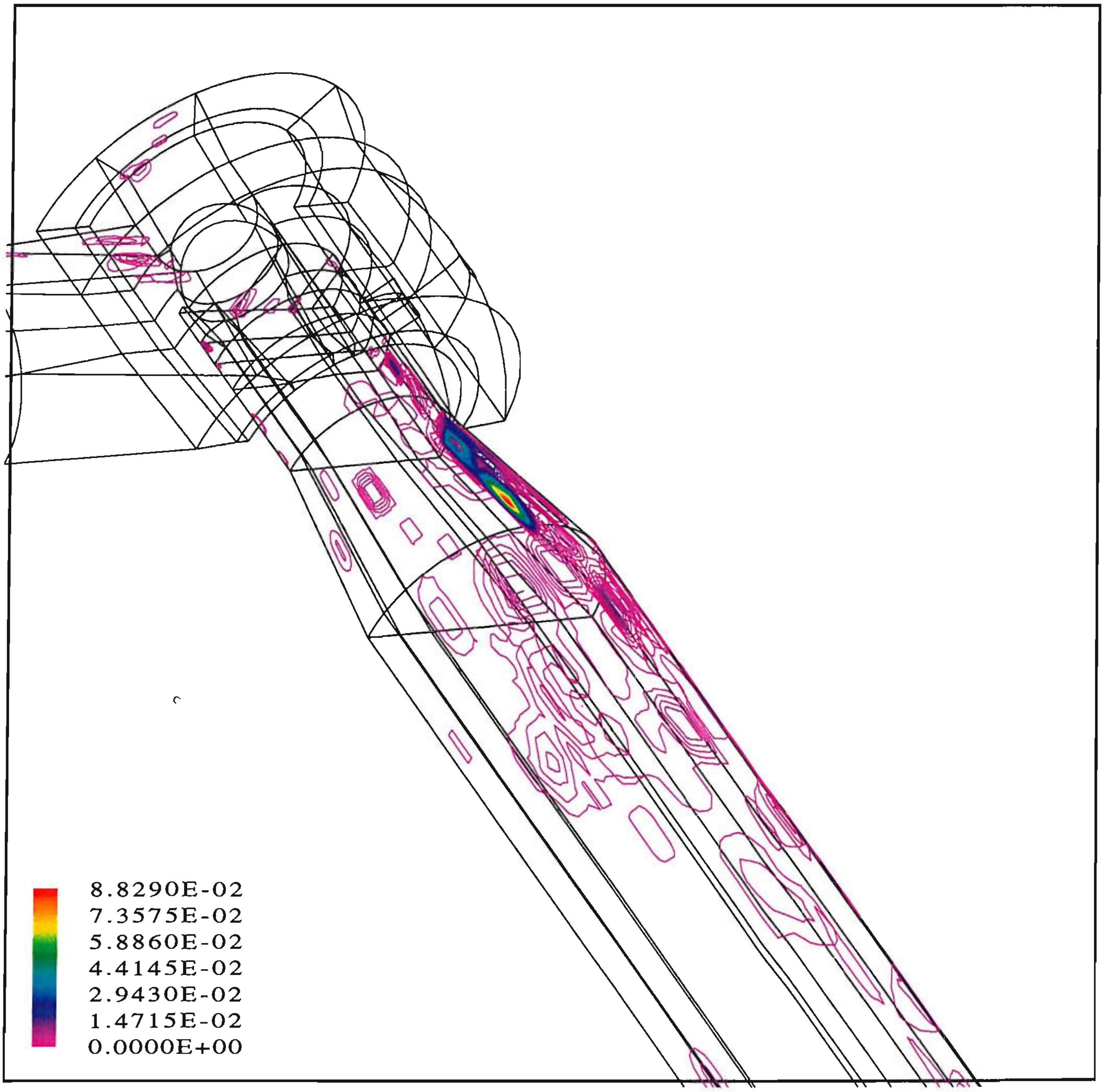

INVESTIGATION OF EROSION WITHIN CAGE TYPE CONTROL CHOKES - LIQUIDS

Particle Type - **Sand** Test No - **4**
Particle Flux Rate - **54** Wppm.
Particle Roundness Factor - **0.5**
Number of Particle Sizes - **8**
Particle Size Range - **170-260** μm
Turbulent Dispersion - **Yes**
Modified Coefficient of Restitution - **Yes**
Squeeze Film Retardation - **Yes**

Appendix Figure 95 - Surface Contour Plot of Internal Plug Particle Impact Velocities (m/s)

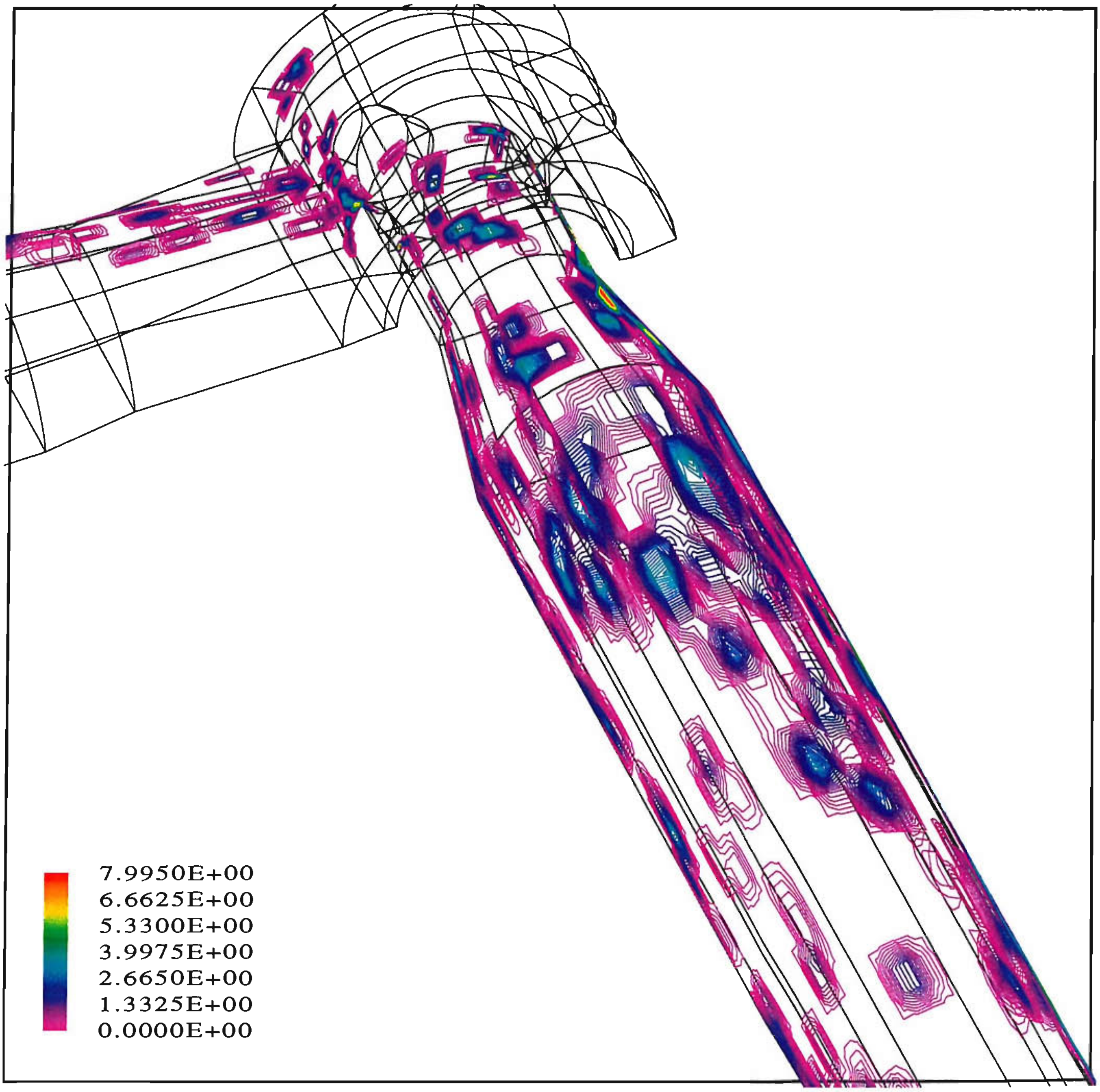

INVESTIGATION OF EROSION WITHIN CAGE TYPE CONTROL CHOKES - LIQUIDS

Particle Type - **Sand** Test No - **4**
Particle Flux Rate - **54** Wppm.
Particle Roundness Factor - **0.5**
Number of Particle Sizes - **8**
Particle Size Range - **170-260** μm
Turbulent Dispersion - **Yes**
Modified Coefficient of Restitution - **Yes**
Squeeze Film Retardation - **Yes**

Appendix Figure 96 - Surface Contour Plot of Internal Plug Particle Impact Angle (deg)

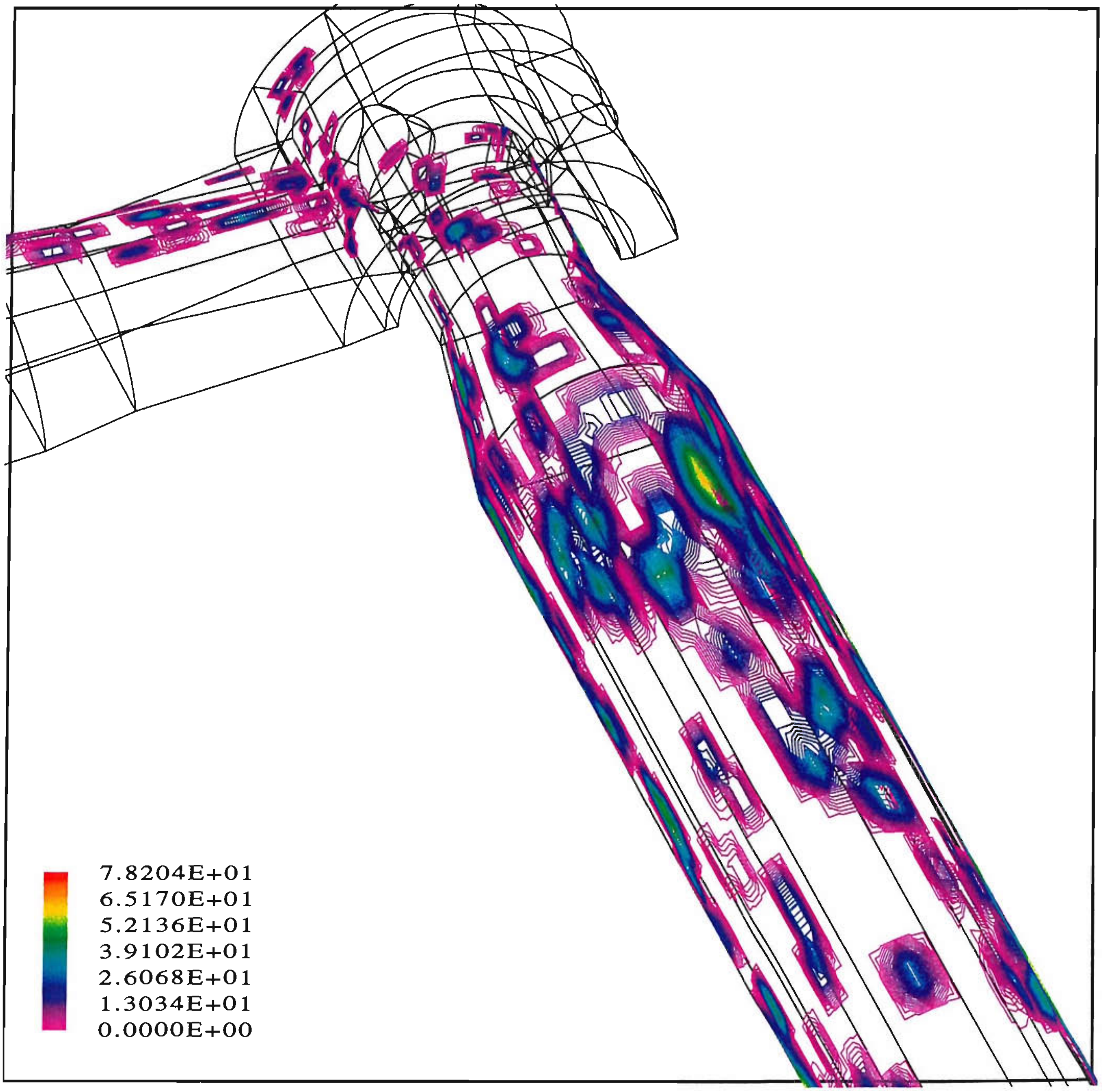

INVESTIGATION OF EROSION WITHIN CAGE TYPE CONTROL CHOKES - LIQUIDS

Particle Type - **Sand**
Test No - **4**
Particle Flux Rate - **54** Wppm.
Particle Roundness Factor - **0.5**
Number of Particle Sizes - **8**
Particle Size Range - **170-260** μm
Turbulent Dispersion - **Yes**
Modified Coefficient of Restitution - **Yes**
Squeeze Film Retardation - **Yes**

Appendix Figure 97 - Surface Contour Plot of Internal Plug Particle Erosion Rates (mm^3/hr)

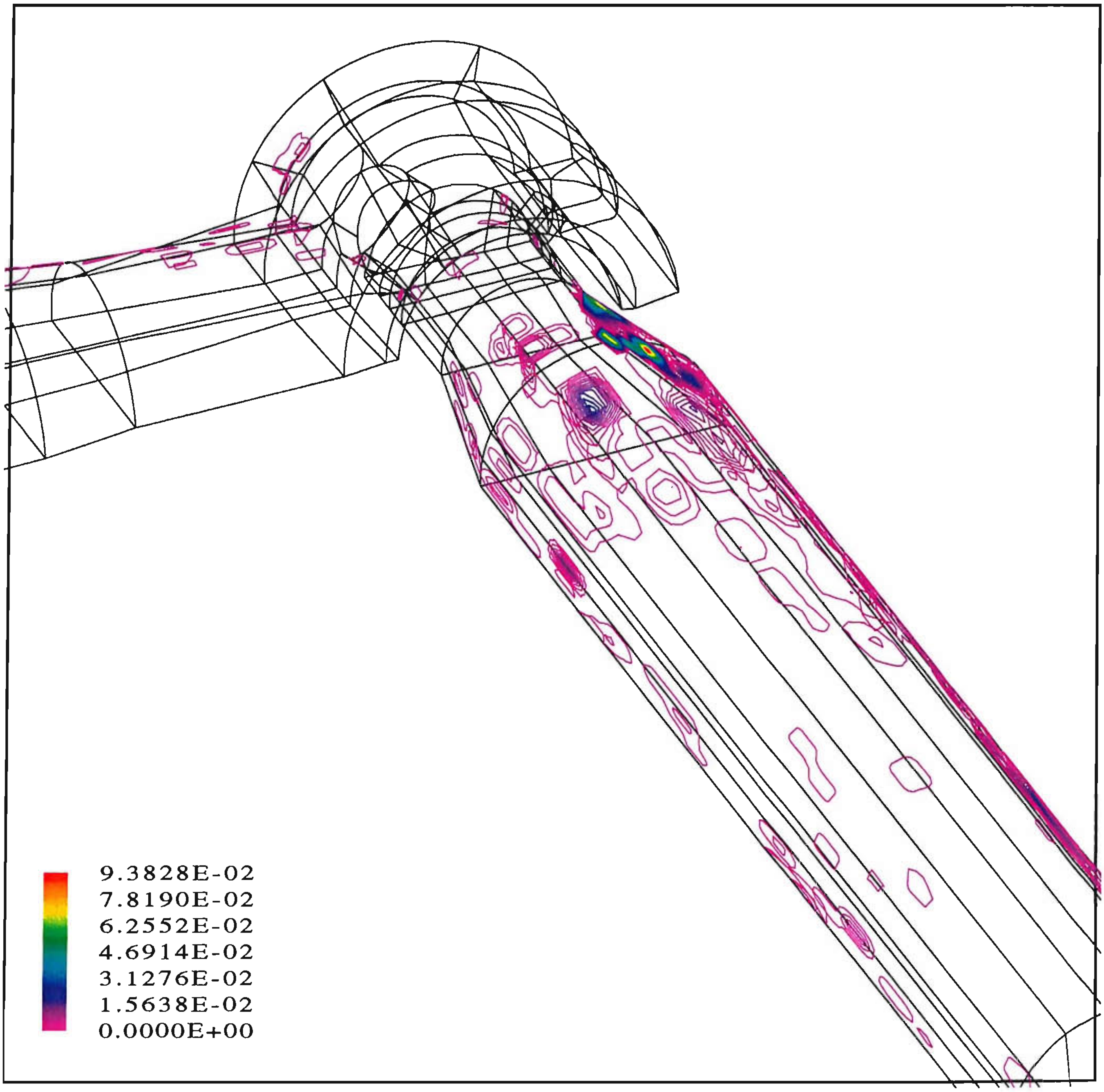

INVESTIGATION OF EROSION WITHIN CAGE TYPE CONTROL CHOKES - LIQUIDS

Particle Type - **Sand** Test No - **4**
Particle Flux Rate - **54** Wppm.
Particle Roundness Factor - **0.5**
Number of Particle Sizes - **8**
Particle Size Range - **170-260** μm
Turbulent Dispersion - **Yes**
Modified Coefficient of Restitution - **Yes**
Squeeze Film Retardation - **Yes**

Appendix Figure 98 - Surface Contour Plot of Internal Plug Particle Erosion Rates (mm^3/hr)

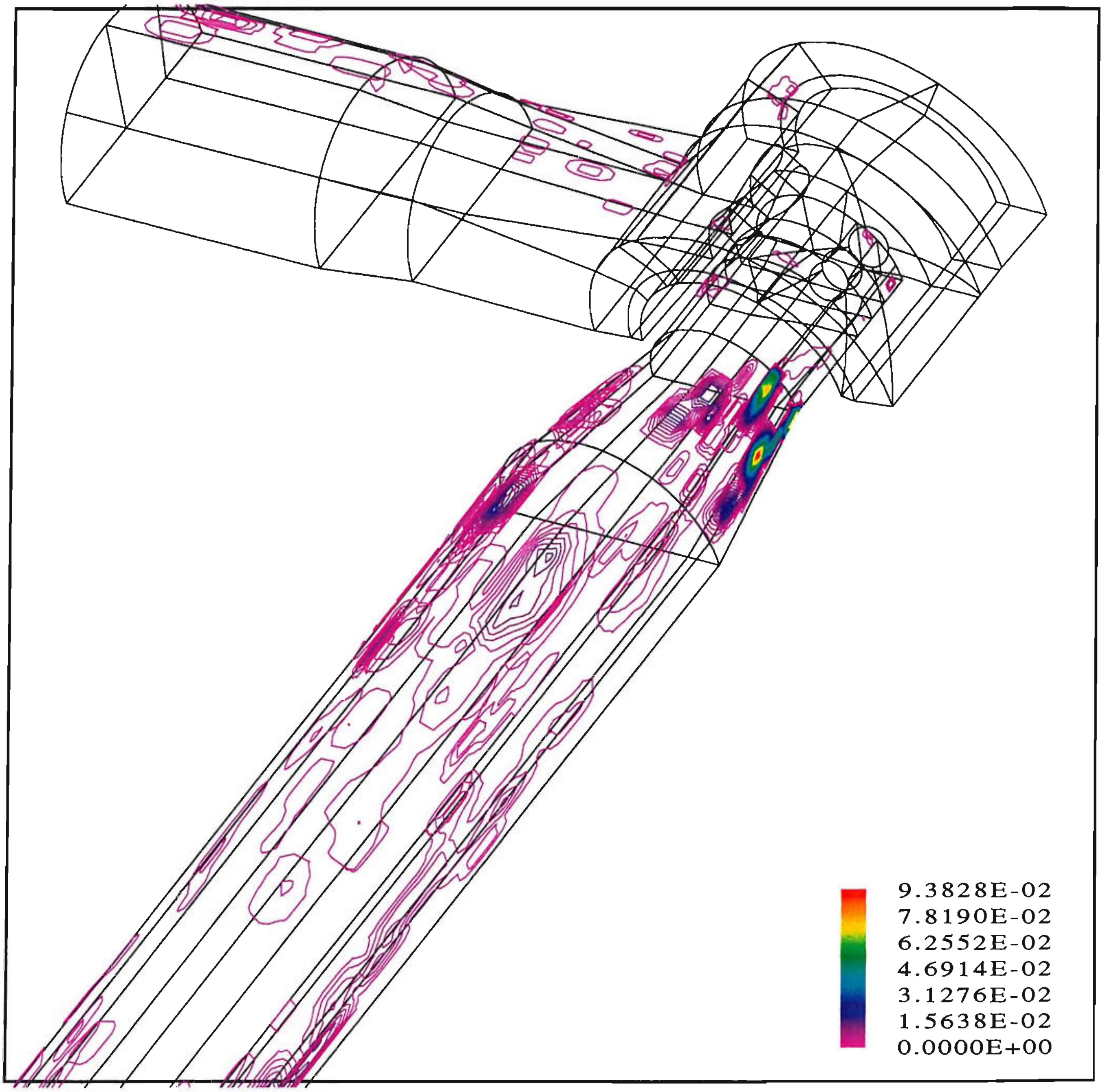

INVESTIGATION OF EROSION WITHIN CAGE TYPE CONTROL CHOKES

Fluid - **Wet Gas**
Inlet Diameter - **75** mm
Port Diameters - **12.5 & 25** mm
Taper Angle on Sleeve - **15°**
Choke Opening - **75** %
Pressure Drop - **50** Bar
Mass Flow Rate (Gas) - **140** kg/hr

Appendix Figure 99 - Velocity Contour Plot of External Sleeve Control Choke (m/s)

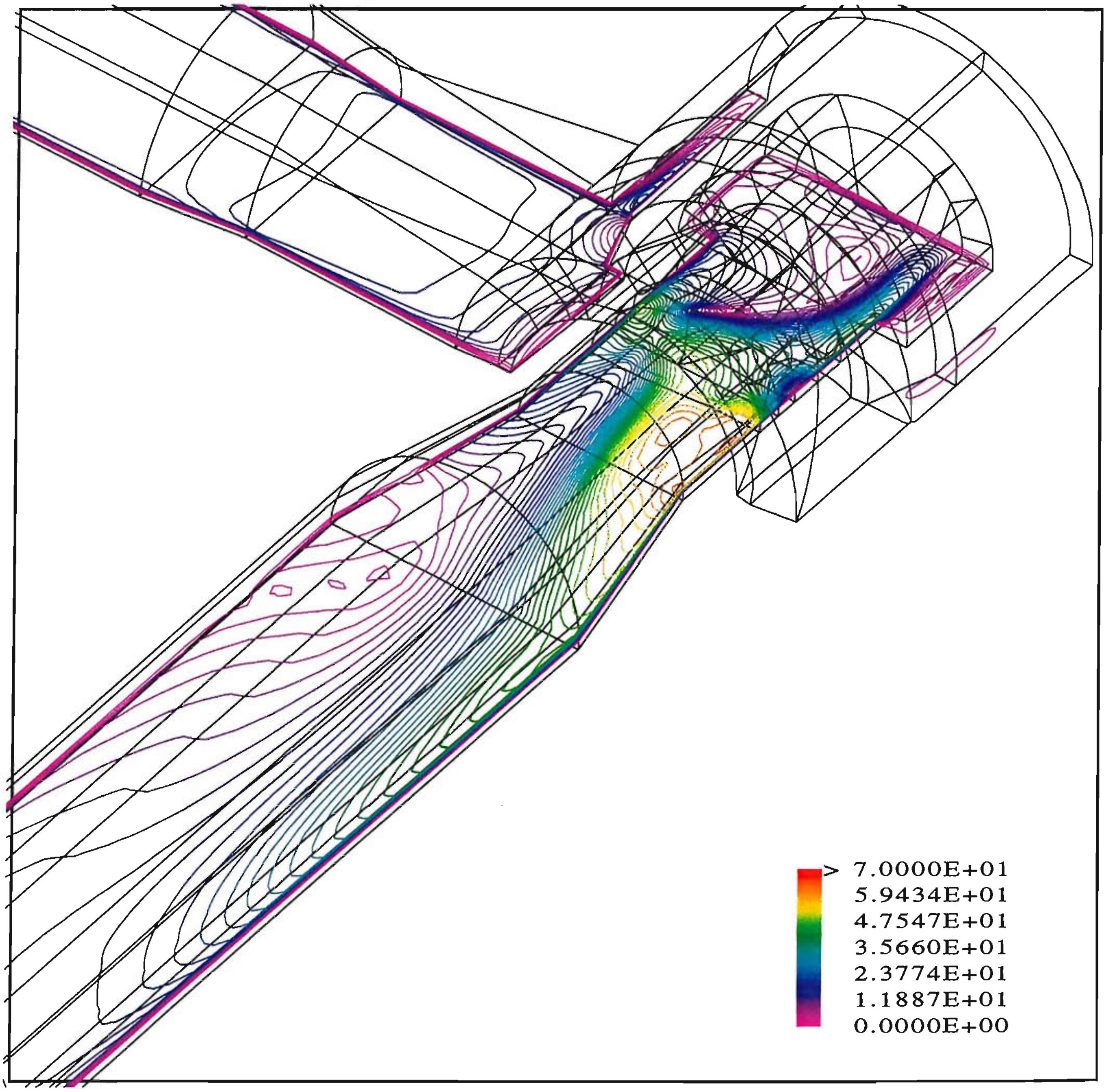

INVESTIGATION OF EROSION WITHIN CAGE TYPE CONTROL CHOKES

Fluid - **Wet Gas**
Inlet Diameter - **75** mm
Port Diameters - **12.5** & **25** mm
Taper Angle on Sleeve - **15°**
Choke Opening - **75** %
Pressure Drop - **50** Bar
Mass Flow Rate (Gas) - **140** kg/hr

Appendix Figure 100 -Turbulent Kinetic Energy Contour Plot of Internal Plug Control Choke

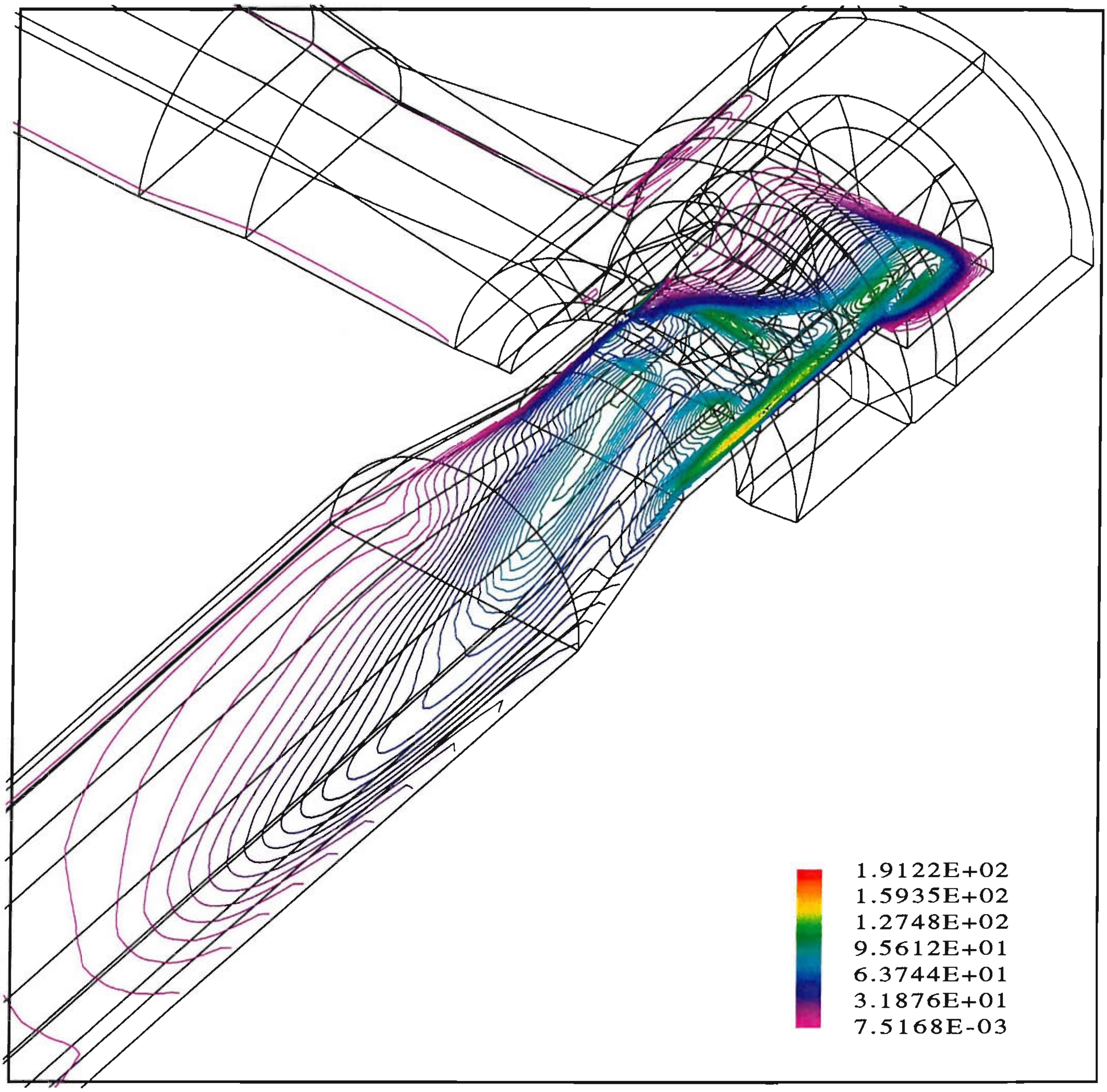

INVESTIGATION OF EROSION WITHIN CAGE TYPE CONTROL CHOKES - WET GAS

Particle Type - **Sand**
Test No - **5**
Particle Flux Rate - **3.7 % by wt.**
Particle Roundness Factor - **0.5**
Number of Particle Sizes - **8**
Particle Size Range - **75-165 μm**
Turbulent Dispersion - **Yes**
Modified Coefficient of Restitution - **Yes**
Squeeze Film Retardation - **Yes**

Appendix Figure 101 - Surface Contour Plot of External Sleeve Particle Impact Velocities (m/s)

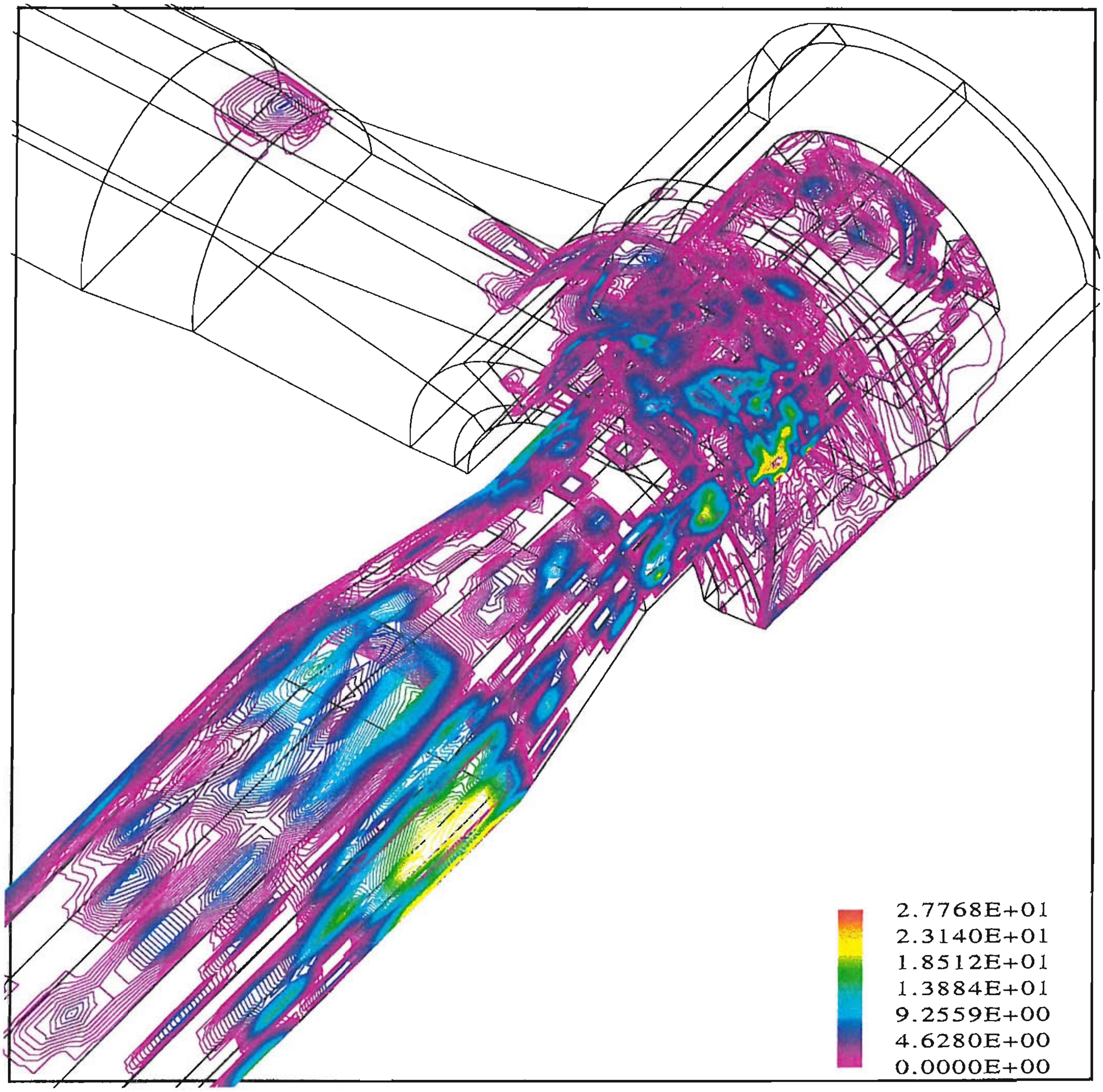

INVESTIGATION OF EROSION WITHIN CAGE TYPE CONTROL CHOKES - WET GAS

Particle Type - **Sand**
Test No - **5**
Particle Flux Rate - **3.7 % by wt.**
Particle Roundness Factor - **0.5**
Number of Particle Sizes - **8**
Particle Size Range - **75-165 μm**
Turbulent Dispersion - **Yes**
Modified Coefficient of Restitution - **Yes**
Squeeze Film Retardation - **Yes**

Appendix Figure 102 - Surface Contour Plot of External Sleeve Particle Impact Angle (deg)

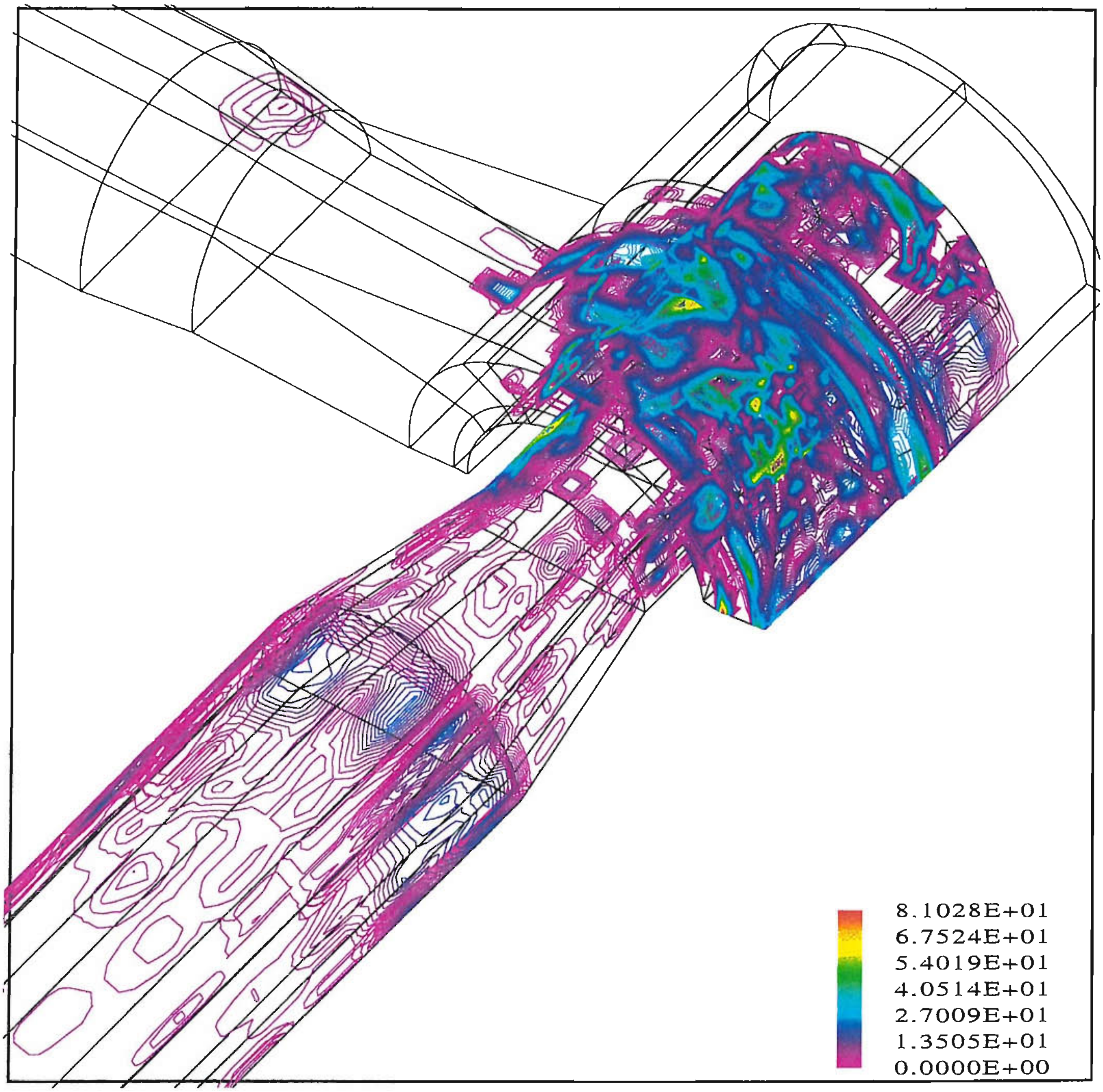

INVESTIGATION OF EROSION WITHIN CAGE TYPE CONTROL CHOKES - WET GAS

Particle Type - **Sand**　　Test No - **5**
Particle Flux Rate - **3.7 % by wt.**
Particle Roundness Factor - **0.5**
Number of Particle Sizes - **8**
Particle Size Range - **75-165** μm
Turbulent Dispersion - **Yes**
Modified Coefficient of Restitution - **Yes**
Squeeze Film Retardation - **Yes**

Appendix Figure 103 - Surface Contour Plot of External Sleeve Particle Erosion Rates (mm^3/hr)

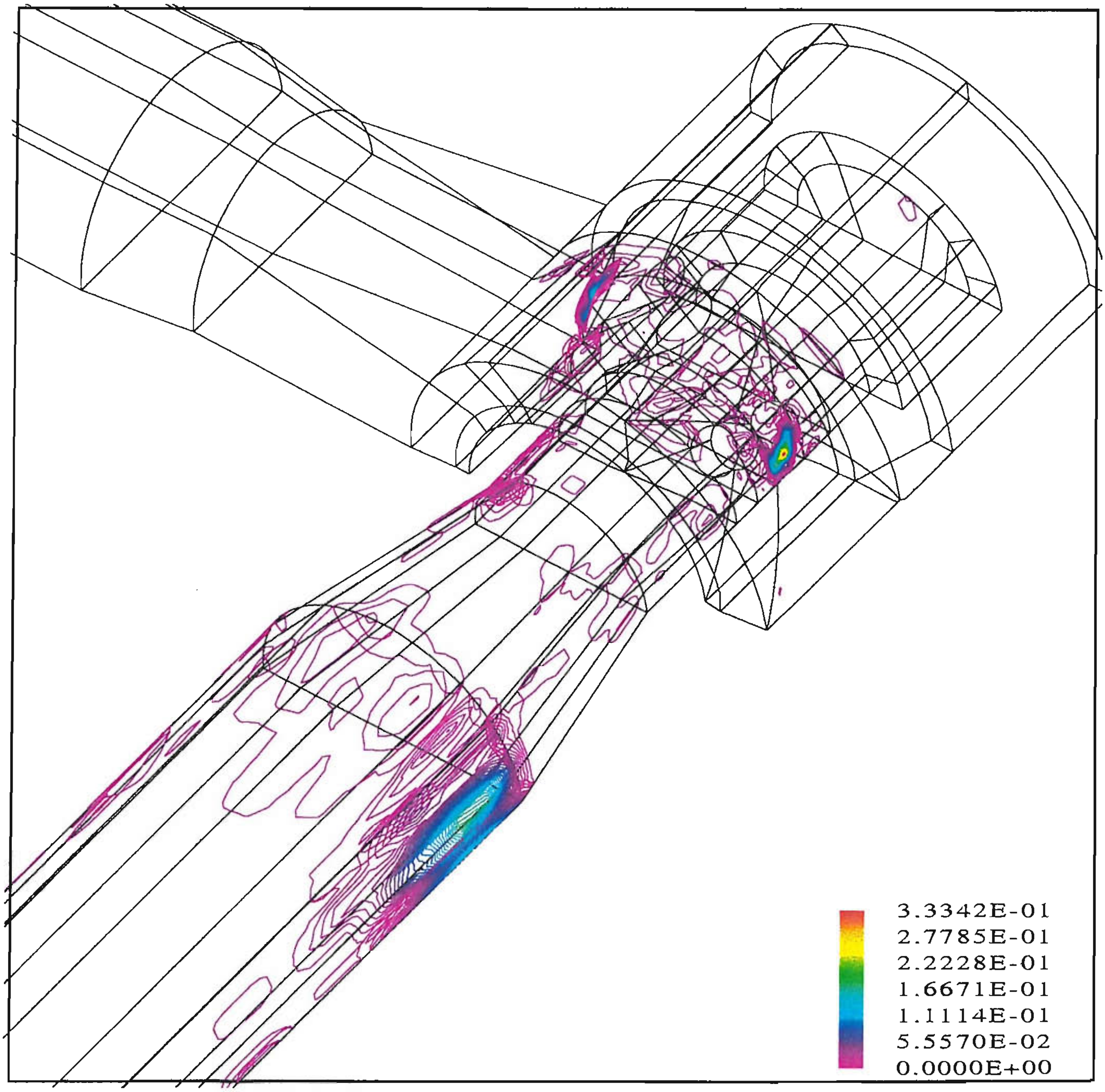

INVESTIGATION OF EROSION WITHIN CAGE TYPE CONTROL CHOKES - WET GAS

Particle Type - **Sand**

Test No - **5**

Particle Flux Rate - **3.7 % by wt.**
Particle Roundness Factor - **0.5**
Number of Particle Sizes - **8**
Particle Size Range - **75-165 μm**
Turbulent Dispersion - **Yes**
Modified Coefficient of Restitution - **Yes**
Squeeze Film Retardation - **Yes**

Appendix Figure 104 - Surface Contour Plot of External Sleeve Particle Erosion Rates (mm^3/hr)

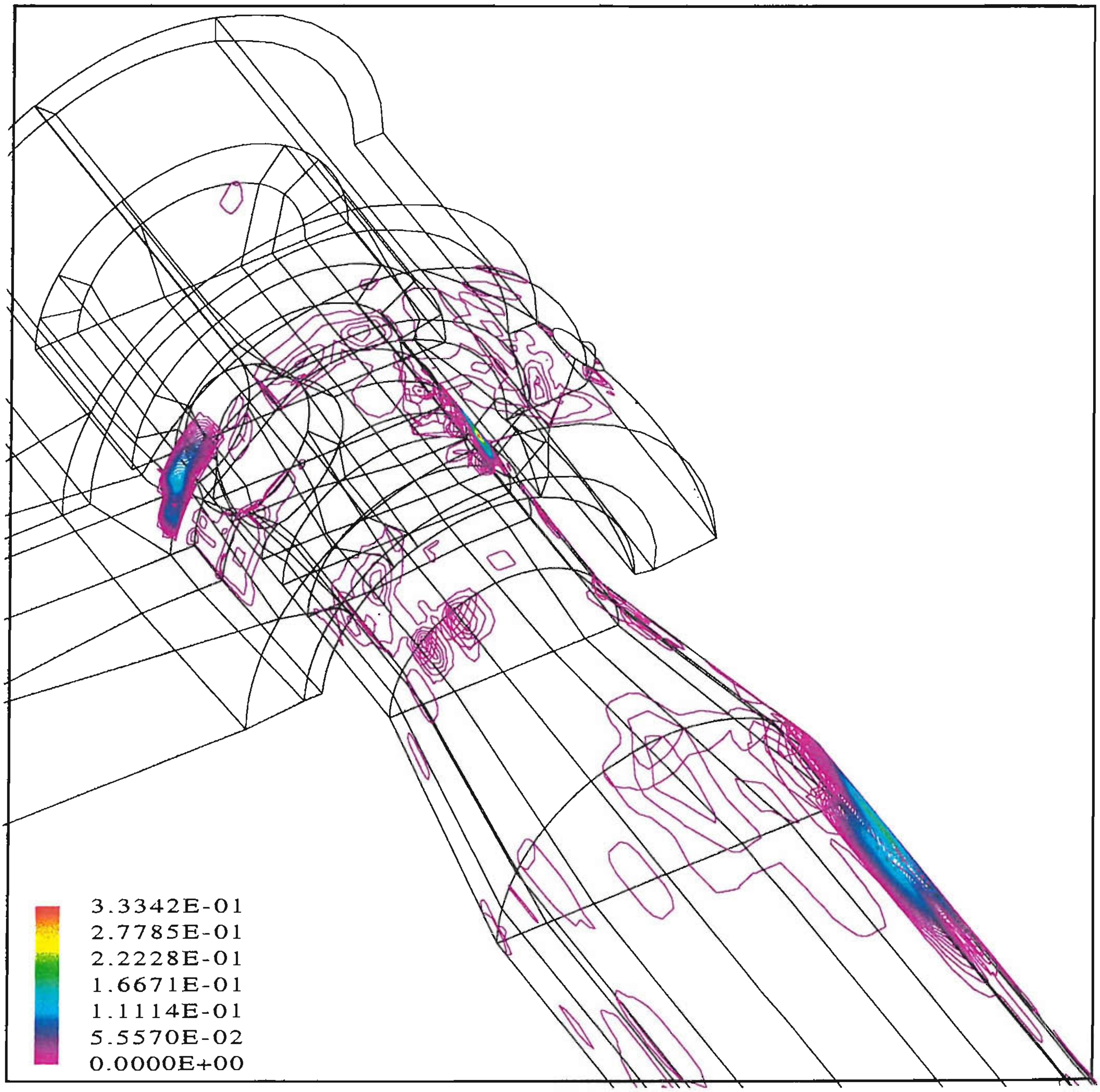

INVESTIGATION OF EROSION WITHIN CAGE TYPE CONTROL CHOKES - WET GAS

Particle Type - **Sand**

Test No - **7**

Particle Flux Rate - **3.7 % by wt.**
Particle Roundness Factor - **0.5**
Number of Particle Sizes - **8**
Particle Size Range - **170-260 μm**
Turbulent Dispersion - **Yes**
Modified Coefficient of Restitution - **Yes**
Squeeze Film Retardation - **Yes**

Appendix Figure 105 - Surface Contour Plot of External Sleeve Particle Impact Velocities (m/s)

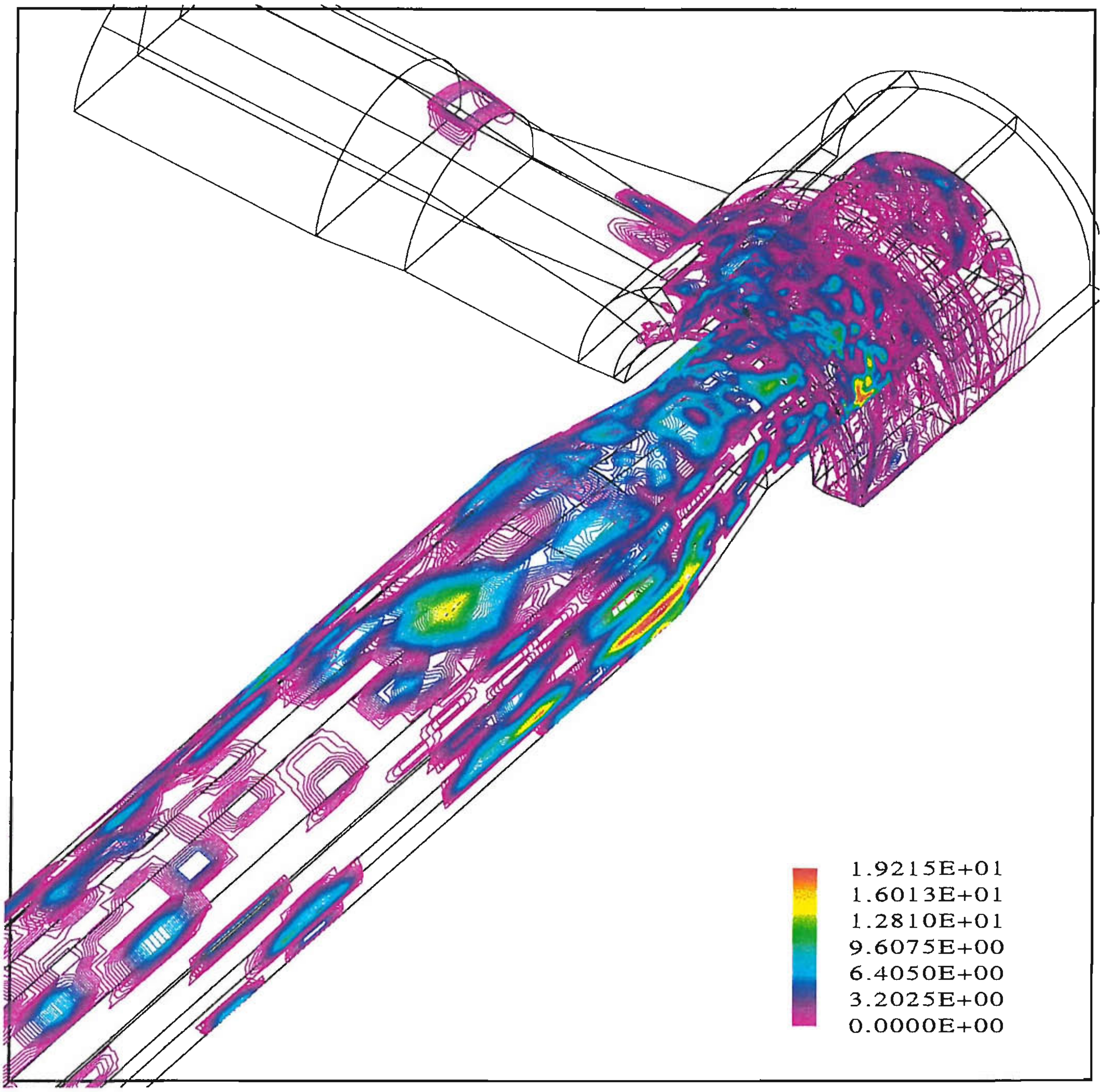

INVESTIGATION OF EROSION WITHIN CAGE TYPE CONTROL CHOKES - WET GAS

Particle Type - **Sand**

Test No - **7**

Particle Flux Rate - **3.7 % by wt.**

Particle Roundness Factor - **0.5**

Number of Particle Sizes - **8**

Particle Size Range - **170-260** μm

Turbulent Dispersion - **Yes**

Modified Coefficient of Restitution - **Yes**

Squeeze Film Retardation - **Yes**

Appendix Figure 106 - Surface Contour Plot of External Sleeve Particle Impact Angle (deg)

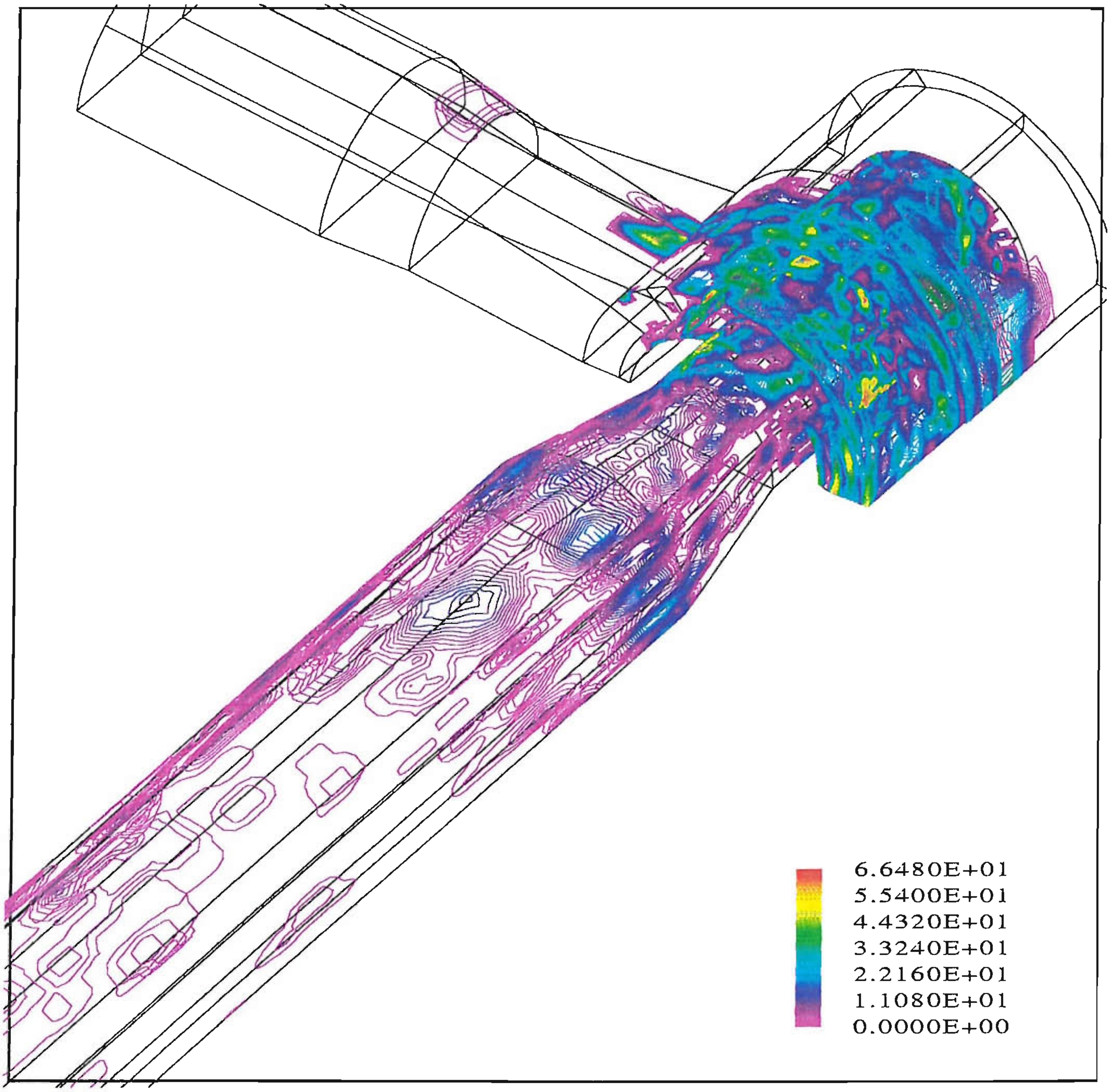

INVESTIGATION OF EROSION WITHIN CAGE TYPE CONTROL CHOKES - WET GAS

Particle Type - **Sand** Test No - **7**
Particle Flux Rate - **3.7 % by wt.**
Particle Roundness Factor - **0.5**
Number of Particle Sizes - **8**
Particle Size Range - **170-260** μm
Turbulent Dispersion - **Yes**
Modified Coefficient of Restitution - **Yes**
Squeeze Film Retardation - **Yes**

Appendix Figure 107 - Surface Contour Plot of External Sleeve Particle Erosion Rates (mm^3/hr)

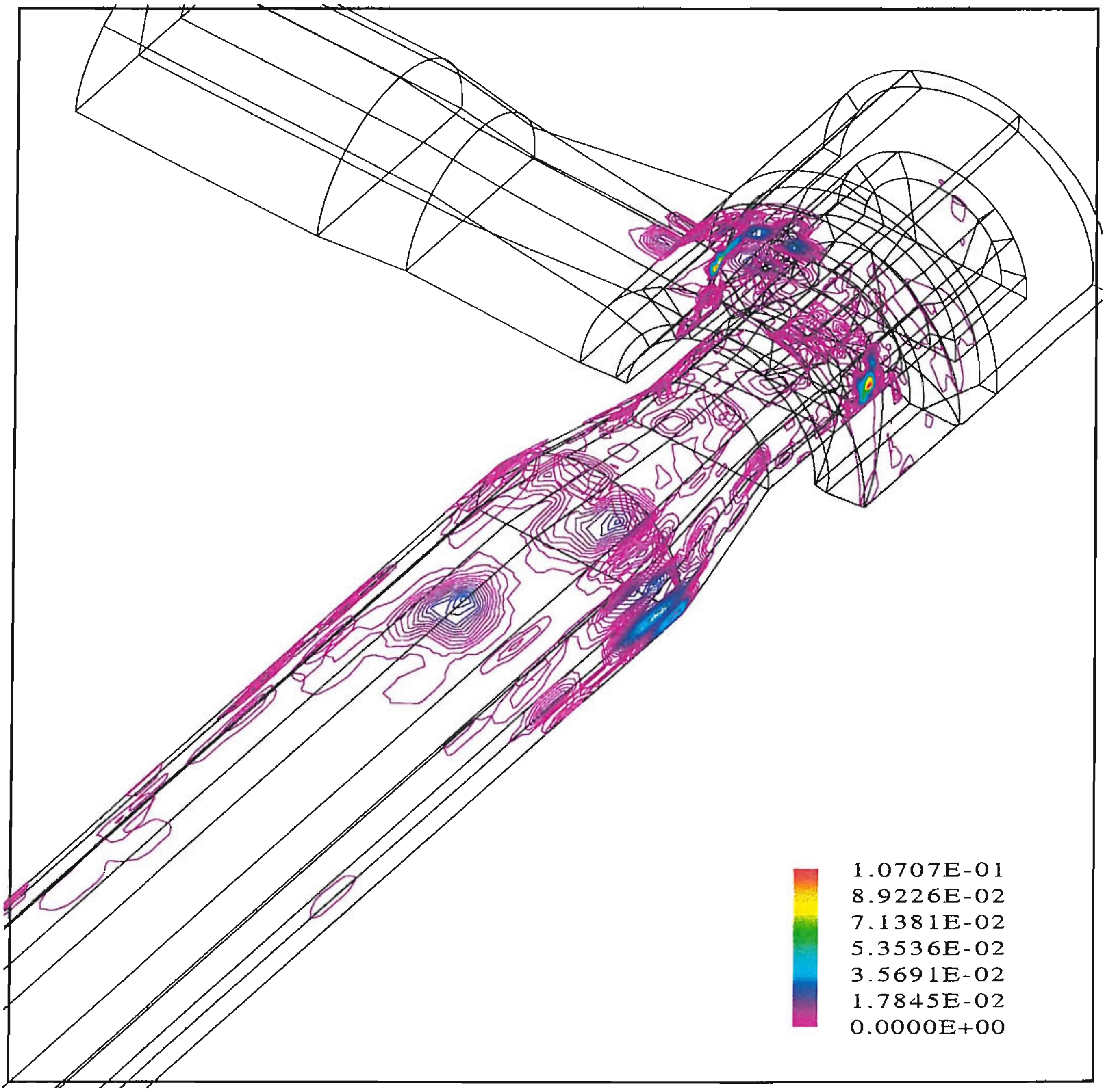

INVESTIGATION OF EROSION WITHIN CAGE TYPE CONTROL CHOKES - WET GAS

Particle Type - **Sand** Test No - **7**
Particle Flux Rate - **3.7 % by wt.**
Particle Roundness Factor - **0.5**
Number of Particle Sizes - **8**
Particle Size Range - **170-260 μm**
Turbulent Dispersion - **Yes**
Modified Coefficient of Restitution - **Yes**
Squeeze Film Retardation - **Yes**

Appendix Figure 108 - Surface Contour Plot of External Sleeve Particle Erosion Rates (mm^3/hr)

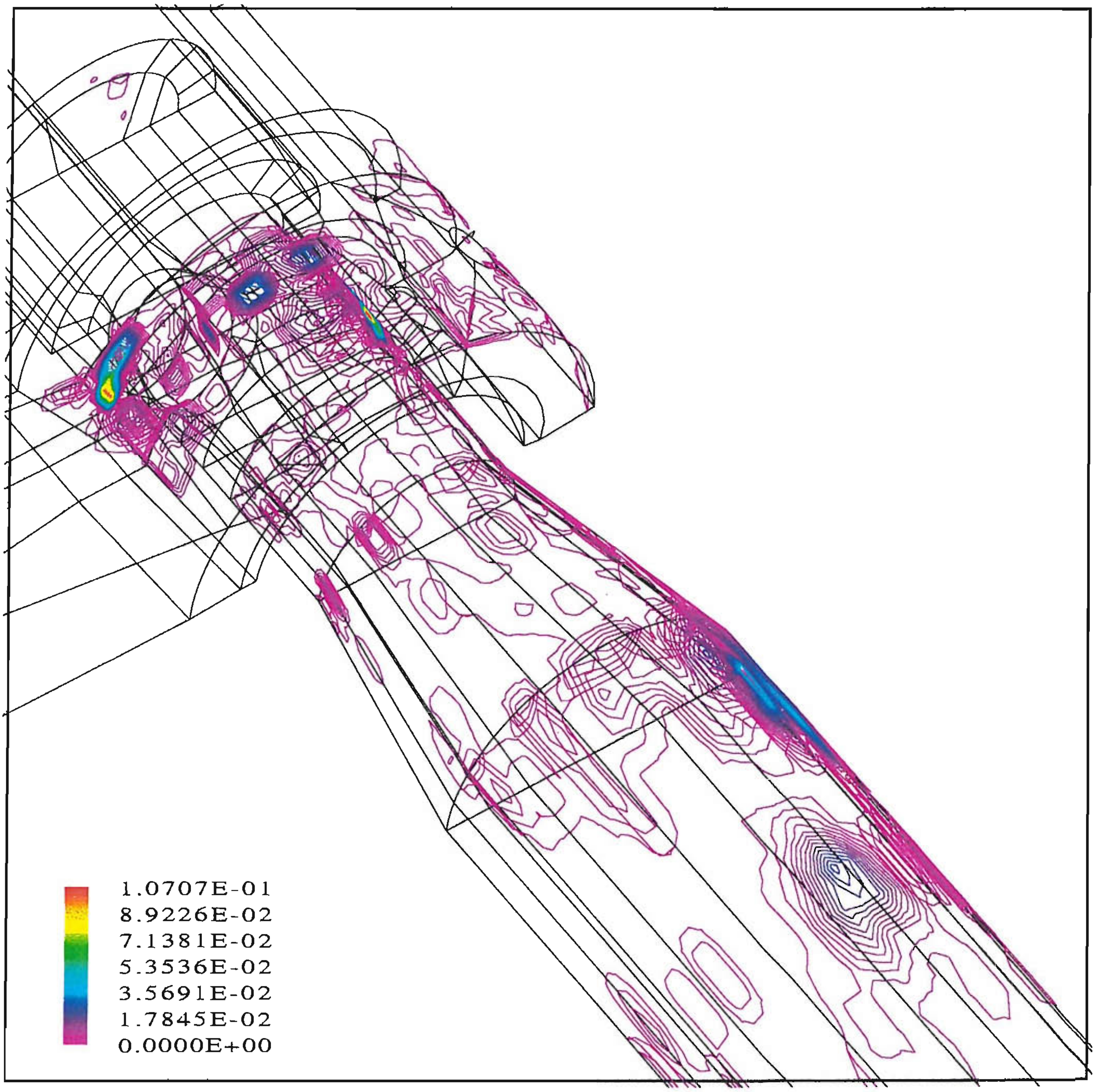

INVESTIGATION OF EROSION WITHIN CAGE TYPE CONTROL CHOKES

Fluid - **Wet Gas**
Inlet Diameter - **75** mm
Port Diameters - **12.5** & **25** mm
Plug Edge - **Sharp**
Choke Opening - **75** %
Pressure Drop - **50** Bar
Mass Flow Rate (Gas) - **140** kg/hr

Appendix Figure 109 - Velocity Contour Plot of Internal Plug Control Choke (m/s)

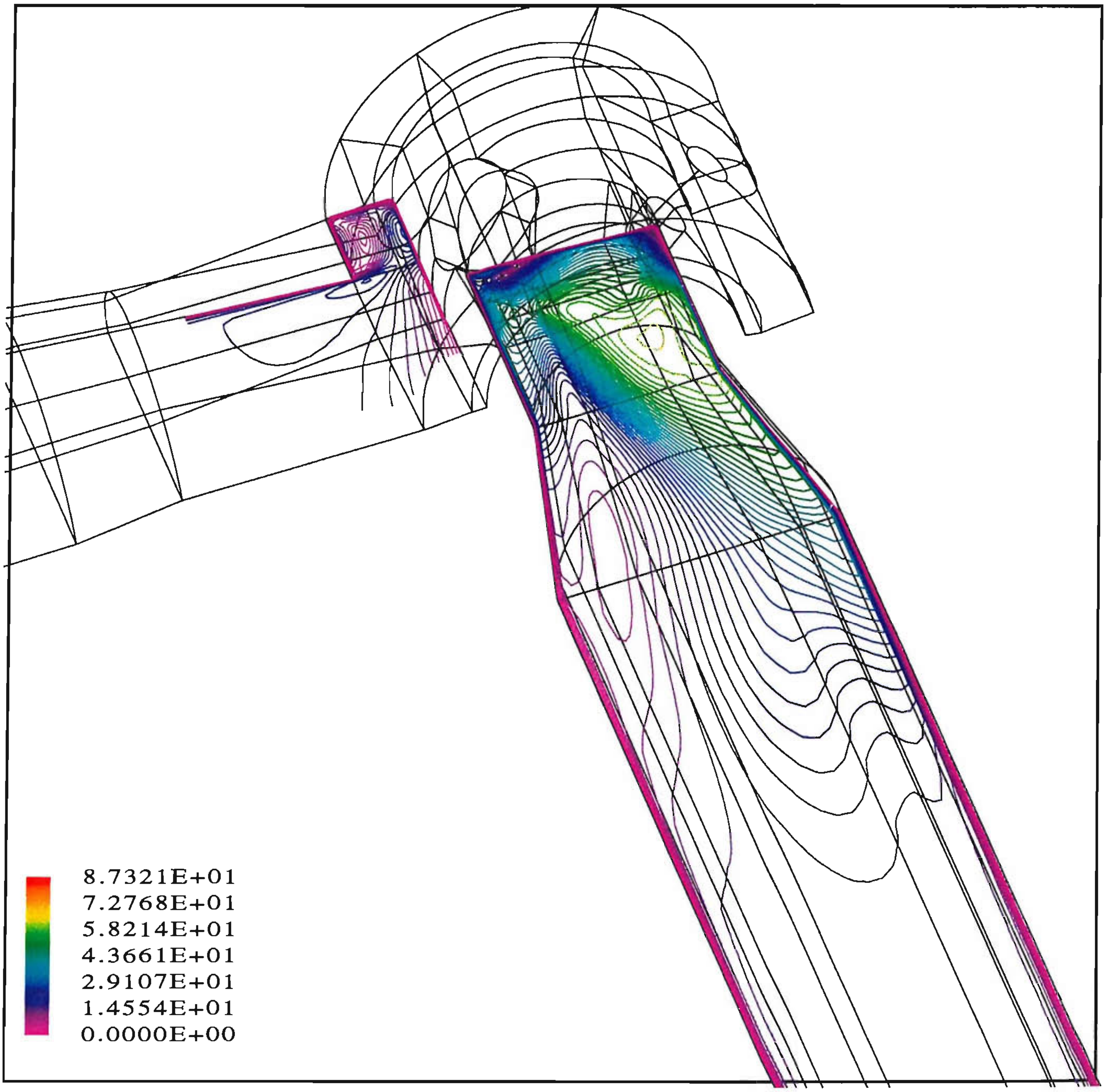

INVESTIGATION OF EROSION WITHIN CAGE TYPE CONTROL CHOKES

Fluid - **Wet Gas**
Inlet Diameter - **75** mm
Port Diameters - **12.5** & **25** mm
Plug Edge - **Sharp**
Choke Opening - **75** %
Pressure Drop - **50** Bar
Mass Flow Rate (Gas) - **140** kg/hr

Appendix Figure 110 - Velocity Contour Plot of Internal Plug Control Choke (m/s)

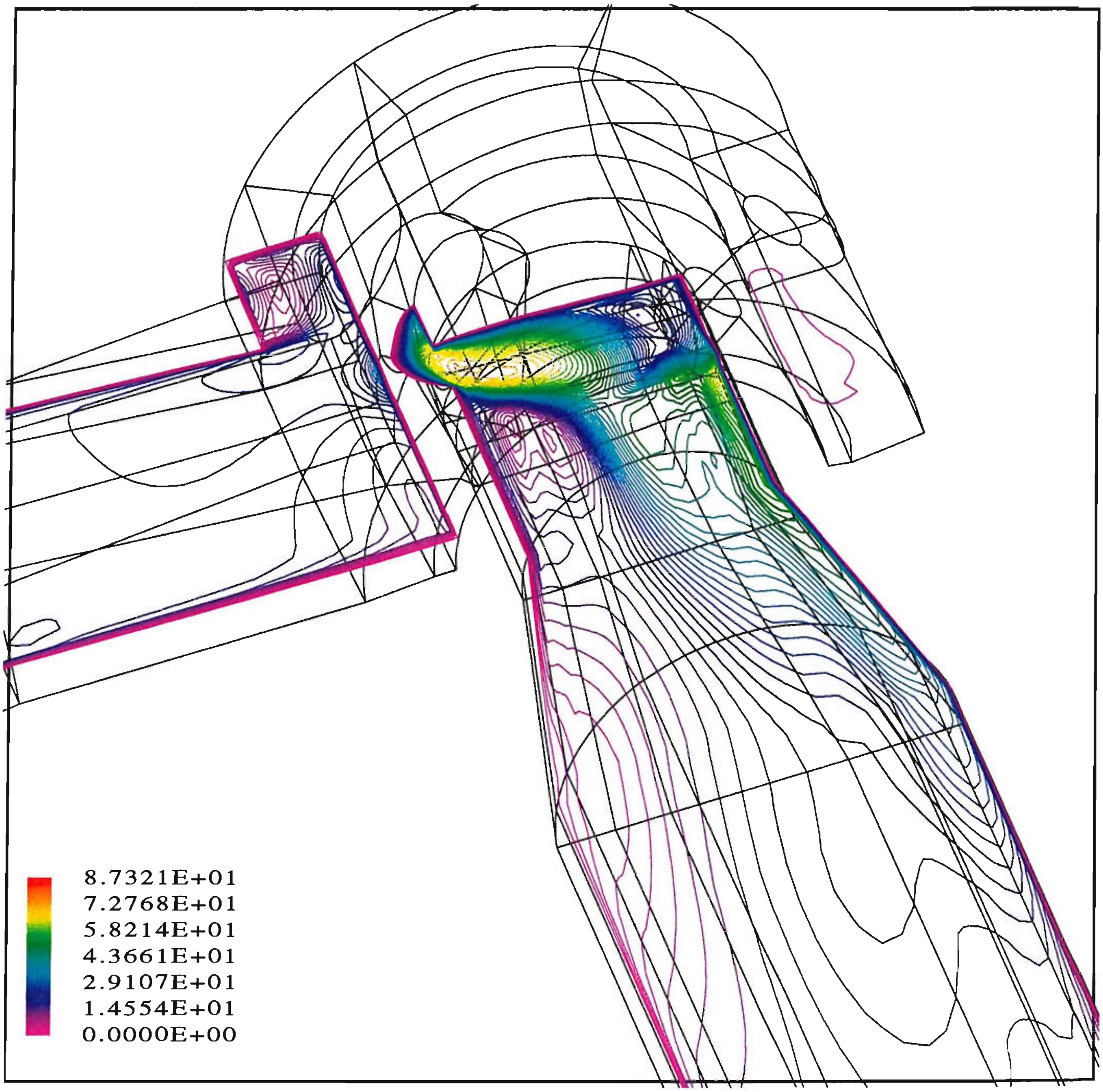

INVESTIGATION OF EROSION WITHIN CAGE TYPE CONTROL CHOKES

Fluid - **Wet Gas**
Inlet Diameter - **75** mm
Port Diameters - **12.5** & **25** mm
Plug Edge - **Sharp**
Choke Opening - **75** %
Pressure Drop - **50** Bar
Mass Flow Rate (Gas) - **140** kg/hr

Appendix Figure 111 - Velocity Contour Plot of Internal Plug Control Choke (m/s)

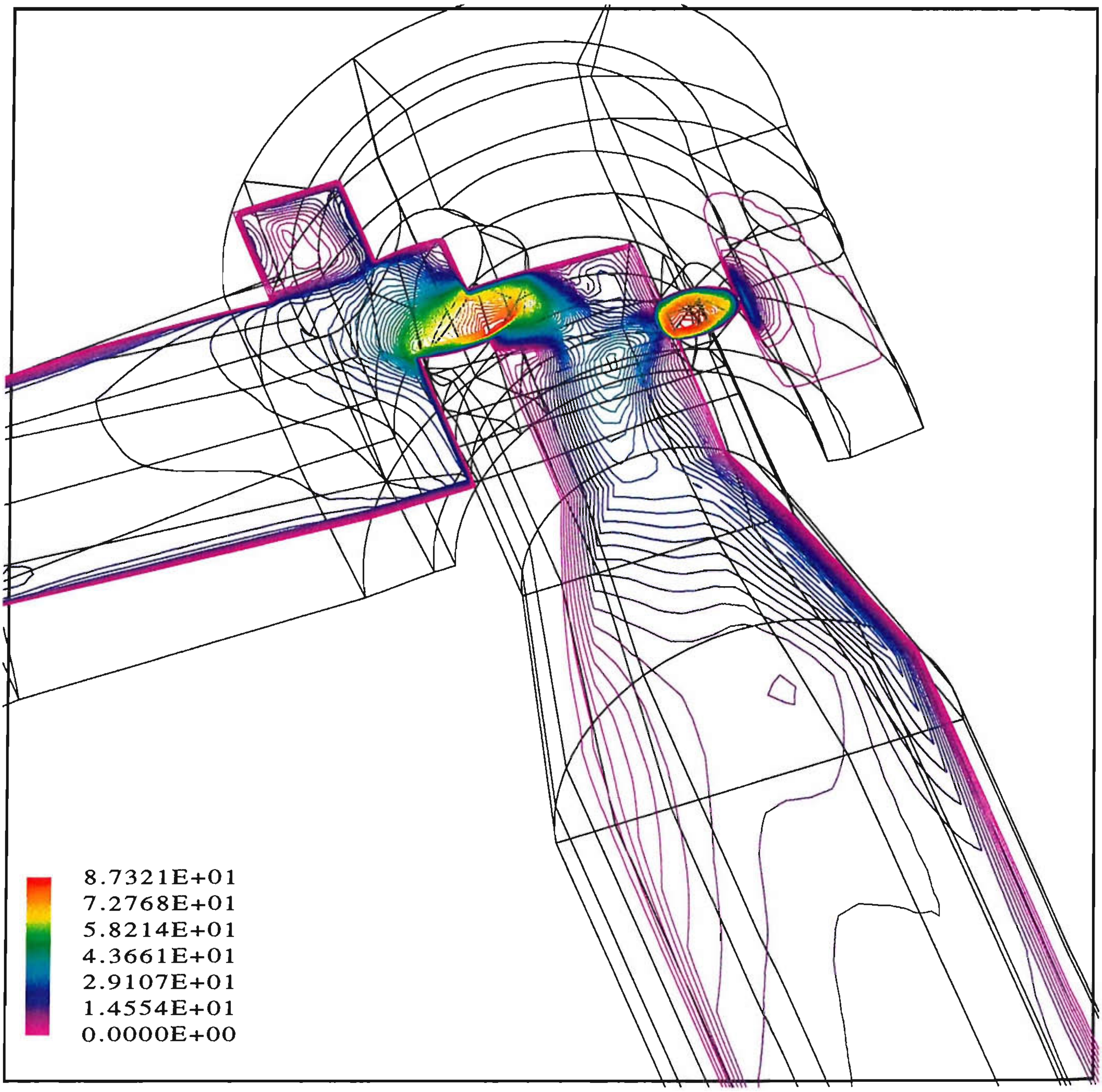

INVESTIGATION OF EROSION WITHIN CAGE TYPE CONTROL CHOKES

Fluid - **Wet Gas**
Inlet Diameter - **75** mm
Port Diameters - **12.5** & **25** mm
Plug Edge - **Sharp**
Choke Opening - **75** %
Pressure Drop - **50** Bar
Mass Flow Rate (Gas) - **140** kg/hr

Appendix Figure 112 - Turbulent Kinetic Energy Contour Plot of Internal Plug Control Choke

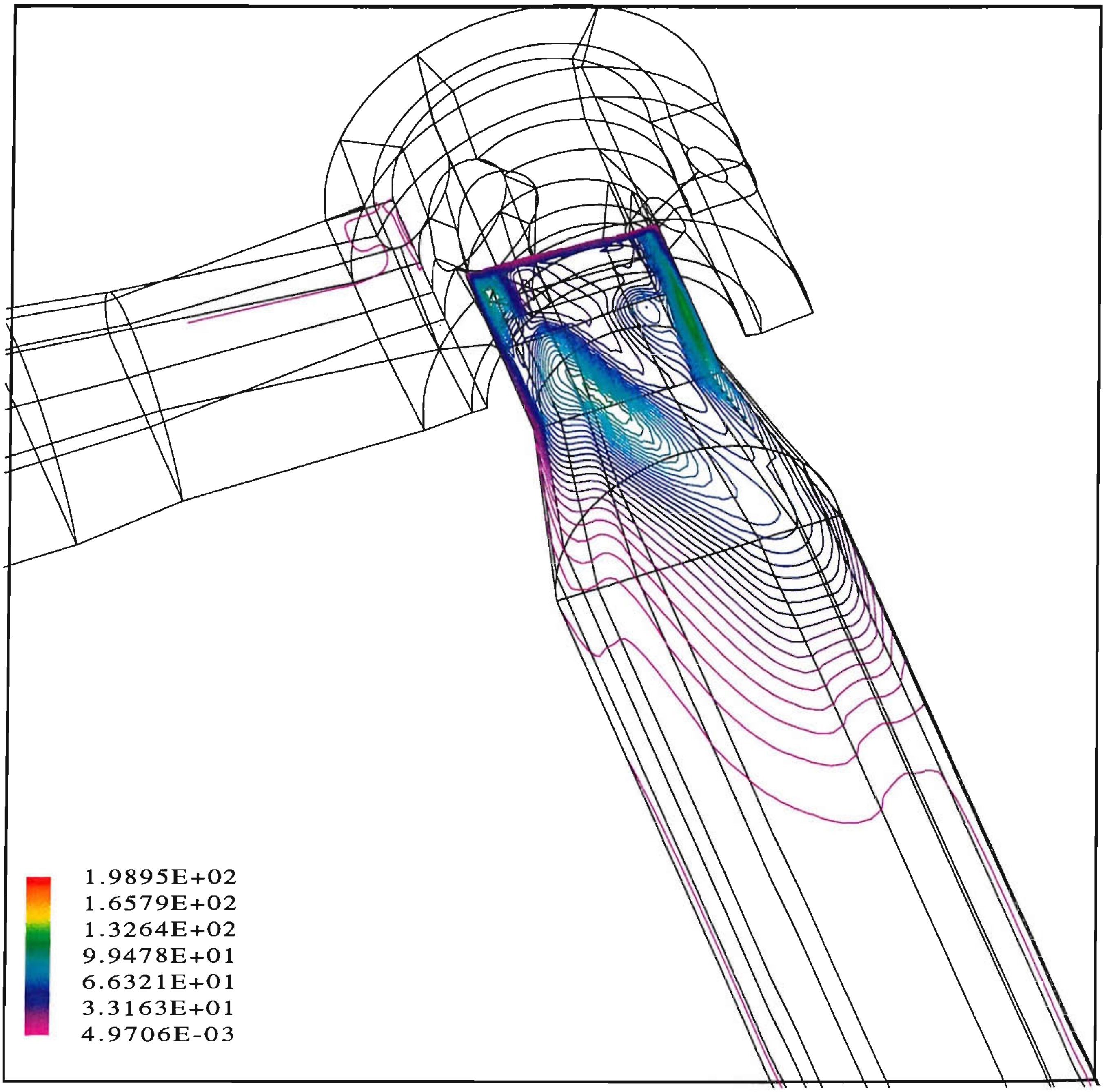

INVESTIGATION OF EROSION WITHIN CAGE TYPE CONTROL CHOKES - WET GAS

Particle Type - **Sand**

Test No - **6**

Particle Flux Rate - **3.7 % by wt.**

Particle Roundness Factor - **0.5**

Number of Particle Sizes - **8**

Particle Size Range - **75-165 μm**

Turbulent Dispersion - **Yes**

Modified Coefficient of Restitution - **Yes**

Squeeze Film Retardation - **Yes**

Appendix Figure 113 - Surface Contour Plot of Internal Plug Particle Impact Velocities (m/s)

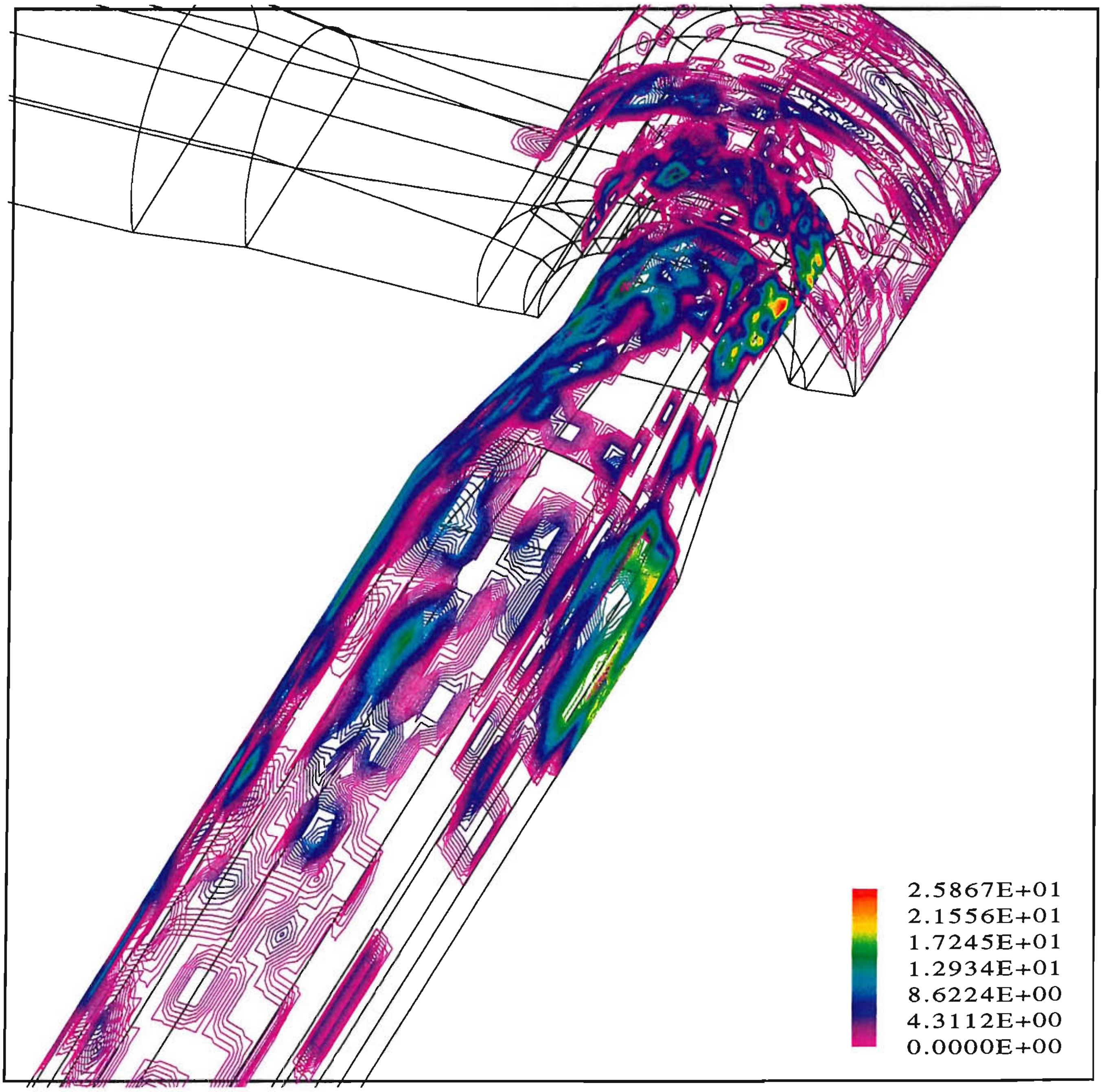

INVESTIGATION OF EROSION WITHIN CAGE TYPE CONTROL CHOKES - WET GAS

Particle Type - **Sand** Test No - **6**
Particle Flux Rate - **3.7 % by wt.**
Particle Roundness Factor - **0.5**
Number of Particle Sizes - **8**
Particle Size Range - **75-165** μm
Turbulent Dispersion - **Yes**
Modified Coefficient of Restitution - **Yes**
Squeeze Film Retardation - **Yes**

Appendix Figure 114 - Surface Contour Plot of Internal Plug Particle Impact Angle (deg)

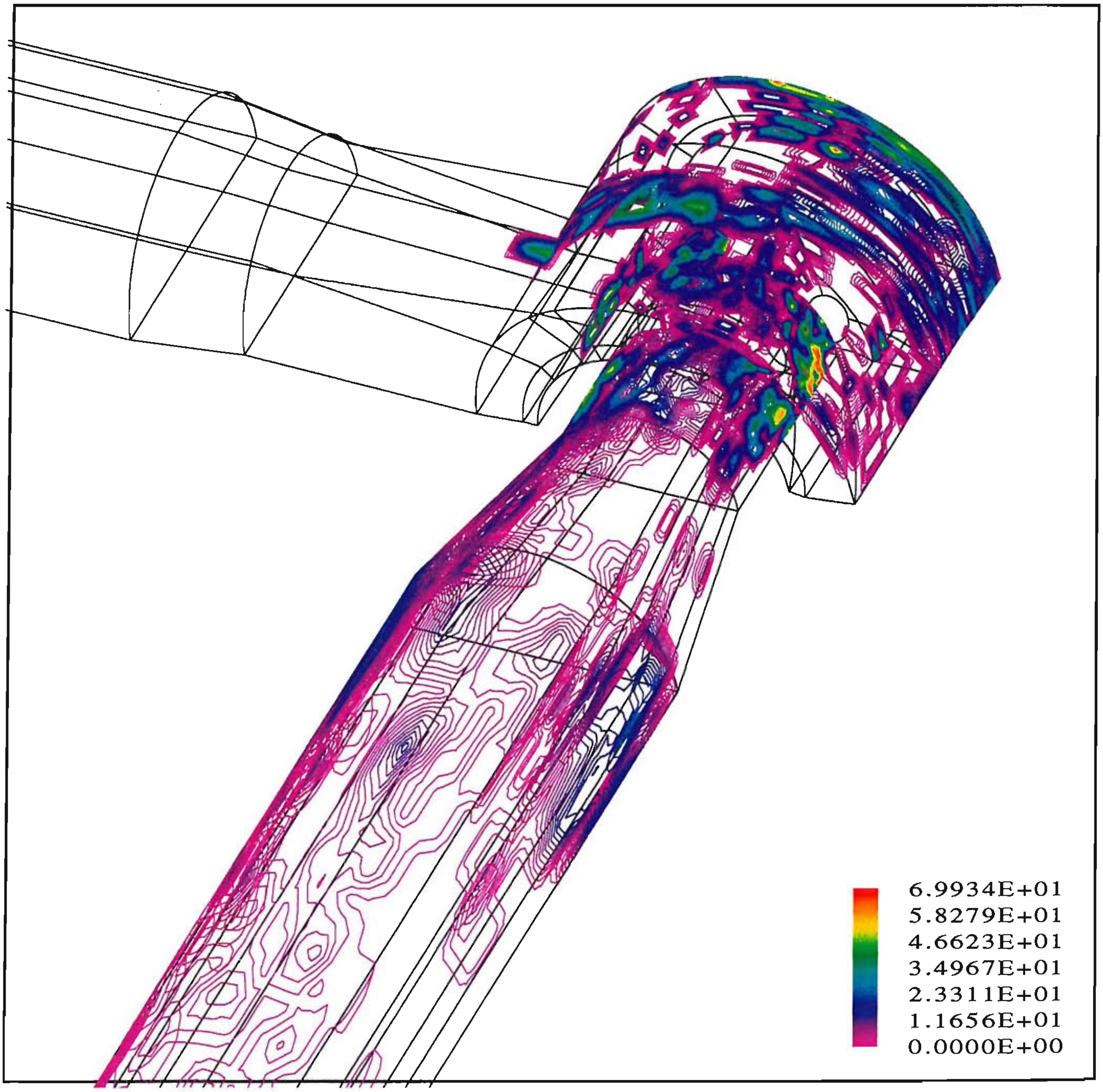

INVESTIGATION OF EROSION WITHIN CAGE TYPE CONTROL CHOKES - WET GAS

Particle Type - **Sand** Test No - **6**
Particle Flux Rate - **3.7 % by wt.**
Particle Roundness Factor - **0.5**
Number of Particle Sizes - **8**
Particle Size Range - **75-165 μm**
Turbulent Dispersion - **Yes**
Modified Coefficient of Restitution - **Yes**
Squeeze Film Retardation - **Yes**

Appendix Figure 115 - Surface Contour Plot of Internal Plug Particle Erosion Rates (mm^3/hr)

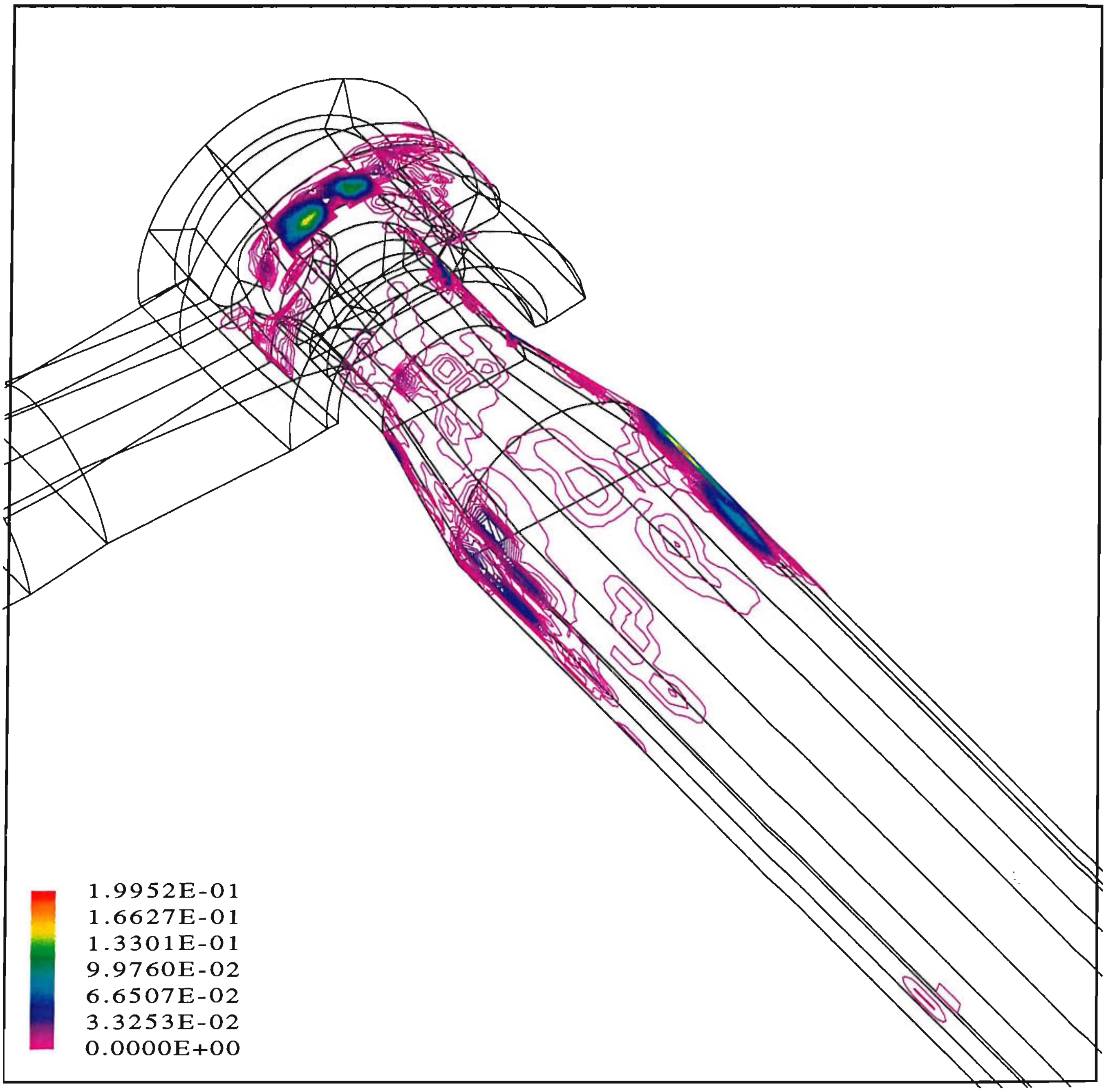

INVESTIGATION OF EROSION WITHIN CAGE TYPE CONTROL CHOKES - WET GAS

Particle Type - **Sand** Test No - **6**
Particle Flux Rate - **3.7 % by wt.**
Particle Roundness Factor - **0.5**
Number of Particle Sizes - **8**
Particle Size Range - **75-165 µm**
Turbulent Dispersion - **Yes**
Modified Coefficient of Restitution - **Yes**
Squeeze Film Retardation - **Yes**

Appendix Figure 116 - Surface Contour Plot of Internal Plug Particle Erosion Rates (mm^3/hr)

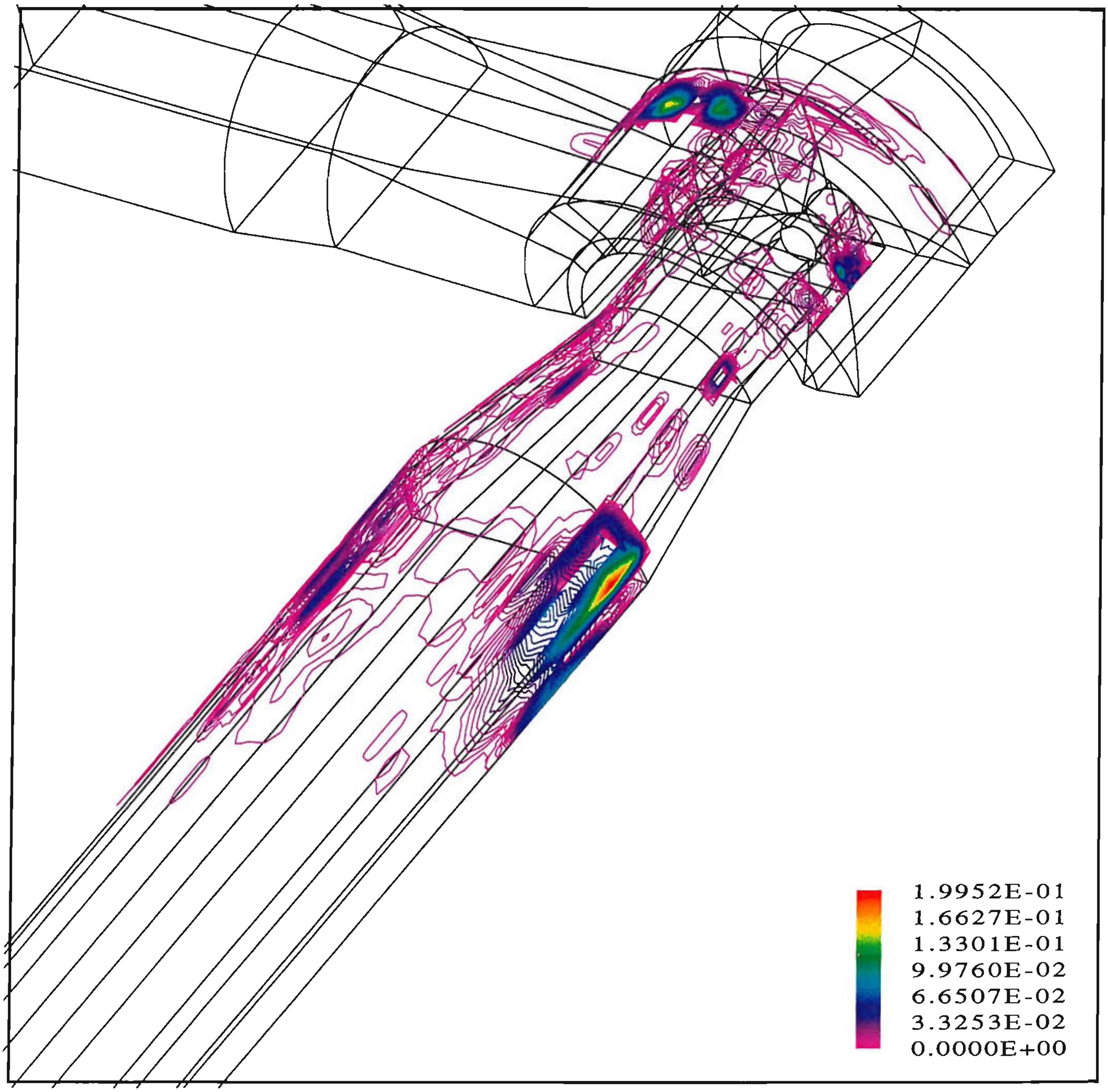

INVESTIGATION OF EROSION WITHIN CAGE TYPE CONTROL CHOKES - WET GAS

Particle Type - **Sand**
Test No - **8**
Particle Flux Rate - **3.7 % by wt.**
Particle Roundness Factor - **0.5**
Number of Particle Sizes - **8**
Particle Size Range - **170-260** μm
Turbulent Dispersion - **Yes**
Modified Coefficient of Restitution - **Yes**
Squeeze Film Retardation - **Yes**

Appendix Figure 117 - Surface Contour Plot of Internal Plug Particle Impact Velocities (m/s)

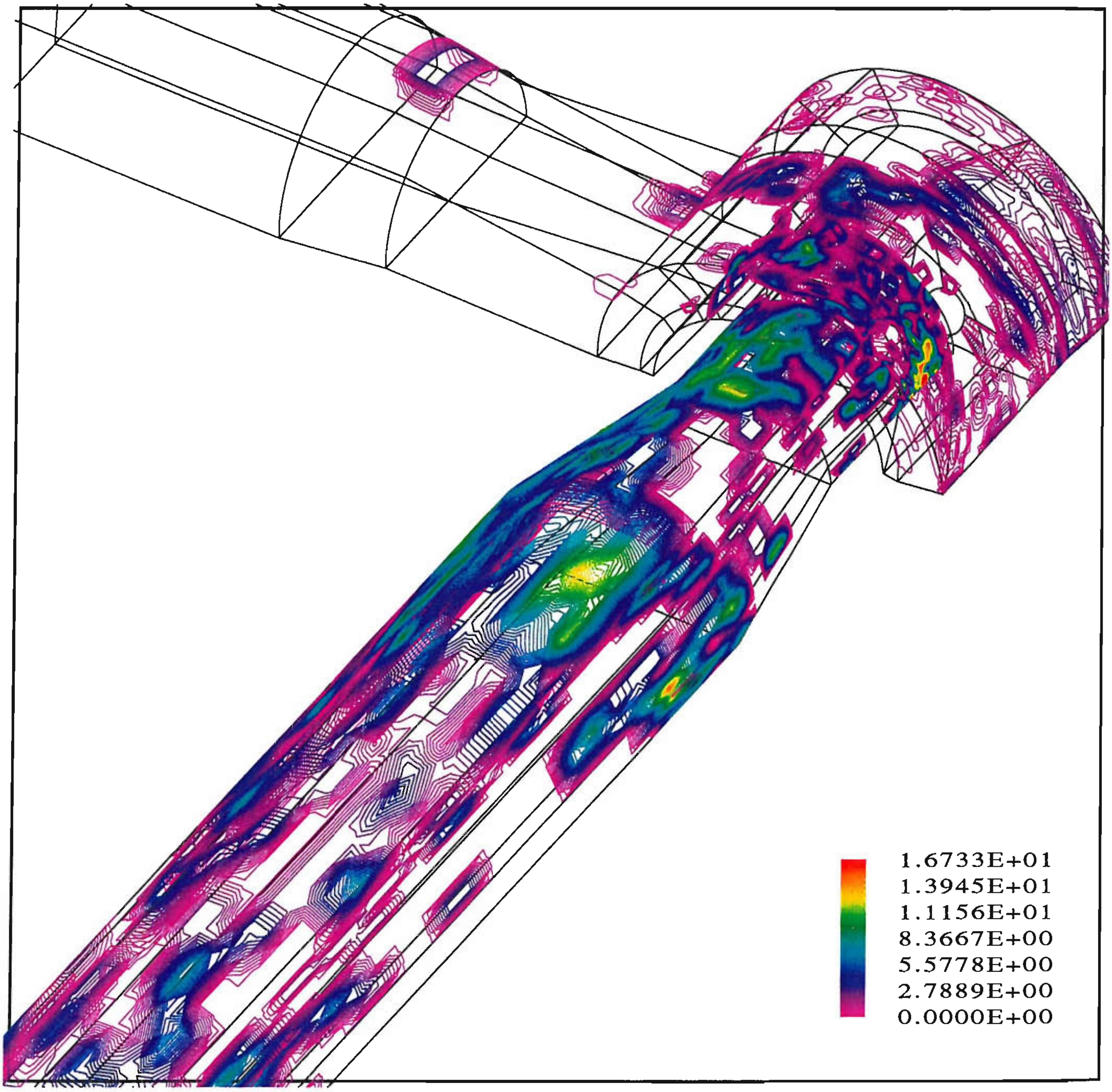

INVESTIGATION OF EROSION WITHIN CAGE TYPE CONTROL CHOKES - WET GAS

Particle Type - **Sand**
Particle Flux Rate - **3.7 % by wt.**
Particle Roundness Factor - **0.5**
Number of Particle Sizes - **8**
Particle Size Range - **170-260 μm**
Turbulent Dispersion - **Yes**
Modified Coefficient of Restitution - **Yes**
Squeeze Film Retardation - **Yes**

Test No - **8**

Appendix Figure 118 - Surface Contour Plot of Internal Plug Particle Impact Angle (deg)

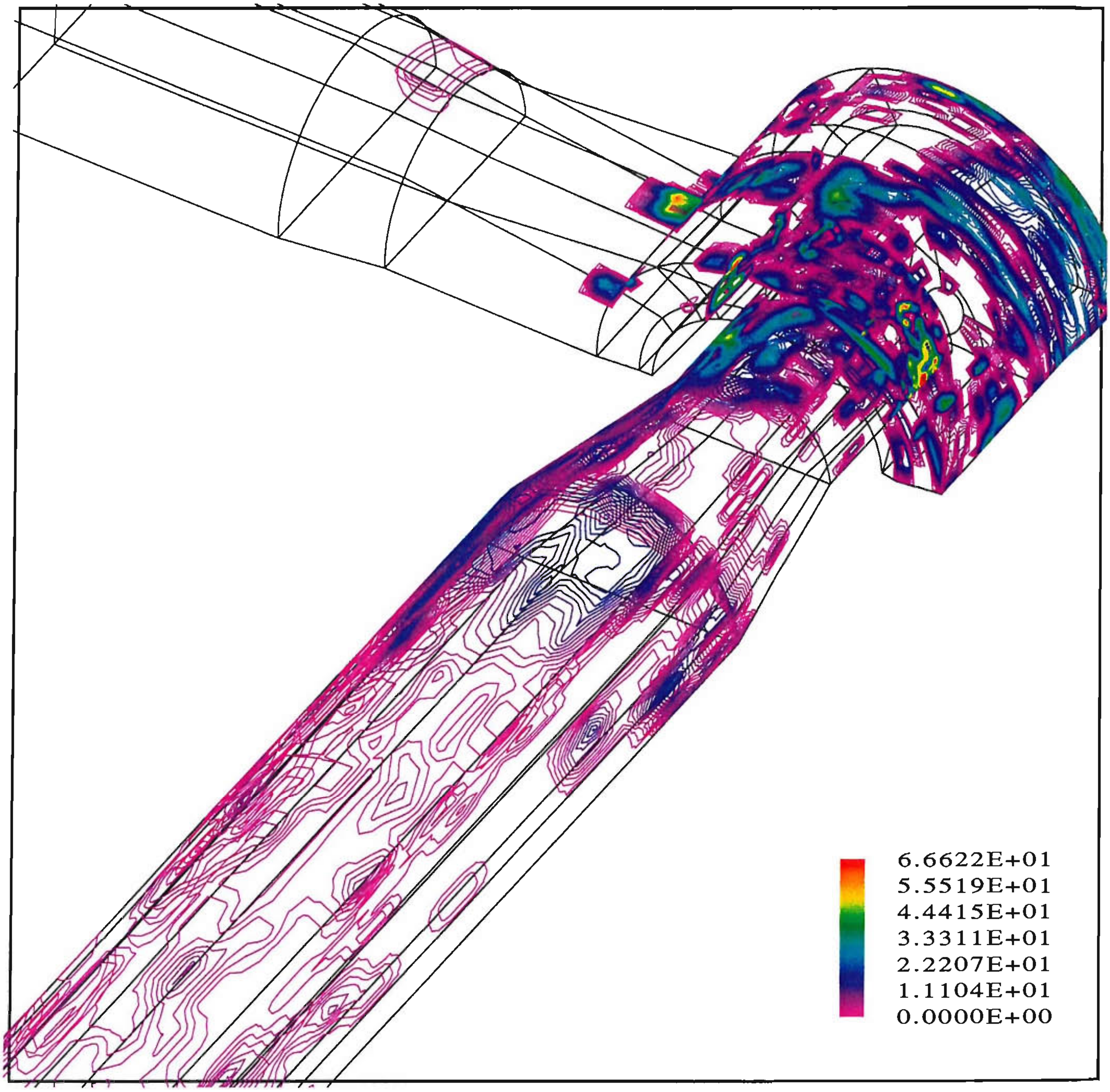

INVESTIGATION OF EROSION WITHIN CAGE TYPE CONTROL CHOKES - WET GAS

Particle Type - **Sand**

Test No - **8**

Particle Flux Rate - **3.7 % by wt.**

Particle Roundness Factor - **0.5**

Number of Particle Sizes - **8**

Particle Size Range - **170-260** μm

Turbulent Dispersion - **Yes**

Modified Coefficient of Restitution - **Yes**

Squeeze Film Retardation - **Yes**

Appendix Figure 119 - Surface Contour Plot of Internal Plug Particle Erosion Rates (mm^3/hr)

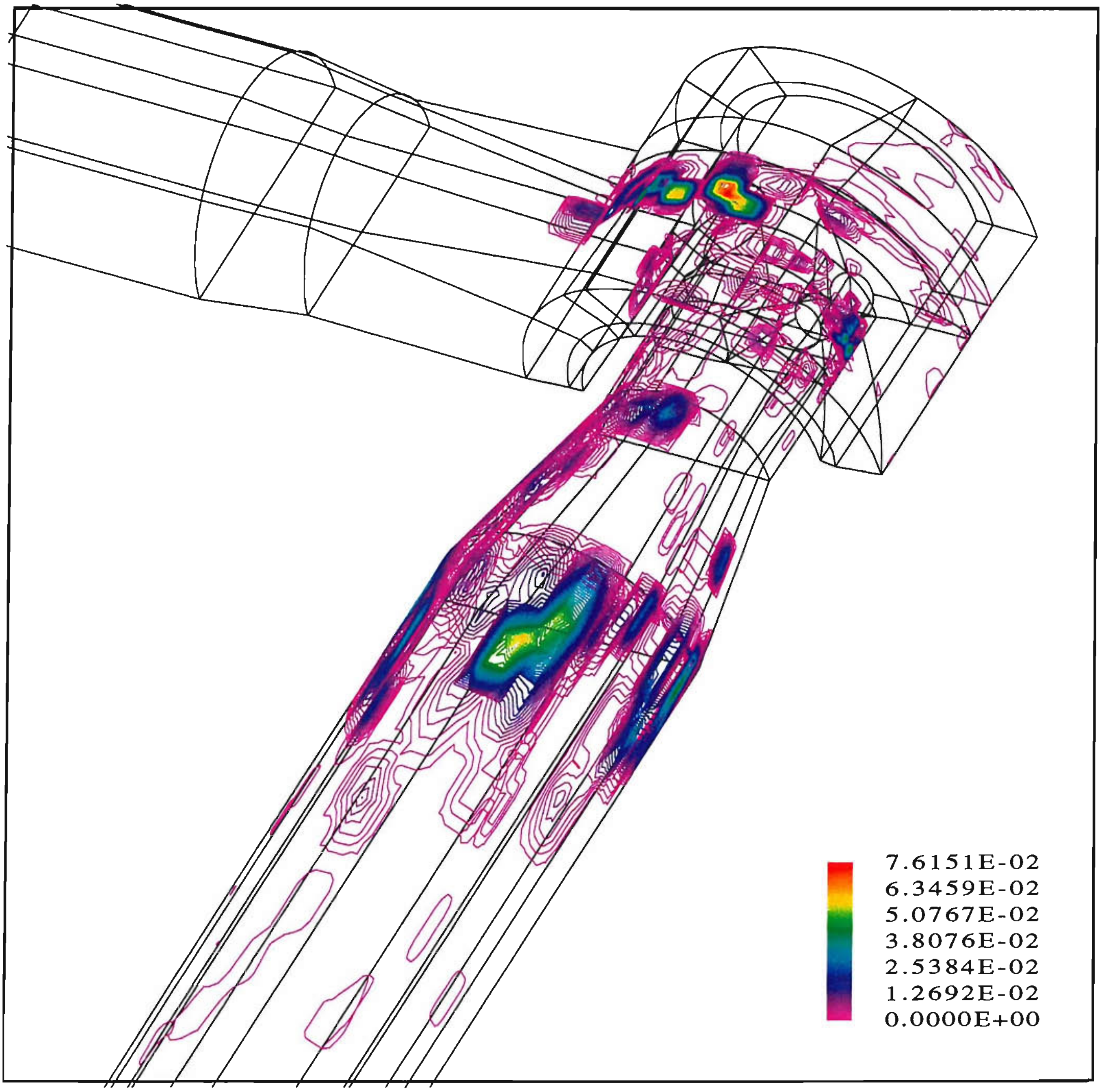

INVESTIGATION OF EROSION WITHIN CAGE TYPE CONTROL CHOKES - WET GAS

Particle Type - **Sand**

Test No - **8**

Particle Flux Rate - **3.7 % by wt.**

Particle Roundness Factor - **0.5**

Number of Particle Sizes - **8**

Particle Size Range - **170-260** μm

Turbulent Dispersion - **Yes**

Modified Coefficient of Restitution - **Yes**

Squeeze Film Retardation - **Yes**

Appendix Figure 120 - Surface Contour Plot of Internal Plug Particle Erosion Rates (mm^3/hr)

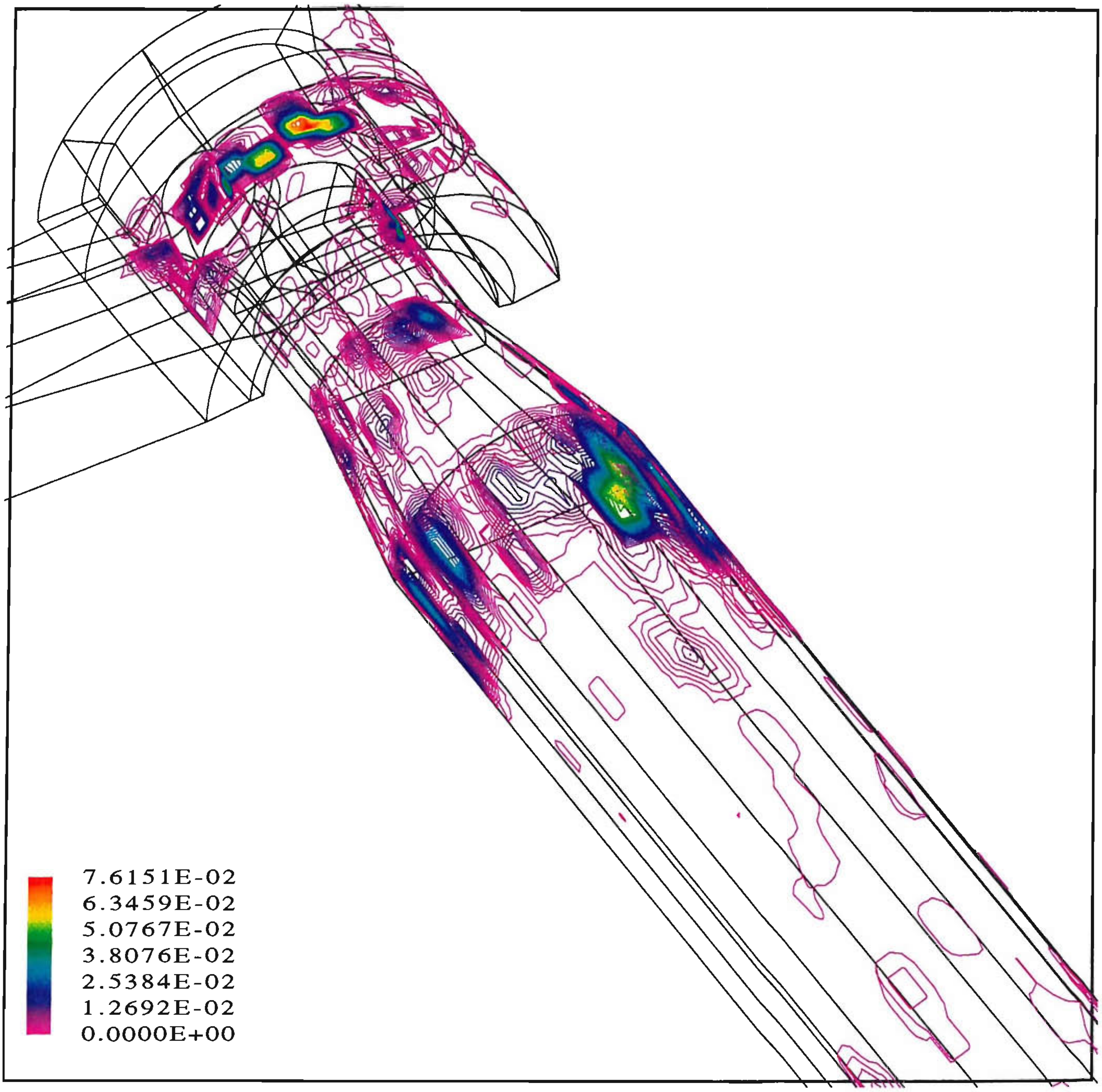

Appendix N Experimental Studies to Evaluate the CFD Erosion Model

Slurry Erosion - Evaluation of Empirical Erosion Constants

Fluid - **Water**
Nozzle Diameter - **5.9** mm
Stand-off Distance - **22** & **30** mm
Liquid Flowrate - **45** l/min
Sand Type - **Redhill 50 (235 μm)**
Sand Loading - **2.0 & 2.5** % by wt.

Appendix Figure 121 - Fluid Velocity Contours Slurry Test Rig - Stand-off Angle 90° (m/s)

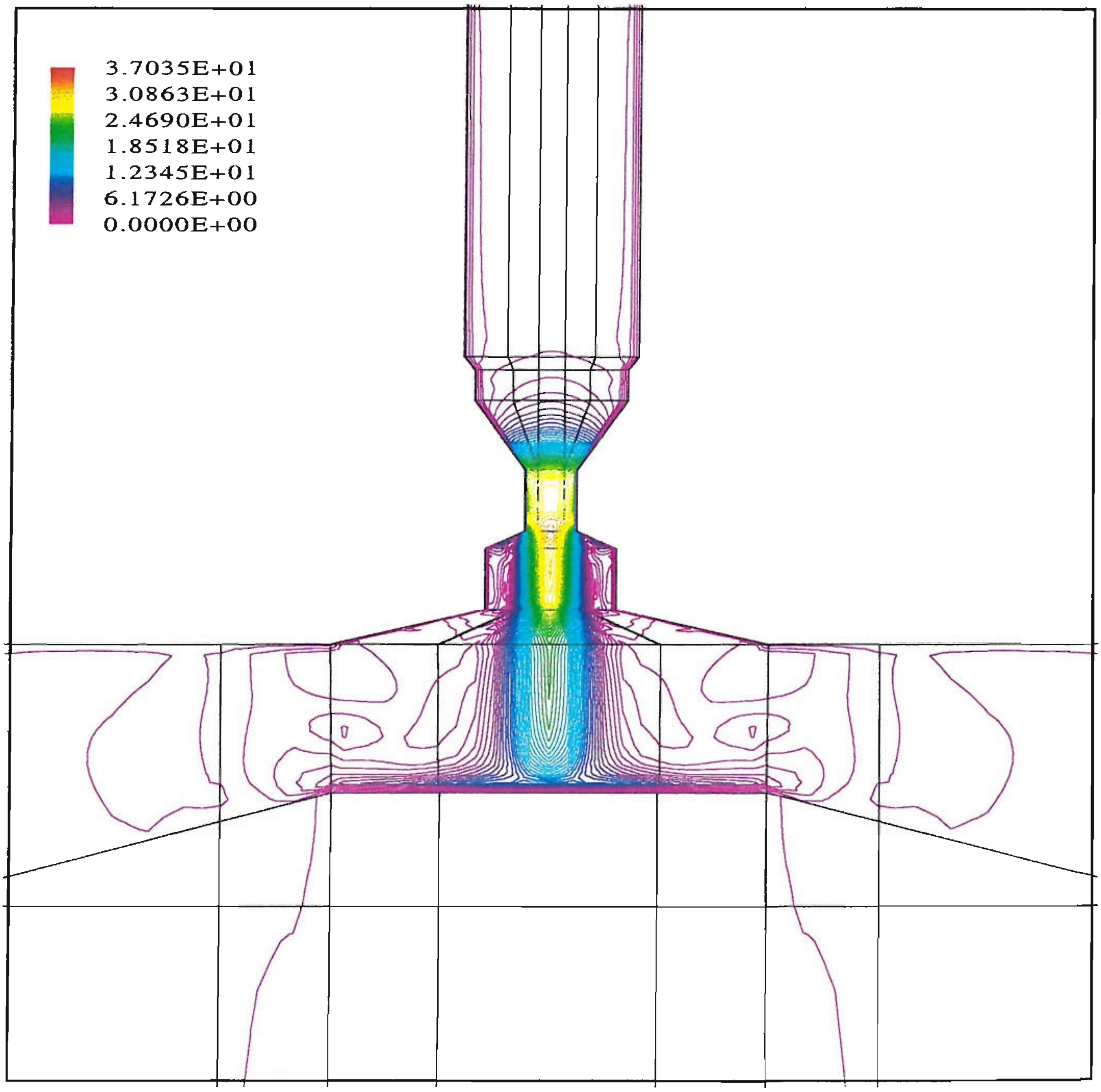

SLURRY EROSION - EVALUATION OF EMPIRICAL EROSION CONSTANTS

Fluid - **Water**
Nozzle Diameter - **5.9** mm
Stand-off Distance - **22** & **30** mm
Liquid Flowrate - **45** l/min
Sand Type - **Redhill 50 (235** μm)
Sand Loading - **2.0** & **2.5** % by wt.

Appendix Figure 122 - Fluid Velocity Contours Slurry Test Rig - Stand-off Angle 75° (m/s)

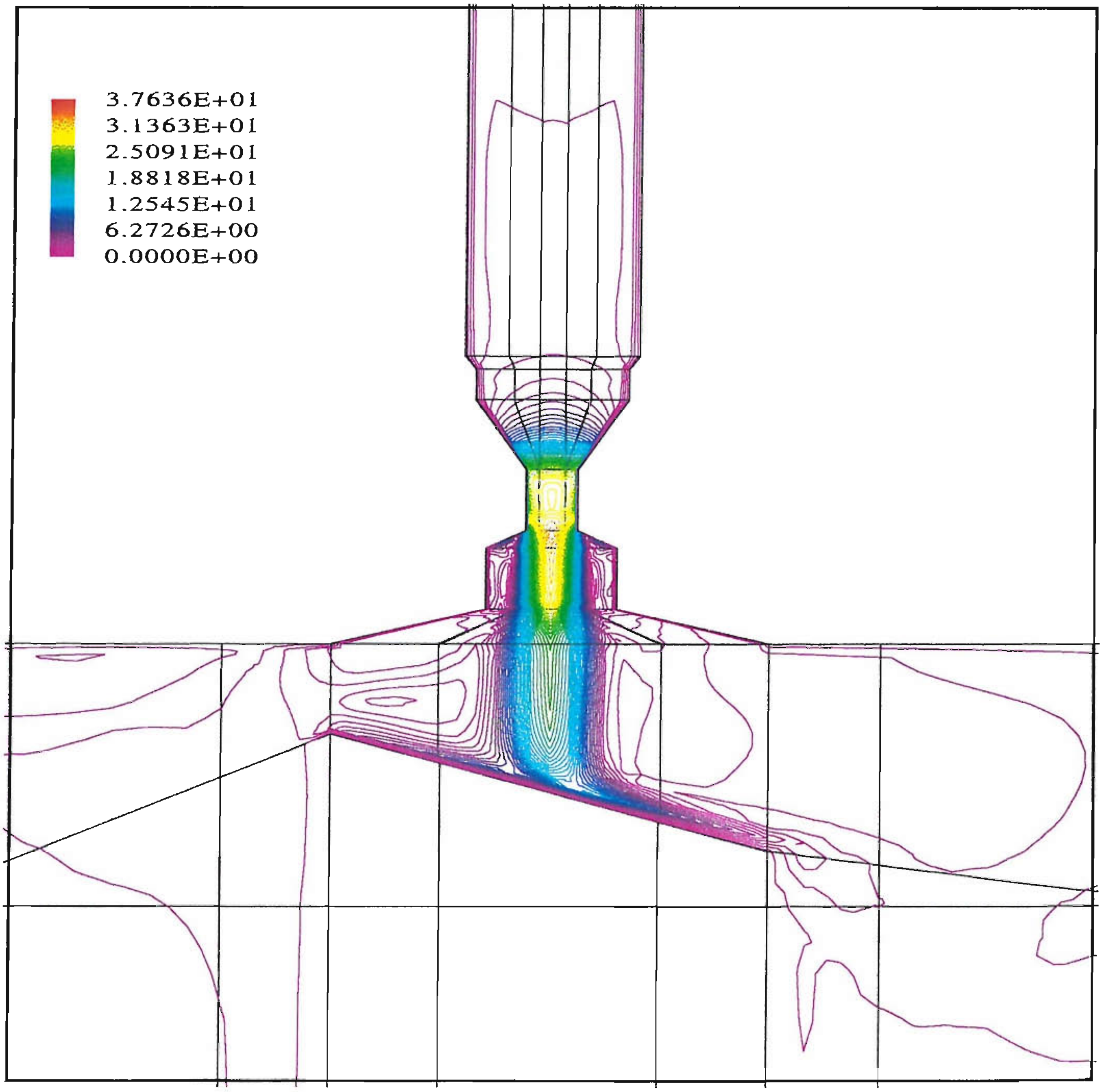

SLURRY EROSION - EVALUATION OF EMPIRICAL EROSION CONSTANTS

Fluid - **Water**
Nozzle Diameter - **5.9** mm
Stand-off Distance - **22** & **30** mm
Liquid Flowrate - **45** l/min
Sand Type - **Redhill 50 (235 μm)**
Sand Loading - **2.0 & 2.5** % by wt.

Appendix Figure 123 - Fluid Velocity Contours Slurry Test Rig - Stand-off Angle 60° (m/s)

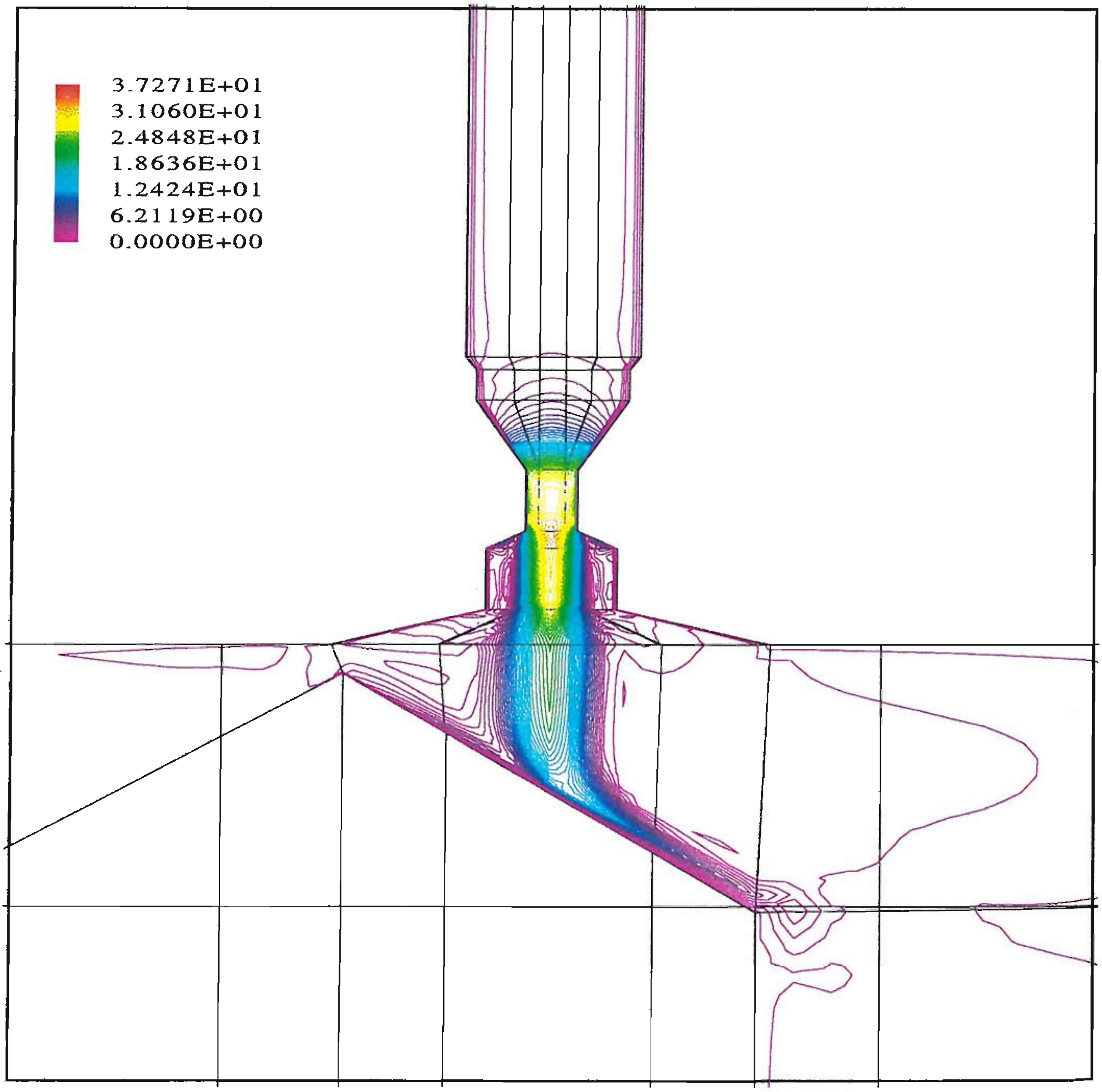

SLURRY EROSION - EVALUATION OF EMPIRICAL EROSION CONSTANTS

Fluid - **Water**
Nozzle Diameter - **5.9** mm
Stand-off Distance - **22** & **30** mm
Liquid Flowrate - **45** l/min
Sand Type - **Redhill 50 (235 μm)**
Sand Loading - **2.0 & 2.5** % by wt.

Appendix Figure 124 - Fluid Velocity Contours Slurry Test Rig - Stand-off Angle 45° (m/s)

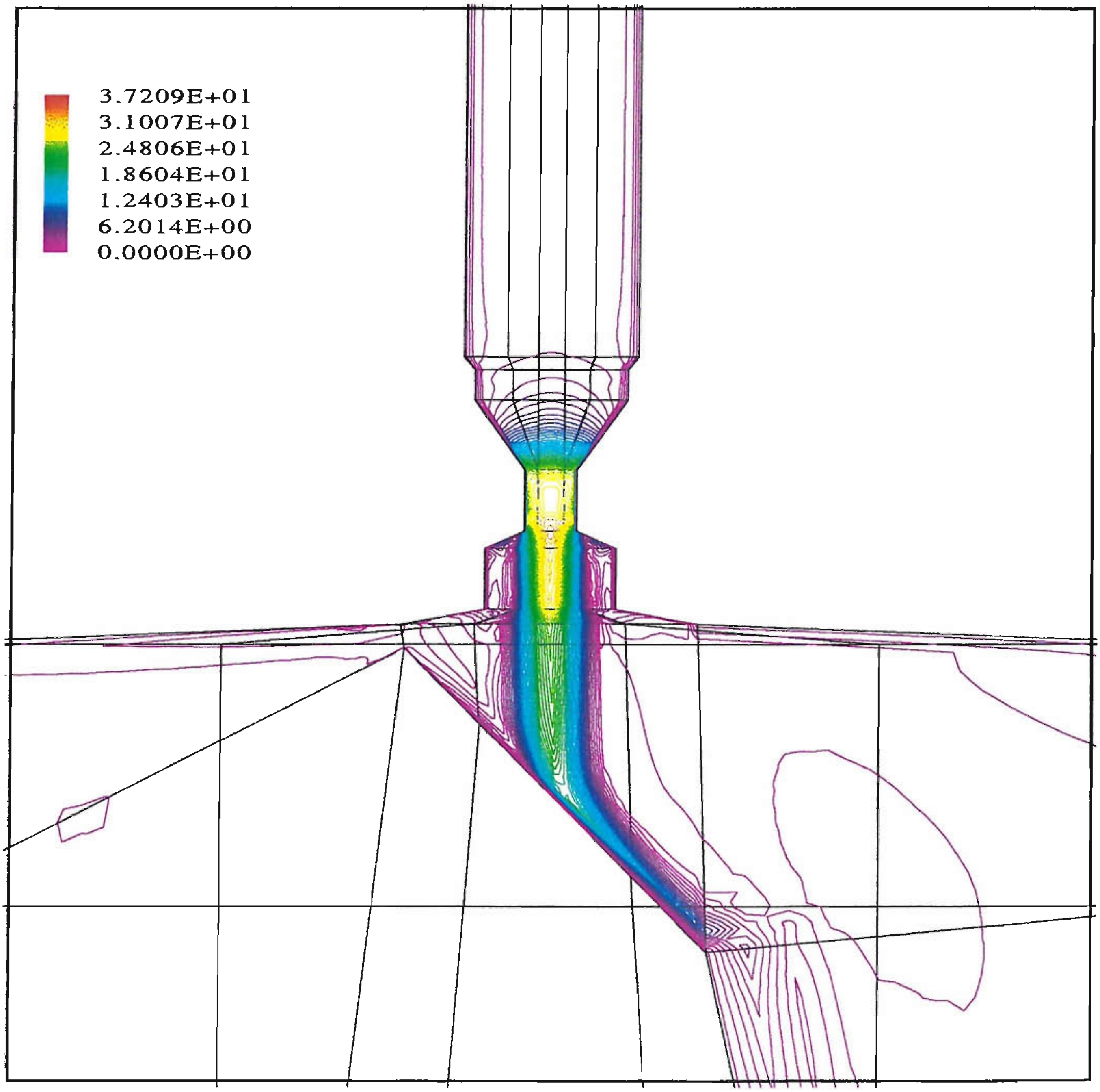

Configuration of Control Chokes Tested

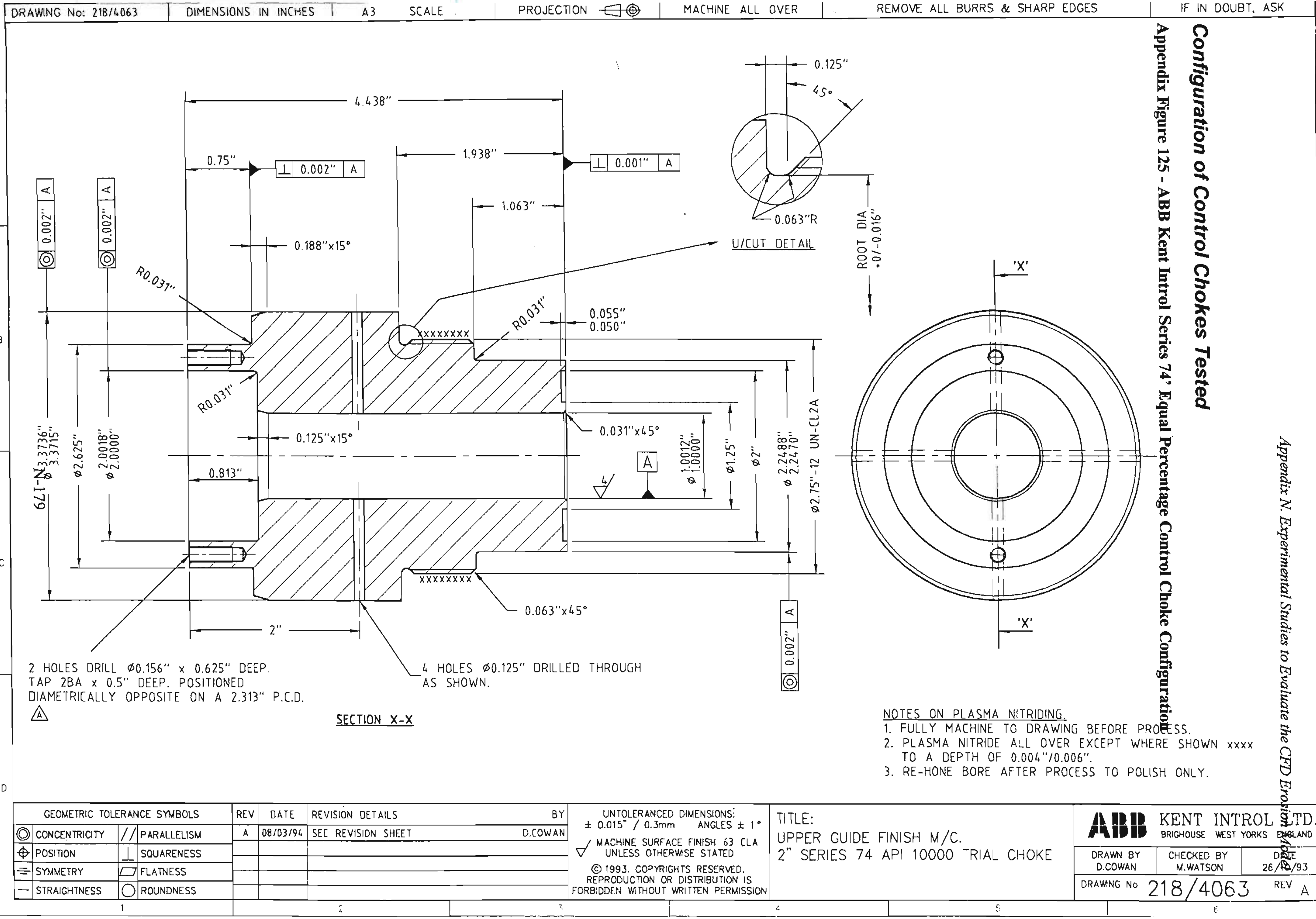

Appendix Figure 125 - ABB Kent Introl Series 74' Equal Percentage Control Choke Configuration

DRAWING No: 208/1519	DIMENSIONS IN INCHES	A2 SCALE 1:	PROJECTION	MACHINE WHERE MARKED	REMOVE ALL BURRS & SHARP EDGES	IF IN DOUBT, ASK

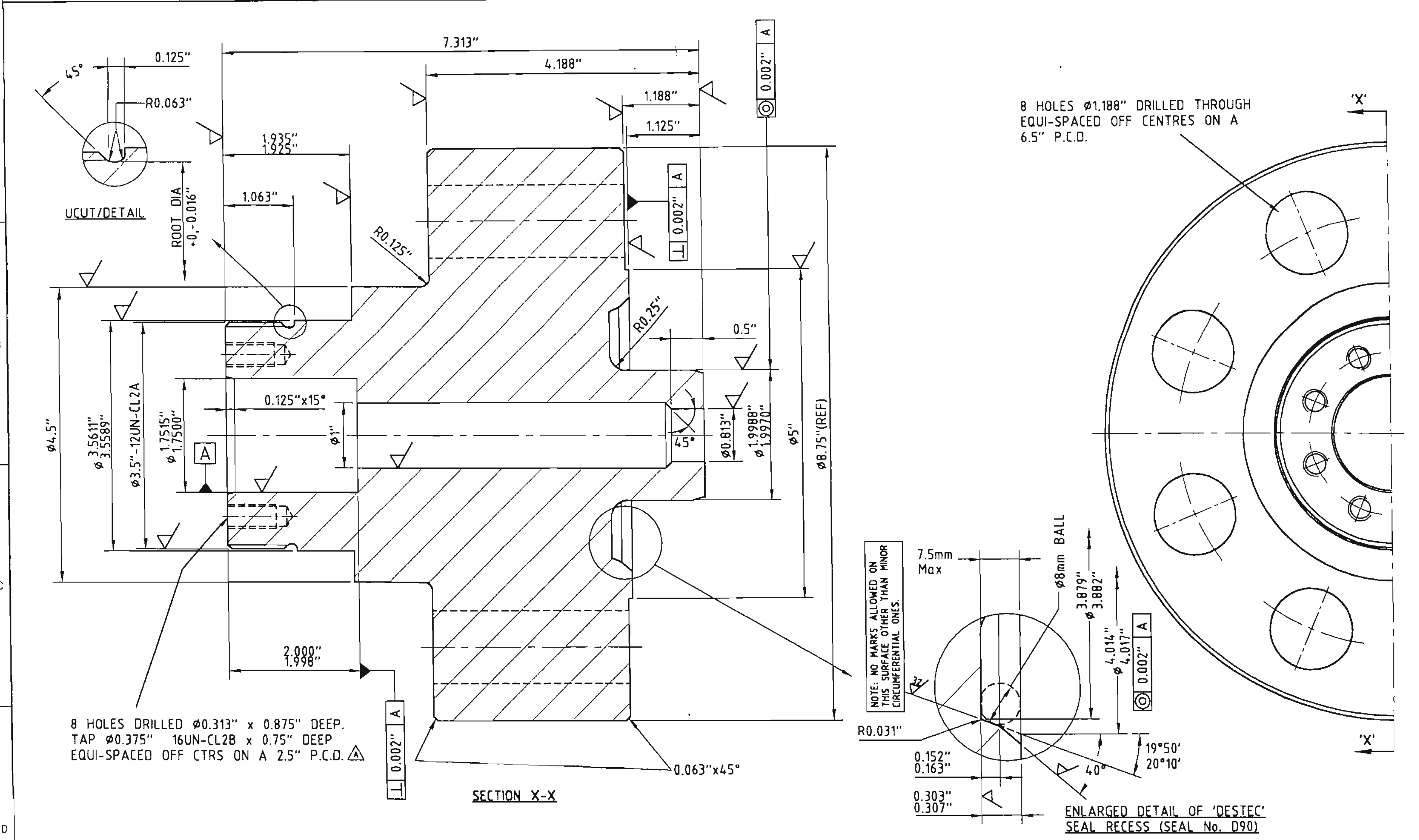

GEOMETRIC TOLERANCE SYMBOLS		REV	DATE	REVISION DETAILS	BY
CONCENTRICITY	PARALLELISM	A	21/02/94	SEE REVISION SHEET	D.COWAN
POSITION	SQUARENESS				
SYMMETRY	FLATNESS				
STRAIGHTNESS	ROUNDNESS				

UNTOLERANCED DIMENSIONS: ± 0.015" / 0.3mm ANGLES ± 1°

MACHINE SURFACE FINISH 63 CLA UNLESS OTHERWISE STATED

© 1993. COPYRIGHTS RESERVED. REPRODUCTION OR DISTRIBUTION IS FORBIDDEN WITHOUT WRITTEN PERMISSION

TITLE:
BONNET FINISH MACHINING
2" SERIES 74 API 10000 TRIAL CHOKE

ABB KENT INTROL LTD.
BRIGHOUSE WEST YORKS ENGLAND

DRAWN BY	CHECKED BY	DATE
D.COWAN	M.WATSON	27/10/93

DRAWING No 208/1519 REV A

DRAWING No: 217/2626	DIMENSIONS IN INCHES	A3 SCALE 1:1	PROJECTION	MACHINE ALL OVER	REMOVE ALL BURRS & SHARP EDGES	IF IN DOUBT, ASK

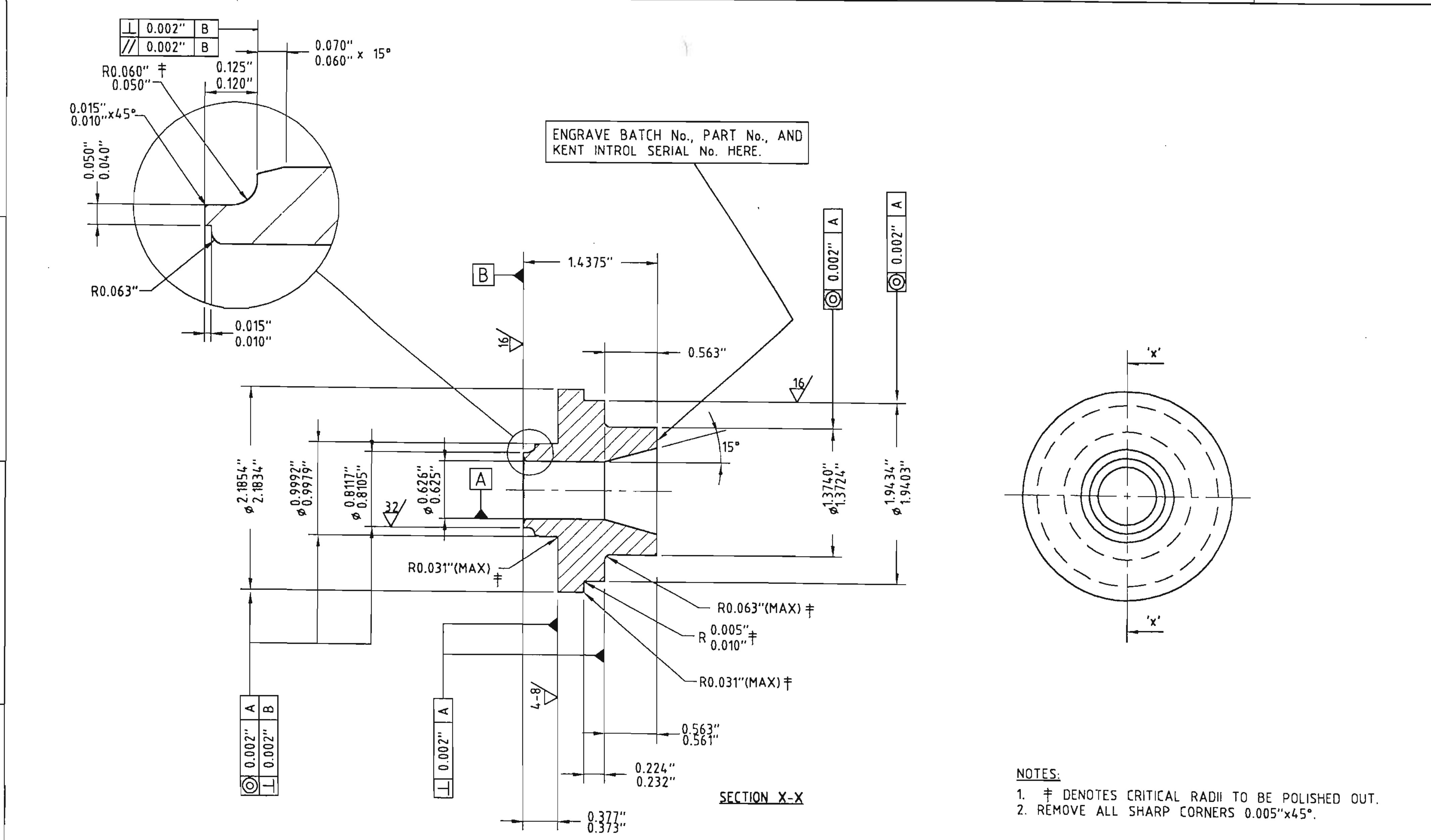

NOTES:

1. ǂ DENOTES CRITICAL RADII TO BE POLISHED OUT.
2. REMOVE ALL SHARP CORNERS 0.005"x45°.

GEOMETRIC TOLERANCE SYMBOLS		REV	DATE	REVISION DETAILS	BY
CONCENTRICITY	PARALLELISM				
POSITION	SQUARENESS				
SYMMETRY	FLATNESS				
STRAIGHTNESS	ROUNDNESS				

UNTOLERANCED DIMENSIONS: ± 0.015" / 0.3mm ANGLES ± 1°

MACHINE SURFACE FINISH 63 CLA UNLESS OTHERWISE STATED

© 1993. COPYRIGHTS RESERVED. REPRODUCTION OR DISTRIBUTION IS FORBIDDEN WITHOUT WRITTEN PERMISSION

TITLE:
1" LCV TRIM SEAT RING FIN. M/C.
2" SERIES 74 2.063" API 10000
TRIAL CHOKE

ABB KENT INTROL LTD.
BRIGHOUSE WEST YORKS ENGLAND

DRAWN BY	CHECKED BY	DATE
D.COWAN	M.WATSON	23/11/93

DRAWING No 217/2626 REV

DRAWING No: 227/4131	DIMENSIONS IN INCHES	DO NOT SCALE	PROJECTION	MACHINE ALL OVER	REMOVE ALL BURRS & SHARP EDGES	IF IN DOUBT, ASK

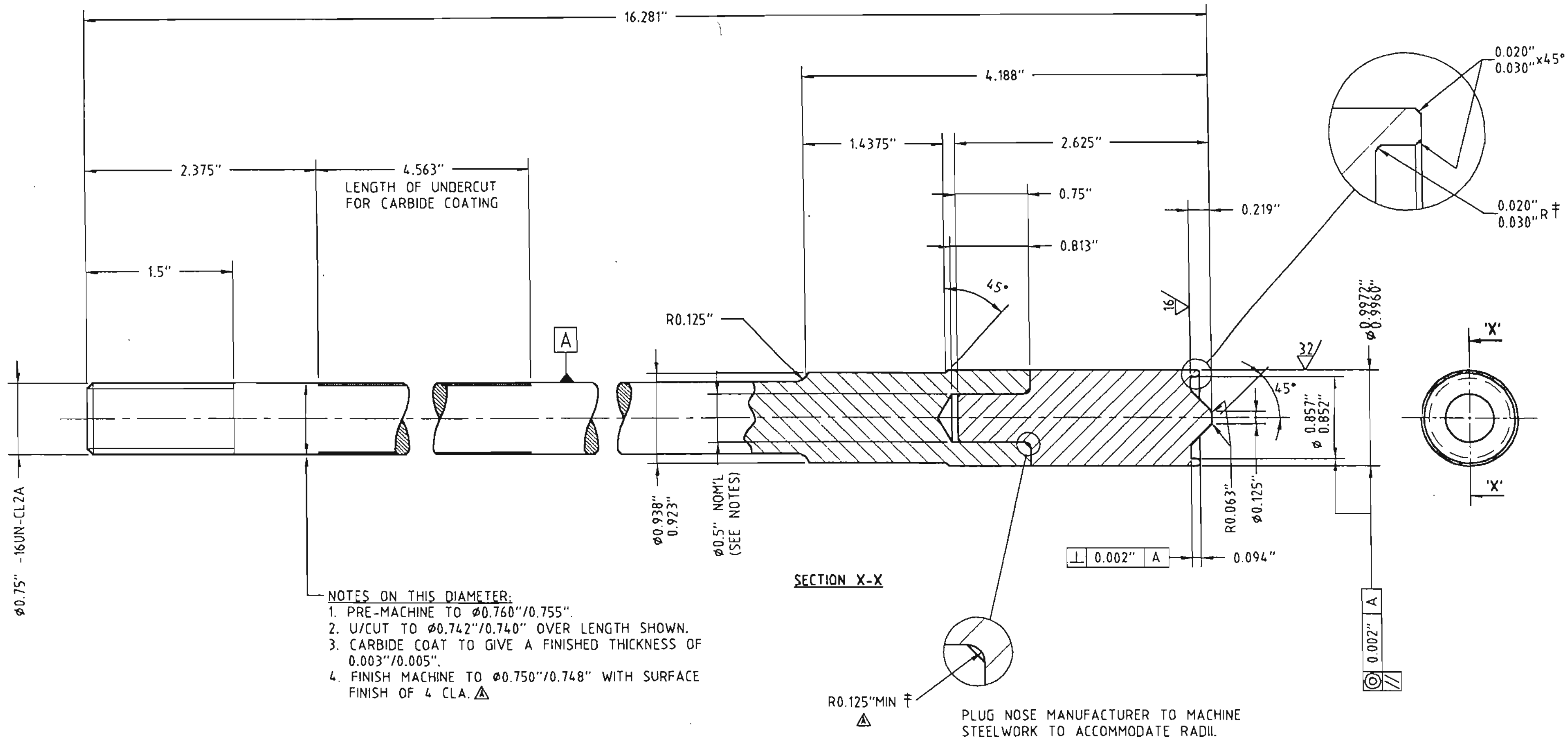

NOTES:
1. PLUG NOSE MANUFACTURER TO MACHINE STEELWORK TO A NOMINAL ø0.5". TOLERANCE AND SURFACE FINISH TO BE SUITABLE FOR A LEAKPROOF SHRINK FIT.
2. ‡ DENOTES CRITICAL RADII TO BE POLISHED OUT.
3. MAXIMUM TEMPERATURE TO BE 100°F.
4. MAXIMUM PRESSURE TO BE 10000 PSIA.
5. BREAK ALL SHARP CORNERS 0.010" x 45° UNLESS OTHERWISE STATED.

GEOMETRIC TOLERANCE SYMBOLS	
CONCENTRICITY	PARALLELISM
POSITION	SQUARENESS
SYMMETRY	FLATNESS
STRAIGHTNESS	ROUNDNESS

REV	DATE	REVISION DETAILS	BY
A	08/03/94	SEE REVISION SHEET	D.COWAN

UNTOLERANCED DIMENSIONS: ± 0.015" / 0.3mm ANGLES ± 1°

MACHINE SURFACE FINISH 63 CLA UNLESS OTHERWISE STATED

© 1993. COPYRIGHTS RESERVED. REPRODUCTION OR DISTRIBUTION IS FORBIDDEN WITHOUT WRITTEN PERMISSION

TITLE:
1" PLUG/STEM FINISH M/C. (LCV)
2" SERIES 74 2.063" API 10000
TRIAL CHOKE

ABB KENT INTROL LTD.
BRIGHOUSE WEST YORKS ENGLAND

DRAWN BY	CHECKED BY	DATE
D.COWAN	M.WATSON	23/11/93

DRAWING No 227/4131 REV A

DRAWING No: 218/4062	DIMENSIONS IN INCHES	A3	SCALE	PROJECTION	MACHINE ALL OVER	REMOVE ALL BURRS & SHARP EDGES	IF IN DOUBT, ASK

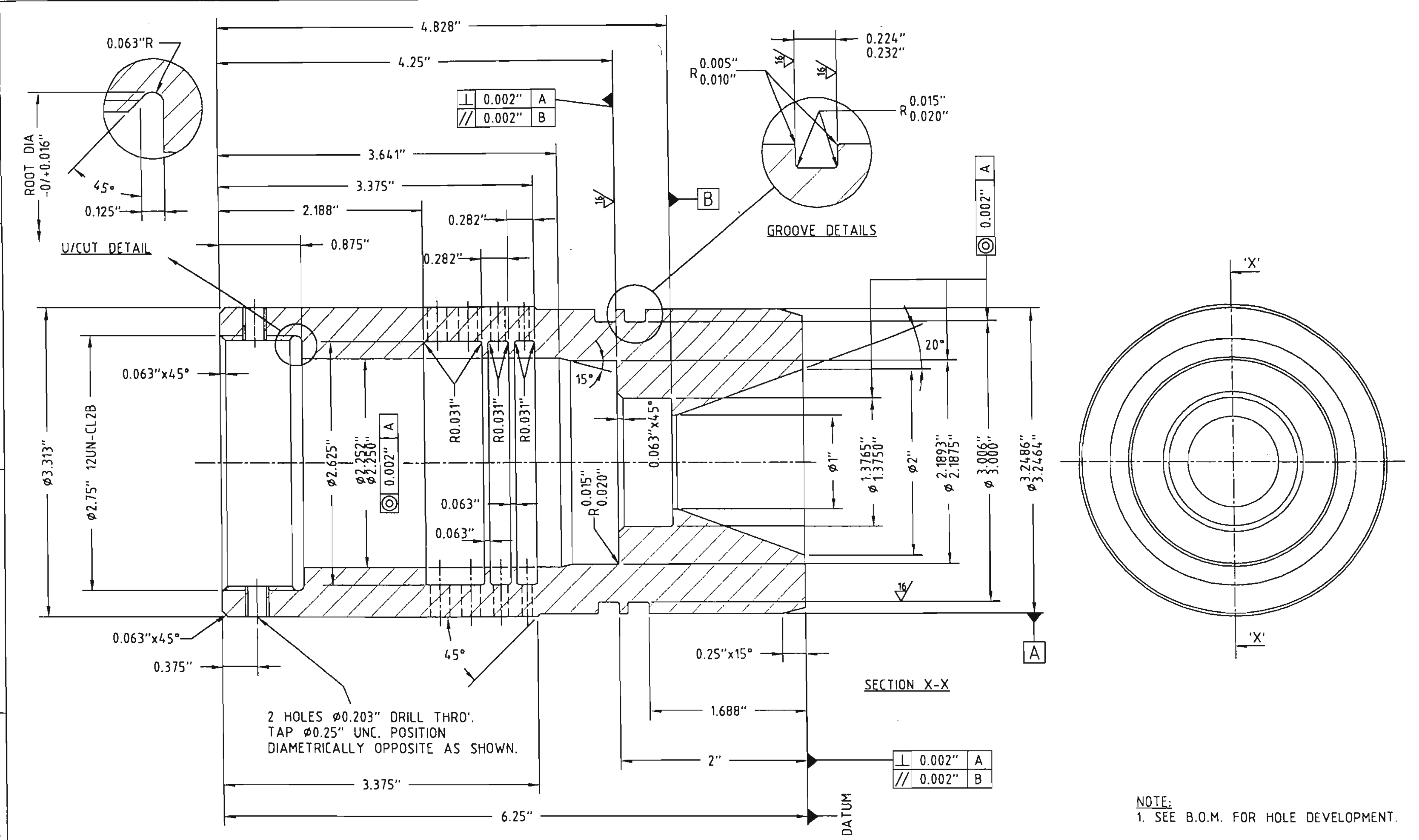

NOTE:
1. SEE B.O.M. FOR HOLE DEVELOPMENT.

GEOMETRIC TOLERANCE SYMBOLS	
◎ CONCENTRICITY	// PARALLELISM
⊕ POSITION	⊥ SQUARENESS
≡ SYMMETRY	▱ FLATNESS
— STRAIGHTNESS	○ ROUNDNESS

REV	DATE	REVISION DETAILS	BY

UNTOLERANCED DIMENSIONS: ± 0.015" / 0.3mm ANGLES ± 1°

MACHINE SURFACE FINISH 63 CLA UNLESS OTHERWISE STATED

© 1993. COPYRIGHTS RESERVED. REPRODUCTION OR DISTRIBUTION IS FORBIDDEN WITHOUT WRITTEN PERMISSION

TITLE:
LOWER GUIDE FINISH M/C.
2" SERIES 74 API 10000 TRIAL CHOKE

ABB KENT INTROL LTD.
BRIGHOUSE WEST YORKS ENGLAND

DRAWN BY	CHECKED BY	DATE
D.COWAN	M.WATSON	26/10/93

DRAWING No 218/4062 REV

DRAWING No: 219/2389	DIMENSIONS IN INCHES	A3 SCALE 1:1	PROJECTION	MACHINE ALL OVER	REMOVE ALL BURRS & SHARP EDGES	IF IN DOUBT, ASK

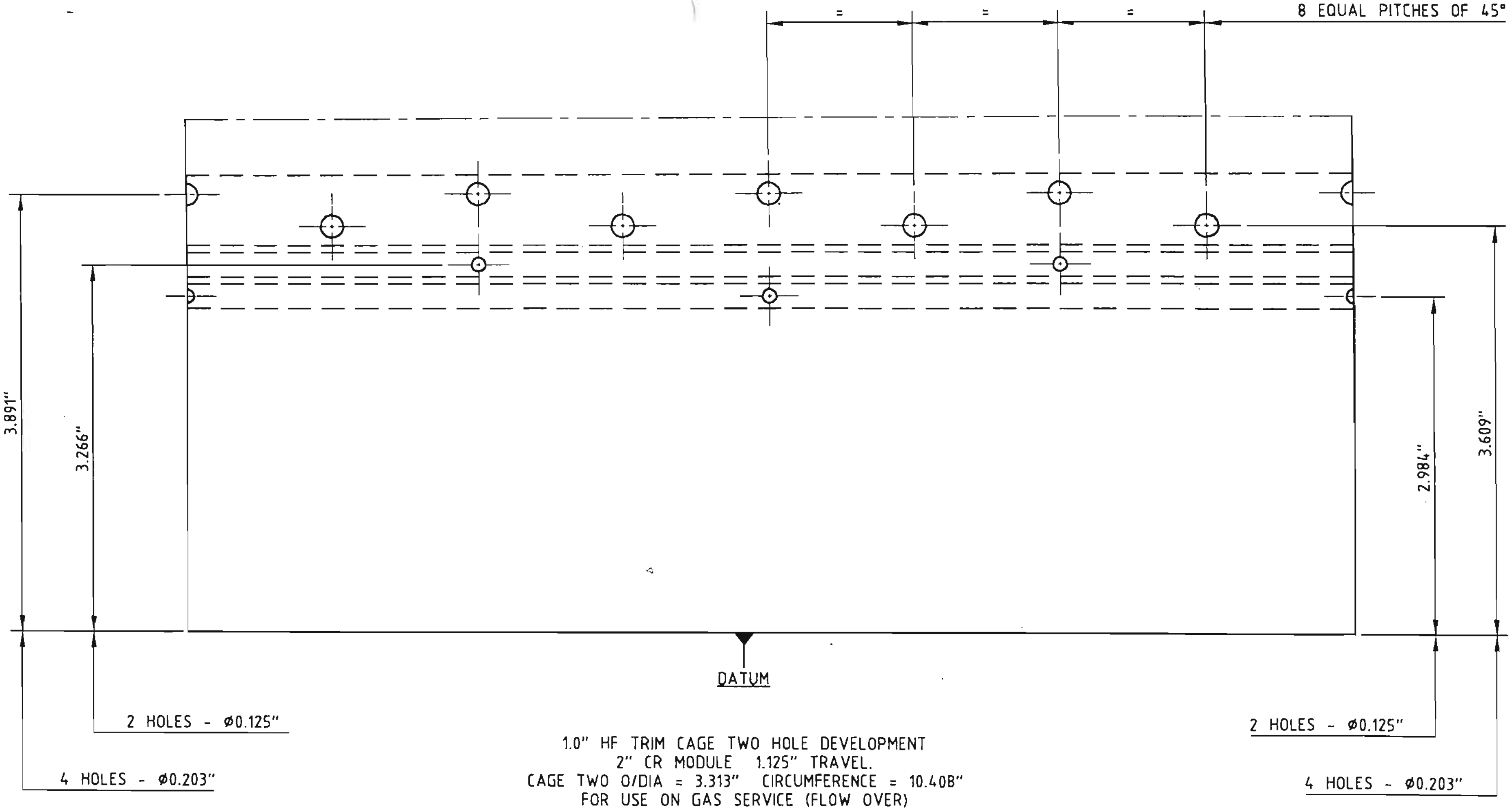

1.0" HF TRIM CAGE TWO HOLE DEVELOPMENT
2" CR MODULE 1.125" TRAVEL.
CAGE TWO O/DIA = 3.313" CIRCUMFERENCE = 10.408"
FOR USE ON GAS SERVICE (FLOW OVER)
FLOW CHARACTERISTIC = EQ. PERCENT
SERIES 74 TRIAL CHOKE

GEOMETRIC TOLERANCE SYMBOLS	
CONCENTRICITY	PARALLELISM
POSITION	SQUARENESS
SYMMETRY	FLATNESS
STRAIGHTNESS	ROUNDNESS

REV	DATE	REVISION DETAILS	BY

UNTOLERANCED DIMENSIONS: ± 0.015" / 0.3mm ANGLES ± 1°
MACHINE SURFACE FINISH 63 CLA UNLESS OTHERWISE STATED

© 1993. COPYRIGHTS RESERVED. REPRODUCTION OR DISTRIBUTION IS FORBIDDEN WITHOUT WRITTEN PERMISSION

TITLE:
SPECIAL HOLE DEVELOPMENT
2" SERIES 74 CHOKE

ABB KENT INTROL LTD.
BRIGHOUSE WEST YORKS ENGLAND

DRAWN BY	CHECKED BY	DATE
D.COWAN	M.WATSON	21/12/93

DRAWING No 219/2389 REV

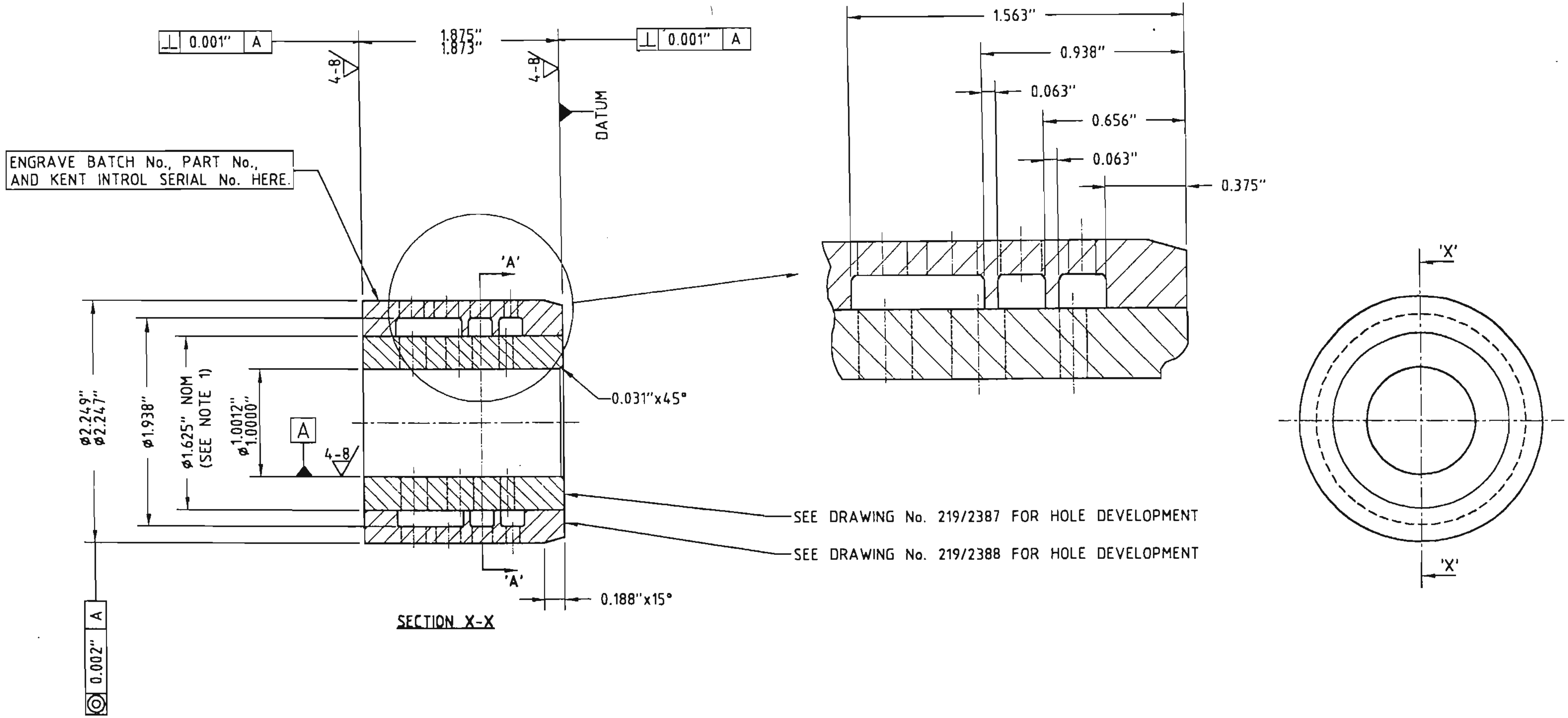

NOTES:

1. ALL RADII TO BE 0.031" UNLESS OTHERWISE STATED.
2. CARBIDE MANUFACTURER TO MACHINE OUTER CAGE & GUIDE TO ø1.625" NOMINAL. TOLERANCE AND SURFACE FINISH TO BE SUITABLE FOR A H7,f6 SLIDING FIT.
3. MAXIMUM TEMPERATURE 100°F.
4. MAXIMUM PRESSURE 10000 PSIA.

GEOMETRIC TOLERANCE SYMBOLS		REV	DATE	REVISION DETAILS	BY
◎ CONCENTRICITY	// PARALLELISM				
⊕ POSITION	⊥ SQUARENESS				
⌯ SYMMETRY	▱ FLATNESS				
— STRAIGHTNESS	○ ROUNDNESS				

UNTOLERANCED DIMENSIONS: ± 0.015" / 0.3mm ANGLES ± 1°

√ MACHINE SURFACE FINISH 63 CLA UNLESS OTHERWISE STATED

© 1993. COPYRIGHTS RESERVED. REPRODUCTION OR DISTRIBUTION IS FORBIDDEN WITHOUT WRITTEN PERMISSION

TITLE:
1" HFT CAGE/GUIDE ASSEMBLY
2" SERIES 74 2.063" API 10000
TRIAL CHOKE (TUNG. CARBIDE TRIM)

ABB KENT INTROL LTD.
BRIGHOUSE WEST YORKS ENGLAND

DRAWN BY	CHECKED BY	DATE
D.COWAN	M.WATSON	22/11/93

DRAWING No 218/4055 REV

DRAWING No: 219/2388	DIMENSIONS IN INCHES	A3 SCALE 1:1	PROJECTION	MACHINE ALL OVER	REMOVE ALL BURRS & SHARP EDGES	IF IN DOUBT, ASK

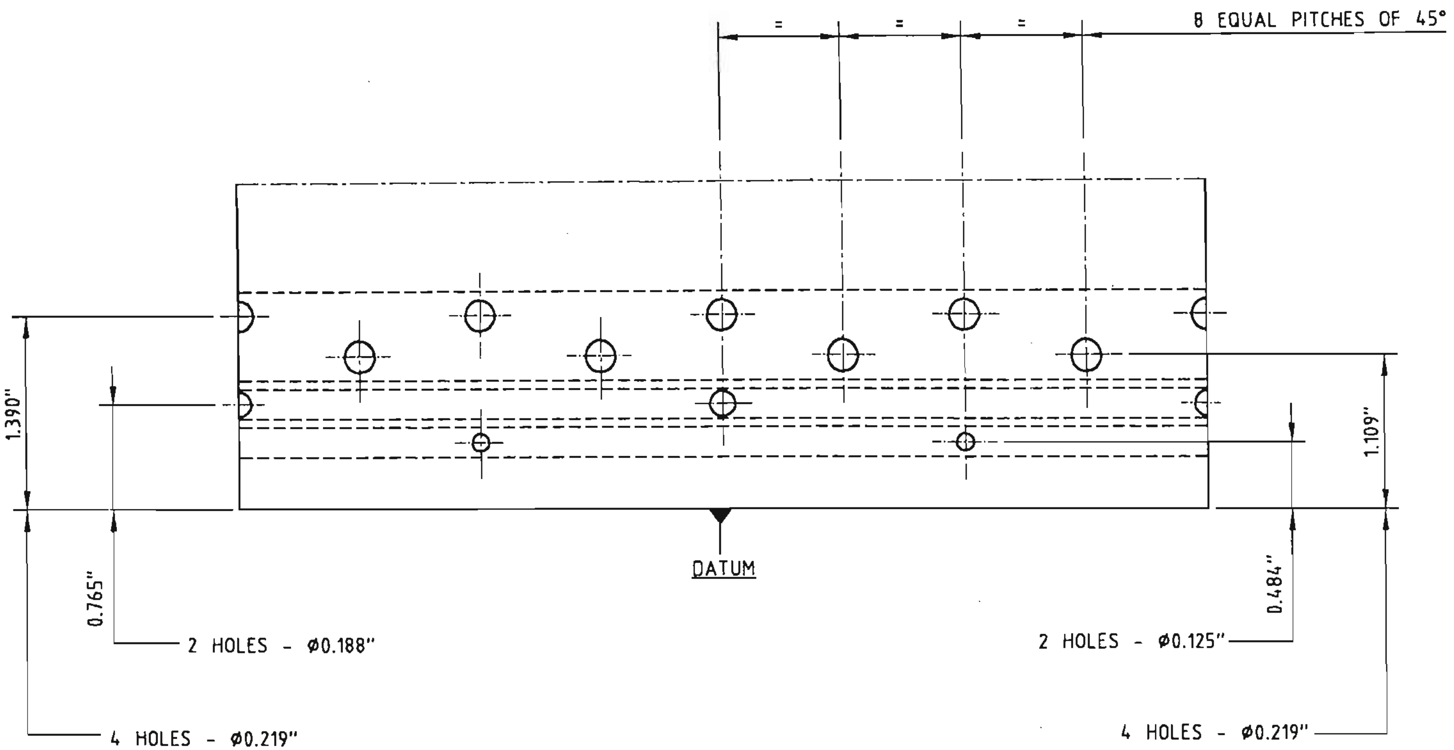

1.0" HF TRIM CAGE 1 HOLE DEVELOPMENT
2" CR MODULE 1.125" TRAVEL.
CAGE O/DIA = 2.250" CIRCUMFERENCE = 7.069"
FOR USE ON GAS SERVICE (FLOW OVER)
FLOW CHARACTERISTIC = EQ. PERCENT
SERIES 74 TRIAL CHOKE

GEOMETRIC TOLERANCE SYMBOLS		REV	DATE	REVISION DETAILS	BY
CONCENTRICITY	PARALLELISM				
POSITION	SQUARENESS				
SYMMETRY	FLATNESS				
STRAIGHTNESS	ROUNDNESS				

UNTOLERANCED DIMENSIONS: ± 0.015" / 0.3mm ANGLES ± 1°
MACHINE SURFACE FINISH 63 CLA UNLESS OTHERWISE STATED

© 1993. COPYRIGHTS RESERVED. REPRODUCTION OR DISTRIBUTION IS FORBIDDEN WITHOUT WRITTEN PERMISSION

TITLE:
SPECIAL HOLE DEVELOPMENT
2" SERIES 74 CHOKE

ABB KENT INTROL LTD.
BRIGHOUSE WEST YORKS ENGLAND

DRAWN BY	CHECKED BY	DATE
D.COWAN	M.WATSON	21/12/93

DRAWING No 219/2388 REV

DRAWING No: 219/2387	DIMENSIONS IN INCHES	A3 SCALE 1:1	PROJECTION	MACHINE ALL OVER	REMOVE ALL BURRS & SHARP EDGES	IF IN DOUBT, ASK

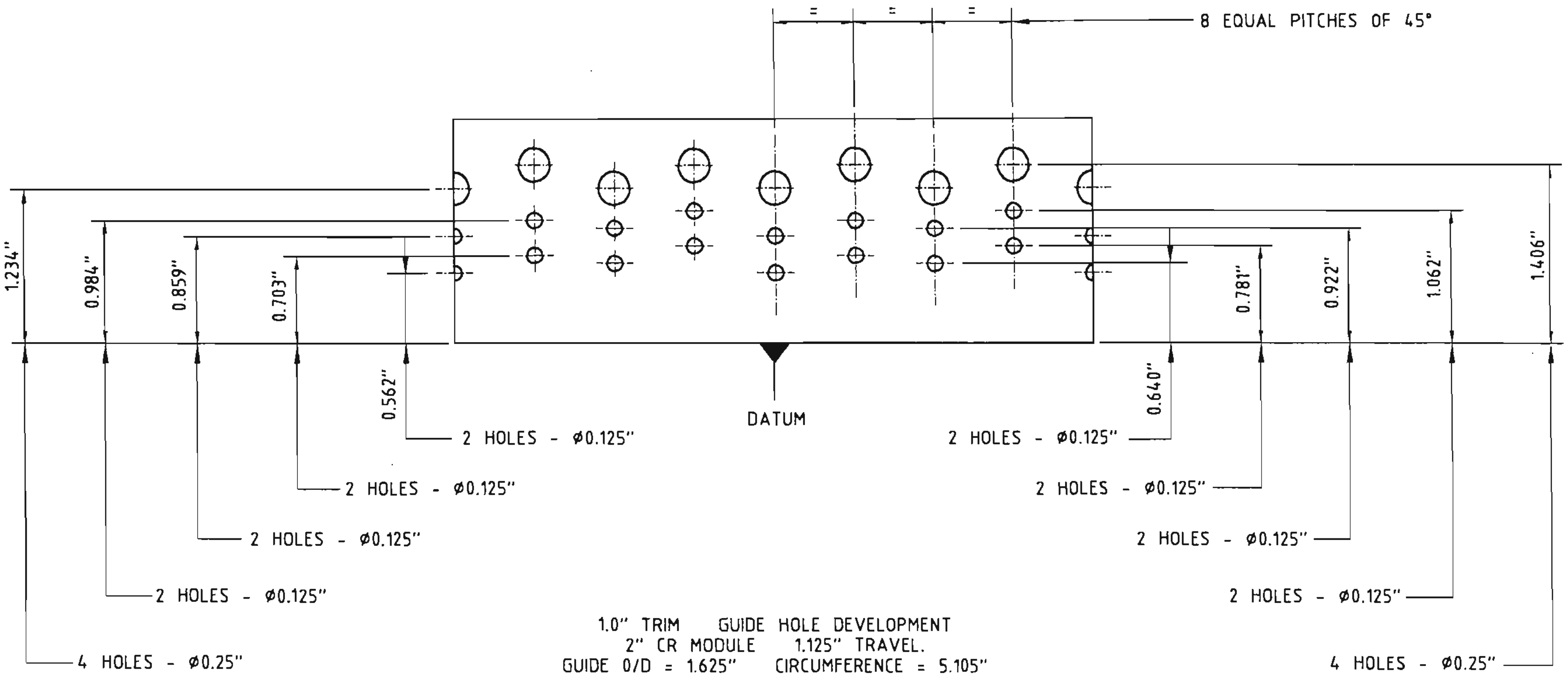

1.0" TRIM GUIDE HOLE DEVELOPMENT
2" CR MODULE 1.125" TRAVEL.
GUIDE O/D = 1.625" CIRCUMFERENCE = 5.105"
VALVE DESIGN Cv (SINGLE STAGE) = 8.5
FLOW CHARACTERISTIC = EQ. PERCENT
SERIES 74 TRIAL CHOKE

GEOMETRIC TOLERANCE SYMBOLS				REV	DATE	REVISION DETAILS	BY
◎	CONCENTRICITY	//	PARALLELISM				
⊕	POSITION	⊥	SQUARENESS				
≡	SYMMETRY	▱	FLATNESS				
—	STRAIGHTNESS	○	ROUNDNESS				

UNTOLERANCED DIMENSIONS:
± 0.015" / 0.3mm ANGLES ± 1°
MACHINE SURFACE FINISH 63 CLA UNLESS OTHERWISE STATED

© 1993. COPYRIGHTS RESERVED. REPRODUCTION OR DISTRIBUTION IS FORBIDDEN WITHOUT WRITTEN PERMISSION

TITLE:
SPECIAL HOLE DEVELOPMENT
2" SERIES 74 CHOKE

ABB KENT INTROL LTD.
BRIGHOUSE WEST YORKS ENGLAND

DRAWN BY	CHECKED BY	DATE
D.COWAN	M.WATSON	20/12/93

DRAWING No 219/2387 REV

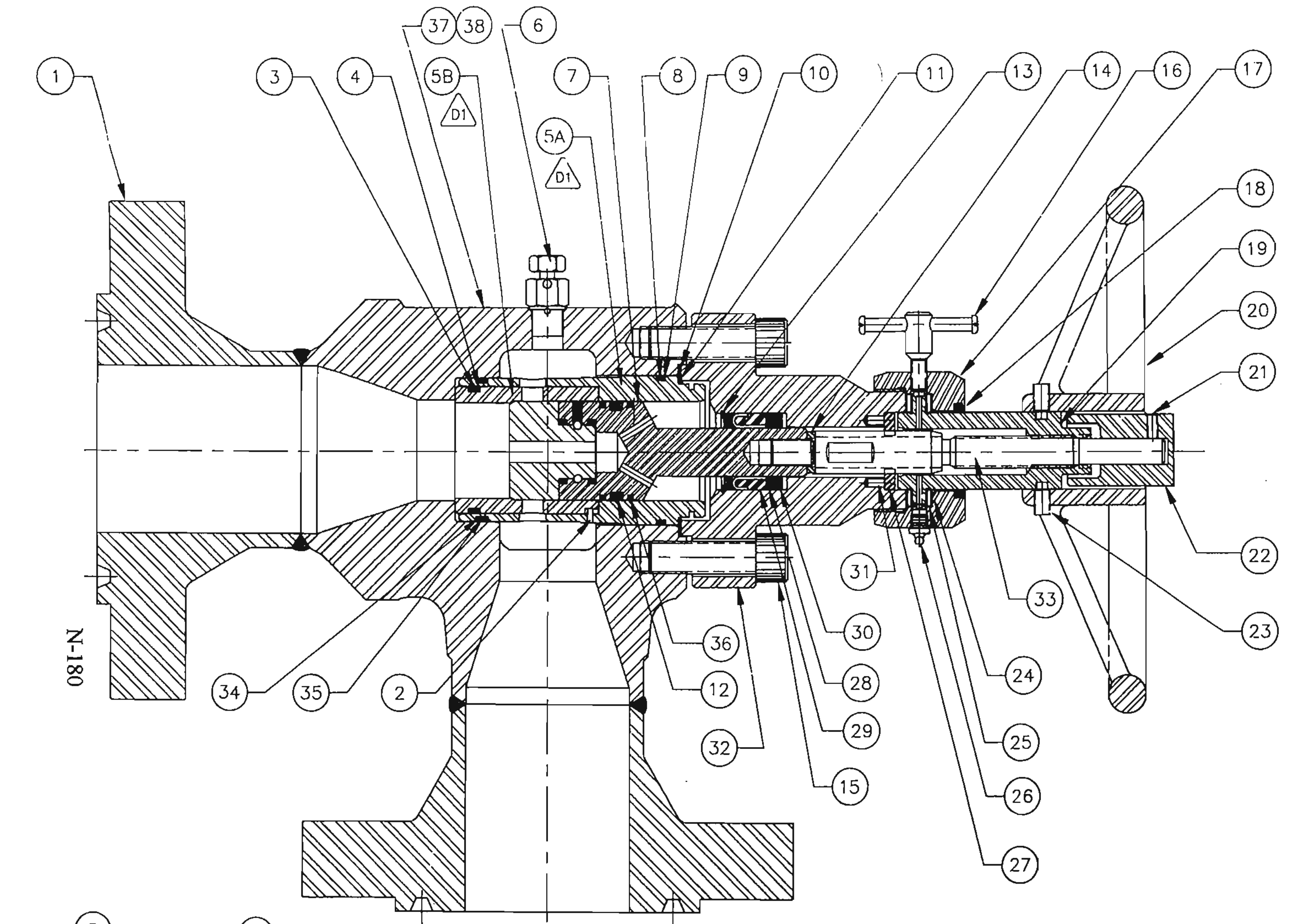

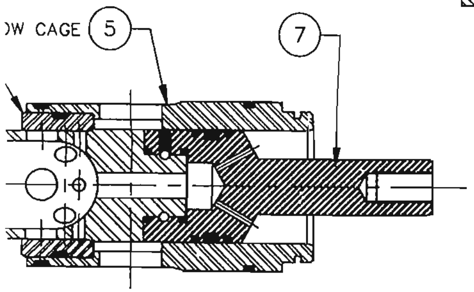

.TERNATIVE INTERNAL SLEEVE TRIM.

ITEM NO.	DESCRIPTION	QTY.
1	BODY ASSEMBLY	1
2	SPRING PIN (P & C)	1
2	SEAT RING (IS)	1
3	O-RING	1
4	BACKUP RING	2
5A	UPPER CAGE	1
5B	LOWER CAGE SLEEVE	1
6	BLEED VALVE	1
7	LOWER STEM ASSEMBLY	1
8	O-RING	1
9	BACKUP RING	1
10	GASKET, METAL SEAL	1
11	GASKET, SLIP-FIT	1
12	T-SEAL	1
13	SNAP RING	1
14	LOCKWASHER	1
15	CAPSCREW	8
16	LOCKING SCREW	1
17	STEM NUT	1
18	WIPER RING	1
19	STEM DRIVE BUSHING	1
20	HANDWHEEL	1
21	SET SCREW	1
22	INDICATOR	1
23	SET SCREW	4
24	THRUST RACE	4
25	THRUST BEARING	2
26	LUBRICATION FITTING	1
27	ANTI-ROTATION RING	1
28	BACKUP RING	1
29	STEM SEAL	1
30	JUNK RING	2
31	SPRING PIN	2
32	BONNET	1
33	UPPER STEM	1
34	O-RING	1
35	BACKUP RING	2
36	WEAR RING	2
37	NAMEPLATE	1
38	SCREW DRIVE	4

NOTE:
DURING ASSEMBLY CAGES ARE TO BE ASSEMBLED WITH THE LEG IN FLOW, IE. HOLES STRADDLE CENTRE LINE OF INLET.

.75	TOLERANCE UNLESS OTHERWISE SPECIFIED	SURFACE TREATMENT	DO NOT SCALE
D	.X ±.1 / ANGLES ±.5°	MATERIAL & HEAT TREAT	G.FARRELL 15/12/89
CAD	.XX ±.02 / .XXX ±.005 / 125		2/11/93

Cooper Industries Cooper Oil Tool Division Aghada, Longford, Ireland.

CC30, WITH BOLTED BONNET, MANUAL.

1 of 1 WMV-948

D1 REV

Appendix Figure 126 - Cameron CC30 Equal Percentage Control Choke Configuration

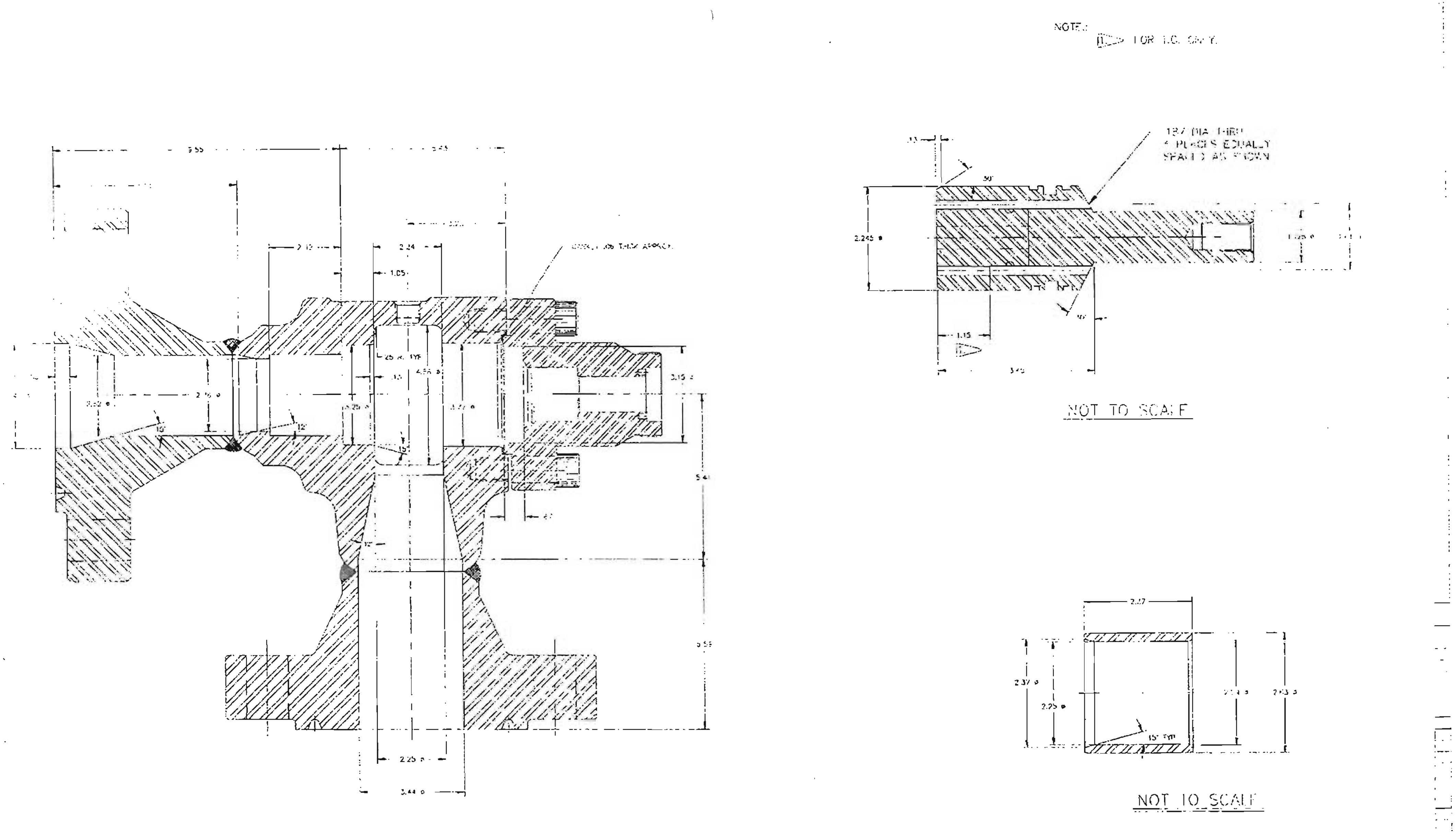

UNLESS OTHERWISE SPECIFIED ALL DIMENSIONS ARE IN INCHES

TOLERANCE UNLESS OTHERWISE SPECIFIED

SURFACE TREATMENT

DO NOT SCALE

MATERIAL & HEAT TREAT

A.DOYLE 21/11/96

CAMERON

MACH DETAIL BODY

BP EROSION TEST

D

CAD

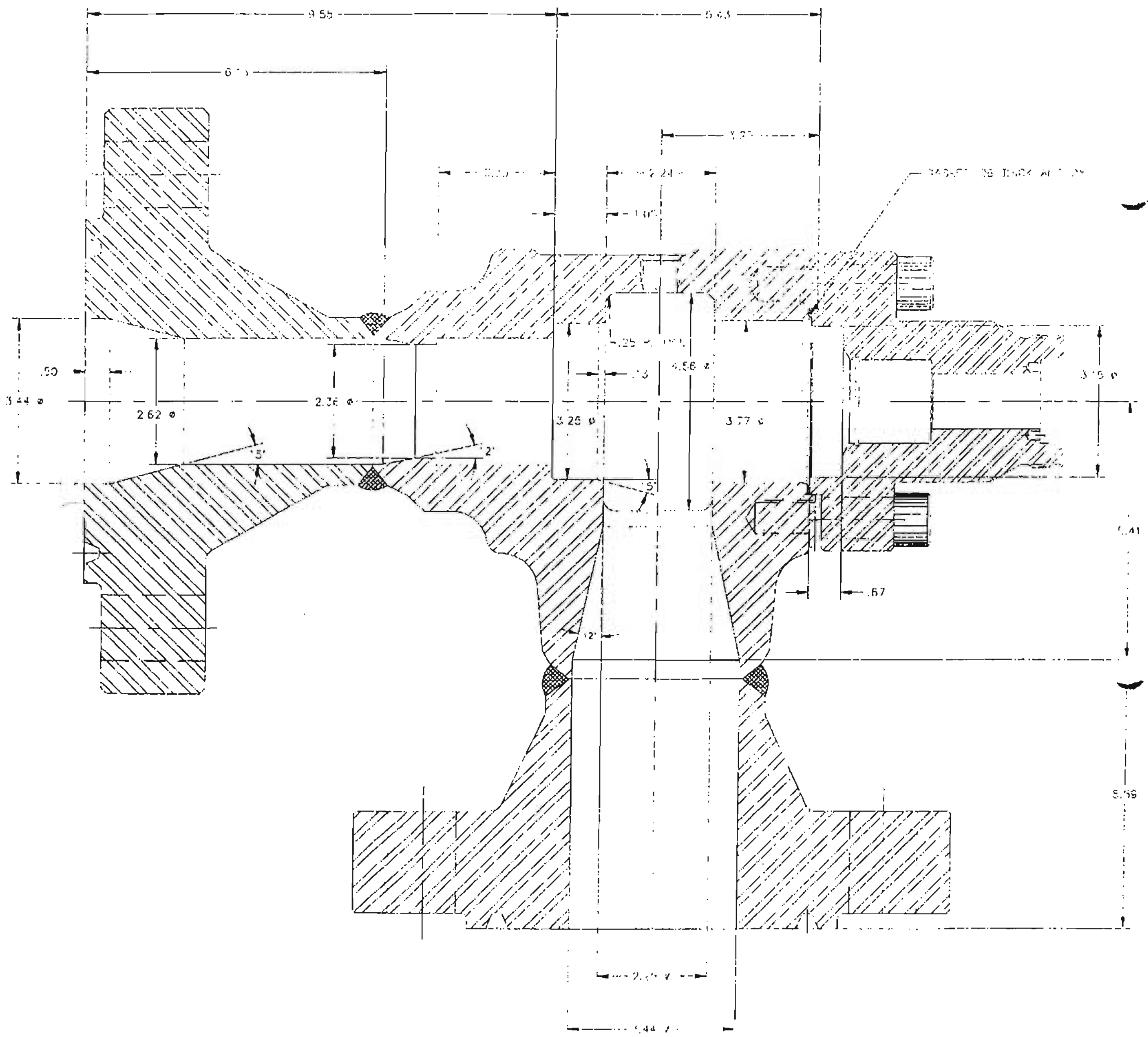
9.55
6.15
2.24
1.00
4.56 ⌀
3.26 ⌀
3.77 ⌀
2.36 ⌀
2.62 ⌀
3.44 ⌀
.50
.67
5.41
5.59
.5°
2°
12°
.5°

FOR I.D. ONLY

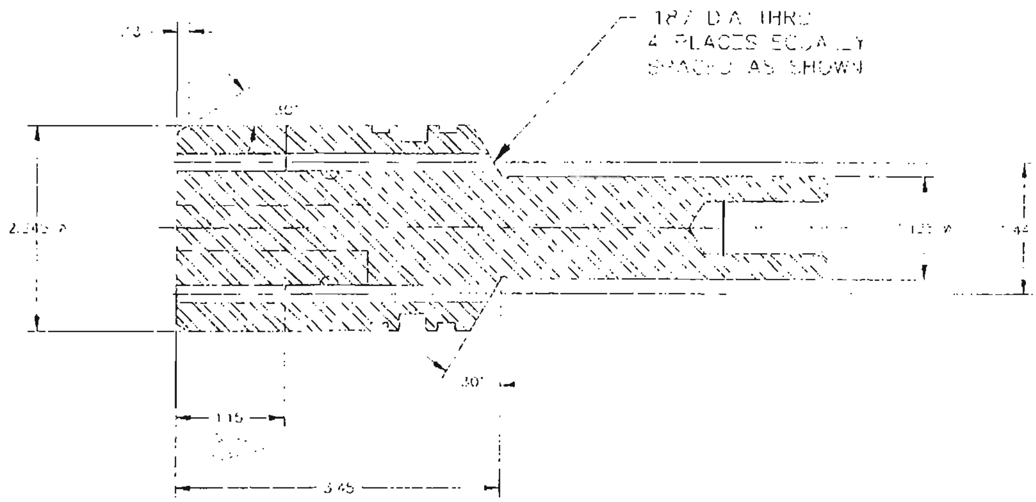

NOT TO SCALE

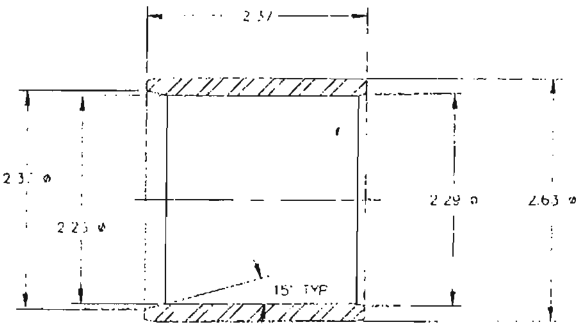

NOT TO SCALE

TOLERANCE UNLESS OTHERWISE SPECIFIED

DO NOT SCALE

CAMERON

CAD

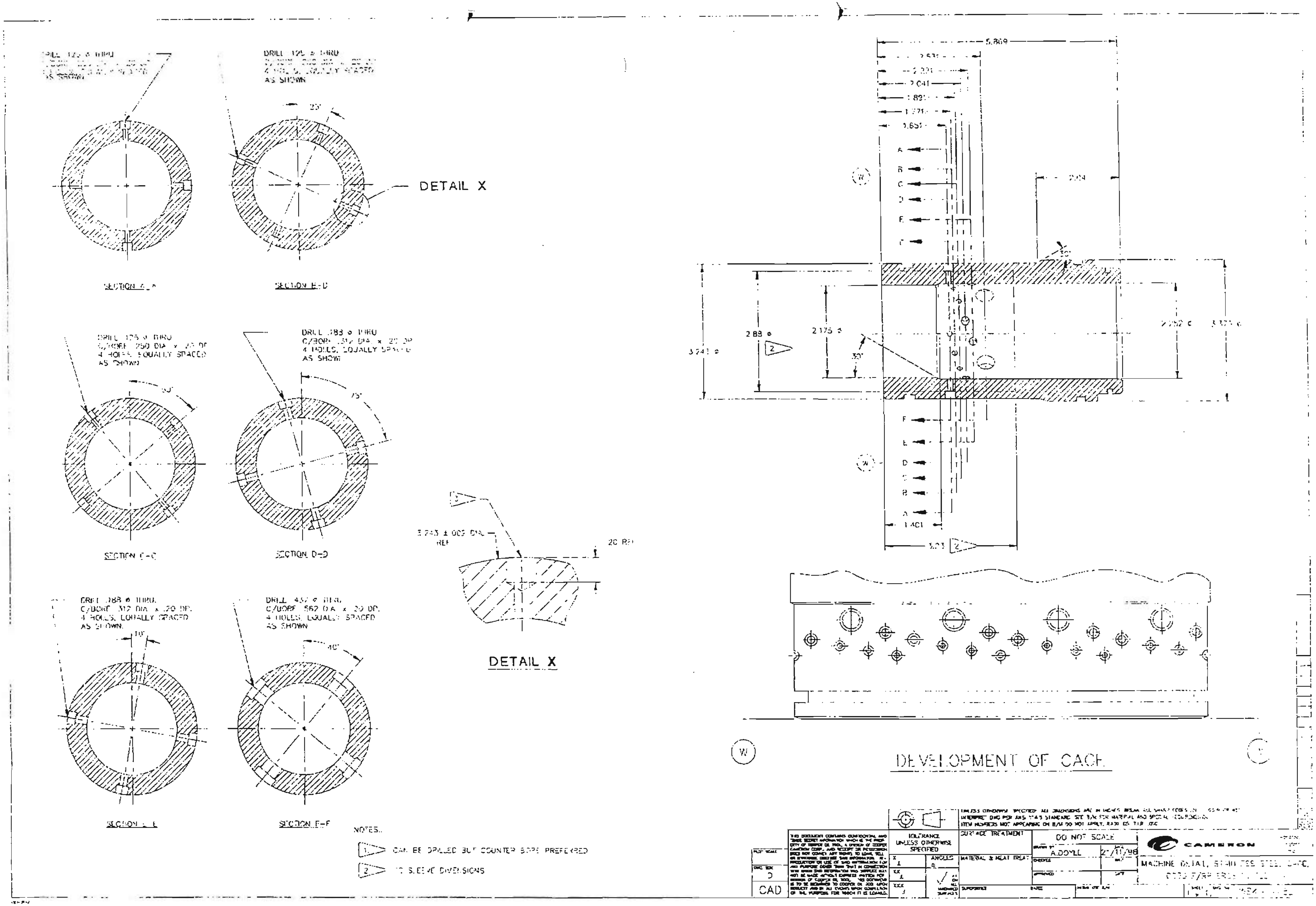

5.809
2.531
2.221
2.041
1.891
1.771
1.651
2.04
30°
2.88 ⌀
2.175 ⌀
3.743 ⌀
2.252 ⌀
3.373 ⌀
1.401
3.23
DRILL .125 ⌀ THRU
AS SHOWN
SECTION A-A
SECTION B-B
DETAIL X
DRILL .125 ⌀ THRU
C/BORE .250 DIA x .20 DP
4 HOLES, EQUALLY SPACED
AS SHOWN
SECTION C-C
DRILL .188 ⌀ THRU
C/BORE .312 DIA x .20 DP
4 HOLES, EQUALLY SPACED
AS SHOWN
SECTION D-D
3.743 ± .002 DIA REF
.20 RAD
DRILL .188 ⌀ THRU
C/BORE .312 DIA x .20 DP.
4 HOLES, EQUALLY SPACED
AS SHOWN.
SECTION E-E
DRILL .437 ⌀ THRU
C/BORE .562 DIA x .20 DP.
4 HOLES, EQUALLY SPACED
AS SHOWN
SECTION F-F
DEVELOPMENT OF CAGE
NOTES.
1 CAN BE DRILLED BUT COUNTER BORE PREFERRED
2 TO SLEEVE DIMENSIONS
TOLERANCE UNLESS OTHERWISE SPECIFIED
ANGLES
SURFACE TREATMENT
MATERIAL & HEAT TREAT
DO NOT SCALE
A.DOYLE
CAMERON
MACHINE DETAIL
CAD

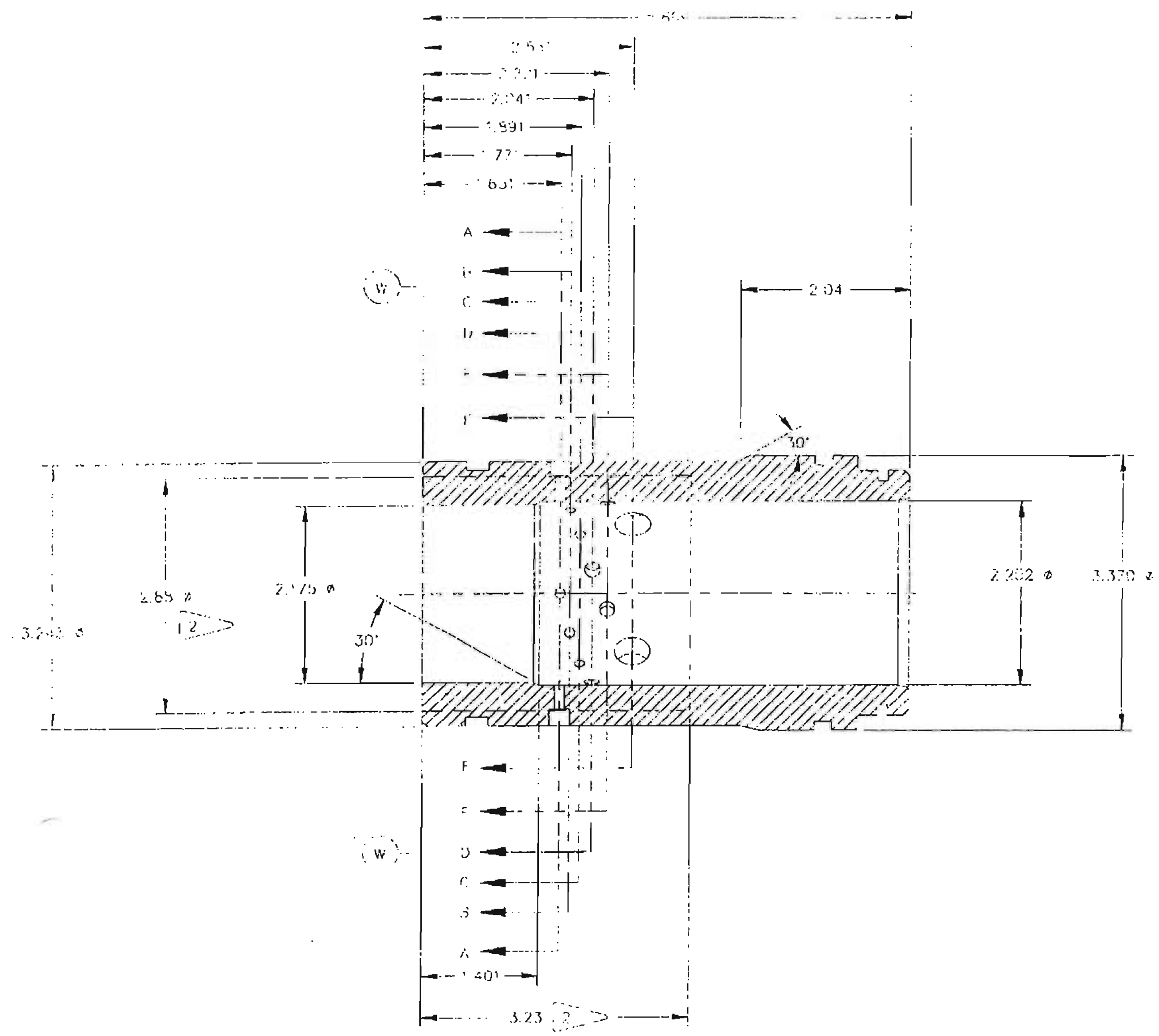

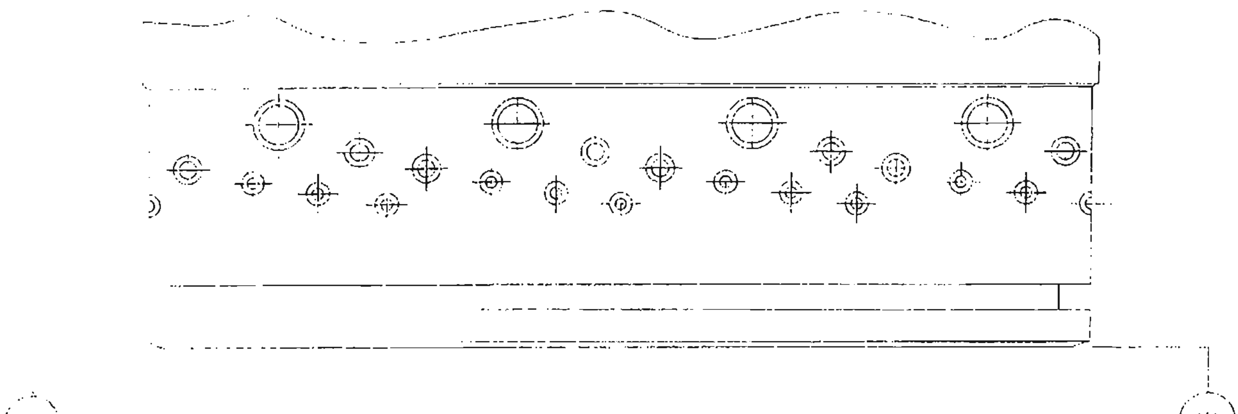

DEVELOPMENT OF CAGE

CAMERON

358-1448

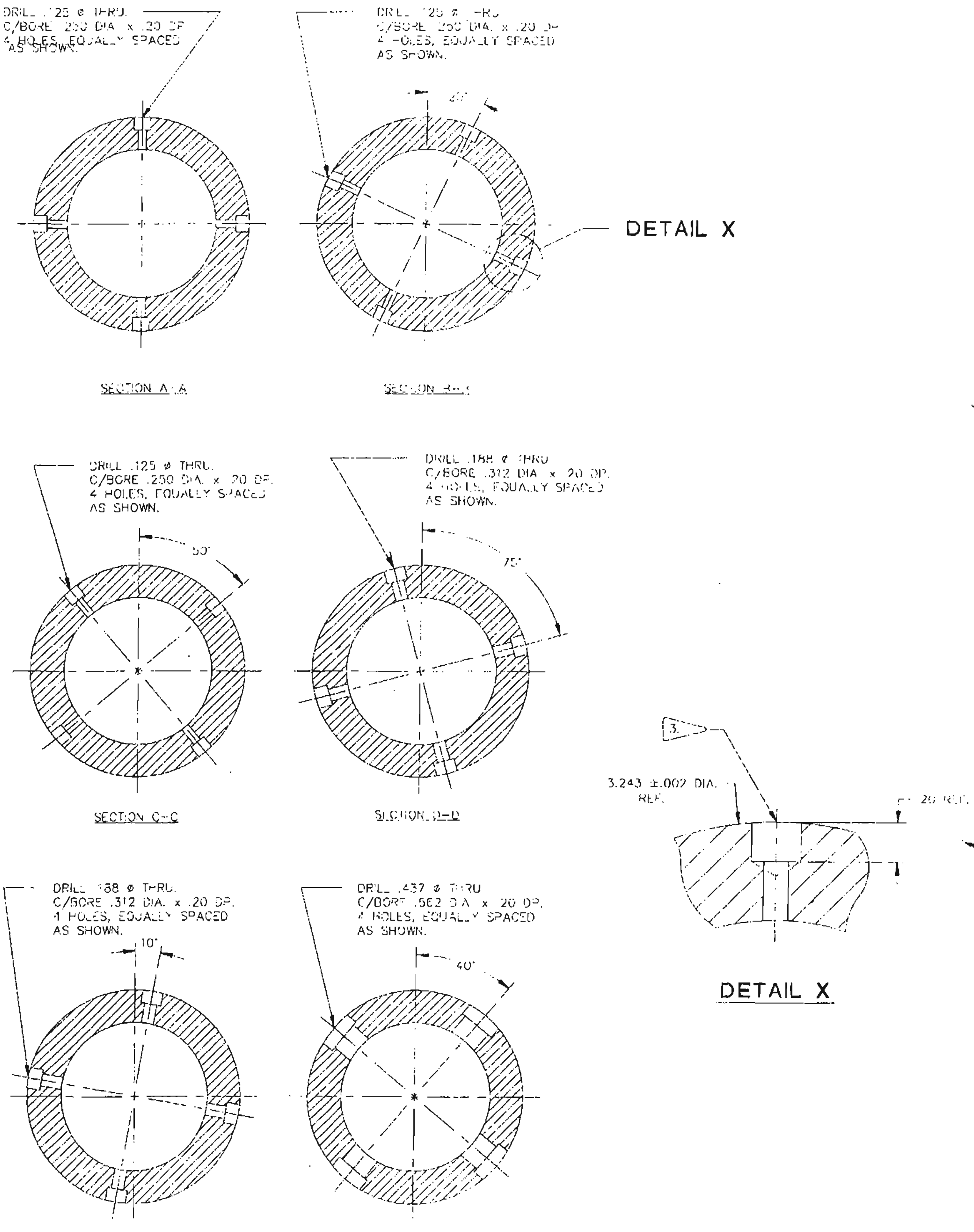

NOTES:

1. ... CAN BE DRILLED BUT COUNTER BORE PREFERRED

2. ... SLEEVE DIMENSIONS

Test Rig Design - Flow Fields within Orifice Plate

Fluid - **Water**
Pipeline Diameter - **75** mm
Orifice Diameter - **18** mm
Taper Length - **One Orifice Diameter**
Restriction Length - **50** mm
Pressure Drop - **25** Bar
Mass Flow Rate - **15.2** kg/hr

Appendix Figure 127 - Fluid Velocity Contours Across Orifice Plate (m/s)

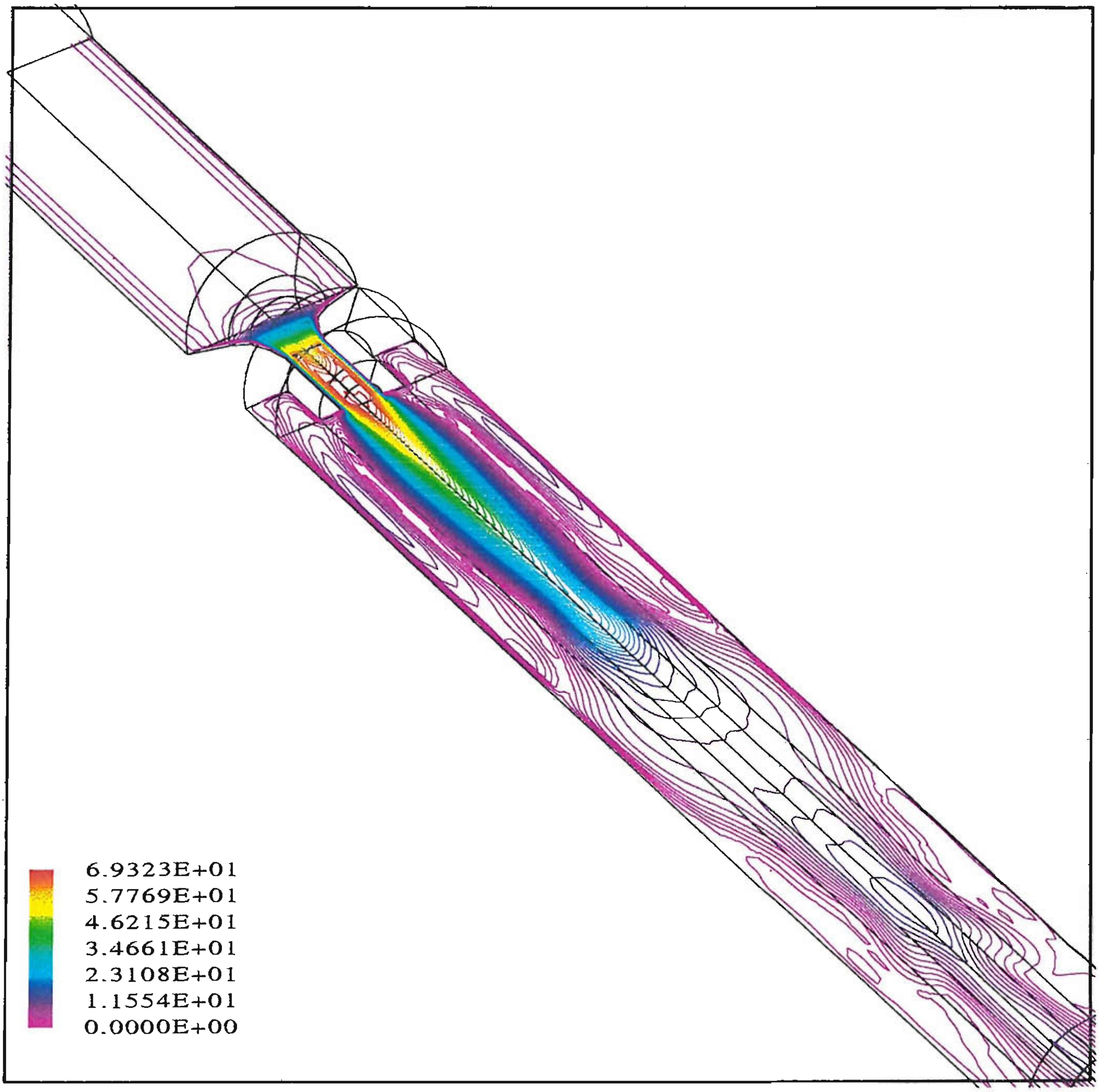

TEST RIG DESIGN - FLOW FIELDS WITHIN ORIFICE PLATE

Particle Type - **Sand**
Particle Flux Rate - **1.0 % by wt.**
Particle Roundness Factor - **0.5**
Number of Particle Sizes - **4**
Particle Size Range - **50-200** μm
Turbulent Dispersion - **Yes**
Modified Coefficient of Restitution - **Yes**
Squeeze Film Retardation - **Yes**

Appendix Figure 128 - Surface Contour Plot of Orifice Plate Particle Impact Velocities (m/s)

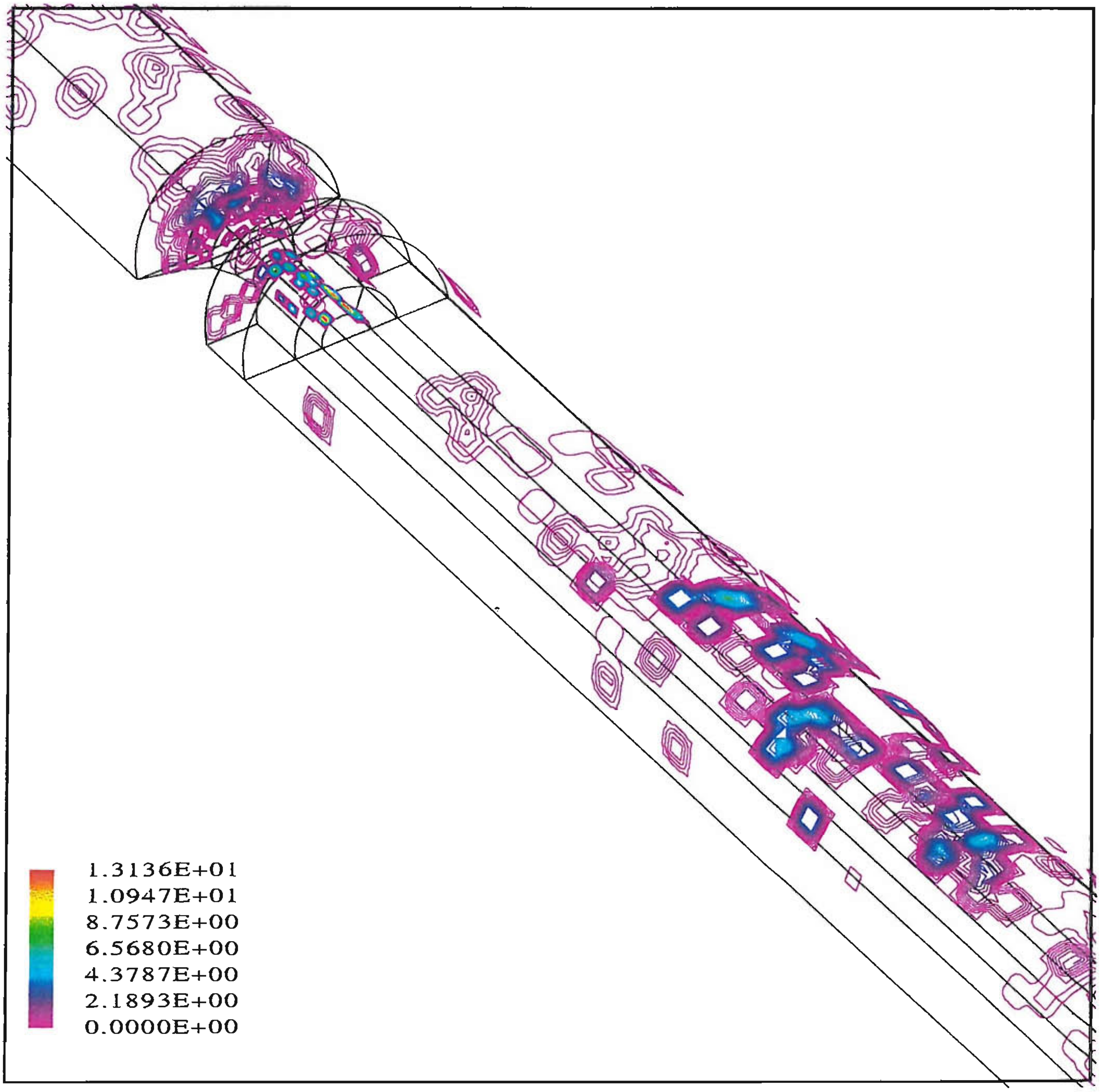

TEST RIG DESIGN - FLOW FIELDS WITHIN ORIFICE PLATE

Particle Type - **Sand**
Particle Flux Rate - **1.0 % by wt.**
Particle Roundness Factor - **0.5**
Number of Particle Sizes - **4**
Particle Size Range - **50-200** μm
Turbulent Dispersion - **Yes**
Modified Coefficient of Restitution - **Yes**
Squeeze Film Retardation - **Yes**

Appendix Figure 129 - Surface Contour Plot of Orifice Plate Particle Impact Angles (deg)

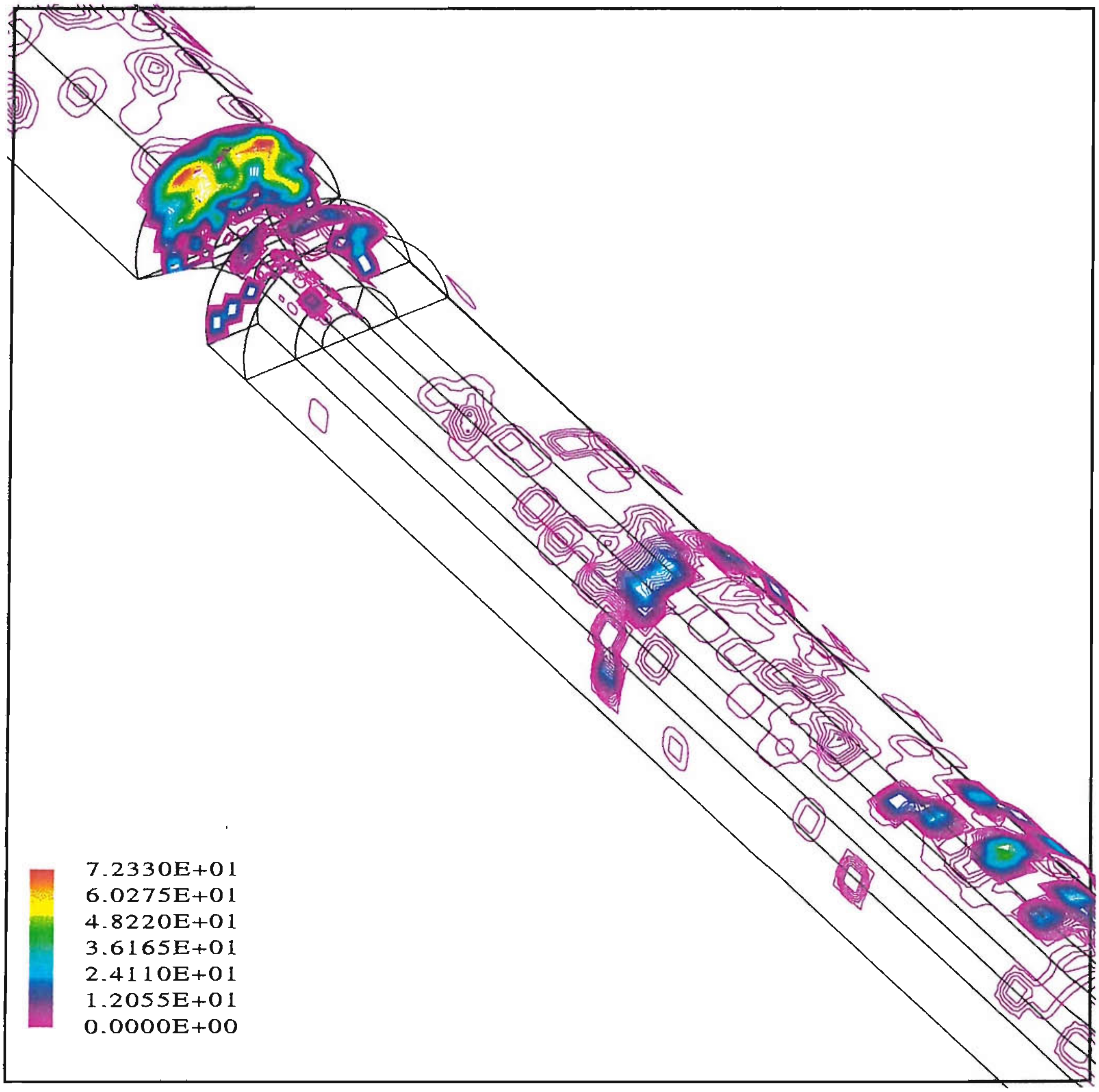

TEST RIG DESIGN - FLOW FIELDS WITHIN ORIFICE PLATE

Particle Type - **Sand**
Particle Flux Rate - **1.0 % by wt.**
Particle Roundness Factor - **0.5**
Number of Particle Sizes - **4**
Particle Size Range - **50-200 μm**
Turbulent Dispersion - **Yes**
Modified Coefficient of Restitution - **Yes**
Squeeze Film Retardation - **Yes**

Appendix Figure 130 - Surface Contour Plot of Orifice Plate Particle Erosion Rates (mm^3/hr)

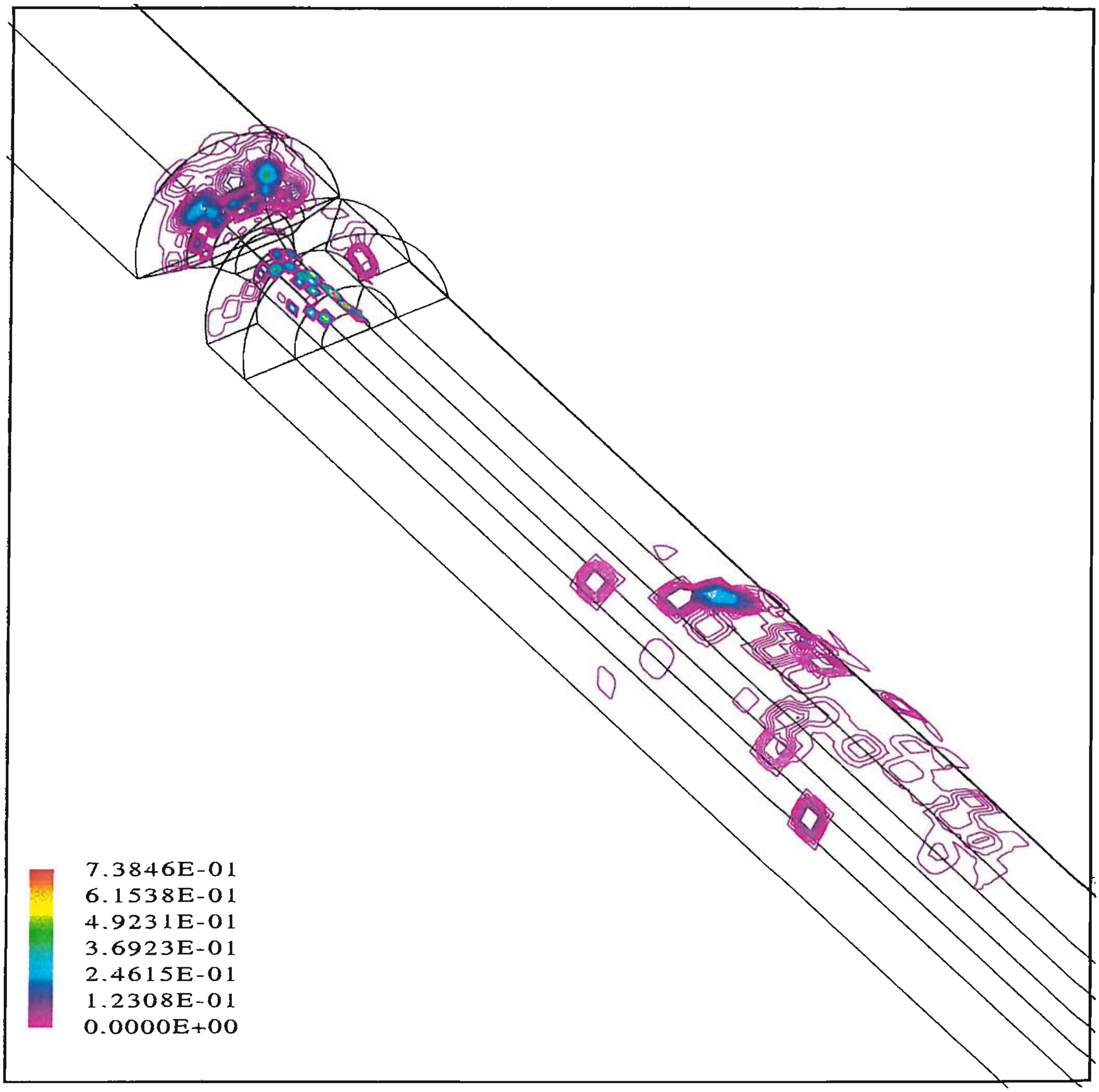

Pressure, Temperature and Flowrate History of Valve Erosion Testing.

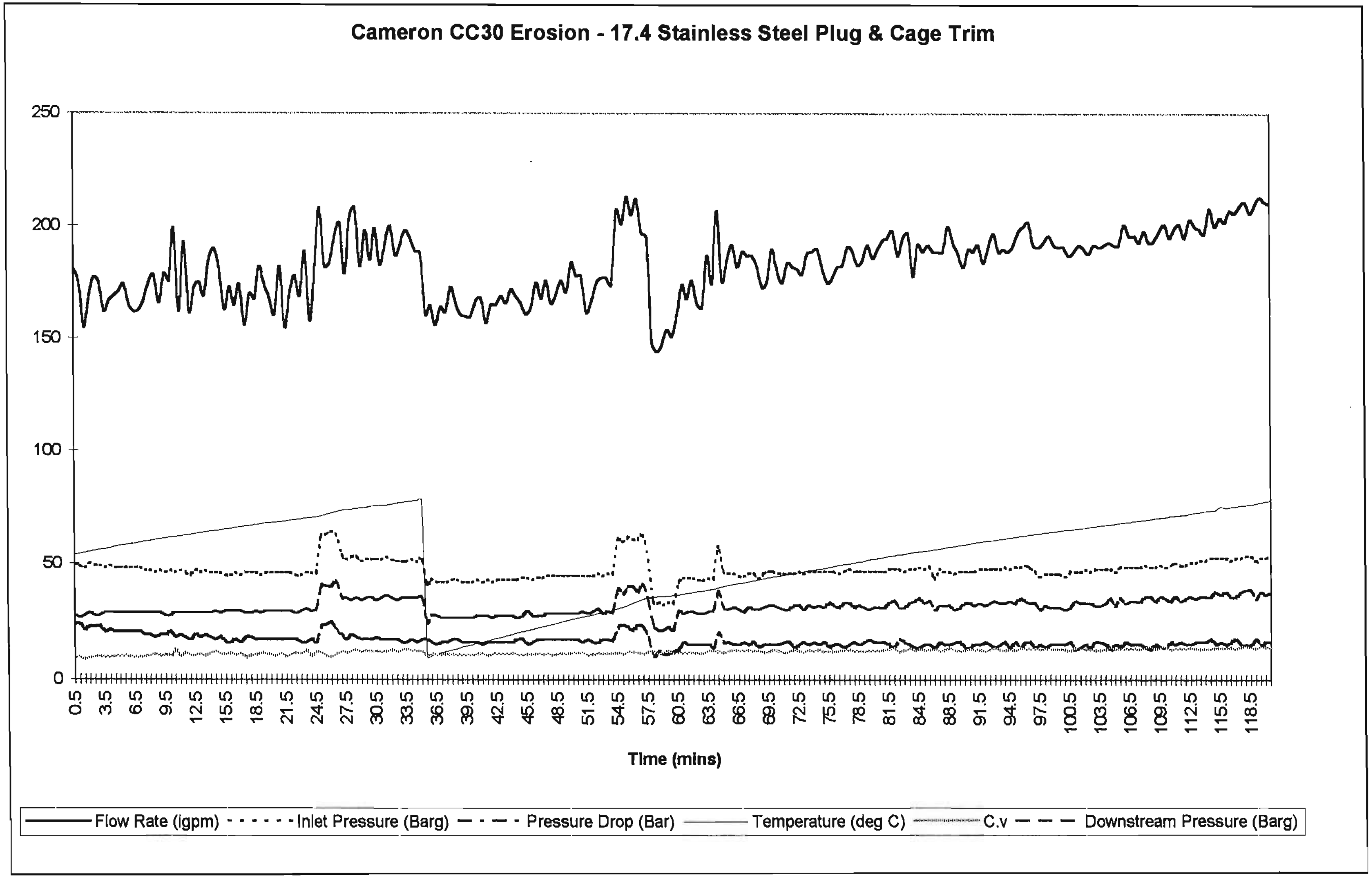

Appendix Figure 131 - Cameron CC30 Equal Percentage Control Choke (17.4 PH Stainless Steel: Test 1 - High Flow)

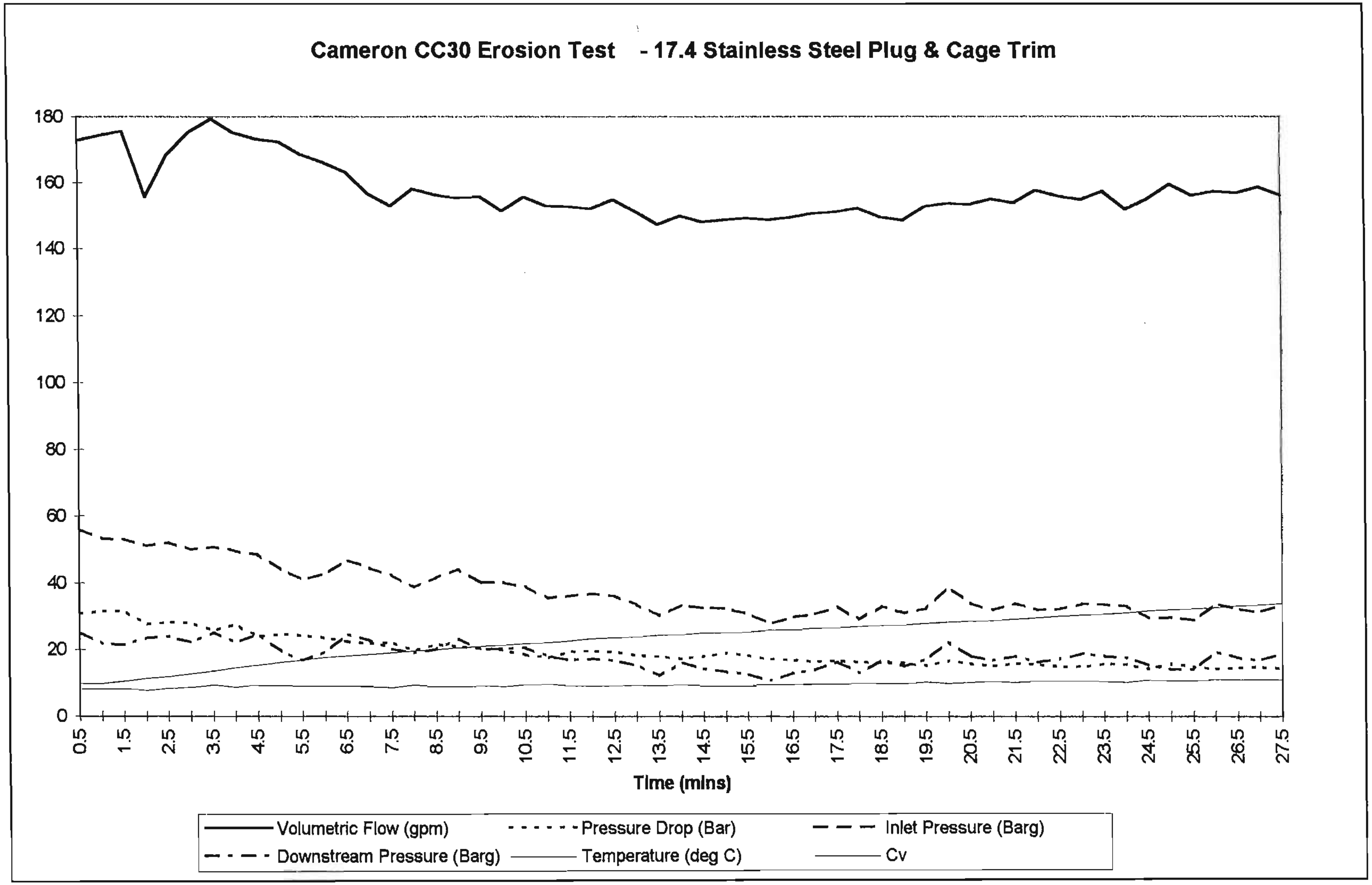

Appendix Figure 132 - Cameron CC30 Equal Percentage Control Choke (17.4 PH Stainless Steel: Test 2 - High Flow)

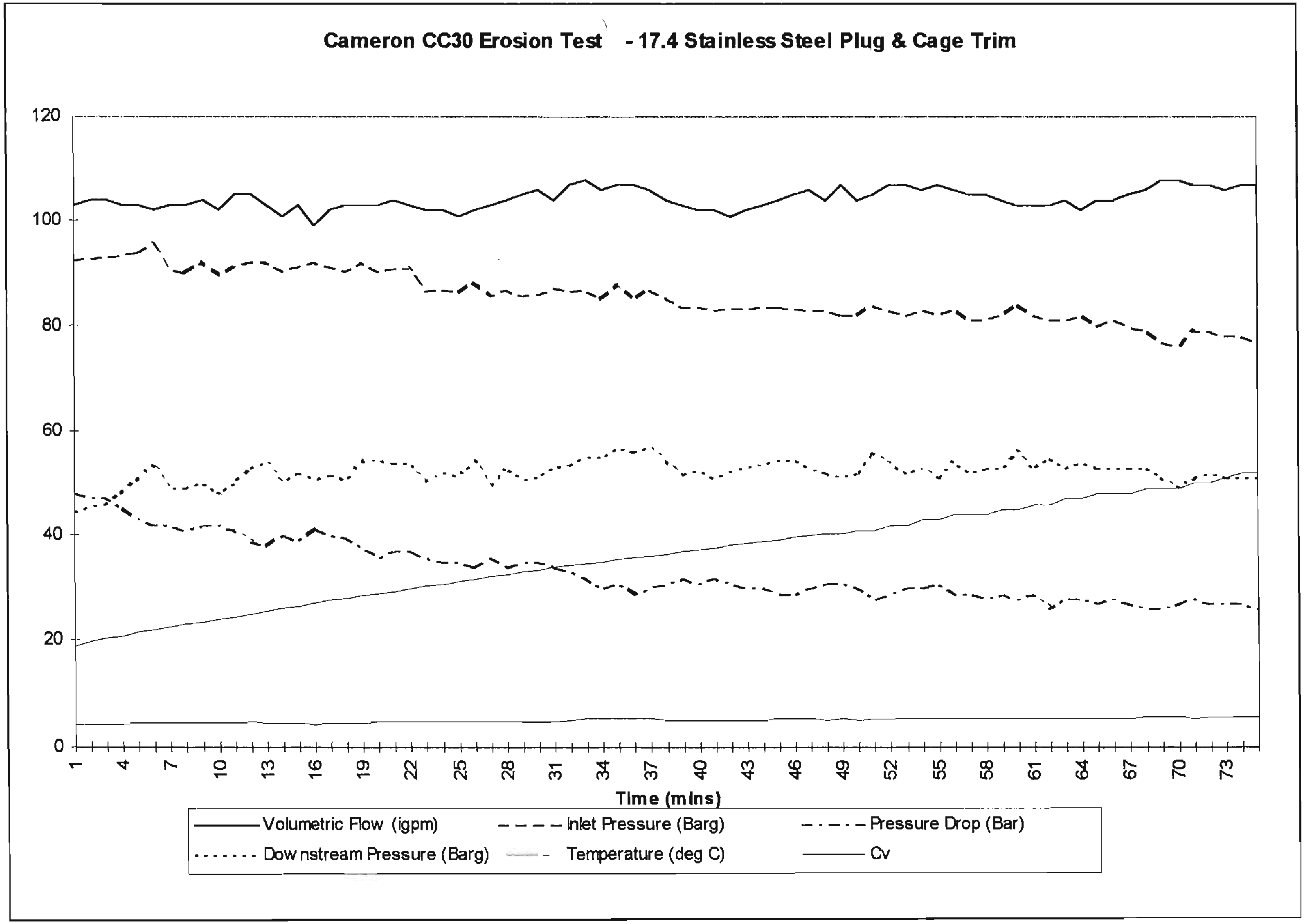

Appendix Figure 133 - Cameron CC30 Equal Percentage Control Choke (17.4 PH Stainless Steel: Test 3 - Low Flow)

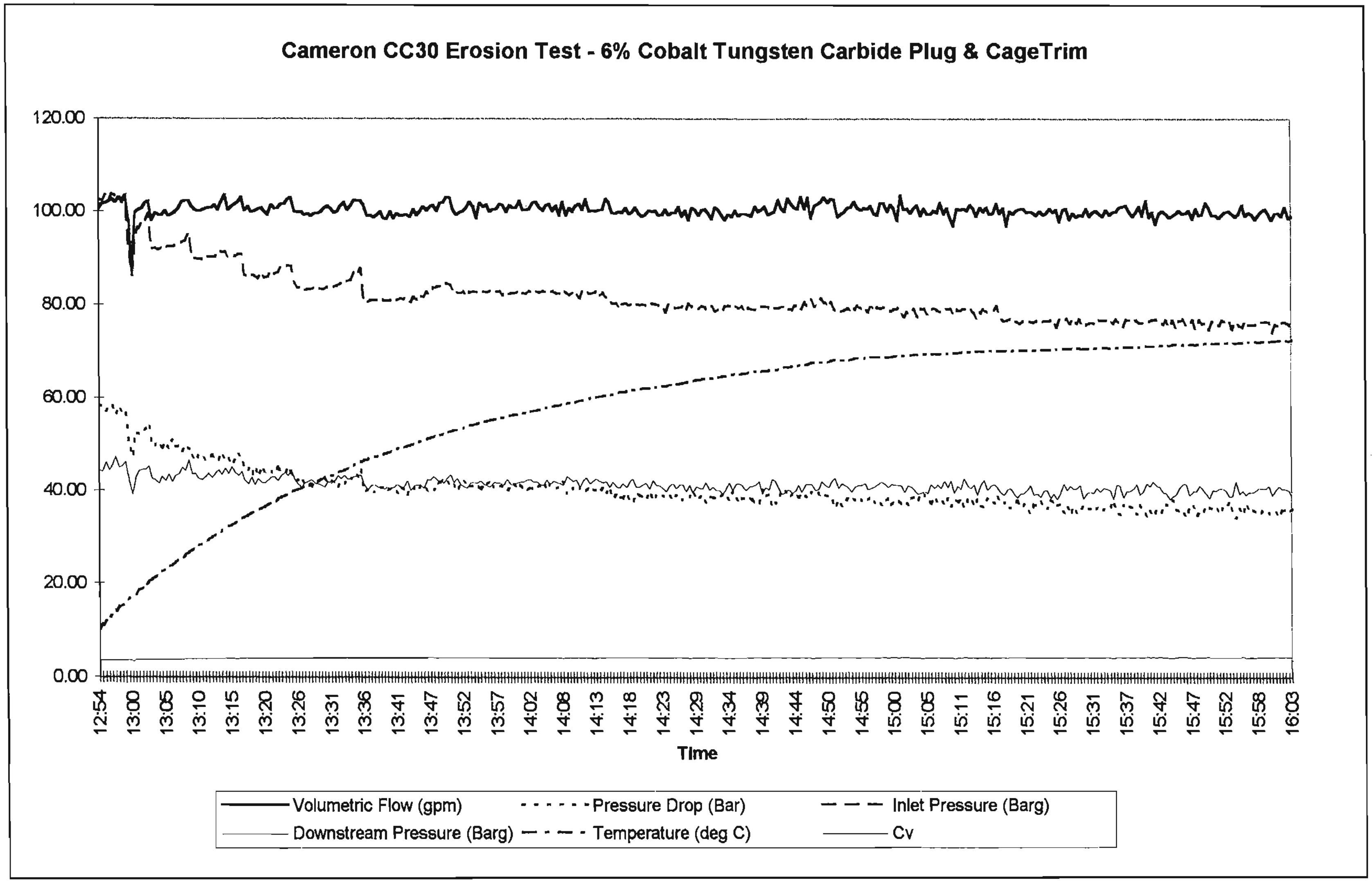

Appendix Figure 134 - Cameron CC30 Equal Percentage Control Choke (6% Cobalt Binder Tungsten Carbide: Test 4 - Low Flow)

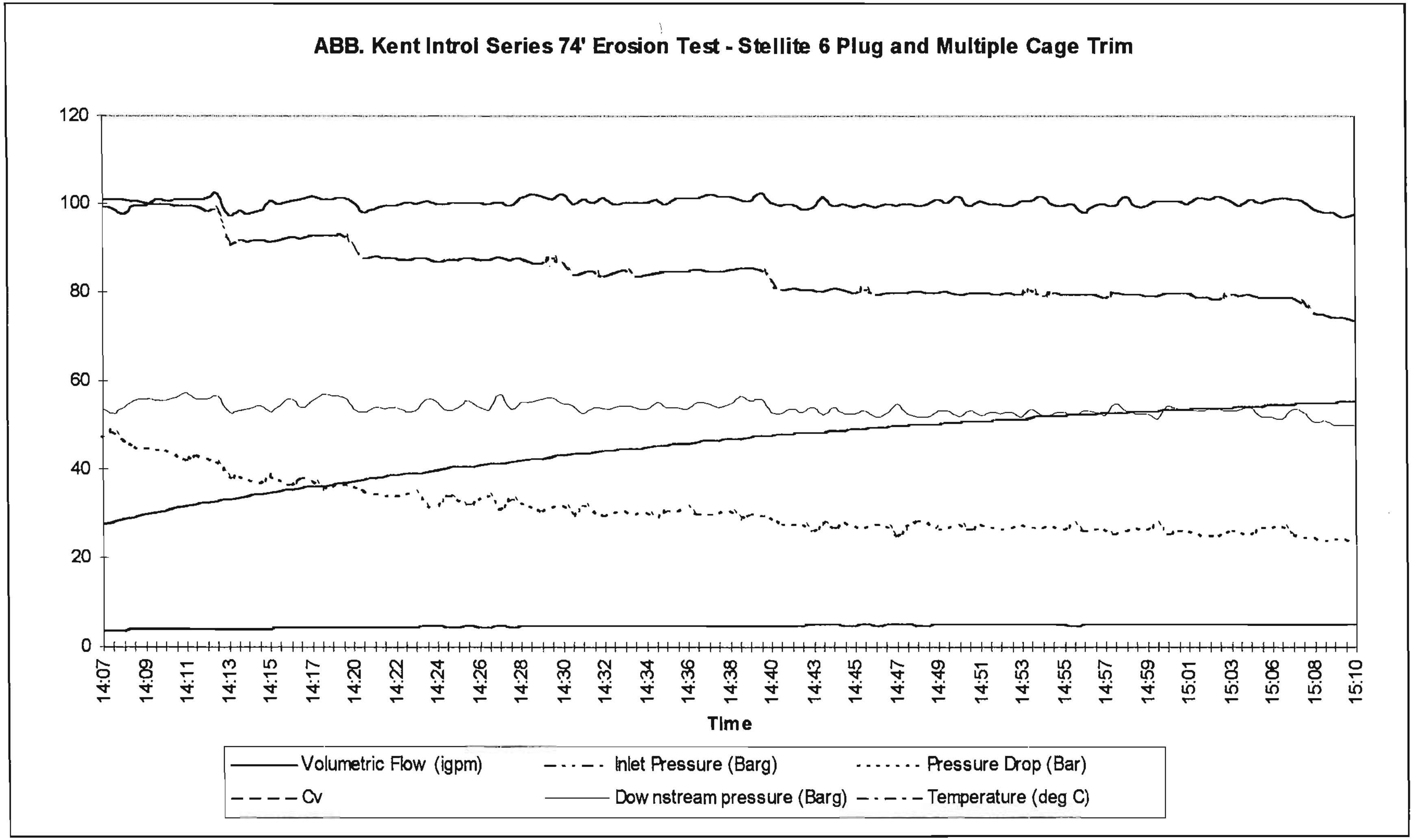

Appendix Figure 135 - ABB Kent Introl Series 74' Equal Percentage Control Choke (Stellite: Test 5 - Low Flow)

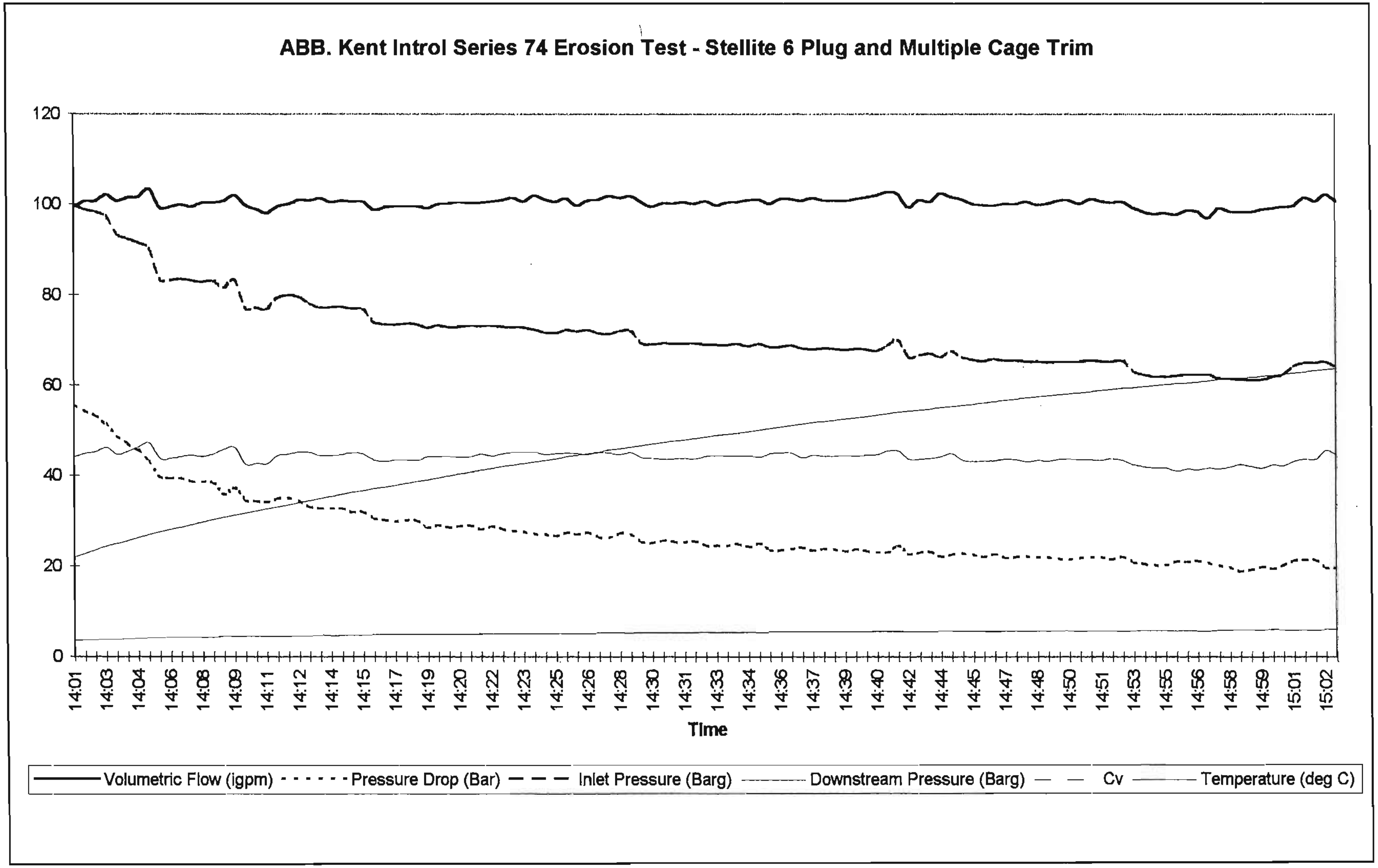

Appendix Figure 136 - ABB Kent Introl Series 74' Equal Percentage Control Choke (Stellite: Test 6 - Low Flow)

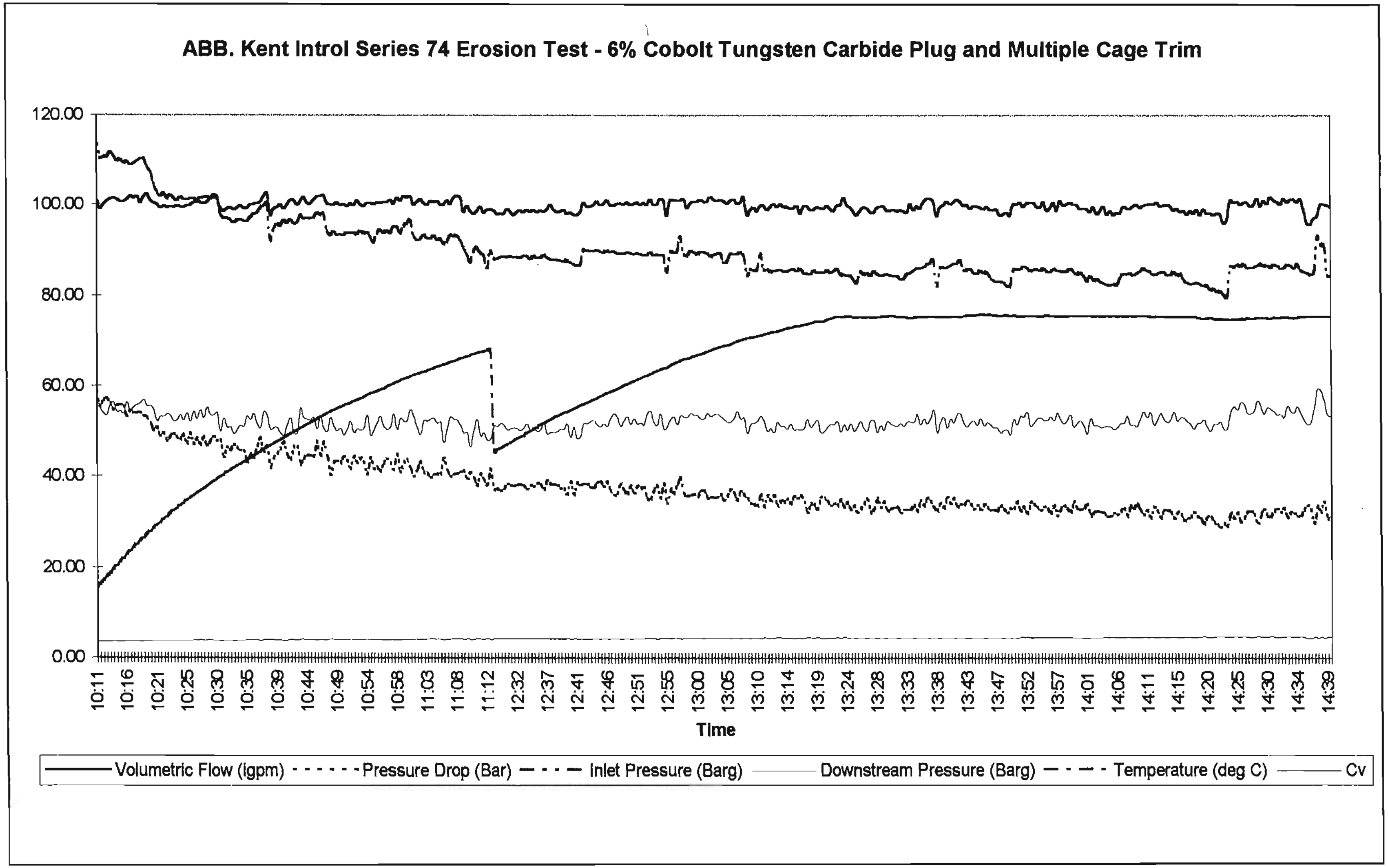

Appendix Figure 137 - ABB Kent Introl Series 74' Equal Percentage Control Choke (6% Cobalt Binder Tungsten Carbide: Test 7 - Low Flow)

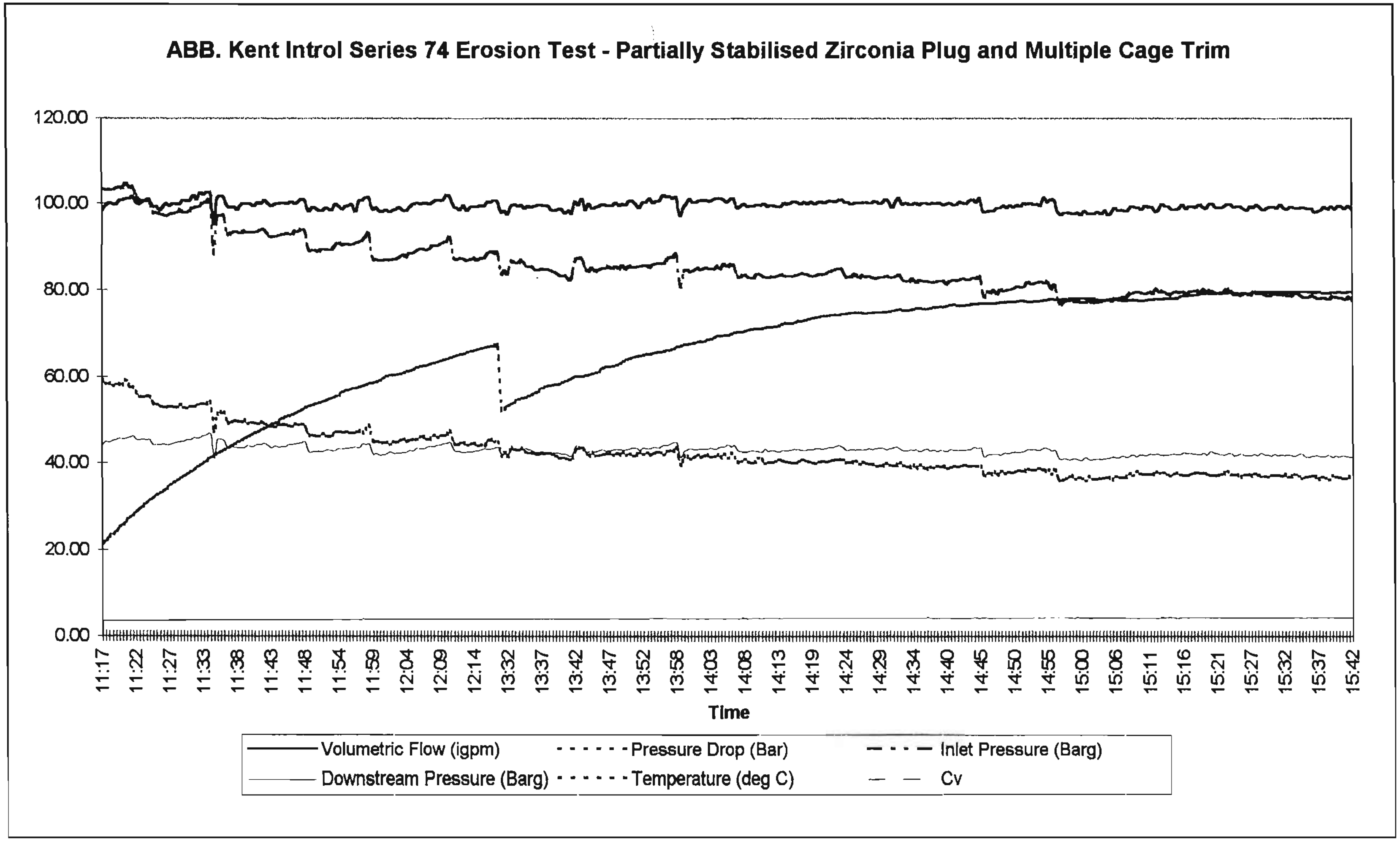

Appendix Figure 138 - ABB Kent Introl Series 74' Equal Percentage Control Choke (Partially Stabilised Zirconia: Test 8 - Low Flow)

Pictorial Record of Choke Valves Tested

Appendix Picture 1 Flow Loop Configuration and Mounting of Cooper Cameron CC30 Test Choke (Bonnet and Actuator Fitted)

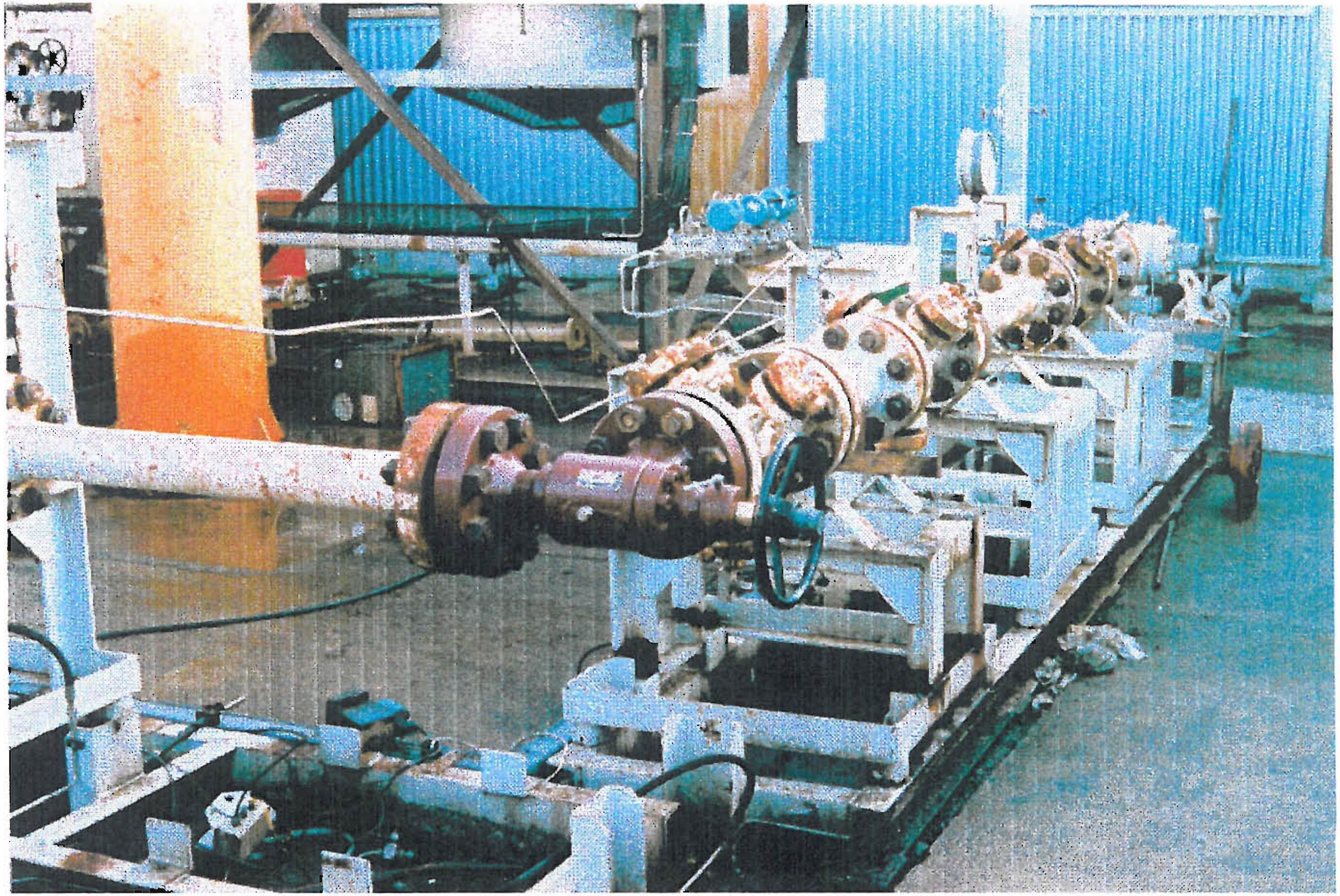

Appendix Picture 2 Flow Loop Configuration and Mounting of ABB. Kent Introl Series 74 Test Choke (Bonnet and Actuator Fitted)

Appendix Picture 3 Flow Loop Configuration and Mounting of ABB. Kent Introl Series 74 Test Choke (Bonnet and Actuator Removed)

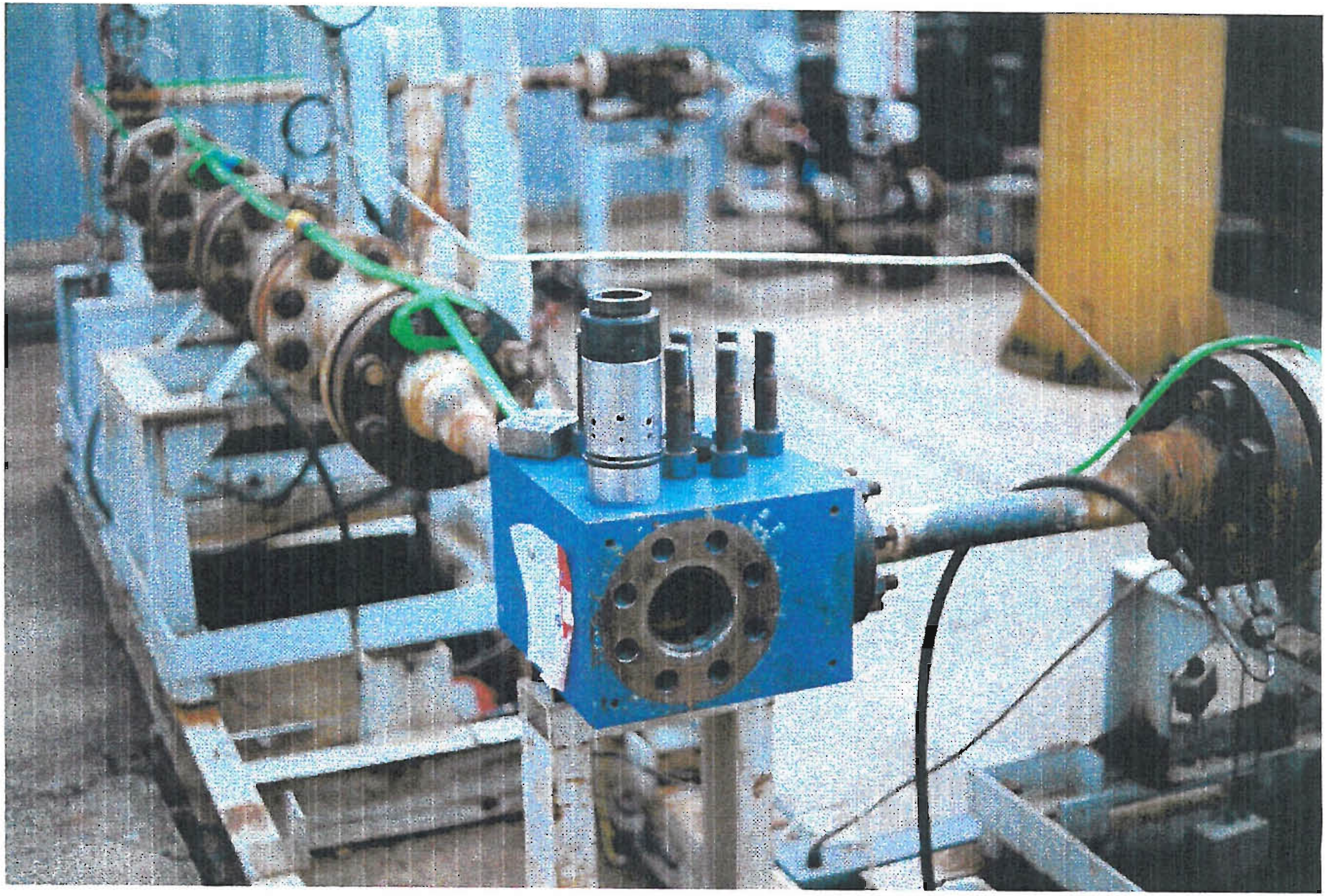

Appendix Picture 4 ABB. Kent Introl Series 74 6% Cobalt Tungsten Carbide Post Test Trim Set - Test 7
(Shrink fit inner/outer cage)

Appendix Picture 5 ABB. Kent Introl Series 74 Stellite Post Test Trim Set - Test 6
(Split inner/outer cage)

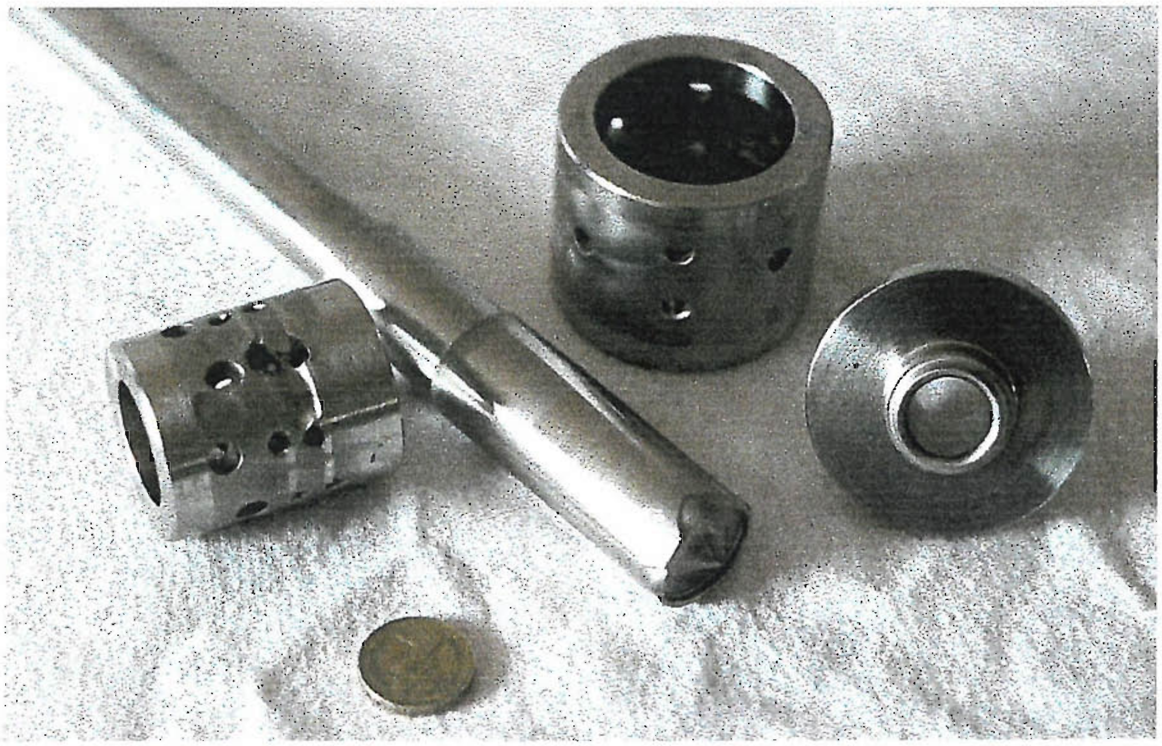

Appendix Picture 6 ABB. Kent Introl Series 74 Stellite Post Test Seat Damage - Test 5

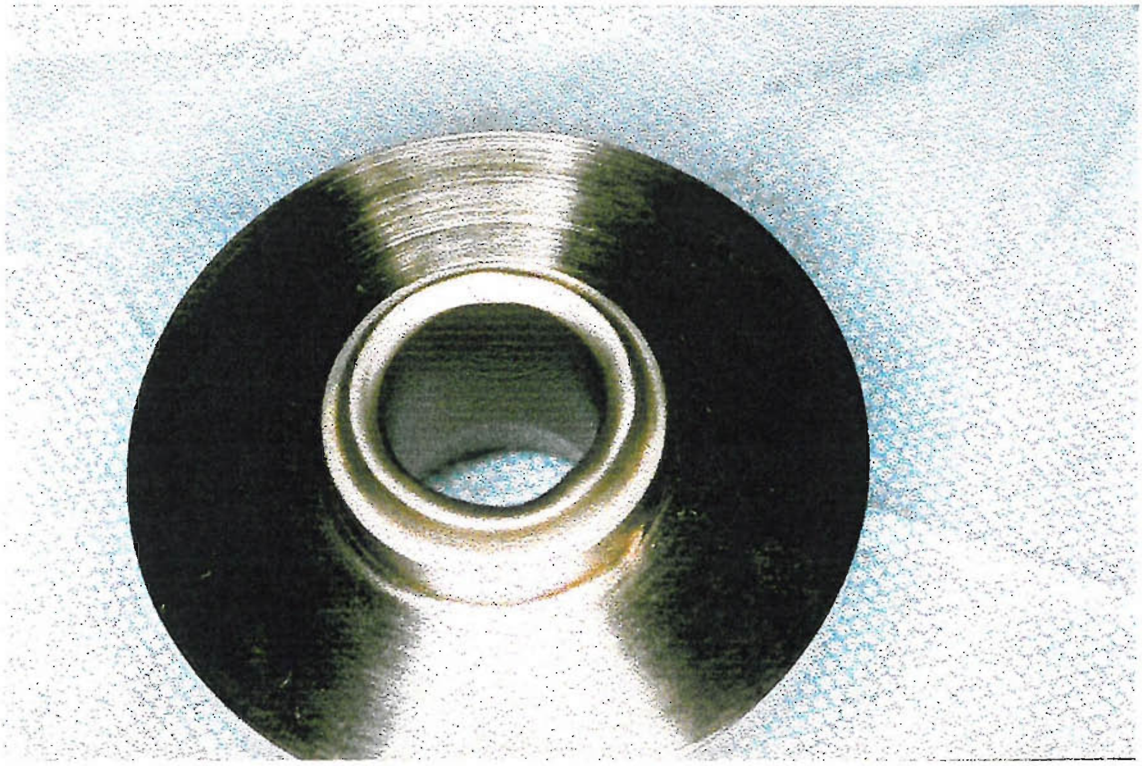

Appendix Picture 7 ABB. Kent Introl Series 74 Stellite Post Test Plug Damage - Test 5

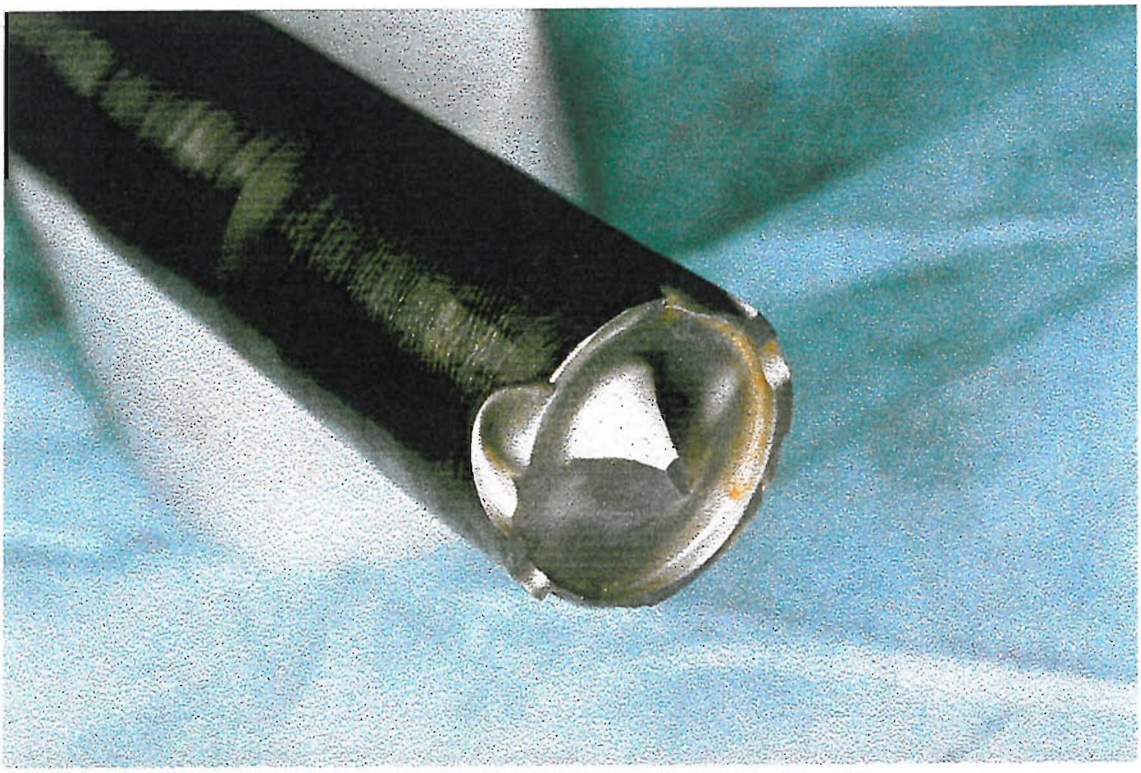

Appendix Picture 8 ABB. Kent Introl Series 74 Stellite Post Test Outer Cage Damage - Test 5

Appendix Picture 9 ABB. Kent Introl Series 74 Stellite Post Test Inner Cage Damage - Test 6

Appendix Picture 10 ABB. Kent Introl Series 74 Stellite Post Test Outer Cage Damage - Test 6

Appendix Picture 11 Cooper Cameron CC30 Stainless Steel Post Test Trim Set - Test 1

High Flowrate Test

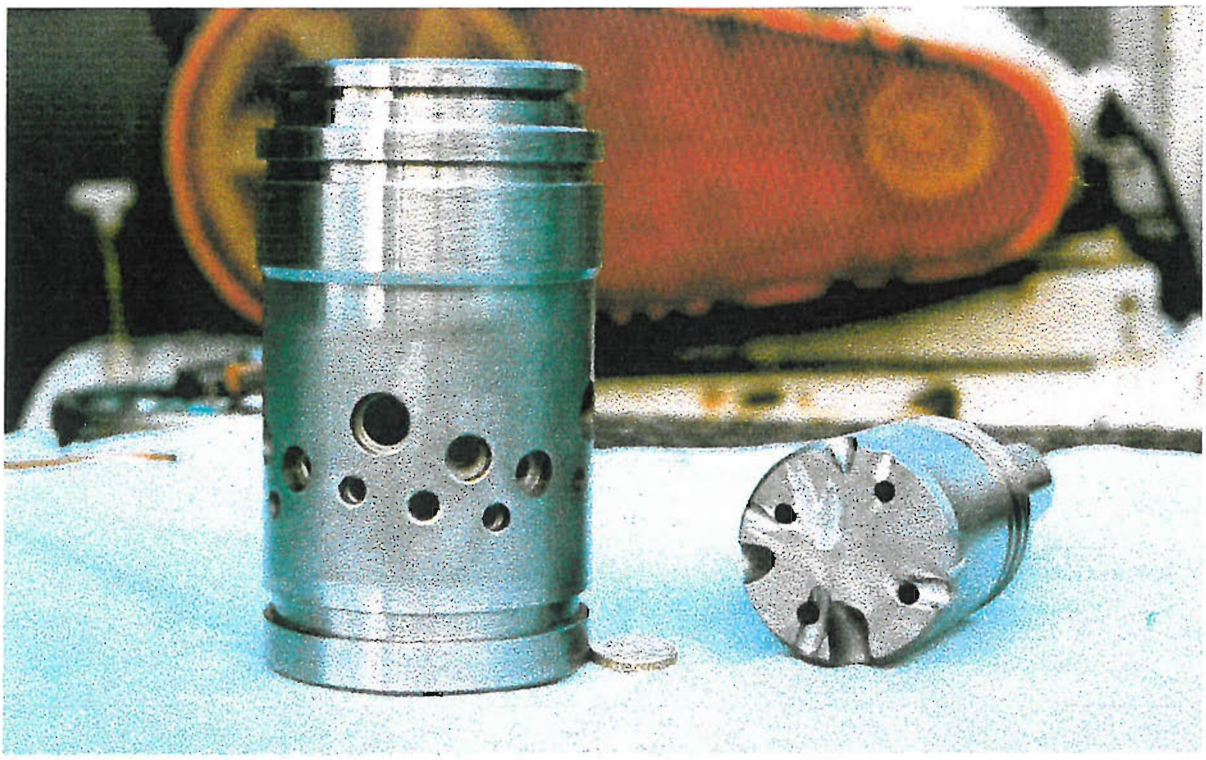

Appendix Picture 12 Cooper Cameron CC30 Stainless Steel and Tungsten Carbide Post Test Plug Damage - Test 1/2/3/4

Left to right - tests 1,2,3 and 4.

Inlet position in each case noted by arrow on test 1 plug.

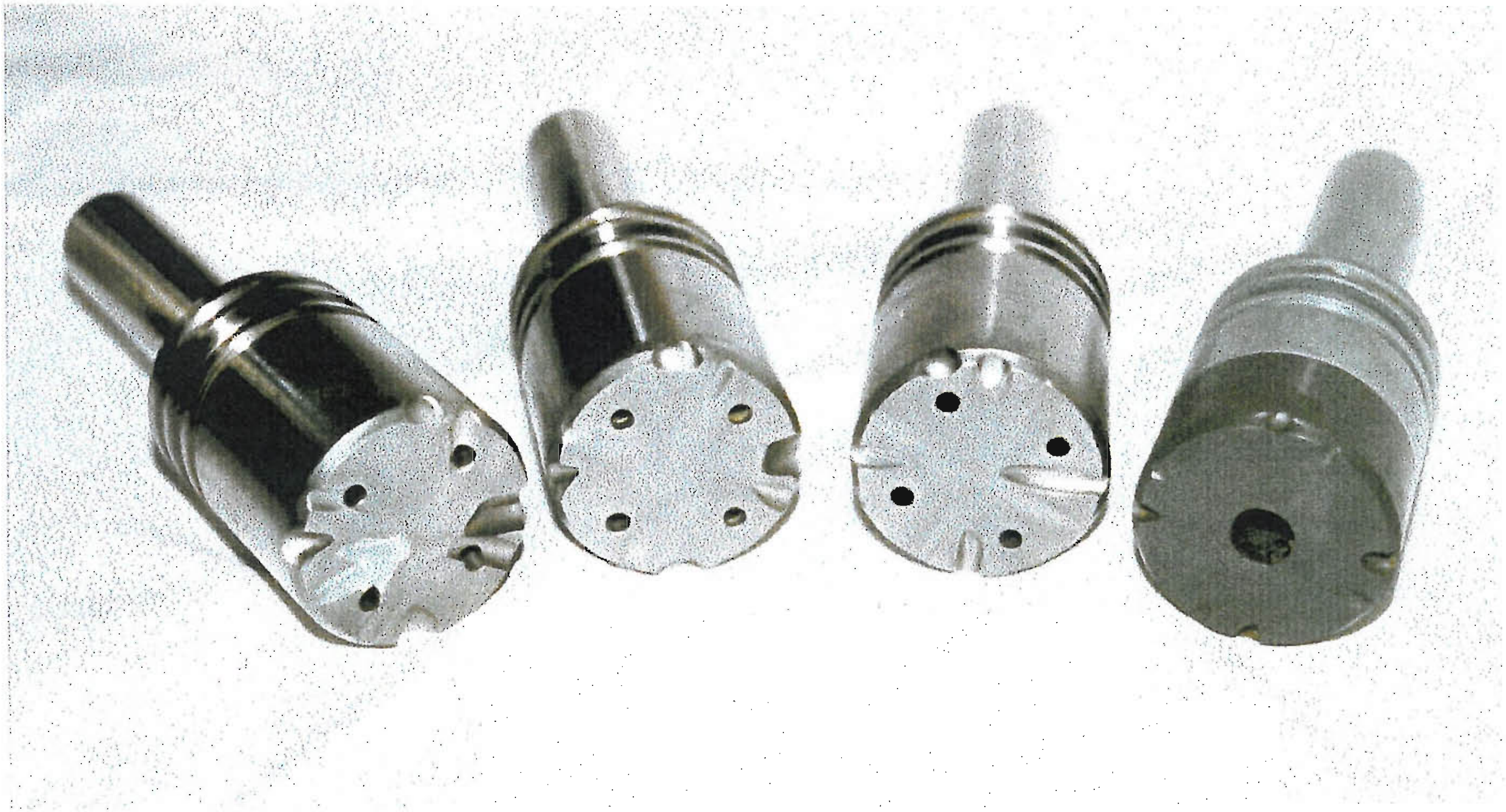

Appendix Picture 13 Cooper Cameron CC30 Stainless Steel Post Test Plug Damage - Test 3

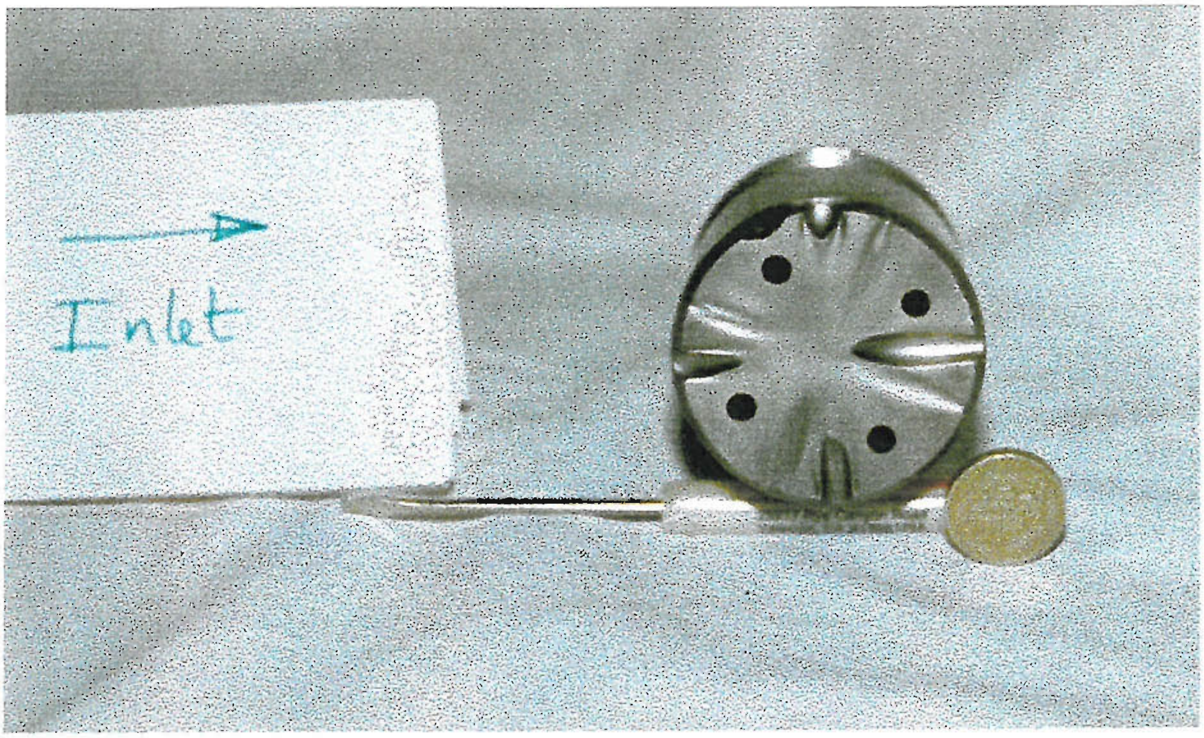

Appendix Picture 14 Cooper Cameron CC30 6% Cobalt Tungsten Carbide Post Test Plug Damage - Test 4

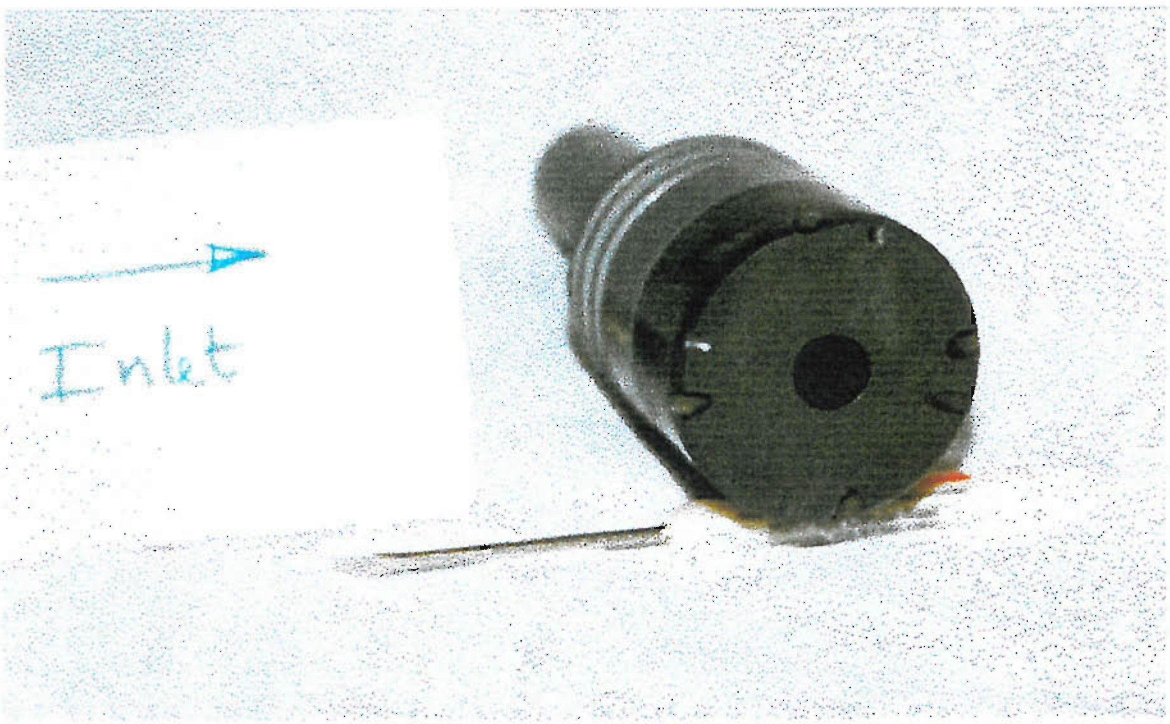

Appendix Picture 15 Cooper Cameron CC30 6% Cobalt Tungsten Carbide Post Test Sand Packing - Test 4

Note sand packed above the plug in the pressure balance cavity within the bonnet.

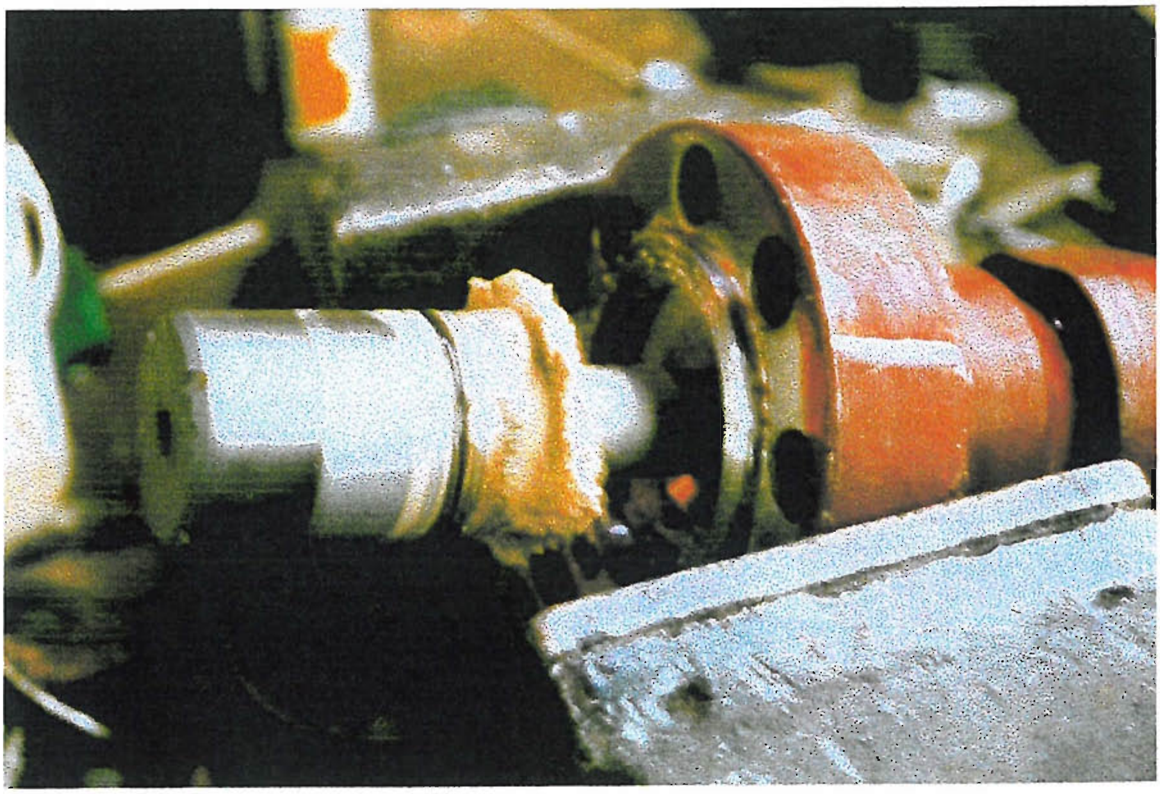

Appendix Picture 16 Sand Attrition SEM investigation, Test 6 after 20 min circulation.

ABB. Kent Introl Series 74 Stellite Test

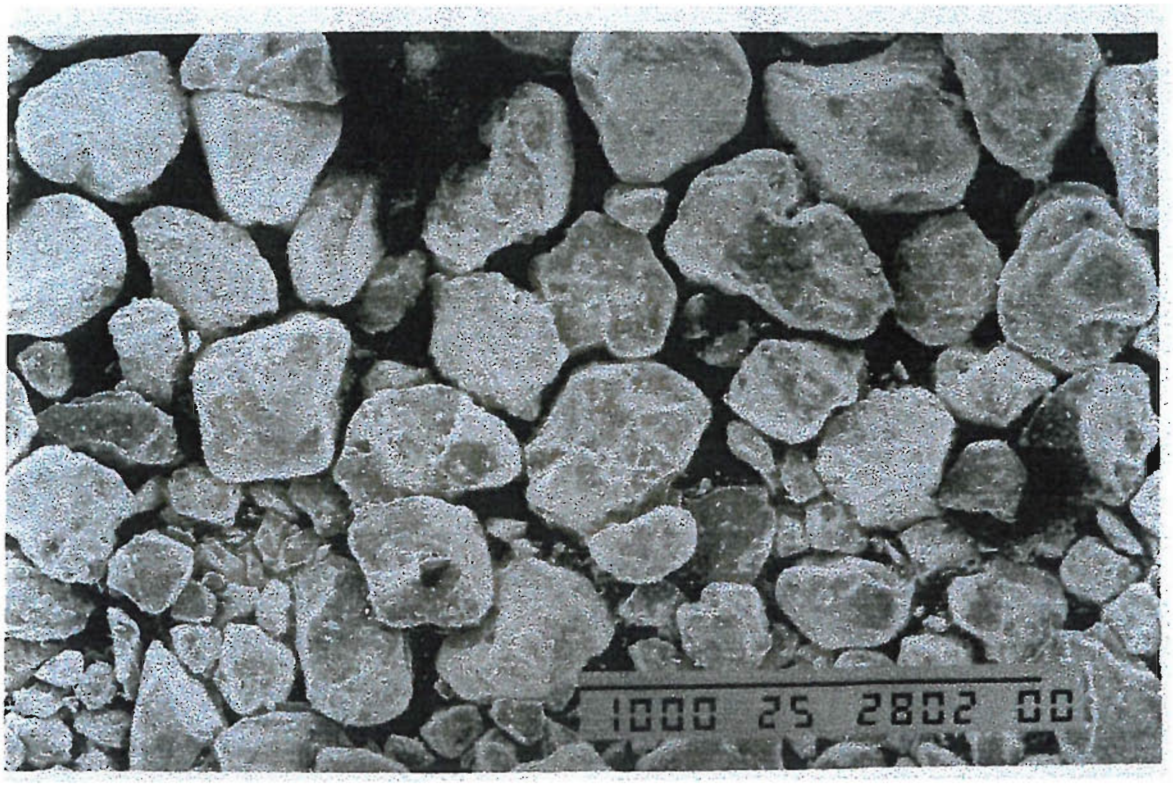

Appendix Picture 17 Sand Attrition SEM investigation, Test 6 after 40 min circulation.

ABB. Kent Introl Series 74 Stellite Test

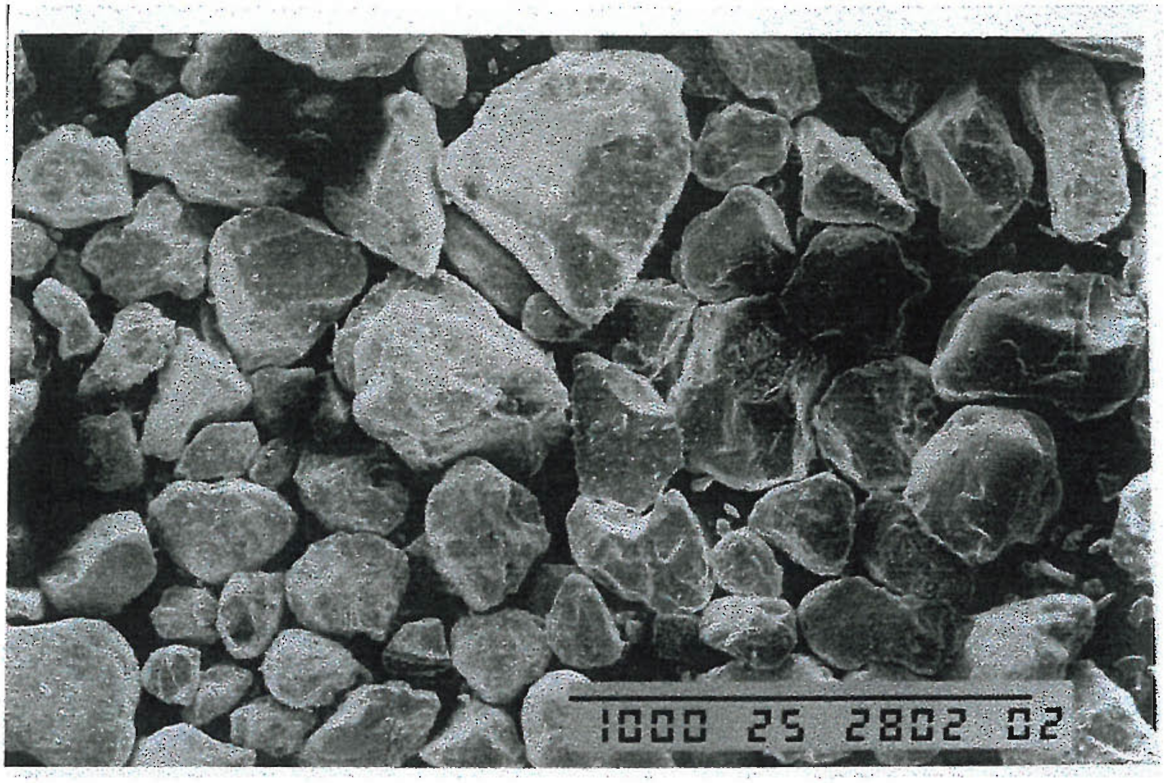

Appendix Picture 18 Sand Attrition SEM investigation, Test 6 after 60 min circulation.

ABB. Kent Introl Series 74 Stellite Test

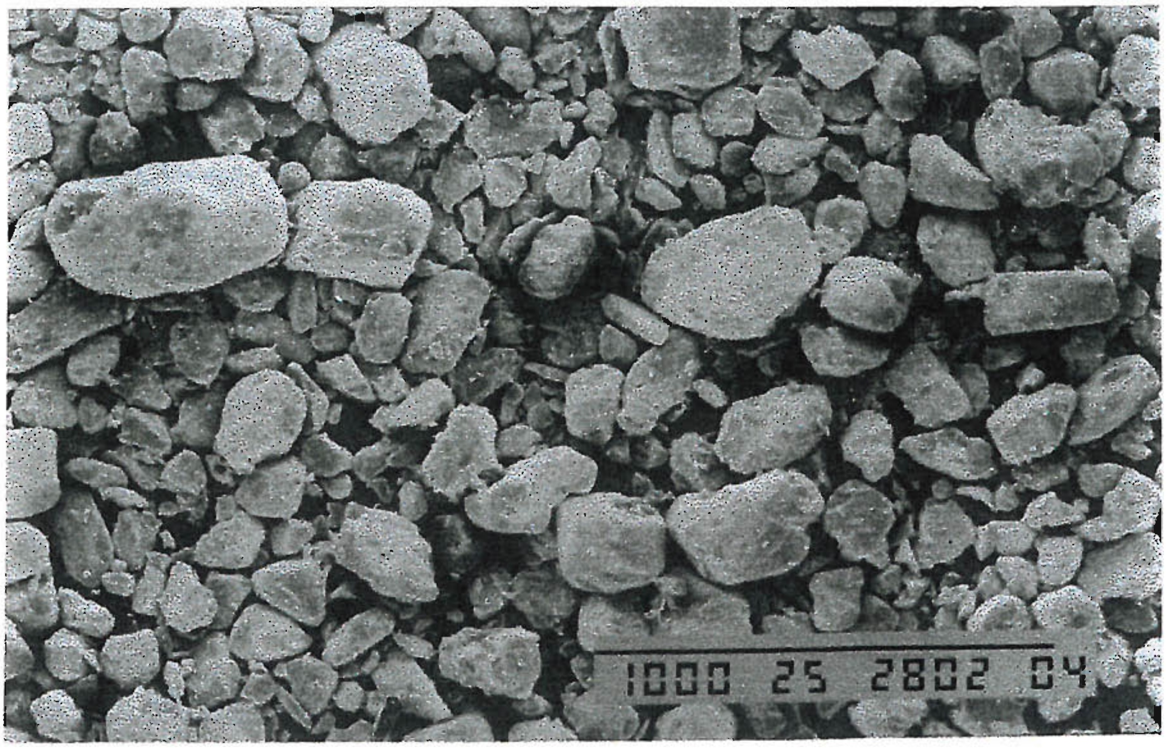

Appendix O Comparison of Numerical and Experimental Erosion Studies. Erosion Model Validation

Particle Distribution on Entry to Test Choke

Fluid - **Water/Sand Slurry**
Pipeline Diameter - **75** mm
Spool Pieces Considered and Length - **7** & **10** m
Consideration Given to Spool Joint - **Yes**
Water Flow Rate - **7.8** kg/s (**100** igpm)
Sand Loading at Entry **1.0** % by wt.
Uniform Entry Conditions and Consideration Given to Gravitational Effects

Appendix Figure 139 - Fluid Velocity Contours Along Pipeline Centre Line (m/s)

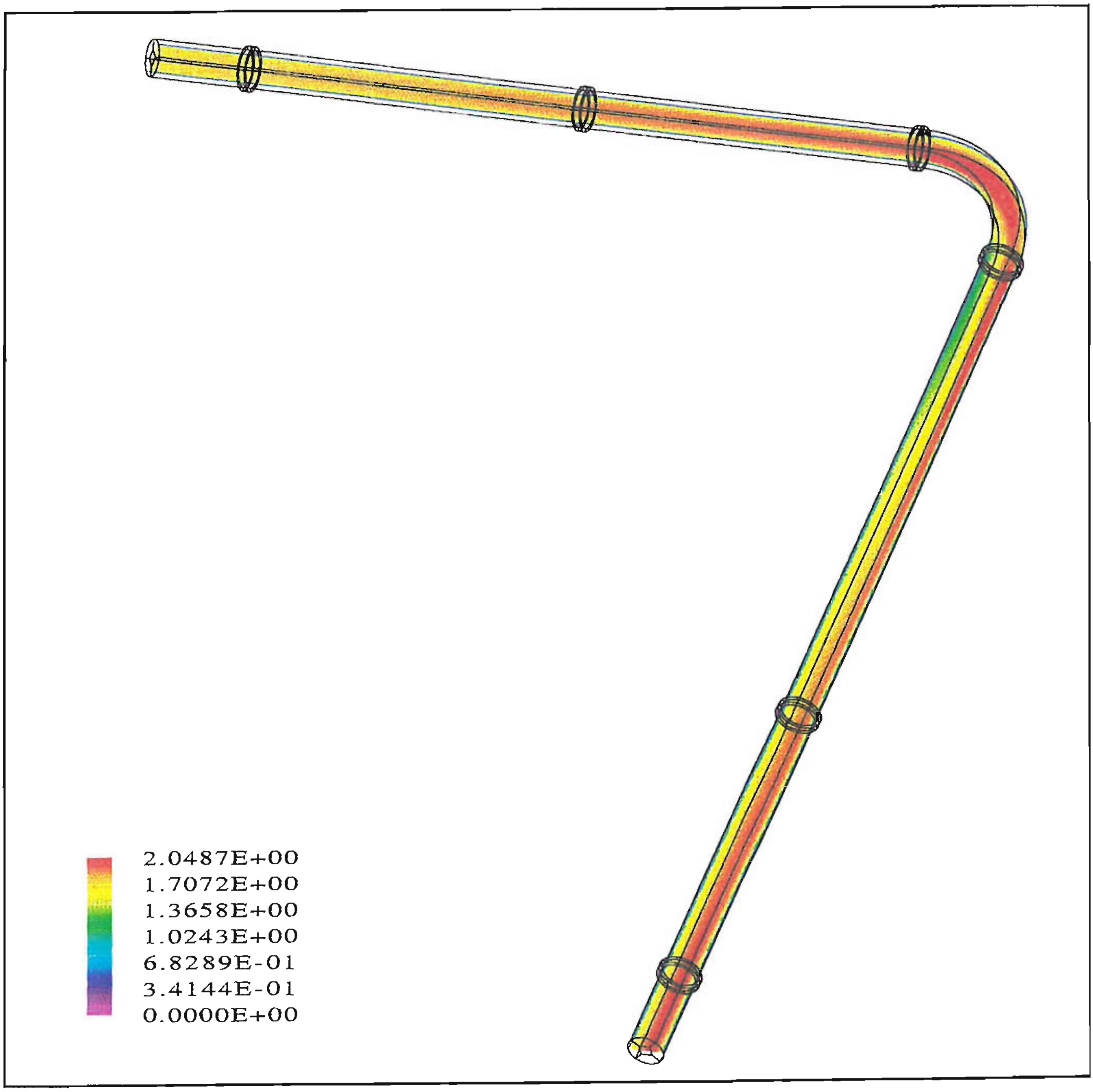

PARTICLE DISTRIBUTION ON ENTRY TO TEST CHOKE

Fluid - **Water/Sand Slurry**
Pipeline Diameter - **75** mm
Spool Pieces Considered and Length - **7** & **10** m
Consideration Given to Spool Joint - **Yes**
Water Flow Rate - **7.8** kg/s (**100** igpm)
Sand Loading at Entry **1.0** % by wt.
Uniform Entry Conditions and Consideration Given to Gravitational Effects

Appendix Figure 140 - Particle Volume Fraction[1] Along Pipeline Centre Line

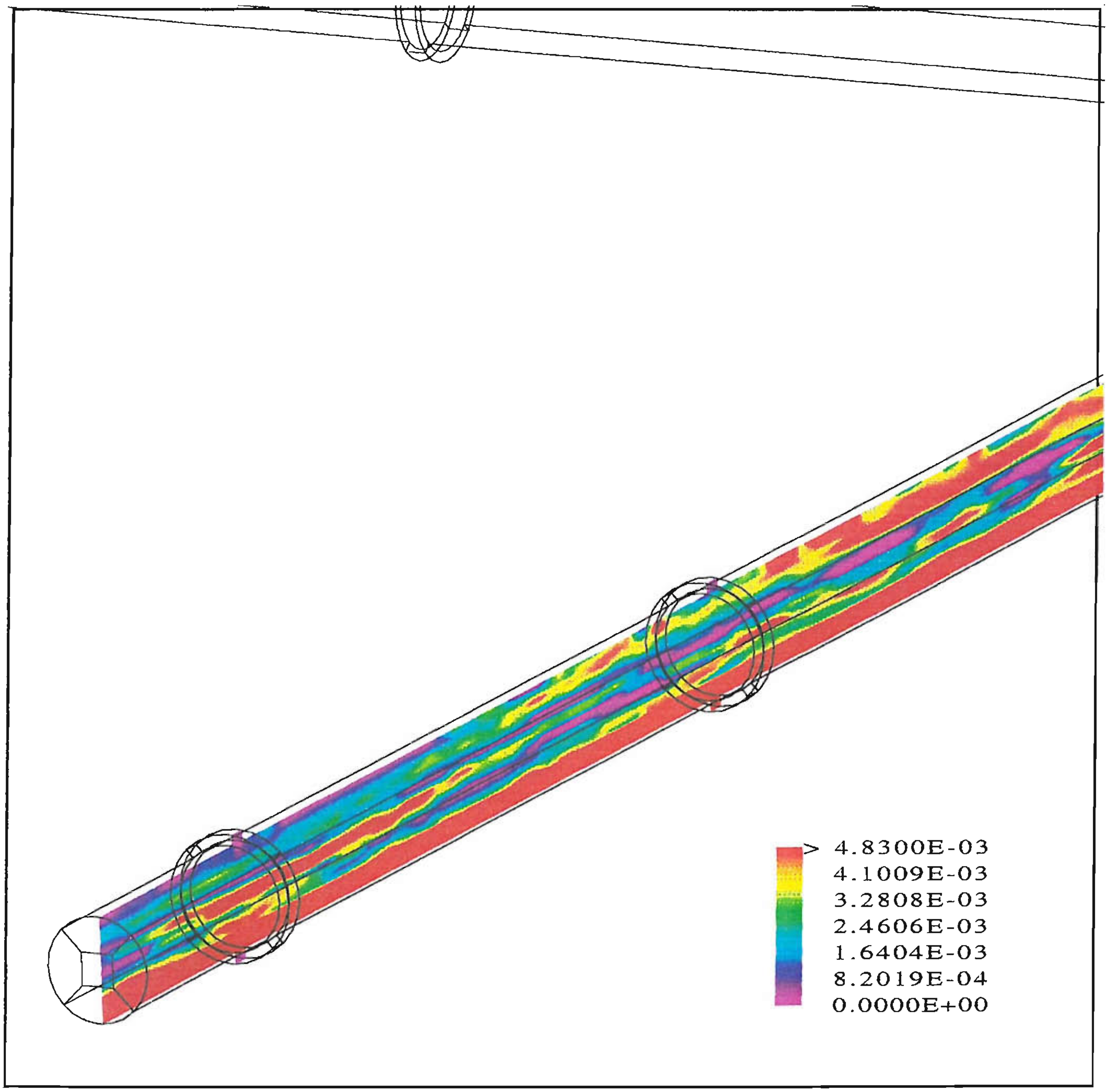

[1] Particle Volume Fraction	0	8.2e-04	1.6e-03	2.5e-03	3.3e-03	4.1e-03	4.8e-03
% by wt.	0	0.22	0.44	0.66	0.88	1.1	1.3

PARTICLE DISTRIBUTION ON ENTRY TO TEST CHOKE

Fluid - **Water/Sand Slurry**
Pipeline Diameter - **75** mm
Spool Pieces Considered and Length - **7** & **10** m
Consideration Given to Spool Joint - **Yes**
Water Flow Rate - **7.8** kg/s (**100** igpm)
Sand Loading at Entry **1.0** % by wt.
Uniform Entry Conditions and Consideration Given to Gravitational Effects

Appendix Figure 141 - Particle Volume Fraction[1] at Entry to the Test Choke

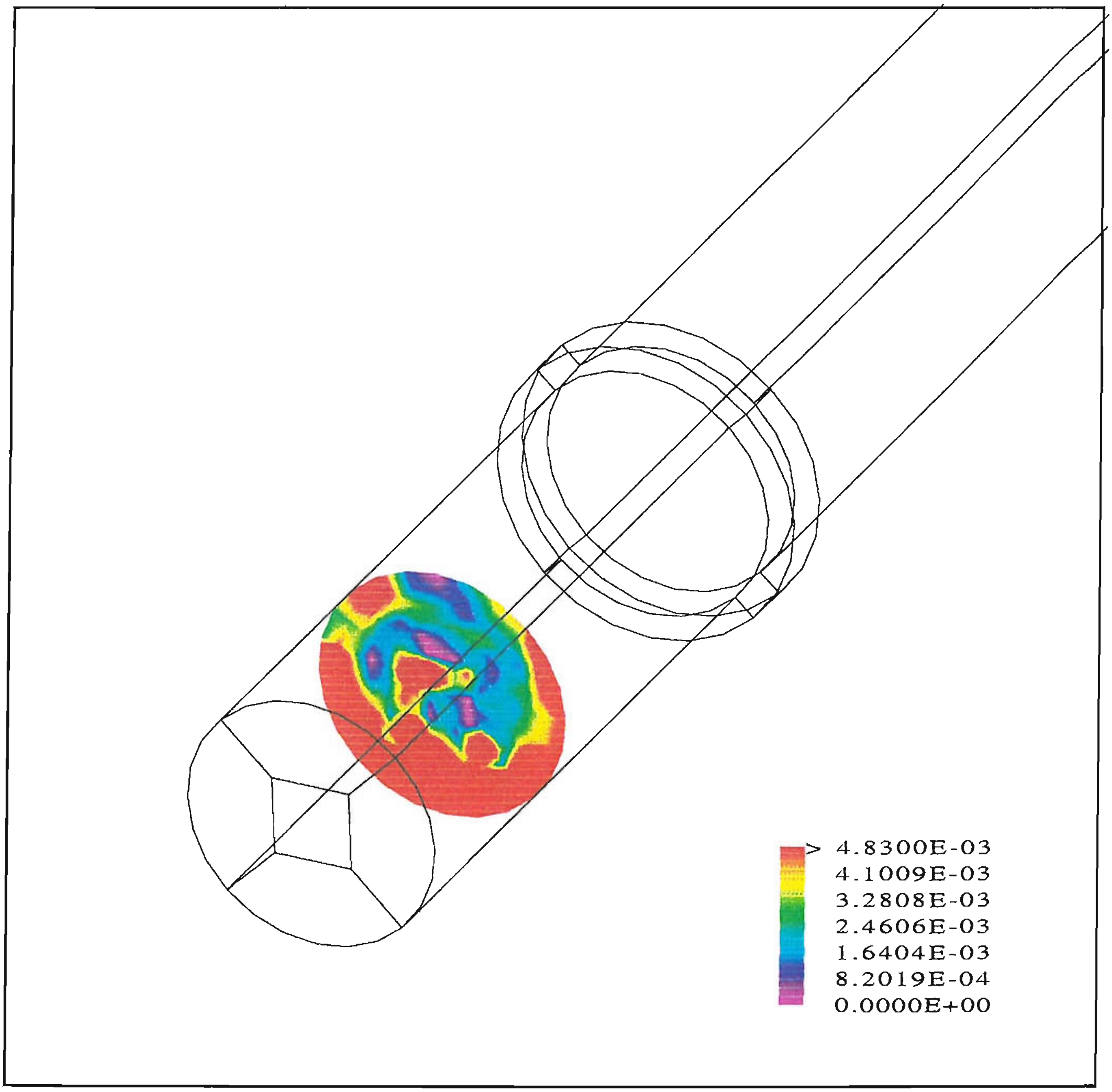

The Flow Field within the CC30 Equal Percentage Control Choke

Fluid - **Water**
Inlet Diameter - **75** mm
Choke Opening - **28**/64ths
Port Diameter & Number of Zones Exposed - **3.175** mm & **3**
Plug Edge - **Taper at 60°**
Inlet Pressure - **58** Barg
Pressure Drop - **40.2** Bar
Fluid Temperature - **57.2** °C
Volumetric Flow Rate - **7.64** kg/s

Appendix Figure 142 - CC30 Velocity Contour Plot Along Centre Line (m/s)

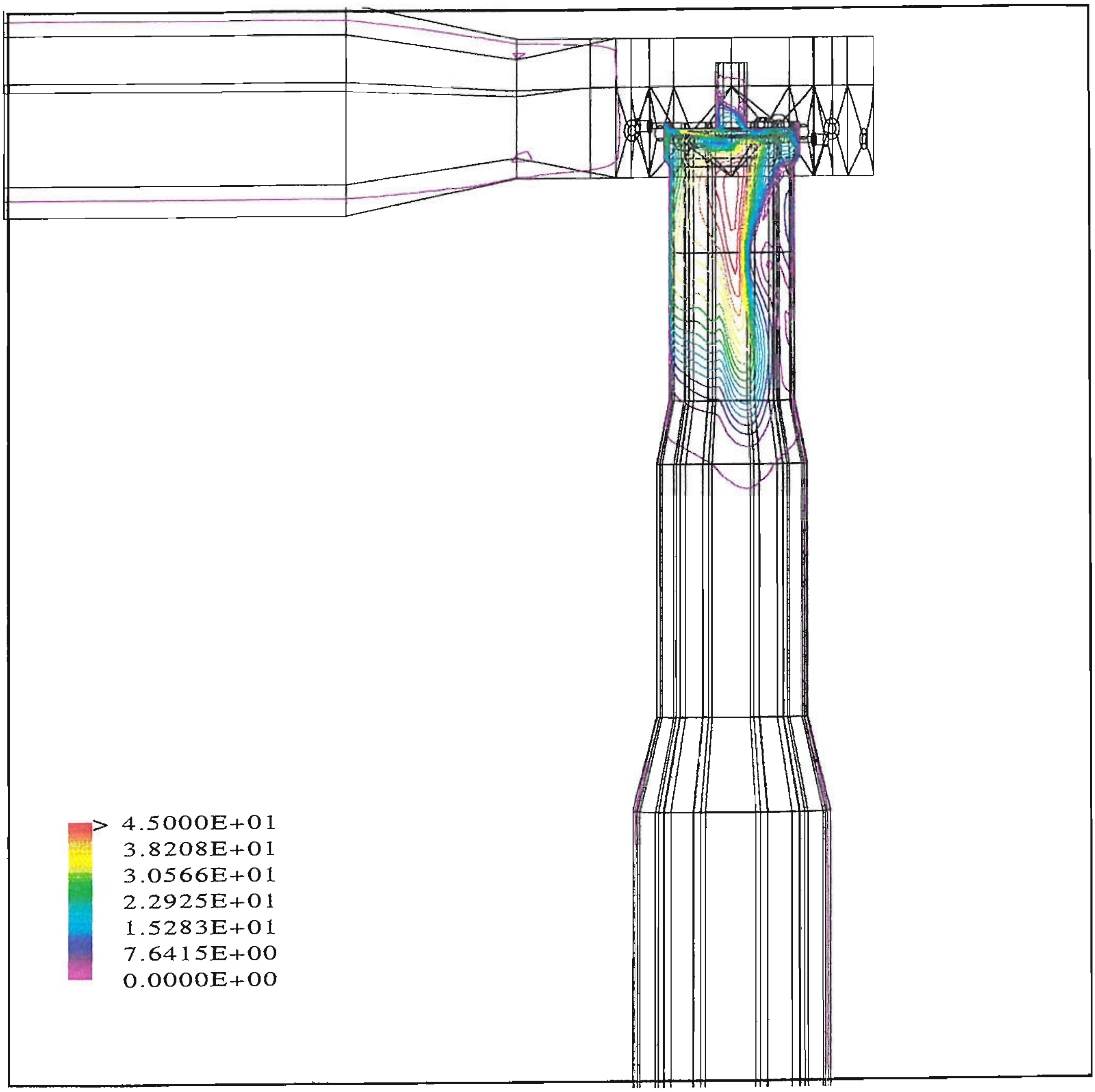

THE FLOW FIELD WITHIN THE CC30 EQUAL PERCENTAGE CONTROL CHOKE

Fluid - **Water**
Inlet Diameter - **75** mm
Choke Opening - **28**/64ths
Port Diameter & Number of Zones Exposed - **3.175** mm & **3**
Plug Edge - **Taper at 60°**
Inlet Pressure - **58** Barg
Pressure Drop - **40.2** Bar
Fluid Temperature - **57.2** °C
Volumetric Flow Rate - **7.64** kg/s

Appendix Figure 143 - CC30 Velocity Contour Plot Along Centre Line (m/s)

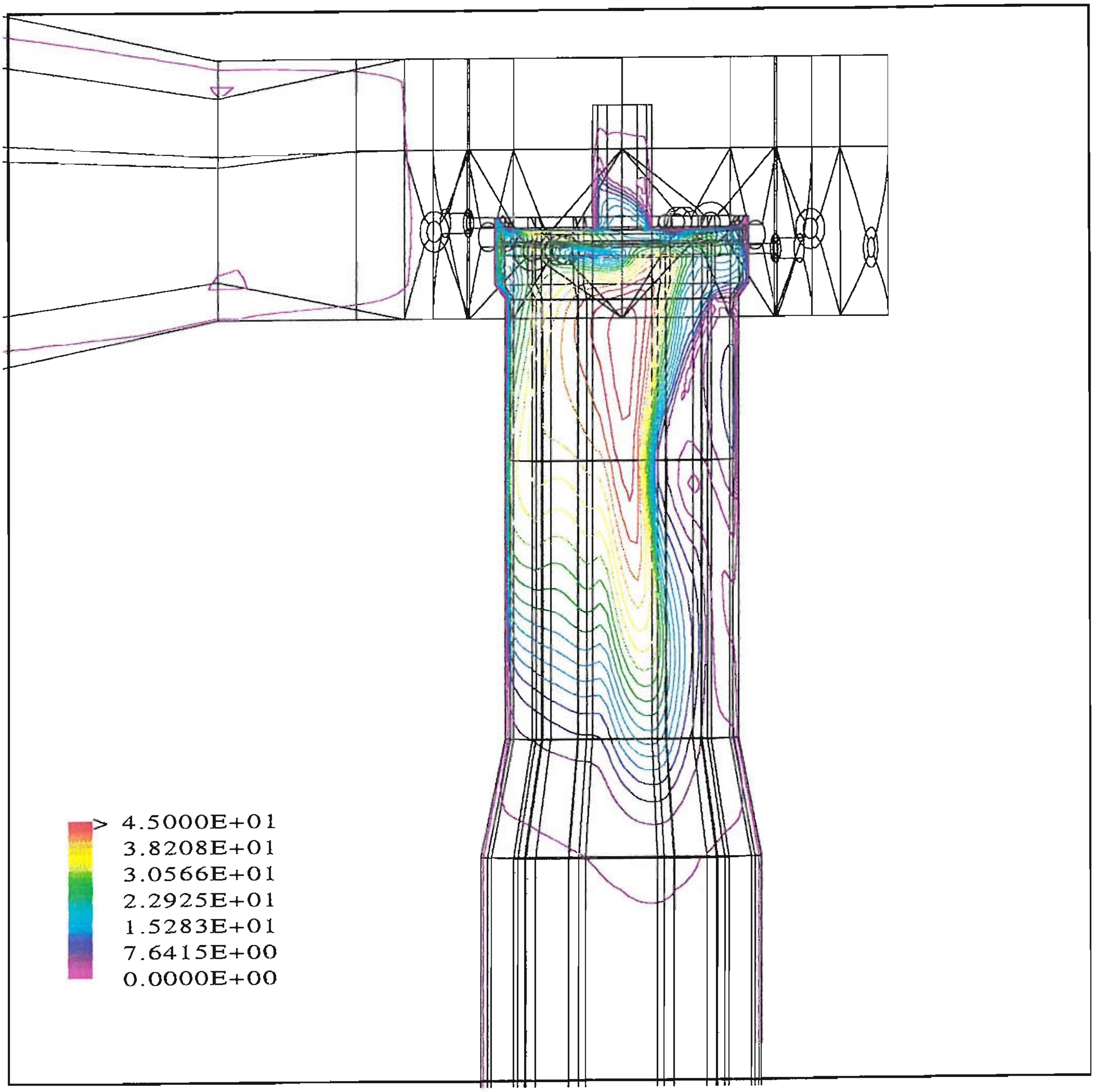

THE FLOW FIELD WITHIN THE CC30 EQUAL PERCENTAGE CONTROL CHOKE

Fluid - **Water**
Inlet Diameter - **75** mm
Choke Opening - **28**/64ths
Port Diameter & Number of Zones Exposed - **3.175** mm & **3**
Plug Edge - **Taper at 60°**
Inlet Pressure - **58** Barg
Pressure Drop - **40.2** Bar
Fluid Temperature - **57.2** °C
Volumetric Flow Rate - **7.64** kg/s

Appendix Figure 144 - CC30 Velocity Contour Plot Along Centre Line (m/s)

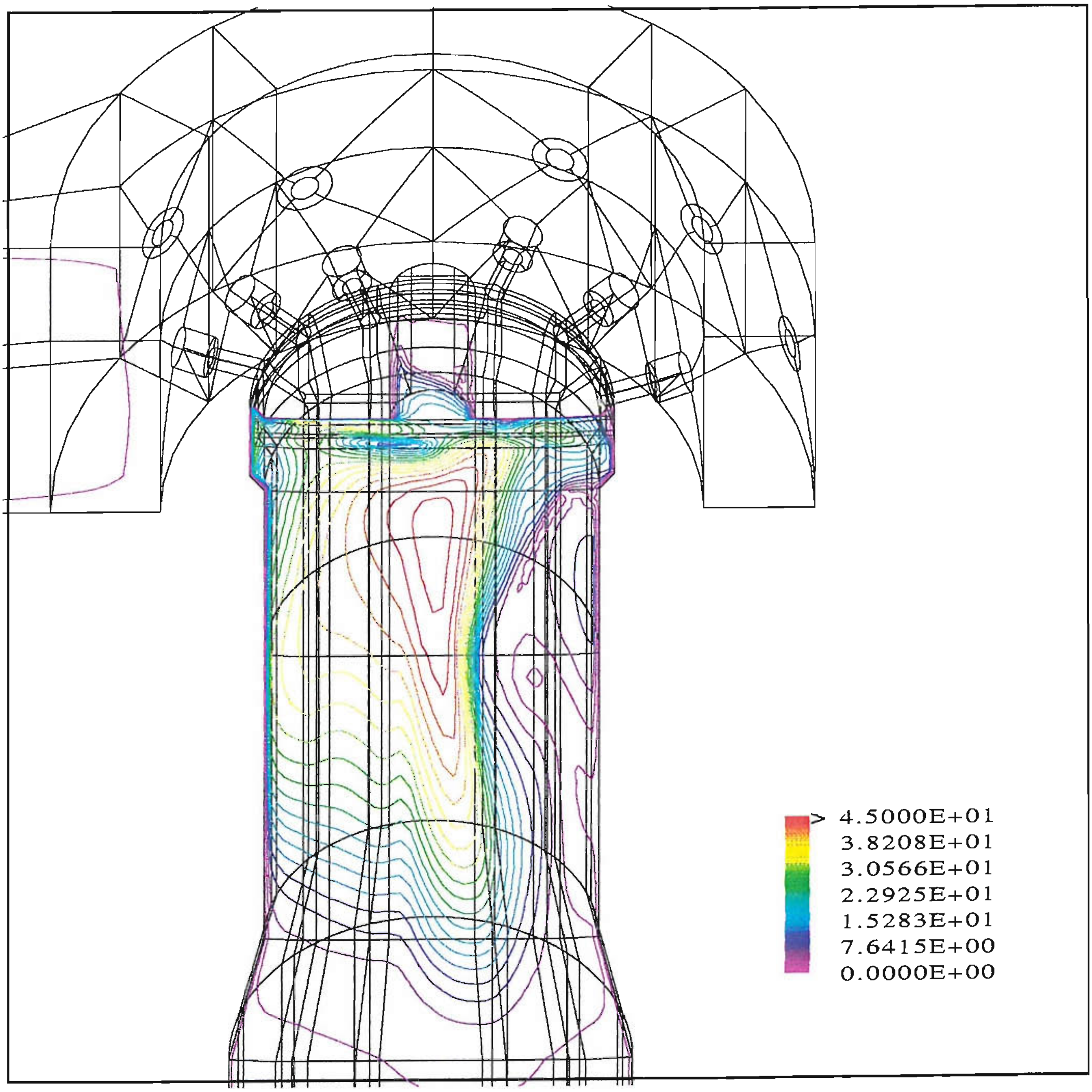

THE FLOW FIELD WITHIN THE CC30 EQUAL PERCENTAGE CONTROL CHOKE

Fluid - **Water**
Inlet Diameter - **75** mm
Choke Opening - **28**/64ths
Port Diameter & Number of Zones Exposed - **3.175** mm & **3**
Plug Edge - **Taper at 60°**
Inlet Pressure - **58** Barg
Pressure Drop - **40.2** Bar
Fluid Temperature - **57.2** °C
Volumetric Flow Rate - **7.64** kg/s

Appendix Figure 145 - CC30 Velocity Vector Plot Along Centre Line (m/s)

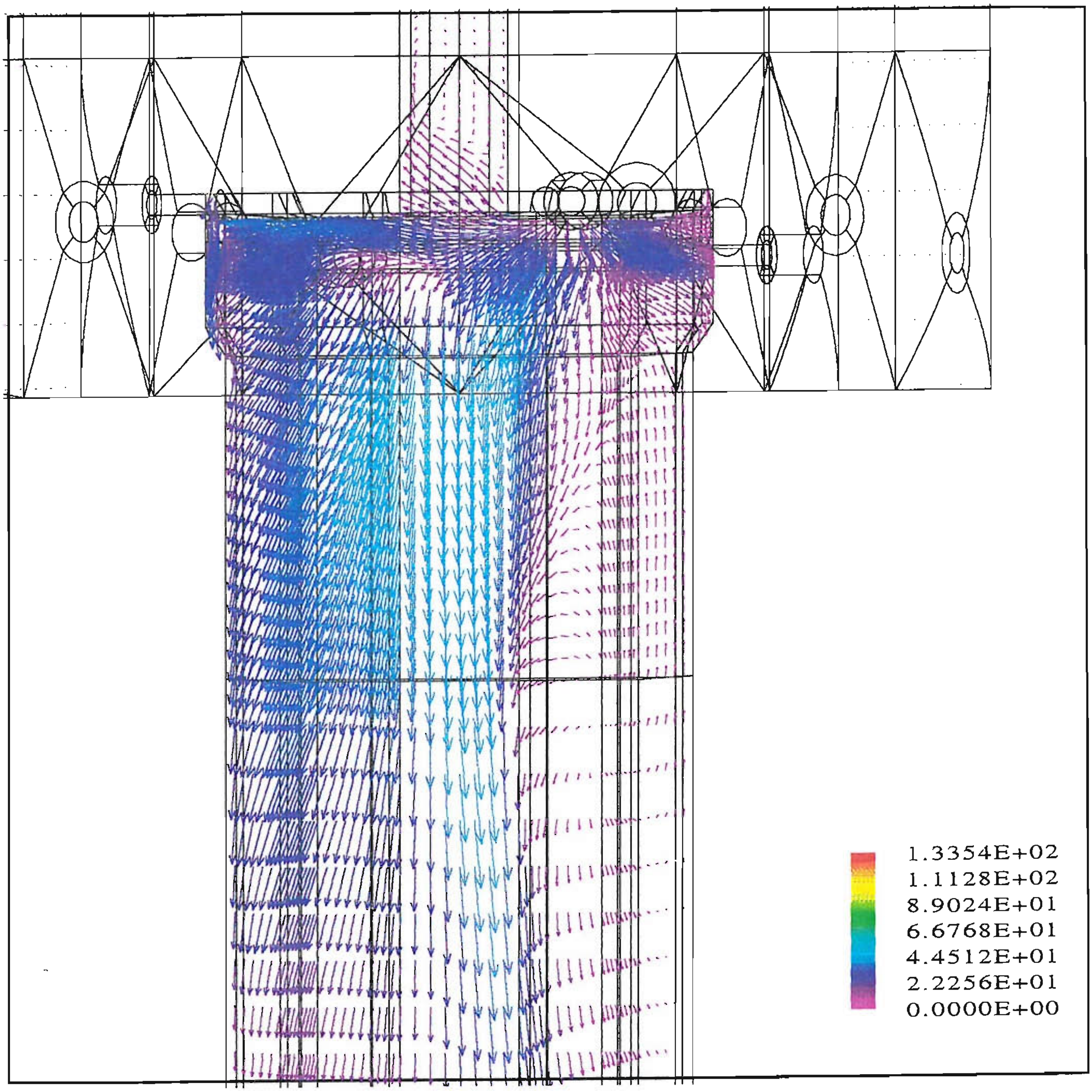

The Flow Field within the CC30 Equal Percentage Control Choke

Fluid - **Water**
Inlet Diameter - **75** mm
Choke Opening - **28**/64ths
Port Diameter & Number of Zones Exposed - **3.175** mm & **3**
Plug Edge - **Taper at 60°**
Inlet Pressure - **58** Barg
Pressure Drop - **40.2** Bar
Fluid Temperature - **57.2** °C
Volumetric Flow Rate - **7.64** kg/s

Appendix Figure 146 - CC30 Velocity Vector Plot at +5 mm from the Centre Line (m/s)

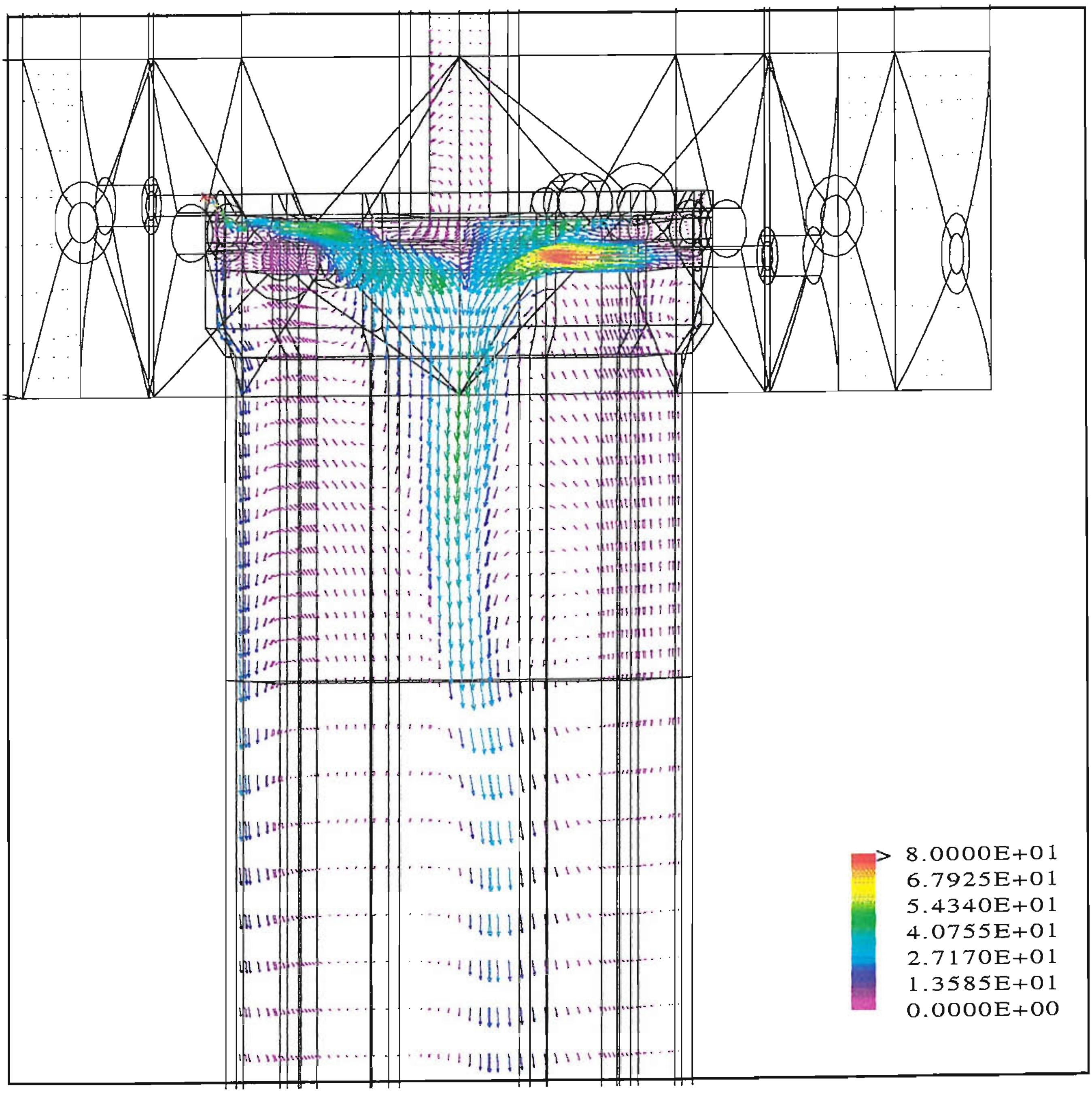

THE FLOW FIELD WITHIN THE CC30 EQUAL PERCENTAGE CONTROL CHOKE

Fluid - **Water**
Inlet Diameter - **75** mm
Choke Opening - **28**/64ths
Port Diameter & Number of Zones Exposed - **3.175** mm & **3**
Plug Edge - **Taper at 60°**
Inlet Pressure - **58** Barg
Pressure Drop - **40.2** Bar
Fluid Temperature - **57.2** °C
Volumetric Flow Rate - **7.64** kg/s

Appendix Figure 147 - CC30 Velocity Vector Plot at +10 mm from the Centre Line (m/s)

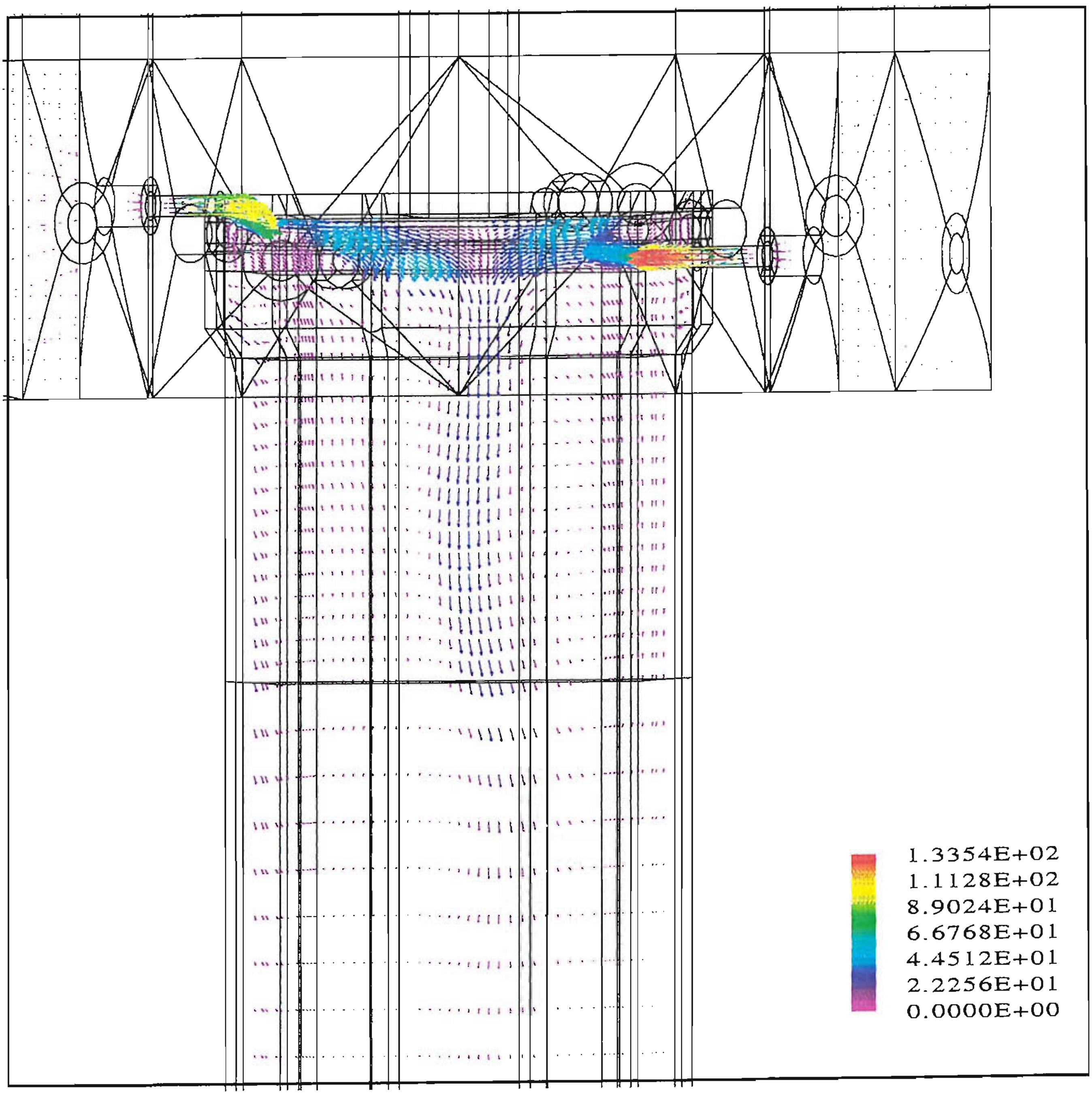

THE FLOW FIELD WITHIN THE CC30 EQUAL PERCENTAGE CONTROL CHOKE

Fluid - **Water**
Inlet Diameter - **75** mm
Choke Opening - **28/64**ths
Port Diameter & Number of Zones Exposed - **3.175** mm & **3**
Plug Edge - **Taper at 60°**
Inlet Pressure - **58** Barg
Pressure Drop - **40.2** Bar
Fluid Temperature - **57.2** °C
Volumetric Flow Rate - **7.64** kg/s

Appendix Figure 148 - CC30 Velocity Vector Plot at +15 mm from the Centre Line (m/s)

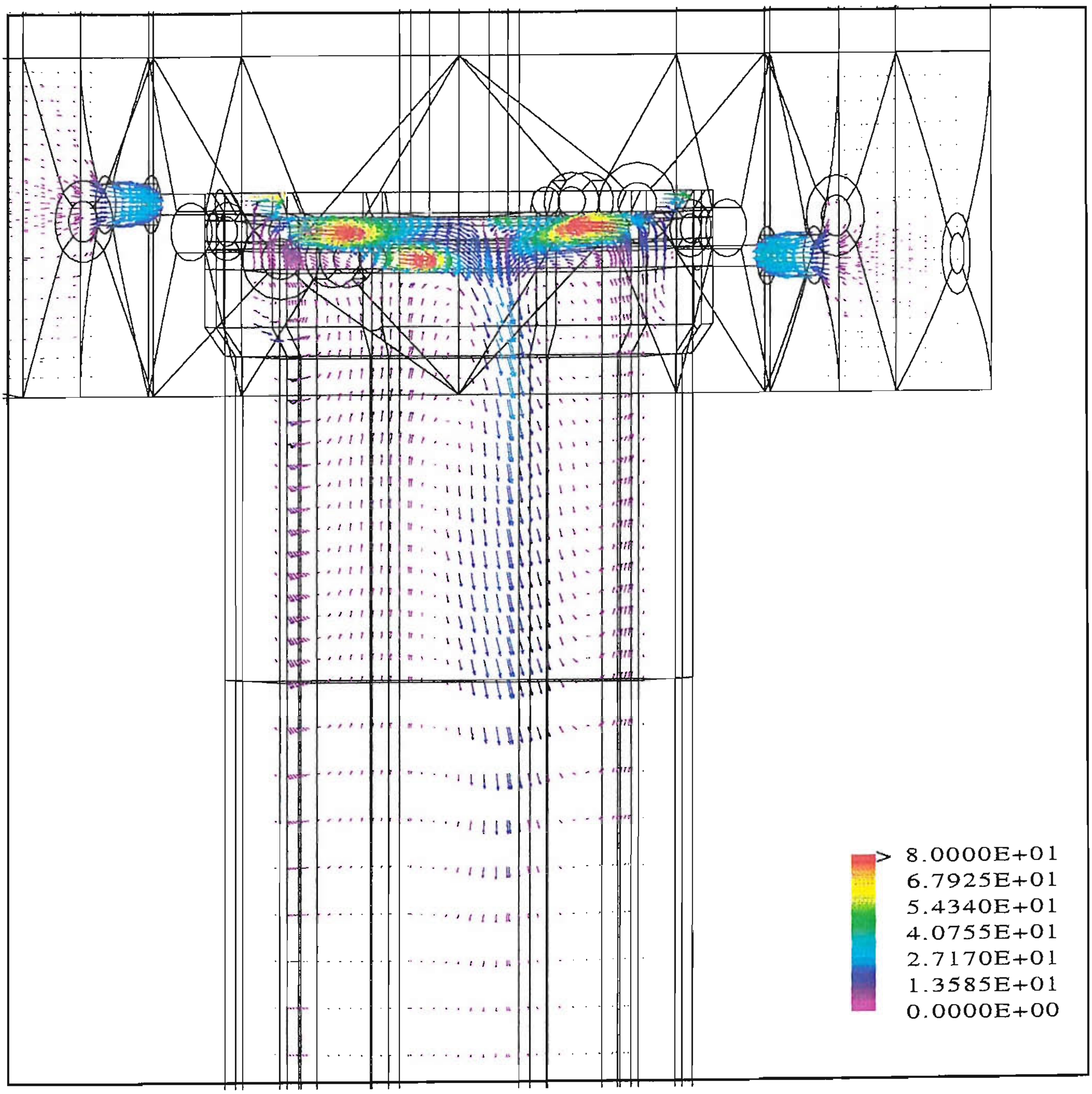

THE FLOW FIELD WITHIN THE CC30 EQUAL PERCENTAGE CONTROL CHOKE

Fluid - **Water**
Inlet Diameter - **75** mm
Choke Opening - **28**/64ths
Port Diameter & Number of Zones Exposed - **3.175** mm & **3**
Plug Edge - **Taper at 60°**
Inlet Pressure - **58** Barg
Pressure Drop - **40.2** Bar
Fluid Temperature - **57.2** °C
Volumetric Flow Rate - **7.64** kg/s

Appendix Figure 149 - CC30 Velocity Vector Plot at Exit from the Flow Cage (m/s)

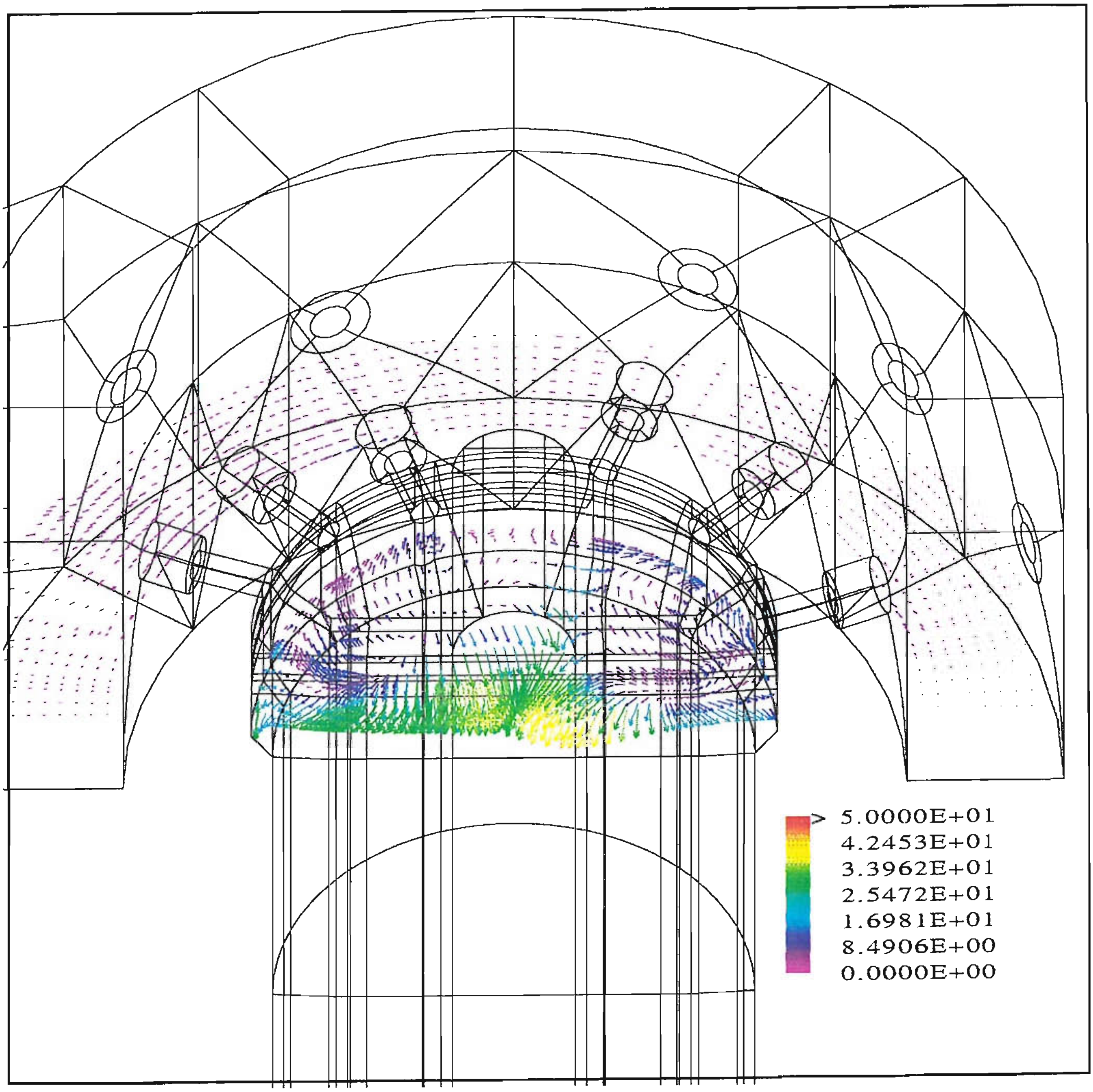

THE FLOW FIELD WITHIN THE CC30 EQUAL PERCENTAGE CONTROL CHOKE

Fluid - **Water**
Inlet Diameter - **75** mm
Choke Opening - **28**/64ths
Port Diameter & Number of Zones Exposed - **3.175** mm & **3**
Plug Edge - **Taper at 60°**
Inlet Pressure - **58** Barg
Pressure Drop - **40.2** Bar
Fluid Temperature - **57.2** °C
Volumetric Flow Rate - **7.64** kg/s

Appendix Figure 150 - CC30 Velocity Vector Plot at Zone 1 within the Flow Cage (m/s)

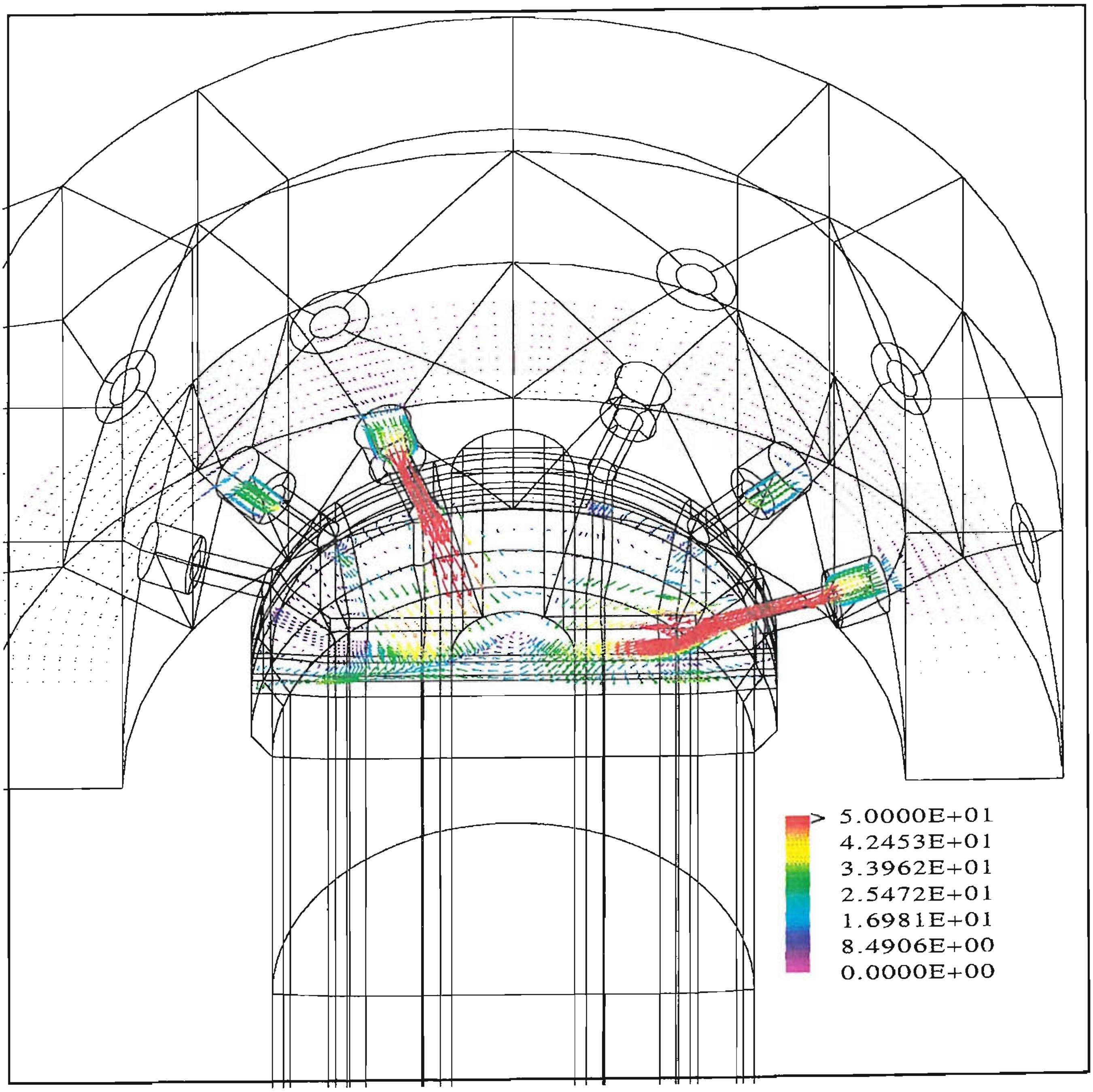

THE FLOW FIELD WITHIN THE CC30 EQUAL PERCENTAGE CONTROL CHOKE

Fluid - **Water**
Inlet Diameter - **75** mm
Choke Opening - **28**/64ths
Port Diameter & Number of Zones Exposed - **3.175** mm & **3**
Plug Edge - **Taper at 60°**
Inlet Pressure - **58** Barg
Pressure Drop - **40.2** Bar
Fluid Temperature - **57.2** °C
Volumetric Flow Rate - **7.64** kg/s

Appendix Figure 151 - CC30 Velocity Vector Plot at Zone 2 within the Flow Cage (m/s)

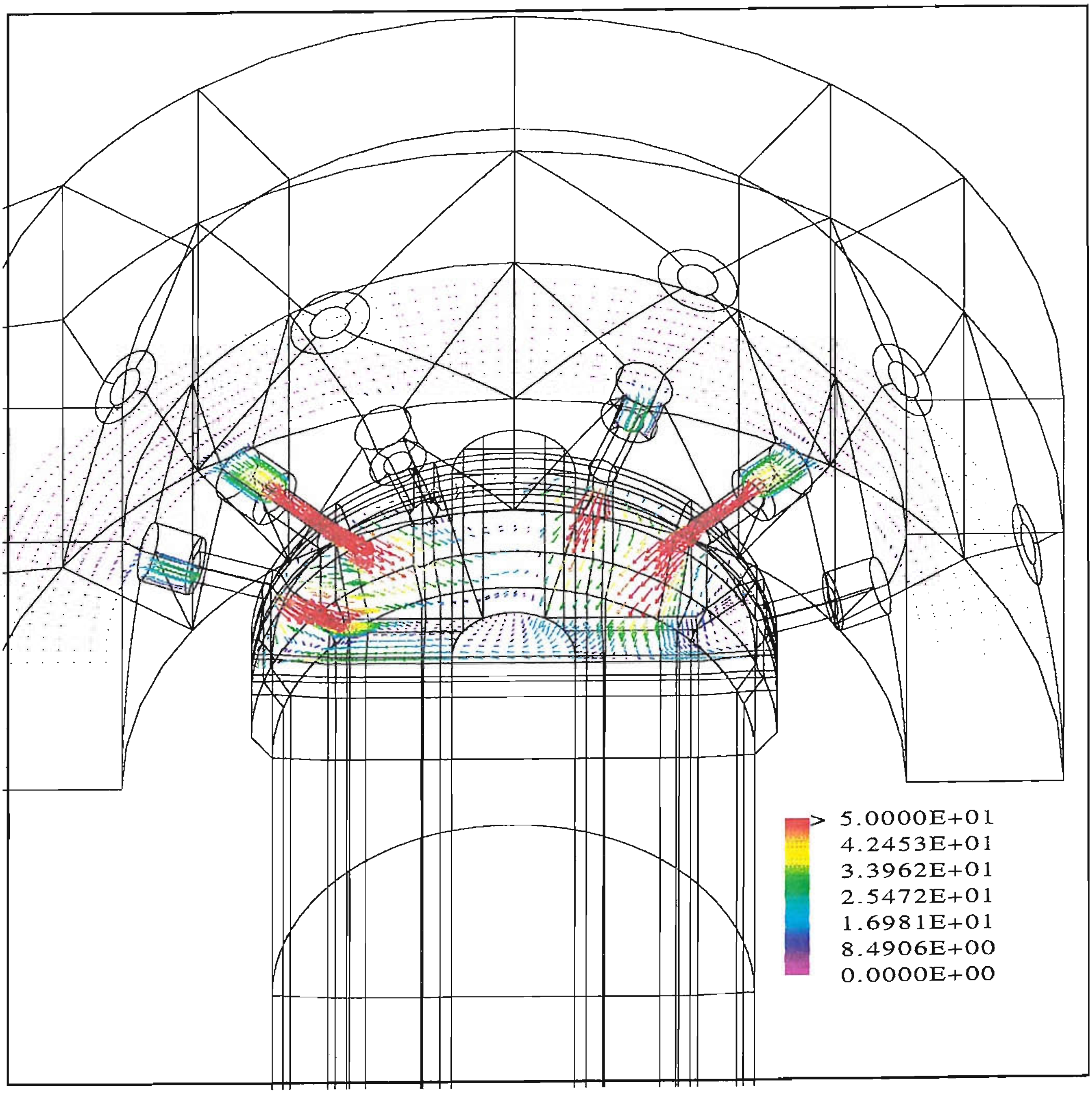

THE FLOW FIELD WITHIN THE CC30 EQUAL PERCENTAGE CONTROL CHOKE

Fluid - **Water**
Inlet Diameter - **75** mm
Choke Opening - **28**/64ths
Port Diameter & Number of Zones Exposed - **3.175** mm & **3**
Plug Edge - **Taper at 60°**
Inlet Pressure - **58** Barg
Pressure Drop - **40.2** Bar
Fluid Temperature - **57.2** °C
Volumetric Flow Rate - **7.64** kg/s

Appendix Figure 152 - CC30 Velocity Vector Plot at Zone 3 within the Flow Cage (m/s)

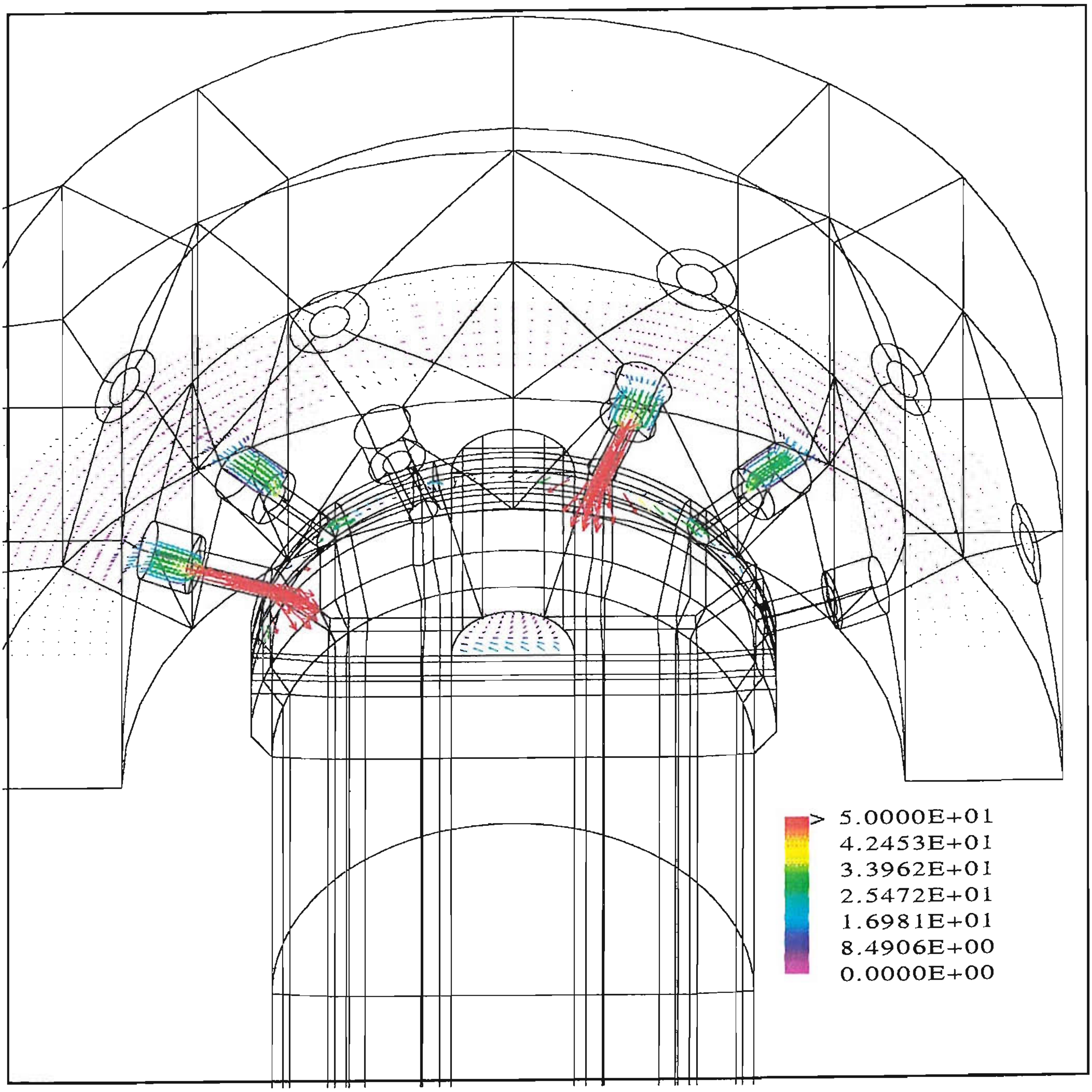

THE FLOW FIELD WITHIN THE CC30 EQUAL PERCENTAGE CONTROL CHOKE

Fluid - **Water**
Inlet Diameter - **75** mm
Choke Opening - **28**/64ths
Port Diameter & Number of Zones Exposed - **3.175** mm & **3**
Plug Edge - **Taper at 60°**
Inlet Pressure - **58** Barg
Pressure Drop - **40.2** Bar
Fluid Temperature - **57.2** °C
Volumetric Flow Rate - **7.64** kg/s

Appendix Figure 153 - CC30 Turbulent Kinetic Energy within the Flow Cage

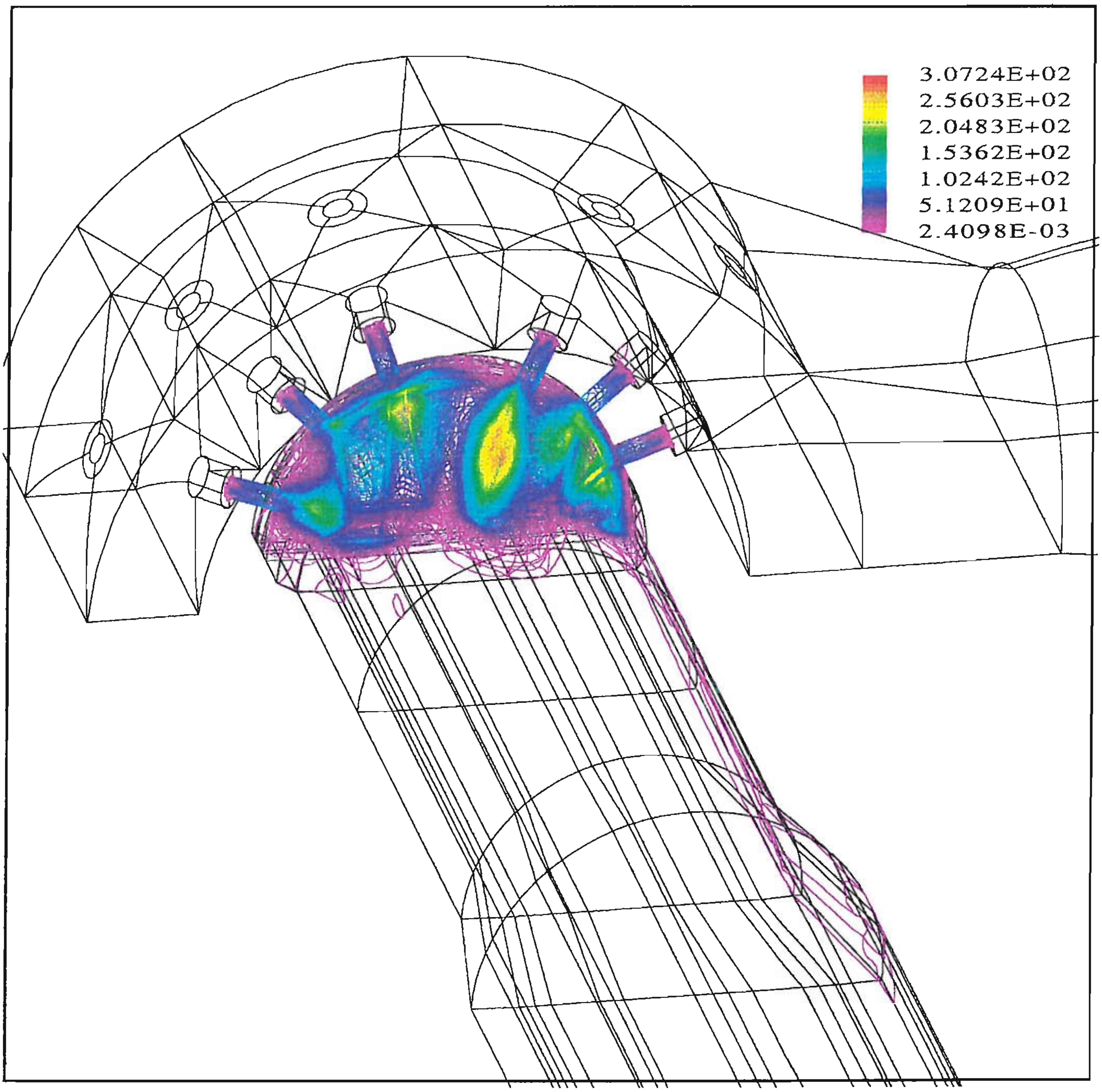

Particle Trajectories within the Tungsten Carbide CC30 Control Choke

Particle Type - **Sand**
Particle Loading and Flux Rate - **1.16** % by wt & **88.7** g/s.
Particle Roundness Factor - **0.5**
Number of Particle Sizes and Total Number of Particles Tracked - **20** & **1440**
Particle Size Range - **20-385** μm
Turbulent Dispersion - **Yes**
Modified Coefficient of Restitution - **Yes**
Squeeze Film Retardation - **Yes**
Gravity Vector Set - **Yes**

Appendix Figure 154 - Particle Trajectories and Trajectory Velocities within the CC30 (m/s)

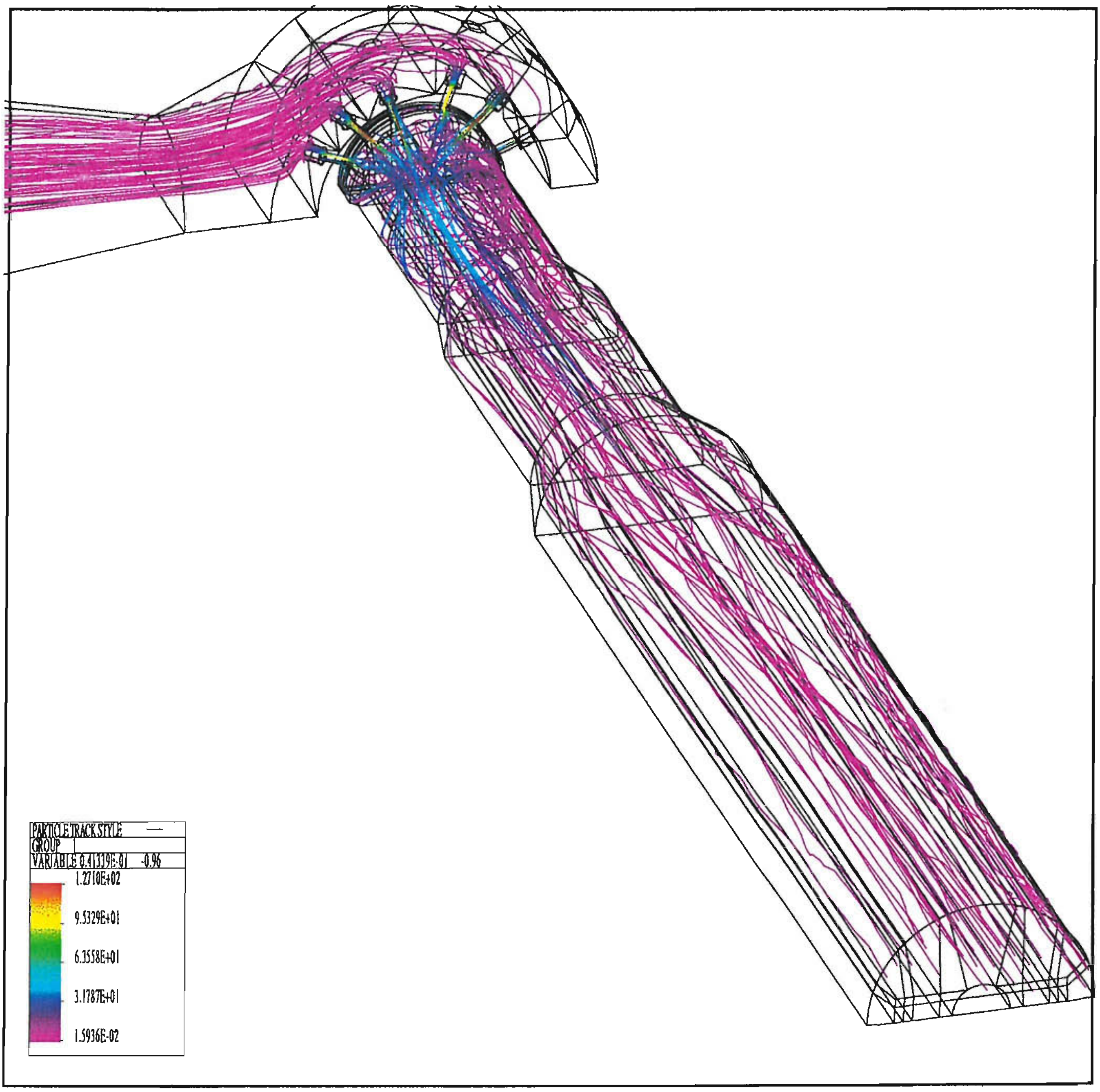

PARTICLE TRAJECTORIES WITHIN THE TUNGSTEN CARBIDE CC30 CONTROL CHOKE

Particle Type - **Sand**
Particle Loading and Flux Rate - **1.16** % by wt & **88.7** g/s.
Particle Roundness Factor - **0.5**
Number of Particle Sizes and Total Number of Particles Tracked - **20** & **1440**
Particle Size Range - **20-385** μm
Turbulent Dispersion - **Yes**
Modified Coefficient of Restitution - **Yes**
Squeeze Film Retardation - **Yes**
Gravity Vector Set - **Yes**

Appendix Figure 155 - Particle Trajectories and Trajectory Velocities within the CC30 (m/s)

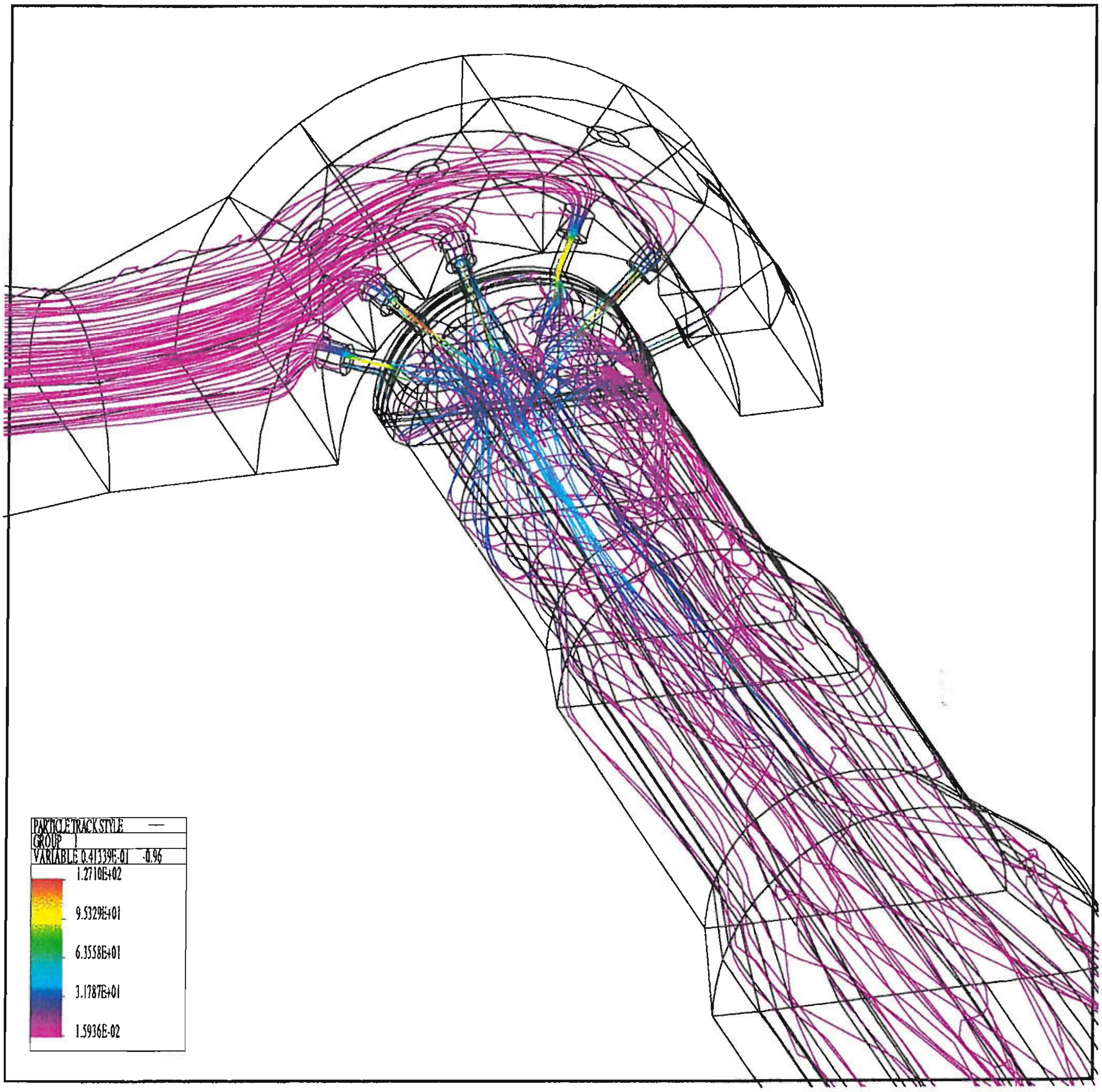

PARTICLE TRAJECTORIES WITHIN THE TUNGSTEN CARBIDE CC30 CONTROL CHOKE

Particle Type - **Sand**
Particle Loading and Flux Rate - **1.16** % by wt & **88.7** g/s.
Particle Roundness Factor - **0.5**
Number of Particle Sizes and Total Number of Particles Tracked - **20** & **1440**
Particle Size Range - **20-385** μm
Turbulent Dispersion - **Yes**
Modified Coefficient of Restitution - **Yes**
Squeeze Film Retardation - **Yes**
Gravity Vector Set - **Yes**

Appendix Figure 156 - Particle Trajectories and Trajectory Velocities within the CC30 (m/s)

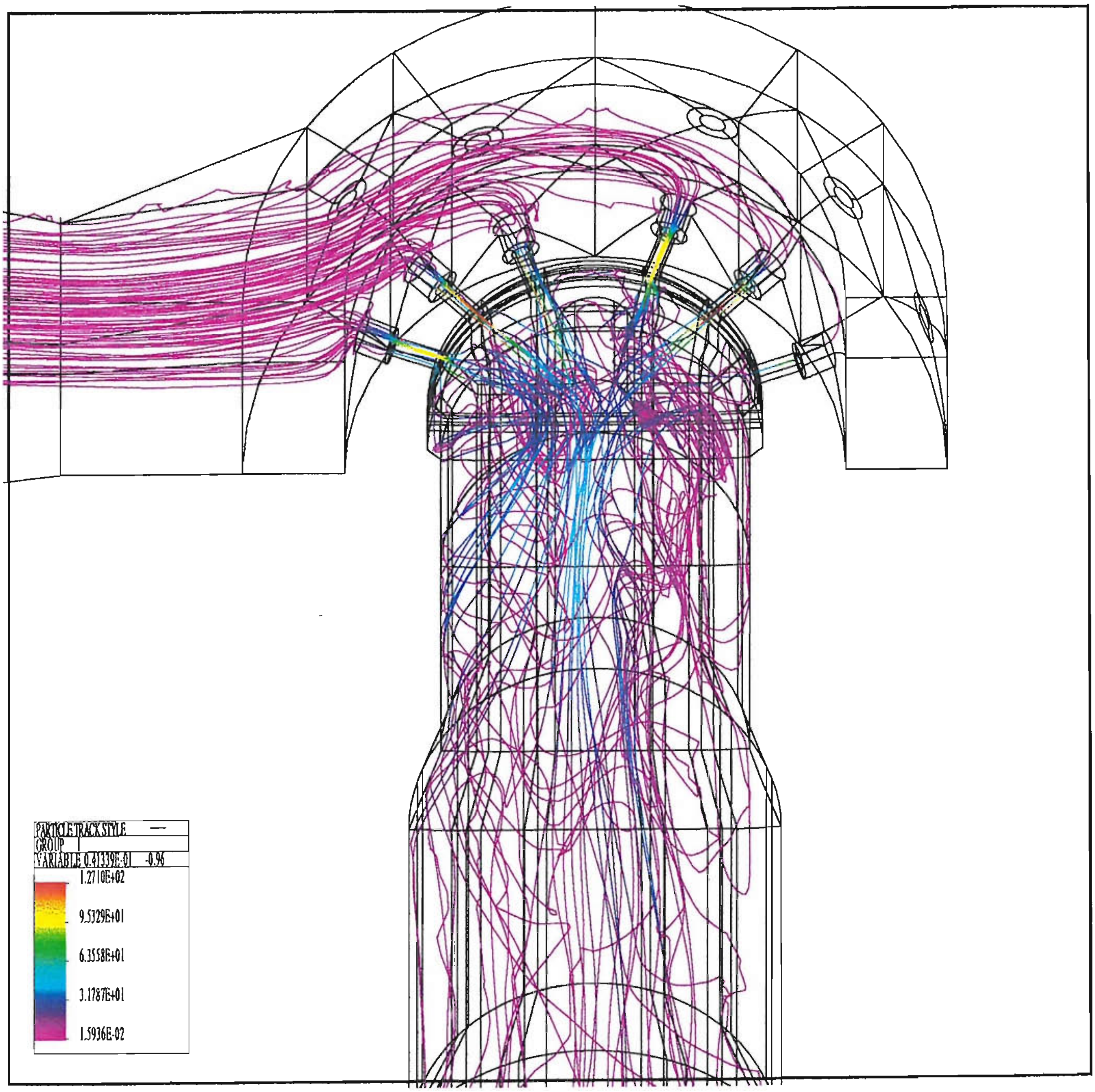

PARTICLE TRAJECTORIES WITHIN THE TUNGSTEN CARBIDE CC30 CONTROL CHOKE

Particle Type - **Sand**
Particle Loading and Flux Rate - **1.16** % by wt & **88.7** g/s.
Particle Roundness Factor - **0.5**
Number of Particle Sizes and Total Number of Particles Tracked - **20** & **1440**
Particle Size Range - **20-385** μm
Turbulent Dispersion - **Yes**
Modified Coefficient of Restitution - **Yes**
Squeeze Film Retardation - **Yes**
Gravity Vector Set - **Yes**

Appendix Figure 157 - Exemplary Particle Trajectories and Velocities within the CC30 (m/s)

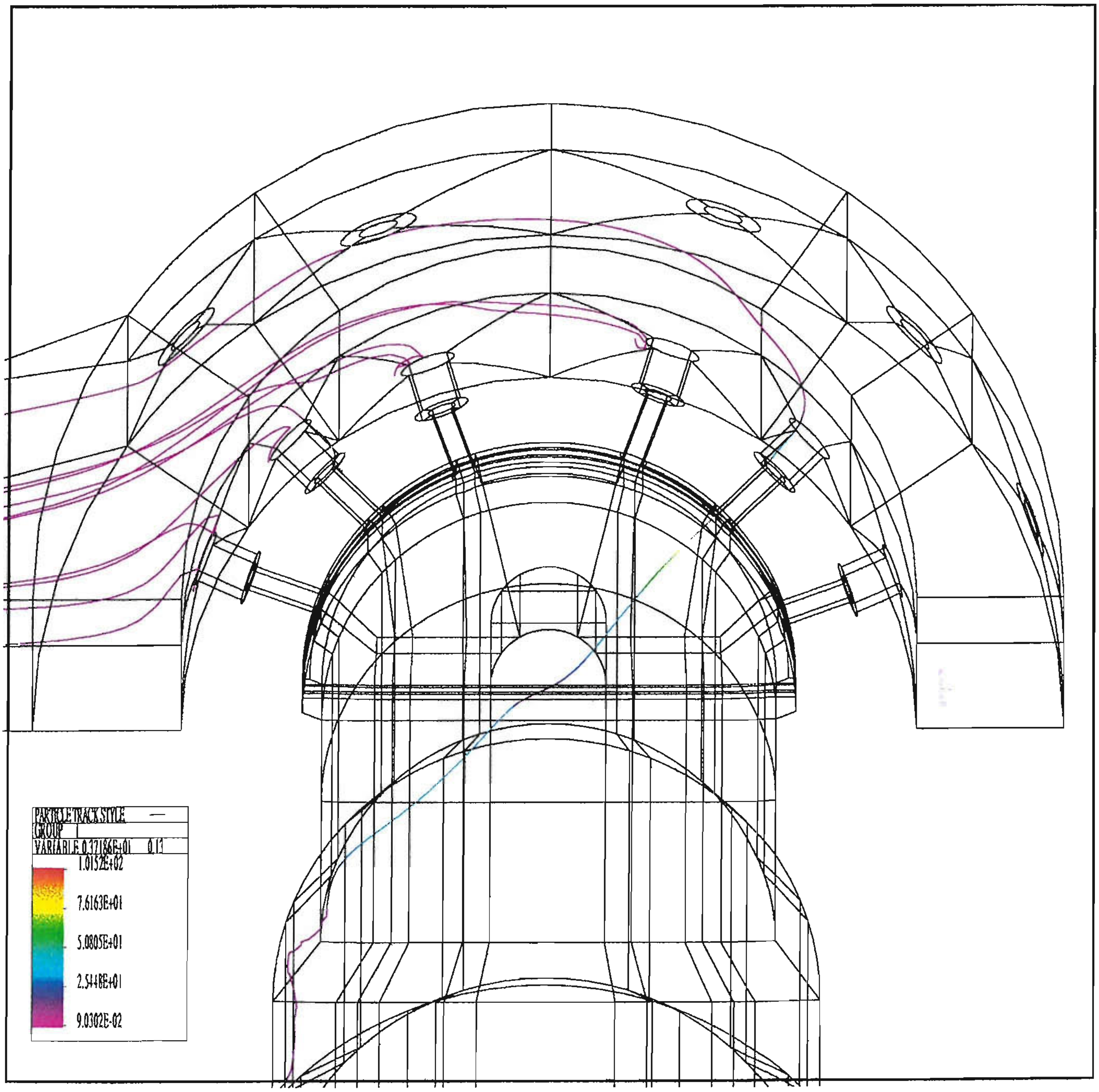

PARTICLE TRAJECTORIES WITHIN THE TUNGSTEN CARBIDE CC30 CONTROL CHOKE

Particle Type - **Sand**
Particle Loading and Flux Rate - **1.16** % by wt & **88.7** g/s.
Particle Roundness Factor - **0.5**
Number of Particle Sizes and Total Number of Particles Tracked - **20** & **1440**
Particle Size Range - **20-385** μm
Turbulent Dispersion - **Yes**
Modified Coefficient of Restitution - **Yes**
Squeeze Film Retardation - **Yes**
Gravity Vector Set - **Yes**

Appendix Figure 158 - Particle Trajectories and Particle Size within the CC30 (μm)

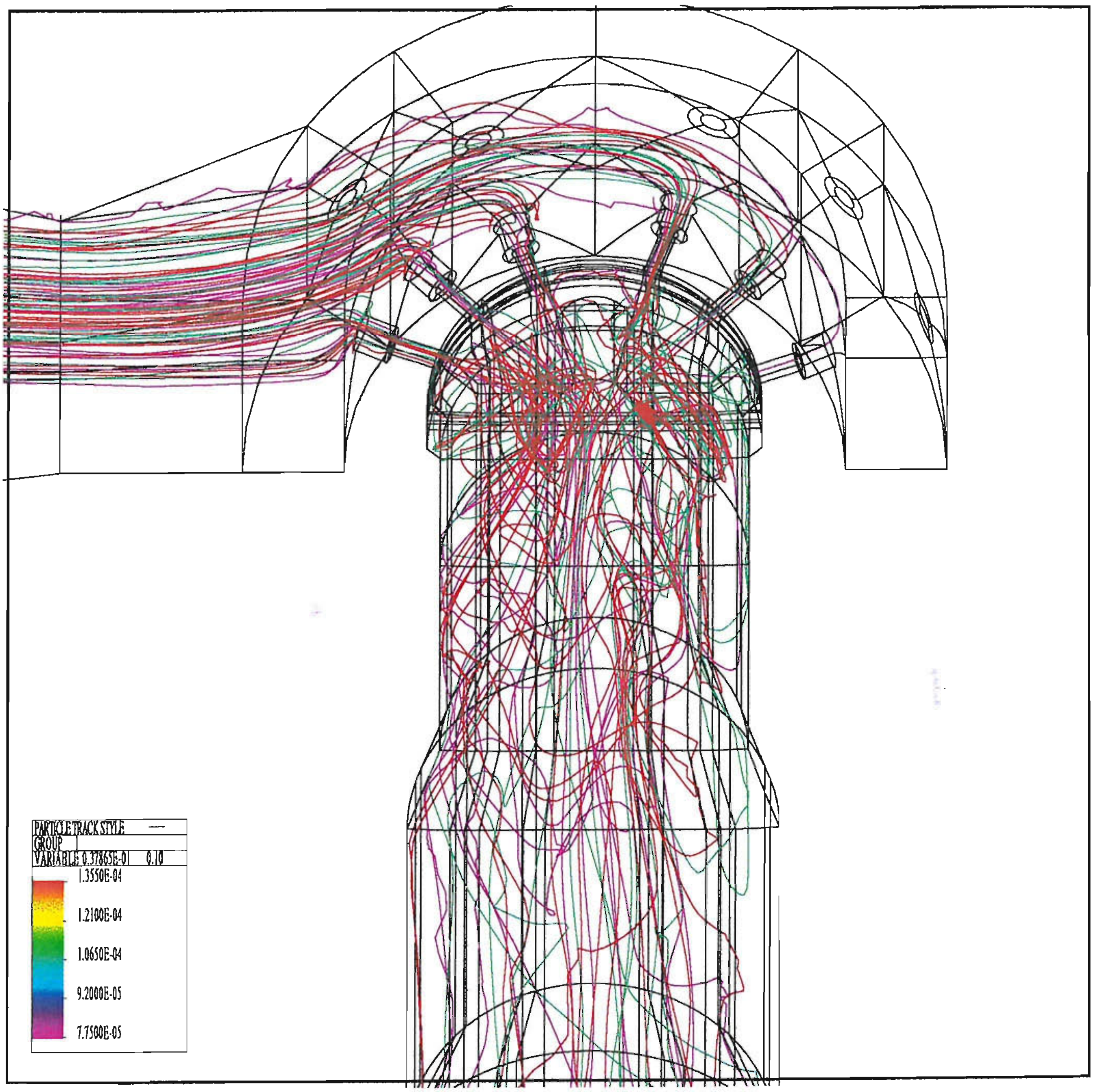

Erosion Characteristics of the Tungsten Carbide CC30 Control Choke

Particle Type - **Sand**
Particle Loading and Flux Rate - **1.16** % by wt & **88.7** g/s.
Particle Roundness Factor - **0.5**
Number of Particle Sizes and Total Number of Particles Tracked - **8** & **576**
Particle Size Range - **212-385** μm
Turbulent Dispersion - **Yes**
Modified Coefficient of Restitution - **Yes**
Squeeze Film Retardation - **Yes**
Gravity Vector Set - **Yes**

Simulation Section - **CC30 Top**

Appendix Figure 159 - WC CC30 Particle Impact Velocity after 2 Calculation Sequences (m/s)

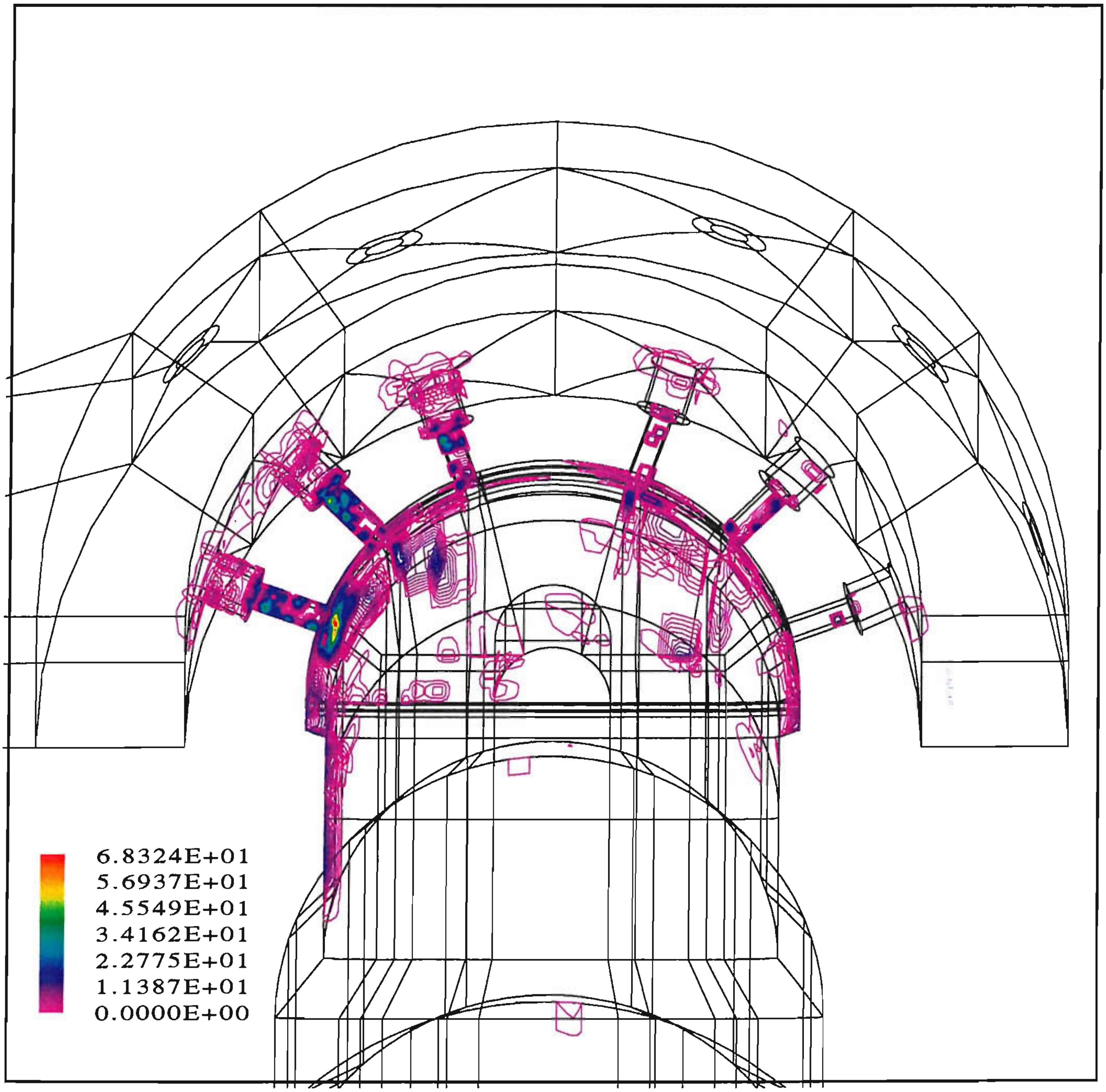

EROSION CHARACTERISTICS OF THE TUNGSTEN CARBIDE CC30 CONTROL CHOKE

Particle Type - **Sand**
Particle Loading and Flux Rate - **1.16** % by wt & **88.7** g/s.
Particle Roundness Factor - **0.5**
Number of Particle Sizes and Total Number of Particles Tracked - **16 & 1152**
Particle Size Range - **63-385** μm
Turbulent Dispersion - **Yes**
Modified Coefficient of Restitution - **Yes**
Squeeze Film Retardation - **Yes**
Gravity Vector Set - **Yes** Simulation Section - **CC30 Top**

Appendix Figure 160 - WC CC30 Particle Impact Velocity after 4 Calculation Sequences (m/s)

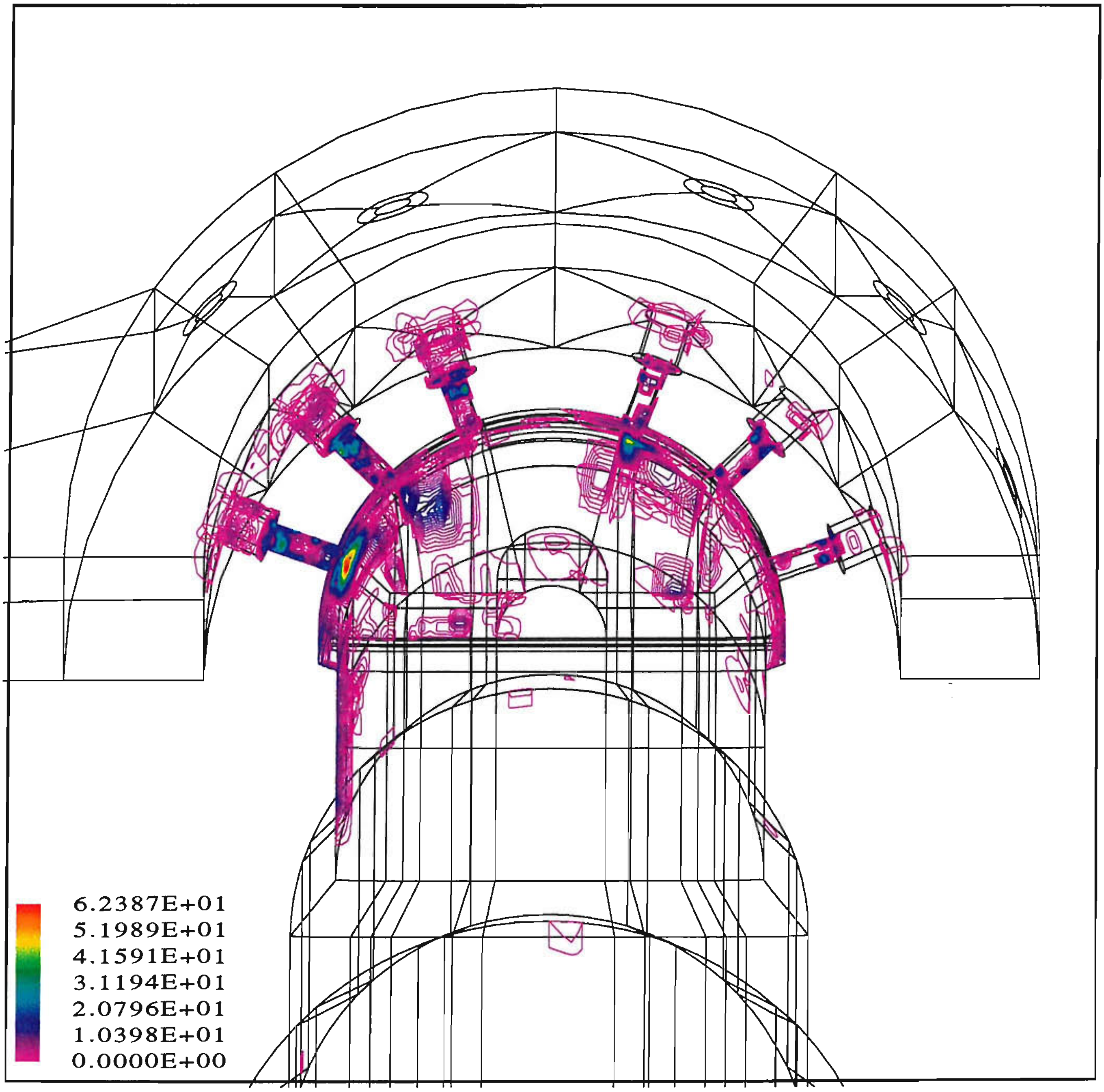

EROSION CHARACTERISTICS OF THE TUNGSTEN CARBIDE CC30 CONTROL CHOKE

Particle Type - **Sand**
Particle Loading and Flux Rate - **1.16** % by wt & **88.7** g/s.
Particle Roundness Factor - **0.5**
Number of Particle Sizes and Total Number of Particles Tracked - **20** & **1440**
Particle Size Range - **20-385** μm
Turbulent Dispersion - **Yes**
Modified Coefficient of Restitution - **Yes**
Squeeze Film Retardation - **Yes**
Gravity Vector Set - **Yes**

Simulation Section - **CC30 Top**

Appendix Figure 161 - WC CC30 Particle Impact Velocity, Complete Calculation Sequence (m/s)

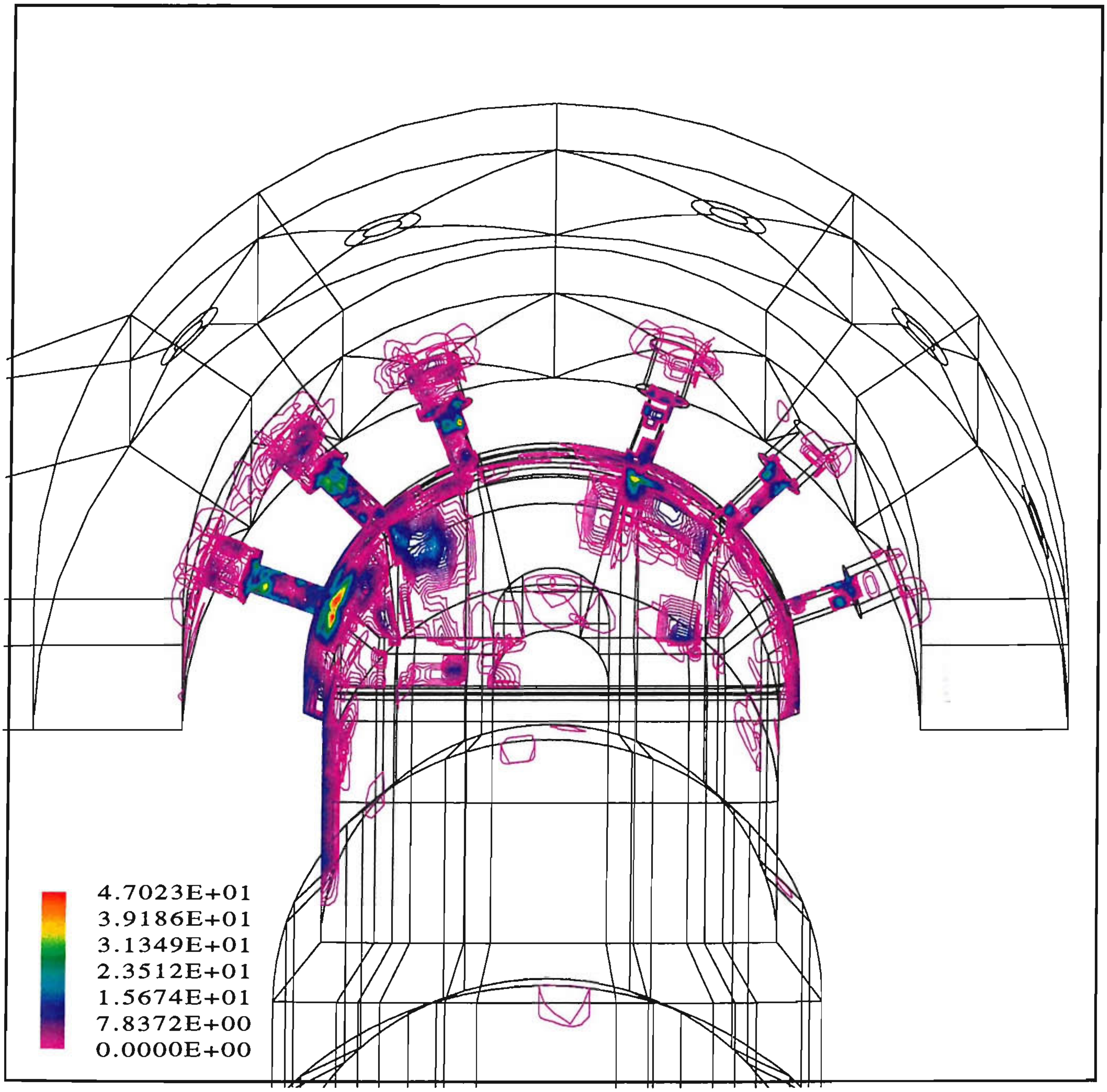

EROSION CHARACTERISTICS OF THE TUNGSTEN CARBIDE CC30 CONTROL CHOKE

Particle Type - **Sand**
Particle Loading and Flux Rate - **1.16** % by wt & **88.7** g/s.
Particle Roundness Factor - **0.5**
Number of Particle Sizes and Total Number of Particles Tracked - **20** & **1440**
Particle Size Range - **20-385** μm
Turbulent Dispersion - **Yes**
Modified Coefficient of Restitution - **Yes**
Squeeze Film Retardation - **Yes**
Gravity Vector Set - **Yes**

Simulation Section - **CC30 Top**

Appendix Figure 162 - WC CC30 Particle Impact Angle, Complete Calculation Sequence (Deg)

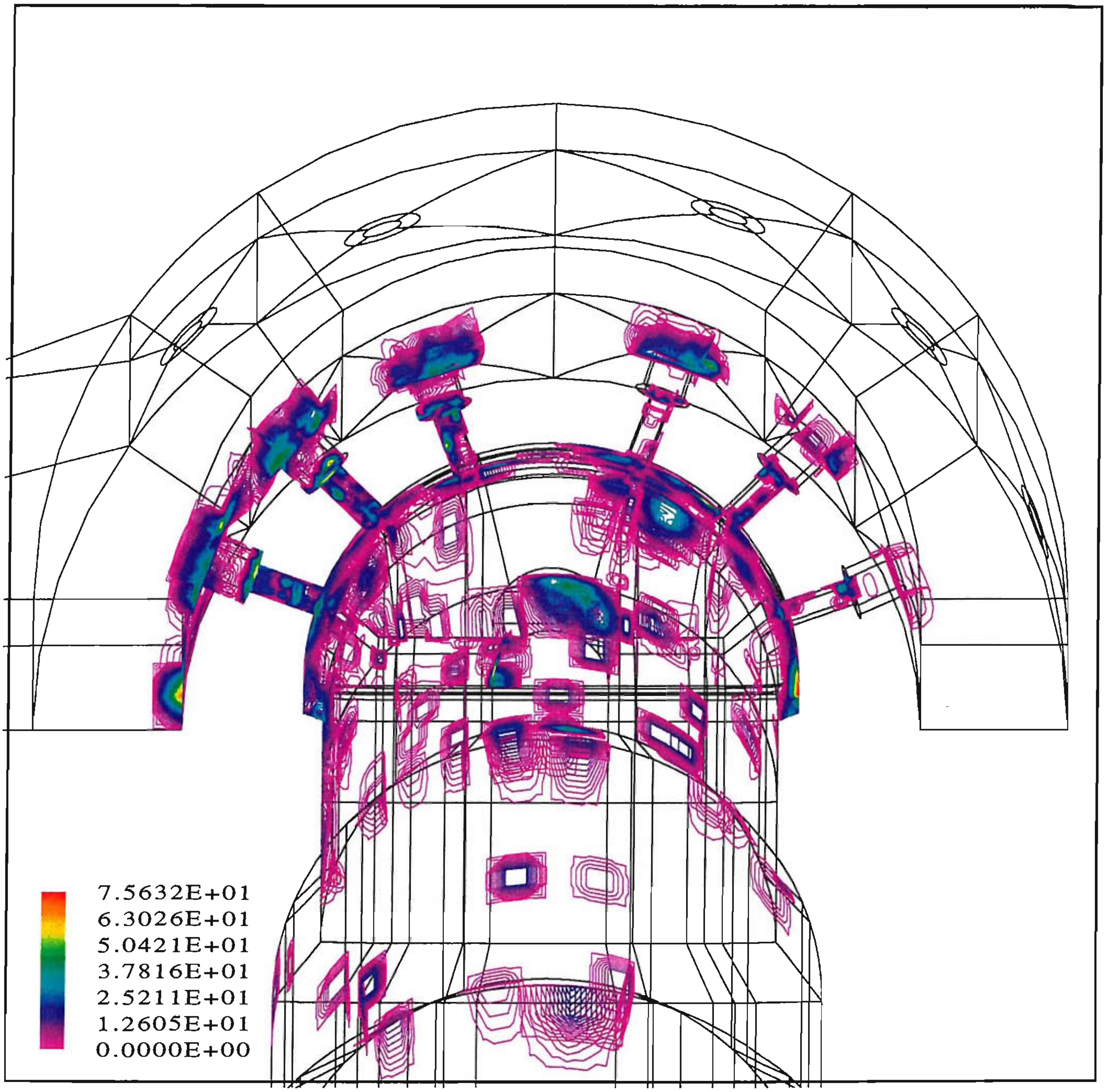

EROSION CHARACTERISTICS OF THE TUNGSTEN CARBIDE CC30 CONTROL CHOKE

Particle Type - **Sand**
Particle Loading and Flux Rate - **1.16** % by wt & **88.7** g/s.
Particle Roundness Factor - **0.5**
Number of Particle Sizes and Total Number of Particles Tracked - **20** & **1440**
Particle Size Range - **20-385** μm
Turbulent Dispersion - **Yes**
Modified Coefficient of Restitution - **Yes**
Squeeze Film Retardation - **Yes**
Gravity Vector Set - **Yes**

Simulation Section - **CC30 Top**

Appendix Figure 163 - WC CC30 Particle Impact Angle, Complete Calculation Sequence (Deg)

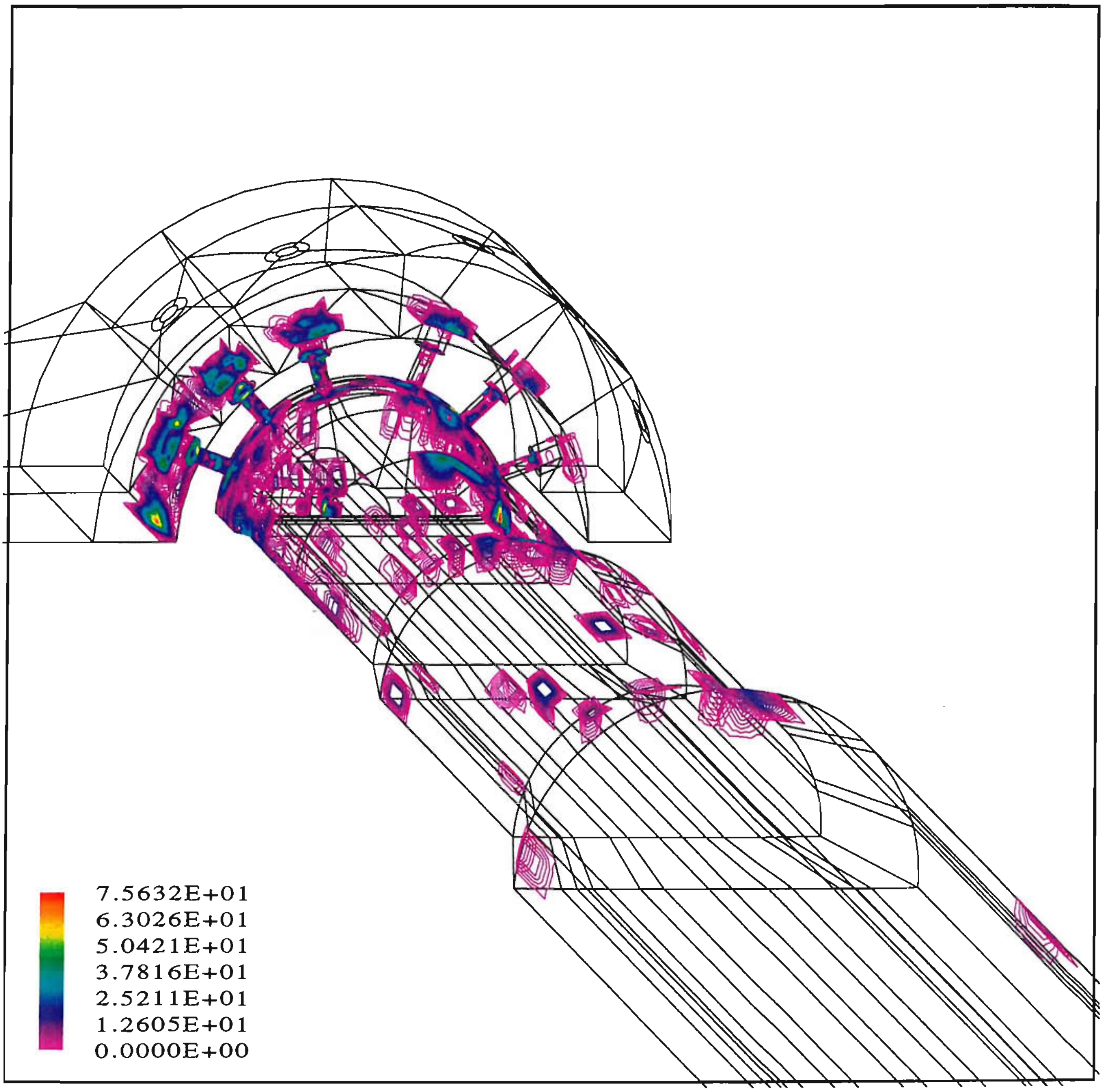

EROSION CHARACTERISTICS OF THE TUNGSTEN CARBIDE CC30 CONTROL CHOKE

Particle Type - **Sand**
Particle Size Mass Flux - **14.5** g/s.
Particle Roundness Factor - **0.5**
Number of Particle Sizes and Total Number of Particles Tracked - **8 & 576**
Particle Size Range - **212-385** μm
Turbulent Dispersion - **Yes**
Modified Coefficient of Restitution - **Yes**
Squeeze Film Retardation - **Yes**
Gravity Vector Set - **Yes** Simulation Section - **CC30 Top**

Appendix Figure 164 - WC CC30 Particle Erosion Rate after 2 Calculation Sequences (mm^2/hr)

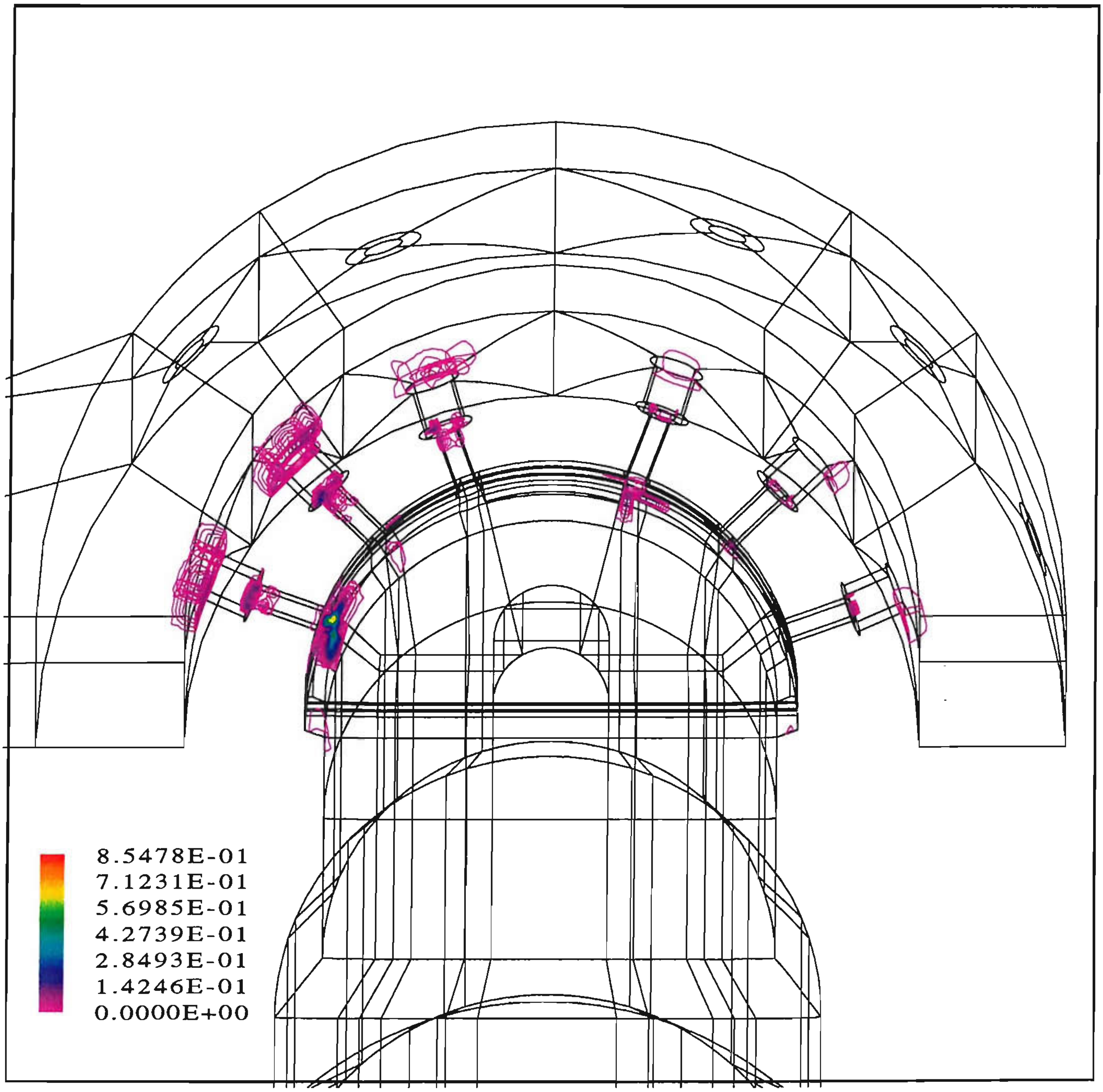

EROSION CHARACTERISTICS OF THE TUNGSTEN CARBIDE CC30 CONTROL CHOKE

Particle Type - **Sand**
Particle Size Mass Flux - **41.5** g/s.
Particle Roundness Factor - **0.5**
Number of Particle Sizes and Total Number of Particles Tracked - **12 & 864**
Particle Size Range - **150-385** μm
Turbulent Dispersion - **Yes**
Modified Coefficient of Restitution - **Yes**
Squeeze Film Retardation - **Yes**
Gravity Vector Set - **Yes**

Simulation Section - **CC30 Top**

Appendix Figure 165 - WC CC30 Particle Erosion Rate after 3 Calculation Sequences (mm^2/hr)

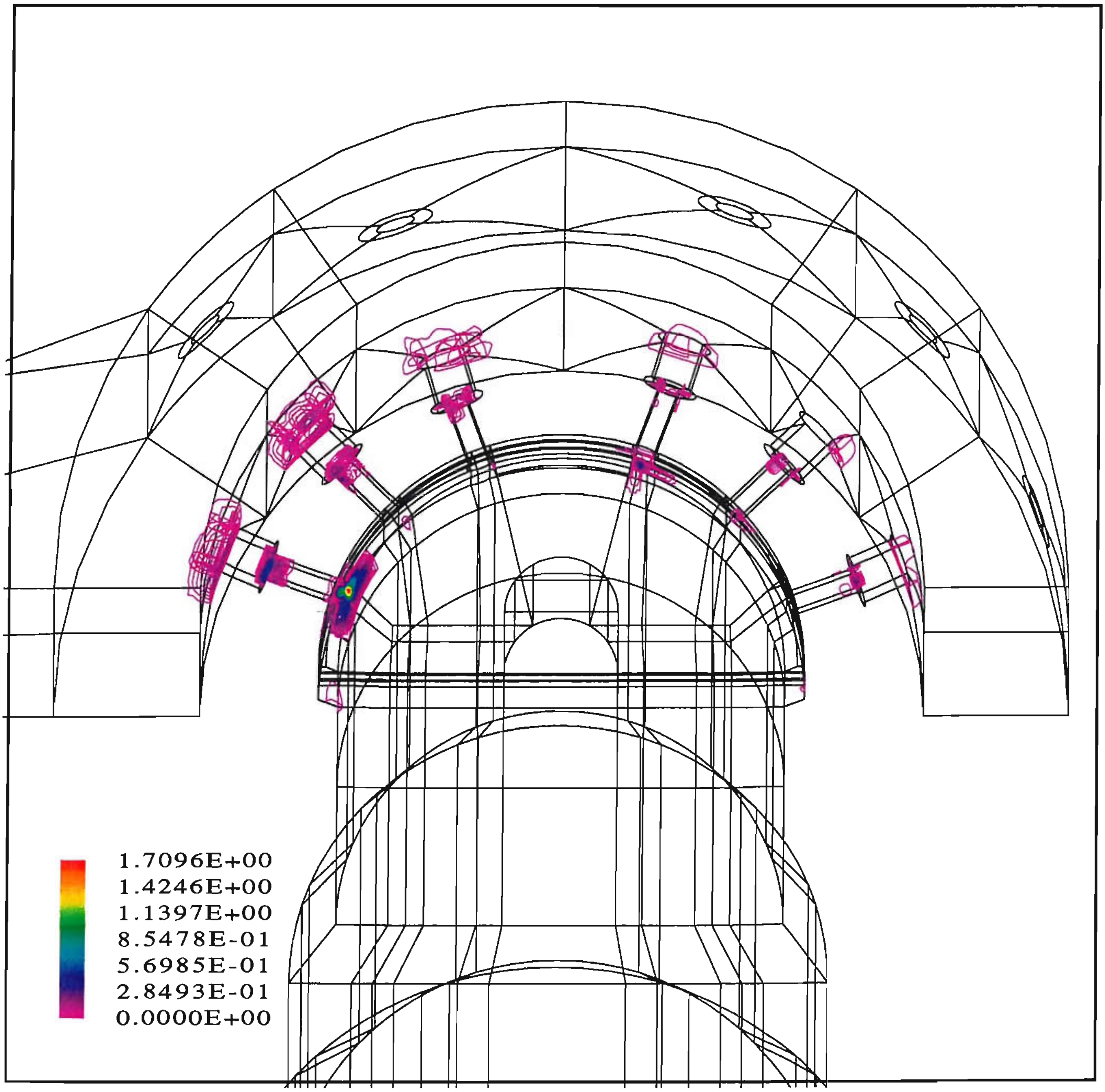

EROSION CHARACTERISTICS OF THE TUNGSTEN CARBIDE CC30 CONTROL CHOKE

Particle Type - **Sand**
Particle Size Mass Flux - **85.4** g/s.
Particle Roundness Factor - **0.5**
Number of Particle Sizes and Total Number of Particles Tracked - **16 & 1152**
Particle Size Range - **63-385** μm
Turbulent Dispersion - **Yes**
Modified Coefficient of Restitution - **Yes**
Squeeze Film Retardation - **Yes**
Gravity Vector Set - **Yes**

Simulation Section - **CC30 Top**

Appendix Figure 166 - WC CC30 Particle Erosion Rate after 4 Calculation Sequences (mm^2/hr)

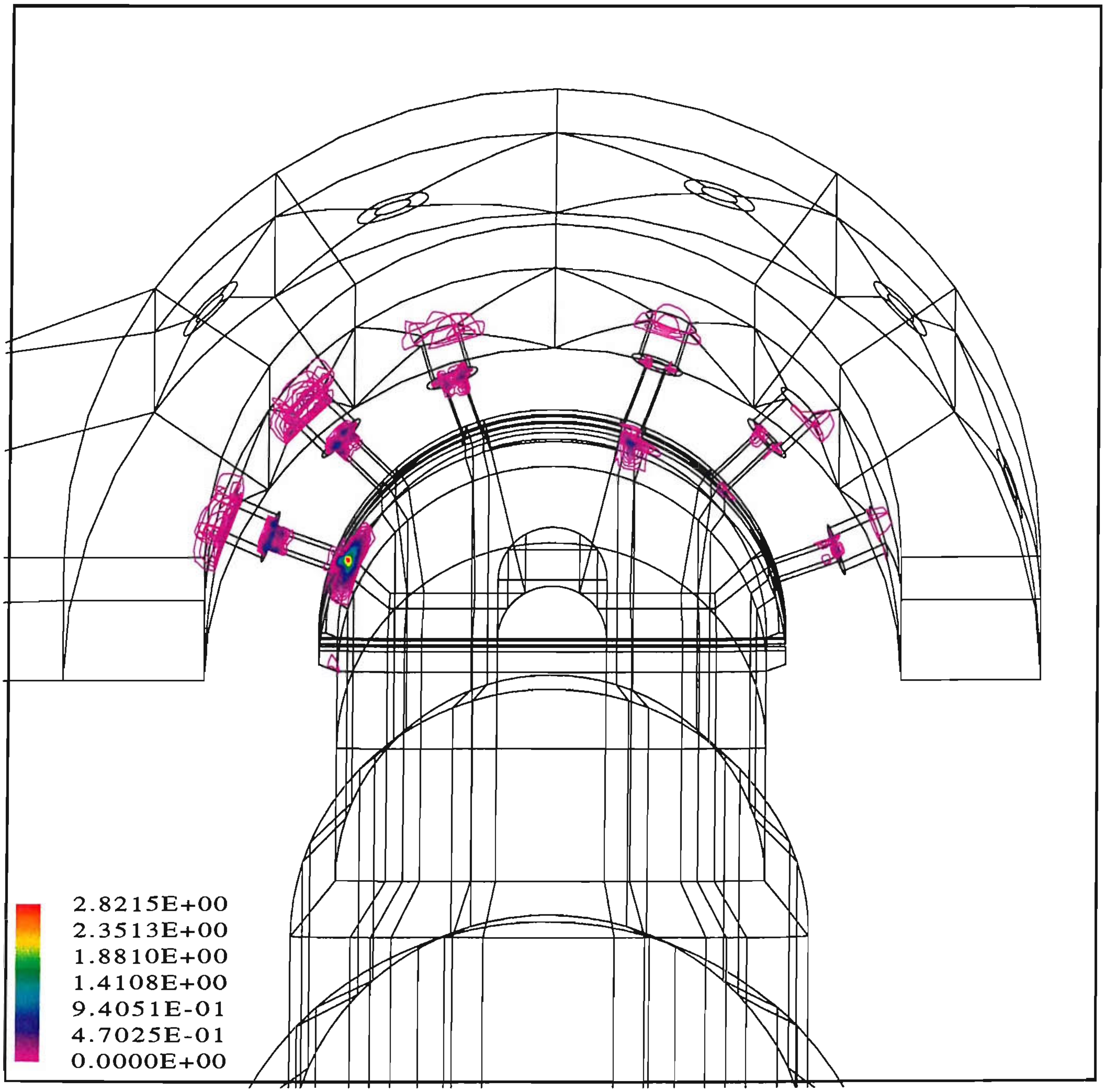

EROSION CHARACTERISTICS OF THE TUNGSTEN CARBIDE CC30 CONTROL CHOKE

Particle Type - **Sand**
Particle Size Mass Flux - **88.7** g/s.
Particle Roundness Factor - **0.5**
Number of Particle Sizes and Total Number of Particles Tracked - **20 & 1440**
Particle Size Range - **20-385** μm
Turbulent Dispersion - **Yes**
Modified Coefficient of Restitution - **Yes**
Squeeze Film Retardation - **Yes**
Gravity Vector Set - **Yes**

Simulation Section - **CC30 Top**

Appendix Figure 167 - WC CC30 Particle Erosion Rate, Complete Calculation Sequence (mm^2/hr)

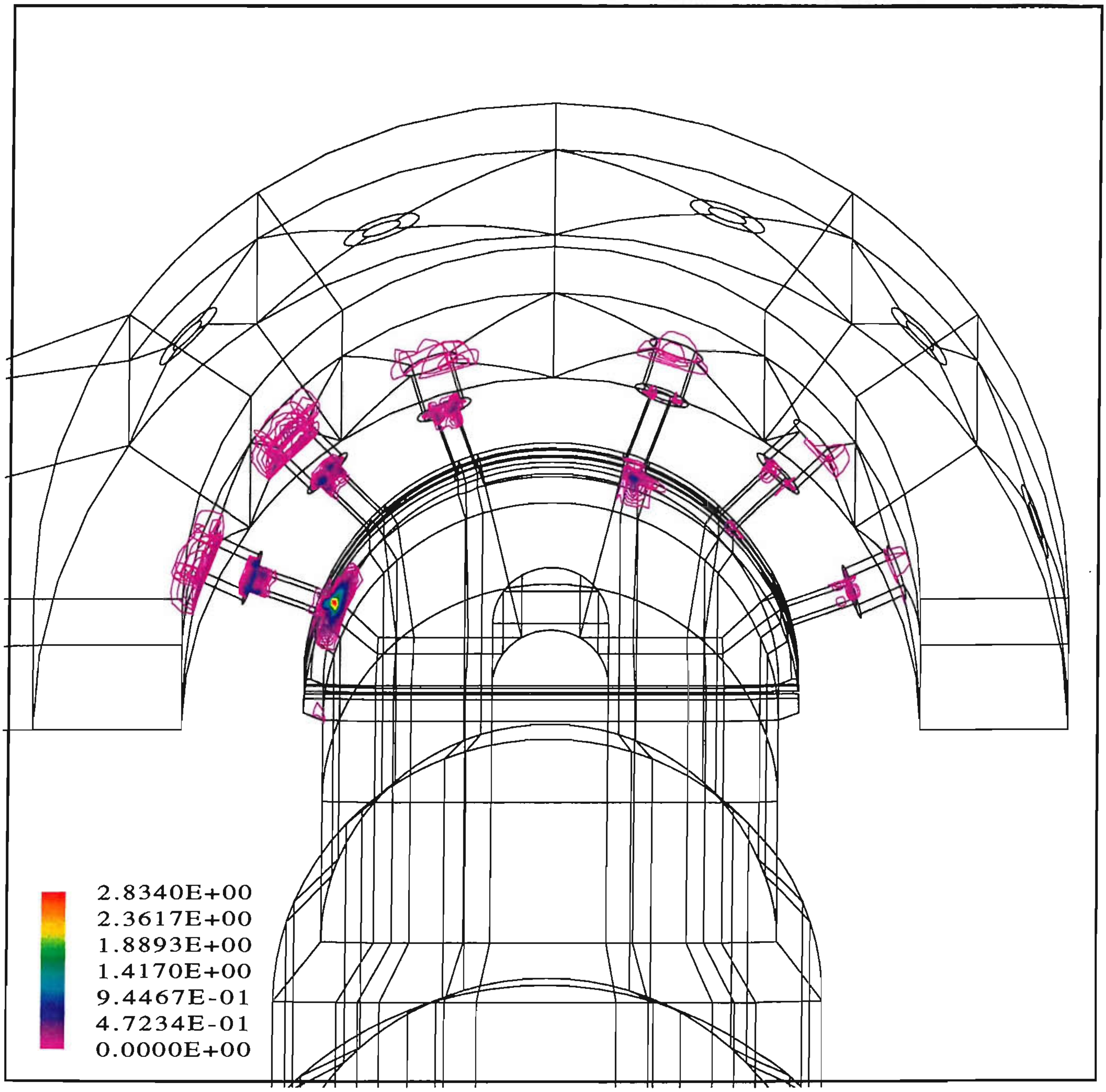

EROSION CHARACTERISTICS OF THE TUNGSTEN CARBIDE CC30 CONTROL CHOKE

Particle Type - **Sand**
Particle Size Mass Flux - **88.7** g/s.
Particle Roundness Factor - **0.5**
Number of Particle Sizes and Total Number of Particles Tracked - **20 & 1440**
Particle Size Range - **20-385** μm
Turbulent Dispersion - **Yes**
Modified Coefficient of Restitution - **Yes**
Squeeze Film Retardation - **Yes**
Gravity Vector Set - **Yes**

Simulation Section - **CC30 Top**

Appendix Figure 168 - WC CC30 Particle Erosion Rate, Complete Calculation Sequence (mm^2/hr)

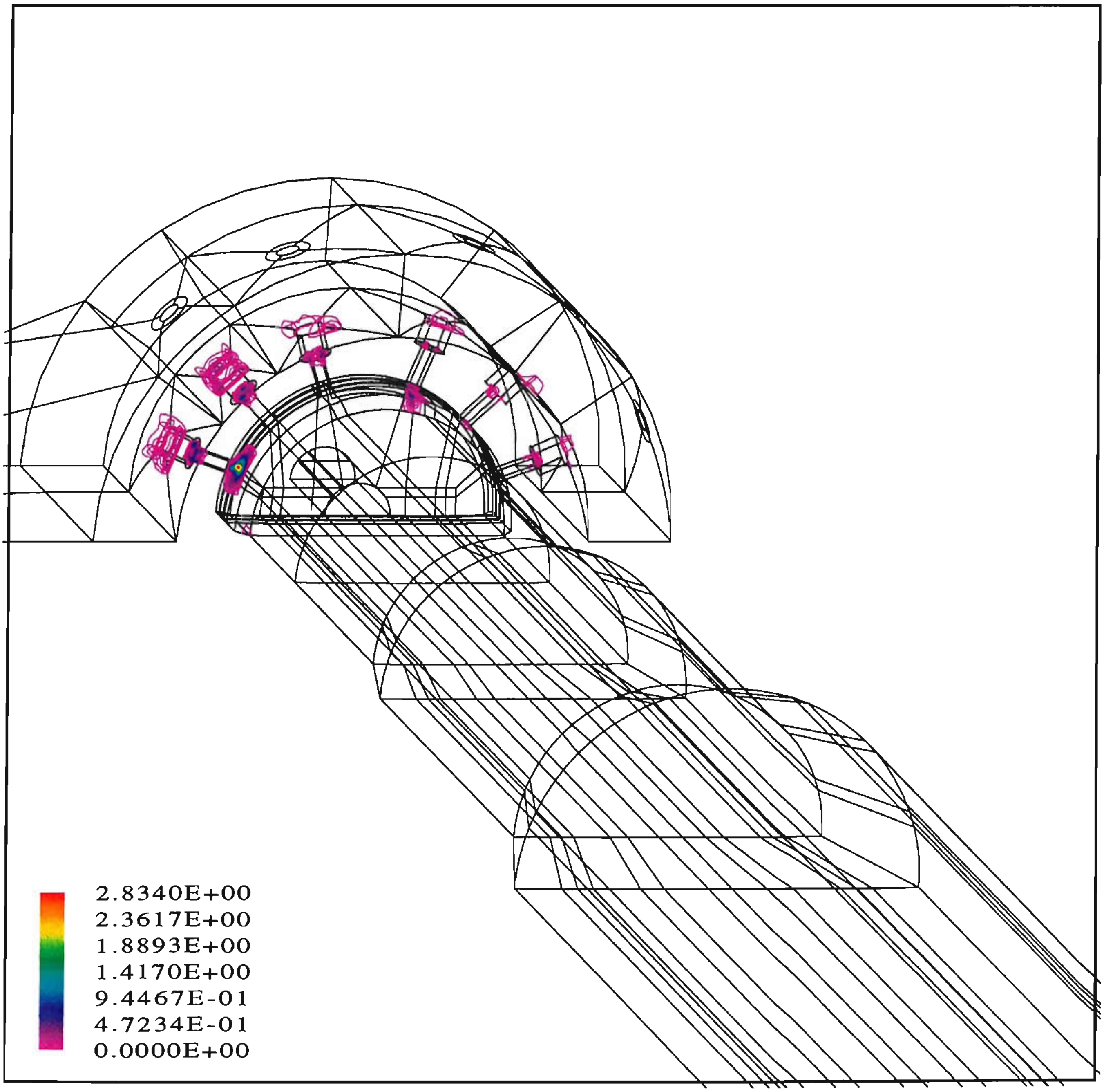

EROSION CHARACTERISTICS OF THE TUNGSTEN CARBIDE CC30 CONTROL CHOKE

Particle Type - **Sand**
Particle Loading and Flux Rate - **1.16** % by wt & **88.7** g/s.
Particle Roundness Factor - **0.5**
Number of Particle Sizes and Total Number of Particles Tracked - **20** & **1440**
Particle Size Range - **20-385** μm
Turbulent Dispersion - **Yes**
Modified Coefficient of Restitution - **Yes**
Squeeze Film Retardation - **Yes**
Gravity Vector Set - **Yes**　　Simulation Section - **CC30 Bottom**

Appendix Figure 169 - WC CC30 Particle Impact Velocity, Complete Calculation Sequence (m/s)

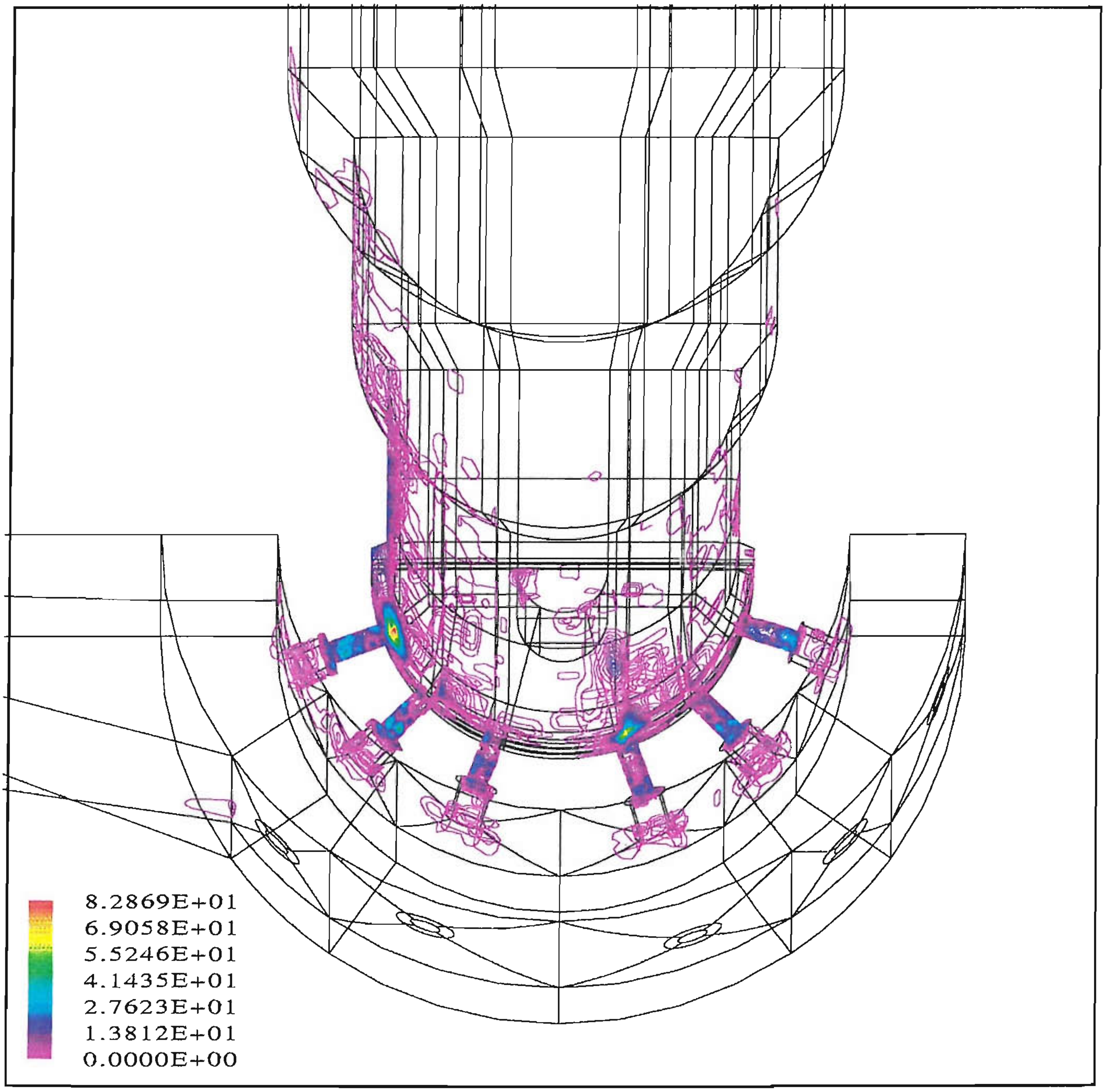

EROSION CHARACTERISTICS OF THE TUNGSTEN CARBIDE CC30 CONTROL CHOKE

Particle Type - **Sand**
Particle Loading and Flux Rate - **1.16** % by wt & **88.7** g/s.
Particle Roundness Factor - **0.5**
Number of Particle Sizes and Total Number of Particles Tracked - **20 & 1440**
Particle Size Range - **20-385** μm
Turbulent Dispersion - **Yes**
Modified Coefficient of Restitution - **Yes**
Squeeze Film Retardation - **Yes**
Gravity Vector Set - **Yes**

Simulation Section - **CC30 Bottom**

Appendix Figure 170 - WC CC30 Particle Impact Velocity, Complete Calculation Sequence (m/s)

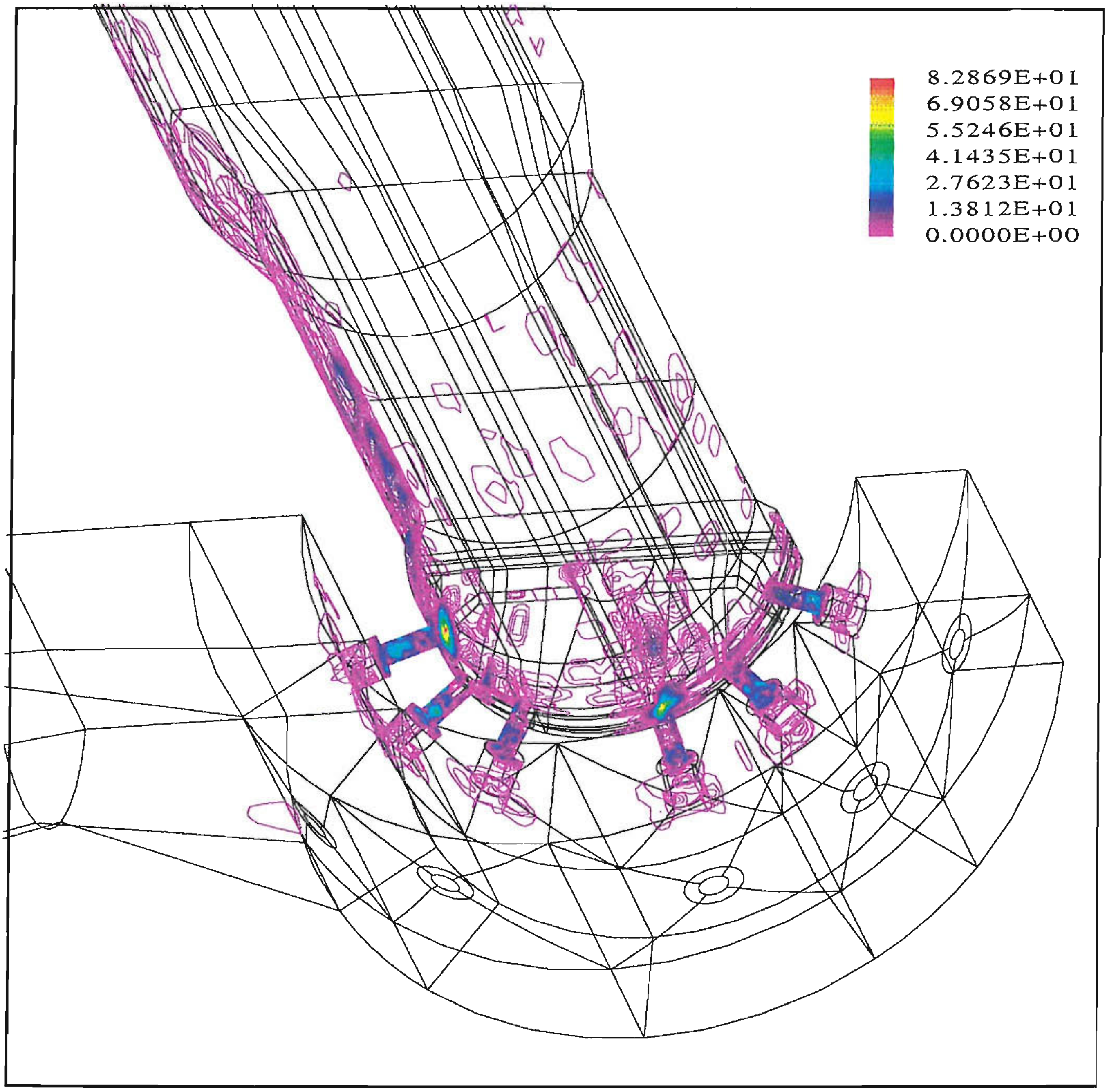

EROSION CHARACTERISTICS OF THE TUNGSTEN CARBIDE CC30 CONTROL CHOKE

Particle Type - **Sand**
Particle Loading and Flux Rate - **1.16** % by wt & **88.7** g/s.
Particle Roundness Factor - **0.5**
Number of Particle Sizes and Total Number of Particles Tracked - **20 & 1440**
Particle Size Range - **20-385** μm
Turbulent Dispersion - **Yes**
Modified Coefficient of Restitution - **Yes**
Squeeze Film Retardation - **Yes**
Gravity Vector Set - **Yes**

Simulation Section - **CC30 Bottom**

Appendix Figure 171 - WC CC30 Particle Impact Angle, Complete Calculation Sequence (Deg)

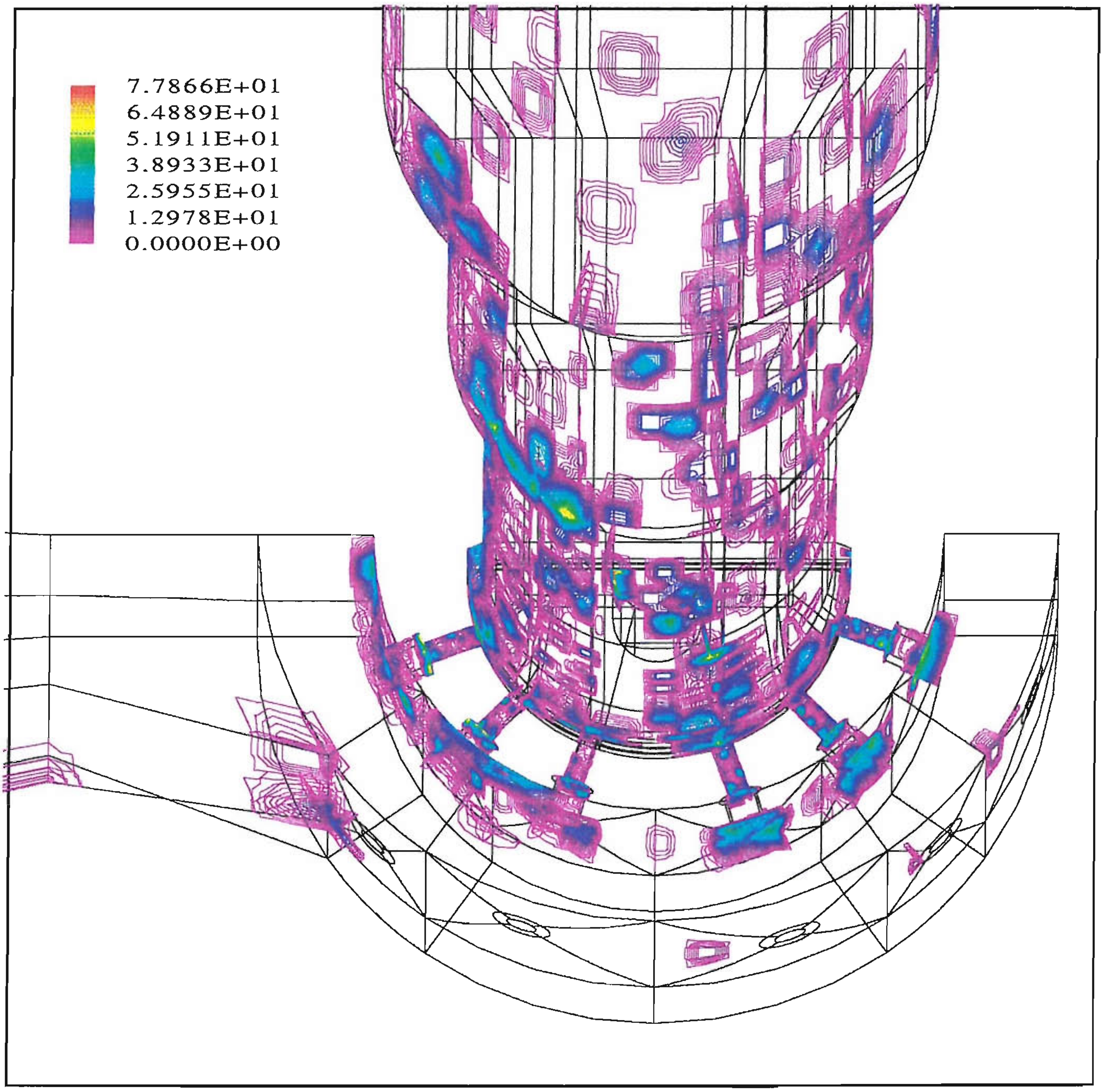

EROSION CHARACTERISTICS OF THE TUNGSTEN CARBIDE CC30 CONTROL CHOKE

Particle Type - **Sand**
Particle Loading and Flux Rate - **1.16** % by wt & **88.7** g/s.
Particle Roundness Factor - **0.5**
Number of Particle Sizes and Total Number of Particles Tracked - **20 & 1440**
Particle Size Range - **20-385** μm
Turbulent Dispersion - **Yes**
Modified Coefficient of Restitution - **Yes**
Squeeze Film Retardation - **Yes**
Gravity Vector Set - **Yes**

Simulation Section - **CC30 Bottom**

Appendix Figure 172 - WC CC30 Particle Impact Angle, Complete Calculation Sequence (Deg)

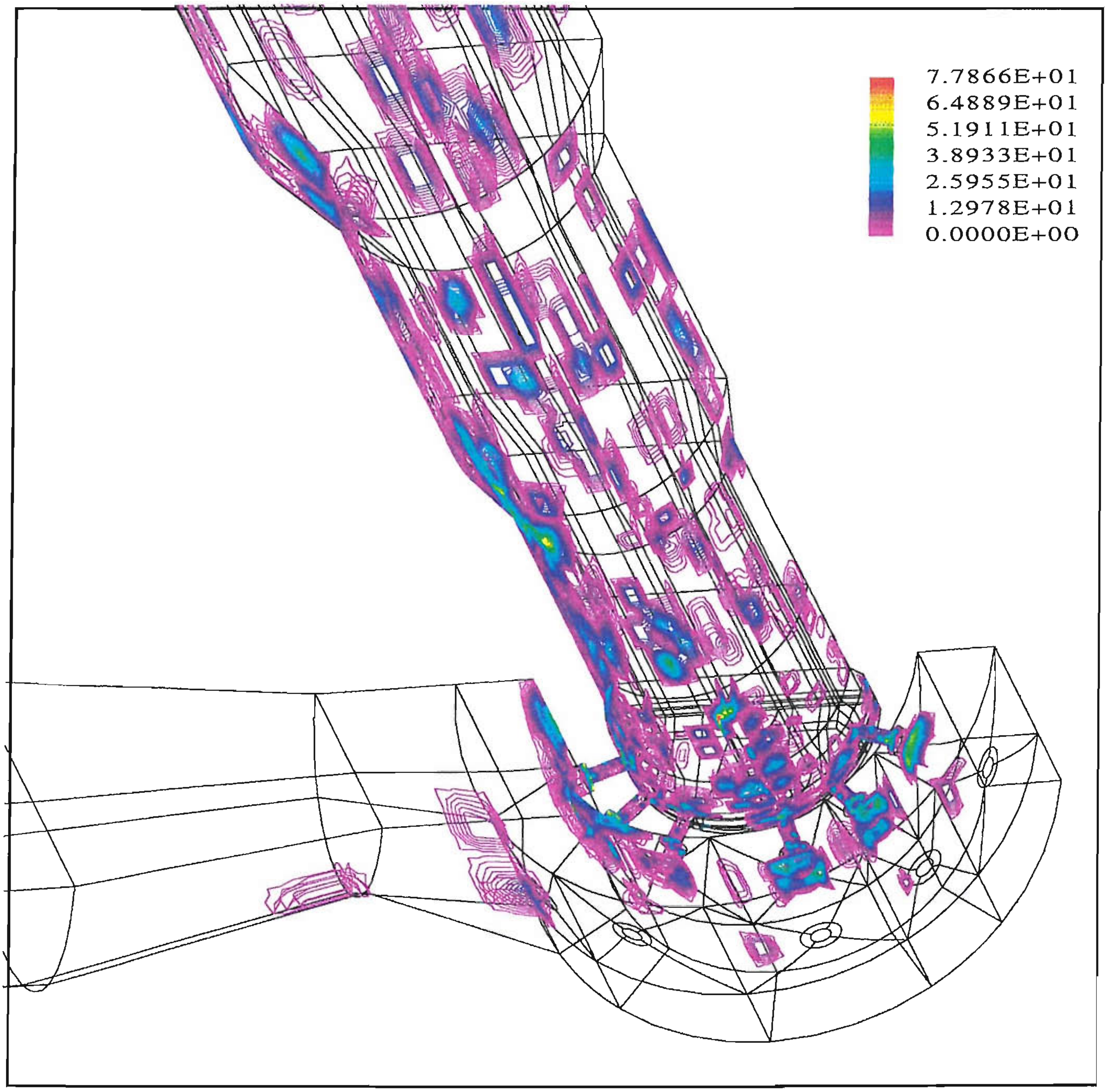

EROSION CHARACTERISTICS OF THE TUNGSTEN CARBIDE CC30 CONTROL CHOKE

Particle Type - **Sand**
Particle Size Mass Flux - **88.7** g/s.
Particle Roundness Factor - **0.5**
Number of Particle Sizes and Total Number of Particles Tracked - **20 & 1440**
Particle Size Range - **20-385** μm
Turbulent Dispersion - **Yes**
Modified Coefficient of Restitution - **Yes**
Squeeze Film Retardation - **Yes**
Gravity Vector Set - **Yes**

Simulation Section - **CC30 Bottom**

Appendix Figure 173 - WC CC30 Particle Erosion Rate, Complete Calculation Sequence (mm^2/hr)

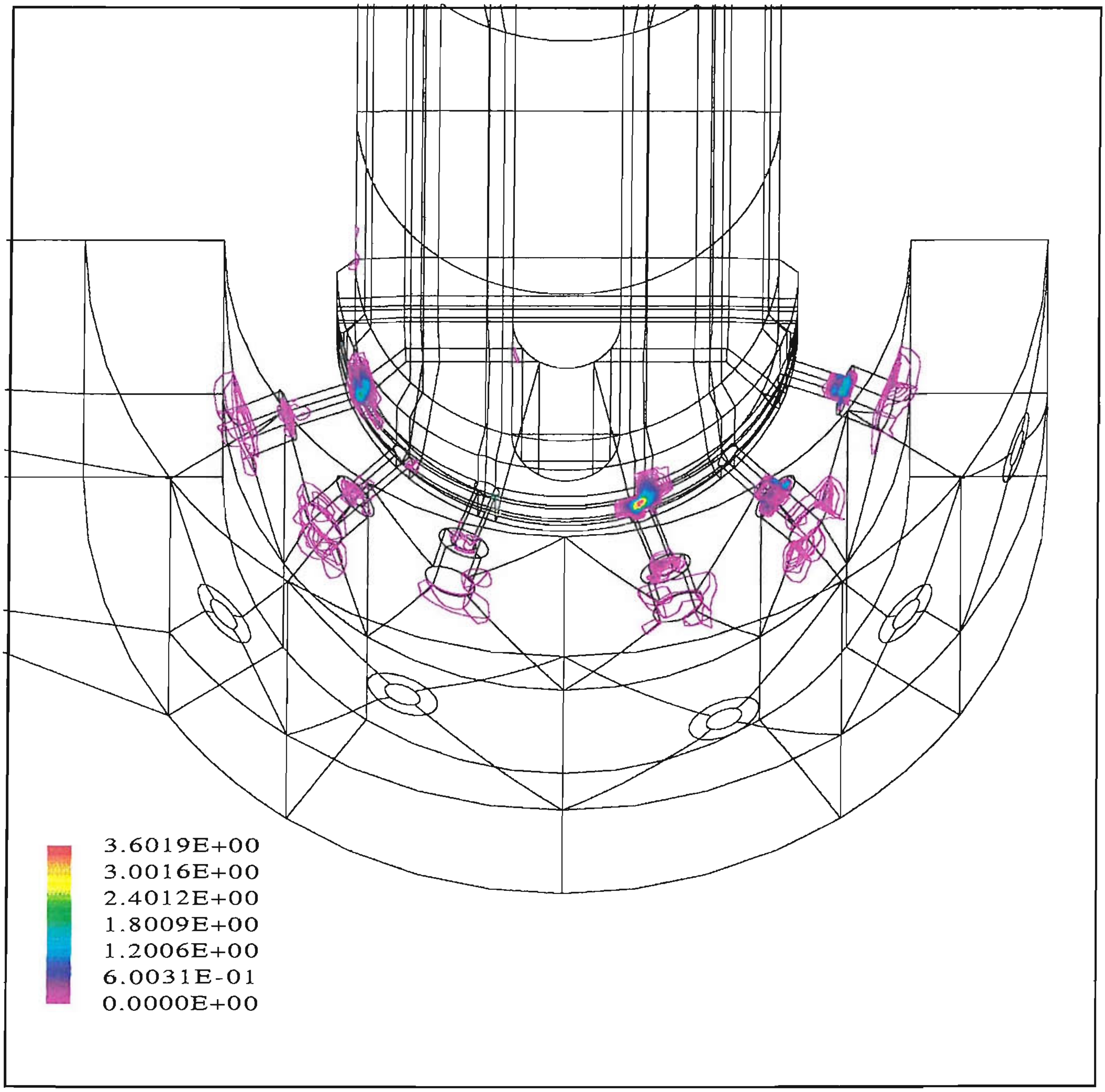

EROSION CHARACTERISTICS OF THE TUNGSTEN CARBIDE CC30 CONTROL CHOKE

Particle Type - **Sand**
Particle Size Mass Flux - **88.7** g/s.
Particle Roundness Factor - **0.5**
Number of Particle Sizes and Total Number of Particles Tracked - **20 & 1440**
Particle Size Range - **20-385** μm
Turbulent Dispersion - **Yes**
Modified Coefficient of Restitution - **Yes**
Squeeze Film Retardation - **Yes**
Gravity Vector Set - **Yes**

Simulation Section - **CC30 Bottom**

Appendix Figure 174 - WC CC30 Particle Erosion Rate, Complete Calculation Sequence (mm^2/hr)

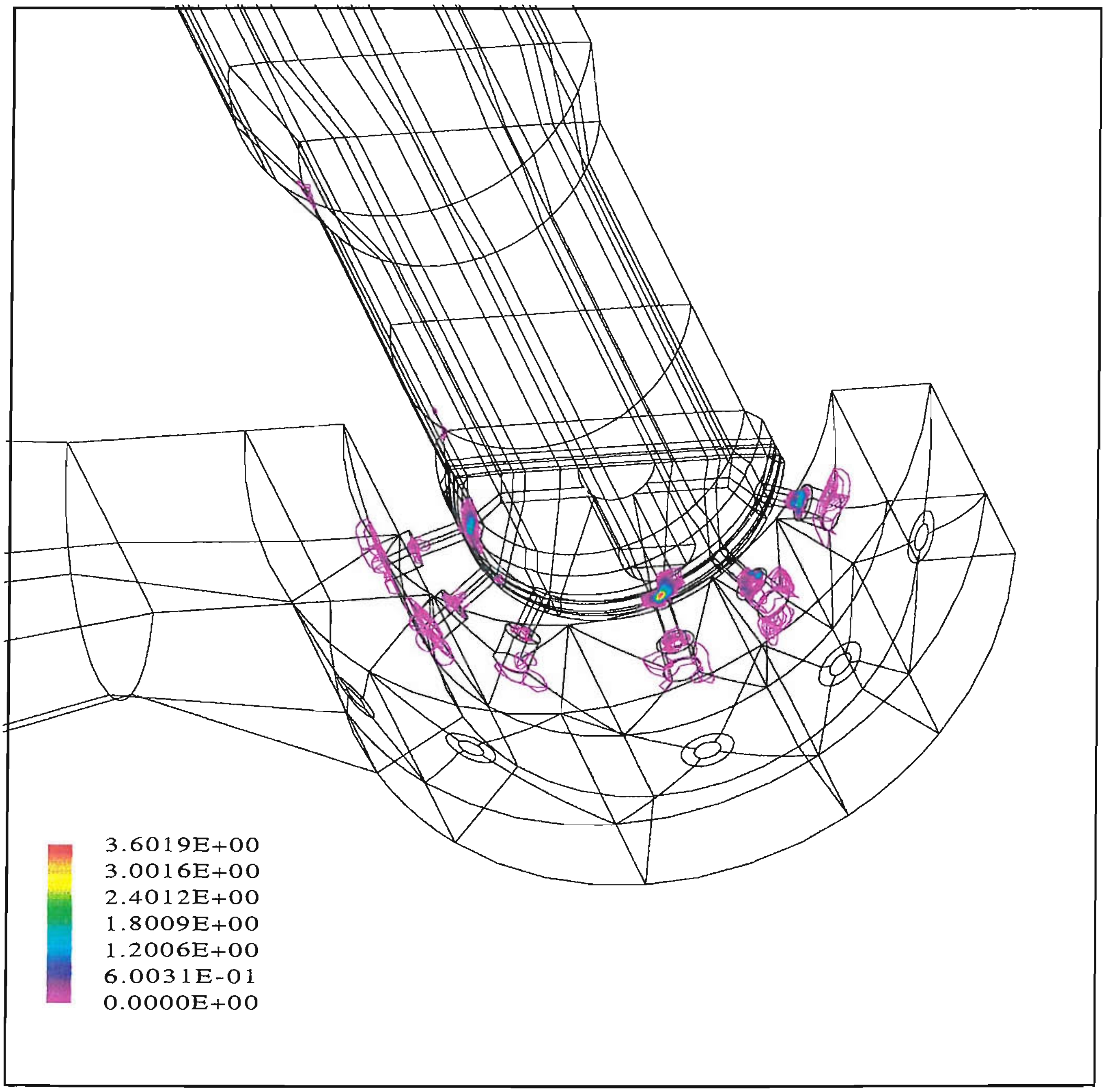

EROSION CHARACTERISTICS OF THE TUNGSTEN CARBIDE CC30 CONTROL CHOKE

Particle Type - **Sand**
Particle Size Mass Flux - **88.7** g/s.
Particle Roundness Factor - **0.5**
Number of Particle Sizes and Total Number of Particles Tracked - **20 & 1440**
Particle Size Range - **20-385** μm
Turbulent Dispersion - **Yes**
Modified Coefficient of Restitution - **Yes**
Squeeze Film Retardation - **Yes**
Gravity Vector Set - **Yes**

Simulation Section - **CC30 Bottom**

Appendix Figure 175 - WC CC30 Particle Erosion Rate, Complete Calculation Sequence (mm^2/hr)

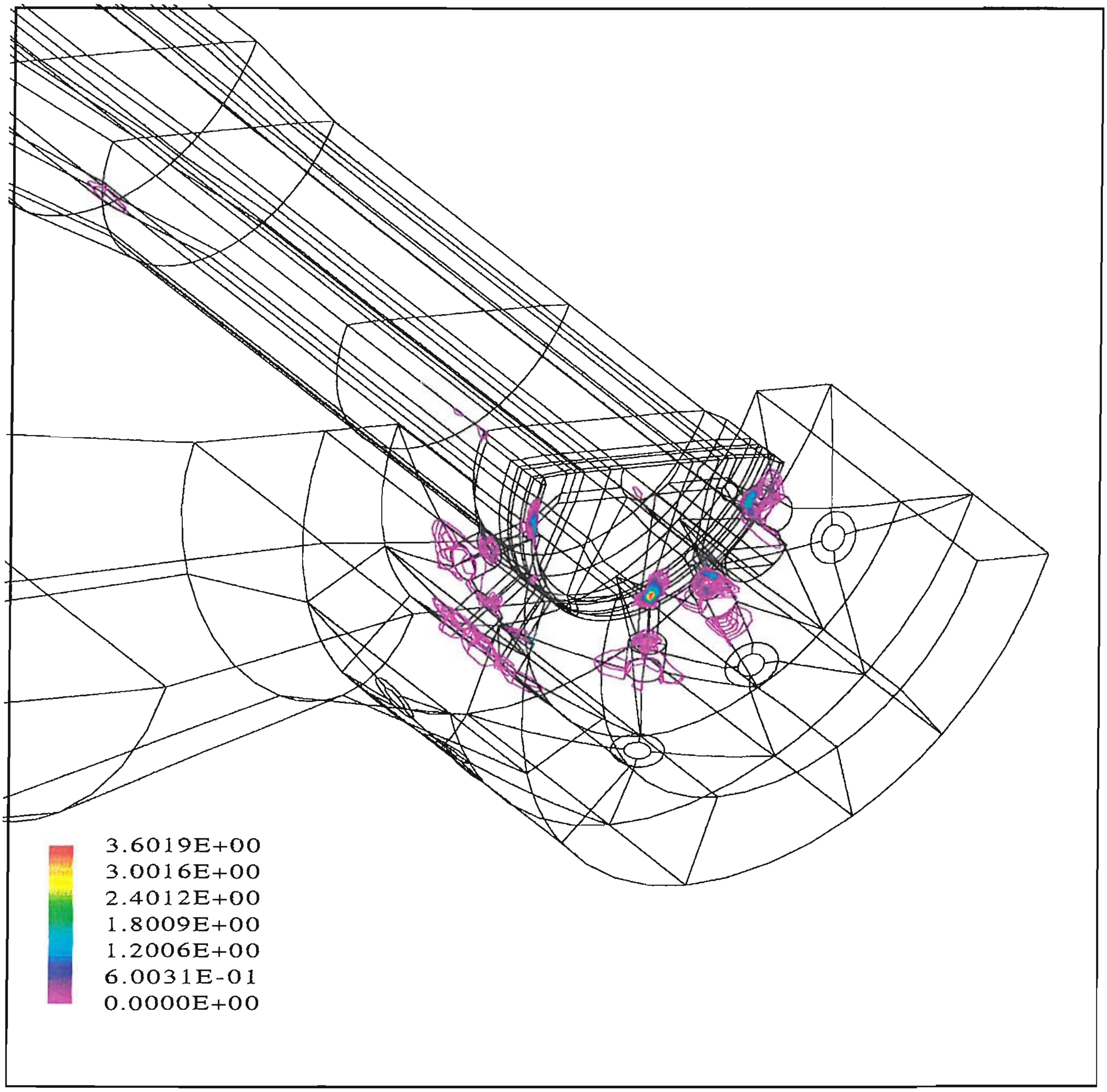

Particle Trajectories within the Stainless Steel CC30 Control Choke

Particle Type - **Sand**
Particle Loading and Flux Rate - **1.16** % by wt & **88.7** g/s.
Particle Roundness Factor - **0.5**
Number of Particle Sizes and Total Number of Particles Tracked - **20** & **1440**
Particle Size Range - **20-385** μm
Turbulent Dispersion - **Yes**
Modified Coefficient of Restitution - **Yes**
Squeeze Film Retardation - **Yes**
Gravity Vector Set - **Yes**

Appendix Figure 176 - Particle Trajectories and Trajectory Velocities within the CC30 (m/s)

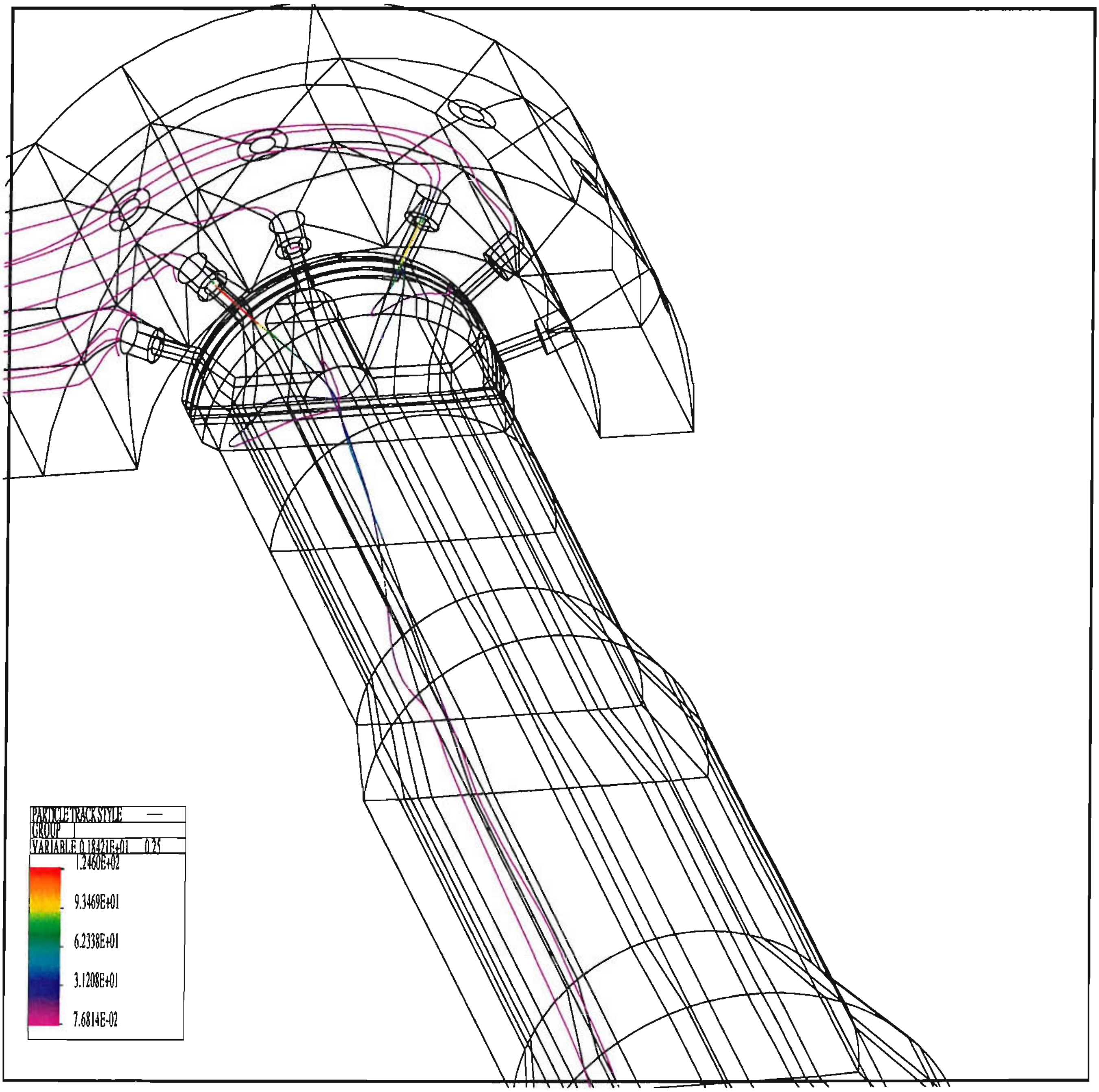

PARTICLE TRAJECTORIES WITHIN THE STAINLESS STEEL CC30 CONTROL CHOKE

Particle Type - **Sand**
Particle Loading and Flux Rate - **1.16** % by wt & **88.7** g/s.
Particle Roundness Factor - **0.5**
Number of Particle Sizes and Total Number of Particles Tracked - **20** & **1440**
Particle Size Range - **20-385** μm
Turbulent Dispersion - **Yes**
Modified Coefficient of Restitution - **Yes**
Squeeze Film Retardation - **Yes**
Gravity Vector Set - **Yes**

Appendix Figure 177 - Particle Trajectories and Trajectory Velocities within the CC30 (m/s)

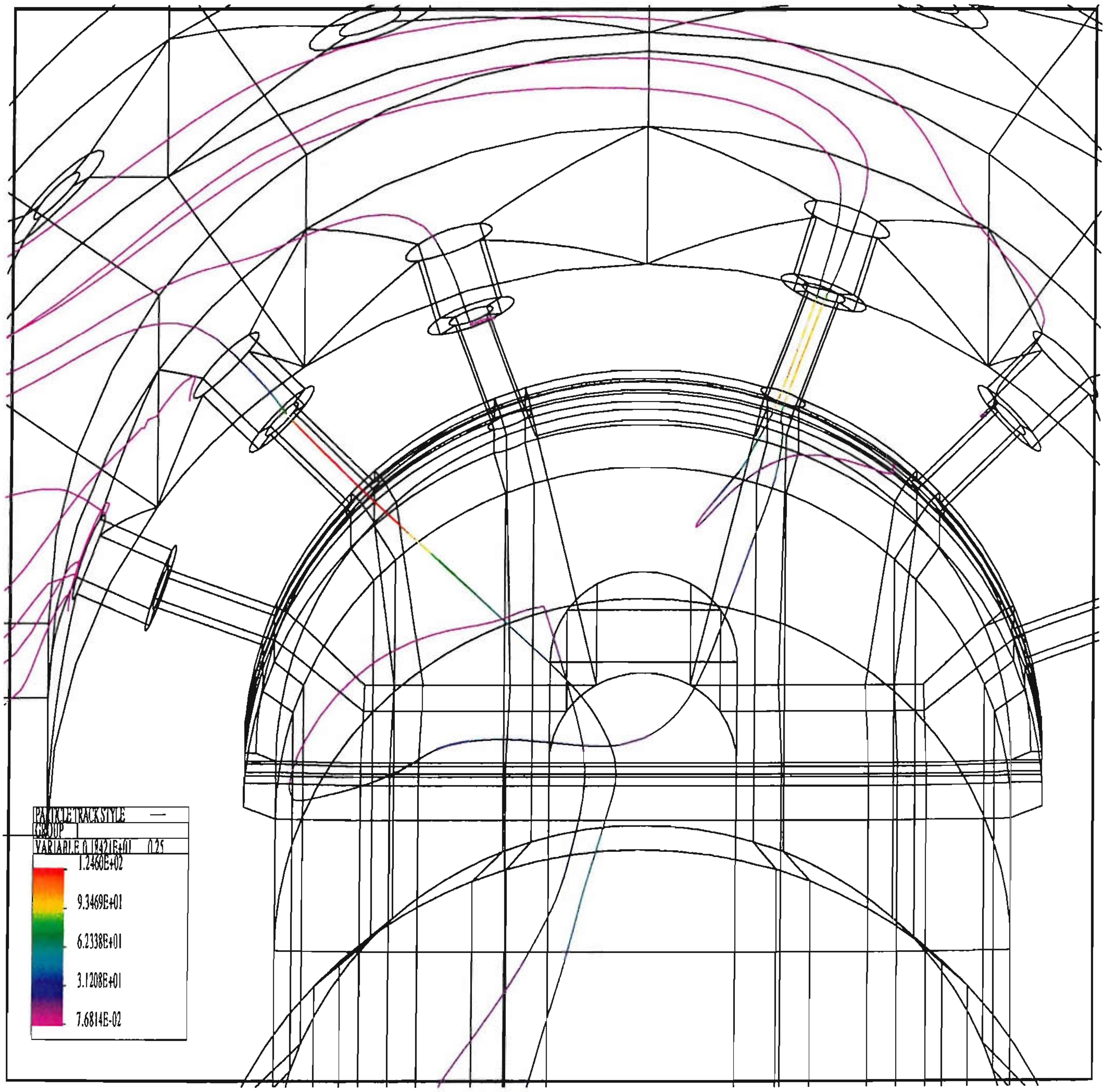

Erosion Characteristics of the Stainless Steel CC30 Control Choke

Particle Type - **Sand**
Particle Loading and Flux Rate - **1.16** % by wt & **88.7** g/s.
Particle Roundness Factor - **0.5**
Number of Particle Sizes and Total Number of Particles Tracked - **12** & **864**
Particle Size Range - **150-385** μm
Turbulent Dispersion - **Yes**
Modified Coefficient of Restitution - **Yes**
Squeeze Film Retardation - **Yes**
Gravity Vector Set - **Yes**

Simulation Section - **CC30 Top**

Appendix Figure 178 - SS CC30 Particle Impact Velocity after 3 Calculation Sequences (m/s)

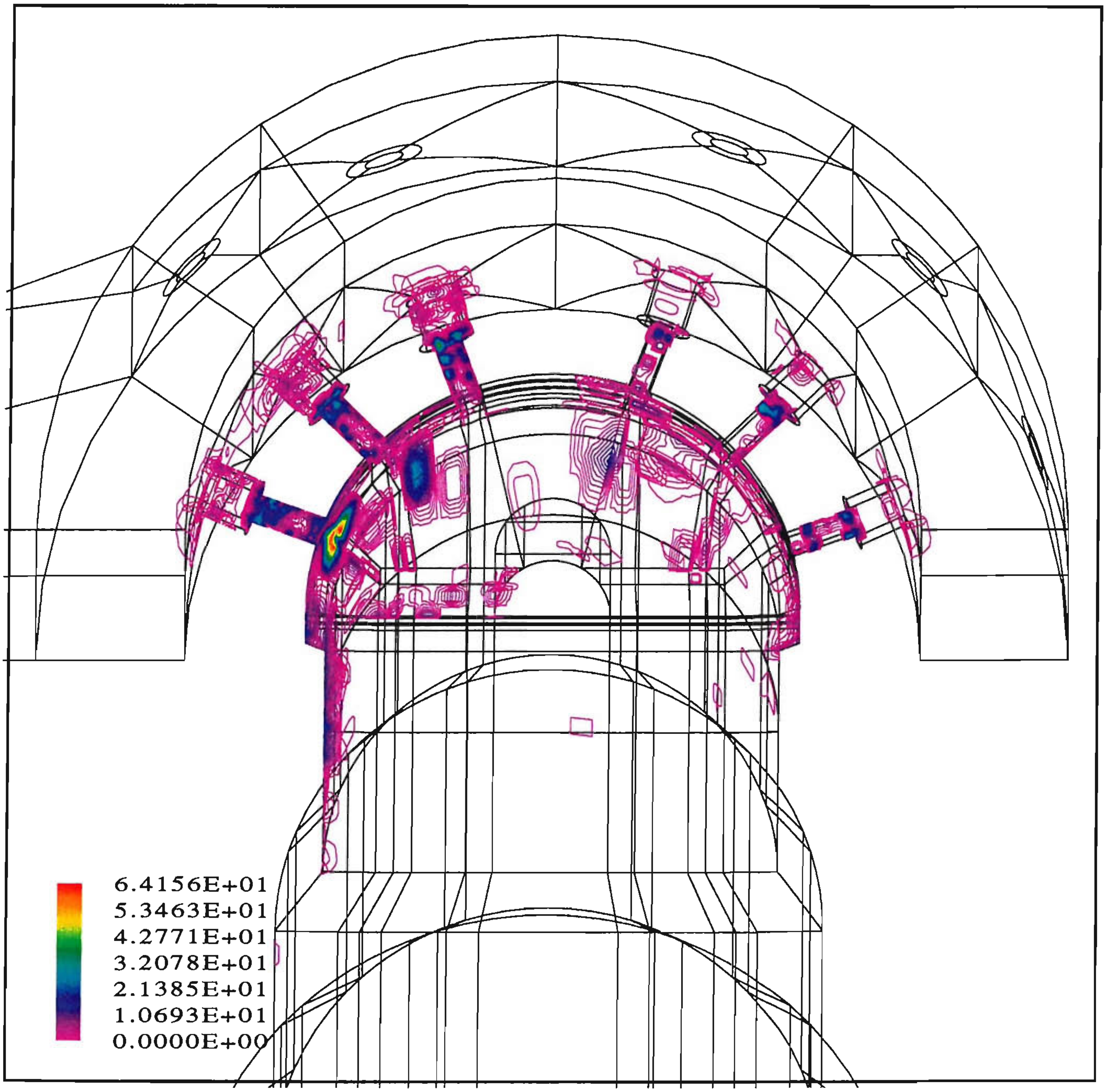

EROSION CHARACTERISTICS OF THE STAINLESS STEEL CC30 CONTROL CHOKE

Particle Type - **Sand**
Particle Loading and Flux Rate - **1.16** % by wt & **88.7** g/s.
Particle Roundness Factor - **0.5**
Number of Particle Sizes and Total Number of Particles Tracked - **16** & **1152**
Particle Size Range - **63-385** μm
Turbulent Dispersion - **Yes**
Modified Coefficient of Restitution - **Yes**
Squeeze Film Retardation - **Yes**
Gravity Vector Set - **Yes**

Simulation Section - **CC30 Top**

Appendix Figure 179 - SS CC30 Particle Impact Velocity after 4 Calculation Sequences (m/s)

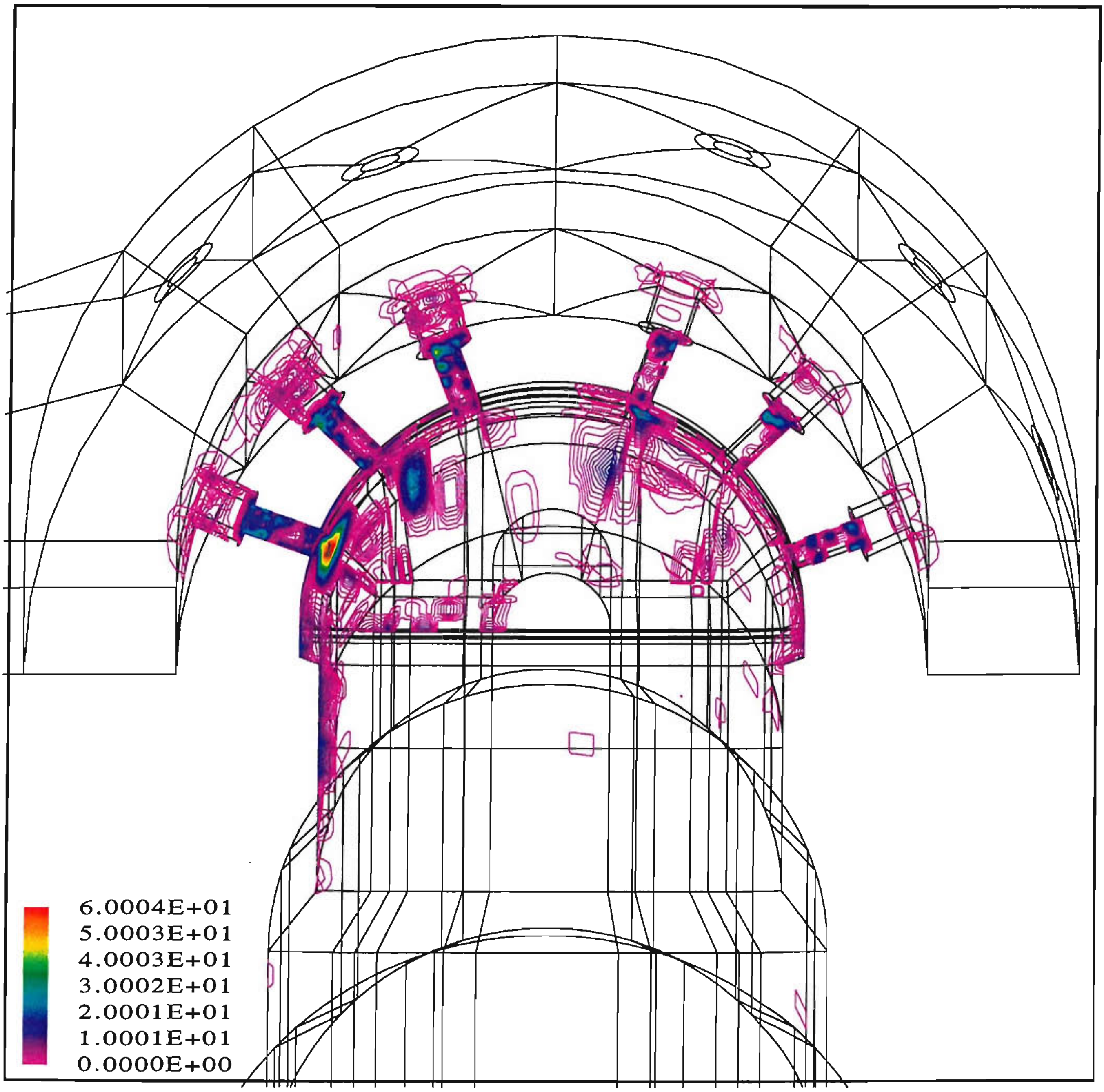

EROSION CHARACTERISTICS OF THE STAINLESS STEEL CC30 CONTROL CHOKE

Particle Type - **Sand**
Particle Loading and Flux Rate - **1.16** % by wt & **88.7** g/s.
Particle Roundness Factor - **0.5**
Number of Particle Sizes and Total Number of Particles Tracked - **20** & **1440**
Particle Size Range - **20-385** μm
Turbulent Dispersion - **Yes**
Modified Coefficient of Restitution - **Yes**
Squeeze Film Retardation - **Yes**
Gravity Vector Set - **Yes** Simulation Section - **CC30 Top**

Appendix Figure 180 - SS CC30 Particle Impact Velocity, Complete Calculation Sequence (m/s)

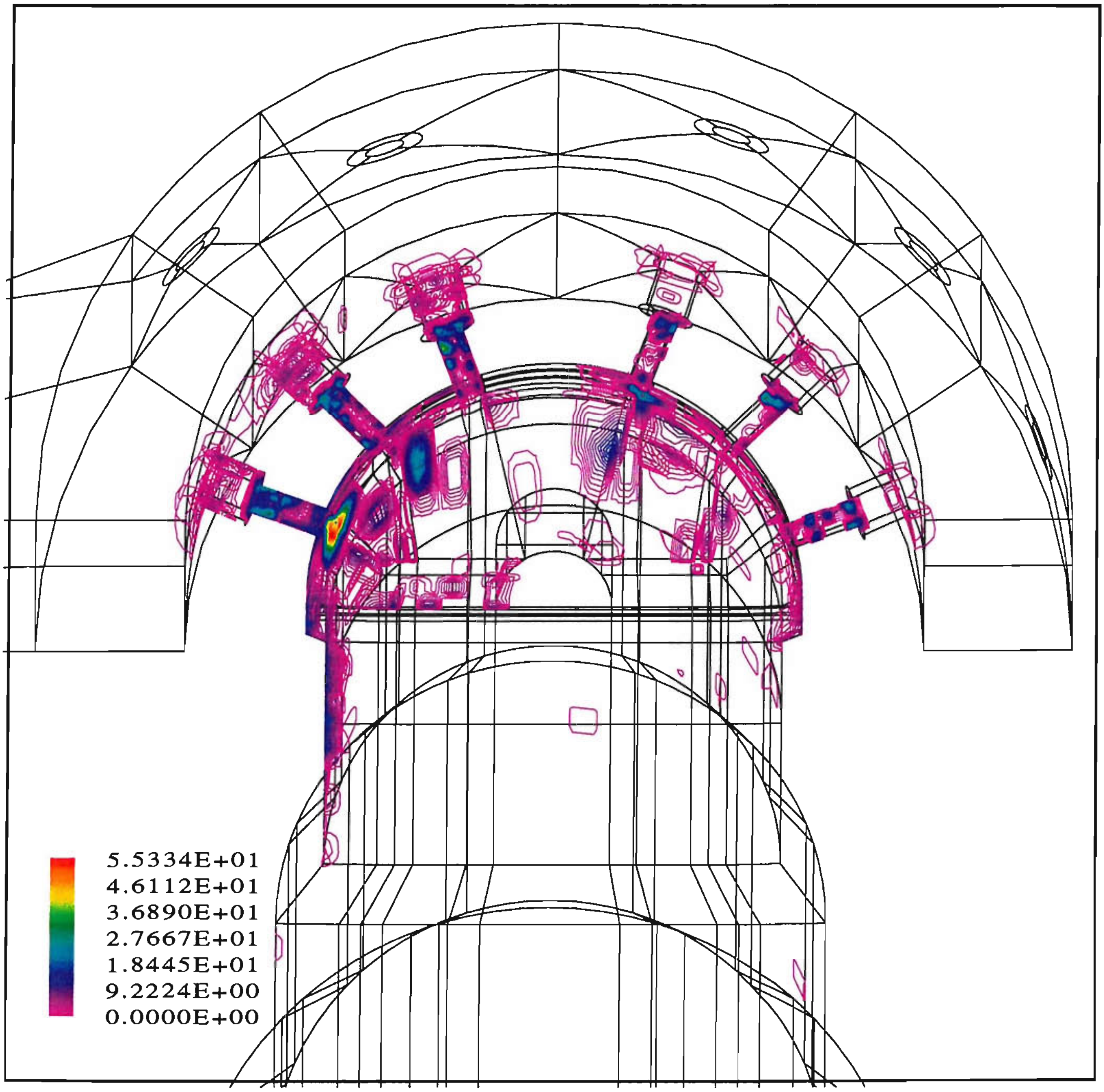

EROSION CHARACTERISTICS OF THE STAINLESS STEEL CC30 CONTROL CHOKE

Particle Type - **Sand**
Particle Loading and Flux Rate - **1.16** % by wt & **88.7** g/s.
Particle Roundness Factor - **0.5**
Number of Particle Sizes and Total Number of Particles Tracked - **20** & **1440**
Particle Size Range - **20-385** μm
Turbulent Dispersion - **Yes**
Modified Coefficient of Restitution - **Yes**
Squeeze Film Retardation - **Yes**
Gravity Vector Set - **Yes**

Simulation Section - **CC30 Top**

Appendix Figure 181 - SS CC30 Particle Impact Velocity, Complete Calculation Sequence (m/s)

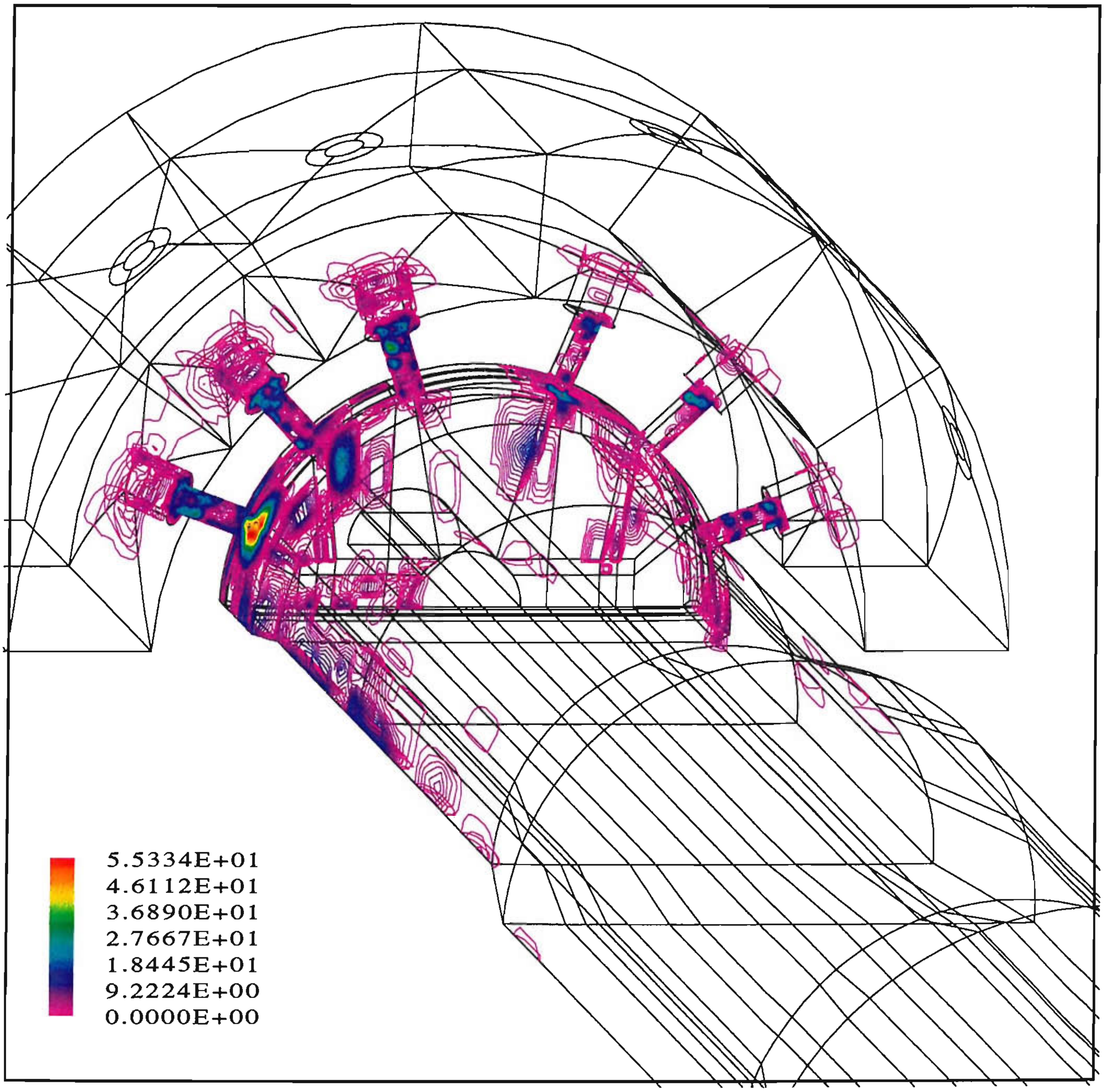

EROSION CHARACTERISTICS OF THE STAINLESS STEEL CC30 CONTROL CHOKE

Particle Type - **Sand**
Particle Loading and Flux Rate - **1.16** % by wt & **88.7** g/s.
Particle Roundness Factor - **0.5**
Number of Particle Sizes and Total Number of Particles Tracked - **20** & **1440**
Particle Size Range - **20-385** μm
Turbulent Dispersion - **Yes**
Modified Coefficient of Restitution - **Yes**
Squeeze Film Retardation - **Yes**
Gravity Vector Set - **Yes**

Simulation Section - **CC30 Top**

Appendix Figure 182 - SS CC30 Particle Impact Angle, Complete Calculation Sequence (Deg)

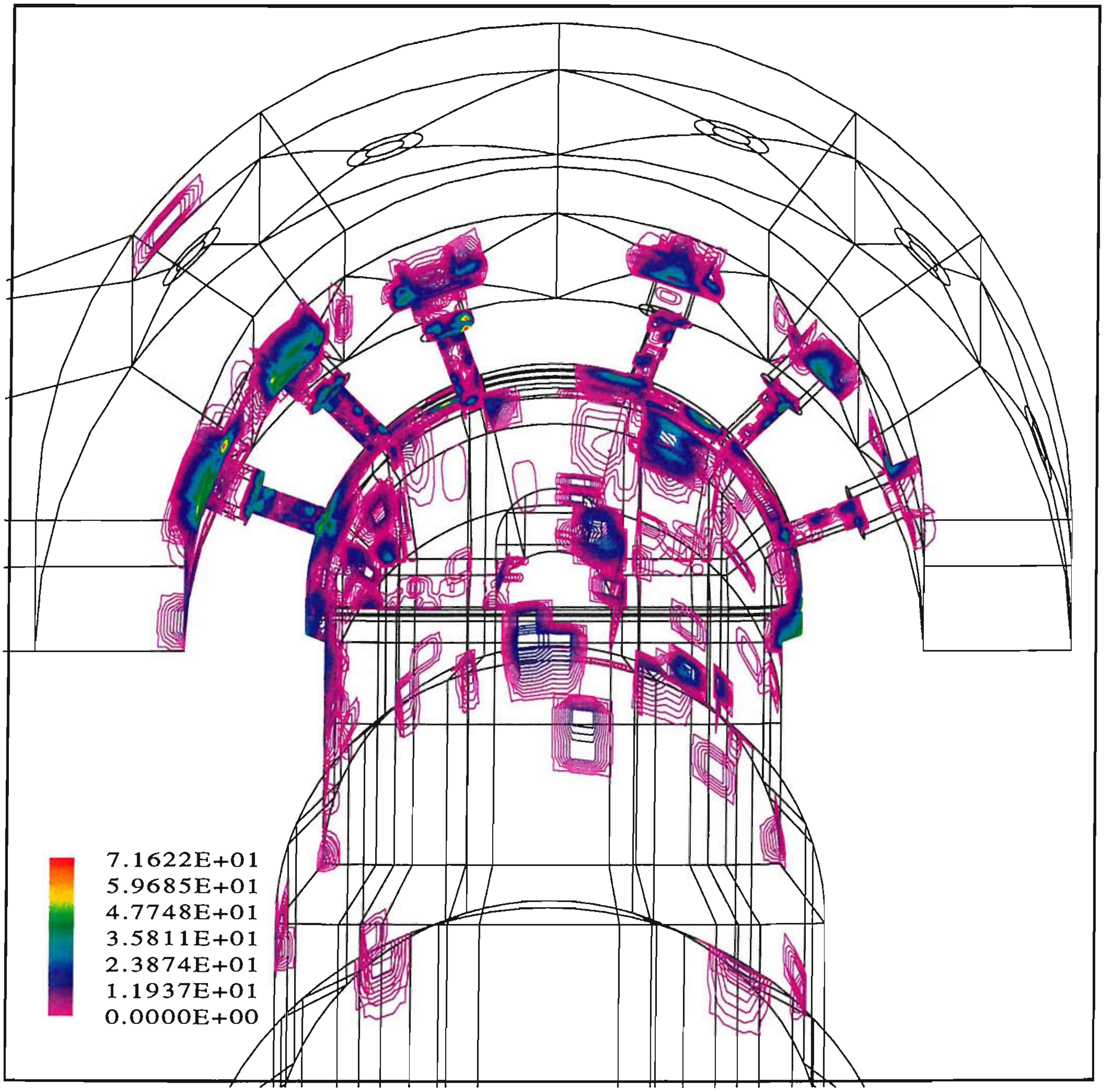

EROSION CHARACTERISTICS OF THE STAINLESS STEEL CC30 CONTROL CHOKE

Particle Type - **Sand**
Particle Size Mass Flux - **41.5** g/s.
Particle Roundness Factor - **0.5**
Number of Particle Sizes and Total Number of Particles Tracked - **12 & 864**
Particle Size Range - **150-385** μm
Turbulent Dispersion - **Yes**
Modified Coefficient of Restitution - **Yes**
Squeeze Film Retardation - **Yes**
Gravity Vector Set - **Yes**

Simulation Section - **CC30 Top**

Appendix Figure 183 - SS CC30 Particle Erosion Rate after 3 Calculation Sequences (mm^2/hr)

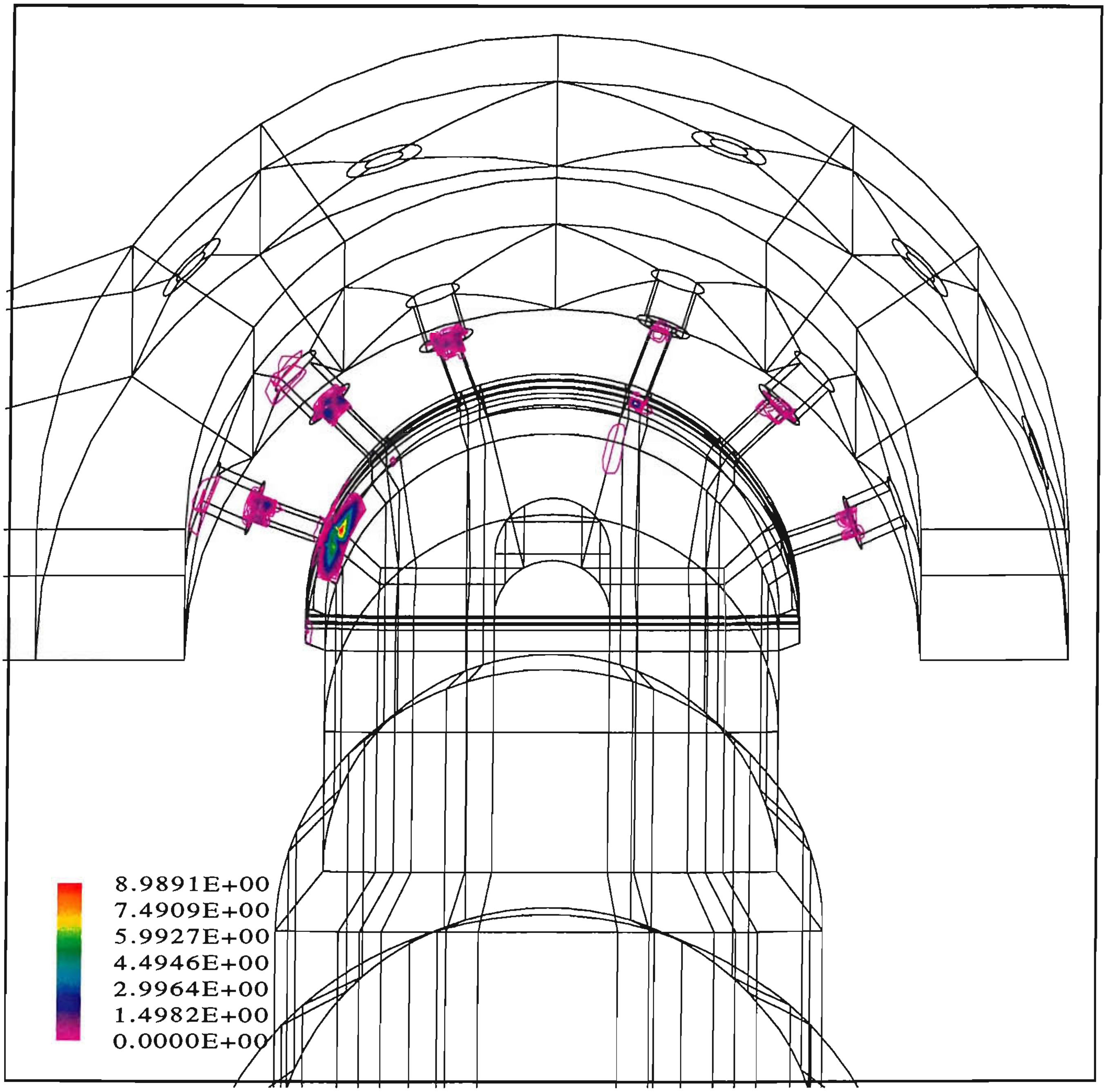

EROSION CHARACTERISTICS OF THE STAINLESS STEEL CC30 CONTROL CHOKE

Particle Type - **Sand**
Particle Size Mass Flux - **85.4** g/s.
Particle Roundness Factor - **0.5**
Number of Particle Sizes and Total Number of Particles Tracked - **16 & 1152**
Particle Size Range - **63-385** μm
Turbulent Dispersion - **Yes**
Modified Coefficient of Restitution - **Yes**
Squeeze Film Retardation - **Yes**
Gravity Vector Set - **Yes**

Simulation Section - **CC30 Top**

Appendix Figure 184 - SS CC30 Particle Erosion Rate after 4 Calculation Sequences (mm²/hr)

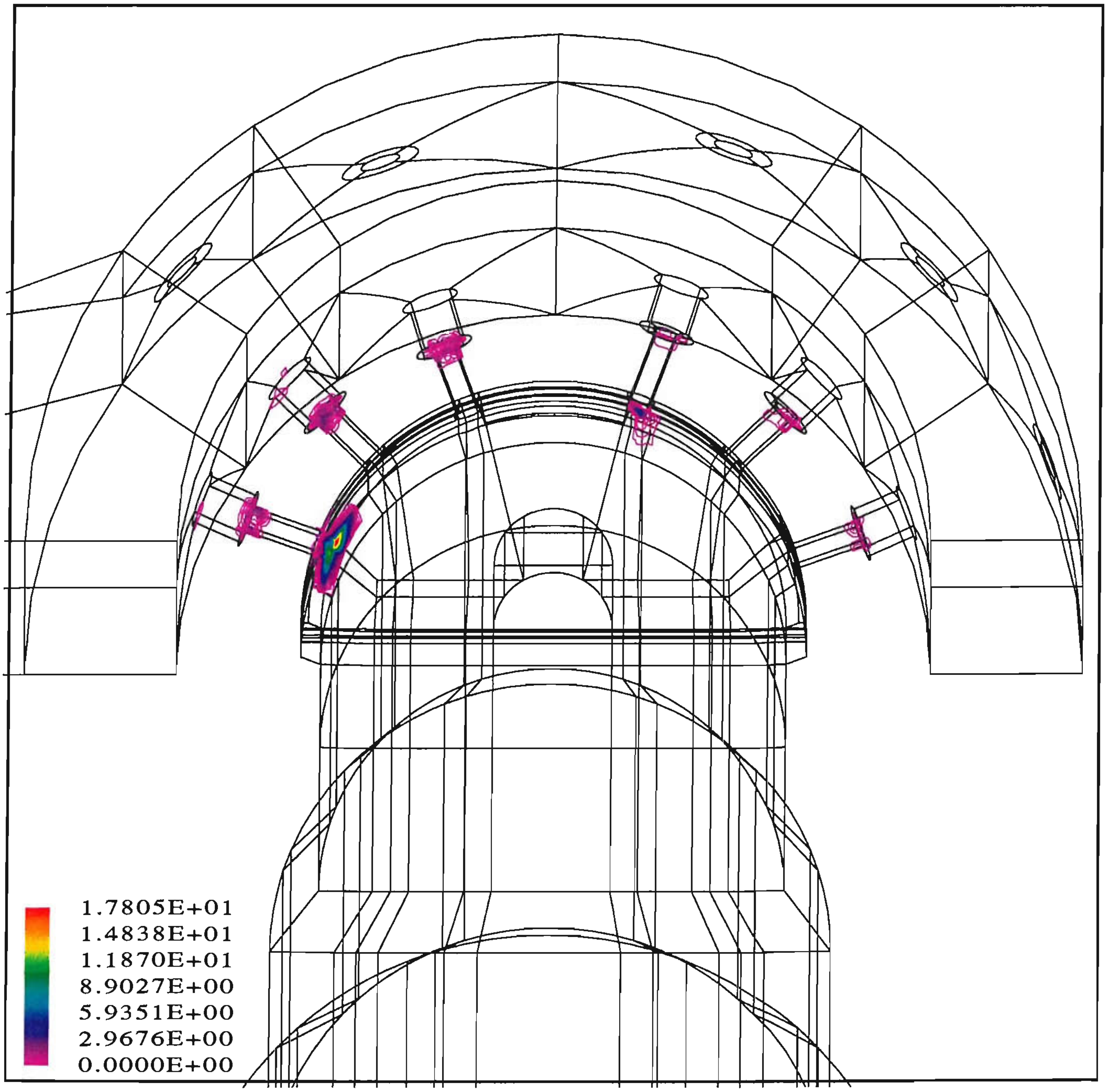

EROSION CHARACTERISTICS OF THE STAINLESS STEEL CC30 CONTROL CHOKE

Particle Type - **Sand**
Particle Size Mass Flux - **88.7** g/s.
Particle Roundness Factor - **0.5**
Number of Particle Sizes and Total Number of Particles Tracked - **20 & 1440**
Particle Size Range - **20-385** μm
Turbulent Dispersion - **Yes**
Modified Coefficient of Restitution - **Yes**
Squeeze Film Retardation - **Yes**
Gravity Vector Set - **Yes** Simulation Section - **CC30 Top**

Appendix Figure 185 - SS CC30 Particle Erosion Rate, Complete Calculation Sequence (mm^2/hr)

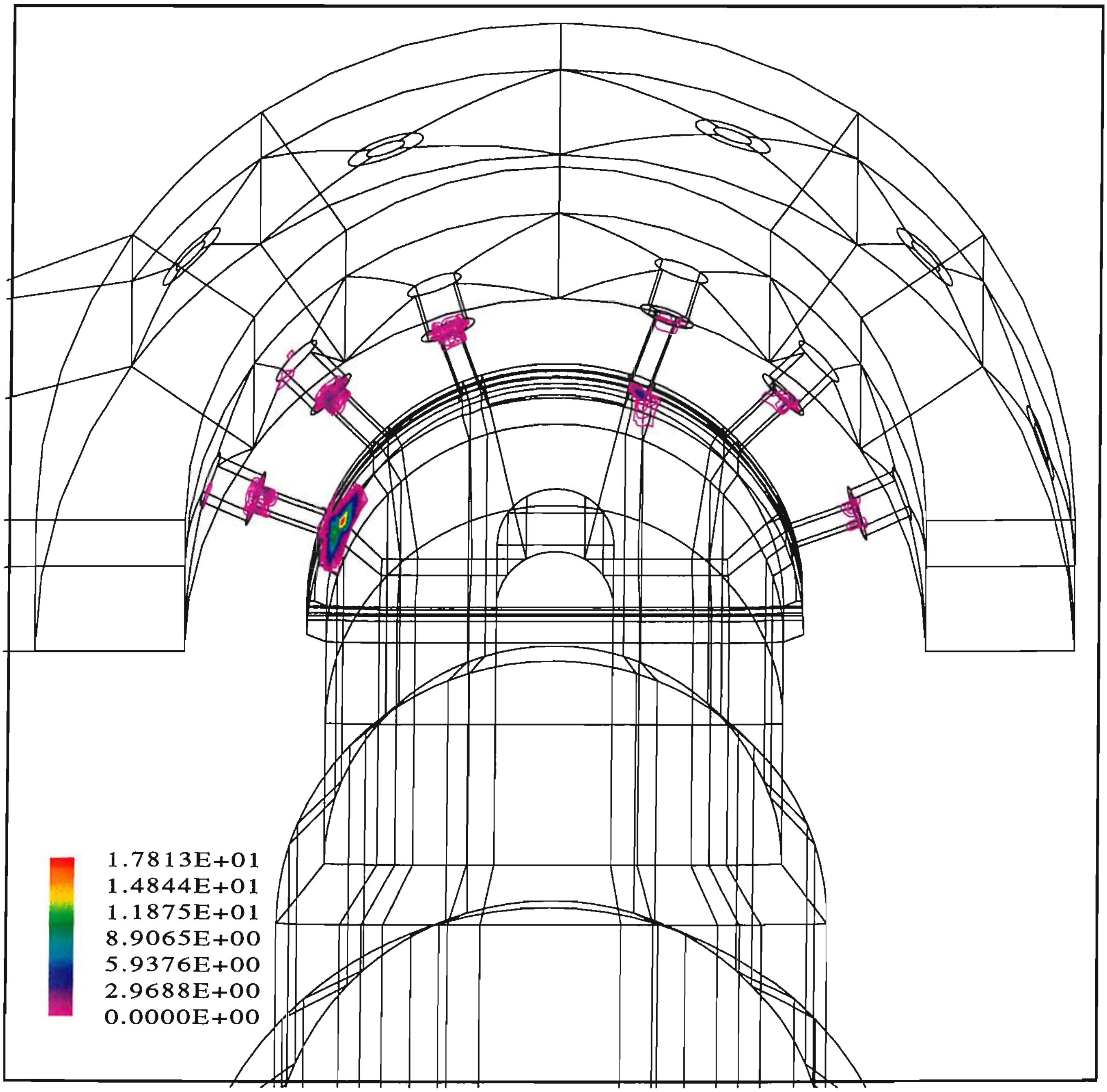

EROSION CHARACTERISTICS OF THE STAINLESS STEEL CC30 CONTROL CHOKE

Particle Type - **Sand**
Particle Size Mass Flux - **88.7** g/s.
Particle Roundness Factor - **0.5**
Number of Particle Sizes and Total Number of Particles Tracked - **20 & 1440**
Particle Size Range - **20-385** μm
Turbulent Dispersion - **Yes**
Modified Coefficient of Restitution - **Yes**
Squeeze Film Retardation - **Yes**
Gravity Vector Set - **Yes**

Simulation Section - **CC30 Top**

Appendix Figure 186 - SS CC30 Particle Erosion Rate, Complete Calculation Sequence (mm^2/hr)